EMERGING TOOLS FOR EMERGING SYMBIOSES — USING GENOMICS APPLICATIONS TO STUDYING ENDOPHYTES

EDITED BY: Mysore V. Tejesvi, Anna Maria Pirttilä and A. Carolin Frank
PUBLISHED IN: Frontiers in Microbiology

frontiers Research Topics

ISSN 1664-8714
ISBN 978-2-88945-219-4
DOI 10.3389/978-2-88945-219-4

About Frontiers

Frontiers is more than just an open-access publisher of scholarly articles: it is a pioneering approach to the world of academia, radically improving the way scholarly research is managed. The grand vision of Frontiers is a world where all people have an equal opportunity to seek, share and generate knowledge. Frontiers provides immediate and permanent online open access to all its publications, but this alone is not enough to realize our grand goals.

Frontiers Journal Series

The Frontiers Journal Series is a multi-tier and interdisciplinary set of open-access, online journals, promising a paradigm shift from the current review, selection and dissemination processes in academic publishing. All Frontiers journals are driven by researchers for researchers; therefore, they constitute a service to the scholarly community. At the same time, the Frontiers Journal Series operates on a revolutionary invention, the tiered publishing system, initially addressing specific communities of scholars, and gradually climbing up to broader public understanding, thus serving the interests of the lay society, too.

Dedication to Quality

Each Frontiers article is a landmark of the highest quality, thanks to genuinely collaborative interactions between authors and review editors, who include some of the world's best academicians. Research must be certified by peers before entering a stream of knowledge that may eventually reach the public - and shape society; therefore, Frontiers only applies the most rigorous and unbiased reviews.
Frontiers revolutionizes research publishing by freely delivering the most outstanding research, evaluated with no bias from both the academic and social point of view.
By applying the most advanced information technologies, Frontiers is catapulting scholarly publishing into a new generation.

What are Frontiers Research Topics?

Frontiers Research Topics are very popular trademarks of the Frontiers Journals Series: they are collections of at least ten articles, all centered on a particular subject. With their unique mix of varied contributions from Original Research to Review Articles, Frontiers Research Topics unify the most influential researchers, the latest key findings and historical advances in a hot research area! Find out more on how to host your own Frontiers Research Topic or contribute to one as an author by contacting the Frontiers Editorial Office: **researchtopics@frontiersin.org**

EMERGING TOOLS FOR EMERGING SYMBIOSES — USING GENOMICS APPLICATIONS TO STUDYING ENDOPHYTES

Topic Editors:
Mysore V. Tejesvi, University of Oulu, Finland
Anna Maria Pirttilä, University of Oulu, Finland
A. Carolin Frank, University of California, Merced, United States

Aspen leaves exhibit beautiful autumn colors of yellow and red, along with brown dots indicating endophyte infection.
Photo by AM Pirttilä

Plants are typically colonized by numerous endophyte species symbiotically without any noticeable disease symptoms. These microbes are abundant, diverse and play critical ecological roles across natural and agricultural ecosystems. Endophytes have attracted the attention of researchers

due to their various beneficial effects on plants, especially in agricultural crop species. Genomic tools will enhance our understanding on the growth and nutrition requirements of this host-symbiont relationship. Recent advances in DNA sequencing technologies and bioinformatic pipelines have allowed analyzing the plant microbiome and host-endophyte interaction more effectively with limited bias. Furthermore, various studies have employed and utilized transcriptomic and genomic tools to understand the role of endophytes and their interaction with plant hosts. This electronic book covers various research articles highlighting the important developments on endophytes using transcriptomics, next generation sequencing and genomic tools.

Citation: Tejesvi, M. V., Pirttilä, A. M., Frank, A. C., eds. (2017). Emerging Tools for Emerging Symbioses — Using Genomics Applications to Studying Endophytes. Lausanne: Frontiers Media. doi: 10.3389/978-2-88945-219-4

Table of Contents

frontiers in Microbiology

EDITORIAL
published: 16 May 2017
doi: 10.3389/fmicb.2017.00859

Editorial: Emerging Tools for Emerging Symbioses—Using Genomics Applications to Studying Endophytes

Mysore V. Tejesvi[1]*, *Anna Maria Pirttilä*[1] and *A. Carolin Frank*[2]

[1] Ecology and Genetics, Faculty of Science, University of Oulu, Oulu, Finland, [2] Life and Environmental Sciences and Sierra Nevada Research Institute, School of Natural Sciences, University of California, Merced, Merced, CA, USA

Keywords: endophytes, trancriptomics, genomics, microarrays, host–endophyte interaction

Editorial on the Research Topic

Emerging Tools for Emerging Symbioses—Using Genomics Applications to Studying Endophytes

OPEN ACCESS

Edited by:
Choong-Min Ryu,
Korea Research Institute of Bioscience and Biotechnology, South Korea

Reviewed by:
Choong-Min Ryu,
Korea Research Institute of Bioscience and Biotechnology, South Korea
Gregor Langen,
University of Cologne, Germany
Henry Mueller,
Graz University of Technology, Austria

***Correspondence:**
Mysore V. Tejesvi
mvtejesvi@gmail.com

Specialty section:
This article was submitted to Plant Microbe Interactions, a section of the journal Frontiers in Microbiology

Received: *14 December 2016*
Accepted: *27 April 2017*
Published: *16 May 2017*

Citation:
Tejesvi MV, Pirttilä AM and Frank AC (2017) Editorial: Emerging Tools for Emerging Symbioses—Using Genomics Applications to Studying Endophytes. Front. Microbiol. 8:859. doi: 10.3389/fmicb.2017.00859

Endophytes, bacteria or fungi colonizing the interior of plants, are abundant, diverse, and play critical ecological roles across natural and agricultural ecosystems. Plants are typically colonized by hundreds of endophyte species without any noticeable disease symptoms. Endophytes have attracted the attention of researchers all over the world due to their various beneficial effects on plants. The rationale for studying endophytes using emerging tools is to better understand the beneficial bacteria and fungi associated with agricultural crops, including their origin, maintenance, and nutritional requirements could help the development of sustainable agricultural systems and the exploitation of various plant–symbiont natural products. Recent advances in DNA sequencing technology and computation now allow more complete descriptions of the endophyte community composition without the biases imposed by culturing. Complementing taxonomic data, community functional traits such as substrate utilization, can be characterized at high throughput using Phenotype MicroArrays (Blumenstein et al.). Comparing whole genomes of endophytes and other symbiotic bacteria with those of pathogens, the factors underlying symbiosis can be identified. Furthermore, analysis of the transcriptomes of both host and microbes can unveil the molecular underpinnings of the interaction.

The studies collected in this ebook advance our knowledge of endophytes and their impact on plants, highlighting the importance of both bacterial and fungal microbiomes on plant health and growth. For example, the largest plants on Earth, *Sequoia sempervirens* and *Sequoiadendron giganteum* host variable communities of bacteria in their foliage, including *Bacillus*, *Burkholderia,* and *Actinomycetes* species that could protect the giant trees against biotic stress was studied using 454 sequencing technology and data was analyzed using Quantitative insights into Microbial Ecology (QIIME) package (Carrell and Frank). It is already known that many endophytes induce resistance and protect the host against diseases. An endophyte of olive, *Pseudomonas fluorescens* PICF7, was found by Gómez-Lama Cabanás et al. antagonistic toward *Verticillium*, triggering a broad range of defense responses in root tissues and was studied using Suppression Subtractive Hybridization" (SSH) technology and quantitative real-time PCR (qRT-PCR). Results indicated that the endophyte triggered defense responses not only locally in roots, but also in other tissues, such as stems and leaves, indicating a systemic response. Host responses by dark septate endophytes (DSEs) were elucidated in the model plants *Arabidopsis thaliana* and *Allium porrum*, showing to be dependent on the plant species and ecotypes. An important finding was that the shifts in the

environmental conditions directed the host responses along the mutualism–parasitism continuum, which confirms earlier understanding of the thin line between an endophyte and a pathogen (Mandyam and Jumpponen).

Interaction and co-existence of endophytes and pathogens often depends on the full plant microbiome and virulence factors. One of the hot topics in our book is the comparative genomics of pathogens and endophytes, which is aimed to get a better grasp of these complex interactions and in turn to lead to a better understanding of plant health. Major differences between genomic virulence factors of endophytes and non-endophytes were analyzed by Lòpez-Fernàndez et al. whereas Sheibani-Tezerji et al. compared the genomes of three strains of *Pantoea ananatis*, isolated from healthy maize seeds, to identify functional genes and the genetic drivers of niche adaption.

Many endophytes have other beneficial effects on the plant host besides protection against diseases, such as growth promotion. Some endophytes can induce development of roots or shoots of the host plant and the composition of the endophytic community may change along with development. For example, *Agrobacterium* and *Erwinia* dominated the seedling stage and members of *Sphingomonas* and *Methylobacterium* were mainly found in the mature leaves of Stevia, positively correlating with *Steviol glycosides* accumulation and was studied using V4 and V6 region of 16S rRNA gene using 454 GS-FLX platform (Yu et al.). Whereas the endophytes typically studied and sequenced are bacteria or fungi, the specific group of endophytic yeasts has largely gone unstudied. The pink-pigmented yeast strain *Rhodotorula graminis* WP1, isolated from *Populus trichocarpa*, was the *first* endophytic yeast genome to be sequenced using the Sanger whole genome shotgun approach (Firrincieli et al.). In comparison with the mycorrhizal fungus *Laccaria bicolor*, *R. graminis* WP1 potentially uses a different signaling pathway to communicate with the host, even though both of these fungi are Basidiomycete symbionts of poplar. Another example is the study by Tadra-Sfeir et al. where RNA-Seq was used to identify the essential genes required for establishment and interaction of endophytes in the transcriptome of the endophytic diazotroph *Herbaspirillum seropedicae*.

The endophytic microbiomes have growing significance in applications such as agriculture and forestry, and may play important but yet unrecognized roles in climate change. In the banana microbiome studied using Illumina MiSeq Sequencing, differences in indicator species associated with legume-based agroforestry (Köberl et al.) suggest that there is a flow between the microbiomes of neighboring plants. This brings the cropping systems to a completely new era as not only nitrogen fixation, but other beneficial traits, such as biocontrol, can be acquired from surrounding plant communities. A serious implication of climate change on methane emissions by rice microbiomes was studied using 454 GS FLX sequencing platform by Okubo et al. The relative abundance of methane-oxidizing *Methylocystaceae* decreased in the rice plants with increased CO_2 levels. As an alarming result, the elevated CO_2 affected the carbon cycle in the rice paddy fields by suppression of methane oxidation and through increased methanogenesis.

This e-book represents an outstanding collection of endophytic research done by various modern molecular biology tools, including next generation sequencing, genome sequencing, and transcriptomics. The book advances our knowledge and understanding on important elements of this symbiosis and provides food for thought for future research. We are grateful to all the authors who have responded to the call and for reviewers for their valuable support.

AUTHOR CONTRIBUTIONS

Editorial was written by MT and subsequent revision, discussion, and modifications were done by MT, AMP, and ACF.

Conflict of Interest Statement: The authors declare that the research was conducted in the absence of any commercial or financial relationships that could be construed as a potential conflict of interest.

frontiers in MICROBIOLOGY

ORIGINAL RESEARCH ARTICLE
published: 11 February 2015
doi: 10.3389/fmicb.2015.00091

Agroforestry leads to shifts within the gammaproteobacterial microbiome of banana plants cultivated in Central America

Martina Köberl[1]*, Miguel Dita[2,3], Alfonso Martinuz[3], Charles Staver[4] and Gabriele Berg[1]

[1] Institute of Environmental Biotechnology, Graz University of Technology, Graz, Austria
[2] Brazilian Agricultural Research Corporation – Embrapa, Brasília, Brazil
[3] Bioversity International Costa Rica, Turrialba, Costa Rica
[4] Bioversity International France, Montpellier, France

Edited by:
Anna Maria Pirttilä, University of Oulu, Finland

Reviewed by:
David John Studholme, University of Exeter, UK
Nai-Chun Lin, National Taiwan University, Taiwan
Reindert Nijland, Wageningen University, Netherlands

***Correspondence:**
Martina Köberl, Institute of Environmental Biotechnology, Graz University of Technology, Petersgasse 12/I, 8010 Graz, Austria
e-mail: martina.koeberl@tugraz.at

Bananas (*Musa* spp.) belong to the most important global food commodities, and their cultivation represents the world's largest monoculture. Although the plant-associated microbiome has substantial influence on plant growth and health, there is a lack of knowledge of the banana microbiome and its influencing factors. We studied the impact of (i) biogeography, and (ii) agroforestry on the banana-associated gammaproteobacterial microbiome analyzing plants grown in smallholder farms in Nicaragua and Costa Rica. Profiles of 16S rRNA genes revealed high abundances of *Pseudomonadales*, *Enterobacteriales*, *Xanthomonadales*, and *Legionellales*. An extraordinary high diversity of the gammaproteobacterial microbiota was observed within the endophytic microenvironments (endorhiza and pseudostem), which was similar in both countries. Enterobacteria were identified as dominant group of above-ground plant parts (pseudostem and leaves). Neither biogeography nor agroforestry showed a statistically significant impact on the gammaproteobacterial banana microbiome in general. However, indicator species for each microenvironment and country, as well as for plants grown in *Coffea* intercropping systems with and without agri-silvicultural production of different *Fabaceae* trees (*Inga* spp. in Nicaragua and *Erythrina poeppigiana* in Costa Rica) could be identified. For example, banana plants grown in agroforestry systems were characterized by an increase of potential plant-beneficial bacteria, like *Pseudomonas* and *Stenotrophomonas*, and on the other side by a decrease of *Erwinia*. Hence, this study could show that as a result of legume-based agroforestry the indigenous banana-associated gammaproteobacterial community noticeably shifted.

Keywords: agroforestry, banana-associated *Gammaproteobacteria*, banana-coffee intercropping, Gros Michel, *Musa*

INTRODUCTION

Musa spp., including dessert and cooking bananas, are large perennial monocotyledonous herbs of the order *Zingiberales*. Their domestication process started about 7000 years ago and involved hybridizations between diverse species and subspecies and the selection of sometimes diploid, but generally triploid seedless, parthenocarpic hybrids, which were thereafter widely dispersed by vegetative propagation (Perrier et al., 2011). The cultigens are landraces and belong to the most important agricultural crops in the tropics and sub-tropics. Worldwide, over 100 million metric tons of fruits are produced annually. Cultivars that enter international commerce are worth $5 billion per year, and locally consumed fruits are major staples for 400 million people in Latin America and Africa (FAOSTAT, 2005).

The *Musa acuminata* cultivar Gros Michel, also known as Big Mike, was the main exported banana variety from the nineteenth century until the late 1950s. However, in response to the susceptibility of this cultivar to the fungal pathogen *Fusarium oxysporum* f. sp. *cubense* (Foc) race 1, Gros Michel was widely replaced by the resistant Cavendish variety (Ploetz, 2006; Butler, 2013). In many countries in Central America, such as Costa Rica and Nicaragua, the Gros Michel variety is still grown, mainly by smallholder farmers in banana-coffee intercropping systems, sometimes in combination with agroforestry systems, where a lower disease incidence is reported in comparison to monocultures. Gros Michel fruits are praised for their fabulous flavor and, due to their thicker skin, for a better robustness to bruises in comparison to Cavendish. Agroforestry in general is a collective name for land-use systems in which woody perennials are grown in association with herbaceous plants or livestock, in spatial arrangement, a rotation or both (Lundgren, 1982). These practices are considered as functionally biodiverse, environmentally friendly and sustainable land-use alternatives. It was shown that such systems were able to enhance soil fertility and productivity by improving certain soil physical properties and protective functions, such as nutrient cycling and carbon sequestration

(Montagnini and Nair, 2004; Seobi et al., 2005; Udawatta et al., 2009). Undeniably, it can be assumed that these environmental benefits are associated with soil microbial activity and soil biological parameters. In addition, the plant-associated microbiome has substantial influence on plant growth, quality, and health (Berg et al., 2014). However, despite the importance of banana for grower's livelihoods on these agroforestry systems in Central America and the hypothesized role of soil and plant microbiome on building healthier environments, knowledge on the microbial diversity of representative productions areas is still scarce.

The objective of this study was to decipher the gammaproteobacterial microbiome of banana plants cultivated in Central America. In order to obtain an almost complete picture of the banana-colonizing *Gammaproteobacteria* under diverse conditions, different plant parts and microenvironments were investigated: the rhizosphere soil surrounding the roots and represents the interface to the bulk soil, the inner tissue of the roots - the endorhiza, the banana leaves, as well as the pseudostem. The cylindrical succulent pseudostem is a peculiarity of the herbaceous banana plant which consists of closely packed leaf-petiole sheaths (Saravanan and Aradhya, 2011). It provides a unique microhabitat for endophytic microorganisms and was recently identified as a bacterial hot spot colonized by an extraordinary high abundance and diversity of enterics (Rossmann et al., 2012). Consequently, we hypothesized a key role of the *Enterobacteriaceae* for plant health especially in the endophytic microenvironments. To additionally capture the group of often plant-beneficial fluorescent pseudomonads (Ayyadurai et al., 2006; Weller, 2007), and at the same time to preserve the necessary sequencing depth, we decided to focus on the whole gammaproteobacterial fraction by employing a comprehensive 16S rRNA gene amplicon sequencing approach. Comparisons between colonization patterns reveal the impact of (i) biogeography (Nicaragua vs. Costa Rica), and (ii) agroforestry conditions (banana-coffee intercropping with vs. without agroforestry) on the banana-associated gammaproteobacterial microbiota.

MATERIALS AND METHODS

EXPERIMENTAL DESIGN AND SAMPLING PROCEDURE

Samples were taken in November 2012 from *M. acuminata* Colla (AAA group) cultivar Gros Michel in Nicaragua and Costa Rica. In each country, samples of banana roots, pseudostem, leaves, and rhizosphere soil were collected from three different farms (Figure S1), where bananas were cultivated in intercropping systems with *Coffea* spp. To understand the effect of agroforestry on the banana-associated microbiome, samples were collected on each farm from sites with and without associated *Fabaceae* trees. The predominant trees were *Inga* spp. in Nicaragua and *Erythrina poeppigiana* in Costa Rica. Each site was under the respective production system since more than 50 years. Composite samples consisting of sub-samples from five appropriate plants without visible infestation of any disease were taken for each microenvironment.

TOTAL COMMUNITY DNA ISOLATION

For extraction of metagenomic DNA from the rhizosphere, 2 g of rhizospheric soil were mixed with 15 ml of 0.85% NaCl for 10 s on the vortex. To isolate total community DNA from the endorhiza, 5 g of roots were surface-sterilized with 4% NaOCl for 5 min. Afterwards, roots were washed three times with sterile distilled water and transferred to sterile WhirlPaks (Nasco, Fort Atkinson, USA), then 10 ml of 0.85% NaCl were added and the surface-sterilized roots were homogenized using mortar and pestle. Pseudostem samples (5 g) were washed with sterile distilled water, transferred to WhirlPaks, and after 10 ml of 0.85% NaCl were added, homogenized with mortar and pestle. From phyllosphere samples, 5 g of leaves were washed three times with sterile distilled water, before homogenization with 10 ml of 0.85% NaCl. From the liquid parts 4 ml were centrifuged at high speed (16,000 × g, 4°C) for 20 min and resulting pellets were stored at −70°C. Total community DNA was extracted using the FastDNA SPIN Kit for Soil (MP Biomedicals, Solon, USA) according to the manufacturer's protocol. Metagenomic DNA samples were encoded using abbreviations indicating: (1) country (N−, Nicaragua; C−, Costa Rica), (2) microenvironment (S, rhizosphere soil; Re, endorhiza; Ps, pseudostem; L, leaves), (3) farm (1–3 in each country; Figure S1) (4) agroforestry conditions (T+, with trees; T−, without trees).

GAMMAPROTEOBACTERIAL 16S rRNA GENE PROFILING BY ILLUMINA MiSeq SEQUENCING

For a deep-sequencing analysis of the banana-associated *Gammaproteobacteria* community, the hypervariable V4 region of the 16S rRNA gene was amplified in a nested PCR approach with the *Gammaproteobacteria* specific primer pair Gamma395f/Gamma871r (Mühling et al., 2008) and the universal primer pair 515F/806R (Caporaso et al., 2011), which carried sample specific tags. The reaction mixture for the first PCR (20 µl) contained 1 × Taq&Go (MP Biomedicals, Eschwege, Germany), 2 mM $MgCl_2$, 0.1 µM of each primer and 1 µl of template DNA dilution (96°C, 4 min; 30 cycles of 96°C, 1 min; 54°C, 1 min; 74°C, 1 min; and elongation at 74°C, 10 min). The second PCR (30 µl) was performed by using 1 × Taq&Go, 0.2 µM of each primer and 1.2 µl from dilutions of the first PCR mixtures (94°C, 3 min; 32 cycles of 94°C, 45 s; 60°C, 1 min; 72°C, 18 s; and elongation at 72°C, 10 min). PCR products of three independent reactions were pooled in equal volumes and purified by employing the Wizard SV Gel and PCR Clean-Up System (Promega, Madison, USA). Sequence libraries were generated by a paired-end approach using the Illumina MiSeq platform (Eurofins MWG, Ebersberg, Germany). The nucleotide sequences are available in the European Nucleotide Archive (www.ebi.ac.uk/ena) under the accession number PRJEB8107.

Data analysis was performed by employing the open source software package QIIME 1.8 (Caporaso et al., 2010a). Sequencing reads with more than three consecutive low quality base calls (Phred quality score ≤ 20) were truncated at the position where their quality began to drop, and only reads with >75% consecutive high quality base calls, without any ambiguous characters, and longer than 200 nucleotides in length were retained for further analyses. All quality sequences were adjusted in the same orientation and clustered into operational taxonomic units (OTUs) with uclust (Edgar, 2010), using 3, 5, and 10% dissimilarity thresholds. From each OTU the most abundant sequence

was selected as the representative one, and the taxonomy of the representative set was assigned with the uclust-based consensus taxonomy assigner using an 80% confidence threshold. The representative sequence set was aligned with PyNAST (Caporaso et al., 2010b). Chimera check was performed with ChimeraSlayer and potentially chimeric sequences were discarded. OTU tables at the different dissimilarity levels were constructed, and OTUs not assigned to the class of *Gammaproteobacteria* as well as singletons were removed from the dataset. For alpha and beta diversity analyses, OTU tables were rarefied at 13,610 reads. Diversity indices Shannon (Shannon, 1997) and Chao1 (Chao and Bunge, 2002) were determined based on the normalized clustering data. Significant differences were calculated with PASW Statistics 18 (SPSS Inc., Chicago, IL, USA) using Tukey and Games-Howell *post hoc* tests, depending on the homogeneity of variances. Beta diversity was analyzed based on weighted UniFrac distances (Lozupone et al., 2007) and 10 jackknife replicates of the total rarefied datasets. Statistical analyses were performed using the adonis test with 999 permutations. Taxonomy based ring-charts were created with Krona 2.2 (Ondov et al., 2011).

Profile clustering network analyses were performed in order to highlight single taxonomic groups corresponding to genus level (OTUs at a dissimilarity level of 3% summarized at taxonomic level 6) with considerable differences between banana plants grown in Nicaragua and in Costa Rica and between those grown with and without associated trees. The network analyses were carried out with taxa exhibiting a mean read change of more than 0.2% of the data set. If the ratio of relative mean abundances exceeded 1.5, the taxa were regarded as altered and assigned to the respective profile. Networks depicting community changes resulting from biogeographical location were restricted to taxa which significantly differed between countries. Significant differences were ascertained with Metastats (White et al., 2009), where *p*-values were computed using a combination of the non-parametric *t*-test, exact Fisher's test, and the false discovery rate with 10^3 permutations. For networks showing differences caused by agroforestry, only taxonomic groups featuring the same pattern in all three farms of a country were considered. Visualization of the networks was carried out using Cytoscape 2.8.3 (Smoot et al., 2011).

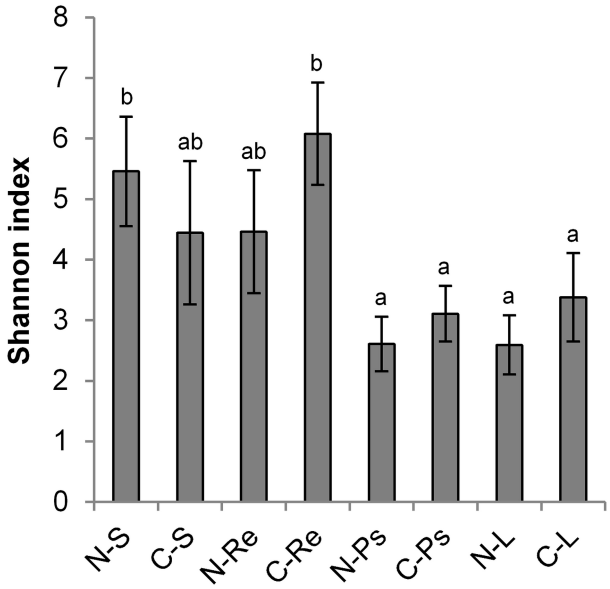

FIGURE 1 | Shannon indices of gammaproteobacterial diversity for different microenvironments (S, rhizosphere soil; Re, endorhiza; Ps, pseudostem; L, leaves) at a genetic distance of 3%, separated in samples from Nicaragua (N–) and Costa Rica (C–). Data were ascertained by 16S rRNA gene profiling and are averages of the three sampling farms of a country ± confidence. Significant differences ($p \leq 0.05$, Tukey *post hoc* test) are indicated by lowercase letters.

RESULTS

RICHNESS AND DIVERSITY OF THE BANANA-ASSOCIATED GAMMAPROTEOBACTERIAL COMMUNITY

The gammaproteobacterial microbiota associated to the rhizosphere, endorhiza, pseudostem, and foliage of healthy banana plants grown under different agroforestry conditions in Nicaragua and Costa Rica analyzed by a barcoded 16S rRNA gene amplicon sequencing approach based on Illumina MiSeq sequencing yielded in 2,234,043 quality sequences with a read length ≥200 nucleotides, between 13,619 and 111,332 quality reads per sample. Rarefaction analyses of the sequencing libraries at a genetic dissimilarity level of 3% are depicted in Figure S2. Comparisons of observed OTUs with their estimated richness by the Chao1 index revealed coverage between 87.3 and 47.4% per sample at order level (Table S1). The sequencing efforts at genus and species level reached 74.1–39.9% and 68.8–31.5%, respectively. The computed Shannon indices of diversity (H′) ranged from 7.56 to 1.47 at a genetic distance of 3% (Table S1). In general, rhizosphere and endorhiza samples exhibited higher gammaproteobacterial diversity than pseudostem and leaves (**Figure 1**). Within samples from Nicaragua, the highest values were observed for the rhizospheric soil (5.46 on average ± 0.90 confidence), but without a significant difference ($p \leq 0.05$, Tukey *post hoc* test) to the endorhiza (4.46 ± 1.02). Significantly lower Shannon indices than in the rhizosphere soil were detected for pseudostem (2.61 ± 0.45) and leaves samples (2.59 ± 0.49). Banana plants from Costa Rica revealed the highest diversity in the endorhiza (6.08 ± 0.85), which not significantly differed from the rhizosphere soil (4.45 ± 1.18). Significantly lower values than in the endorhiza were observed for leaves (3.38 ± 0.73) and pseudostem (3.11 ± 0.46). Between the same microenvironments of banana plants from the two countries, no significant differences were observed. Agroforestry did not show a significant impact ($p \leq 0.05$, Games-Howell *post hoc* test) on the gammaproteobacterial diversity of the different microenvironments.

TAXONOMIC COMPOSITION OF THE GAMMAPROTEOBACTERIAL BANANA MICROBIOME

Nearly all quality sequences could be assigned below the class level, and over all banana-associated communities, high abundances of *Pseudomonadales*, *Enterobacteriales*, *Xanthomonadales*, and *Legionellales* were found (**Figures 2**, **3**). The rhizosphere

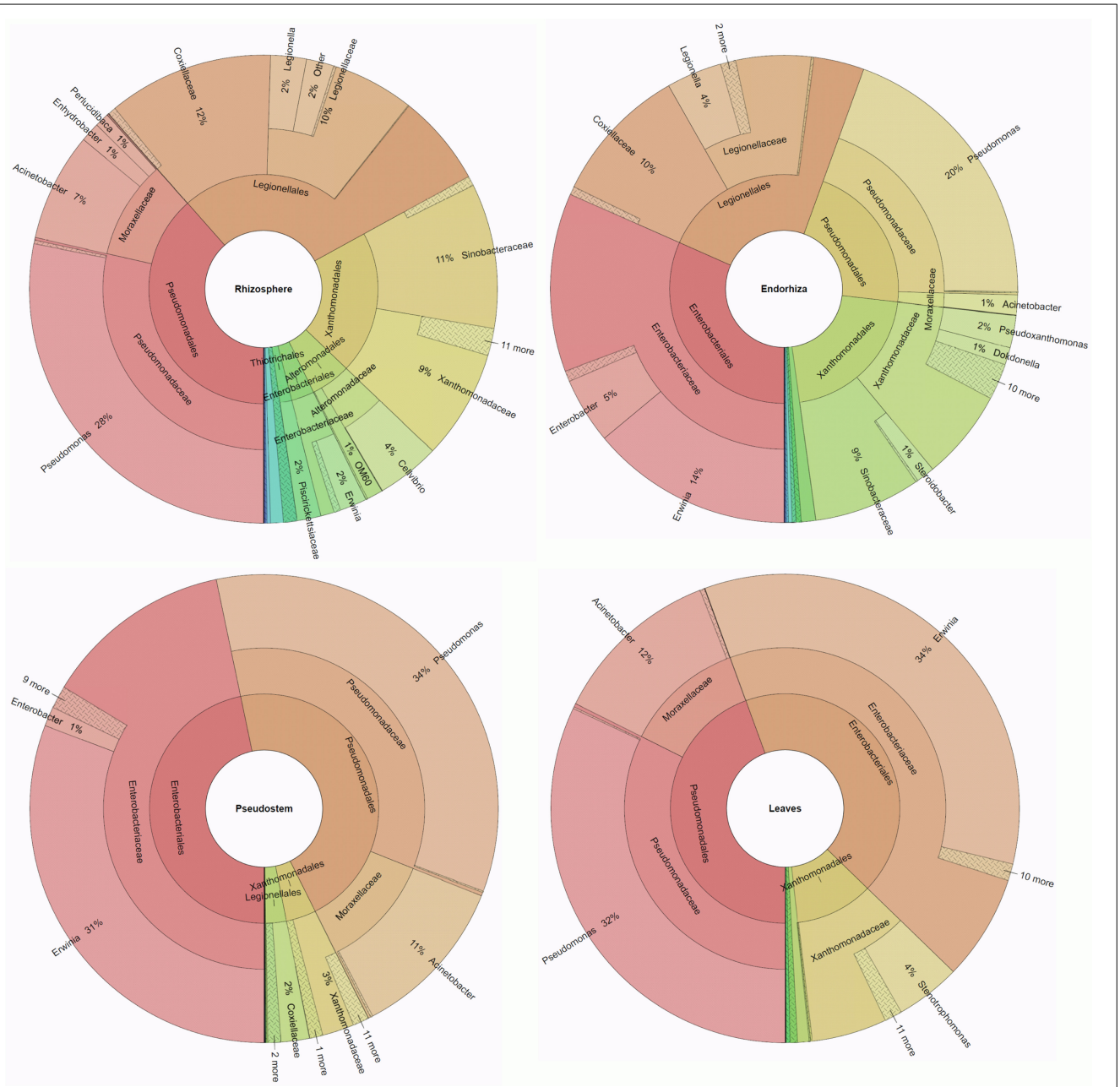

FIGURE 2 | Taxonomic composition of the gammaproteobacterial banana microbiome. Ring-charts for each microenvironment depict the mean values of 12 composite samples from healthy plants grown on six different smallholder farms in Nicaragua and Costa Rica, independent of their agroforestry conditions and biogeographical differences.

of bananas from Nicaragua was colonized by a significantly higher abundance ($p \leq 0.05$, Metastats) of *Pseudomonadales*, *Thiotrichales*, as well as of unclassified *Gammaproteobacteria* than the rhizosphere soil of Costa Rica. Conversely, the plant rhizosphere from Costa Rica was inhabited to a greater extent of *Legionellales* and *Enterobacteriales*. The endorhiza of bananas from Nicaragua exhibited significantly higher relative abundances of *Pseudomonadales*, while *Xanthomonadales* occurred in higher abundances in endorhiza samples from Costa Rica. The pseudostem in general was highly dominated by *Enterobacteriales* and *Pseudomonadales* and showed no significant differences between countries at order level. The foliage exhibited a similar gammaproteobacterial colonization to the pseudostem. However, the leaves from Costa Rica revealed in addition to the dominant orders higher abundances of *Oceanospirillales* than those from Nicaragua.

At lower taxonomic levels, *Pseudomonadales* could be assigned to *Pseudomonadaceae* (genus *Pseudomonas*) and *Moraxellaceae*

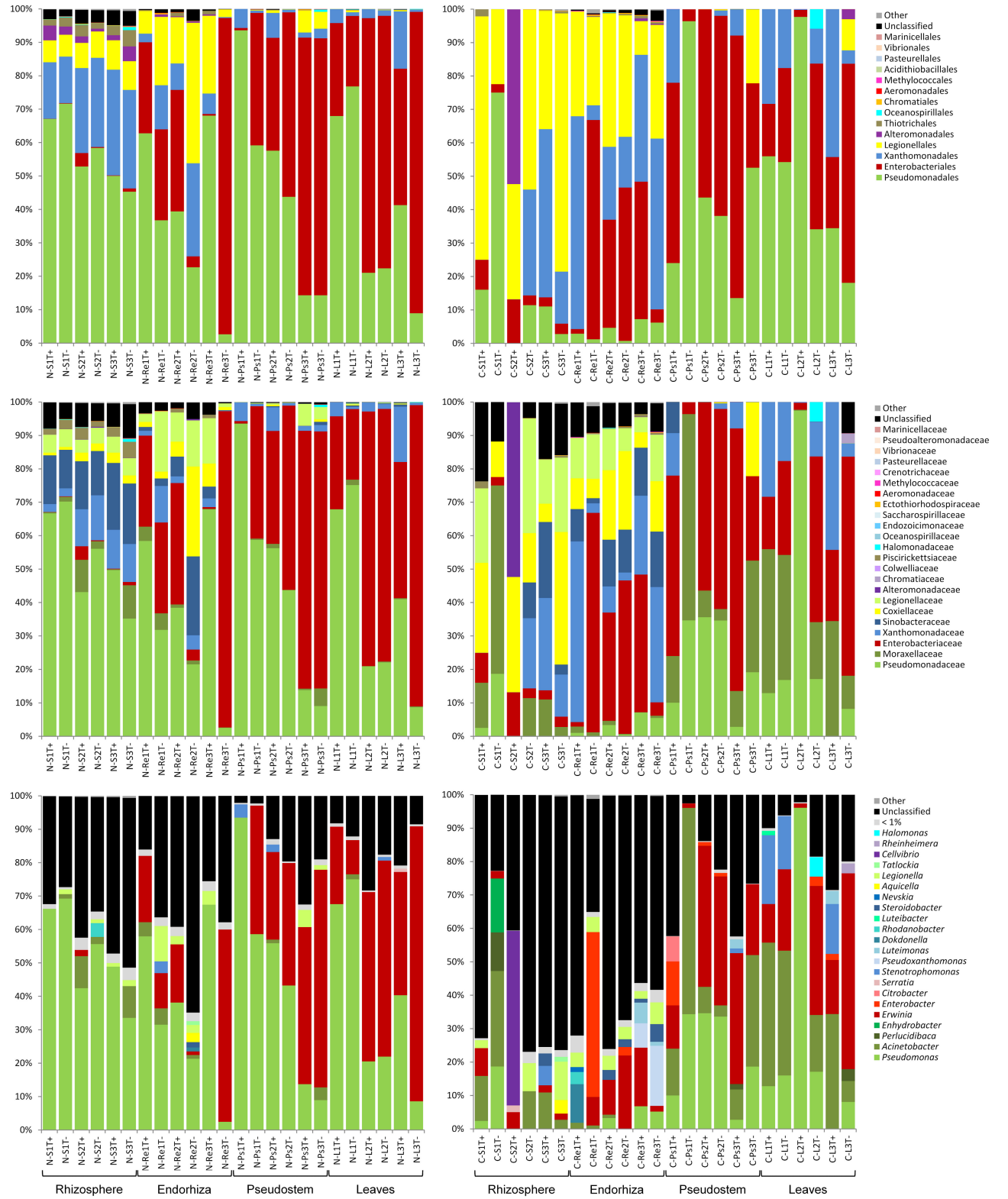

FIGURE 3 | Taxonomic composition of *Gammaproteobacteria* communities inhabiting rhizosphere, endorhiza, pseudostem, and leaves of banana plants from Nicaragua (left) and Costa Rica (right) grown under different agroforestry conditions. Sequences obtained by Illumina MiSeq sequencing were classified at order, family and genus level. Samples were encoded using abbreviations indicating: (1) country (N–, Nicaragua; C–, Costa Rica), (2) microenvironment (S, rhizosphere soil; Re, endorhiza; Ps, pseudostem; L, leaves), (3) farm (1, 2, 3), and (4) agroforestry conditions (T+, with trees; T–, without trees).

(genera *Acinetobacter*, *Perlucidibaca*, and *Enhydrobacter*), whereby in general Nicaragua samples were highly dominated by *Pseudomonadaceae* and samples from Costa Rica revealed a high abundance of *Moraxellaceae*. The enterobacterial fraction was dominated by *Erwinia* with lower abundances of *Enterobacter*, *Citrobacter*, and *Serratia*. *Xanthomonadales* sequences could be assigned to different *Xanthomonadaceae* (*Stenotrophomonas*, *Pseudoxanthomonas*, *Luteimonas*, *Dokdonella*, *Rhodanobacter*, and *Luteibacter*) and *Sinobacteraceae* (*Steroidobacter*, and *Nevskia*). *Legionellales* could be divided into the families *Coxiellaceae* (*Aquicella*) and *Legionellaceae* (*Legionella*, and *Tatlockia*). Further genera identified for taxonomic groups with a relative abundance over 1% per sample belonged to *Alteromonadales* (*Cellvibrio*, and *Rheinheimera*) and to *Oceanospirillales* (*Halomonas*).

IMPACT OF BIOGEOGRAPHY AND AGROFORESTRY

Considering the total gammaproteobacterial community, no significant differences ($p \leq 0.05$, adonis test) based on weighted UniFrac distances could be calculated for individual microenvironments between banana plants grown in Nicaragua and Costa Rica (Table S2), and for none of the countries a significant impact on the banana-colonizing *Gammaproteobacteria* resulting from tree presence was found (Table S3). However, profile clustering network analyses revealed differences of individual taxonomic groups in the colonization patterns between banana plants of the two Central American countries as well as between plants grown in agroforestry systems and those grown without associated trees (**Figure 4**). Each network subdivides the four investigated microenvironments (rhizosphere soil, endorhiza, pseudostem, and leaves), leaving out taxonomic groups without considerable differences between different conditions. In the networks visualizing the impact of biogeography, only taxa with significant differences ($p \leq 0.05$, Metastats) between the sampling countries were shown, while in the networks depicting the impact of agroforestry, only taxa featuring the same pattern in all three farms of the respective country were considered.

Without the influence of different agroforestry trees, banana plants from Nicaragua revealed a significantly higher abundance of *Pseudomonas*, unclassified *Sinobacteraceae*, *Piscirickettsiaceae*, and other unclassified *Gammaproteobacteria* in their rhizosphere (**Figure 4A**), while the rhizosphere and also the endorhiza from plants in Costa Rica was colonized to a greater extent by *Legionellales* (unclassified *Coxiellaceae* and others). The pseudostem did not show significant differences in its gammaproteobacterial colonization between the two countries in plants grown without associated trees. However, the leaves from plants grown in Nicaragua exhibited higher numbers of unclassified *Enterobacteriaceae*, while those of plants from Costa Rica had higher abundances of *Acinetobacter* and unclassified *Xanthomonadaceae*. Under agroforestry conditions, the below-ground habitats of banana plants grown in Nicaragua in association with *Inga* spp. were characterized by much higher abundances of *Pseudomonas* than bananas cultivated under agroforestry conditions with *E. poeppigiana* in Costa Rica (**Figure 4B**). The rhizosphere of plants grown in the *Inga* agroforestry system further revealed higher abundances of unclassified *Alteromonadales* and other unclassified *Gammaproteobacteria*, while banana plants grown in the *Erythrina* agroforestry system were more inhabited by unclassified *Sinobacteraceae* in their endorhiza and by *Erwinia* in their rhizosphere. Conversely, banana leaves from the *Inga* agroforestry system in Nicaragua showed a significantly higher number of *Erwinia*, while the aerial plant parts of Costa Rica's bananas from the *Erythrina* agroforestry system were colonized to a greater extent by *Acinetobacter*. In comparison to banana plants grown without associated trees, plants cultivated in agro-ecosystems in Nicaragua harbored an increased number of *Pseudomonas* (species unclassified) in their endorhiza (**Figure 4C**), as well as of *Xanthomonadaceae* (*Stenotrophomonas* and others) in their above-ground parts. Costa Rica's plants grown in a system without trees revealed a significantly higher number of *Erwinia* in their phyllosphere than appropriate plants grown in an agroforestry system (**Figure 4D**).

DISCUSSION

A deep sequencing analysis of the gammaproteobacterial microbiome associated with the Gros Michel banana variety in Central America revealed an extraordinary high diversity within the endophytic community. Considering the below-ground microhabitats, the endorhiza of plants grown in Nicaragua unveiled a diversity comparable to that of the rhizosphere soil. The succulent pseudostem which can be considered as an above-ground endophytic microhabitat revealed a diversity comparable to that of the leaves encompassing endo- as well as ectophytes. A 16S rRNA gene amplicon sequencing approach targeting only the enterobacterial community of the banana plant revealed a strikingly diverse colonization of its endosphere with a Shannon diversity index for the pseudostem ($H' = 0.55$) similar to those of rhizosphere samples ($H' = 0.40$–0.55), even though based on only one pseudostem sample (Rossmann et al., 2012). But normally, what we know from other plants, we face a contrasting picture; due to root exudates and the resulting high nutrient content, the rhizosphere represents a favored microenvironment for microbial colonization and is characterized by a high abundance and diversity (Berendsen et al., 2012; Berg et al., 2014), and only a fraction of this root-associated microorganisms is able to invade, compete with other well-adapted endophytes, and successfully colonize the inner plant tissue (Germaine et al., 2004; Chi et al., 2005). Several endophytes are known for their advantageous associations and close interactions with their host plants. They have been shown to enhance plant growth and quality (Berg et al., 2005a; Köberl et al., 2013), increase plant resistance to abiotic stresses, pathogens and even herbivores (Rodriguez et al., 2009; Marasco et al., 2012; Yi et al., 2013), and contribute to plant-assisted bioremediation (Lodewyckx et al., 2001; Siciliano et al., 2001). The generally high diversity within the endophytic community of the banana plant can be explained by the permanent nature of its corm serving as a reservoir for endophytic diversity and the transmission to following generations via vegetative suckers.

In addition to the diversity, the gammaproteobacterial taxonomic composition was highly similar between the endophytic pseudostem and banana leaves as well, revealing a predominant

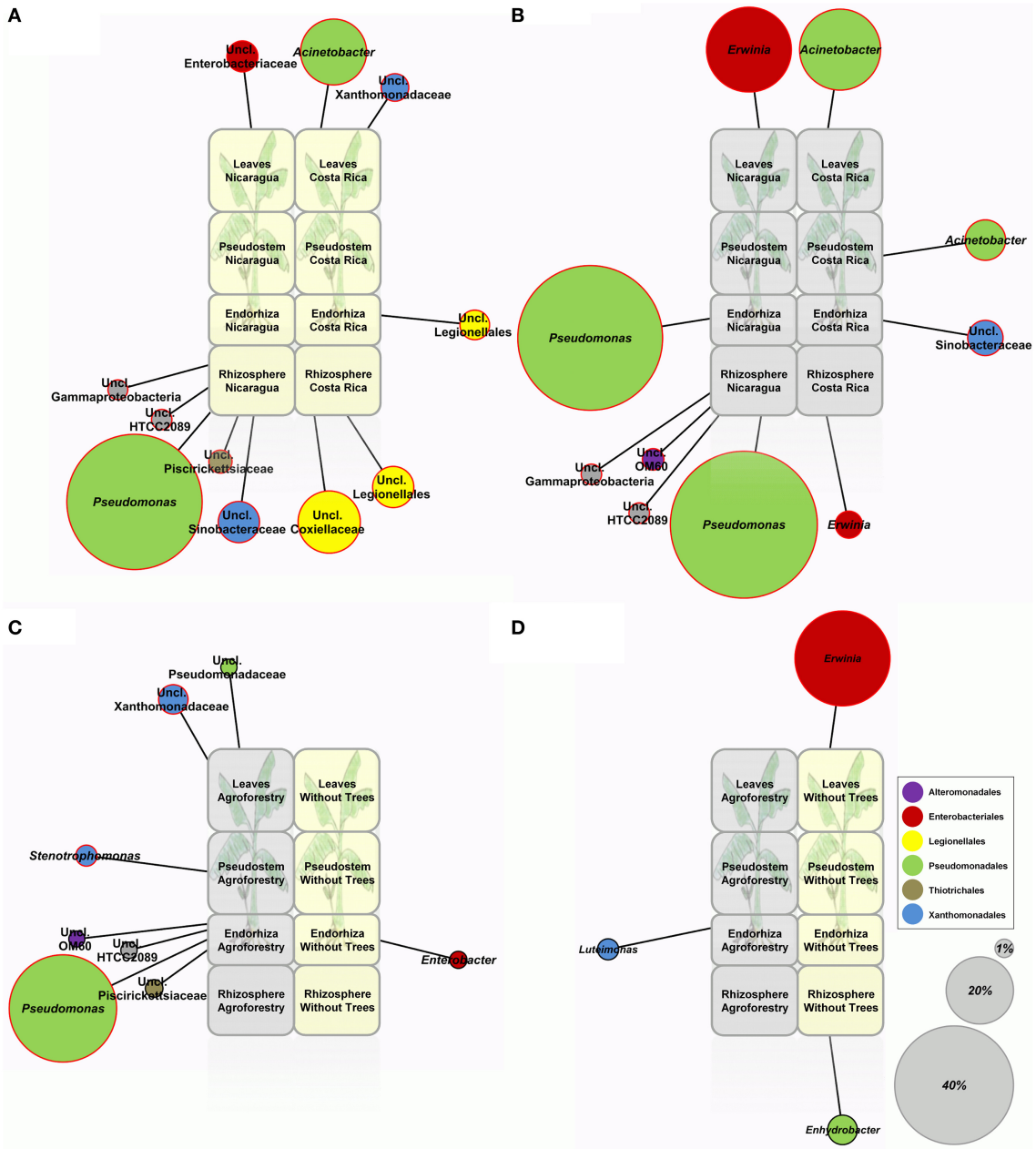

FIGURE 4 | Profile clustering network analyses depicting the impact of biogeography and agroforestry on the gammaproteobacterial microbiome of banana plants cultivated in Nicaragua and Costa Rica. **(A)** Impact of biogeography without agroforestry, **(B)** Impact of biogeography and different agroforestry systems (*Inga* spp. in Nicaragua; *Erythrina poeppigiana* in Costa Rica), **(C)** Impact of agroforestry in Nicaragua, **(D)** Impact of agroforestry in Costa Rica. The relative abundances of OTUs at a dissimilarity level of 3% summarized at genus level with a mean read change between different conditions of more than 0.2% of the data set were used. If the ratio of relative mean abundances exceeded 1.5, the taxa were regarded as altered and assigned to the respective profile. Node sizes correspond to the abundance change between conditions; nodes matching to changes of 1, 20, and 40% of the data set were added as reference points. **(A,B)** Number of depicted nodes was reduced to taxa with significant differences between countries ($p \leq 0.05$, Metastats). **(C,D)** Only those taxonomic groups that featured the same pattern in all three farms of the respective country are shown. Significant differences are indicated by red node borders.

colonization by *Enterobacteriaceae* and *Pseudomonadales*. *Pseudomonadales*, in particular the genus *Pseudomonas* but also *Acinetobacter* (both identified as dominant groups in this study), are well-known plant colonizers and among others often accountable for beneficial plant-microbe interactions (Weller, 2007; Rolli et al., 2015). Interestingly, while the *Pseudomonadales* community in samples from Nicaragua was highly dominated by the genus *Pseudomonas*, banana plants from Costa Rica revealed significantly higher relative abundances of *Acinetobacter*. Although it is well-known that the plant microbiome is shaped

by both soil community and the plant cultivar (Berg and Smalla, 2009), the dominance of enterics in the banana pseudostem described for the East African Highland banana of Uganda (Rossmann et al., 2012) could be confirmed for the Gros Michel variety cultivated in Central America as well and could be extended to the entire perennial above-ground plant parts of the banana. However, while the colonization study of the East African Highland banana in Uganda (Rossmann et al., 2012) revealed *Enterobacter* as the predominant enterobacterial genus in plant-associated microenvironments, *Erwinia* was identified as the most dominant genus in the Central American Gros Michel variety. In contrast to *Enterobacter* which comprises several opportunistic human pathogenic strains (*E. aerogenes*, *E. cloacae*) (Berg et al., 2015), *Erwinia* is mainly known as plant pathogen (*E. amylovora*, *E. tracheiphila*) (Eastgate, 2000; Rojas et al., 2013). However, as this study encompassed only healthy banana plants without symptoms of *Fusarium* wilt or any other disease, there is no indication that the *Erwinia* strains observed within the banana-associated microbiome are in any manner harmful to the plant. A recent study of the lettuce (*Lactuca sativa*) microbiome also revealed a preferential occurrence of enterics in the phyllosphere (Erlacher et al., 2014).

In general, a higher impact on the banana-associated gammaproteobacterial microbiome was observed for the biogeographical location than for the agroforestry conditions. The biggest differences between the sampling countries were observed for the rhizosphere communities, representing the most probable source of all other plant colonizers. Consequently, based on the different rhizosphere microbiomes, disparities were found for all investigated microenvironments, whereby above-ground plant parts shared higher similarities, possibly due to a rigorous selection process with subsequent enrichment especially of enterics and pseudomonads. In addition to generally high contents of polyphenols and antioxidants in the succulent banana pseudostem, Saravanan and Aradhya (2011) could recently measure high concentrations of flavonoid compounds. Flavonoids are widely distributed secondary metabolites with diverse metabolic functions in plants; among several others, some of them are well-known for their antimicrobial activity (Falcone Ferreyra et al., 2012) and have been identified to be involved in the plant-driven selection of microbes (Bais et al., 2006; Weston and Mathesius, 2013).

For both countries and different agroforestry systems, a slight shift of the gammaproteobacterial microbiome resulting from associated *Fabaceae* trees could be observed. Banana plants grown in the agroforestry system with *Inga* trees in Nicaragua revealed significantly higher abundances of *Pseudomonas* and *Stenotrophomonas*. Both genera comprise several potential plant-beneficial species. For instance, *Stenotrophomonas rhizophila* has become a model bacterium among the plant growth-promoters and stress protecting agents (Alavi et al., 2013), particularly because of its beneficial effects on plants in salinated soils (Egamberdieva et al., 2011). Positive *Pseudomonas*-plant interactions are well-known (Weller, 2007) and have already been discussed. However, the genus *Pseudomonas* also includes some species with potential deleterious effects on plants (*P. syringae*, *P. viridiflava*) (Jakob et al., 2002), and moreover some species of *Pseudomonas* and also of *Stenotrophomonas* are known as opportunistic pathogens in humans as well (*P. aeruginosa*, *S. maltophilia*). Several studies provided evidence that similar or even identical functions are responsible for the beneficial interactions with plants and virulence in other eukaryotic hosts (Berg et al., 2005b; Alavi et al., 2014). For banana plants grown in association with *E. poeppigiana* in Costa Rica, a significant decrease of *Erwinia* spp. was recorded. Although this study targeted exclusively the gammaproteobacterial fraction, results could show that as a consequence of legume-based agroforestry the indigenous banana-associated microbial community was noticeably shifted.

AUTHOR CONTRIBUTIONS

Conceived and designed the experiments: GB, CS, MD. Performed the experiments: MK, AM. Analyzed the data: MK, MD, GB. Contributed reagents/materials/analysis tools: CS, GB. Wrote the paper: MK, GB.

ACKNOWLEDGMENTS

This study was supported by the Federal Ministry for Europe, Integration and Foreign Affairs (BMEIA) of the Republic of Austria through the Austrian Development Agency (ADA).

SUPPLEMENTARY MATERIAL

The Supplementary Material for this article can be found online at: http://www.frontiersin.org/journal/10.3389/fmicb.2015.00091/abstract

REFERENCES

Alavi, P., Starcher, M. R., Thallinger, G. G., Zachow, C., Müller, H., and Berg, G. (2014). *Stenotrophomonas* comparative genomics reveals genes and functions that differentiate beneficial and pathogenic bacteria. *BMC Genomics* 15:482. doi: 10.1186/1471-2164-15-482

Alavi, P., Starcher, M. R., Zachow, C., Müller, H., and Berg, G. (2013). Root-microbe systems: the effect and mode of interaction of stress protecting agent (SPA) *Stenotrophomonas rhizophila* DSM14405(T.). *Front. Plant Sci.* 4:141. doi: 10.3389/fpls.2013.00141

Ayyadurai, N., Ravindra Naik, P., Sreehari Rao, M., Sunish Kumar, R., Samrat, S. K., Manohar, M., et al. (2006). Isolation and characterization of a novel banana rhizosphere bacterium as fungal antagonist and microbial adjuvant in micropropagation of banana. *J. Appl. Microbiol.* 100, 926–937. doi: 10.1111/j.1365-2672.2006.02863.x

Bais, H. P., Weir, T. L., Perry, L. G., Gilroy, S., and Vivanco, J. M. (2006). The role of root exudates in rhizosphere interactions with plants and other organisms. *Annu. Rev. Plant Biol.* 57, 233–266. doi: 10.1146/annurev.arplant.57.032905.105159

Berendsen, R. L., Pieterse, C. M., and Bakker, P. A. (2012). The rhizosphere microbiome and plant health. *Trends Plant Sci.* 17, 478–486. doi: 10.1016/j.tplants.2012.04.001

Berg, G., Eberl, L., and Hartmann, A. (2005b). The rhizosphere as a reservoir for opportunistic human pathogenic bacteria. *Environ. Microbiol.* 7, 1673–1685. doi: 10.1111/j.1462-2920.2005.00891.x

Berg, G., Erlacher, A., and Grube, M. (2015). "The edible plant microbiome: importance and health issues," in *Principles of Plant-Microbe Interactions – Microbes for Sustainable Agriculture,* ed B. Lugtenberg (Cham: Springer), 419–426.

Berg, G., Grube, M., Schloter, M., and Smalla, K. (2014). Unraveling the plant microbiome: looking back and future perspectives. *Front. Microbiol.* 5:148. doi: 10.3389/fmicb.2014.00148

Berg, G., Krechel, A., Ditz, M., Sikora, R. A., Ulrich, A., and Hallmann, J. (2005a). Endophytic and ectophytic potato-associated bacterial communities differ in structure and antagonistic function against plant pathogenic

fungi. *FEMS Microbiol. Ecol.* 51, 215–229. doi: 10.1016/j.femsec.2004.08.006

Berg, G., and Smalla, K. (2009). Plant species and soil type cooperatively shape the structure and function of microbial communities in the rhizosphere. *FEMS Microbiol. Ecol.* 68, 1–13. doi: 10.1111/j.1574-6941.2009.00654.x

Butler, D. (2013). Fungus threatens top banana. *Nature* 504, 195–196. doi: 10.1038/504195a

Caporaso, J. G., Bittinger, K., Bushman, F. D., DeSantis, T. Z., Andersen, G. L., and Knight, R. (2010b). PyNAST: a flexible tool for aligning sequences to a template alignment. *Bioinformatics* 26, 266–267. doi: 10.1093/bioinformatics/btp636

Caporaso, J. G., Kuczynski, J., Stombaugh, J., Bittinger, K., Bushman, F. D., Costello, E. K., et al. (2010a). QIIME allows analysis of high-throughput community sequencing data. *Nat. Methods* 7, 335–336. doi: 10.1038/nmeth.f.303

Caporaso, J. G., Lauber, C. L., Walters, W. A., Berg-Lyons, D., Lozupone, C. A., Turnbaugh, P. J., et al. (2011). Global patterns of 16S rRNA diversity at a depth of millions of sequences per sample. *Proc. Natl. Acad. Sci. U.S.A.* 108(Suppl. 1), 4516–4522. doi: 10.1073/pnas.1000080107

Chao, A., and Bunge, J. (2002). Estimating the number of species in a stochastic abundance model. *Biometrics* 58, 531–539. doi: 10.1111/j.0006-341X.2002.00531.x

Chi, F., Shen, S. H., Cheng, H. P., Jing, Y. X., Yanni, Y. G., and Dazzo, F. B. (2005). Ascending migration of endophytic rhizobia, from roots to leaves, inside rice plants and assessment of benefits to rice growth physiology. *Appl. Environ. Microbiol.* 71, 7271–7278. doi: 10.1128/AEM.71.11.7271-7278.2005

Eastgate, J. A. (2000). *Erwinia amylovora*: the molecular basis of fireblight disease. *Mol. Plant Pathol.* 1, 325–329. doi: 10.1046/j.1364-3703.2000.00044.x

Edgar, R. C. (2010). Search and clustering orders of magnitude faster than BLAST. *Bioinformatics* 26, 2460–2461. doi: 10.1093/bioinformatics/btq461

Egamberdieva, D., Kucharova, Z., Davranov, K., Berg, G., Makarova, N., Azarova, T., et al. (2011). Bacteria able to control foot and root rot and to promote growth of cucumber in salinated soils. *Biol. Fertil. Soils* 47, 197–205. doi: 10.1007/s00374-010-0523-3

Erlacher, A., Cardinale, M., Grosch, R., Grube, M., and Berg, G. (2014). The impact of the pathogen *Rhizoctonia solani* and its beneficial counterpart *Bacillus amyloliquefaciens* on the indigenous lettuce microbiome. *Front. Microbiol.* 5:175. doi: 10.3389/fmicb.2014.00175

Falcone Ferreyra, M. L., Rius, S. P., and Casati, P. (2012). Flavonoids: biosynthesis, biological functions, and biotechnological applications. *Front. Plant Sci.* 3:222. doi: 10.3389/fpls.2012.00222

FAOSTAT (2005). *Statistical Database of the Food and Agriculture Organization of the United Nations*. Available online at: www.fao.org

Germaine, K., Keogh, E., Garcia-Cabellos, G., Borremans, B., Lelie, D., Barac, T., et al. (2004). Colonisation of poplar trees by *gfp* expressing bacterial endophytes. *FEMS Microbiol. Ecol.* 48, 109–118. doi: 10.1016/j.femsec.2003.12.009

Jakob, K., Goss, E. M., Araki, H., Van, T., Kreitman, M., and Bergelson, J. (2002). *Pseudomonas viridiflava* and *P. syringae* – natural pathogens of *Arabidopsis thaliana*. *Mol. Plant Microbe Interact.* 15, 1195–1203. doi: 10.1094/MPMI.2002.15.12.1195

Köberl, M., Schmidt, R., Ramadan, E. M., Bauer, R., and Berg, G. (2013). The microbiome of medicinal plants: diversity and importance for plant growth, quality and health. *Front. Microbiol.* 4:400. doi: 10.3389/fmicb.2013.00400

Lodewyckx, C., Taghavi, S., Mergeay, M., Vangronsveld, J., Clijsters, H., and van der Lelie, D. (2001). The effect of recombinant heavy metal resistant endophytic bacteria in heavy metal uptake by their host plant. *Int. J. Phytoremed.* 3, 173–187. doi: 10.1080/15226510108500055

Lozupone, C. A., Hamady, M., Kelley, S. T., and Knight, R. (2007). Quantitative and qualitative beta diversity measures lead to different insights into factors that structure microbial communities. *Appl. Environ. Microbiol.* 73, 1576–1585. doi: 10.1128/AEM.01996-06

Lundgren, B. (1982). Introduction – what is agroforestry? *Agrofor. Syst.* 1, 3–12.

Marasco, R., Rolli, E., Ettoumi, B., Vigani, G., Mapelli, F., Borin, S., et al. (2012). A drought resistance-promoting microbiome is selected by root system under desert farming. *PLoS ONE* 7:e48479. doi: 10.1371/journal.pone.0048479

Montagnini, F., and Nair, P. K. R. (2004). Carbon sequestration: an underexploited environmental benefit of agroforestry systems. *Agrofor. Syst.* 61, 281–295. doi: 10.1023/B:AGFO.0000029005.92691.79

Mühling, M., Woolven-Allen, J., Murrell, J. C., and Joint, I. (2008). Improved group-specific PCR primers for denaturing gradient gel electrophoresis analysis of the genetic diversity of complex microbial communities. *ISME J.* 2, 379–392. doi: 10.1038/ismej.2007.97

Ondov, B. D., Bergman, N. H., and Phillippy, A. M. (2011). Interactive metagenomic visualization in a web browser. *BMC Bioinformatics* 12:385. doi: 10.1186/1471-2105-12-385

Perrier, X., De Langhe, E., Donohue, M., Lentfer, C., Vrydaghs, L., Bakry, F., et al. (2011). Multidisciplinary perspectives on banana (*Musa* spp.) domestication. *Proc. Natl. Acad. Sci. U.S.A.* 108, 11311–11318. doi: 10.1073/pnas.1102001108

Ploetz, R. C. (2006). *Fusarium* wilt of banana is caused by several pathogens referred to as *Fusarium oxysporum* f. sp. *cubense*. *Phytopathology* 96, 653–656. doi: 10.1094/PHYTO-96-0653

Rodriguez, R. J., White, J. F. Jr., Arnold, A. E., and Redman, R. S. (2009). Fungal endophytes: diversity and functional roles. *New Phytol.* 182, 314–330. doi: 10.1111/j.1469-8137.2009.02773.x

Rojas, E. S., Dixon, P. M., Batzer, J. C., and Gleason, M. L. (2013). Genetic and virulence variability among *Erwinia tracheiphila* strains recovered from different cucurbit hosts. *Phytopathology* 103, 900–905. doi: 10.1094/PHYTO-11-12-0301-R

Rolli, E., Marasco, R., Vigani, G., Ettoumi, B., Mapelli, F., Deangelis, M. L., et al. (2015). Improved plant resistance to drought is promoted by the root-associated microbiome as a water stress-dependent trait. *Environ. Microbiol.* doi: 10.1111/1462-2920.12439. [Epub ahead of print].

Rossmann, B., Müller, H., Smalla, K., Mpiira, S., Tumuhairwe, J. B., Staver, C., et al. (2012). Banana-associated microbial communities in Uganda are highly diverse but dominated by *Enterobacteriaceae*. *Appl. Environ. Microbiol.* 78, 4933–4941. doi: 10.1128/AEM.00772-12

Saravanan, K., and Aradhya, S. M. (2011). Polyphenols of pseudostem of different banana cultivars and their antioxidant activities. *J. Agric. Food Chem.* 59, 3613–3623. doi: 10.1021/jf103835z

Seobi, T., Anderson, S. H., Udawatta, R. P., and Gantzer, C. J. (2005). Influence of grass and agroforestry buffer strips on soil hydraulic properties for an Albaqualf. *Soil Sci. Soc. Am. J.* 69, 893–901. doi: 10.2136/sssaj2004.0280

Shannon, C. E. (1997). The mathematical theory of communication. 1963. *MD Comput.* 14, 306–317.

Siciliano, S. D., Fortin, N., Mihoc, A., Wisse, G., Labelle, S., Beaumier, D., et al. (2001). Selection of specific endophytic bacterial genotypes by plants in response to soil contamination. *Appl. Environ. Microbiol.* 67, 2469–2475. doi: 10.1128/AEM.67.6.2469-2475.2001

Smoot, M. E., Ono, K., Ruscheinski, J., Wang, P. L., and Ideker, T. (2011). Cytoscape 2.8: new features for data integration and network visualization. *Bioinformatics* 27, 431–432. doi: 10.1093/bioinformatics/btq675

Udawatta, R. P., Kremer, R. J., Garrett, H. E., and Anderson, S. H. (2009). Soil enzyme activities and physical properties in a watershed managed under agroforestry and row-crop systems. *Agri. Ecosyst. Environ.* 131, 98–104. doi: 10.1016/j.agee.2008.06.001

Weller, D. M. (2007). *Pseudomonas* biocontrol agents of soilborne pathogens: looking back over 30 years. *Phytopathology* 97, 250–256. doi: 10.1094/PHYTO-97-2-0250

Weston, L. A., and Mathesius, U. (2013). Flavonoids: their structure, biosynthesis and role in the rhizosphere, including allelopathy. *J. Chem. Ecol.* 39, 283–297. doi: 10.1007/s10886-013-0248-5

White, J. R., Nagarajan, N., and Pop, M. (2009). Statistical methods for detecting differentially abundant features in clinical metagenomic samples. *PLoS Comput. Biol.* 5:e1000352. doi: 10.1371/journal.pcbi.1000352

Yi, H. S., Yang, J. W., and Ryu, C. M. (2013). ISR meets SAR outside: additive action of the endophyte *Bacillus pumilus* INR7 and the chemical inducer, benzothiadiazole, on induced resistance against bacterial spot in field-grown pepper. *Front. Plant Sci.* 4:122. doi: 10.3389/fpls.2013.00122

Conflict of Interest Statement: The authors declare that the research was conducted in the absence of any commercial or financial relationships that could be construed as a potential conflict of interest.

Received: 13 November 2014; accepted: 24 January 2015; published online: 11 February 2015.
*Citation: Köberl M, Dita M, Martinuz A, Staver C and Berg G (2015) Agroforestry leads to shifts within the gammaproteobacterial microbiome of banana plants cultivated in Central America. Front. Microbiol. **6**:91. doi: 10.3389/fmicb.2015.00091*
This article was submitted to Plant-Microbe Interaction, a section of the journal Frontiers in Microbiology.

frontiers in Microbiology

ORIGINAL RESEARCH
published: 22 September 2015
doi: 10.3389/fmicb.2015.01008

Bacterial endophyte communities in the foliage of coast redwood and giant sequoia

*Alyssa A. Carrell[1,2,3] and Anna C. Frank[1,4]**

[1] Life and Environmental Sciences, School of Natural Sciences, University of California, Merced, Merced, CA, USA, [2] Department of Biology, Duke University, Durham, NC, USA, [3] Environmental Sciences Division, Oak Ridge National Laboratory, Oak Ridge, TN, USA, [4] Sierra Nevada Research Institute, University of California, Merced, Merced, CA, USA

The endophytic bacterial microbiome, with an emerging role in plant nutrient acquisition and stress tolerance, is much less studied in natural plant populations than in agricultural crops. In a previous study, we found consistent associations between trees in the pine family and acetic acid bacteria (AAB) occurring at high relative abundance inside their needles. Our objective here was to determine if that pattern may be general to conifers, or alternatively, is more likely restricted to pines or conifers growing in nutrient limited and exposed environments. We used 16S rRNA pyrosequencing to characterize the foliar endophyte communities of two conifers in the *Cupressaceae* family: Two coast redwood (CR; *Sequoia sempervirens*) populations and one giant sequoia (GS; *Sequoiadendron giganteum*) population were sampled. Similar to the pines, the endophyte communities of the giant trees were dominated by Proteobacteria, Firmicutes, Acidobacteria, and Actinobacteria. However, although some major operational taxonomic units (OTUs) occurred at a high relative abundance of 10–40% in multiple samples, no specific group of bacteria dominated the endophyte community to the extent previously observed in high-elevation pines. Several of the dominating bacterial groups in the CR and GS foliage (e.g., *Bacillus*, *Burkholderia*, Actinomycetes) are known for disease- and pest suppression, raising the possibility that the endophytic microbiome protects the giant trees against biotic stress. Many of the most common and abundant OTUs in our dataset were most similar to 16S rRNA sequences from bacteria found in lichens or arctic plants. For example, an OTU belonging to the uncultured Rhizobiales LAR1 lineage, which is commonly associated with lichens, was observed at high relative abundance in many of the CR samples. The taxa shared between the giant trees, arctic plants, and lichens may be part of a broadly defined endophyte microbiome common to temperate, boreal, and tundra ecosystems.

Keywords: bacterial endophytes, 16S rRNA, foliage, microbiome, giant sequoia, redwood, *Sequoia sempervirens*, *Sequoiadendron giganteum*

OPEN ACCESS

Edited by:
Mysore V. Tejesvi, University of Oulu, Finland

Reviewed by:
Raffaella Balestrini, Consiglio Nazionale delle Ricerche, Italy
Oswaldo Valdes-Lopez, National Autonomous University of Mexico, Mexico

****Correspondence:***
Anna C. Frank, Life and Environmental Sciences, School of Natural Sciences, University of California, Merced, 5200 North Lake Road, Merced, CA 95343, USA
cfrank3@ucmerced.edu

Specialty section:
This article was submitted to Plant Biotic Interactions, a section of the journal Frontiers in Microbiology

Received: *19 June 2015*
Accepted: *07 September 2015*
Published: *22 September 2015*

Citation:
Carrell AA and Frank AC (2015) Bacterial endophyte communities in the foliage of coast redwood and giant sequoia. Front. Microbiol. 6:1008. doi: 10.3389/fmicb.2015.01008

Introduction

The plant microbiome is essential to plant health (Turner et al., 2013; Berg, 2014; Peñuelas and Terradas, 2014), but the role of microbes colonizing most wild plants still remains unknown. For example, while a number of studies have examined the fungal endophyte communities inside the leaves of forest trees (Ganley et al., 2004; Arnold et al., 2007; Oono et al., 2014; Qadri et al., 2014),

less is known about the role and diversity of their bacterial counterparts. The motivation for studying endophytic microbiomes comes mainly from studies of agricultural crops: Over the last two decades or so, a number of studies—most of them focused on bacterial isolates—have demonstrated that endophytes can benefit plants and crop yield through enhanced nutrient uptake, disease suppression, increased abiotic stress tolerance, and direct stimulation of plant growth, all from within the plant tissues (Rosenblueth and Martinez-Romero, 2006; Hardoim et al., 2008; Reinhold-Hurek and Hurek, 2011). In addition, a few studies on natural plant populations suggest that the bacterial endophytes associated with wild plants can affect plant traits, for example by fixing nitrogen (N), altering soil geochemical cycles to enable plant persistence, and producing compounds that are antagonistic against fungal pests (Adams et al., 2008; Anand et al., 2013; Rout et al., 2013; Knoth et al., 2014).

A better appreciation of how wild plants interact with their native microbiomes may be critical for understanding and predicting how terrestrial ecosystems will respond to current and projected global change (Rodriguez et al., 2004; Porras-Alfaro and Bayman, 2011; Berg, 2014). The coniferous forests in the Northern Hemisphere are potential major carbon (C) sinks, and their response to warming, elevated CO_2, and increased disease pressure will influence the amount of C they can store. Many of the traits that influence this response can be microbially mediated, including defense, N-fixation, and abiotic stress tolerance (Friesen et al., 2011).

Community 16S rRNA sequencing can yield some insight into the relationship between a plant host and its associated microbiome, as well as detect endophyte community members with potential functional importance. Recent work on model-, agricultural-, and biofuel plants (e.g., *Arabidopsis, Oryza, Zea,* and *Populus*) suggests that bacterial endophyte communities are generally influenced by a combination of host species identity, host genotype, season, and environment, with substantial variation in taxonomic composition across plant individuals or species (Gottel et al., 2011; Bulgarelli et al., 2012; Lundberg et al., 2012; Shakya et al., 2013; Schlaeppi et al., 2014; Aleklett et al., 2015; Edwards et al., 2015; Müller et al., 2015; Shen and Fulthorpe, 2015). There are exceptions to this pattern, for example in *Sphagnum* mosses, where *Burkholderia* sp. dominate across individual plants as well as plant species, likely due to their vertical transmission (Bragina et al., 2013). Similarly, our recent study of limber pine (*Pinus flexilis*) and Engelmann spruce (*Picea engelmannii*) growing at high elevation (3000–3400 m), showed that their foliar endophyte microbiomes were consistently dominated by a few operational taxonomic units (OTUs) in the *Acetobacteraceae*, or acetic acid bacteria (AAB), a family of Alphaproteobacteria commonly associated with N_2-fixation (Fuentes-Ramirez et al., 2001; Kersters et al., 2006; Dutta and Gachhui, 2007).

In order to determine whether the pattern we observed in the high elevation conifers—recurring dominance by a few endophytic taxa—is unique to trees in the pine family, and/or the extreme subalpine environment, or alternatively, is common to conifer species across habitats, we here explore the foliar bacterial endophytic communities of coast redwood (CR) and giant sequoia (GS).

Coast redwood and giant sequoia are the tallest and largest living tree species on Earth, respectively. The oldest known GS individuals are about 3,500 years old, and CR individuals have life spans that can extend 2000 years. Both are the only extant species in their respective genera, with extremely restricted distributions; CR occurs exclusively in the cloud-inundated humid areas along the coast of central and northern California; GS occurs in scattered groves along a narrow belt along the western Sierra Nevada, California, at elevations that generally range from 1400 to 2000 m. While fungal endophytes of CR have received some attention, to our knowledge, no studies of bacterial endophytes in CR or GS exist. The investigation of fungal endophytes in CR was pioneered by Carroll and Carroll (1978), who isolated four different endophyte species. A follow-up study that also examined spatial patterns in fungal endophyte communities found a higher diversity of fungal species (Espinosa-Garcia and Langenheim, 1990). The most extensive study to date documented 16 different endophyte species, and found that the fungal endophyte community was stable among host individuals and along a north to south distribution of CR, with dominance of *Pleuroplacoema* sp. (Rollinger and Langenheim, 1993).

Here, we used 16S rRNA pyrosequencing to characterize the taxonomic composition of bacteria in surface-sterilized foliage of two populations of CR (one in Northern California and one in Central California), and one population of GS. At each site, we sampled three individuals. To contrast inter- and intra tree variation in the endophytic community, we took samples from the lower, middle, and upper canopy of each tree.

Materials and Methods

Sample Collection and Sterilization

We collected CR needles from a Northern California site (Samuel P. Taylor State Park, Lagunitas) in November 2011 and a Central California site (Big Creek UC Natural Reserve, in Big Sur) in October 2011. We collected GS needles from trees growing at Freeman Creek Grove in Sequoia National Monument, Porterville, CA, USA in August 2011. To assess the difference in endophytic communities across individuals, locations, and species, we collected needles from three individuals trees in each of the three locations; GS trees A, B, and C from Freeman Creek Grove, CR trees D, E, and F from Big Creek, and trees G, I, and H from Samuel P. Taylor SP). To investigate intra-tree variation in the endophytic community, we sampled needles from three canopy heights (lower, middle, and upper) from each tree. For all downstream processing and analysis, we treated the resulting 27 samples individually (i.e., we did not pool them). For each sample, we removed approximately 10 g of needles with a sterile razor blade, placed them in a ziplock bag, and transported them to the University of California, Merced at 4°C. We sterilized the needles via submersion in ethanol for 1 min, 30% hydrogen peroxide for three minutes, followed by three rinses with sterile de-ionized water, and stored them at −20°C. We confirmed surface sterility of foliage by

negative PCR amplification (but not sequencing) of the final rinse.

DNA Extraction

We pulverized the needles to a fine powder using liquid nitrogen in a sterile mortar. We extracted DNA from 0.6 g of the pulverized tissue in a 2 ml screw cap tube containing 800 μl of CTAB solution (1 ml CTAB buffer, 0.04 g of polyvinylpyrrolidone, 5 μl of 2-mercaptoethanol), incubated in a dry bath at 60°C for 2 h, and then homogenized with 0.3 g of 0.11 mm sterile glass beads with a bead beater for 3 min. We removed proteins by adding an equal amount of chloroform and centrifuged the sample for 10 min at 16 rcf. We placed the aqueous top phase in a sterile 2 ml snap cap tube with 1/10 volume of cold 3 M sodium acetate and 1/2 volume cold isopropanol and placed it in a –20°C freezer overnight to precipitate the nucleic acids. We then centrifuged the sample for 30 min at 16 rcf, decanted the supernatant, added 700 μl of 70% ethanol, and centrifuged the sample for 10 min. We resuspended the air-dried pellet with 30 μl of DNA resuspension fluid (1.0 M Tris-HCL, 0.1 M EDTA) and stored it at –20°C.

DNA Amplification

We amplified DNA using methods previously described (Carrell and Frank, 2014). Briefly, we used a nested PCR using a thermocycle profile with reduced PCR cycles to minimize PCR bias (Jiao et al., 2006). For the initial PCR, we used the chloroplast excluding primer 16S 799f (AACMGGATTAGATACCCKG) and 16S 1492r (TACGGHTACCTTGTTACGACTT) which resulted in a mitochondrial product of about 1000 bp and a bacterial product of about 750 bp as described by Chelius and Triplett (2001). We then separated the bacterial product from the mitochondrial product and extracted the bacterial product using E-Gel® SizeSelect™ Gels (Life Technologies, Carlsbad, CA, USA). We then used the extracted bacterial product as a template for PCR using the thermocycle profile described by Jiao et al. (2006) and the Golay-barcoded primer set 799f and 1115r (AGGGTTGCGCTCGTTG) (Redford et al., 2010). We performed a negative PCR control the same way, but with no template DNA added (but this control was not sequenced). We cleaned the final product with the QIAquick PCR cleanup kit, quantified the DNA concentration using Nanodrop, and pooled equal amounts of all 27 samples for pyrosequencing. The pooled product was sequenced at the Environmental Genomics Core Facility at the University of South Carolina for pyrosequencing on a 454 Life Sciences Genome Sequencer FLX machine.

OTU Generation

We analyzed and processed the sequences using the QIIME package (Caporaso et al., 2010b). We quality filtered the sequences (minimum quality score of 25, minimum length of 200 bp, and no ambiguity in primer sequence) and assigned them to their corresponding sample by the barcode sequences. We removed sample EU (CR tree E, upper canopy) due to an insufficient number of sequences (59 sequences). One GS sample (tree A, middle canopy), was dominated by *Staphylococcus epidermis*, a common member of the skin microbiota, at high relative abundance (40%), and we discarded it due to likely contamination. We clustered the remaining sequences into OTUs using UCLUST, with a minimum coverage of 99% and a minimum similarity of 97%. A representative sequence was chosen for each OTU by selecting the longest sequence that had the highest number of hits to other sequences of that particular OTU. We detected chimeric sequences with ChimeraSlayer and removed them before taxonomic analysis (Edgar et al., 2011). We aligned representative sequences using PyNAST (Caporaso et al., 2010a) against the Greengenes core set (DeSantis et al., 2006). We made taxonomic assignments for the representative sequences using the Ribosomal Database Project (RDP) classifier (Wang et al., 2007) with greengenes representative set of sequences as reference. We removed sequences classified as "Chloroplast" (0.5%), "Mitochondria" (10%), or "Unassigned" from the alignment. We generated heatmaps using in-house perl/perl Tk scripts. We identified core OTUs using the script compute_core_microbiome.py in QIIME.

Community Analysis

To evaluate communities at an equal sequencing depth, we rarified all samples to the lowest number of sequences occurring in a sample (594). We inferred an approximate maximum-likelihood phylogeny with FastTree (Price et al., 2009). We constructed unweighted and weighted UniFrac distance matrices from the phylogenetic tree to analyze dissimilarity of sample communities (Lozupone and Knight, 2005). To analyze the strength and statistical significance of sample groupings, we used Anosim and PERMANOVA as implemented in QIIME. We used the Kruskal–Wallis test as implemented in QIIME to determine whether differences in the relative abundances of individual bacterial taxa across sample types were significant.

Phylogenetic Tree

To build a phylogenetic tree of the Alphaproteobacteria in our dataset, we created a dataset that contained only OTUs corresponding to Alphaproteobacteria present more than 50 times in our samples (34 OTUs total). First, we used this dataset as a query for BLAST searches against the NCBI 16S rRNA and GenBank non-redundant (nr) databases to identify the five top matching isolates or uncultured taxa that matched each OTU at or above 96% identity. We added matching sequences to our dataset, and aligned the sequences using infernal (Nawrocki et al., 2009). We removed highly variable regions and gap-only sites from the alignment using the filer_alignment.py script in the QIIME package and trimmed it to the ∼300 nucleotides covered by our 16S rRNA pyrosequences. We used RAxML (Stamatakis et al., 2005) to infer a maximum likelihood tree with 1000 bootstrap replicates, and plotted it using the Interactive Tree of Life tool (Letunic and Bork, 2011).

Results

A total of 26 out of our 27 samples were successfully amplified and sequenced, and the negative PCR control was blank. One CR

sample (from the Central CA location) had only 59 sequences, and was discarded from further analysis. We also removed one sample due to likely contamination (see Materials and Methods), giving us eight sequenced samples from GS, eight sequenced samples from the Central CA CR population, and nine sequenced samples from the Northern CA CR population (25 sequenced samples total). The samples yielded an average of 1741 sequences after plant DNA was removed. Rarefaction plots did not saturate, indicating that we under-sampled the bacterial communities at the 97% OTU level (data not shown). The sequence data have been submitted to the GenBank databases under project accession number SRP045230.

Across all samples, the most abundant phyla in all samples were Proteobacteria and Firmicutes, followed by Acidobacteria, Actinobacteria, TM7, and Bacteroidetes. The relative abundance of bacterial phyla varied among samples, but Proteobacteria or Firmicutes dominated most samples (**Figure 1**). Firmicutes were significantly more abundant in GS (35% of the sequences on average) than in CR (13% of the sequences on average; $P < 0.05$), and significantly different across locations (35, 22, and 6% of sequences from Freeman Creek, Central CA, and Northern CA, respectively; $P < 0.005$). Among the Proteobacteria, Alphaproteobacteria was the most prominent class, followed by Betaproteobacteria. Among the Firmicutes, Bacilli dominated.

We used principal coordinate analysis (PCoA) of weighted and unweighted UniFrac distances to investigate patterns of separation between endophyte communities in samples from the different locations (**Figure 2**). We found that unweighted UniFrac identified clustering by species (**Figure 2B**: Permanova: Pseudo-F statistic = 3.2009, $P = 0.001$; Anosim: $R = 0.4557$, $P < 0.001$). The CR communities formed two clusters that largely separated Northern and Central CA populations (Permanova: Pseudo-F statistic = 2.7375, $P < 0.001$; Anosim: $R = 0.5349$, $P < 0.001$), with some overlap. When we took into account the relative abundance of taxa in addition to the presence of bacterial taxa (using weighted UniFrac distance matrices) clustering by species still occurred (**Figure 2B**: Permanova: Pseudo-F statistic = 6.12, $P = 0.001$; Anosim: $R = 0.5464$, $P < 0.001$).

Next, we examined our sequences for high-level taxonomic groups that consistently dominated our samples within or across locations. There were no significant differences in the distribution of the most common bacterial orders between locations or tree species (**Figure 3**). Acidobacteriales, Actinomycetales, Bacillales, Rhizobiales, Rhodospirillales, and Burkholderiales were the most abundant and diverse orders, each represented by over 100 OTUs, many of which could not be classified below the order level (e.g., 43% of the Actinomycetales OTUs, 35% of the Bacillales OTUs, 70% of the Rhizobiales OTUs).

To identify dominant members of the endophyte communities and their distribution across samples, we looked for OTUs that were present in both high relative abundance and were consistently present (i.e., in >85% of samples) within a species

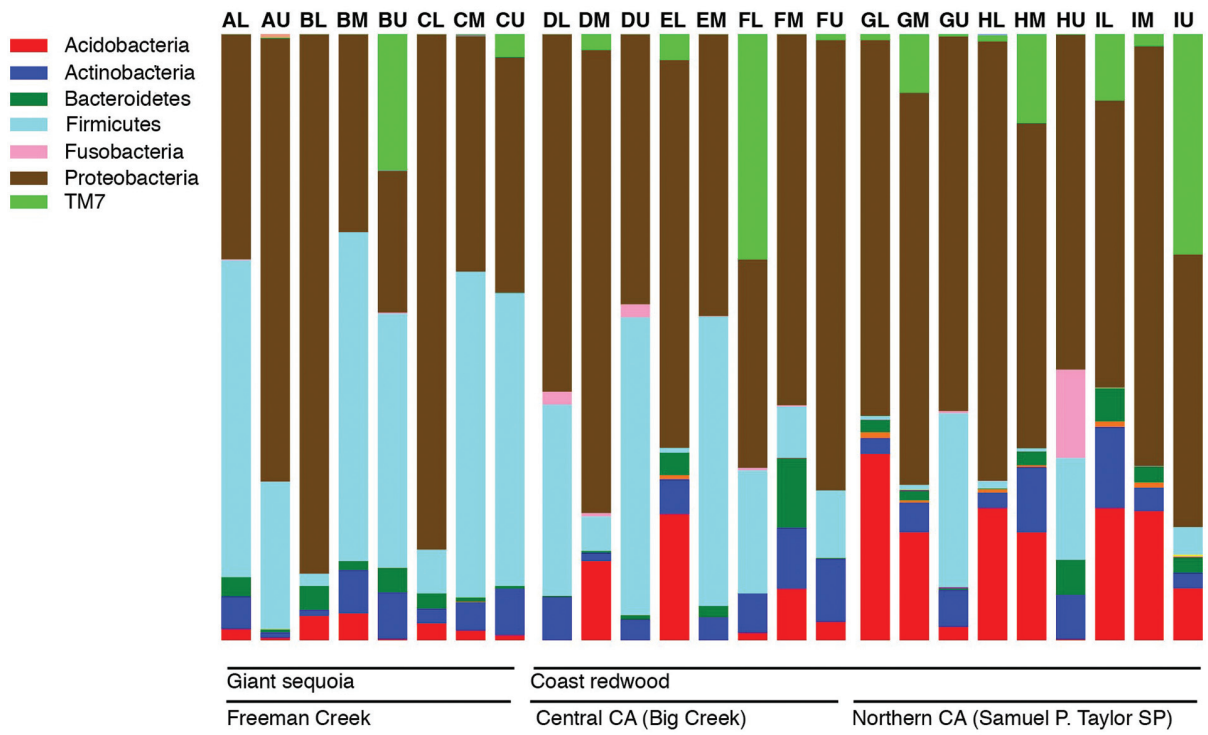

FIGURE 1 | Bar chart showing the relative abundance of major phyla in all the samples as percentages of all 16S rRNA gene sequences recovered in our foliage samples. Each bar represents a sample, and letters A–I indicate individual trees (nine total), while L, M, and U indicate the canopy location from which the sample was taken (lower, middle, or upper).

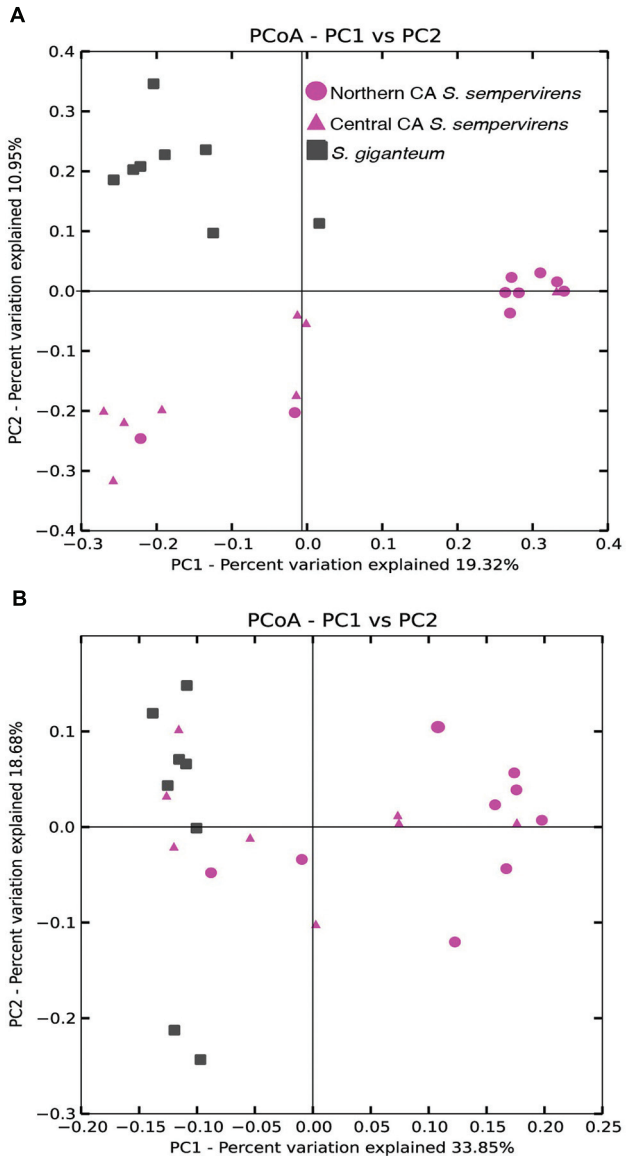

FIGURE 2 | Principal coordinate analysis (PCoA) of the (A) unweighted and (B) weighted UniFrac distance matrices. Points that are closer together on the ordination have communities that are more similar. Each point corresponds to a sample, and shapes correspond to host tree populations. Coast redwood (CR) samples are shown in pink, and giant sequoia (GS) samples are shown in gray.

or population (hereafter referred to as core OTUs). **Figure 4** shows the overall 20 most common OTUs in our dataset, along with their status as core OTUs across all samples or within a population. In addition, to capture the dominance and variation of OTUs within major groups (**Figure 4**), but that were not necessarily among the 20 top OTUs in the entire dataset, we did this separately for the OTU-rich classes Acidobacteria, Actinobacteriia, Bacilli, Alphaproteobacteria, and Betaproteobacteria (**Figure 4**). The results are shown in **Figure 5**, where the relative abundance of each OTU is calculated as the percentages of total OTUs within each class. In both cases (**Figures 4** and **5**), the resulting OTU sequences were used to query the NCBI 16S rRNA and nr databases for matches to isolates or uncultured sequences described in peer-reviewed manuscripts.

In contrast to the endophyte communities from high elevation pines in our previous study, where single AAB OTUs made up at least 15% in Engelmann spruce and 19% in limber pine (Carrell and Frank, 2014), no single taxon was consistently present with a relative abundance above 15% across the samples from within a site. The most common OTUs belonged to genera previously identified as endophytes, e.g., *Bacillus*, *Herbaspirillum*, *Pseudomonas*, and *Acetobacteraceae* (Elbeltagy et al., 2001; Cocking et al., 2006; Bacon and Hinton, 2011; Bordiec et al., 2011; **Figures 4** and **5**). Many of our dominant OTUs in the classes Acidobacteriia and Alphaproteobacteria (but not *Bacillus*) were most similar to sequences from one of two particular studies; a study of lichen-associated bacteria (Hodkinson et al., 2012), and a study of endophytes of the cold-tolerant arctic plants Alpine sorrel (*Oxyria digyna*), pincushion plant (*Diapensia lapponica*), and highland rush (*Juncus trifidus*) (Nissinen et al., 2012; **Figures 4** and **5**).

The most common OTU in our dataset (1726, **Figure 4**) was present in 85% of all CR samples, and in 100% of samples from the Northern CA population, where it was found in high relative abundance (6–34%) in all but one sample. This OTU is not closely related to any known isolate, but shares 99% identity to uncultured clones in the Lichen-Associated Rhizobiales-1 (LAR1) lineage. Taxa in this lineage are prevalent and recurring in the lichen microbiome (Hodkinson and Lutzoni, 2009; Hodkinson et al., 2012). While this OTU was not completely absent from our GS samples, it was only present in a few samples, and only at low relative abundance (**Figure 4**). In GS, several top OTUs were present across all samples (i.e., OTU 3293, 3526, 2805, 348; **Figure 5**). OTU 3293, which belongs to the genus *Bacillus*, was also present in all CR samples from the Central CA population; in a few of the samples at high relative abundance (20-40%; **Figure 4**). AAB, the family that was found to recur at high relative abundance in the subalpine conifers (Carrell and Frank, 2014), did not consistently dominate the foliar endophyte community of CR and GS, although taxa belonging to this group were present in many samples. For example, OTUs 2805 and 509 (**Figure 4**) belong to this group. OTU 2805 was found in the majority of samples from both species, while OTU 509 was absent from most of the CR samples (**Figure 4**). Also notable, half of the sequences from one of the GS samples fell within an OTU with 99% identity to database sequences from to the insect symbiont *Sodalis glossinidus*.

We looked for dominant OTUs that were significantly more common in a particular location and/or species, but found no significant differences in the distribution of the 20 most dominant OTUs between locations or tree species (Kruskal–Wallis). Only five *Bacillus* OTUs that were not among the most dominant overall, but which were dominant within the class *Bacilli*, were significantly more common in GS than in CR (indicated in **Figure 5**).

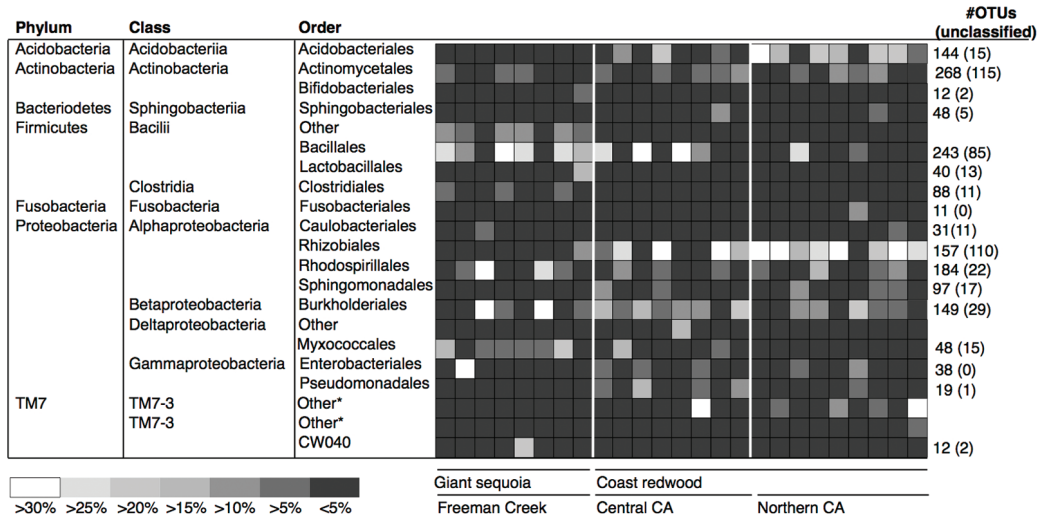

FIGURE 3 | Heatmap showing the 20 most dominant orders in our dataset and their average relative abundances as percentages of all 16S rRNA gene sequences recovered in our foliage samples, along with the total number of operational taxonomic units (OTUs) in each order. The number of OTUs in each order that could not be classified below the order level is shown within parenthesis. Color tones range from white to dark gray to indicate the highest to lowest relative abundance values.

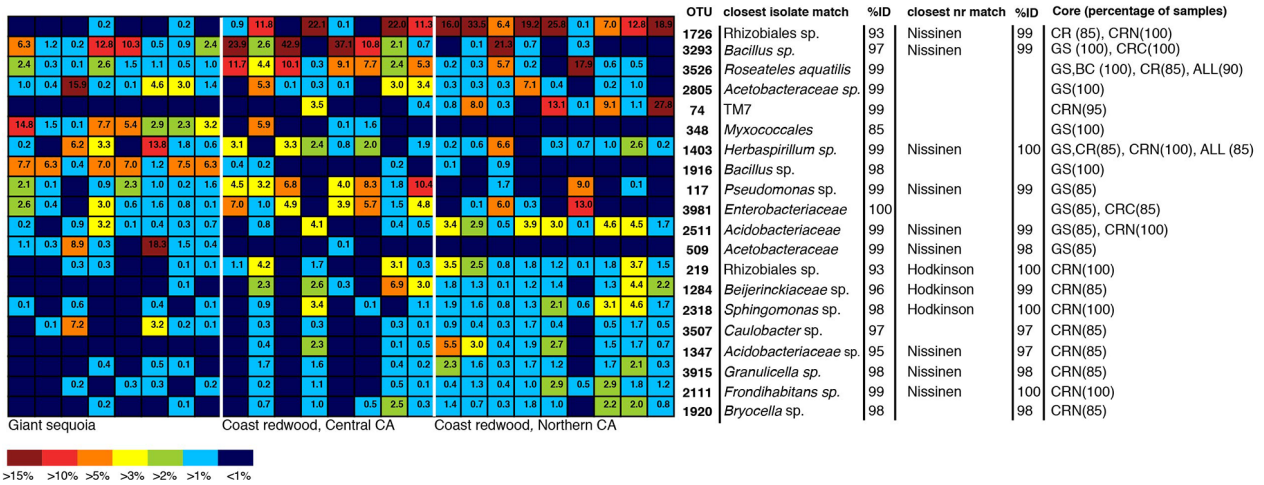

OTU	closest isolate match	%ID	closest nr match	%ID	Core (percentage of samples)
1726	Rhizobiales sp.	93	Nissinen	99	CR (85), CRN(100)
3293	*Bacillus sp.*	97	Nissinen	99	GS (100), CRC(100)
3526	*Roseateles aquatilis*	99			GS,BC (100), CR(85), ALL(90)
2805	*Acetobacteraceae sp.*	99			GS(100)
74	TM7	99			CRN(95)
348	*Myxococcales*	85			GS(100)
1403	*Herbaspirillum sp.*	99	Nissinen	100	GS,CR(85), CRN(100), ALL (85)
1916	*Bacillus* sp.	98			GS(100)
117	*Pseudomonas* sp.	99	Nissinen	99	GS(85)
3981	*Enterobacteriaceae*	100			GS(85), CRC(85)
2511	*Acidobacteriaceae*	99	Nissinen	99	GS(85), CRN(100)
509	*Acetobacteraceae*	99	Nissinen	98	GS(85)
219	Rhizobiales sp.	93	Hodkinson	100	CRN(100)
1284	*Beijerinckiaceae* sp.	96	Hodkinson	99	CRN(85)
2318	*Sphingomonas* sp.	98	Hodkinson	100	CRN(100)
3507	*Caulobacter* sp.	97		97	CRN(85)
1347	*Acidobacteriaceae* sp.	95	Nissinen	97	CRN(85)
3915	*Granulicella sp.*	98	Nissinen	98	CRN(85)
2111	*Frondihabitans sp.*	99	Nissinen	100	CRN(100)
1920	*Bryocella* sp.	98		98	CRN(85)

FIGURE 4 | Heatmap showing the 20 most dominant OTUs in our dataset, along with best matches in the GenBank 16S rRNA database, an indication if the top GenBank nr match was a sequence from the Hodkinson et al. (2012) or Nissinen et al. (2012) studies, and their status as core OTUs across all samples (ALL), GS samples, CR samples, Coast redwood from Northern CA (CRN) or Coast redwood from Central CA (CRC). Within parenthesis, the percentage of samples above which the OTU is present. Color tones range from warm (red) to cool (blue) to indicate the highest to lowest relative abundance values.

To gain better taxonomic resolution for dominant Alphaproteobacterial OTUs (such as those belonging to LAR1 and AAB discussed above), we constructed a maximum likelihood phylogenetic tree from the Alphaproteobacterial sequences occurring more than 50 times in our samples, along with similar sequences in GenBank (≥96% identity). The phylogeny is shown in **Figure 6**. All Rhodospirillales sequences fell within the family *Acetobacteraceae* but could not be classified below the family level. Many were similar to sequences from Nissinen et al.'s (2012) study on arctic plants. Similarly, Rhizobiales sequences fell in uncultured lineages with the majority putatively in the LAR1 lineage commonly associated with lichens (Hodkinson et al., 2012). This includes some of the most common OTUs in our dataset (e.g., 1726 and 1284), which fell within clades together with LAR1 sequences. The sequences classified as belonging to the order Sphingomonadales also had matches to sequences from the study on arctic plants (Nissinen et al., 2012). While several of the Sphingomonadales OTUs were closely related (≥97% identity) to isolated bacteria (in the genus *Sphingomonas*), only one OTU in the Rhizobiales was closely related to known isolates (in the genus *Methylobacterium*). Similarly, only one OTU in the Rhodospirillales was closely

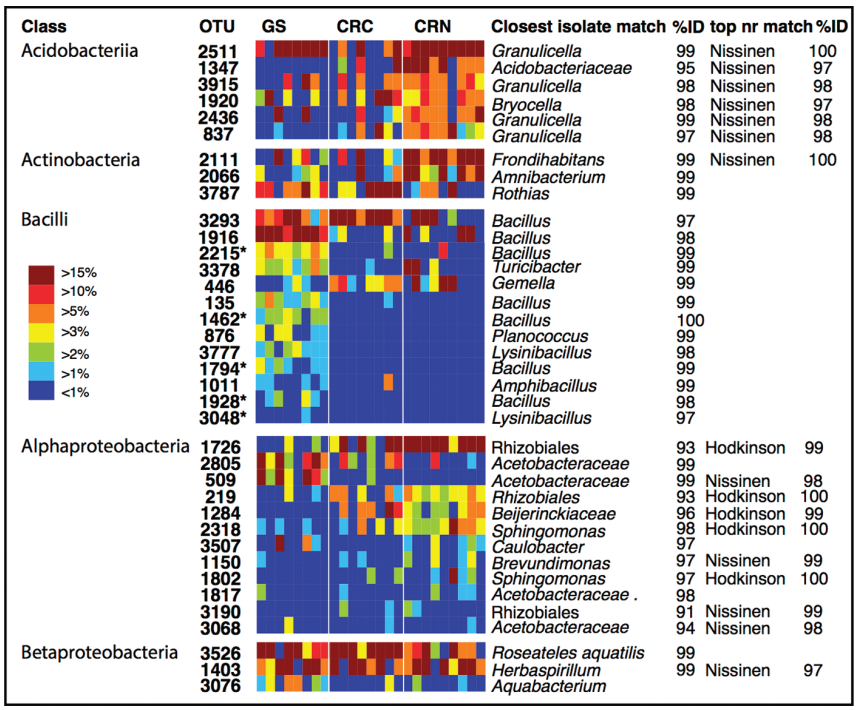

FIGURE 5 | Individual OTU heatmaps for dominant and diverse classes, along with best matches in the GenBank 16S rRNA database and an indication when the top match to GenBank nr was to sequences from the Hodkinson et al. (2012) or Nissinen et al. (2012) studies. Here, colors represent the relative abundance of each OTU as a percentage of the total OTUs within each class. Color tones range from warm (red) to cool (blue) to indicate the highest to lowest relative abundance values. GS: Giant sequoia; CRN: Coast redwood from Northern CA; CRC: Coast redwood from Central CA. Five OTUs which were significantly more common in giant sequoia than in CR are marked with an asterisk.

related to an organism that has been cultured (in the genus *Neoasaia*).

Discussion

The four phyla that dominated the CR and GS communities in this study— Proteobacteria, Firmicutes, Acidobacteria, Actinobacteria —are the same that constitute the majority of bacterial communities associated with the high elevation pines limber pine and Engelmann spruce (Carrell and Frank, 2014). This suggests that lineages within these phyla may be adapted to the conifer foliage endosphere and to the plant interior in general. These phyla have been found to dominate the endophyte communities of various plants (Gottel et al., 2011; Lundberg et al., 2012; Schlaeppi et al., 2014; Shen and Fulthorpe, 2015). Overall, the CR and GS communities were significantly different (**Figure 2**), but at the level of individual taxonomic lineages, few significant differences were observed. There were exceptions, such as the phylum Firmicutes, as well as individual OTUs within the Firmicutes, which were significantly more abundant in GS. It is possible that with more samples, we would see more significant differences in community composition between the two conifer species.

However, in contrast to the endophyte communities from limber pine and Engelmann spruce, no single taxon was consistently present above ∼15% within all samples from either CR or GS or from one of the three locations, and this result would likely not change with an increased sample size. In addition, AAB, while present in many samples, were not dominant taxa in CR and GS foliage. This difference is not due to batch effects associated with different sample processing or sequencing runs, since the samples in this study were prepared and sequenced at the same time as the Engelmann spruce (but not limber pine) samples from our previous study (Carrell and Frank, 2014). Thus, unless our DNA extraction method is not equally efficient in leaves from *Cupressaceae* and *Pinaceae* species, the differences observed here between trees in the two families are real, reflecting either the different environment in which the trees grow, the host species identity of the samples, or most likely, a combination of the two. The conifer leaf endophyte community could also be subject to seasonal or year-to-year variation (Shen and Fulthorpe, 2015), which might influence both the difference observed here between GS (which were sampled in August) and CR (which were sampled in October and November), and between the two conifer families, as the pines were sampled in September (Carrell and Frank, 2014). However, more recent data demonstrate that at least the relationship between AAB and pine is stable across years (Moyes et al., unpublished).

In both GS and CR, multiple OTUs were present in all samples from within a location (but at lower relative abundances

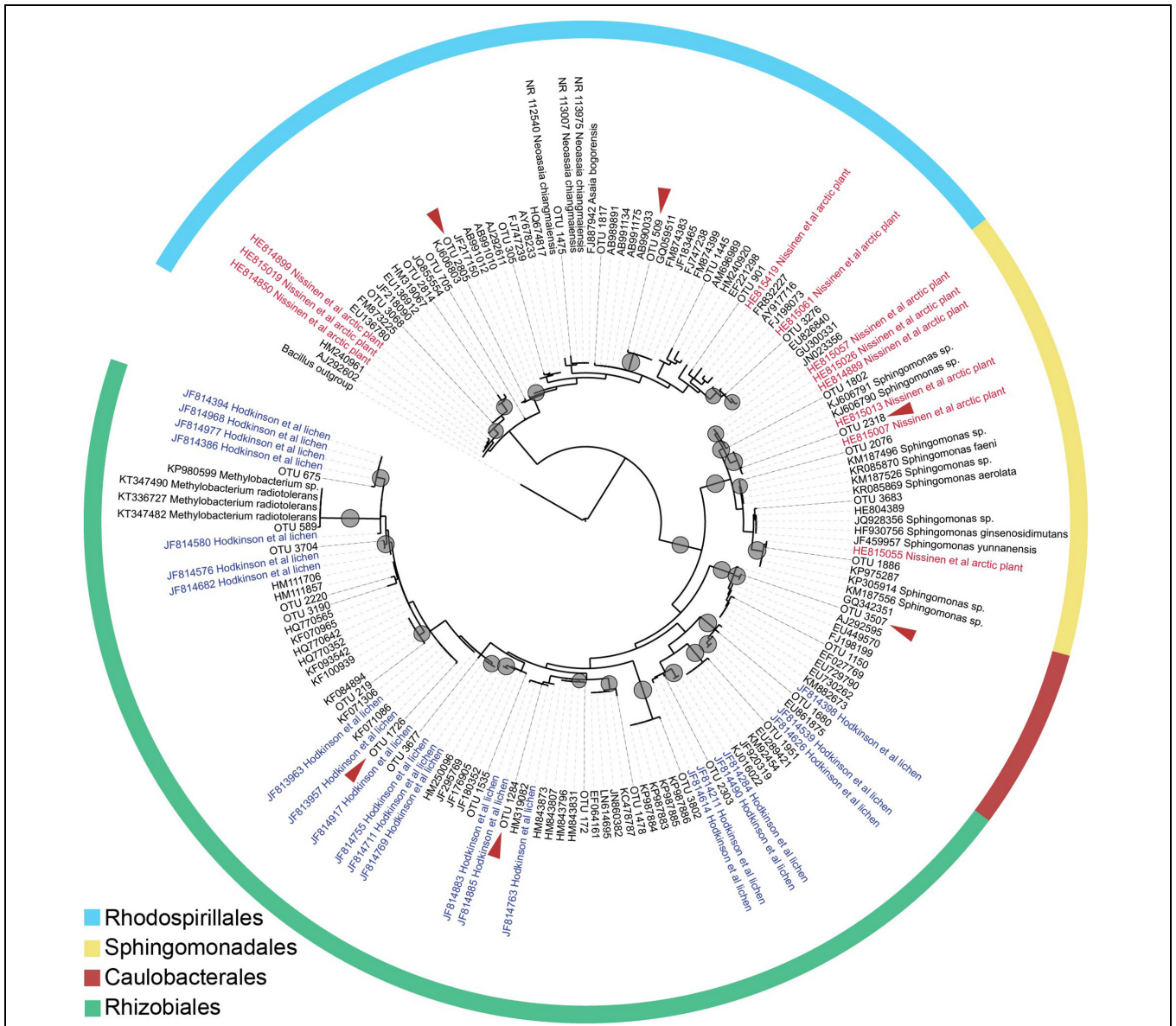

FIGURE 6 | Maximum likelihood tree inferred using the Alphaproteobacterial sequences in our dataset that occur above 50 times total. Nodes with bootstrap support at or above 80 are indicated with a gray circle. Taxa named 'OTU' and with terminal branches shown in solid lines are OTUs from our dataset. Other taxa are indicated by their GenBank accession number, and in the case of isolates of known species, by species name. Taxa from the Hodkinson et al. (2012) study of lichen-associated bacteria are marked 'Hodkinson' and appear in blue, and taxa from the Nissinen et al. (2012) study on endophytes of arctic plants are marked 'Nissinen' and appear in red. A red arrow indicates that the OTU is among the 20 most abundant in the dataset (**Figure 4**).

than observed in the pines in our previous study). Such core OTUs may represent bacteria that are selected by the host, adapted to the environment inside the foliage, or present in high abundance in the source community (e.g., leaf surface, dust, or soil). Most notably, in CR foliage, an OTU belonging to the uncultured LAR1 lineage, which previously has only been described associated with the lichen symbiosis (Hodkinson et al., 2012), was present in all samples from the Northern CA population, and in most samples from the Central CA population. Our phylogenetic analysis of Alphaproteobacterial sequences, while limited by the length of the alignment (~300 nt), suggests that our CR samples contain a wide a diversity of taxa belonging to LAR1 and/or other uncultured lineages in the Rhizobiales (**Figure 1**).

Interestingly, many of the dominant OTUs in the classes Acidobacteriia, Alphaproteobacteria, and Betaproteobacteria were most similar to uncultured endophytes of arctic plants (Nissinen et al., 2012), and several Alphaproteobacterial OTUs—in addition to those belonging to the LAR1 lineage—were most similar to uncultured bacteria associated with the lichen symbiosis (Hodkinson et al., 2012; **Figures 5** and **6**). Nissinen et al. (2012) demonstrated that many of their isolates from arctic

plants were cold-tolerant. Endophytic mediation of plant tolerance to low-temperature stress has been reported in grapevine (Theocharis et al., 2012), however cold-tolerant endophytes do not necessarily provide cold-tolerance to the host plant.

Some possible functions of the CR and GS endophyte microbiome are protection against host biotic and abiotic stress, and N_2 fixation. Several of the major and diverse bacterial groups in the CR and GS foliage (e.g., *Bacillus*, *Burkholderia*, Actinomycetes) are among those known to provide defense to plant hosts though, e.g., antimicrobial and antifungal activity (Mendes et al., 2011; Raaijmakers and Mazzola, 2012). Taxa belonging to the class Bacilli were present in all three populations, but were especially prominent in GS; several OTUs from this class were significantly more common in GS than in CR (**Figure 5**). Bacteria in the genus *Bacillus* show antagonistic activity to a wide range of potential phytopathogens, stimulate plant host defense, and are consequently exploited for biological control of plant diseases (Ongena and Jacques, 2008; Raaijmakers and Mazzola, 2012). For example, a *Bacillus pumilus* endophyte isolated from phloem of healthy lodgepole pine (*Pinus contorta*) is antagonistic against the fungal symbionts of the bark beetle (*Dendroctonus ponderosae*) (Adams et al., 2008). Likewise, Actinomycetes are well-known for their wide diversity of secondary metabolite production, many of which include antibiotic compounds (Tiwari and Gupta, 2012), including strains isolated from plants (Qin et al., 2011). Actinomycetes have been found to dominate the culturable antifungal population in the roots of Douglas fir (*Pseudotsuga menziesii*) (Axelrood et al., 1996). The *Burkholderiaceae* and *Pseudomonadacae* also harbor genera and species with activity against plant pathogenic fungi (Postma et al., 2010; Kwak et al., 2012; Suárez-Moreno et al., 2012).

The presence of these bacterial lineages in the foliage along with the lack of reported outbreaks of pests or diseases on CR and giant foliage is an incentive to further study their foliar bacterial microbiomes. For example, while redwood forests are one of the ecosystems most threatened by the oomycete sudden oak death agent *Phytophthora ramorum*, infection of CR is much lower than in co-occurring species such as tanoak (*Lithocarpus densiflorus)* and California–laurel (*Umbellularia californica*) and results in substantially less sporulation from infected needles (Davidson et al., 2008). Foliar endophytic fungi may contribute heterogeneity in defense chemicals that allows the giant trees to resist disease over centuries to millennia; unlike the host tree, their short life cycle should allow them to respond on ecological timescales to short-cycle pathogens and pests (Carroll, 1988). The bacterial community present within the foliage is another potential source of defense with high potential for spatial and temporal variability.

We previously hypothesized that AAB endophytes fix atmospheric N_2 inside the needles of high elevation pines (Carrell and Frank, 2014). While AAB bacterial were only present at low relative abundance in CR and GS, we found that LAR1, a potential N_2 fixing lineage associated with lichen thalli (Hodkinson and Lutzoni, 2009), was both consistently associated with CR (**Figure 5**), and represented by diverse taxa (**Figure 6**). Based on the phylogenetic affiliation of the *nifH* sequences from lichen, it has been hypothesized that lichen-associated bacteria in the LAR1 lineage fix and contribute atmospheric N_2 to the lichen symbiosis (Grube et al., 2009; Hodkinson and Lutzoni, 2009). Endophytic N_2-fixation may be a source of N_2 to CRs, in addition to other suspected N sources such as fog (Ewing et al., 2009). Moreover, the presence of LAR1 taxa as endophytes in CR could reflect the high abundance of epiphytic lichens in the CR canopy (Williams and Sillett, 2007), which may share endophytic communities with their substrate tree. Redwoods, with their complex branch architecture and long lifespan, support large communities of epiphytic ferns, shrubs, and even trees (Sillett and Pelt, 2007; Williams and Sillett, 2007), all potential hosts of endophytic communities that could be shared with the redwood. Given the phylogenetic affinity of many of our dominant OTUs with endophytes from distant environments and hosts (i.e., arctic plants and lichens), the potential for endophyte sharing among partners in the redwood canopy ecosystem is probably high.

Conclusion

The GS and CR trees we sampled did not host specific recurring bacterial taxa to the extent observed in high elevation conifers (Carrell and Frank, 2014); major OTUs were present but their relative abundance was more variable among samples. Bacterial groups known to be involved in plant defense were major members of the CRs and GS microbiomes, suggesting a potential role in host defense. Further studies using culturing protocols designed to maximize the recovery of specific bacteria such as Actinomycetes (Kaewkla and Franco, 2013) could be done to assess the antimicrobial and antifungal potential of bacteria isolated from surface-sterilized CR and GS foliage.

Author Contributions

AC and AF conceived and designed the sampling and experiments. AC performed the DNA extraction, and PCR amplification. AC and AF analyzed the data and wrote the article.

Acknowledgments

The authors thank Anthony Ambrose, Rikke R. Naesborg, Cameron Williams, Wendy Baxter, Chris Wong, and Todd Dawson at UC Berkeley for providing us with samples, and Jason Sexton, Lara Kueppers, Dana Carper, and Mike Beman at UC Merced, as well as the two reviewers for giving constructive comments on the manuscript. This research was supported by a grant from the Save-the-Redwoods League.

References

Adams, A. S., Six, D. L., Adams, S. M., and Holben, W. E. (2008). In vitro interactions between yeasts and bacteria and the fungal symbionts of the mountain pine beetle (*Dendroctonus ponderosae*). *Microb. Ecol.* 56, 460–466. doi: 10.1007/s00248-008-9364-0

Aleklett, K., Leff, J. W., Fierer, N., and Hart, M. (2015). Wild plant species growing closely connected in a subalpine meadow host distinct root-associated bacterial communities. *Peer J.* 3:e804. doi: 10.7717/peerj.804

Anand, R., Grayston, S., and Chanway, C. (2013). N2-Fixation and seedling growth promotion of lodgepole pine by endophytic *Paenibacillus polymyxa*. *Microb. Ecol.* 66, 369–374. doi: 10.1007/s00248-013-0196-1

Arnold, A. E., Henk, D. A., Eells, R. L., Lutzoni, F., and Vilgalys, R. (2007). Diversity and phylogenetic affinities of foliar fungal endophytes in loblolly pine inferred by culturing and environmental PCR. *Mycologia* 99, 185–206. doi: 10.3852/mycologia.99.2.185

Axelrood, P. E., Clarke, A. M., Radley, R., and Zemcov, S. J. (1996). Douglas-fir root-associated microorganisms with inhibitory activity towards fungal plant pathogens and human bacterial pathogens. *Can. J. Microbiol.* 42, 690–700. doi: 10.1139/m96-094

Bacon, C. W., and Hinton, D. M. (2011). In planta reduction of maize seedling stalk lesions by the bacterial endophyte *Bacillus mojavensis*. *Can. J. Microbiol.* 57, 485–492. doi: 10.1139/w11-031

Berg, G. (2014). The plant microbiome and its importance for plant and human health. *Front. Microbiol.* 5:491. doi: 10.3389/fmicb.2014.00491

Bordiec, S., Paquis, S., Lacroix, H., Dhondt, S., Ait Barka, E., Kauffmann, S., et al. (2011). Comparative analysis of defence responses induced by the endophytic plant growth-promoting rhizobacterium *Burkholderia phytofirmans* strain PsJN and the non-host bacterium *Pseudomonas* syringae pv. pisi in grapevine cell suspensions. *J. Exp. Bot.* 62, 595–603. doi: 10.1093/jxb/erq291

Bragina, A., Cardinale, M., Berg, C., and Berg, G. (2013). Vertical transmission explains the specific *Burkholderia* pattern in *Sphagnum mosses* at multi-geographic scale. *Front. Microbiol.* 4:394. doi: 10.3389/fmicb.2013.00394

Bulgarelli, D., Rott, M., Schlaeppi, K., Ver Loren van Themaat, E., Ahmadinejad, N., Assenza, F., et al. (2012). Revealing structure and assembly cues for *Arabidopsis* root-inhabiting bacterial microbiota. *Nature* 488, 91–95. doi: 10.1038/nature11336

Caporaso, J. G., Bittinger, K., Bushman, F. D., DeSantis, T. Z., Andersen, G. L., and Knight, R. (2010a). PyNAST: a flexible tool for aligning sequences to a template alignment. *Bioinformatics* 26, 266–267. doi: 10.1093/bioinformatics/btp636

Caporaso, J. G., Kuczynski, J., Stombaugh, J., Bittinger, K., Bushman, F. D., Costello, E. K., et al. (2010b). QIIME allows analysis of high-throughput community sequencing data. *Nat. Methods* 7, 335–336. doi: 10.1038/nmeth.f.303

Carrell, A. A., and Frank, A. C. (2014). *Pinus flexilis* and *Picea engelmannii* share a simple and consistent needle endophyte microbiota with a potential role in nitrogen fixation. *Front. Microbiol.* 5:333. doi: 10.3389/fmicb.2014.00333

Carroll, G. (1988). Fungal endophytes in stems and leaves: from latent pathogen to mutualistic symbiont. *Ecology* 69, 2–9. doi: 10.2307/1943154

Carroll, G. C., and Carroll, F. E. (1978). Studies on the incidence of coniferous needle endophytes in the Pacific Northwest. *Can. J. Bot.* 56, 3034–3043. doi: 10.1139/b78-367

Chelius, M. K., and Triplett, E. W. (2001). The diversity of archaea and bacteria in association with the roots of *Zea mays* L. *Microb. Ecol.* 41, 252–263. doi: 10.1007/s002480000087

Cocking, E. C., Stone, J. T., and Davey, M. R. (2006). Intracellular colonization of roots of arabidopsis and crop plants by *Gluconacetobacter diazotrophicus*. *In Vitro Cell. Dev. Biol.* 42, 74–82. doi: 10.1079/IVP2005716

Davidson, J. M., Patterson, H. A., and Rizzo, D. M. (2008). Sources of inoculum for *Phytophthora ramorum* in a redwood forest. *Phytopathology* 98, 860–866. doi: 10.1094/PHYTO-98-8-0860

DeSantis, T. Z., Hugenholtz, P., Larsen, N., Rojas, M., Brodie, E. L., Keller, K., et al. (2006). Greengenes, a chimera-checked 16S rRNA gene database and workbench compatible with ARB. *Appl. Environ. Microbiol.* 72, 5069–72. doi: 10.1128/AEM.03006-05

Dutta, D., and Gachhui, R. (2007). Nitrogen-fixing and cellulose-producing *Gluconacetobacter kombuchae* sp. nov., isolated from Kombucha tea. *Int. J. Syst. Evol. Microbiol.* 57, 353–7. doi: 10.1099/ijs.0.64638-0

Edgar, R. C., Haas, B. J., Clemente, J. C., Quince, C., and Knight, R. (2011). UCHIME improves sensitivity and speed of chimera detection. *Bioinformatics* 27, 2194–2200. doi: 10.1093/bioinformatics/btr381

Edwards, J., Johnson, C., Santos-Medellín, C., Lurie, E., Podishetty, N. K., Bhatnagar, S., et al. (2015). Structure, variation, and assembly of the root-associated microbiomes of rice. *Proc. Natl. Acad. Sci. U.S.A.* 112, E911–E920. doi: 10.1073/pnas.1414592112

Elbeltagy, A., Nishioka, K., Sato, T., Suzuki, H., Ye, B., Hamada, T., et al. (2001). Endophytic colonization and in planta nitrogen fixation by a *Herbaspirillum* sp. isolated from wild rice species. *Appl. Environ. Microbiol.* 67, 5285–5293. doi: 10.1128/AEM.67.11.5285-5293.2001

Espinosa-Garcia, F. J., and Langenheim, J. H. (1990). The endophytic fungal community in leaves of a coastal redwood population diversity and spatial patterns. *New Phytol.* 116, 89–97. doi: 10.1111/j.1469-8137.1990.tb00513.x

Ewing, H. A., Weathers, K. C., Templer, P. H., Dawson, T. E., Firestone, M. K., Elliott, A. M., et al. (2009). Fog water and ecosystem function: heterogeneity in a california redwood forest. *Ecosystems* 12, 417–433. doi: 10.1007/s10021-009-9232-x

Friesen, M. L., Porter, S. S., Stark, S. C., von Wettberg, E. J., Sachs, J. L., and Martinez-Romero, E. (2011). Microbially mediated plant functional traits. *Annu. Rev. Ecol. Evol. Syst.* 42, 23–46. doi: 10.1146/annurev-ecolsys-102710-145039

Fuentes-Ramirez, L. E., Bustillos-Cristales, R., Tapia-Hernandez, A., Jimenez-Salgado, T., Wang, E. T., Martinez-Romero, E., et al. (2001). Novel nitrogen-fixing acetic acid bacteria, *Gluconacetobacter johannae* sp. nov. and *Gluconacetobacter azotocaptans* sp. nov., associated with coffee plants. *Int. J. Syst. Evol. Microbiol.* 51, 1305–1314

Ganley, R. J., Brunsfeld, S. J., and Newcombe, G. (2004). A community of unknown, endophytic fungi in western white pine. *Proc. Natl. Acad. Sci. U.S.A.* 101, 10107–10112. doi: 10.1073/pnas.0401513101

Gottel, N. R., Castro, H. F., Kerley, M., Yang, Z., Pelletier, D. A., Podar, M., et al. (2011). Distinct microbial communities within the endosphere and rhizosphere of *Populus deltoides* roots across contrasting soil types. *Appl. Environ. Microbiol.* 77, 5934–44. doi: 10.1128/AEM.05255-11

Grube, M., Cardinale, M., de Castro, J. V., Müller, H., and Berg, G. (2009). Species-specific structural and functional diversity of bacterial communities in lichen symbioses. *ISME J.* 3, 1105–1115. doi: 10.1038/ismej.2009.63

Hardoim, P. R., van Overbeek, L. S., and Elsas, J. D. (2008). Properties of bacterial endophytes and their proposed role in plant growth. *Trends Microbiol.* 16, 463–471. doi: 10.1016/j.tim.2008.07.008

Hodkinson, B. P., Gottel, N. R., Schadt, C. W., and Lutzoni, F. (2012). Photoautotrophic symbiont and geography are major factors affecting highly structured and diverse bacterial communities in the lichen microbiome. *Environ. Microbiol.* 14, 147–161. doi: 10.1111/j.1462-2920.2011.02560.x

Hodkinson, B. P., and Lutzoni, F. (2009). A microbiotic survey of lichen-associated bacteria reveals a new lineage from the Rhizobiales. *Symbiosis* 49, 163–180. doi: 10.1007/s13199-009-0049-3

Jiao, J. Y., Wang, H. X., Zeng, Y., and Shen, Y. M. (2006). Enrichment for microbes living in association with plant tissues. *J. Appl. Microbiol.* 100, 830–837. doi: 10.1111/j.1365-2672.2006.02830.x

Kaewkla, O., and Franco, C. M. (2013). Rational approaches to improving the isolation of endophytic actinobacteria from Australian native trees. *Microb. Ecol.* 65, 384–393. doi: 10.1007/s00248-012-0113-z

Kersters, K., Lisdiyanti, P., Komagata, K., and Swings, J. (2006). "The family acetobacteraceae: the genera acetobacter, acidomonas, asaia, gluconacetobacter, gluconobacter, and kozakia," in *The prokaryotes*, eds M. Dworkin, S. Falkow, E. Rosenberg, K. H. Schleifer, and E. Stackebrandt (New York, NY: Springer), 163–200.

Knoth, J. L., Kim, S.-H., Ettl, G. J., and Doty, S. L. (2014). Biological nitrogen fixation and biomass accumulation within poplar clones as a result of inoculations with diazotrophic endophyte consortia. *New Phytol.* 201, 599–609. doi: 10.1111/nph.12536

Kwak, M. -J., Song, J. Y., Kim, S.-Y., Jeong, H., Kang, S. G., Kim, B. K., et al. (2012). Complete genome sequence of the endophytic bacterium *Burkholderia* sp. strain KJ006. *J. Bacteriol.* 194, 4432–4433. doi: 10.1128/JB.00821-12

Letunic, I., and Bork, P. (2011). Interactive Tree Of Life v2: online annotation and display of phylogenetic trees made easy. *Nucleic Acids Res.* 39, W475–W478. doi: 10.1093/nar/gkr201

Lozupone, C., and Knight, R. (2005). UniFrac: a new phylogenetic method for comparing microbial communities. *Appl. Environ. Microbiol.* 71, 8228–8235. doi: 10.1128/AEM.71.12.8228-8235.2005

Lundberg, D. S., Lebeis, S. L., Paredes, S. H., Yourstone, S., Gehring, J., Malfatti, S., et al. (2012). Defining the core *Arabidopsis thaliana* root microbiome. *Nature* 488, 86–90. doi: 10.1038/nature11237

Mendes, R., Kruijt, M., de Bruijn, I., Dekkers, E., van der Voort, M., Schneider, J. H., et al. (2011). Deciphering the rhizosphere microbiome for disease-suppressive bacteria. *Science* 332, 1097–1100. doi: 10.1126/science.1203980

Müller, H., Berg, C., Landa, B. B., Auerbach, A., Moissl-Eichinger, C., and Berg, G. (2015). Plant genotype-specific archaeal and bacterial endophytes but similar *Bacillus antagonists* colonize Mediterranean olive trees. *Front. Microbiol.* 6:138. doi: 10.3389/fmicb.2015.00138

Nawrocki, E. P., Kolbe, D. L., and Eddy, S. R. (2009). Infernal 1.0: inference of RNA alignments. *Bioinformatics* 25, 1335–1337. doi: 10.1093/bioinformatics/btp157

Nissinen, R. M., Männistö, M. K., and van Elsas, J. D. (2012). Endophytic bacterial communities in three arctic plants from low arctic fell tundra are cold-adapted and host-plant specific. *FEMS Microbiol. Ecol.* 82, 510–522. doi: 10.1111/j.1574-6941.2012.01464.x

Ongena, M., and Jacques, P. (2008). Bacillus lipopeptides: versatile weapons for plant disease biocontrol. *Trends Microbiol.* 16, 115–125. doi: 10.1016/j.tim.2007.12.009

Oono, R., Lutzoni, F., Arnold, A. E., Kaye, L., U'Ren, J. M., May, G., et al. (2014). Genetic variation in horizontally transmitted fungal endophytes of pine needles reveals population structure in cryptic species. *Am. J. Bot.* 101, 1362–1374. doi: 10.3732/ajb.1400141

Peñuelas, J., and Terradas, J. (2014). The foliar microbiome. *Trends Plant Sci.* 19, 278–280. doi: 10.1016/j.tplants.2013.12.007

Porras-Alfaro, A., and Bayman, P. (2011). Hidden fungi, emergent properties: endophytes and microbiomes. *Annu. Rev. Phytopathol.* 49, 291–315. doi: 10.1146/annurev-phyto-080508-081831

Postma, J., Scheper, R. W. A., and Schilder, M. T. (2010). Effect of successive cauliflower plantings and *Rhizoctonia solani* AG 2-1 inoculations on disease suppressiveness of a suppressive and a conducive soil. *Soil Biol. Biochem.* 42, 804–812. doi: 10.1016/j.soilbio.2010.01.017

Price, M. N., Dehal, P. S., and Arkin, A. P. (2009). FastTree: computing large minimum evolution trees with profiles instead of a distance matrix. *Mol. Biol. Evol.* 26, 1641–1650. doi: 10.1093/molbev/msp077

Qadri, M., Rajput, R., Abdin, M. Z., Vishwakarma, R. A., and Riyaz-Ul-Hassan, S. (2014). Diversity, molecular phylogeny, and bioactive potential of fungal endophytes associated with the himalayan blue pine (*Pinus wallichiana*). *Microb. Ecol.* 67, 877–887. doi: 10.1007/s00248-014-0379-4

Qin, S., Xing, K., Jiang, J.-H., Xu, L.-H., and Li, W.-J. (2011). Biodiversity, bioactive natural products and biotechnological potential of plant-associated endophytic actinobacteria. *Appl. Microbiol. Biotechnol.* 89, 457–473. doi: 10.1007/s00253-010-2923-6

Raaijmakers, J. M., and Mazzola, M. (2012). Diversity and natural functions of antibiotics produced by beneficial and plant pathogenic bacteria. *Annu. Rev. Phytopathol.* 50, 403–424. doi: 10.1146/annurev-phyto-081211-172908

Redford, A. J., Bowers, R. M., Knight, R., Linhart, Y., and Fierer, N. (2010). The ecology of the phyllosphere: geographic and phylogenetic variability in the distribution of bacteria on tree leaves. *Environ. Microbiol.* 12, 2885–2893. doi: 10.1111/j.1462-2920.2010.02258.x

Reinhold-Hurek, B., and Hurek, T. (2011). Living inside plants: bacterial endophytes. *Curr. Opin. Plant Biol.* 14, 435–443. doi: 10.1016/j.pbi.2011.04.004

Rodriguez, R. J., Redman, R. S., and Henson, J. M. (2004). the role of fungal symbioses in the adaptation of plants to high stress environments. *Mitig. Adapt. Strateg. Glob. Change* 9, 1573–1596. doi: 10.1023/B:MITI.0000029922.31110.97

Rollinger, J. L., and Langenheim, J. H. (1993). Geographic survey of fungal endophyte community composition in leaves of coastal redwood. *Mycologia* 85, 149. doi: 10.2307/3760450

Rosenblueth, M., and Martinez-Romero, E. (2006). Bacterial endophytes and their interactions with hosts. *Mol. Plant Microbe Interact.* 19, 827–837. doi: 10.1094/MPMI-19-0827

Rout, M. E., Chrzanowski, T. H., Westlie, T. K., Deluca, T. H., Callaway, R. M., and Holben, W. E. (2013). Bacterial endophytes enhance competition by invasive plants. *Am. J. Bot.* 100, 1726–1737. doi: 10.3732/ajb.1200577

Schlaeppi, K., Dombrowski, N., Oter, R. G., Ver Loren van Themaat, E., and Schulze-Lefert, P. (2014). Quantitative divergence of the bacterial root microbiota in *Arabidopsis thaliana* relatives. *Proc. Natl. Acad. Sci. U.S.A.* 111, 585–592. doi: 10.1073/pnas.1321597111

Shakya, M., Gottel, N., Castro, H., Yang, Z. K., Gunter, L., LabbÃ, J., et al. (2013). A multifactor analysis of fungal and bacterial community structure in the root microbiome of mature populus deltoides trees. *PLoS ONE* 8:e76382 doi: 10.1371/journal.pone.0076382

Shen, S. Y., and Fulthorpe, R. (2015). Seasonal variation of bacterial endophytes in urban trees. *Front. Microbiol.* 6:427. doi: 10.3389/fmicb.2015.00427

Sillett, S. C., and Pelt, R. V. (2007). Trunk reiteration promotes epiphytes and water storage in an old-growth redwood forest canopy. *Ecol. Monogr.* 77, 335–359. doi: 10.1890/06-0994.1

Stamatakis, A., Ludwig, T., and Meier, H. (2005). RAxML-III: a fast program for maximum likelihood-based inference of large phylogenetic trees. *Bioinformatics* 21, 456–463. doi: 10.1093/bioinformatics/bti191

Suárez-Moreno, Z. R., Caballero-Mellado, J., Coutinho, B. G., Mendonça-Previato, L., James, E. K., and Venturi, V. (2012). Common features of environmental and potentially beneficial plant-associated burkholderia. *Microb. Ecol.* 63, 249–266. doi: 10.1007/s00248-011-9929-1

Theocharis, A., Bordiec, S., Fernandez, O., Paquis, S., Dhondt-Cordelier, S., Baillieul, F., et al. (2012). *Burkholderia phytofirmans* PsJN primes *Vitis vinifera* L. and confers a better tolerance to low nonfreezing temperatures. *Mol. Plant Microbe Interact.* 25, 241–249. doi: 10.1094/MPMI-05-11-0124

Tiwari, K., and Gupta, R. K. (2012). Rare actinomycetes: a potential storehouse for novel antibiotics. *Crit. Rev. Biotechnol.* 32, 108–132. doi: 10.3109/07388551.2011.562482

Turner, T. R., James, E. K., and Poole, P. S. (2013). The plant microbiome. *Genome Biol.* 14, 209. doi: 10.1186/gb-2013-14-6-209

Wang, Q., Garrity, G. M., Tiedje, J. M., and Cole, J. R. (2007). Naive Bayesian classifier for rapid assignment of rRNA sequences into the new bacterial taxonomy. *Appl. Environ. Microbiol.* 73, 5261–5267. doi: 10.1128/AEM.00062-07

Williams, C. B., and Sillett, S. C. (2007). Epiphyte communities on redwood (*Sequoia sempervirens*) in northwestern California. *Bryologist* 110, 420–452. doi: 10.1639/0007-2745(2007)11

Conflict of Interest Statement: The Guest Associate Editor Mysore Tejesvi declares that despite having hosted a Frontiers Research Topic with the author Anna C. Frank, the review process was handled objectively. The authors declare that the research was conducted in the absence of any commercial or financial relationships that could be construed as a potential conflict of interest.

frontiers in Microbiology

ORIGINAL RESEARCH
published: 25 August 2015
doi: 10.3389/fmicb.2015.00867

Effects of growth stage and fulvic acid on the diversity and dynamics of endophytic bacterial community in *Stevia rebaudiana* Bertoni leaves

Xuejian Yu[1], *Jinshui Yang*[1], *Entao Wang*[2], *Baozhen Li*[1] *and Hongli Yuan*[1]*

[1] State Key Laboratory of Agrobiotechnology, MOA Key Laboratory of Soil Microbiology, College of Biological Sciences, China Agricultural University, Beijing, China, [2] Departamento de Microbiología, Escuela Nacional de Ciencias Biológicas, Instituto Politécnico Nacional, Mexico City, Mexico

The aim of this study was to learn the interactions among the endophytic bacteria, the plant growth, the foliar spray of fulvic acid, and the accumulation of steviol glycosides in the leaves of *Stevia rebaudiana*. Metagenomic DNA was extracted from the *Stevia* leaves at different growth stages with or without the fulvic acid treatment; and the diversity of endophytic bacteria in *Stevia* leaves was estimated by pyrosequencing of 16S rRNA genes. As results, Proteobacteria, Actinobacteria, Bacteroidetes, and Firmicutes were found to be the dominant phyla despite the growth stages and fulvic acid application. *Stevia* growth stages strongly regulated composition of endophytic community. The genera *Agrobacterium* (12.3%) and *Erwinia* (7.2%) dominated in seedling stage were apparently declined in the vegetable and initial flowering stages, while *Sphingomonas* and *Methylobacterium* increased in mature leaves at harvest time, which showed that the mature leaves of *Stevia* preferred to accumulate some certain endophytic bacteria. *Sphingomonas* and *Methylobacterium* constituted an important part of the core endophytic community and were positively correlated with the stevioside content and *UGT74G1* gene expression, respectively; while *Erwinia*, *Agrobacterium*, and *Bacillus* were negatively correlated with the stevioside accumulation. Fulvic acid treatment accelerated the variation of endophytes along the growth stages and increased the steviol glycosides content. This is the first study to reveal the community composition of endophytic bacteria in the *Stevia* leaves, to evidence the strong effects of growth stage and fulvic acid application on the endophytes of *Stevia*, and to demonstrate the correlation between the endophytic bacteria and the steviol glycosides accumulation.

Keywords: endophytes, *Stevia rebaudiana* Bertoni, bacterial diversity, pyrosequencing, growth stage, fulvic acid

OPEN ACCESS

Edited by:
Mysore V. Tejesvi, University of Oulu, Finland

Reviewed by:
Raffaella Balestrini, Consiglio Nazionale delle Ricerche, Italy
Arijit Mukherjee, University of Central Arkansas, USA

***Correspondence:**
Hongli Yuan, Center for Life Sciences, College of Biological Sciences, China Agricultural University, 2 Yuanmingyuan Xilu, Haidian, Beijing 100193, China
hlyuan@cau.edu.cn

Specialty section:
This article was submitted to Plant Biotic Interactions, a section of the journal Frontiers in Microbiology

Received: *15 May 2015*
Accepted: *10 August 2015*
Published: *25 August 2015*

Citation:
Yu X, Yang J, Wang E, Li B and Yuan H (2015) Effects of growth stage and fulvic acid on the diversity and dynamics of endophytic bacterial community in Stevia rebaudiana Bertoni leaves. Front. Microbiol. 6:867. doi: 10.3389/fmicb.2015.00867

Introduction

Being a part of the plant associated microorganisms, endophytic bacteria live intercellular spaces or inside the plant cells (Hallmann et al., 1997; Lucero et al., 2011) at least part of their lifetime without causing visibly harmful effects on the host (Sturz et al., 2000). Although the endophytes are ubiquitous in plants, only a small fraction of the plants have been involved in the study of endophytic biology (Strobel et al., 2004; Ryan et al., 2008). As the majority of terrestrial

carbon fixation and a strong biotic link between the biosphere and atmosphere, the plant leaves provide a special habitat for microorganisms, with intense solar radiation, and dramatic change of temperature (Hunter et al., 2010). Therefore, the leaves present a valuable context for investigating the relationships among the endophytic microbes, their hosts and the biotic/abiotic environmental factors (Meyer and Leveau, 2012; Zimmerman and Vitousek, 2012).

It has been reported that the endophytic communities in leaves varied with the host plant species (Yang et al., 2001) or genotype (van Overbeek and van Elsas, 2008; Hunter et al., 2010), the plant growth stage (van Overbeek and van Elsas, 2008), and the plant morphology (Elvira-Recuenco and van Vuurde, 2000; Yang et al., 2001), referring to the differences in leaf structure (shape, thickness, and stomata) and chemical properties (water and nutrients contents, secondary metabolites, Rodriguez et al., 2009; Hunter et al., 2010; Arturo et al., 2012). Furthermore, abiotic factors such as temperature, solar radiant intensity, rainfall, soil quality, and especially the fertilization have been proven to play a momentous role in regulating the modes of leaf endophytic bacterial colonization (Pedraza et al., 2009; Hunter et al., 2010). Among these factors, the plant growth stage was found overwhelming the effect of plant genotype on the total bacterial communities associated with potato (van Overbeek and van Elsas, 2008). In addition, it has been proved that the plant growth regulators could simulate lots of physiological processes in plants and improve the plant performance (Ren et al., 2011; Luczkiewicz et al., 2014). However, little information is available about the effects of growth regulators on the endophytes associated with plant leaves.

Stevia rebaudiana Bertoni is an important economic plant for producing steviol glycosides (SGs), a kind of natural, non-caloric, high-intensity sweeteners approved as natural sweeteners beneficial to health (Yadav et al., 2011). In China, this plant has been extensively cultivated in last decades as the third most popular natural sugar source, just after cane and beet (Yang et al., 2013). In *Stevia* leaves, eight kinds of SGs have been detected, with stevioside (ST), rebaudioside A (RA), and rebaudioside C (RC) as the major ones (Yadav et al., 2011), in which RC has an undesirable bitter aftertaste, which restricts its application in the food industry for human direct consumption; while RA has a higher sweetness rating and better taste than RC. The SGs are accumulated in the *Stevia* leaves and their concentration varies widely depending on the genotype, fertilization level and growth stages (Yadav et al., 2011; Yan et al., 2012) via their effects on the 17-step biosynthetic pathway of SGs (Kumar et al., 2012; Madhav et al., 2013; Chen et al., 2014). For the biosynthesis of SGs in *Stevia*, the last five steps are specific and catalyzed by at least three UDP-glycosyltransferases genes: *UGT85C2* gene responsible for the addition of C-13-glucose to steviol; *UGT74G1* responsible for addition of glycosyl to steviolbioside; and *UGT76G1* coding the key enzyme for transferring a glucose residue to the ST molecule for synthesizing RA (**Supplementary Figure S1**) (Kumar et al., 2012; Madhav et al., 2013; Chen et al., 2014). Thus, enhancing the expression level of the *UGT* genes through certain treatments might be a possible way to increase the RA content in the *Stevia* leaves. Previously, we found that the spread of fulvic acid (FA), an eco-friendly plant regulator (Nardi et al., 2002), could increase *Stevia* leaf biomass. However, the biological mechanism of this effect was unclear. Considering the economic importance of *S.rebaudiana* and the special characters of its leaves (high RA content), these plants could be considered as a valuable model for investigating the diversity and dynamics of endophytic bacteria in leaves, and for evaluating the interactions among the endophytic community, the metabolites accumulation and the application of growth regulator. Therefore, we performed this study to compare the endophytic bacterial communities in *Stevia* leaves with or without plant regulator (FA) treatment at different growth stages, using the 454 pyrosequencing of 16S rRNA gene. In addition, we also investigated the relationships among the endophytic communities, the SGs content and *UGT* genes expression. The aim was to provide a potential insight into the plant-microorganism interactions in *Stevia*. It was the first study on the endophytic bacterial community in *Stevia* leaves and on the correlation between the endophytes and the accumulation of SGs.

Materials and Methods

Plant Growth Conditions and Treatments

Rooted plantlets of a high-RA-yielding variety of *Stevia rebaudiana* Bertoni, Xinguang No. 3, purchased from Lvyuan *Stevia* Co. Ltd. (Mingguang, Anhui, China) were transplanted in plots (20 m^2 for each) in the fields at Shangzhuang experimental station of China Agricultural University (116.18°E, 40.14°N) in May 8 of 2012. The experiment consisted of a randomized block design with four biological replications for the control and the FA treatments, respectively; therefore, a total of eight plots were included. The described field study did not require specific permits and did not involve endangered or protected species.

The plants were put in the plots with ∼30 cm of space between plants in the rows and with distance of 45 cm between two rows. Urea (15 g m^{-2}) was supplied as the basic fertilizer in soil for all the experiments. Treatment F was applied with a foliar spray of FA solution (500 mg l^{-1}) at the dose of 75 ml m^{-2} once every 2 weeks after transplanting; while water was applied for the control group. The FA solution was obtained from the biodegradation of leonardite with the bacterial community MCSL-2 (Gao et al., 2012) by centrifugation at 8000 × *g* for 15 min and filtered through Whatman No. 1 to remove cells and residual leonardite after 21 days of incubation. The supernatant was dried at 60°C and dissolved in water at the concentration of 500 mg l^{-1} (Gao et al., 2012).

Leaf Sampling and Metagenomic DNA Extraction

In this analysis, *Stevia* plants from control and FA treatments were collected at three growth stages: the seedling stage (coded as C-0), the vegetable growing stage (after 2 months of growth, coded as C-2 for control and F-2 for FA treatment), and the initial flowering stage (after 4 months of growth, coded as C-4 for control and F-4 for FA treatment). From each plot, 10 randomly selected plants were uprooted. The leaves of sampled plants were cut off immediately using a razor blade and all the leaves from the same plot were stored in a paper bag as a single sample. During all

the sampling procedure, sterile gloves were used by the workers to avoid bacterial contamination. The samples were transported to the laboratory on ice, and then stored at −80°C before further processing.

To isolate the metagenomic DNA, all the sampled leaves were surface cleaned to reduce the presence of surface microorganisms by the following procedure: simply rinsed in sterilized deionized H_2O; immersed in 70% (v/v) ethanol (2 min); immersed in sterilized deionized H_2O (2 min); immersed in 5% (w/v) NaClO (3 min), and finally received three sequential 1 min rinses in sterilized H_2O (Bodenhausen et al., 2013). The leaves were dried at 37°C for 4 h and then the samples from the same treatments at the same stage were compiled and ground in liquid nitrogen. A modified endophytic DNA enrichment method (Wang et al., 2008b) was employed to avoid the influence of leaf chloroplast DNA. The metagenomic DNA was extracted from 0.5 g of each enriched endophytic bacterial sample using an E. Z. N. A.TM Soil DNA Kit according to the manufacturer's instructions (Omega Bio-tek, Inc., USA).

PCR Amplification and Pyrosequencing Analysis

Primer set 515F/926R was used to amplify the 16S rRNA gene fragment (V4 and V6 region) from the samples on the 454 GS-FLX pyrosequencing platform and duplicate was employed for each sample. The universal primer set 515F/926R specific to V4 and V5 regions and PCR protocol describe previously and the reverse primer included a 7 bp barcode (Quince et al., 2011). The PCR conditions used were 95°C for 5 min, 30 cycles of 95°C for 40 s, 55°C for 40 s, and 72°C for 1 min, followed by 72°C for 7 min (Andersson et al., 2008; Lopez-Velasco et al., 2011). The sequencing data were processed using the Quantitative Insights Into Microbial Ecology (QIIME) software (Caporaso et al., 2011), and suspected chimeras were detected using the QIIME chimera with a denoising step. To compare the samples, sequences below a quality score of 25 and <200 bp were removed, and the adapters, barcodes and primers were trimmed using default parameters. Sequences representing chloroplast or mitochondrial DNA were eliminated from further analysis (Bodenhausen et al., 2013). The obtained sequences were assigned into operational taxonomic units (OTUs) using 97% identity clustering, and the most abundant sequence from each OTU was selected as the representative sequence for that OTU. Taxonomy was assigned from the RDP database with 80% confidence. Sequences were assigned to phylotype clusters at two cut-off levels of species, 3 and 5%. Based on the sequences and/or OTUs obtained, rarefaction curves, ACE, Chao1 richness and the Shannon index were calculated. UPGMA clustering analysis, PCoA, CCA were performed to evaluate the similarities and to correlate the microbial distribution with the environmental factors for the five samples. The pyrosequencing reads have been deposited at the GenBank under accession number SRR1552085.

Determination of Biomass Yield and Content of SGs in *Stevia* Leaves

After 4 months growth, the control and FA treated plants were harvested separately for each plot, and the leaves obtained from each plot were dried in an oven at 50°C to a constant weight. The dried leaves from each plot were then weighted and ground separately using a high-speed grinder. An aliquot of 0.25 g of the ground leaves from each sample was extracted in a 150-mL Erlenmeyer flasks with 25 mL of 70% (v/v) ethanol in a 70°C water bath by shaking (150 rpm) for 30 min (Moraes et al., 2013; Serfaty et al., 2013). After cooling, aliquot of 1 mL was filtered with 0.22 μm filter (Beihua Sunrise Barrier Separation Technology, Beijing, China) and 20 μL of the filtrated extract were analyzed by high-performance liquid chromatography (HPLC; Shimadzu Essentia LC-15C, Shimadzu Corporation, Kyoto, Japan) using a Phenomenex Luna-NH_2 column (5 μm, 250 × 4.6 mm; Phenomenex Inc., Torrance, CA, USA). A mixture of acetonitrile and water (75:25, v/v) was used as the eluent at a flow rate of 1 mL min^{-1}, and the compounds were detected with ultraviolet (UV) light at 210 nm. For quantitative analysis, pure ST and RA obtained from Liaoning Qianqian biotechnology Co., Ltd were separately used to prepare the standard solutions in ethanol at the concentrations of 0.3, 0.6, 0.9, and 1.2 g l^{-1}. The parameters of external calibration curves were obtained by fitting experimental data through linear regression from replicate injections of standard solutions (Kolb et al., 2001).

UGT Genes Expression

In this assay, 10 plants from each plot were randomly selected and 5 g of the leaves were mixed as one sample for RNA isolation (Brandle et al., 2002; Madhav et al., 2013) with TRI gene reagent (Genstar), according to the manufacturer's instructions. After quality control, 1 μg of the high purity RNA samples ($A_{260/280} > 1.8$) was used for cDNA synthesis with PrimeScript cDNA Synthesis Kit (Takara, Japan) following the manufacturer's instructions.

For real-time quantitative polymerase chain reaction (RT-q PCR), the *β-actin* and 18S rRNA genes, which are expressed at a constant level across all samples, were used to normalize the data individually for more reliability (Mohamed et al., 2011). Primers for both *UGT*, *β-actin* and 18S rRNA genes were designed according to Mohamed et al. (2011) (sequences in 5′–3′, the annealing temperature of the primers was listed in the parenthesis):

UGT76G1 (60°C):
f-GCAGCTTACTAGACCACGATC
r-CTCATCCACTTCACTAGTACTAC
UGT74G1 (60°C):
f-TGCATGAACTGGTTAGACGATAAG
r-GCATCCTACTGATTCGTGTGCTA
UGT85C2 (60°C):
f-TCGATGAGTTGGAGCCTAGTATT
r-CTAAACTGTATCCATGGAGACTC
β-actin (60°C):
f-AGCAACTGGGATGACATGGAA
r-GGAGCGACACGAAGTTCATTG
18S rRNA (60°C):
f-CCGGCGACGCATCATT
r-AGGCCACTATCCTACCATCGAA

The PCR reaction was performed in 20 μl containing 8.2 μl H_2O, 10 μl SYBR green mix, 0.4 μl of each primer (10 μmol l^{-1})

and 1 μl of cDNA obtained as mentioned above. The reactions were applied as quadruplicates in an ABI PRISM 7500 sequence detection system (ABI, Applied Biosystems) with the following thermal cycles: 95°C for 10 min, followed by 40 cycles of 95°C for 30 s and 60°C for 30 s.

Statistical Analysis

To estimate the effects of FA treatment, the data of leaf yields and contents of SGs were statistically analyzed using the software package of Microsoft Excel and SPSS 17.0 for Windows (IBM Corp., Armonk, NY, USA). To examine the statistical significance of differences between treatment and control groups, a One-Way analysis of variance (ANOVA) was conducted through the Tukey HSD-test.

Results

Overall Diversity of the Endophytic Bacteria in *Stevia* Leaves

After quality control, a total of 49,289 sequences were obtained from all the five samples in the pyrosequencing analysis (**Table 1**). Excluding the potential chimeras, 2164 bacterial OTUs were obtained from the leaf endophytic samples, at the 0.03 distance cutoff. The average number of OTUs observed in the samples was 690.8 ($SD = 101.5$). The coverage parameters OTUs/Chao1 and OTUs/ACE were about 60 and 50%, respectively. The species richness (OTU numbers and Simpson index) of leaf endophytes was apparently increased along the growth of plant: 38.6 and 29.9% greater than that in C-0 after 2 (C-2) and 4 (C-4) months growth, respectively, as shown in **Table 1**. However, the Shannon index was decreased. In comparison with the control samples (C-2 and C-4), the fulvic acid treatment (F-2 and F-4) decreased both the species richness and the diversity index: −23.8 and −18.2% for OTU number; −1.76 and −0.9 for Shannon index, respectively.

Among these OTUs, 2048 (94.6%) were identified into 12 phyla and only six of them presented an average abundance >1% of the OTUs (covering 0.24–79.32% of reads) (**Figures 1A**, **2A**, details available as **Supplementary Table S1**): 58.09% of OTUs covering 79.32% of reads were Proteobacteria; 19.09% of OTUs corresponding to 14.32% of reads were Actinobacteria; 9.01% of OTUs with 3.09% of reads were Bacteroidetes; 5.73% of OTUs with 1.94% of reads were Firmicutes; 1.39% of OTUs covering 0.24% of reads were Gemmatimonadetes; 1.34% of OTUs with 0.30% of reads were Acidobacteria, and 1–4 OTUs (<0.2%) covering 2–7 (≤0.014%) of reads belonged to each of the Candidate division TM7, Chlorobi, Chloroflexi, Planctomycetes, Thermi, and Armatimonadetes. At the family level, 71.49% of OTUs were identified into 131 taxa, with Sphingomonadaceae (15.26% for OTUs and 41.59% for reads) and Methylobacteriaceae (8.02% for OTUs and 19.19% for reads) as the most abundant ones, followed by Enterobacteriaceae (6.59% for OTUs and 6.52% for reads), Microbacteriaceae (3.30% for OTUs and 4.69% for reads), and Kineosporiaceae (0.97% for OTUs and 3.26% for reads); while each of the other families occupied <3% of the reads (**Figure 2B**, **Supplementary Table S2**).

TABLE 1 | General data of pyrosequencing results of leaf endophytic bacteria and growth/quality characters of *Stevia* in different growth stage and treatments.

Characters	Growth stage and treatment[#]				
	C-0	C-2	C-4	F-2	F-4
PYROSEQUENCING DATA					
Reads	3670	10,228	10,752	8210	16,429
OTUs	595	825	773	629	632
Chao1[§]	1073	1256	1467	928	1006
ACE[¶]	1492	1264	1900	1219	983
Shannon	6.68	4.73	5.24	2.97	4.34
Simpson	0.032	0.211	0.101	0.461	0.163
GROWTH AND QUALITY*					
Plant height (cm)	12.60 e	38.10 d	89.40 b	41.9 c	99.00 a
RA content (%)	8.08 c	10.20 b	11.95 ab	13.20 a	13.65 a
ST content (%)	0.50 c	0.80 bc	1.77 ab	0.97 bc	2.28 a
RC content (%)	0.23 c	0.96 ab	1.42 a	0.70 bc	1.31 a
SGs content (%)	8.81 c	11.96 b	15.14 a	14.87 a	17.24 a
76G1 gene expression	1.00 c	0.46 d	0.16 e	2.04 b	4.34 a
85C2 gene expression	1.00 b	0.50 c	0.04 d	2.52 a	0.25 cd
74G1 gene expression	1.00 d	9.40 ab	3.67 c	10.49 a	8.52 b

**Data were average of four replicates and numbers in the same line followed by different letters presented significant difference at P = 0.05.*

[#]C, control; F, fulvic acid treatment; 0, seedling stage; 2, middle vegetable growth stage; 4, initial flowering stage.

[§]Calculated at a distance level of 0.03.

[¶]Ninety-five percent confidence interval. ACE, abundance-based coverage estimators.

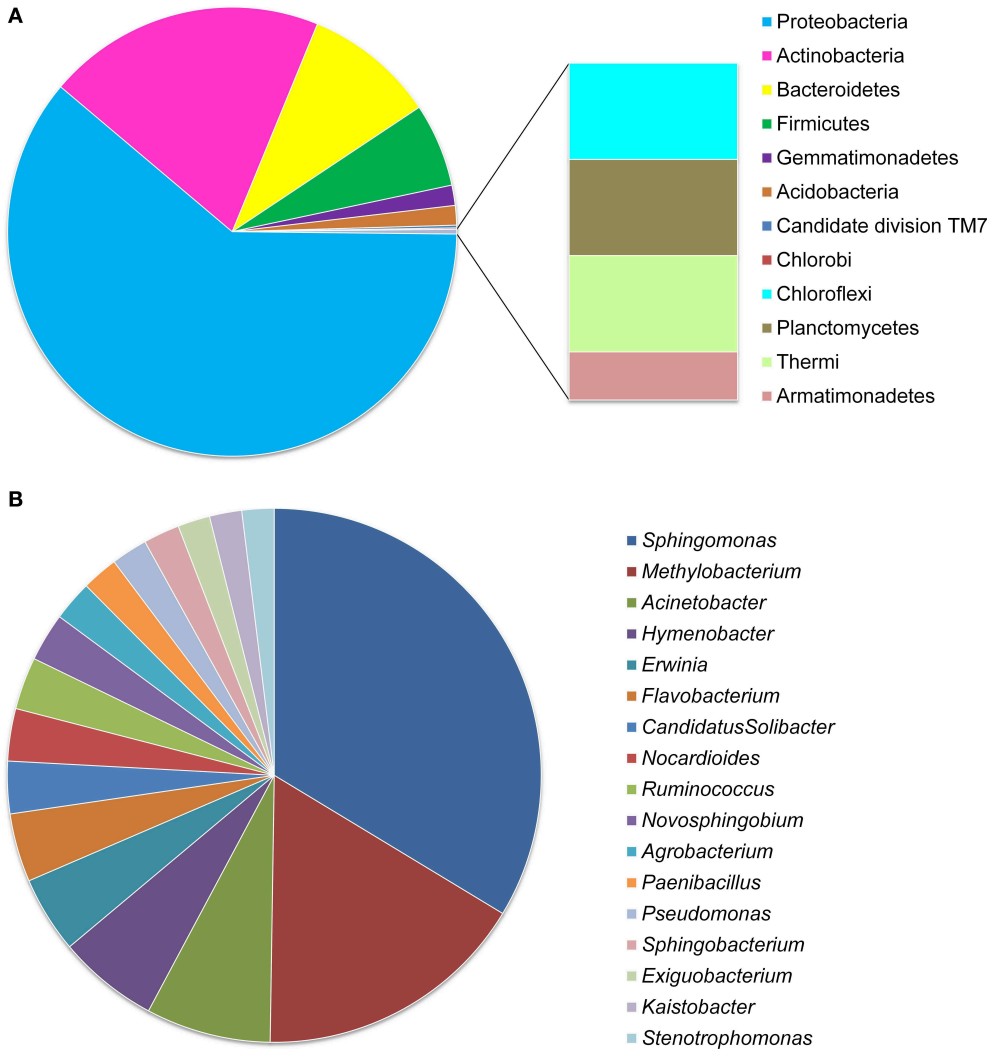

FIGURE 1 | OTU distribution of *Stevia* leaf endophytic bacteria at phylum (A) and genus (B) levels. Data were obtained from all the five samples of the two treatments and three growth stages.

At the genus level, only 813 (37.6%) OTUs were identified into 187 taxa (**Figure 1B**, **Supplementary Figure S2**), including *Sphingomonas* (16.97% for OTUs and 36.77% for reads) and *Methylobacterium* (8.36% for OTUs and 11.62% for reads) as the most abundant ones, followed by the genera *Acinetobacter* (3.81% for OTUs), *Hymenobacter* (3.08%), *Pseudomonas* (2.58%), *Erwinia* (2.34%), *Flavobacterium* (1.60%), *Nocardioides* (1.60%), and *Paenibacillus* (1.11%) etc.; while each of the other genera occupied <1.25% of the reads (**Figure 1B**, **Supplementary Figure S2** and **Supplementary Table S3**).

Variation of Endophytic Bacterial Communities along Growth Stage

The variation of community composition in leaf endophytes was estimated at the levels of OTU (**Supplementary Figure S3**), phylum, and genus (**Figure 2A**, **Supplementary Figure S2**). Among the 1700 OTUs, only 96 (5.65%) were found in all the three growth stages (samples C-0, C-2, and C-4) (**Supplementary Figure S3**), which comprised 71.61% of the total pyrosequencing reads and formed the core microbiome of the leaf endophytes for *Stevia*. Among the core microbiome, Proteobacteria (85.72%), and Actinobacteria (13.77%) are the dominant groups, followed by Bacteroidetes, Acidobacteria, and Firmicutes, which occupied less than 0.20% of the reads (**Figure 3**, **Supplementary Table S4**). Furthermore, 43 genera, dominated by *Sphingomonas*, *Methylobacterium, Acinetobacter, Bacillus*, *Nocardioides,* and *Pseudomonas,* were found in the core microbiome (**Supplementary Table S3**). Similar core microbiome was also found in the fulvic acid treatments (F-2 and F-4).

The change of relative abundance for each of the phyla, especially the six principle ones mentioned above was obvious in the three growth stages (**Figure 3**). Many of the stage specific OTUs were found as rare and high diverse sequences. The C-0, C-2, and C-4 samples harbored 337 (19.82%), 499 (29.35%), and 467 (27.47%) unique OTUs,

FIGURE 2 | Relative abundance of bacterial phyla (A) and families (B, taxa represented occurred at >1% abundance in at least one sample) associated with *Stevia* leaves as determined from pyrosequencing. Percentages represent the portion of 16S rRNA gene 454 reads which were classified to that phylum and family.

respectively (**Supplementary Figure S3**). These unique fractions comprised a major proportion (76.65%) of OTUs, but merely proportion (14.70%) of the reads. The stage specific OTUs were dominated by the Proteobacteria (5.3%), Actinobacteria (2.0%), Bacteroidetes (1.3%), and Firmicutes (1.0%), in which the proportions of Bacteroidetes and Firmicutes were much higher than those in the common OTUs (**Figure 3**). Candidate division TM7, Planctomycetes, Chlorobi, Chloroflexi, and Gemmatimonadetes were specifically presented in the unique OTUs and the high variety of stage specific OTUs lead to the differences among the community structure of endophytic bacteria in various growth stages.

At the family level, different trends of species abundance were observed in the three growth stages (**Figure 2B**, **Supplementary Table S2**). Enterobacteriaceae (18.43%) was the most abundant family followed by Rhizobiaceae (17.46%), Sphingomonadaceae (10.52%), Micrococcaceae (8.92%), and Methylobacteriaceae (6.01%) in sample C-0. In the sample C-2, Methylobacteriaceae (27.68%) and Sphingomonadaceae (22.67%) were the dominant families; while in the sample C-4, the most abundant families were Sphingomonadaceae (53.20%), followed by Methylobacteriaceae (18.04%). The relative abundance of different families varied from stage to stage. The dominated taxa shifted dynamically along the growth stage: the relative abundance of Enterobacteriaceae and Rhizobiaceae fell from 18.43 and 17.46% in C-0 to 4.3 and 1.6% in C-4, respectively. On the other hand, the abundance of Sphingomonadaceae showed a substantial increase from 10.5% at seedling stage to 22.7% at the vegetable stage, and then to 53.2% at flowering stage. Compared to the samples of C-2 and

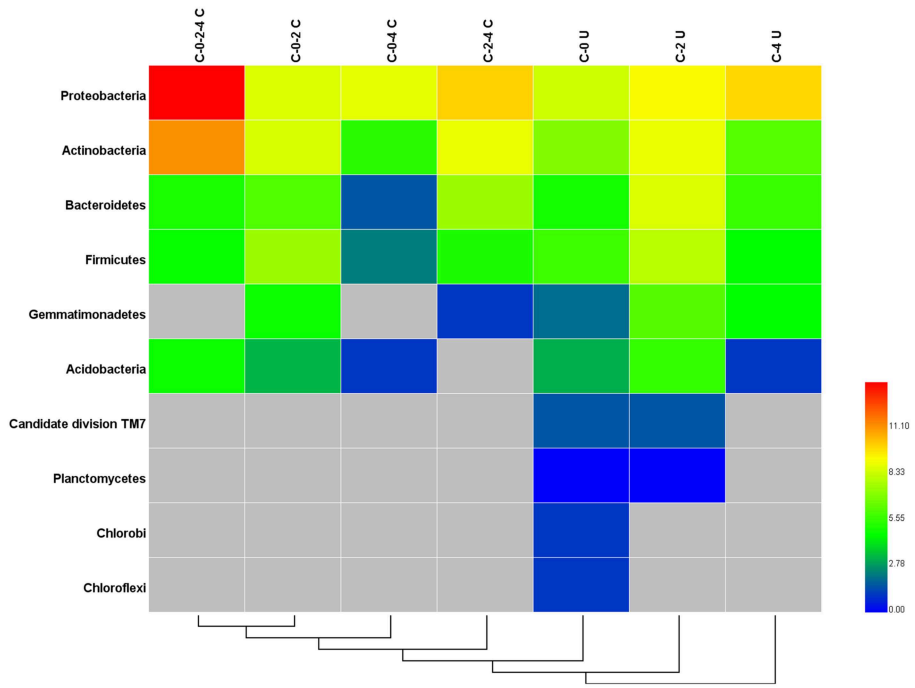

FIGURE 3 | Heatmap of the shared and unique phyla in *Stevia* leaf samples at different growth stages. C-0-2-4 C: common phyla for stages C-0, C-2, and C-4; C-0-2 C: common phyla for stages; C-0-4 C: common phyla for stages C-0 and C-4; C-2-4 C: common phyla for stages C-2 and C-4; C-0 U: unique phyla for stage C-0; C-2 U: unique phyla for stage C-2; C-4 U: unique phyla for stage C-4.

C-4, Micrococcaceae was much more enriched in the C-0 sample and the relative abundance reached to 8.92% of the reads while the average abundance in the other two samples was <1%. Overall, the taxonomic distribution of leaf endophytes in C-0 was much more scattered than those in C-2 and C-4. In other words, the community composition of endophytes in mature leaves was more centralized and the two most abundant families comprised over 50 and 70% reads in C-2 and C-4, respectively.

The community composition at the genus level was consistent to that at the family level (**Supplementary Figure S2**). Many of the identified genera, like *Actinomadura* in the seedling stage (C-0), *Agromyces* in the vegetable stage (C-2), *Hyphomonas* in the initial of flowering stage (C-4), were recorded.

Effects of Fulvic Acid on Production and Endophytic Communities of *Stevia*

In this study, the final dry weight of *Stevia* leaves was significantly increased (26.2%, $P < 0.05$) in the fulvic acid treatment (2801.2 kg ha^{-1}) compared with that of the control (2219.5 kg ha^{-1}). Similar effects were also detected in the plant height, *UGT* gene expression and contents of RA and ST in the FA treatment (**Table 1**, **Supplementary Figure S4**). Corresponding to the increases in leaf biomass and plant height, the community composition of the leaf endophytes was also dramatically modified by the FA treatment. The data of OTU numbers and indices of Chao1, ACE and Shanon (**Table 1**) showed a clear decrease in diversity of endophytes. The shifting in community composition caused by the FA treatment can be observed from **Figure 2** (**Supplementary Tables S1**, **S2**). FA treatment reduced the abundances of Sphingomonadaceae, Microbacteriaceae, Comamonadaceae, Nocardiodaceae, but increased the abundances of Methylobacteriaceae, Psuedomonadaceae, Enterobacteriaceae, and Xanthomonadaceae in the vegetable growth stage. In the initial flowering stage, the abundances of Sphingomonadaceae and Kineosporiaceae were increased; companying with the decrease in abundances of Methylobacteriaceae, Aurantimonadaceae, and Psuedomonadaceae. These effects can also be found at the genus level, such as presence of *Aerococcus* and absence of *Aquicella* in the FA treatment (**Supplementary Table S3**).

PCoA/CCA Analysis of Endophytic Communities

The PCA analysis revealed that the growth stage was a strong interpretive factor for the variation in community composition of the leaf endophytes (**Figure 4A**). The first principal coordinate separated the samples based on the growth stage, the seedling stage clearly separated from the other growth stages along PC1 which showed an obvious difference among the samples. Samples at the same growth stage with or without FA treatment (C-2/F-2, C-4/F-4) were separated from each other, and the FA treated samples formed a close cluster, indicating that the FA treatment was also a factor to shape the community composition.

The relevance of the OTUs for community composition was better explained through the networks (**Figure 5**), which was characterized by edges linking the OTUs (shown in yellow) with the corresponding samples (shown in red). The distribution

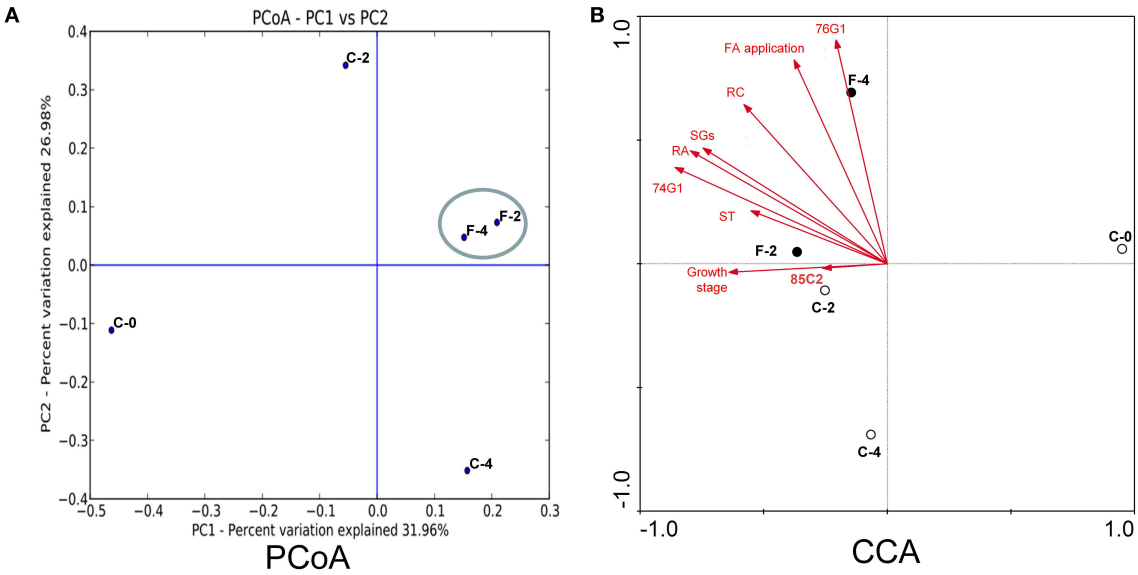

FIGURE 4 | PCoA (A) and CCA (B) analysis of the endophytic samples in *Stevia* leaves with different growth stages with or without FA treatment.

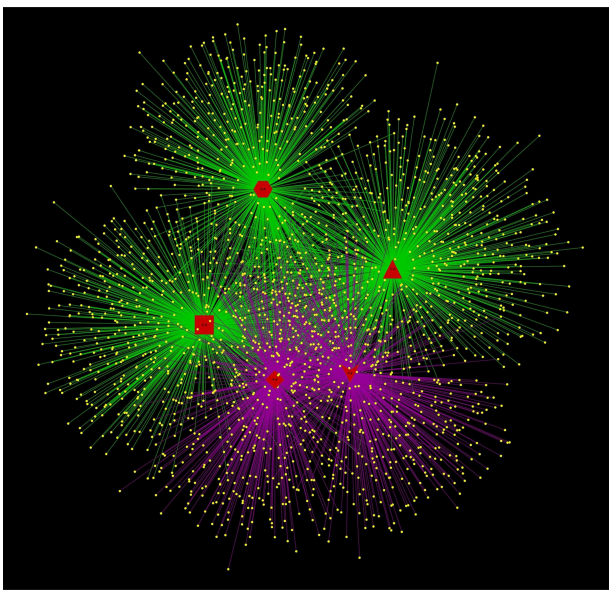

FIGURE 5 | Networks representing sample/OTU interaction. OTU nodes are yellow, with edges indicated according to FA treatment (purple: with FA treatment; green: without FA treatment). Sample nodes are shown in red color with different shapes according to growth time and FA treatment (Hexagon, C-0; Triangle, C-2; Rect, C-4; Vee, F-2; diamond, F-4).

of sample nodes in the networks highlighted the separation according to growth stage and FA treatment. The samples treated by FA were clustered closer and shared more common OTUs than the controls, proving again that the FA treatment was highly involved in shaping the endophytic bacterial communities in *Stevia* leaves.

The relationship between leaf endophyte community structure and biotic/abiotic factors (steviol glycosides content, growth stage, *UGT* gene expression, and FA application) was revealed by the canonical correspondence analysis (**Figure 4B**). The first two CCA axes explained as high as 57.0 and 28.3% of the total variance in the bacterial community data, and significant species–environment correlations were observed, indicating that the CCA result was reliable. According to CCA analysis, the *UGT74G1* gene expression, contents of RA and SGs were best correlated with axis 1 ($r = -0.8588, -0.7963, -0.7461$, respectively), while *UGT76G1* gene expression and FA application were best correlated with axis 2 ($r = 0.9057, 0.8238$, respectively).

Relationship between the Core Community and Plant Performances

To construct a core bacterial community of *Stevia* leaf endophytes, we pooled the 10 most abundant genera in each of the five samples (C-0, C-2, C-4, F-2, F-4), resulting in 20 genera altogether (**Supplementary Table S5**). Although it was a small portion compared to the entire community, the core community constituted 55.6% of the total sequences. Overall, *Sphingomonas* (45.7%) and *Methylobacterium* (17.9%) were the most abundant genera (**Figure 6**).

The correlation analysis between the relative abundance of the 20 genera constituting the core community and the plant performances (**Table 2**) showed that the relative abundances of *Sphingomonas* and *Salinibacterium* were positively correlated with ST content and plant height at the $r > 0.8$ ($P < 0.05$) level. The genera *Methylobacterium* and *Acinetobacter* were positively correlated with *UGT74G1* and *76G1* gene expression, respectively, while *Agrobacterium* and *Erwinia* were negatively correlated with *UGT74G1* gene expression. Moreover, as growth stage of *Stevia* extended, there were remarkable increases of the relative abundances for positively correlated taxa while the negatively correlated taxa had a sharply decrease. The relative abundance of *Sphingomonas* increased from 7.2 to 47.3% during

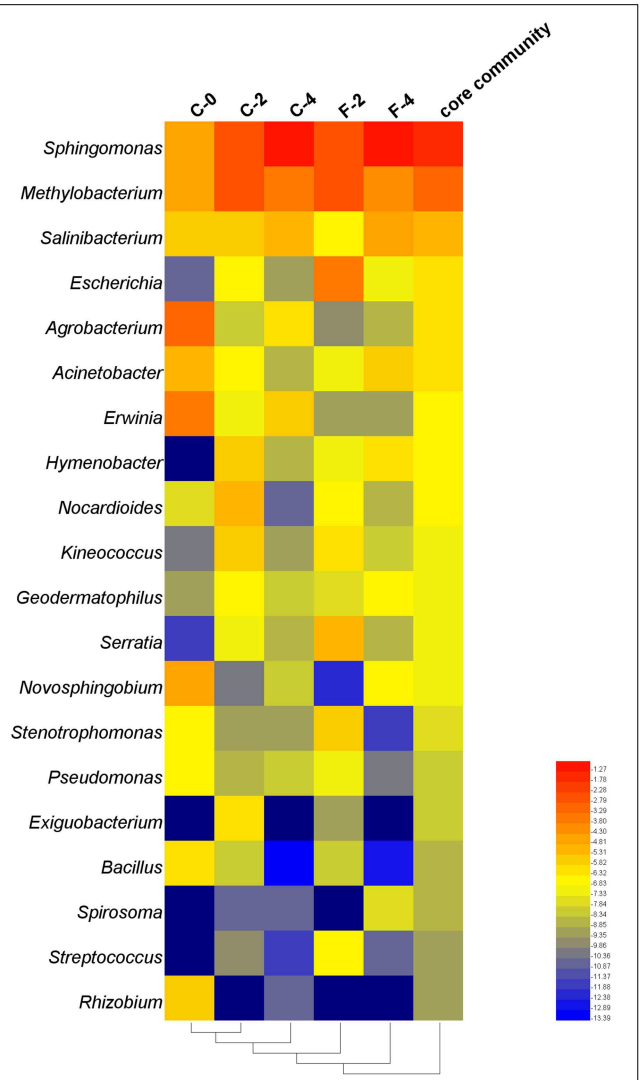

FIGURE 6 | Heatmap of taxonomic distribution of the core community of the endophytic samples in *Stevia* leaves with different growth time at the genus level.

4 months of growth which was 5.6 times greater compared to the seedling stage. On the other hand, the relative abundance of *Bacillus* (negatively correlated taxa) decreased from 1.44 to 0.01% during 4 months of growth. Interestingly, FA treatment could strengthen the trend of these changes. At the flowering stage, the relative abundance of *Sphingomonas* was up to 54.4% in F-4 which increased by 15.0% compared to C-4 sample, while the potential plant pathogens (*Erwinia* and *Agrobacterium*) had a clearly decrease.

Discussion

The present study is the first investigation on the diversity and community composition of endophytic bacteria associated with *S. Rebaudiana.* Comparing with the previous study on leaf endophytes of tomato (Romero et al., 2014), the diversity of the endophytic bacteria in *Stevia* leaves was greater, since the rarefaction curve was saturated at 80 OTUs for endophytic bacteria of tomato, while 595–825 OTUs were detected in the *Stevia* endophytes. This great number of OTUs revealed in the present study also was a little surprise considering the low abundance of endophytic bacteria in leaves (10^3–10^5 CFU g^{-1} of fresh leaf for rice, Ferrando et al., 2012) or the low frequencies of isolation 1.6–13.6% for *Trichilia elegans* (Rhoden et al., 2015). The great diversity of endophytic bacteria implied that the leaves of *Stevia* may present a habitat more adequate for the bacteria than those of other plants.

This study revealed that the endophytic bacteria in the *Stevia* leaves were super-dominated by Proteobacteria, followed by Actinobacteria, Bacteroides, Firmicutes, Gemmatemonadetes, and Acidobacteria etc. (**Figures 1**, **2**). This community structure was typical for the phyllosphere of tomato, soybean, clover, *Arabidopsis thaliana*, and *Citrus sinesis* (Yang et al., 2001; Delmotte et al., 2009; Vorholt, 2012; Bodenhausen et al., 2013; Romero et al., 2014), suggesting a common overlay in the key community members at phylum level across host plants. However, the bacterial communities in *Stevia* leaves showed its own specificity compared to other host plants. Gammaproteobacteria was the most abundant class in both the potato and *Arabidopsis thaliana* plants (Berg et al., 2005; Bodenhausen et al., 2013), but Alphaproteobacteria was the most abundant class in the *S. rebaudiana* leaves. Furthermore, the most abundant genera in *Stevia* leaves were *Sphingomonas, Methylobacterium,* and *Acinetobacter* etc. (**Supplementary Figure S2**); but *Massilia* and *Flavobacterium* were prevalent in *Arabidopsis thaliana* (Bodenhausen et al., 2013) and *Bacillus, Stenotrophomonas,* and *Acinetobacter* etc. were dominant in tomato leaves (Romero et al., 2014). The heavily populated taxon of Candidate division TM7 from tree leaves (Redford et al., 2010) was <0.5% in our samples; and no sequences corresponding to *Pantoea* was observed, which was abundant in the lettuce phyllosphere (Rastogi et al., 2012). On the other hand, the dominance of Enterobacteriaceae in seedling *Stevia* leaves was similar to that of the spinach phyllosphere (Lopez-Velasco et al., 2011) but was different from that in *Arabidopsis thaliana* (Bodenhausen et al., 2013). These variations between host species could be ascribed to the differences in plant characteristics (morphology, physiology, metabolic profile) (Whipps, 2001; Lopez-Velasco et al., 2011). Although some conditions were common for the phyllosphere, such as exposure to UV light, temperature fluctuations, and low nutrient availability (Delmotte et al., 2009), the accumulation of SGs made the *Stevia* leaves more selective for the endophytes, since SGs could be used by some bacteria (Kunova et al., 2014) and inhibit other bacteria (Gamboa and Chaves, 2012). Therefore, our results support the previous estimation that the host species strongly shaped the leaf endophytic community (Ding et al., 2013). As the first study about endophytic bacterial community in *Stevia* leaves, variations in the taxon composition and the proportions of the dominant taxa were observed due to the changes of growth stages. The dominance of Enterobacteriaceae and Rhizobiaceae in seedling leaves and Methylobacteriaceae and Sphingomonadaceae in mature leaves showed a highly dynamic

TABLE 2 | Correlation analysis of the core community and steviol glycoside content.

Genus	C-0	C-2	C-4	F-2	F-4	Plant height	Content of			Gene expression		
							ST	RC	SGs	76G1	85C2	74G1
	Relative abundance (%)					Pearson correlation coefficients*						
Sphingomonas	4.28	19.2	46.6	16.2	58.8	0.926	0.970					
Methylobacterium	4.74	16.5	9.89	20.3	6.92							0.917
Salinibacterium	2.48	2.39	3.34	1.16	4.02	0.883	0.925					
Escherichia	0.05	1.06	0.19	7.28	0.77						0.883	
Agrobacterium	12.4	0.33	1.32	0.12	0.30							−0.914
Acinetobacter	3.02	0.97	0.26	0.74	1.92					0.882		
Erwinia	7.28	0.63	2.00	0.18	0.19							−0.981
Hymenobacter	0.00	1.86	0.28	0.83	1.51							
Nocardioides	0.54	2.65	0.07	1.23	0.29							
Kineococcus	0.08	1.83	0.21	1.36	0.43							
Geodermatophilus	0.16	1.18	0.35	0.55	1.12							
Serratia	0.03	0.66	0.25	3.03	0.29							
Novosphingobium	3.57	0.08	0.41	0.02	0.96						0.968	
Stenotrophomonas	1.09	0.2	0.2	2.03	0.03							
Pseudomonas	1.17	0.29	0.31	0.82	0.09						0.907	
Exiguobacterium	0	1.59	0	0.16	0							
Bacillus	1.44	0.33	0.01	0.39	0.02	−0.990	−0.949	−0.960	−0.884			
Spirosoma	0	0.06	0.07	0	0.57							
Streptococcus	0	0.11	0.04	0.91	0.07						0.893	
Rhizobium	2.13	0	0.06	0	0							

**Only significant ($P < 0.05$) correlations with a Pearson correlation coefficient >0.600 or <−0.600 for the dependent variables are shown.*

influence on endophytic bacterial communities by plant growth stages. The increase of species richness and decrease of Shannon index in mature leaves (**Table 1**) also confirmed the great effects of growth stages. These changes might demonstrate that more bacterial species have been harbored, but the dominance of some taxa (*Sphingomonas, Methylobacterium*) was very high in the bacterial community of flowering plants (**Table 2**). Moreover, the results of principal coordinate analysis (**Figure 4**) also proved the huge influences of growth stages on the endophytic community. Previously, the variation of endophytic communities related to the plant growth stages have been explicated by temporal changes in abiotic conditions such as temperature, sun exposure, and soil fertilization (Wang et al., 2008a). Moreover, the changes in biotic factors during the plant growth, such as capability of nutrients, leaf size, and glycosides content may also cause the alternation of bacterial endophytes, since the colonization space of endophytes trended to increase as *Stevia* leaf expanding with longer growth time.

Previously, it has been estimated that some of the endophytic bacteria, such as *Sphingomonas* (Innerebner et al., 2011) and *Methylobacterium* (Ardanov et al., 2012), might have potential benefits on plant growth and health. Interestingly, both *Sphingomonas* and *Methylobacterium* were detected as increased and predominant groups in the leaf endophytic community along the growth of *Stevia*, which means they may contribute to the host some kind of benefits. Moreover, a clear decline of highly potential plant pathogens such as *Erwinia* (Toth et al., 2003) and *Agrobacterium* (Pitzschke and Hirt, 2010) was observed, indicating that the plant-endophyte communication trends to form a better relationship for plant health as *Stevia* grew stronger. This study is also the first one to report the regulation of leaf endophytic community structure by fulvic acid. As a plant growth regulator, FA treatment could accelerate the enrichment of beneficial bacteria and decline the potential phytopathogens (**Table 2**, **Figure 4**). The decrease of diversity index in the FA treatments (**Table 1**) was a result of enhanced predominance of some taxa by the application of fulvic acid, mainly the beneficial bacteria *Sphingomonas* and *Salinibacterium* etc. (**Table 2**). The decrease of *Erwinia* and *Agrobacterium* richness implied that FA treatment may decrease the infection of fire blight diseases and crown gall/hairy root diseases caused by these bacteria (Toth et al., 2003; Pitzschke and Hirt, 2010). This regulation by FA treatment might contribute to the establishment of a harmonious relationship between *Stevia* leaf and endophytic community, and then improve the yield and quality of *Stevia* leaves, such as enhancing the high sweetness and good taste RA content (**Table 1**).

The CCA results revealed strong correlation between some biotic/abiotic factors, (such as FA treatment and SGs contents) and the endophytic communities. These correlations further confirmed that both the plant (biotic) factors and the abiotic environmental factors could regulate the endophytic microbial community, and in turn the variations of plant endophytes might alter the plant performance as revealed in previous studies on

other plants such as *Potato* and *Arabidopsis thaliana* (Berg et al., 2005; Manter et al., 2010; Fernandes et al., 2012; Bodenhausen et al., 2013). The real meaning of the interactions among the FA treatment, the alternation of endophytic bacterial communities, and the plant growth/accumulation of SGs in leaves is still unclear and needs further research. To explain the effects of plant growth and FA treatment on the diversity of endophytic bacteria, the following aspects may be considered: the possible effects of some FA compounds or the metabolites of endophytes induced by the FA on the infection pathways and the establishment of mutualistic relationship (Azevedo et al., 2000); the effects of FA on the chemical and physical states of the wounds or stomata of leaves (Gough et al., 1997; Redford et al., 2010), as well as the stimulation for growth of some plant bacteria, similar to the root exudates for *Bacillus subtilis* (Bais et al., 2006; Rudrappa et al., 2007). The mutualistic relationship between endophytes and plant host suggested a promising potential system for promoting plant performance.

Conclusively, this study provided a general description of the diversity and community shift in the endophyte populations in *Stevia* leaves along the growth stages with/without plant regulator application for the first time. A huge phylogenetic diversity was observed through pyrosequencing technology. The genera *Sphingomonas* and *Methylobacterium* were found as the principal components of the core endophytic community in *Stevia* leaves and presented positive correlations with the stevioside content and *UGT74G1* gene expression. The *Stevia* growth stages could alter the endophytic bacterial community in the *Stevia* leaves, and the FA treatment could accelerate these variations, without changing the pattern of variations along growth period. A significant correlation between some certain species with specific biotic/abiotic factors was also demonstrated. These results demonstrated that the endophytes of *Stevia* leaves might represent a valuable resource for plant growth and steviol glycosides accumulation, and regulation of certain specific plant endophytes to promote plant growth and health might be a reliable option. Further studies on the interactions between the endophytes and plant host should be implemented.

Acknowledgments

This work was supported by the National High Technology Research and Development Program of China (No. 2011AA10A206). EW was supported by the project SIP 20140124 authorized by IPN.

Supplementary Material

The Supplementary Material for this article can be found online at: http://journal.frontiersin.org/article/10.3389/fmicb.2015.00867

Supplementary Figure S1 | The biosynthetic pathway of steviol glycosides.

Supplementary Figure S2 | Heatmap of taxonomic distribution in *Stevia* leaf samples at different growth stages at the genus level.

Supplementary Figure S3 | Distribution of the shared and unique OTUs in *Stevia* leaf samples at different growth stages (C-0; C-2; C-4). Numbers of sequenced reads were presented in parenthesis.

Supplementary Figure S4 | The expression of *UGT* genes relative to β-actin in both control group and FA treated leaves at different growth stages. Mean gene expression followed by an asterisk (*) is significant relative to control groups and normalized to β-actin gene ($P < 0.05$). Error bars represent SEM.

Supplementary Table S1 | Community structure of leaf endophytic bacteria at phylum level.

Supplementary Table S2 | Community structure of leaf endophytic bacteria at family level.

Supplementary Table S3 | Community structure of leaf endophytic bacteria at genus level.

Supplementary Table S4 | Distribution of the shared and unique OTUs (at phylum level) in *Stevia* leaf samples at different growth stages.

Supplementary Table S5 | Distribution of the core biome of endophytic bacteria (at genus level) in *Stevia* leaf samples at different growth stages.

References

Andersson, A. F., Lindberg, M., Jakobsson, H., Bäckhed, F., Nyrén, P., and Engstrand, L. (2008). Comparative analysis of human gut microbiota by barcoded pyrosequencing. *PLoS ONE* 3:e2836. doi: 10.1371/journal.pone.0002836

Ardanov, P., Sessitsch, A., Häggman, H., Kozyrovska, N., and Pirttilä, A. M. (2012). Methylobacterium-induced endophyte community changes correspond with protection of plants against pathogen attack. *PLoS ONE* 7:e46802. doi: 10.1371/journal.pone.0046802

Arturo, S.-A., Yumi, O., Fernandes, G. W., Ronald Aaron, B., and John, G. (2012). Relationships between endophyte diversity and leaf optical properties. *Trees* 26, 291–299. doi: 10.1007/s00468-011-0591-5

Azevedo, J., Maccheroni, W., Pereira, J., and de Araújo, W. L. (2000). Endophytic microorganisms: a review on insect control and recent advances on tropical plants. *Electron J. Biotechnol.* 3, 40–65. doi: 10.2225/vol3-issue1-fulltext-4

Bais, H. P., Weir, T. L., Perry, L. G., Gilroy, S., and Vivanco, J. M. (2006). The role of root exudates in rhizosphere interactions with plants and other organisms. *Annu. Rev. Plant Biol.* 57, 233–266. doi: 10.1146/annurev.arplant.57.032905.105159

Berg, G., Krechel, A., Ditz, M., Sikora, R. A., Ulrich, A., and Hallmann, J. (2005). Endophytic and ectophytic potato-associated bacterial communities differ in structure and antagonistic function against plant pathogenic fungi. *FEMS Microbiol. Ecol.* 51, 215–229. doi: 10.1016/j.femsec.2004.08.006

Bodenhausen, N., Horton, M. W., and Bergelson, J. (2013). Bacterial communities associated with the leaves and the roots of *Arabidopsis thaliana*. *PLoS ONE* 8:e56329. doi: 10.1371/journal.pone.0056329

Brandle, J. E., Richman, A., Swanson, A. K., and Chapman, B. P. (2002). Leaf ESTs from *Stevia rebaudiana*: a resource for gene discovery in diterpene synthesis. *Plant Mol. Biol.* 50, 613–622. doi: 10.1023/A:1019993221986

Caporaso, J., Lauber, C., Walters, W., Berg-Lyons, D., Lozupone, C., Turnbaugh, P., et al. (2011). Global patterns of 16S rRNA diversity at a depth of millions of sequences per sample. *Proc. Natl. Acad. Sci. U.S.A.* 108(Suppl. 1), 4516–4522. doi: 10.1073/pnas.1000080107

Chen, J., Hou, K., Qin, P., Liu, H., Yi, B., Yang, W., et al. (2014). RNA-Seq for gene identification and transcript profiling of three *Stevia rebaudiana* genotypes. *BMC Genomics* 15:571. doi: 10.1186/1471-2164-15-571

Delmotte, N., Knief, C., Chaffron, S., Innerebner, G., Roschitzki, B., Schlapbach, R., et al. (2009). Community proteogenomics reveals insights into the physiology

of phyllosphere bacteria. *Proc. Natl. Acad. Sci. U.S.A.* 106, 16428–16433. doi: 10.1073/pnas.0905240106

Ding, T., Palmer, M. W., and Melcher, U. (2013). Community terminal restriction fragment length polymorphisms reveal insights into the diversity and dynamics of leaf endophytic bacteria. *BMC Microbiol.* 13:1. doi: 10.1186/1471-2180-13-1

Elvira-Recuenco, M., and van Vuurde, J. W. (2000). Natural incidence of endophytic bacteria in pea cultivars under field conditions. *Can. J. Microbiol.* 46, 1036–1041. doi: 10.1139/w00-098

Fernandes, N., Steinberg, P., Rusch, D., Kjelleberg, S., and Thomas, T. (2012). Community structure and functional gene profile of bacteria on healthy and diseased thalli of the red seaweed *Delisea pulchra*. *PLoS ONE* 7:e50854. doi: 10.1371/journal.pone.0050854

Ferrando, L., Fernández Mañay, J., and Fernández Scavino, A. (2012). Molecular and culture-dependent analyses revealed similarities in the endophytic bacterial community composition of leaves from three rice (*Oryza sativa*) varieties. *FEMS Microbiol. Ecol.* 80, 696–708. doi: 10.1111/j.1574-6941.2012.01339.x

Gamboa, F., and Chaves, M. (2012). Antimicrobial potential of extracts from *Stevia rebaudiana* leaves against bacteria of importance in dental caries. *Acta Odontol. Latinoam.* 25, 171–175.

Gao, T. G., Jiang, F., Yang, J. S., Li, B. Z., and Yuan, H. L. (2012). Biodegradation of Leonardite by an alkali-producing bacterial community and characterization of the degraded products. *Appl. Microbiol. Biotechnol.* 93, 2581–2590. doi: 10.1007/s00253-011-3669-5

Gough, C., Galera, C., Vasse, J., Webster, G., Cocking, E. C., and Dénarié, J. (1997). Specific flavonoids promote intercellular root colonization of *Arabidopsis thaliana* by *Azorhizobium caulinodans* ORS571. *Mol. Plant Microbe Interact.* 10, 560–570. doi: 10.1094/MPMI.1997.10.5.560

Hallmann, J., QuadtHallmann, A., Mahaffee, W. F., and Kloepper, J. W. (1997). Bacterial endophytes in agricultural crops. *Can. J. Microbiol.* 43, 895–914. doi: 10.1139/m97-131

Hunter, P. J., Hand, P., Pink, D., Whipps, J. M., and Bending, G. D. (2010). Both leaf properties and microbe-microbe interactions influence within-species variation in bacterial population diversity and structure in the lettuce (*Lactuca Species*) phyllosphere. *Appl. Environ. Microbiol.* 76, 8117–8125. doi: 10.1128/AEM.01321-10

Innerebner, G., Knief, C., and Vorholt, J. A. (2011). Protection of *Arabidopsis thaliana* against leaf-pathogenic *Pseudomonas syringae* by *Sphingomonas* strains in a controlled model system. *Appl. Environ. Microbiol.* 77, 3202–3210. doi: 10.1128/AEM.00133-11

Kolb, N., Herrera, J. L., Ferreyra, D. J., and Uliana, R. F. (2001). Analysis of sweet diterpene glycosides from *Stevia rebaudiana*: improved HPLC method. *J. Agric. Food Chem.* 49, 4538–4541. doi: 10.1021/jf010475p

Kumar, H., Kaul, K., Bajpai-Gupta, S., Kaul, V. K., and Kumar, S. (2012). A comprehensive analysis of fifteen genes of steviol glycosides biosynthesis pathway in *Stevia rebaudiana* (Bertoni). *Gene* 492, 276–284. doi: 10.1016/j.gene.2011.10.015

Kunová, G., Rada, V., Vidaillac, A., and Lisova, I. (2014). Utilisation of steviol glycosides from *Stevia rebaudiana* (Bertoni) by Lactobacilli and Bifidobacteria in *in vitro* conditions. *Folia Microbiol. (Praha)* 59, 251–255. doi: 10.1007/s12223-013-0291-1

Lopez-Velasco, G., Welbaum, G. E., Boyer, R. R., Mane, S. P., and Ponder, M. A. (2011). Changes in spinach phylloepiphytic bacteria communities following minimal processing and refrigerated storage described using pyrosequencing of 16S rRNA amplicons. *J. Appl. Microbiol.* 110, 1203–1214. doi: 10.1111/j.1365-2672.2011.04969.x

Lucero, M., Unc, A., Cooke, P., Dowd, S., and Sun, S. (2011). Endophyte microbiome diversity in micropropagated *Atriplex canescens* and *Atriplex torreyi* var griffithsii. *PLoS ONE* 6:e17693. doi: 10.1371/journal.pone.0017693

Luczkiewicz, M., Kokotkiewicz, A., and Glod, D. (2014). Plant growth regulators affect biosynthesis and accumulation profile of isoflavone phytoestrogens in high-productive *in vitro* cultures of *Genista tinctoria*. *Plant Cell Tissue Organ Cult.* 118, 419–429. doi: 10.1007/s11240-014-0494-4

Madhav, H., Bhasker, S., and Chinnamma, M. (2013). Functional and structural variation of uridine diphosphate glycosyltransferase (UGT) gene of *Stevia rebaudiana*-UGTSr involved in the synthesis of rebaudioside A. *Plant Physiol. Biochem.* 63, 245–253. doi: 10.1016/j.plaphy.2012.11.029

Manter, D., Delgado, J., Holm, D., and Stong, R. (2010). Pyrosequencing reveals a highly diverse and cultivar-specific bacterial endophyte community in potato roots. *Microb. Ecol.* 60, 157–166. doi: 10.1007/s00248-010-9658-x

Meyer, K., and Leveau, J. (2012). Microbiology of the phyllosphere: a playground for testing ecological concepts. *Oecologia* 168, 621–629. doi: 10.1007/s00442-011-2138-2

Mohamed, A. A., Ceunen, S., Geuns, J., van den Ende, W., and De Ley, M. (2011). UDP-dependent glycosyltransferases involved in the biosynthesis of steviol glycosides. *J. Plant Physiol.* 168, 1136–1141. doi: 10.1016/j.jplph.2011.01.030

Moraes, R. M., Donega, M. A., Cantrell, C. L., Mello, S. C., and McChesney, J. D. (2013). Effect of harvest timing on leaf production and yield of diterpene glycosides in *Stevia rebaudiana* Bert: a specialty perennial crop for Mississippi. *Ind. Crops Prod.* 51, 385–389. doi: 10.1016/j.indcrop.2013.09.025

Nardi, S., Pizzeghello, D., Muscolo, A., and vianello, A. (2002). Physiological effects of humic substances on higher plants. *Soil Biol. Biochem.* 34, 1527–1536. doi: 10.1016/S0038-0717(02)00174-8

Pedraza, R. O., Bellone, C. H., de Bellone, S., Sorte, P. M. B., and Teixeira, K. R. D. (2009). Azospirillum inoculation and nitrogen fertilization effect on grain yield and on the diversity of endophytic bacteria in the phyllosphere of rice rainfed crop. *Eur. J. Soil Biol.* 45, 36–43. doi: 10.1016/j.ejsobi.2008.09.007

Pitzschke, A., and Hirt, H. (2010). New insights into an old story: *Agrobacterium*-induced tumour formation in plants by plant transformation. *EMBO J.* 29, 1021–1032. doi: 10.1038/emboj.2010.8

Quince, C., Lanzen, A., Davenport, R. J., and Turnbaugh, P. J. (2011). Removing noise from pyrosequenced amplicons. *BMC Bioinformatics* 12:38. doi: 10.1186/1471-2105-12-38

Rastogi, G., Sbodio, A., Tech, J. J., Suslow, T. V., Coaker, G. L., and Leveau, J. H. (2012). Leaf microbiota in an agroecosystem: spatiotemporal variation in bacterial community composition on field-grown lettuce. *ISME J.* 6, 1812–1822. doi: 10.1038/ismej.2012.32

Redford, A. J., Bowers, R. M., Knight, R., Linhart, Y., and Fierer, N. (2010). The ecology of the phyllosphere: geographic and phylogenetic variability in the distribution of bacteria on tree leaves. *Environ. Microbiol.* 12, 2885–2893. doi: 10.1111/j.1462-2920.2010.02258.x

Ren, G., Liu, X, and Shi, Y. (2011). Effects of plant growth regulator S-Y on diurnal changes in photosynthetic parameters and yield of *Stevia rebaudina* Bertoni. *Energy Proc.* 5, 429–434. doi: 10.1016/j.egypro.2011.03.074

Rhoden, S. A., Garcia, A., Santos e Silva, M. C., Azevedo, J. L., and Pamphile, J. A. (2015). Phylogenetic analysis of endophytic bacterial isolates from leaves of the medicinal plant *Trichilia elegans* A. Juss. (Meliaceae). *Genet. Mol. Res.* 14, 1515–1525. doi: 10.4238/2015.February.20.7

Rodriguez, R. J., White, J. F. Jr., Arnold, A. E., and Redman, R. S. (2009). Fungal endophytes: diversity and functional roles. *New Phytol.* 182, 314–330. doi: 10.1111/j.1469-8137.2009.02773.x

Romero, F. M., Marina, M., and Pieckenstain, F. L. (2014). The communities of tomato (*Solanum lycopersicum* L.) leaf endophytic bacteria, analyzed by 16S-ribosomal RNA gene pyrosequencing. *FEMS Microbiol. Lett.* 351, 187–194. doi: 10.1111/1574-6968.12377

Rudrappa, T., Quinn, W. J., Stanley-Wall, N. R., and Bais, H. P. (2007). A degradation product of the salicylic acid pathway triggers oxidative stress resulting in down-regulation of *Bacillus subtilis* biofilm formation on *Arabidopsis thaliana* roots. *Planta* 226, 283–297. doi: 10.1007/s00425-007-0480-8

Ryan, R. P., Germaine, K., Franks, A., Ryan, D. J., and Dowling, D. N. (2008). Bacterial endophytes: recent developments and applications. *FEMS Microbiol. Lett.* 278, 1–9. doi: 10.1111/j.1574-6968.2007.00918.x

Serfaty, M., Ibdah, M., Fischer, R., Chaimovitsh, D., Saranga, Y., and Dudai, N. (2013). Dynamics of yield components and stevioside production in *Stevia rebaudiana* grown under different planting times, plant stands and harvest regime. *Ind. Crops Prod.* 50, 731–736. doi: 10.1016/j.indcrop.2013.08.063

Strobel, G., Daisy, B., Castillo, U., and Harper, J. (2004). Natural products from endophytic microorganisms. *J. Nat. Prod.* 67, 257–268. doi: 10.1021/np030397v

Sturz, A. V., Christie, B. R., and Nowak, J. (2000). Bacterial endophytes: potential role in developing sustainable systems of crop production. *Crit. Rev. Plant Sci.* 19, 1–30. doi: 10.1016/S0735-2689(01)80001-0

Toth, I. K., Bell, K. S., Holeva, M. C., and Birch, P. R. J. (2003). Soft rot erwiniae: from genes to genomes. *Mol. Plant Pathol.* 4, 17–30. doi: 10.1046/j.1364-3703.2003.00149.x

van Overbeek, L., and van Elsas, J. D. (2008). Effects of plant genotype and growth stage on the structure of bacterial communities associated with potato (*Solanum tuberosum* L.). *FEMS Microbiol. Ecol.* 64, 283–296. doi: 10.1111/j.1574-6941.2008.00469.x

Vorholt, J. (2012). Microbial life in the phyllosphere. *Nat. Rev. Microbiol.* 10, 828–840. doi: 10.1038/nrmicro2910

Wang, G., Xu, Y., Jin, J., Liu, J., Zhang, Q., and Liu, X. (2008a). Effect of soil type and soybean genotype on fungal community in soybean rhizosphere during reproductive growth stages. *Plant Soil* 317, 135–144. doi: 10.1007/s11104-008-9794-y

Wang, H. X., Geng, Z. L., Zeng, Y., and Shen, Y. M. (2008b). Enriching plant microbiota for a metagenomic library construction. *Environ. Microbiol.* 10, 2684–2691. doi: 10.1111/j.1462-2920.2008.01689.x

Whipps, J. M. (2001). Microbial interactions and biocontrol in the rhizosphere. *J. Exp. Bot.* 52, 487–511. doi: 10.1093/jexbot/52.suppl_1.487

Yadav, A. K., Singh, S., Dhyani, D., and Ahuja, P. S. (2011). A review on the improvement of stevia [*Stevia rebaudiana* (Bertoni)]. *Can. J. Plant Sci.* 91, 1–27. doi: 10.4141/cjps10086

Yan, L., Liu, X., and Shi, Y. (2012). "Effect of different mixed fertilizers on the growth and development in *Stevia rebaudiana* Bertoni," in *Proceedings of the 2012 International Conference on Biomedical Engineering and Biotechnology*, (Macau: IEEE Computer Society), 198–201. doi: 10.1109/iCBEB.2012.478

Yang, C. H., Crowley, D. E., Borneman, J., and Keen, N. T. (2001). Microbial phyllosphere populations are more complex than previously realized. *Proc. Natl. Acad. Sci. U.S.A.* 98, 3889–3894. doi: 10.1073/pnas.051633898

Yang, J., Liu, X., and Shi, Y. (2013). Effect of different mixed fertilizer on yield, quality and economic benefits in *Stevia rebaudiana Bertoni*. *Adv. J. Food Sci. Technol.* 5, 588–591.

Zimmerman, N., and Vitousek, P. (2012). Fungal endophyte communities reflect environmental structuring across a Hawaiian landscape. *Proc. Natl. Acad. Sci. U.S.A.* 109, 13022–13027. doi: 10.1073/pnas.1209872109

Conflict of Interest Statement: The authors declare that the research was conducted in the absence of any commercial or financial relationships that could be construed as a potential conflict of interest.

frontiers in MICROBIOLOGY

ORIGINAL RESEARCH ARTICLE
published: 20 February 2015
doi: 10.3389/fmicb.2015.00136

Elevated atmospheric CO_2 levels affect community structure of rice root-associated bacteria

Takashi Okubo[1,2], Dongyan Liu[3], Hirohito Tsurumaru[2], Seishi Ikeda[4], Susumu Asakawa[3], Takeshi Tokida[5], Kanako Tago[1], Masahito Hayatsu[1], Naohiro Aoki[6], Ken Ishimaru[7], Kazuhiro Ujiie[7], Yasuhiro Usui[8], Hirofumi Nakamura[9], Hidemitsu Sakai[8], Kentaro Hayashi[5], Toshihiro Hasegawa[8] and Kiwamu Minamisawa[2]*

[1] Environmental Biofunction Division, National Institute for Agro-Environmental Sciences, Tsukuba, Japan
[2] Department of Environmental Life Sciences, Graduate School of Life Sciences, Tohoku University, Sendai, Japan
[3] Division of Bioresource Functions, Graduate School of Bioagricultural Sciences, Nagoya University, Nagoya, Japan
[4] Large-scale Farming Research Division, Hokkaido Agricultural Research Center, National Agriculture and Food Research Organization, Hokkaido, Japan
[5] Carbon and Nutrient Cycles Division, National Institute for Agro-Environmental Sciences, Tsukuba, Japan
[6] Department of Agricultural and Environmental Biology, Graduate School of Agricultural and Life Sciences, The University of Tokyo, Tokyo, Japan
[7] Division of Plant Sciences, National Institute of Agrobiological Sciences, Tsukuba, Japan
[8] Agro-Meteorology Division, National Institute for Agro-Environmental Sciences, Tsukuba, Japan
[9] Taiyo-Keiki Co., Ltd., Tokyo, Japan

Edited by:
Mysore V. Tejesvi, University of Oulu, Finland

Reviewed by:
Yusuke Saijo, Max Planck Institute for Plant Breeding Research, Germany
Hossein Borhan, Agriculture and Agri-Food Canada, Canada

***Correspondence:**
Kiwamu Minamisawa, Department of Environmental Life Sciences, Graduate School of Life Sciences, Tohoku University, Katahira 2-1-1, Aoba-ku, Sendai, Miyagi 980-8577, Japan
e-mail: kiwamu@ige.tohoku.ac.jp

A number of studies have shown that elevated atmospheric CO_2 ($[CO_2]$) affects rice yields and grain quality. However, the responses of root-associated bacteria to $[CO_2]$ elevation have not been characterized in a large-scale field study. We conducted a free-air CO_2 enrichment (FACE) experiment (ambient + 200 μmol.mol^{-1}) using three rice cultivars (Akita 63, Takanari, and Koshihikari) and two experimental lines of Koshihikari [chromosome segment substitution and near-isogenic lines (NILs)] to determine the effects of $[CO_2]$ elevation on the community structure of rice root-associated bacteria. Microbial DNA was extracted from rice roots at the panicle formation stage and analyzed by pyrosequencing the bacterial 16S rRNA gene to characterize the members of the bacterial community. Principal coordinate analysis of a weighted UniFrac distance matrix revealed that the community structure was clearly affected by elevated $[CO_2]$. The predominant community members at class level were Alpha-, Beta-, and Gamma-proteobacteria in the control (ambient) and FACE plots. The relative abundance of Methylocystaceae, the major methane-oxidizing bacteria in rice roots, tended to decrease with increasing $[CO_2]$ levels. Quantitative PCR revealed a decreased copy number of the methane monooxygenase (*pmoA*) gene and increased methyl coenzyme M reductase (*mcrA*) in elevated $[CO_2]$. These results suggest elevated $[CO_2]$ suppresses methane oxidation and promotes methanogenesis in rice roots; this process affects the carbon cycle in rice paddy fields.

Keywords: rice, root, 16S rRNA gene, FACE, methane

INTRODUCTION

Atmospheric concentration of carbon dioxide, ($[CO_2]$), is expected to continue to rise during the next several decades (Fisher et al., 2007). Many studies have been conducted to understand the effects of elevated $[CO_2]$ on rice (e.g., yield and grain quality; Hasegawa et al., 2013; Usui et al., 2014) and on the paddy field ecosystem (e.g., methane emission; Tokida et al., 2010, 2011) using free-air $[CO_2]$ enrichment (FACE). Understanding the bacterial response to increased $[CO_2]$ is necessary to predict its effects on the rice and paddy ecosystem because rice-associated bacteria produce plant hormones, fix nitrogen, and oxidize methane (Bao et al., 2014; Ikeda et al., 2014). The relative abundances and activities of these bacteria are affected by field management (Bao et al., 2013, 2014; Ikeda et al., 2014), rice genotype (Sasaki et al., 2013; Okubo et al., 2014a), and growth stage (Okubo et al., 2014b).

It has been reported that elevated $[CO_2]$ levels affect the community structures and/or abundances of microorganisms in rhizosphere of grassland (Hayden et al., 2012), cropland (Schortemeyer et al., 1996), and marsh (Lee et al., in press). Since $[CO_2]$ in soil is much higher than in the atmosphere, it is likely that these changes were indirectly induced by elevated $[CO_2]$ through increased root growth and changes of the quality and quantity of root exudates (Drigo et al., 2008). Elevated $[CO_2]$ significantly increases root biomass and total organic carbon in rice root exudates (Bhattacharyya et al., 2013), which may influence the activity of rhizospheric and root-associated bacteria. We

Abbreviations: AMBI, ambient levels of CO_2; CSSL, chromosome segment substitution line; FACE, free-air CO_2 enrichment; NIL, near-isogenic line; OUT, operational taxonomic unit; PCoA, principal coordinates analysis; $[CO_2]$, atmospheric CO_2 concentration.

previously reported that the bacterial community associated with roots and shoots of Koshihikari (a widely planted rice cultivar in Japan) might be affected by increasing [CO_2] (Okubo et al., 2014b; Ikeda et al., in press). However, we could not draw strong conclusions at the time due to limited sample size. Meanwhile, many other studies have shown that the effects of [CO_2] elevation on rice yield and grain quality differ between cultivars (Hasegawa et al., 2013; Myers et al., 2014; Usui et al., 2014), suggesting that the response of rice-associated bacteria also differs.

In the present study, we assessed the effects of elevated [CO_2] on community structure in the root-associated bacteria of five rice genotypes: Akita 63 (Mae et al., 2006), Takanari (Taylaran et al., 2009), Koshihikari, a chromosome segment substitution line (CSSL) of Koshihikari that carries chromosomal segment from Kasalath for increasing the grain number (designated as CSSL-Gn1; Madoka et al., 2008), and a near-isogenic line (NIL) of Koshihikari that carries chromosomal segments from Kasalath containing the sucrose phosphate synthase gene (designated as NIL-SPS1; Hashida et al., 2013). Akita 63 and Takanari tend to produce a greater yield enhancement rate as a result of [CO_2] elevation than does Koshihikari (Hasegawa et al., 2013). The productivity of CSSL-Gn1 and NIL-SPS1 is greater than that of Koshihikari under ambient [CO_2] levels (Madoka et al., 2008; Hashida et al., 2013). These traits make these rice genotypes suitable for managing the growing demand for food by the world's growing population.

MATERIALS AND METHODS

STUDY SITE

The study was conducted during the 2012 growth season as part of an ongoing rice FACE study at Tsukubamirai, Ibaraki, Japan (35°58′27″N, 139°59′32″E, 10 m above sea level). The soil of the experimental site is fluvisol, which is typical in alluvial areas. Bulk density is 0.87×10^6 g.m^{-3}. Total C and N content is 21.4 and 1.97 mg.g^{-1}, respectively. Cation exchange capacity is 202 μmolc.g^{-1} (Hasegawa et al., 2013). The experimental site was established in 2010, and the control protocols for FACE were described previously (Nakamura et al., 2012). Briefly, four rice paddy fields were used as replicates, each with two areas at ambient levels of CO_2 (AMBI) and elevated [CO_2] (FACE). Each treatment area was a 240-m^2 octagon (hereafter "a ring"). The FACE rings had emission tubes on all eight sides that released pure CO_2 from the windward sides to maintain a stable concentration at the ring's center. The CO_2 level was set to 200 μmol.mol^{-1} above the ambient concentration (Nakamura et al., 2012). The AMBI and FACE rings were separated by at least by 70 m (center to center), which is sufficient to prevent cross-contamination by CO_2 (Heim et al., 2009).

RICE CULTIVATION AND FERTILIZATION

We tested five rice (*Oryza sativa* L.) genotypes: Akita 63, Takanari, Koshihikari, CSSL-Gn1, and NIL-SPS1. The CSSL-Gn1 (Madoka et al., 2008) carries a chromosomal segment of Kasalath on the Koshihikari genetic background to increase the grain number; the substituted region is located on chromosome 1 approximately between restriction fragment length polymorphism (RFLP) markers R687 and C178 (Ebitani et al., 2005). The NIL-SPS1 (Hashida et al., 2013) carries two chromosomal segments of Kasalath on chromosome 1 containing *OsSPS1* (1.1 centimorgans) and chromosome 10 (4.1 centimorgans) on the genetic background of Koshihikari. Rice was sown on April 24, 2012 in seedling trays with 448 cells (Minoru Pot 448, Minoru Industrial Co., Ltd., Okayama, Japan). Three seeds were sown in each cell. After emergence, we raised the seedlings in a puddled open field with a tunnel cloche or floating mulch for the first two weeks. On May 23 and 24, seedlings at the five-leaf stage were manually transplanted into the rings, at three seedlings per hill ("hill" is a group of seedlings transplanted to one spot). Hills and rows were 15 and 30 cm apart, respectively, with a resultant density of 22.2 hills.m^{-2}. Fertilizers were applied as basal dressing. Phosphate and potassium were added on April 9 as a compound fertilizer (Sumitomo Chemical Co., Ltd., Tokyo, Japan) containing 4.36 (g P).m^{-2} and 8.30 (g K).m^{-2}. Nitrogen was added on May 14 at 8 g.m^{-2} (2 and 6 g.m^{-2} as urea and coated urea, respectively; 4 g of LP-100 and 2 g of LP-140; JCAM-Agri Co., Ltd., Tokyo, Japan). The method of rice cultivation and fertilization was as described previously (Hasegawa et al., 2013). Immediately after the nitrogen application, the field was puddled for uniformity on May 17, 2012.

RICE SAMPLING AND MICROBIAL DNA PREPARATION

Plants were collected from three hills from each treatment plot on July 18 and 19, 2012 (56–57 days after transplanting), corresponding to the panicle formation stage. At each hill, a block of plow layer soil (30 cm length × 15 cm length × 15 cm depth) was taken with the plants and immediately transported to the laboratory. The soil was washed away with tap water and the roots were separated from the aboveground parts and stored at −80°C. The root samples were manually ground to a fine powder in liquid nitrogen using a mortar and pestle. Three ground-root samples collected from the same ring of the same genotypes and treatment (FACE or AMBI) were composited and homogenized in a blender. Microbial cells including endophytes and epiphytes were extracted by density gradient ultracentrifugation as described (Ikeda et al., 2009). Total DNA was prepared as described (Ikeda et al., 2009).

16S rRNA GENE SEQUENCE ANALYSIS

These genes were amplified as follows: 10 ng total bacterial DNA was used as a template in a final reaction volume of 50 μL including 0.1 μM of each primer and 2 U of Ex Taq DNA polymerase (Takara Bio, Shiga, Japan) with the universal primers 27F (5′-AGAGTTTGATCMTGGCTCAG-3′) and 518R (5′-TTACCGCGGCTGCTGG-3′), containing the 454 FLX adaptors and a sample-specific multiplex identifier (Okubo et al., 2012; Ikeda et al., 2014). The cycling conditions were as follows: initial denaturation for 2 min at 94°C; 25 cycles of 30 s at 94°C, 30 s at 55°C, and 1.5 min at 72°C; and the final extension step of 8 min at 72°C. PCR products of the predicted size (∼500 bp) were purified using the Wizard SV Gel and PCR Clean-Up System (Promega Japan, Tokyo, Japan). Sequencing was performed on 454 GS FLX+ (Roche Diagnostics K.K., Tokyo, Japan). The pyrosequencing reads were processed using the Quantitative Insights Into Microbial Ecology (QIIME) software

package (Caporaso et al., 2010). The sequences were assigned to each sample according to the sample-specific multiplex identifier. Low-quality sequences shorter than 300 bp, with an average quality score lower than 25, with mismatching primer sequences, or with ambiguous bases (marked as "N"), were eliminated from downstream analyses. The forward and reverse primer regions were removed from the quality-filtered sequences. Potentially chimeric sequences were removed using the USEARCH6.1 software (Edgar, 2010). Potentially contaminated sequences classified as *chloroplast*, *mitochondria*, or unassigned by the RDP Classifier software (Wang et al., 2007) were removed. The remaining sequences were clustered into operational taxonomic units (OTUs) at 97% similarity using the pick_de_novo_otus command with default parameters. Principal coordinates analysis (PCoA) was performed on weighted and unweighted UniFrac distance matrixes (Lozupone and Knight, 2005) using a random sample of 2000 sequences for data normalization. For statistical testing, to determine the effects of the $[CO_2]$ elevation, rice genotype, and their interaction, permutational multivariate analysis of variance (PERMANOVA) was conducted on the UniFrac distance matrixes using the *adonis* function in the R software package vegan (http://vegan.r-forge.r-project.org/). The numbers of OTUs and Chao1 as well as Shannon, and Simpson's indexes were calculated with 10 replicates using a random sample of 2000 sequences for data normalization. Statistical analysis was performed on the mean values of 10 replicates to determine the effects of the $[CO_2]$ elevation, rice genotype, and their interaction using linear mixed model of the SPSS Statistics software, version 22 (IBM Japan, Tokyo, Japan). $[CO_2]$ and rice genotype were treated as fixed effects, while field and field × $[CO_2]$ were treated as random effects. The phylogenetic composition of the sequences was evaluated using the RDP classifier (Wang et al., 2007), with confidence levels of 80%. Statistical analysis was also performed on the relative abundance of each taxonomic group to determine the effects of the $[CO_2]$ elevation, rice genotype, and their interaction.

QUANTIFICATION OF *pmoA* AND *mcrA* GENES

The copy numbers of *pmoA* and *mcrA* in the microbial DNA were determined using a Thermal Cycler Dice Real Time System (TaKaRa, Shiga, Japan) with primers A189f/mb661r (Holmes et al., 1995; Costello and Lidstrom, 1999) for the *pmoA* gene and mcrA-f/mcrA-r (Luton et al., 2002) for the *mcrA* gene. For both genes, reactions were performed in a total volume of 25 μL containing 12.5 μL SYBR Premix ExTaq, 0.1 μL each primer (50 mM), 10 ng template DNA, and 12.3 μL sterilized ultrapure water. The PCR conditions were as follows: 40 cycles of denaturation at 95°C for 30 s, annealing at 65.5°C for 30 s, and extension at 72°C for 45 s for *pmoA* and 45 cycles of denaturation at 95°C for 40 s, annealing at 55°C for 30 s, and extension at 72°C for 60 s for *mcrA*. Clones of the *pmoA* genes derived from *Methylosinus trichosporium* strain OB3b (GenBank accession number U31650) and *Methylomonas koyamae* strain Fw12E-Y (GenBank accession number AB538965) were used to generate a standard curve for the quantification of *pmoA* gene copies. For the quantification of *mcrA* gene copies, *mcrA* gene fragments derived from *Methanobrevibacter arboriphilus* strain SA (GenBank accession number AB300777), *Methanosarcina mazei* strain TMA (GenBank accession number AB300778), and *Methanoculleus chikugoensis* strain MG62 (GenBank accession number AB300779) were used to construct a standard curve. The copy numbers of *pmoA* and *mcrA* were processed by means of linear mixed model in the SPSS Statistics software, version 22. Outliers were excluded from the statistical analysis.

THE NUCLEOTIDE SEQUENCE ACCESSION NUMBER

Raw sequence data were deposited in the DNA Data Bank of Japan (DDBJ) Sequence Read Archive under accession number: DRA002644.

RESULTS

RICHNESS AND DIVERSITY INDICES OF A BACTERIAL COMMUNITY

The number of 16S rRNA gene sequences analyzed in the present study is shown in Table S1. The rarefaction curves for the number of OTUs are shown in Figure S1. Richness and diversity of a root-associated bacterial community were evaluated using the 16S rRNA gene sequences with the number of OTUs and Chao1 as well as Shannon and Simpson's (1 − Dominance) indices. The effects of the $[CO_2]$ elevation were not statistically significant with regard to the number of OTUs ($p = 0.1$, **Figure 1A**) and Chao1 ($p = 0.1$, **Figure 1B**), suggesting that the $[CO_2]$ elevation had little or no effect on the richness of root-associated bacterial communities. Shannon (**Figure 1C**) and Simpson's (**Figure 1D**) indices were significantly decreased by the $[CO_2]$ elevation ($p < 0.05$), indicating that the $[CO_2]$ elevation decreased the diversity of root-associated bacterial communities. The $[CO_2]$ × rice genotype interaction was not statistically significant for all indices (**Figure 1**, $p = 0.1$), suggesting that bacterial communities associated with rice roots showed similar responses to the $[CO_2]$ elevation regardless of genotype. The effect of rice genotype was almost significant for all indices (**Figure 1**, $p = 0.051$).

AN OVERVIEW OF BACTERIAL COMMUNITY STRUCTURES

PCoA based on weighted and unweighted UniFrac distance matrices was performed to obtain an overview of changes in the bacterial community structure caused by $[CO_2]$ elevation, rice genotype, and $[CO_2]$ × rice genotype interaction. In the weighted UniFrac analysis, the $[CO_2]$ elevation separated samples along the axis of the first principal component (PC1; **Figure 2A**). The adonis test yielded a p value of 0.003, indicating that the community structures of root-associated bacteria were significantly affected by the $[CO_2]$ elevation. In contrast, the effects of rice genotype (**Figure 2B**) and $[CO_2]$ × rice genotype interaction (**Figures 2A,B**) on community structure were not statistically significant ($p = 0.1$). Statistical analysis suggested that the changes in a bacterial community caused by the $[CO_2]$ elevation represented a general response of rice plants, regardless of genotype. Akita 63, however, tended to show a smaller response to the $[CO_2]$ elevation, compared to the other rice genotypes (**Figure 2B** and Figure S2). In unweighted UniFrac analysis, the $[CO_2]$ elevation (Figure S3A), rice genotype (Figure S3B), and $[CO_2]$ × rice genotype interaction (Figures S3A,B) had no significant

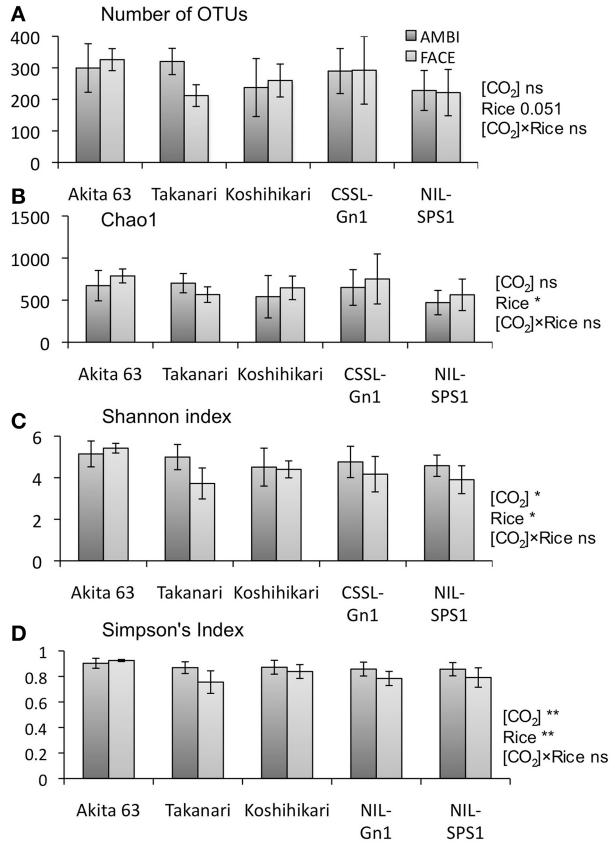

FIGURE 1 | The effects of $[CO_2]$ elevation and rice cultivar on the richness and diversity indices of a root-associated bacterial community ($n = 4$). **(A)** Number of OTUs; **(B)** Chao1; **(C)** Shannon index; **(D)** Simpson's index. Error bars represent standard deviation. Statistically significant effects are indicated: $^{**}p < 0.01$ and $^{*}p < 0.05$. The value indicates the probability between 0.05 and 0.1; ns, not significant ($p > 0.1$); OTU, operational taxonomic unit; AMBI, ambient levels of CO_2; CSSL, chromosome segment substitution line; FACE, free-air CO_2 enrichment; NIL, near-isogenic line.

effect on community structure ($p = 0.1$). These results suggest that $[CO_2]$ elevation affected the relative abundance of bacterial species rather than which bacterial species were present or absent because unweighted UniFrac analysis ignores the information on abundance of OTUs and takes into account only data on the presence and absence of OTUs.

PHYLOGENETIC COMPOSITION

Class-level data on rice root-associated bacterial communities are depicted in **Figure 3A** and Table S2. Alphaproteobacteria (38.0–70.0%) and Betaproteobacteria (16.0–48.9%) were the predominant classes followed by Gammaproteobacteria, Deltaproteobacteria, Clostridia, Planctomycetia, and Actinobacteria. The relative abundance of Alphaproteobacteria tended to be reduced by the $[CO_2]$ elevation (**Figure 3A**, Table S2; $p = 0.085$), whereas the Betaproteobacteria increased (**Figure 3A**, Table S2; $p < 0.05$). Other classes were not clearly affected by the $[CO_2]$ elevation (**Figure 3A**, Table S2; $p = 0.1$). The effect of $[CO_2]$ on the relative abundance of Alphaproteobacteria and Betaproteobacteria was not observed in Akita 63 (Table S2). At the family level, Burkholderiaceae were predominant, representing 13.7–46.5% of all sequences (**Figure 3B**, Table S3). The relative abundance of Burkholderiaceae was significantly increased by the $[CO_2]$ elevation (**Figure 3B**, Table S3; $p < 0.05$). In Alphaproteobacteria, the families of Bradyrhizobiaceae (15.5–30.8%), Rhizobiaceae (5.6–15.2%), and Methylocystaceae (5.4–13.0%) were predominant (**Figure 3B**, Table S3); their relative abundance showed a decreasing trend by the $[CO_2]$ elevation. Although the decreases of Bradyrhizobiaceae and Rhizobiaceae were not statistically significant ($p = 0.1$), those might be due to the limited sample size in our study, given the large standard deviation (**Figure 3B**). In all samples, Methylocystaceae were the dominant methane-oxidizing bacteria under both AMBI and FACE conditions, representing 5.4–13.0% of all sequences (**Figure 3B**, Table S3), followed by Methylophilaceae (0–0.1%) and Methylococcaceae (0–0.05%). It is worth mentioning that Methylacidiphilales, which are often found in acidic geothermal environments (Sharp et al., 2014), were also detected in root-associated bacterial communities, with a relative abundance of 0–0.05% under both AMBI and FACE conditions.

COPY NUMBERS OF THE *pmoA* AND *mcrA* GENES

QPCR was performed to estimate methane monooxygenase (*pmoA*) and methyl coenzyme M reductase (*mcrA*) gene copy number in the DNA of microbial communities extracted from rice roots. The copy number of *pmoA* was significantly reduced by the $[CO_2]$ elevation (**Figure 4A**, $p < 0.01$). The effect of the $[CO_2] \times$ rice genotype interaction was not statistically significant in relation to the *pmoA* copy number (**Figure 4A**, $p = 0.1$). The effect of rice genotype on *pmoA* copy number was marginally significant ($p = 0.055$). NIL-SPS1 tended to show a higher copy number than CSSL-Gn1 (**Figure 4A**). Compared to Koshihikari, the average *pmoA* copy number was higher in NIL-SPS1 but lower in CSSL-Gn1, suggesting that those substituted genomic regions had the opposite effect on the relative abundance of root-associated methane-oxidizing bacteria. The *mcrA* copy number was significantly increased by $[CO_2]$ elevation (**Figure 4B**, $p < 0.01$). The effect of the rice genotype on the copy number of *mcrA* was also significant (**Figure 4B**, $p < 0.01$). NIL-SPS1 showed a significantly higher *mcrA* copy number than the other rice genotypes ($p < 0.001$). Although the *mcrA* copy number showed a trend for an increase in all rice genotypes under the influence of $[CO_2]$ elevation, the rate of increase differed among the genotypes (a significant $[CO_2] \times$ rice genotype interaction, $p < 0.01$). For example, in NIL-SPS1, this copy number was increased by 89.9%, whereas in CSSL-Gn1 and Koshihikari, the copy number increased only by 7.9 and 37.7%, respectively.

DISCUSSION

The structure of root-associated bacterial communities is clearly affected by an increase in $[CO_2]$ (**Figure 2A**). The results of PCoA based on weighted (**Figure 2A**) and unweighted (Figure S3A) UniFrac distances suggest that the $[CO_2]$ elevation affects the relative abundance of bacteria rather than which bacterial

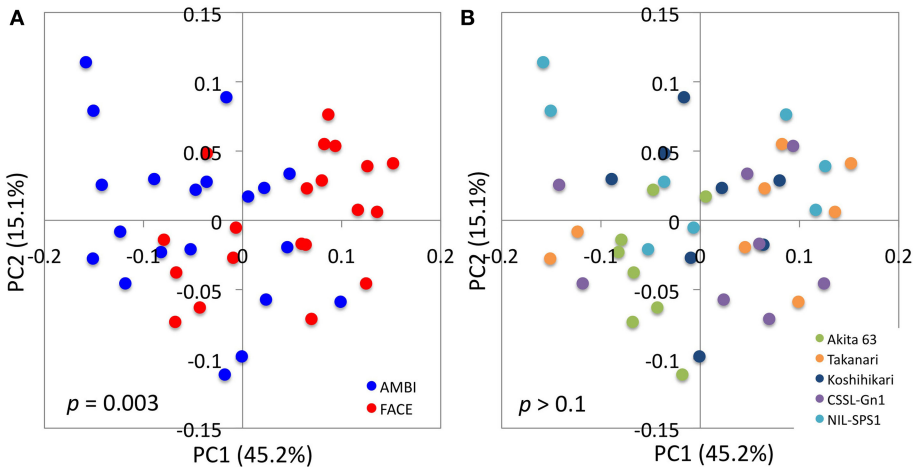

FIGURE 2 | UniFrac principal coordinates analysis plots illustrating the effects of the [CO_2] elevation and rice cultivar on the structure of root-associated bacterial communities. Distance matrices were defined by a weighted UniFrac distance. Data points are colored according to [CO_2] treatment in **(A)** or by rice cultivar in **(B)**. The results of statistical tests of differences between treatments are indicated in each plot. The [CO_2] × rice genotype interaction was not statistically significant ($p > 0.1$). PC, principal component; AMBI, ambient levels of CO_2; CSSL, chromosome segment substitution line; FACE, free-air CO_2 enrichment; NIL, near-isogenic line.

linages are present or absent in rice roots. Shannon (**Figure 1C**) and Simpson's (**Figure 1D**) indices show that the [CO_2] elevation significantly reduces bacterial diversity. This decrease could be partially explained by the very high relative abundance of Burkholderiaceae (14.9–46.5%) under elevated [CO_2] (**Figure 3B** and Table S3). In contrast, the [CO_2] elevation had little or no effect on the richness of a bacterial community, according to the number of OTUs (**Figure 1A**) and Chao1 (**Figure 1B**). Thus, the results on richness and diversity indices are consistent with the UniFrac PCoA plots with regard to the responses to [CO_2] elevation.

The effects of the [CO_2] × rice genotype interaction on UniFrac PCoA plots (**Figure 2** and Figure S3) and on the richness and diversity indices of a bacterial community (**Figure 1**) are not statistically significant, suggesting that bacterial communities associated with rice roots show similar responses to [CO_2] regardless of the genotype. Nevertheless, the effects of the [CO_2] × rice genotype interaction need to be examined in more detail because the bacterial community associated with Akita 63 tends to show a smaller response to the [CO_2] elevation than the bacterial communities associated with the other rice genotypes (**Figure 2** and Figure S2). The statistically insignificant effects of the [CO_2] × rice genotype interaction might be due to the limited sample sizes, considering the large standard variations that we observed (Figure S2).

The copy number of *pmoA* (**Figure 4A**) and the relative abundance of Methylocystaceae (the dominant methanotrophs in rice roots; **Figure 3B**) were reduced by the [CO_2] elevation. The decrease in the relative abundance of Methylocystaceae was observed in another FACE study (Okubo et al., 2014b). These results suggest the methane-oxidizing activity in rice roots is downregulated by [CO_2] elevation. In contrast, the copy number for *mcrA* was significantly increased by the [CO_2] elevation (**Figure 4B**), suggesting that the abundance of methanogenic Archaea associated with rice roots increases under elevated [CO_2]; this change may lead to upregulation of methanogenesis in rice roots. Other FACE studies showed that the elevated [CO_2] stimulates photosynthesis in plants (Sasaki et al., 2005). Additional assimilated carbon under elevated [CO_2] increases the carbon content of root exudates (a potential carbon source for root-associated microorganisms; Bhattacharyya et al., 2013); this change may increase the abundance of root-associated methanogenic Archaea. The present study demonstrates that the copy number of *mcrA* is higher in NIL-SPS1 than in Koshihikari. One study showed that the SPS activity in NIL-SPS1 is higher than that in Koshihikari at the panicle formation stage (Hashida et al., 2013). It is likely that the SPS activity correlates with the amount of the sucrose pool available for transport (Huber, 1983). The difference in photosynthetic carbon allocation between NIL-SPS1 and Koshihikari may influence *mcrA* copy number in root-associated microbial communities.

We originally hypothesized that the copy number of *pmoA* correlates with that of *mcrA* because methane is the major substrate for methanotrophs. Nevertheless, the copy number of *pmoA* was reduced by the [CO_2] elevation, whereas *mcrA* copy number increased (**Figures 4A,B**). These results are suggestive of the existence of other factors limiting the population of methanotrophs in rice roots. Other FACE studies revealed that [CO_2] elevation decreases N and Cu concentrations in rice plants (Myers et al., 2014). These chemical elements are known to be important for methane oxidation (Semrau et al., 2010). If N and Cu are less available for rice root-associated bacteria under elevated [CO_2], then this situation may decrease the rate of methane oxidation in rice roots, leading to a decrease in the relative abundance of methane-oxidizing bacteria.

Although our results showed that [CO_2] elevation shifts the community structure of rice root-associated bacteria, the mechanism of that shift remains unclear. Previous studies

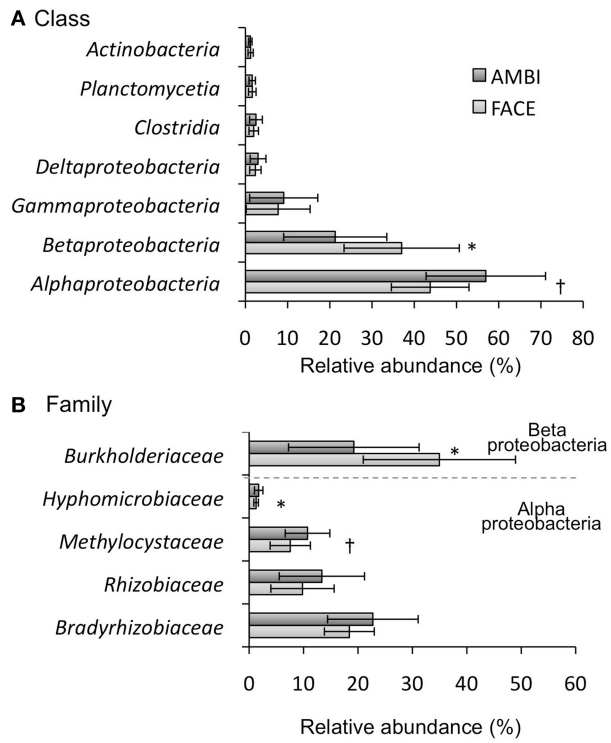

FIGURE 3 | Phylogenetic composition of root-associated bacteria at the class level in (A) and at the family level in (B) ($n = 4$). The relative abundance is shown in averages for five rice genotypes. Error bars represent standard deviation. Statistically significant effects of the [CO_2] elevation: $^{*}p < 0.05$ and $^{\dagger}p < 0.1$. AMBI, ambient levels of CO_2; FACE, free-air CO_2 enrichment.

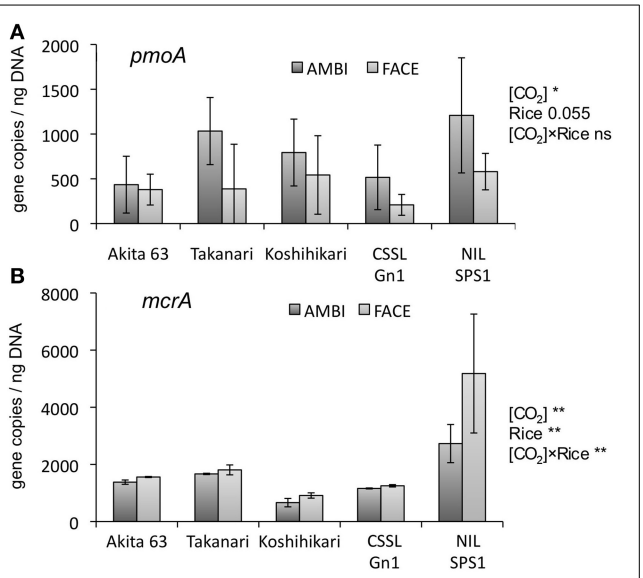

FIGURE 4 | The effects of the [CO_2] elevation and rice cultivar on *pmoA* (A) and *mcrA* (B) gene copy number in a root-associated bacterial community ($n = 4$, except $n = 3$ for the *pmoA* copy number of Akita 63). Error bars show standard deviation. Statistically significant effects are indicated: $^{**}p < 0.01$, and $^{*}p < 0.05$. The value indicates the probability between 0.05 and 0.1; ns, not significant ($p > 0.1$); AMBI, ambient levels of CO_2; CSSL, chromosome segment substitution line; FACE, free-air CO_2 enrichment; NIL, near-isogenic line.

reported that elevated [CO_2] increases the carbon content of root exudates (Bhattacharyya et al., 2013). This increase will affect the community, activity, and food webs of rhizosphere microorganisms, which may contribute to the community shift of root-associated bacteria. Thus, ecological complexities in rhizosphere processes make it difficult to produce a straightforward explanation.

In the present study, we described a shift in the community structure of rice root-associated bacteria under the influence of [CO_2] elevation. There are still some challenges to elucidating the secondary effects of the changes in bacterial community structure on the rice yield and paddy ecosystem. Changes in the relative abundance of methanotrophs and methanogens will affect the carbon cycle in a rice paddy. In addition, metaproteomic analysis of rice root-associated bacteria revealed that Methylocystaceae are typical nitrogen-fixing bacteria in rice roots (Bao et al., 2014). The [CO_2] elevation may reduce the amount of N_2 fixed by Methylocystaceae in rice roots; this change is expected to aggravate the N deficiency in rice under elevated [CO_2], in addition to the dilution effect due to the greater production of dry matter.

As far as we know, ours is the first study to compare the structure of root-associated bacterial communities with the copy number analysis of microbial functional genes in NIL, CSSL, and their recurrent parent. Although statistically significant community differences were not observed by PCoA analysis (**Figures 2A,B**), the copy number of *pmoA* (**Figure 4A**) and *mcrA* (**Figure 4B**) varied, suggesting genomic substitution affects the activity of root-associated microorganisms. Over the past few decades, quantitative trait loci and chromosomal regions affecting traits have been screened for genes that enhance the physiological and morphological contributors to rice productivity (Madoka et al., 2008; Ujiie et al., 2012). NILs and CSSLs are also powerful tools for elucidating the genetic basis underlying the influence of rice plants on the activity of the associated microorganisms. Analysis of chromosomal regions affecting traits in the associated microbial communities should allow us to develop new cultivars that accommodate microorganisms that are more beneficial for the plants.

ACKNOWLEDGMENTS

This work was supported by Grants-in-Aid for Scientific Research (C) 22580074, (A) 23248052, and (A) 26252065 from the Ministry of Education, Science, Sports and Culture of Japan; and JSPS KAKENHI Grant Number 269473 and 247071. TO is a Research Fellow of the Japan Society for the Promotion of Science.

SUPPLEMENTARY MATERIAL

The Supplementary Material for this article can be found online at: http://www.frontiersin.org/journal/10.3389/fmicb.2015.00136/abstract

REFERENCES

Bao, Z., Okubo, T., Kubota, K., Kasahara, Y., Tsurumaru, H., Anda, M., et al. (2014). Metaproteomic identification of diazotrophic methanotrophs and their localization in root tissues of field-grown rice plants. *Appl. Environ. Microbiol.* 80, 5043–5052. doi: 10.1128/AEM.00969-14

Bao, Z., Sasaki, K., Okubo, T., Ikeda, S., Anda, M., Hanzawa, E., et al. (2013). Impact of *Azospirillum* sp. B510 inoculation on rice-associated bacterial communities in a paddy field. *Microbes Environ.* 28, 487–490. doi: 10.1264/jsme2.ME13049

Bhattacharyya, P., Roy, K. S., Neogi, S., Manna, M. C., Adhya, T. K., Rao, K. S., et al. (2013). Influence of elevated carbon dioxide and temperature on below-ground carbon allocation and enzyme activities in tropical flooded soil planted with rice. *Environ. Monit. Assess.* 185, 8659–8671. doi: 10.1007/s10661-013-3202-7

Caporaso, J. G., Kuczynski, J., Stombaugh, J., Bittinger, K., Bushman, F. D., Costello, E. K., et al. (2010). QIIME allows analysis of high-throughput community sequencing data. *Nat. Methods* 7, 335–336. doi: 10.1038/nmeth.f.303

Costello, A. M., and Lidstrom, M. E. (1999). Molecular characterization of functional and phylogenetic genes from natural populations of methanotrophs in lake sediments. *Appl. Environ. Microbiol.* 65, 5066–5074.

Drigo, B., Kowalchuk, G. A., and van Veen, J. A. (2008). Climate change goes underground: effects of elevated atmospheric CO_2 on microbial community structure and activities in the rhizosphere. *Biol. Fertil. Soils* 44, 667–679. doi: 10.1007/s00374-008-0277-3

Ebitani, T., Takeuchi, Y., Nonoue, Y., Yamamoto, T., Takeuchi, K., and Yano, M. (2005). Construction and evaluation of chromosome segment substitution lines carrying overlapping chromosome segment of *indica* rice cultivar "Kasalath" in a genetic background of *japonica* elite cultivar "Koshihikari." *Breed. Sci.* 55, 65–73. doi: 10.1270/jsbbs.55.65

Edgar, R. C. (2010). Search and clustering orders of magnitude faster than BLAST. *Bioinformatics* 26, 2460–2461. doi: 10.1093/bioinformatics/btq461

Fisher, B. S., Nakicenovic, N., Alfsen, K., Corfee Morlot, J., de la Chesnaye, F., Hourcade, J.-Ch., et al. (2007). "Issues related to mitigation in the long term context," in *Climate change 2007: mitigation. Contribution of Working Group III to the Fourth Assessment Report of the Inter-Governmental Panel on Climate Change*, eds B. Metz, O. R. Davidson, P. R. Bosch, R. Dave, and L. A. Meyer (Cambridge: Cambridge University Press), 169–250.

Hasegawa, T., Sakai, H., Tokida, T., Nakamura, H., Zhu, C., Usui, Y., et al. (2013). Rice cultivar responses to elevated CO_2 at two free-air CO_2 enrichment (FACE) sites in Japan. *Funct. Plant Biol.* 40, 148–159. doi: 10.1071/FP12357

Hashida, Y., Aoki, N., Kawanishi, H., Okamura, M., Ebitani, T., Hirose, T., et al. (2013). A near isogenic line of rice carrying chromosome segments containing OsSPS1 of Kasalath in the genetic background of Koshihikari produces an increased spikelet number per panicle. *Field Crop. Res.* 149, 56–62. doi: 10.1016/j.fcr.2013.04.020

Hayden, H. L., Mele, P. M., Bougoure, D. S., Allan, C. Y., Norng, S., Piceno, Y. M., et al. (2012). Changes in the microbial community structure of bacteria, archaea and fungi in response to elevated CO_2 and warming in an Australian native grassland soil. *Environ. Microbiol.* 12, 3081–3096. doi: 10.1111/j.1462-2920.2012.02855.x

Heim, A., Moser, N., Blum, H., and Schmidt, M. W. I. (2009). How far do experimentally elevated CO_2 levels reach into the surrounding? – An example using the ^{13}C label of soil organic matter as an archive. *Global Change Biol.* 15, 1598–1602. doi: 10.1111/j.1365-2486.2009.01843.x

Holmes, A. J., Costello, A., Lindstrom, M. E., and Murrell, J. C. (1995). Evidence that particulate methane monooxygenase and ammonia monooxygenase may be evolutionarily related. *FEMS Microbiol. Lett.* 132, 203–208. doi: 10.1111/j.1574-6968.1995.tb07834.x

Huber, S. C. (1983). Role of sucrose-phosphate synthase in partitioning of carbon in leaves. *Plant Physiol.* 71, 818–821. doi: 10.1104/pp.71.4.818

Ikeda, S., Kaneko, T., Okubo, T., Rallos, L. E., Eda, S., Mitsui, H., et al. (2009). Development of a bacterial cell enrichment method and its application to the community analysis in soybean stems. *Microbial. Ecol.* 58, 703–714. doi: 10.1007/s00248-009-9566-0

Ikeda, S., Sasaki, K., Okubo, T., Yamashita, A., Terasawa, K., Bao, Z., et al. (2014). Low nitrogen fertilization adapts rice root microbiome to low nutrient environment by changing biogeochemical functions. *Microbes Environ.* 29, 50–59. doi: 10.1264/jsme2.ME13110

Ikeda, S., Tokida, T., Nakamura, H., Sakai, H., Usui, Y., Okubo, T., et al. (in press). Characterization of leaf blade- and leaf sheath-associated bacterial communities and assessment of their responses to environmental changes in CO_2, temperature, and nitrogen levels under field conditions. *Microbes Environ.* doi: 10.1264/jsme2.ME14117

Lee, S. H., Kim, S. Y., Ding, W., and Kang, H. (in press). Impact of elevated CO_2 and N addition on bacteria, fungi, and archaea in a marsh ecosystem with various types of plants. *Appl. Microbiol. Biotechnol.* doi: 10.1007/s00253-015-6385-8. [Epub ahead of print].

Lozupone, C., and Knight, R. (2005). UniFrac: a new phylogenetic method for comparing microbial communities. *Appl. Environ. Microbiol.* 71, 8228–8235. doi: 10.1128/AEM.71.12.8228-8235.2005

Luton, P. E., Wayne, J. M., Sharp, R. J., and Riley, P. W. (2002). The *mcrA* gene as an alternative to 16S rRNA in the phylogenetic analysis of methanogen populations in landfill. *Microbiology* 148, 3521–3530.

Madoka, Y., Kashiwagi, T., Hirotsu, N., and Ishimaru, K. (2008). Indian rice "Kasalath" contains genes that improve traits of Japanese premium rice "Koshihikari." *Theor. Appl. Genet.* 116, 603–612. doi: 10.1007/s00122-007-0693-z

Mae, T., Inaba, A., Kaneta, Y., Masaki, S., Sasaki, M., Aizawa, M., et al. (2006). A large-grain rice cultivar, Akita 63, exhibits high yields with high physiological N-use efficiency. *Field Crops Res.* 97, 227–237. doi: 10.1016/j.fcr.2005.10.003

Myers, S. S., Zanobetti, A., Kloog, I., Huybers, P., Leakey, A. D., Bloom, A. J., et al. (2014). Increasing CO2 threatens human nutrition. *Nature* 510, 139–142. doi: 10.1038/nature13179

Nakamura, H., Tokida, T., Yoshimoto, M., Sakai, H., Fukuoka, M., and Hasegawa, T. (2012). Performance of the enlarged rice-FACE system using pure-CO_2 installed in Tsukuba, Japan. *J. Agric. Meteorol.* 68, 15–23. doi: 10.2480/agrmet.68.1.2

Okubo, T., Ikeda, S., Sasaki, K., Ohshima, K., Hattori, M., Sato, T., et al. (2014a). Phylogeny and functions of bacterial communities associated with field-grown rice shoots. *Microbes Environ.* 29, 329–332. doi: 10.1264/jsme2.ME14077

Okubo, T., Ikeda, S., Yamashita, A., Terasawa, K., and Minamisawa, K. (2012). Pyrosequence read length of 16S rRNA gene affects phylogenetic assignment of plant-associated bacteria. *Microbes Environ.* 27, 204–208. doi: 10.1264/jsme2.ME11258

Okubo, T., Tokida, T., Ikeda, S., Bao, Z., Tago, K., Hayatsu, M., et al. (2014b). Effects of elevated carbon dioxide, elevated temperature, and rice growth stage on the community structure of rice root-associated bacteria. *Microbes Environ.* 29, 184–190. doi: 10.1264/jsme2.ME14011

Sasaki, H., Hara, T., Ito, S., Miura, S., Hoque, M. M., Lieffering, M., et al. (2005). Seasonal changes in canopy photosynthesis and respiration, and partitioning of photosynthate, in rice (*Oryza sativa* L.) grown under free-air CO_2 enrichment. *Plant Cell Physiol.* 46, 1704–1712. doi: 10.1093/pcp/pci186

Sasaki, K., Ikeda, S., Ohkubo, T., Kisara, C., Sato, T., and Minamisawa, K. (2013). Effects of plant genotype and nitrogen level on bacterial communities in rice shoots and roots. *Microbes Environ.* 28, 391–395. doi: 10.1264/jsme2.ME12212

Schortemeyer, M., Hartwig, U. A., Hendrey, G. R., and Sadowsky, M. J. (1996). Microbial community changes in the rhizospheres of white clover and perennial ryegrass exposed to free air carbon dioxide enrichment (FACE). *Soil Biol. Biochem.* 28, 1717–1724. doi: 10.1016/S0038-0717(96)00243-X

Semrau, J. D., DiSpirito, A. A., and Yoon, S. (2010). Methanotrophs and copper. *FEMS Microbiol. Rev.* 34, 496–531. doi: 10.1111/j.1574-6976.2010.00212.x

Sharp, C. E., Smirnova, A. V., Graham, J. M., Stott, M. B., Khadka, R., Moore, T. R., et al. (2014). Distribution and diversity of Verrucomicrobia methanotrophs in geothermal and acidic environments. *Environ. Microbiol.* 16, 1867–1878. doi: 10.1111/1462-2920.12454

Taylaran, R. D., Ozawa, S., Miyamoto, N., Ookawa, T., Motobayashi, T., and Hirasawa, T. (2009). Performance of a high-yielding modern rice cultivar Takanari and several old and new cultivars grown with and without chemical fertilizer in a submerged paddy field. *Plant Prod. Sci.* 12, 365–380. doi: 10.1626/pps.12.365

Tokida, T., Adachi, M., Cheng, W., Nakajima, Y., Fumoto, T., Matsushima, M., et al. (2011). Methane and soil CO_2 production from current-season photosynthates in a rice paddy exposed to elevated CO_2 concentration and soil temperature. *Global Change Biol.* 17, 3327–3337. doi: 10.1111/j.1365-2486.2011.02475.x

Tokida, T., Fumoto, T., Cheng, W., Matsunami, T., Adachi, M., Katayanagi, N., et al. (2010). Effects of free-air CO_2 enrichment (FACE) and soil warming on CH_4 emission from a rice paddy field: impact assessment and stoichiometric evaluation. *Biogeosciences* 7, 2639–2653. doi: 10.5194/bg-7-2639-2010

Ujiie, K., Kashiwagi, T., and Ishimaru, K. (2012). Identification and functional analysis of alleles for productivity in two sets of chromosome segment substitution lines of rice. *Euphytica* 187, 325–337. doi: 10.1007/s10681-012-0660-x

Usui, Y., Sakai, H., Tokida, T., Nakamura, H., Nakagawa, H., and Hasegawa, T. (2014). Heat-tolerant rice cultivars retain grain appearance quality under free-air CO_2 enrichment. *Rice* 7, 6. doi: 10.1186/s12284-014-0006-5

Wang, Q., Garrity, G. M., Tiedje, J. M., and Cole, J. R. (2007). Naive Bayesian classifier for rapid assignment of rRNA sequences into the new bacterial taxonomy. *Appl. Environ. Microbiol.* 73, 5261–5267. doi: 10.1128/AEM.00062-07

Conflict of Interest Statement: The authors declare that the research was conducted in the absence of any commercial or financial relationships that could be construed as a potential conflict of interest.

Received: 23 November 2014; accepted: 05 February 2015; published online: 20 February 2015.

Citation: Okubo T, Liu D, Tsurumaru H, Ikeda S, Asakawa S, Tokida T, Tago K, Hayatsu M, Aoki N, Ishimaru K, Ujiie K, Usui Y, Nakamura H, Sakai H, Hayashi K, Hasegawa T and Minamisawa K (2015) Elevated atmospheric CO_2 levels affect community structure of rice root-associated bacteria. Front. Microbiol. ***6****:136. doi: 10.3389/fmicb.2015.00136*

This article was submitted to Plant-Microbe Interaction, a section of the journal Frontiers in Microbiology.

frontiers in Microbiology

DATA REPORT
published: 17 September 2015
doi: 10.3389/fmicb.2015.00978

Genome sequence of the plant growth promoting endophytic yeast *Rhodotorula graminis* WP1

*Andrea Firrincieli[1], Robert Otillar[2], Asaf Salamov[2], Jeremy Schmutz[2,3], Zareen Khan[4], Regina S. Redman[5], Neil D. Fleck[4], Erika Lindquist[2], Igor V. Grigoriev[2] and Sharon L. Doty[4]**

[1] Department for Innovation Biological, Agro-Food and Forest System, University of Tuscia, Tuscia, Italy, [2] U.S. Department of Energy Joint Genome Institute, Walnut Creek, CA, USA, [3] HudsonAlpha Institute for Biotechnology, Huntsville, AL, USA, [4] School of Environmental and Forest Sciences, University of Washington, Seattle, WA, USA, [5] Adaptive Symbiotic Technologies, Seattle, WA, USA

Keywords: symbiosis, endophytes, populus, plant-microbe interactions, endophytic yeast, endophyte genomics, microbiome, phytobiome

OPEN ACCESS

Edited by:
Carolin Frank, University of California, Merced, USA

Reviewed by:
Eric Kemen, Max Planck Institute for Plant Breeding Research, Germany
Wei Qian, Institute of Microbiology, Chinese Academy of Sciences, China

****Correspondence:***
Sharon L. Doty, sldoty@u.washington.edu

Specialty section:
This article was submitted to Plant Biotic Interactions, a section of the journal Frontiers in Microbiology

Received: *30 May 2015*
Accepted: *03 September 2015*
Published: *17 September 2015*

Citation:
Firrincieli A, Otillar R, Salamov A, Schmutz J, Khan Z, Redman RS, Fleck ND, Lindquist E, Grigoriev IV and Doty SL (2015) Genome sequence of the plant growth promoting endophytic yeast Rhodotorula graminis WP1. Front. Microbiol. 6:978. doi: 10.3389/fmicb.2015.00978

Background

Here we present the genome sequence of *Rhodotorula graminis* WP1, a pink-pigmented, encapsulated yeast strain belonging to the Basidiomycota phylum that was isolated from within stems of *Populus trichocarpa* growing in its native riparian environment alongside the Snoqualmie River in Western Washington state(Xin et al., 2009). Although numerous bacterial endophytes, the microorganisms living fully within plants, have been characterized, relatively few endophytic yeast strains have been studied (Doty, 2011). The genome of strain WP1 was the first endophytic yeast to be sequenced, and has been included in several genomic analyses (Spatafora et al., 2013; Nagy et al., 2014; Pendleton et al., 2014). Although originally isolated from poplar, WP1 has a broad host range, providing growth benefits not only to poplar (Knoth et al., 2014; Khan et al. in review) but also to grasses and agricultural crop species (Khan et al., 2012; Knoth et al., 2013). Strain WP1 improves plant vigor and has useful biochemical properties (Doty, 2014) including the ability to ferment both pentoses and hexoses and to degrade fermentation inhibitors (Xu et al., 2011). Genomic analysis of bacterial endophytes has revealed certain features in common including genes for phytohormone synthesis, adhesion, colonization, stress reduction, and iron and phosphate acquisition (Fouts et al., 2008; Taghavi et al., 2010; Sessitsch et al., 2012; Witzel et al., 2012). We analyzed the genome of WP1 with a focus on genes potentially involved in plant-microbe interactions.

Methods

DNA Purification

Rhodotorula graminis strain WP1 was isolated from surface-sterilized shoot cuttings of poplar (*P. trichocarpa*) collected at the Three Forks Natural Area in King County, WA in the riparian zone of the Snoqualmie River (+47° 31′ 14.30″, −121° 46′ 28.32″) in August 2002, and glycerol stocks were frozen at −70°C. All subsequent studies were done using samples from these cryo-stocks. For DNA extraction, WP1 was grown in 300 ml YPD (yeast extract, peptone, dextrose) broth, pelleted, washed twice in sterile water, frozen, and freeze-dried. Cells were lysed with glass beads and the genomic DNA purified as previously described (Pitkin et al., 1996).

RNA Extraction

A single WP1 colony from solid NFMS [Nitrogen-Free Murashige and Skoog medium (Murashige and Skoog, 1962); Caisson] was used to inoculate 100 ml of liquid NFMS, and grown with agitation (200–250 rpm) for 24 h at RT. Cells were harvested and resuspended in 100 ml YPD broth and grown with agitation at RT. After 2 days, cells were centrifuged at 1300 × g and washed twice with NFMS medium. Cell density was adjusted to an OD_{600} 0.4 in fresh NFMS and grown with agitation (200–250 rpm) at RT until the cell density reached an OD_{600} of 1.2. Cells were centrifuged at 1300 × g, washed twice in NFMS media, frozen at −80°C overnight, and lyophilized. Cells were ground in liquid nitrogen until a fine powder was achieved, and RNA extracted using standard protocols as suggested by the manufacturers of the reagent TRlzol (Life Technologies).

Genome Sequencing

The *Rhodotorula graminis* strain WP1 genome was sequenced by the Joint Genome Institute (JGI) using the Sanger whole genome shotgun approach. Three (3, 6, and 33.8 kb insert size) libraries were sequenced. Sequenced reads were QC filtered for vector sequence, mitochondria, unanchored rDNA, and assembled with the Arachne assembler (Jaffe et al., 2003). The 21,013,998 bp assembly resulted in 26 scaffolds comprising 323 contigs with average read depth coverage of 8.55x (**Table 1**).

Transcriptome Sequencing

For analysis of the *R. graminis* transcriptome, polyA mRNA was used to construct cDNA libraries and these were sequenced using the Roche-454 GS-FLX platform. The 1.9 million reads were filtered and screened for quality and contamination and were assembled into contigs using Newbler (v2.3-PreRelease-6/30/2009) with default parameters.

Genome Annotation

The *R. graminis* genome assembly was annotated using the JGI Annotation Pipeline (Grigoriev et al., 2006), which combines several gene prediction and functional annotation methods, and integrates the annotated genome into JGI web-based resource for fungal comparative genomics, MycoCosm (http://jgi.doe.gov/fungi) (Grigoriev et al., 2014). Before gene prediction, assembly scaffolds were masked using RepeatMasker (Smit et al., 2010), RepBase library (Jurka et al., 2005), and the most frequent (>150 times) repeats recognized by RepeatScout (Price et al., 2005). The following combination of gene predictors was run on the masked assembly: ab initio including Fgenesh (Salamov and Solovyev, 2000) and GeneMark (Ter-Hovhannisyan et al., 2008); homology-based including Fgenesh+ (Salamov and Solovyev, 2000) and Genewise (Birney and Durbin, 2000) seeded by BLASTx alignments against the NCBI NR database; and transcriptome-based using Fgenesh package. In addition to protein-coding genes, tRNAs were predicted using tRNAscan-SE (Lowe and Eddy, 1997). For each genomic locus, the best representative gene model was selected based on a combination of protein homology and transcriptome support. All predicted proteins were functionally annotated using SignalP (Nielsen et al., 1997) for signal sequences, TMHMM (Melén et al., 2003) for transmembrane domains, interProScan (Quevillon et al., 2005) for integrated collection of functional and structural protein domains, and protein alignments to NCBI nr, SwissProt (Boeckmann et al., 2003), KEGG (Kanehisa et al., 2004) for metabolic pathways, and KOG (Koonin et al., 2004) for eukaryotic clusters of orthologs. InterPro and SwissProt hits were used to map Gene Ontology terms (Ashburner et al., 2000).

Results

Genome Characteristics

The 21.01 Mbp genome of *Rhodotorula graminis* strain WP1 was assembled in 28 scaffolds and 323 contigs with 1.13% in scaffold gaps (**Table 1**). The genome contains 3.63% repetitive DNA and 7283 predicted genes, supported by transcriptomics and homology to proteins from other fungi (**Table 2**). Three thousand five hundred and fifty-two predicted proteins form 929 multigene families based on MCL clustering, the largest of which include protein kinases, transporters, and transcription factors (http://genome.jgi.doe.gov/Rhoba1_1).

R. graminis has one of the highest GC-rich genomes (67%) among the all publicly available fungal genomes and while expectedly its intron content is also GC-rich, a significant imbalance in the C (42.7%) and G (23%) content of introns is surprising. This 19.7% deviation is the largest asymmetry

TABLE 1 | Genome assembly statistics for *R. graminis* strain WP1.

Assembly length, bp	21,031,998
Number of scaffolds	26
Scaffold N50	7
Scaffold L50, bp	1,420,730
Number of contigs	323
Contig N50	38
Contig L50, bp	167,432
%GC	67.76

TABLE 2 | Gene content of *R. graminis* strain WP1.

	Annotation results	
Number of genes	7283	100%
Avg. gene length, bp	2126	
Avg. protein length, aa	501	
Avg. exon length, bp	254	
Avg. intron length, bp	105	
Avg. exons per gene	6.2	
PROTEINS WITH:		
Similarity to KEGG	6384	88%
Similarity to KOG	5910	81%
Similarity to Swissprot	5989	82%
Similarity to NCBI NR	5724	79%
Pfam domain	4545	62%
Complete CDS	6415	88%
Transmembrane helices	1283	18%
Signal peptide	1626	22%

in C/G content observed among the introns of all fungal genomes in MycoCosm (Grigoriev et al., 2014), where the average asymmetry is 1.8 ± 3.1%, and the second highest asymmetry of 7.3% (29.5% C and 22.2% G) was identified in the related Pucciniomycotina yeast *Sporobolomyces roseus*. Additionally, an extended donor splice consensus observed in introns of *R. graminis* is likely due to the high C content of introns. Most eukaryotes have a conserved consensus at positions +1 to +6 of introns (Rogozin and Milanesi, 1997; Bhasi et al., 2007). In *R. graminis*, positions +7 to +10 have a predominantly C nucleotide, with positions +3 and +4 also having stronger consensus relative to what is observed in other basidiomycetes.

Phytohormones, Volatile Organic Compounds (VOCs), Capsule Production and Small Secreted Proteins (SSPs)

A common feature of endophytic bacteria and fungi is the production of phytohormones (Hardoim et al., 2008; Bulgarelli et al., 2013; Sukumar et al., 2013; Duca et al., 2014). Many of the beneficial plant-associated microorganisms that produce auxin rely on plant-exuded tryptophan as the precursor for biosynthesis of the auxin, indole-3-acetic acid (IAA) (Hardoim et al., 2008). Since auxins stimulate plant growth and there is a higher prevalence of auxin-producing microorganisms within plants than in the rhizosphere, it has been proposed that the plant host environment selects for endophytes with this trait (Patten and Glick, 2002). Genomic analysis of several bacterial endophytes, including *Enterobacter* from poplar stems (Taghavi et al., 2010), *Gluconacetobacter diazotrophicus* from sugarcane (Bertalan et al., 2009), and the endophyte community of rice (Sessitsch et al., 2012) provided evidence of multiple microbial pathways for auxin biosynthesis. Although less is known about endophytic yeast than endophytic bacteria, there is evidence of plant growth promotion by auxin-producing yeasts (Doty, 2011). Eight of the *Williopsis saturnus* endophytic yeast strains of maize roots produced the auxins IAA and IPYA (Nassar et al., 2005). Since WP1 has strong root-promoting activity on recalcitrant poplar clones (Doty, unpublished) and overall plant growth-promoting activity (Khan et al., 2012; Knoth et al., 2014), we analyzed the genome for evidence of auxin and other phytohormone biosynthesis capabilities, putative effectors involved in plant-microbe interaction, and antitoxin systems.

The WP1 genome lacks the standard genes encoding for proteins involved in the biosynthesis of IAA via indole-3-pyruvate (KEGG Entry: R00677; R00684) and indole-3-acetamide (KEGG Entry: R00679). However, three putative proteins, an aromatic-L-amino-acid decarboxylase (Protein ID: 35429), a monoamine oxidase (Protein ID: 54216) and an indol-3-acetaldehyde dehydrogenase (Protein ID: 14581) can be involved in the conversion of L-tryptophan to IAA via tryptamine. In this pathway, trp is first decarboxylated to tryptamine (KEGG Entry: R00685) which is subsequently oxidized into indole-3-acetaldehyde and then to IAA through two consecutive oxidation steps carried out by an amine oxidase (KEGG Entry: R02173) and an aldehyde dehydrogenase, respectively (KEGG Entry: R02678). Furthermore, two putative hydrolases (Protein ID: 34153; 66162) belonging to the nitrilase superfamily, which are important for the microbial colonization of plants due to their role in nitriles detoxification and utilization of plant nitriles as carbon and nitrogen source (Howden and Preston, 2009; Howden et al., 2009), can also convert the indole-3-acetonitrile (IAN) into IAA (KEGG Entry: R03093). However, IAN synthesis occurring in microbes is still unclear (Fu and Wang, 2011).

From research for functional domains, 15 proteins in WP1 were annotated as containing a 2OG-Fe(II) oxygenase domain (IPR005123) which are primarily involved in the biosynthesis of gibberellins and other plant hormones (Prescott and Lloyd, 2000; Zhao et al., 2013; Farrow and Facchini, 2014). WP1 was shown to produce the phytohormones GA3, IAA, JA, ABA, and Br *in vitro* (Khan et al. in review).

R. graminis WP1 has a set of genes involved in the synthesis of (R)-acetoin and (R,R)-2,3-butandiol, two well-known VOCs that increase resistance to plant pathogens and also act as growth promoting factors (Johnston-Monje and Raizada, 2011; D'Alessandro et al., 2014; Taghavi et al., 2015). In WP1, a putative metabolic pathway which leads to the synthesis of (R)-acetoin and (R,R)-2,3-butandiol starts with the decarboxylation of pyruvate into 2-acetolactate (KEGG Entry: R00006) by a putative acetolactate synthase (Protein ID: 32290; 35922). Under aerobic conditions, the synthesis of (R,R)-2,3-butandiol (KEGG Entry: R02946) from (R)-acetoin by two putative NADH-dependent dehydrogenase (Protein ID: 39181; 46342) occurs through the spontaneous decarboxylation of 2-acetolactate into (R)-acetoin (Atsumi et al., 2009).

In order to offer a more in depth overview about the presence of putative SSPs (aminoacidic seq. <300) encoding genes, as supposed effectors involved in plant-microbe interactions (Rafiqi et al., 2013), we data mined the annotation file "SignalP" as described in Pendleton et al. (2014) but with slight modification. The following file, accessible from the download section through the sub-directory path: Files > Annotation > Filtered Models > Functional Annotation > Signalp, were analyzed through the TargetP 1.1 Server (Emanuelsson et al., 2000). Among 208 putative SSPs, two coding sequences (Protein ID: 43059 and 46692) for extracellular membrane proteins with a cysteine-rich domain (CFEM domain: IPR008427) were detected. Moreover, through the Search tool, three secreted proteins (Protein ID: 55573, 55528, and 50767) with a Carbohydrate-binding WSC domain (IPR013994) were also detected.

Inoculation of roots with WP1 results in colonization of the plant, including the shoots, possibly through the formation of a yeast-form biofilm (unpublished data). Unlike bacteria that could colonize plants using flagella, most yeasts, just like filamentous fungi, may colonize, and interact with the plant through a filamentous form. The passage from a yeast-form to a filamentous stage can be triggered by a wide range of environmental stimuli or as a result of the interactions with other microorganisms within multispecies biofilms (Lengeler et al., 2000). In a study on the sexuality and life cycle in *Rhodotorula glutinis* strains, the capability to form filamentous mycelia was reported (Banno, 1967). Although we have not seen a filamentous form of WP1

under culture conditions, we cannot exclude the possibility that WP1 is able to form mycelia under specific environmental conditions.

An interesting feature of WP1 is the presence of a polysaccharidic capsule that surrounds the cellular body (**Figure 1**). A well-studied encapsulated yeast is represented by *Cryptococcus neoformans*, an opportunistic pathogen that causes meningoencephalitis in immunocompromised patients (Mitchell and Perfect, 1995). *C. neoformans* is ubiquitous in nature and the survival under different environmental conditions can be due to his biofilmogenic property. Within biofilms, microbial cells not only have an increased resistance and tolerance against a wide range of biotic and abiotic stress but also, under specific physiological and environmental conditions, can disperse and colonize new ecological niches (Ramage et al., 2009). The capability of *C. neoformans* to form a biofilm is dependent on the presence of the capsule. Deletion mutants in cap59 and cap10, two genes involved in the capsule synthesis and virulence, are unable to form biofilms, implicating that this structure exerts an important role in the adhesion and subsequent formation of cells aggregates (Garcia-Rivera et al., 2004; Martinez and Casadevall, 2005). Since a putative CAP59 (Protein ID: 4796) and CAP10 (Protein ID: 7100) were detected in WP1, the genome sequence of non-pathogenic encapsulated yeast would be interesting for a comparative analysis between the capsule synthesis in WP1 and *C. neoformans*.

Finally, the WP1 genome was data-mined for functional domains related to notable antitoxin systems. A set of antitoxin systems including multi antimicrobial extrusion protein (MATE), multidrug resistance efflux transporters (EmrE) and putative proteins with a multidrug resistance protein MdtG (IPR001958) domain was observed in the WP1 genome. The WP1 capsule in conjunction with these antitoxin systems represent important features that may be important for competition against other endophytes, plant colonization, and survival under different biotic and abiotic stresses.

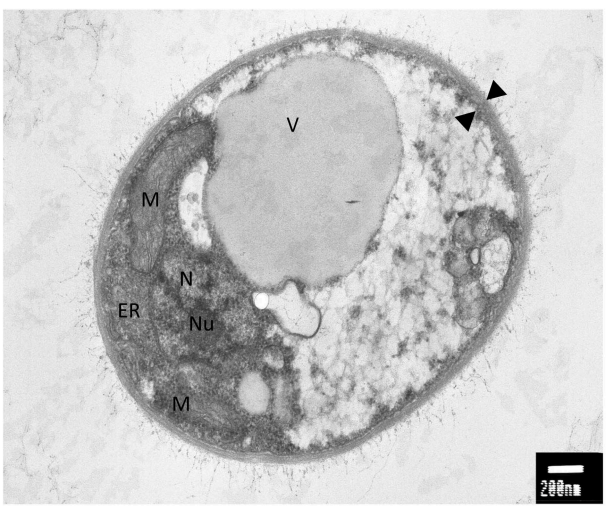

FIGURE 1 | Electron microscopy analysis of *Rhodotorula graminis* strain WP1; M, mitochondria; ER, endoplasmic reticulum; N, nucleus; Nu, nucleulus; V, vacuole; black triangles, capsule. Photo credit: Prof. Jimmie Lara, Department of Microbiology, University of Washington.

Other Symbiotic Traits

Endophytes often share in common sets of genes that are thought to confer symbiotic abilities (Sessitsch et al., 2012; Bulgarelli et al., 2013). These beneficial genes could be acquired by horizontal gene transfer (HGT) (Taghavi et al., 2005; Aminov, 2011). There has been some indication of HGT between bacteria and fungi (Marcet-Houben and Gabaldon, 2010). However, when compared via BLAST against other databases of endophyte-associate genes (Sessitsch et al., 2012), WP1 shares only minimal homology with a few highly conserved bacterial endophyte genes such as catalase (Protein ID: 47984), as well as a gene involved in cofactor-A transport (Protein ID: 66591), and a glutathione S-transferase family protein (Protein ID: 54692). All of these matches, however, are all core metabolism/housekeeping proteins, and had less than 50% identity to the bacterial query proteins. Additionally, the WP1 genome was run through an in-house pipeline designed to identify genes acquired via transdomain HGT (Thomas, unpublished), but the results were negative. This lack of significant evidence of HGT could suggest that this endophytic yeast evolved most of its plant interaction and symbiosis genes independently from its bacterial counterparts. The well-studied symbiotic Basidiomycota, *Laccaria bicolor*, begins the colonization of poplar roots using an array of effector proteins known as mycorrhiza-induced-cysteine-rich SSPs (MiSSPs) (Martin et al., 2008). A domain of the WP1 mRNA splicing factor Prp8 (ProteinID 49541) is partially homologous to the *L. bicolor* LbMiSSP17 effector protein (Protein ID: 332226). Otherwise, no homology with the other 22 *L. bicolor* MiSSPs exists. Despite the fact that both WP1 and *L. bicolor* are both Basidiomycetes which symbiotically colonize poplar, this lack of homology could suggest WP1 uses an entirely different signaling pathway to communicate with the host.

Conclusions

There is a growing interest in the plant microbiome and its impacts on plant health and growth. With the sequence of the poplar genome (Tuskan et al., 2006) and multiple studies of the poplar microbiome (Hacquard and Schadt, 2015), poplar can become a model system for studying tree-microbiome interactions. The *Laccaria-Populus* interaction is a well-studied mycorrhizal mutualism at the molecular level (Podila et al., 2009; Aminov, 2011; Larsen et al., 2011; Plett et al., 2015). With comparative genomics studies of the bacteria, mycorrhizae, and yeast associated with *Populus*, an understanding of common themes in plant-mutualist interactions may emerge.

Data Access

The genome version discussed in this paper is the *Rhodotorula graminis* strain WP1 v1.1. Assembled scaffolds and all predicted genes and annotations are available at JGI fungal genome portal

Mycocosm (http://genome.jgi.doe.gov/Rhoba1_1) and deposited to GenBank under accession JTAO00000000.

Acknowledgments

The work conducted by the U.S. Department of Energy Joint Genome Institute is supported by the Office of Science of the U.S. DOE under contract DE-AC02-05 CH11231. Partial research support was provided by NSF SGER # 0838091, NIFA grant # 2012-00931, AFRI grant # 2010-05080, and the Byron and Alice Lockwood Professorship. We thank Prof. Jim Lara for the electron microscopy figure, Shaoqun (Simon) Zhou and Dr. James H. Thomas for helpful discussions, and Dr. Stephen Mondo for assistance with the GenBank submission.

References

Aminov, R. I. (2011). Horizontal gene exchange in environmental microbiota. *Front. Microbiol.* 2:158. doi: 10.3389/fmicb.2011.00158

Ashburner, M., Ball, C. A., Blake, J. A., Botstein, D., Butler, H., Cherry, J. M., et al. (2000). Gene ontology: tool for the unification of biology. The gene ontology consortium. *Nat. Genet*. 25, 25–29. doi: 10.1038/75556

Atsumi, S., Li, Z., and Liao, J. C. (2009). Acetolactate synthase from Bacillus subtilis serves as a 2-ketoisovalerate decarboxylase for isobutanol biosynthesis in Escherichia coli. *Appl. Environ. Microbiol.* 75, 6306–6311. doi: 10.1128/AEM.01160-09

Banno, I. (1967). Studies on the sexuality of Rhodotorula. *J. Gen. Appl. Microbiol*. 13, 167–196.

Bertalan, M., Albano, R., de, P. V., Rouws, L., Rojas, C., Hemerly, A., et al. (2009). Complete genome sequence of the sugarcane nitrogen-fixing endophyte Gluconacetobacter diazotrophicus Pal5. *BMC Genomics* 10:450. doi: 10.1186/1471-2164-10-450

Bhasi, A., Pandey, R. V., Utharasamy, S. P., and Senapathy, P. (2007). EuSplice: a unified resource for the analysis of splice signals and alternative splicing in eukaryotic genes. *Bioinformatics* 23, 1815–1823. doi: 10.1093/bioinformatics/btm084

Birney, E., and Durbin, R. (2000). Using GeneWise in the Drosophila annotation experiment. *Genome. Res*. 10, 547–548. doi: 10.1101/gr.10.4.547

Boeckmann, B., Bairoch, A., Apweiler, R., Blatter, M. C., Estreicher, A., Gasteiger, E., et al. (2003). The SWISS-PROT protein knowledgebase and its supplement TrEMBL in 2003. *Nucleic Acids Res.* 31, 365–370. doi: 10.1093/nar/gkg095

Bulgarelli, D., Schlaeppi, K., Spaepen, S., Ver Loren van, T. E., and Schulze-Lefert, P. (2013). Structure and functions of the bacterial microbiota of plants. *Annu. Rev. Plant Biol*. 64, 807–838. doi: 10.1146/annurev-arplant-050312-120106

D'Alessandro, M., Erb, M., Ton, J., Brandenburg, A., Karlen, D., Zopfi, J., et al. (2014). Volatiles produced by soil-borne endophytic bacteria increase plant pathogen resistance and affect tritrophic interactions. *Plant Cell Environ*. 37, 813–826. doi: 10.1111/pce.12220

Doty, S. L. (2011). "Growth-promoting endophytic fungi of forest trees," in *Endophytes of Forest Trees: Biology and Applications*, eds A. M. Pirttilä and A. C. Carolin (Dordrecht; Heidelberg; London, UK; New York, NY: Springer), 151–156.

Doty, S. L. (2014). *Endophytic Yeast Strains, Methods for Ethanol and Xylitol Production, Methods for Biological Nitrogen Fixation, and a Genetic Source for Improvement of Industrial Strains*. Patent No. 8,728,781.

Duca, D., Lorv, J., Patten, C. L., Rose, D., and Glick, B. R. (2014). Indole-3-acetic acid in plant-microbe interactions. *Anton. Leeuwen.* 106, 85–125. doi: 10.1007/s10482-013-0095-y

Emanuelsson, O., Nielsen, H., Brunak, S., and von, H. G. (2000). Predicting subcellular localization of proteins based on their N-terminal amino acid sequence. *J. Mol. Biol*. 300, 1005–1016. doi: 10.1006/jmbi.2000.3903

Farrow, S. C., and Facchini, P. J. (2014). Functional diversity of 2-oxoglutarate/Fe(II)-dependent dioxygenases in plant metabolism. *Front. Plant Sci.* 5:524. doi: 10.3389/fpls.2014.00524

Fouts, D. E., Tyler, H. L., DeBoy, R. T., Daugherty, S., Ren, Q., Badger, J., et al. (2008). Complete genome sequence of the N2-fixing broad host range endophyte Klebsiella pneumoniae 342 and virulence predictions verified in mice. *PLoS. Genet*. 4:e1000141. doi: 10.1371/journal.pgen.1000141

Fu, J., and Wang, S. (2011). Insights into auxin signaling in plant-pathogen interactions. *Front. Plant Sci.* 2:74. doi: 10.3389/fpls.2011.00074

García-Rivera, J., Chang, Y. C., Kwon-Chung, K. J., and Casadevall, A. (2004). Cryptococcus neoformans CAP59 (or Cap59p) is involved in the extracellular trafficking of capsular glucuronoxylomannan. *Eukaryot. Cell* 3, 385–392. doi: 10.1128/EC.3.2.385-392.2004

Grigoriev, I. V., Martinez, D. A., and Salamov, A. A. (2006). Fungal genomic annotation. *Appl. Mycol. Biotechnol.* 6, 123–142. doi: 10.1016/S1874-5334(06)80008-0

Grigoriev, I. V., Nikitin, R., Haridas, S., Kuo, A., Ohm, R., Otillar, R., et al. (2014). MycoCosm portal: gearing up for 1000 fungal genomes. *Nucleic Acids Res*. 42, D699–D704. doi: 10.1093/nar/gkt1183

Hacquard, S., and Schadt, C. W. (2015). Towards a holistic understanding of the beneficial interactions across the Populus microbiome. *New Phytol*. 205, 1424–1430. doi: 10.1111/nph.13133

Hardoim, P. R., van Overbeek, L. S., and Elsas, J. D. (2008). Properties of bacterial endophytes and their proposed role in plant growth. *Trends Microbiol.* 16, 463–471. doi: 10.1016/j.tim.2008.07.008

Howden, A. J., Harrison, C. J., and Preston, G. M. (2009). A conserved mechanism for nitrile metabolism in bacteria and plants. *Plant J*. 57, 243–253. doi: 10.1111/j.1365-313X.2008.03682.x

Howden, A. J., and Preston, G. M. (2009). Nitrilase enzymes and their role in plant-microbe interactions. *Microb. Biotechnol*. 2, 441–451. doi: 10.1111/j.1751-7915.2009.00111.x

Jaffe, D. B., Butler, J., Gnerre, S., Mauceli, E., Lindblad-Toh, K., Mesirov, J., et al. (2003). Whole-genome sequence assembly for mammalian genomes: arachne 2. *Genome. Res*. 13, 91–96. doi: 10.1101/gr.828403

Johnston-Monje, D., and Raizada, M. N. (2011). Conservation and diversity of seed associated endophytes in Zea across boundaries of evolution, ethnography and ecology. *PLoS ONE* 6:e20396. doi: 10.1371/journal.pone.0020396

Jurka, J., Kapitonov, V. V., Pavlicek, A., Klonowski, P., Kohany, O., and Walichiewicz, J. (2005). Repbase Update, a database of eukaryotic repetitive elements. *Cytogenet. Genome. Res*. 110, 462–467. doi: 10.1159/000084979

Kanehisa, M., Goto, S., Kawashima, S., Okuno, Y., and Hattori, M. (2004). The KEGG resource for deciphering the genome. *Nucleic Acids Res*. 32, D277–D280. doi: 10.1093/nar/gkh063

Khan, Z., Guelich, G., Phan, H., Redman, R. S., and Doty, S. L. (2012). Bacterial and yeast endophytes from poplar and willow promote growth in crop plants and grasses. *ISRN Agron.* 2012:890280. doi: 10.5402/2012/890280

Knoth, J., Kim, S.-H., Ettl, G., and Doty, S. L. (2013). Effects of cross host species inoculation of nitrogen-fixing endophytes on growth and leaf physiology of maize. *GCB Bioenery* 5, 408–418. doi: 10.1111/gcbb.12006

Knoth, J. L., Kim, S. H., Ettl, G. J., and Doty, S. L. (2014). Biological nitrogen fixation and biomass accumulation within poplar clones as a result of inoculations with diazotrophic endophyte consortia. *New Phytol*. 201, 599–609. doi: 10.1111/nph.12536

Koonin, E. V., Fedorova, N. D., Jackson, J. D., Jacobs, A. R., Krylov, D. M., Makarova, K. S., et al. (2004). A comprehensive evolutionary classification of proteins encoded in complete eukaryotic genomes. *Genome. Biol*. 5:R7. doi: 10.1186/gb-2004-5-2-r7

Larsen, P. E., Sreedasyam, A., Trivedi, G., Podila, G. K., Cseke, L. J., and Collart, F. R. (2011). Using next generation transcriptome sequencing to predict an ectomycorrhizal metabolome. *BMC Syst. Biol*. 5:70. doi: 10.1186/1752-0509-5-70

Lengeler, K. B., Davidson, R. C., D'souza, C., Harashima, T., Shen, W. C., Wang, P., et al. (2000). Signal transduction cascades regulating fungal development and virulence. *Microbiol. Mol. Biol. Rev*. 64, 746–785. doi: 10.1128/MMBR.64.4.746-785.2000

Lowe, T. M., and Eddy, S. R. (1997). tRNAscan-SE: a program for improved detection of transfer RNA genes in genomic sequence. *Nucleic Acids Res*. 25, 955–964. doi: 10.1093/nar/25.5.0955

Marcet-Houben, M., and Gabaldon, T. (2010). Acquisition of prokaryotic genes by fungal genomes. *Trends Genet*. 26, 5–8. doi: 10.1016/j.tig.2009.11.007

Martin, F., Aerts, A., Ahren, D., Brun, A., Danchin, E. G., Duchaussoy, F., et al. (2008). The genome of Laccaria bicolor provides insights into mycorrhizal symbiosis. *Nature* 452, 88–92. doi: 10.1038/nature06556

Martinez, L. R., and Casadevall, A. (2005). Specific antibody can prevent fungal biofilm formation and this effect correlates with protective efficacy. *Infect. Immun*. 73, 6350–6362. doi: 10.1128/IAI.73.10.6350-6362.2005

Melén, K., Krogh, A., and von, H. G. (2003). Reliability measures for membrane protein topology prediction algorithms. *J. Mol. Biol*. 327, 735–744. doi: 10.1016/S0022-2836(03)00182-7

Mitchell, T. G., and Perfect, J. R. (1995). Cryptococcosis in the era of AIDS–100 years after the discovery of *Cryptococcus neoformans*. *Clin. Microbiol. Rev*. 8, 515–548.

Murashige, T., and Skoog, F. (1962). A revised medium for rapid growth and bioassays with tobacco tissue culture. *Physiol. Plant* 15, 473–497. doi: 10.1111/j.1399-3054.1962.tb08052.x

Nagy, L. G., Ohm, R. A., Kovács, G. M., Floudas, D., Riley, R., Gácser, A., et al. (2014). Latent homology and convergent regulatory evolution underlies the repeated emergence of yeasts. *Nat. Commun*. 5, 4471. doi: 10.1038/ncomms5471

Nassar, A. H., El-Tarabily, K. A., and Sivasithamparam, K. (2005). Promotion of plant growth by an auxin-producing isolate of the yeast Williopsis saturnus endophytic in maize (Zea mays L.) roots. *Biol. Fertil. Soils* 42, 97–108. doi: 10.1007/s00374-005-0008-y

Nielsen, H., Engelbrecht, J., Brunak, S., and von, H. G. (1997). Identification of prokaryotic and eukaryotic signal peptides and prediction of their cleavage sites. *Protein Eng*. 10, 1–6. doi: 10.1093/protein/10.1.1

Patten, C. L., and Glick, B. R. (2002). Role of Pseudomonas putida indoleacetic acid in development of the host plant root system. *Appl. Environ. Microbiol.* 68, 3795–3801. doi: 10.1128/AEM.68.8.3795-3801.2002

Pendleton, A. L., Smith, K. E., Feau, N., Martin, F. M., Grigoriev, I. V., Hamelin, R., et al. (2014). Duplications and losses in gene families of rust pathogens highlight putative effectors. *Front. Plant Sci.* 5:299. doi: 10.3389/fpls.2014.00299

Pitkin, J. W., Panaccione, D. G., and Walton, J. D. (1996). A putative cyclic peptide efflux pump encoded by the TOXA gene of the plant-pathogenic fungus Cochliobolus carbonum. *Microbiology* 142(Pt 6), 1557–1565. doi: 10.1099/13500872-142-6-1557

Plett, J. M., Tisserant, E., Brun, A., Morin, E., Grigoriev, I. V., Kuo, A., et al. (2015). The mutualist laccaria bicolor expresses a core gene regulon during the colonization of diverse host plants and a variable regulon to counteract host-specific defenses. *Mol. Plant Microbe Interact*. 28, 261–273. doi: 10.1094/MPMI-05-14-0129-FI

Podila, G. K., Sreedasyam, A., and Muratet, M. (2009). *Populus* rhizosphere and the ectomycorrhizal interactome. *Crit. Rev. Plant Sci*. 28, 359–367. doi: 10.1080/07352680903241220

Prescott, A. G., and Lloyd, M. D. (2000). The iron(II) and 2-oxoacid-dependent dioxygenases and their role in metabolism. *Nat. Prod. Rep*. 17, 367–383. doi: 10.1039/a902197c

Price, A. L., Jones, N. C., and Pevzner, P. A. (2005). De novo identification of repeat families in large genomes. *Bioinformatics* 21(Suppl. 1), i351–i358. doi: 10.1093/bioinformatics/bti1018

Quevillon, E., Silventoinen, V., Pillai, S., Harte, N., Mulder, N., Apweiler, R., et al. (2005). InterProScan: protein domains identifier. *Nucleic Acids Res*. 33, W116–W120. doi: 10.1093/nar/gki442

Rafiqi, M., Jelonek, L., Akum, N. F., Zhang, F., and Kogel, K. H. (2013). Effector candidates in the secretome of Piriformospora indica, a ubiquitous plant-associated fungus. *Front. Plant Sci.* 4:228. doi: 10.3389/fpls.2013.00228

Ramage, G., Mowat, E., Jones, B., Williams, C., and Lopez-Ribot, J. (2009). Our current understanding of fungal biofilms. *Crit. Rev. Microbiol.* 35, 340–355. doi: 10.3109/10408410903241436

Rogozin, I. B., and Milanesi, L. (1997). Analysis of donor splice sites in different eukaryotic organisms. *J. Mol. Evol*. 45, 50–59. doi: 10.1007/PL00006200

Salamov, A. A., and Solovyev, V. V. (2000). Ab initio gene finding in Drosophila genomic DNA. *Genome. Res*. 10, 516–522. doi: 10.1101/gr.10.4.516

Sessitsch, A., Hardoim, P., Döring, J., Weilharter, A., Krause, A., Woyke, T., et al. (2012). Functional characteristics of an endophyte community colonizing rice roots as revealed by metagenomic analysis. *Mol. Plant Microbe Interact*. 25, 28–36. doi: 10.1094/MPMI-08-11-0204

Smit, A. F. A., Hubley, R., and Green, P. (2010). *Repeat Masker Open-3.0*. Available online at: http://www.repeatmasker.org

Spatafora, J. W., Stajich, J. E., and Grigoriev, I. (2013). 1000 fungal genomes project. *Phytopathology* 103, 137. Available online at: http://1000.fungalgenomes.org/home/webcite

Sukumar, P., Legué, V., Vayssierès, A., Martin, F., Tuskan, G. A., and Kalluri, U. C. (2013). Involvement of auxin pathways in modulating root architecture during beneficial plant-microorganism interactions. *Plant Cell Environ*. 36, 909–919. doi: 10.1111/pce.12036

Taghavi, S., Barac, T., Greenberg, B., Borremans, B., Vangronsveld, J., and van der Lelie, D. (2005). Horizontal gene transfer to endogenous endophytic bacteria from poplar improves phytoremediation of toluene. *Appl. Environ. Microbiol*. 71, 8500–8505. doi: 10.1128/AEM.71.12.8500-8505.2005

Taghavi, S., van der Lelie, D., Hoffman, A., Zhang, Y. B., Walla, M. D., Vangronsveld, J., et al. (2010). Genome sequence of the plant growth promoting endophytic bacterium *Enterobacter* sp. 638. *PLoS. Genet*. 6:e1000943. doi: 10.1371/journal.pgen.1000943

Taghavi, S., Wu, X., Ouyang, L., Zhang, Y. B., Stadler, A., McCorkle, S., et al. (2015). Transcriptional responses to sucrose mimic the plant-associated life style of the plant growth promoting endophyte *Enterobacter* sp. 638. *PLoS ONE* 10:e0115455. doi: 10.1371/journal.pone.0115455

Ter-Hovhannisyan, V., Lomsadze, A., Chernoff, Y. O., and Borodovsky, M. (2008). Gene prediction in novel fungal genomes using an ab initio algorithm with unsupervised training. *Genome. Res*. 18, 1979–1990. doi: 10.1101/gr.081612.108

Tuskan, G. A., Difazio, S., Jansson, S., Bohlmann, J., Grigoriev, I., Hellsten, U., et al. (2006). The genome of black cottonwood, Populus trichocarpa (Torr. & Gray). *Science* 313, 1596–1604. doi: 10.1126/science.1128691

Witzel, K., Gwinn-Giglio, M., Nadendla, S., Shefchek, K., and Ruppel, S. (2012). Genome sequence of Enterobacter radicincitans DSM16656(T), a plant growth-promoting endophyte. *J. Bacteriol*. 194, 5469. doi: 10.1128/JB.01193-12

Xin, G., Glawe, D., and Doty, S. L. (2009). Characterization of three endophytic, indole-3-acetic acid-producing yeasts occurring in Populus trees. *Mycol. Res.* 113, 973–980. doi: 10.1016/j.mycres.2009.06.001

Xu, P., Bura, R., and Doty, S. L. (2011). Genetic analysis of D-xylose metabolism by endophytic yeast strains of *Rhodotorula graminis* and *Rhodotorula mucilaginosa*. *Genet. Mol. Biol*. 34, 471–478. doi: 10.1590/S1415-47572011000300018

Zhao, Z., Zhang, Y., Liu, X., Zhang, X., Liu, S., Yu, X., et al. (2013). A role for a dioxygenase in auxin metabolism and reproductive development in rice. *Dev. Cell* 27, 113–122. doi: 10.1016/j.devcel.2013.09.005

Conflict of Interest Statement: The authors declare that the research was conducted in the absence of any commercial or financial relationships that could be construed as a potential conflict of interest.

frontiers in Microbiology

ORIGINAL RESEARCH
published: 21 May 2015
doi: 10.3389/fmicb.2015.00491

Genome wide transcriptional profiling of *Herbaspirillum seropedicae* SmR1 grown in the presence of naringenin

*Michelle Z. Tadra-Sfeir[1], Helisson Faoro[1,2], Doumit Camilios-Neto[3], Liziane Brusamarello-Santos[1], Eduardo Balsanelli[1], Vinicius Weiss[1], Valter A. Baura[1], Roseli Wassem[4], Leonardo M. Cruz[1], Fábio De Oliveira Pedrosa[1], Emanuel M. Souza[1] and Rose A. Monteiro[1]**

[1] Nitrogen Fixation group, Department of Biochemistry and Molecular Biology, Universidade Federal do Paraná, Curitiba, Brazil, [2] Instituto Carlos Chagas, Fundação Oswaldo Cruz, Fiocruz-PR, Curitiba, Brazil, [3] Department of Biochemistry and Biotechnology, Universidade Estadual de Londrina, Londrina, Brazil, [4] Department of Genetics, Universidade Federal do Paraná, Curitiba, Brazil

OPEN ACCESS

Edited by:
Carolin Frank,
University of California, Merced, USA

Reviewed by:
David Baltrus,
University of Arizona, USA
Yumiko Sakuragi,
University of Copenhagen, Denmark

***Correspondence:**
Rose A. Monteiro,
Department of Biochemistry and Molecular Biology, Centro Politecnico - Setor de Ciências Biológicas, Universidade Federal do Paraná, C. Postal 19046, CEP81531980, Curitiba, PR, Brazil
roseadele@gmail.com

Specialty section:
This article was submitted to Plant-Microbe Interaction, a section of the journal Frontiers in Microbiology

Received: 29 January 2015
Accepted: 04 May 2015
Published: 21 May 2015

Citation:
Tadra-Sfeir MZ, Faoro H, Camilios-Neto D, Brusamarello-Santos L, Balsanelli E, Weiss V, Baura VA, Wassem R, Cruz LM, De Oliveira Pedrosa F, Souza EM and Monteiro RA (2015) Genome wide transcriptional profiling of Herbaspirillum seropedicae SmR1 grown in the presence of naringenin. Front. Microbiol. 6:491. doi: 10.3389/fmicb.2015.00491

Herbaspirillum seropedicae is a diazotrophic bacterium which associates endophytically with economically important *gramineae*. Flavonoids such as naringenin have been shown to have an effect on the interaction between *H. seropedicae* and its host plants. We used a high-throughput sequencing based method (RNA-Seq) to access the influence of naringenin on the whole transcriptome profile of *H. seropedicae.* Three hundred and four genes were downregulated and seventy seven were upregulated by naringenin. Data analysis revealed that genes related to bacterial flagella biosynthesis, chemotaxis and biosynthesis of peptidoglycan were repressed by naringenin. Moreover, genes involved in aromatic metabolism and multidrug transport efflux were actived.

Keywords: *H. seropedicae*, naringenin, RNAseq, plant-bacteria interaction, transcription regulation

Introduction

Beneficial plant–bacterial interactions promote plant growth and development. During this process molecular changes occur in both partners, and signal molecules are involved in partner communication. In legume-*Rhizobium* interactions, flavonoids released by plant roots induce sets of genes involved in nodulation (Broughton et al., 2000). In addition, flavonoids seem to play a role in other plant bacterial associations. Naringenin stimulates lateral root crack (LRC) colonization of *Arabidopsis thaliana* by *Azorhizobium caulinodans* and *H. seropedicae* a process independent of the *nod* genes (Gough et al., 1997). This flavonoid, secreted by some plants, is a signal molecule that regulates gene expression in bacteria such as *H. seropedicae* (Tadra-Sfeir et al., 2011) and *A. caulinodans* (Webster et al., 1998).

The diazotroph *H. seropedicae* is frequently found in endophytic association with maize (*Zea mays*), rice (*Oryza sativa*), sorghum (*Sorghum bicolor*), sugar cane (*Saccharum officinarum*) and other plants. Inoculation of rice with *H. seropedicae* strains resulted in plant growth promotion and increase in productivity (Baldani et al., 2000; Gyaneshwar et al., 2002). This effect may be due in part to transfer of fixed nitrogen, since ^{15}N dilution assays indicate significant N transfer to the host plant (Baldani et al., 2000), and production of phytohormones by the bacteria (Bastián et al., 1998). However, the bacterial genes necessary for the establishment of endophytic interaction

and the molecular cues that direct their expression are largely unkown. Previously, we isolated 16 *H. seropedicae* mutant strains in genes regulated by the plant-derived flavonoid naringenin; 12 of these were downregulated and 4 upregulated. Four of these genes are involved in the synthesis of the outer membrane of the cell wall, suggesting that changes in the cell surface probably occur during the interaction between *H. seropedicae* and its host plants (Tadra-Sfeir et al., 2011).

To explore which other genes are regulated by naringenin, we determined the transcriptional profile of *H. seropedicae* grown in NFBHP malate medium in the presence or absence of naringenin using RNA-seq.

Materials and Methods

Bacterial Growth

H. seropedicae SmR1, a streptomycin resistant strain, was grown at 30°C and 120 rpm in NFbHPN medium (Klassen et al., 1997) in the presence (+Nar) or absence (–Nar) of 100 μM of naringenin containing streptomycin (80 $\mu g.mL^{-1}$)for 6 h (optical density at 600 nm of 0.8).

Transcriptome Profiling Experiments Design and Analyses

The total RNA was isolated using RiboPure™-Bacteria Kit (Ambion) and treated with DNase I (Ambion) for removal of the remaining genomic DNA. Seven micrograms of total RNA were rRNA-depleted using two rounds of the MICROBExpress™ Bacterial mRNA Enrichment Kit (Ambion). The efficiency of the depletion was evaluated in agarose gel 1% and all RNA preparations were quantified with a Nanodrop 1000 spectrophotometer. After rRNA depletion, 500 ng of depleted rRNA was used to construct the sequencing libraries following standard protocols using the SOLiD Total RNA-Seq Kit (Life Technologies). The libraries were barcoded by using the SOLiD Transcriptome Multiplexing Kit (Life Technologies). The emulsion PCR and SOLiD sequencing were performed according to standard Life Technologies protocols. Two independent samples were used to prepare replicate libraries resulting in a total of 4 libraries. Mapping of the reads against the *H. seropedicae* genome sequence, data processing and statistical analysis were performed using the CLC Genomics Workbench 5.1 and the results were expressed in RPKM (Reads Per Kilobase of exon model per Million mapped reads) (Mortazavi et al., 2008). The sequence data are available in the ArrayExpress database (www.ebi.ac.uk/arrayexpress) under accession number E-MTAB-3435.

A gene was considered expressed when read coverage was equal to or higher than 3-fold, and differentially expressed when RPKM value was 2-fold higher/smaller in +Nar compared to -Nar and *p*-value higher than 0.05 by the Baggerley's test as implemented in CLC Workbench. The Baggerley's test (Baggerly et al., 2003) compares the proportion of counts in a group of replicates (+Nar) against those of another group of replicates (−Nar), comprising a weighted *t*-type test statistic. The samples are given different weights depending on their sizes (total counts). The weights are obtained by assuming a Beta distribution on the proportions in a group, and estimating these, along with the proportion of a binomial distribution, by the method of moments. RNAseq statistical analyses were also made using the R package DESeq, which performs a negative binomial distribution and a shrinkage estimator for the distribution's variance and size-factor normalization (Anders and Huber, 2010).

Motility Assay

The motility assay was performed on NFbHPN-malate semi-solid agar (0.25%) plates supplemented with 100 μM naringenin. Overnight culture of *H. seropedicae* was inoculated in the center of the plate and incubated at 30°C. The plates were photographed after 12 h and motility halos were measured by using ImageJ (Rasband, 1997). Ten replicates with 10^8 bacteria were inoculated in both plates.

RT-qPCR

For validation with RT-qPCR, total RNA was isolated from cultures grown in the presence and absence of naringenin (100 μM) using the Ribominus (Ambion), the cDNAs were synthesized using the High-capacity cDNA Reverse Transcription kit (Applied Biosystems), and quantified using the Power SYBR-Green PCR Master Mix on a Step One Plus Real Time-PCR System (Applied Biosystems). The Primer express 3.0 software was used to design the primers. The 16S rRNA gene was used as internal control, and the relative gene expression was determined using the $2^{-\Delta\Delta Ct}$ method (Livak and Schmittgen, 2008).

Colonization Assay

H. seropedicae SmR1 cells were grown in NFbHPN medium at 30°C, 120 rpm, until $OD_{600nm} = 1$. The culture was diluted to $OD_{600nm} = 0.2$ in fresh medium, and grown in the same conditions in the presence or absence of 100 μM naringenin for 6 h. These cells were washed with saline buffer and 10^5 cells were inoculated per maize plantlet (samples in triplicate). Quantification of bacterial root endophytic populations was performed according to Balsanelli et al. (2013), every 12 h until 3 days after inoculation. Endophytic bacteria at time zero is too low to count (REF).

Results and Discussion

Early *Herbaspirillum* seropedicae Smr1 Maize Root Colonization Is Stimulated by Naringenin

Flavonoids constitute a large part of root exudates (Cesco et al., 2010), being involved in root colonization. Previously results showed that the plant-derived flavonoid naringenin regulated the expression of *H. seropedicae* genes. Maize roots were inoculated with *H. seropedicae* in the presence of naringenin (100 μM) to determine the effect of this flavonoid in colonization pattern. The results showed that the endophytic population in the first 36 h is higher in the presence of naringenin (**Figure 1**). After 36 h the endophytic population is the same in the absence and in the presence of naringenin. These results indicate that naringenin affects early endophytic colonization. Naringenin stimulation of

root colonization was also observed during the colonization of *Arabidopsis thaliana* by *H. seropedicae* (Gough et al., 1997), and wheat by *Azorhizobium caulinodans* (Webster et al., 1998).

Changes in the *Herbaspirillum seropedicae* SmR1 Transcriptome in Response to Naringenin

RNA-seq profiling of *H. seropedicae* cells grown in the presence (+Nar) or absence (−Nar) of 100 μM of naringenin for 6 h was performed as described in Bacterial growth in Material and Methods. Sixty four million and fifty eight million reads were obtained for −Nar and +Nar conditions, respectively, and of those 2.7 million and 2.5 million were mapped uniquely to the *H. seropedicae* genome. As expected, biological replicates showed a very high level of correlation ($r^2 > 0.97$) (**Table 1**), thus all the libraries of each condition were used for further analysis.

The genes that showed fold change greater than 2.0 (+Nar relative to −Nar) and a $p = 0.05$ were considered to be regulated by naringenin. Three hundred and four genes were downregulated and 77 were upregulated by naringenin by CLC Workbench. Fifty-three percent of these were also differentially regulated by the DESeq analysis (Table S1). The regulation of *flhB*, *flgE*, Hsero_2564 and *murF* genes are confirmed by qPCR (**Table 2**). Some genes with fold changes marginally lower than 2.0 fold or p higher than 0.05 were also considered regulated if neighborhood analysis suggested that they are part of an operon with genes regulated according to the previous criteria. The majority of the upregulated genes belong to the following functional gene categories: lipid transport and metabolism, energy production and conversion, inorganic ion transport and metabolism and unknown function (**Figure 2A**). The downregulated genes belong mainly to the categories aminoacid transport and metabolism, carbohydrate transport and metabolism, motility and unknown function (**Figure 2B**).

We found some groups of genes whose expression were regulated based on both CLC Workbench and DESeq analyses by naringenin that may be involved in plant-bacterial interaction. These genes are mainly involved with cell wall and motility. We also noticed an increase in the expression of genes that could be involved in naringenin degradation.

H. seropedicae Cell Wall Is Altered in the Presence of Naringenin

Peptidoglycan is an essential component for synthesis of the bacterial cell wall and the biosynthesis of this molecule is

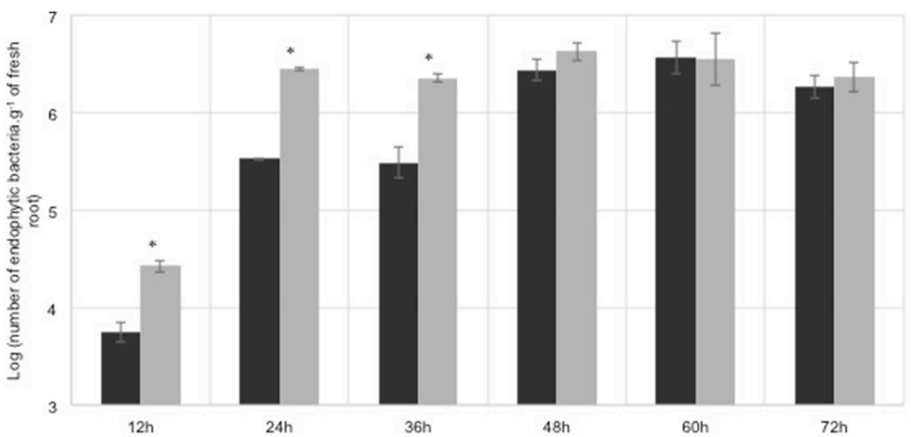

FIGURE 1 | Maize root endophytic colonization by *H. seropedicae* wild-type. *H. seropedicae* SmR1 cells were grown in the presence (gray bars) or absence (black bars) of 100 μM naringenin for 6 h, and 10^5 cells were inoculated on maize plantlets. The number of root endophytic bacteria was determined after the periods indicated. Results are shown as means of Log_{10} (number of endophytic bacteria.g^{-1} of fresh root) ± standard deviation. Asterisk indicates significant differences at $p < 0.0083$ (Student *t*-test with Bonferroni correction) of endophytic colonization between naringenin treated and non-treated bacteria.

TABLE 1 | Summary of RNA-seq data.

Sample	Reads in biological replicates	Total reads	Reads mapped unambiguously[a]	Total reads mapped unambiguously replicates	Correlation (R^2)
−Naringenin 1	34,539,083	64,757,598	1,429,789	2,718,964	0.97
−Naringenin 2	30,218,515		1,289,175		
+Naringenin 1	14,525,262	58,754,928	683,731	2,478,145	0.98
+Naringenin 2	32,189,749		1,029,225		
+Naringenin 3	12,039,917		765,189		

[a] *The reads were uniquely mapped to the H. seropedicae genome using CLC Genomics Workbench 5.1 will 90% of minimum length and 80% of similarity. The numbers 1 and 2 refer to biological replicates and the number 3 is technical replicate of the condition +Naringenin.*

a complex process that proceeds in several stages (Ramos et al., 2004; Patin et al., 2010; Muchova et al., 2011). The assembly of the peptidoglycan involves, the Mur ligases (MurC, MurD, MurE, and MurF) that catalyze the first step of the synthesis the UDP-N-acetylmuramoyl-pentapeptide precursor (Patin et al., 2010). Three genes that encode the enzymes MurC, MurD, and MurF were downregulated in the presence of naringenin (**Figure 3**). Other *mur* genes were also inhibited by naringenin such as genes encoding the enzymes MraY and MurG (**Figure 3**). MraY catalyzes the transfer of the phospho-N-acetyl-muramoyl-pentapeptide from UDP-N-acetyl-muramoyl-pentapeptide to a membrane acceptor to form lipid I. The final step of the peptidoglycan subunit biosynthesis is the addition of N-acetylglucosamine (GlcNAc) to lipid I catalyzed by MurG producing lipid II (Muchova et al., 2011).

Interestingly the genes *ddlB* and *ftsQAZ* were also downregulated by naringenin and found in the same operon as the *mur* genes (**Figure 3**, Figure S1A). D-Alanine–D-alanine ligase (coded by *ddlB*) is an enzyme involved in peptidoglycan biosynthesis and the proteins FtsQ, FtsA, and FtsZ are involved in septum formation in cell-division (Jofré et al., 2009). Mutations in *ddlB* and *ftsQAZ* genes in *Azospirillum brasilense* resulted in overproduction of exopolysaccharides, decreased bacterial tolerance to saline stress and alteration in cell morphology (Jofré et al., 2009).

A decrease in level of peptidoglycan synthesis enzyme GlmU was observed in the proteome of *H. seropedicae* grown in the presence of sugarcane extract (Cordeiro et al., 2013). In our study the expression of *glmU* was slightly decreased (−1.3-fold, $p = 0$) in the presence of naringenin, a decrease similar to that was observed by RT-PCR (-1.6-fold) in *H. seropedicae* grown in the presence of the sugarcane extract (Cordeiro et al., 2013). Peptidoglycan may act as elicitors of plant innate immunity, being recognized as a microbe-associated molecular pattern (MAMP) (Erbs and Newman, 2012). For example purified peptidoglycans from *Xanthomonas campestris* pv. *Campestris* and *Agrobacterium tumefaciens* act as MAMPs, inducing immune responses in *Arabidopsis thaliana*. The results suggest that the *H. seropedicae* is capable of controlling peptidoglycan synthesis in response to plant signals. A similar strategy has been described for *Listeria monocytogenes* that can N-deacetylate its peptidoglycan, avoiding the recognition and killing by host cells (Boneca et al., 2007). *Agrobacterium tumefaciens* also alters its peptidoglycan to reduce elicitation of plant defense (Erbs et al., 2008). Tadra-Sfeir et al. (2011) showed that the *ampG* gene of *H. seropedicae* is downregulated by naringenin), and the mutation in this gene alters the cell morphology. *ampG* codes for a muropeptide permease that is involved in the recycling of peptidoglycan. In the present transcriptome analysis the expression of this gene was slightly decreased (−1.2). It is possible that this difference is due to distinct growth condition used in the present work.

The genes *rfbG galE rfbBC* and *wcaGA* involved in lipopolyssacharide (LPS) biosynthesis were also downregulated by naringenin. Alterations in cell surface are common in other bacteria when they interact with plants or in the presence of plant compounds. *Rhizobium* sp. strain NGR234 synthesizes a new LPS in the presence of flavonoids and this LPS is important for the colonization of NGR234 in leguminous plants (Ardissone et al., 2011).

TABLE 2 | Genes differentially expressed in the presence of naringenin.

Gene	Fold Change Transcriptome[a]	qPCR[b]
*flh*B	−2.65	0.599
*flg*E	−2.33	0.618
Hsero 2564	−7.37	0.476
*mur*F	−2.08	0.64

[a] *The Fold change was determined by CLC Workbench 5.1.*
[b] *Relative expression in the presence of naringenin.*

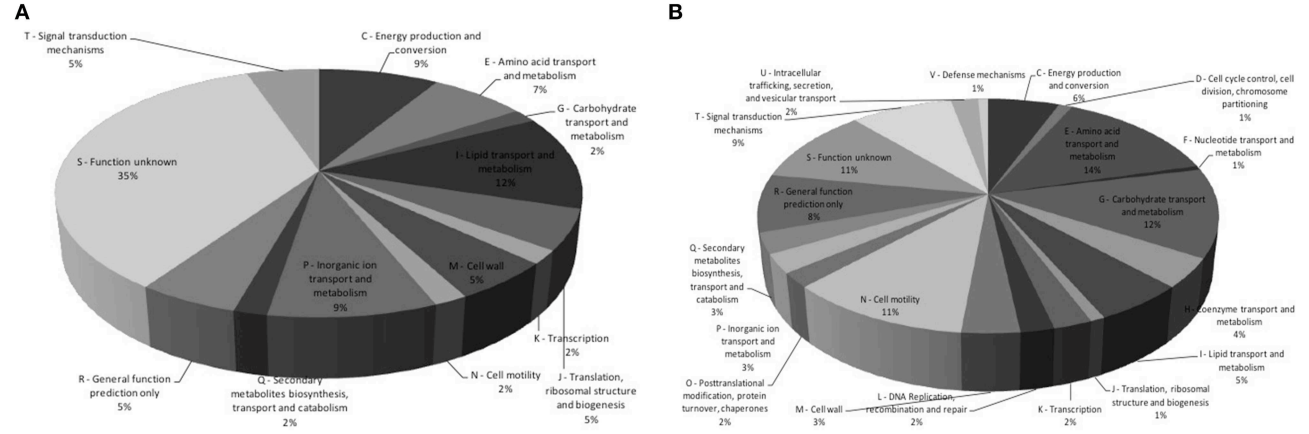

FIGURE 2 | Functional classification of genes upregulated and downregulated by naringenin. Three hundred and four genes were upregulated **(A)** and 77 were downregulated **(B)** in the presence of naringenin. The genes were functional classificated by COG (Clusters if Orthologous Groups of proteins Tatusov et al., 1997) (http://www.ncbi.nlm.nih.gov/COG).

Chemotaxis and Flagella

Bacteria can sense the environment and rapidly respond to environmental changes through the action of specific signaling pathways. The chemotaxis signal begins with the binding of molecules on membrane receptors. Chemoreceptors are encoded by the *tsr, tar, trg* and *tap* genes, that code for methyl-accepting chemotaxis proteins (MCPs) (Pereira et al., 2004).

We identified forty-one genes involved in the chemotaxis transduction pathways in *Herbaspirillum seropedicae* genome. Twenty nine of these are found in five clusters and the other genes are monocistronics with 6 homologous to *cheA*, 5 to *cheB*, 10 to *cheD*, 5 to *cheR*, 1 to *cheM*, 9 to *cheY*, 1 to *cheZ*, and 5 to *cheW* (Pedrosa et al., 2011). Cluster I has five genes, *Hsero_0623* (methyl-accepting chemotaxis transducer transmembrane protein), *cheWRB* and the *Hsero_0627*. Cluster III of *H. seropedicae* contains *tar, cheRDBYZ* and *flhBA, three cheD*-like and eight genes coding for methyl-accepting chemotaxis proteins (*tsr*, Hsero_0538, 1262, 1556, 3234, 4019, 4543, and 4615) all these were repressed in the presence of naringenin. In contrast the *cheR* and *cheY* genes of the cluster II *cheWBRYA* were activated in the presence of the flavonoid. Cluster IV has *cheYAW* genes and the cluster V contains eight genes, one encoding a methyl-accepting chemotaxis protein (*Hsero_3022*), one a chemotaxis signal transduction protein (*Hsero_3021*), one a response regulator protein (*Hsero_3016*), one an acyl dehydratase protein (*Hsero_3015*), and the genes *cheRWAB*. The expression of the gene clusters I, IV, and V did not change in the presence of naringenin. In *Pseudomonas aeruginosa* the *che* genes are also organized in five gene clusters, which have different responses depending

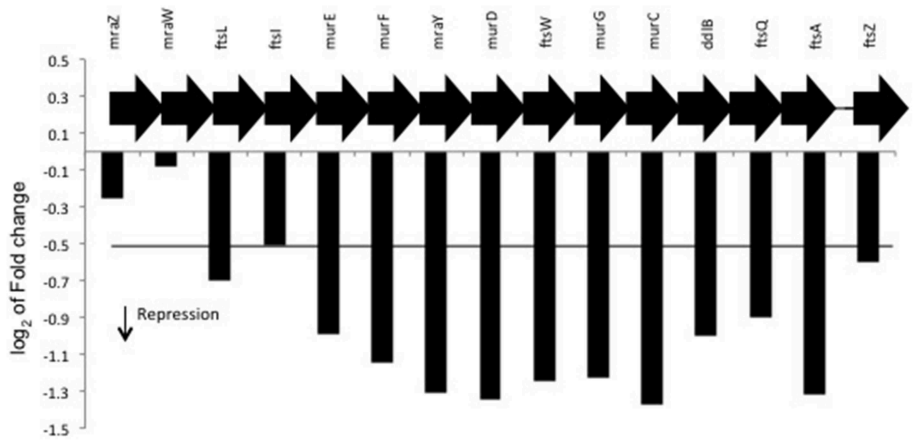

FIGURE 3 | Differential expression of region of *mur* genes in the presence of naringenin. Region of *mur* genes in *H. seropedicae* genome. The value represents the $\log_2$ of fold change of genes.

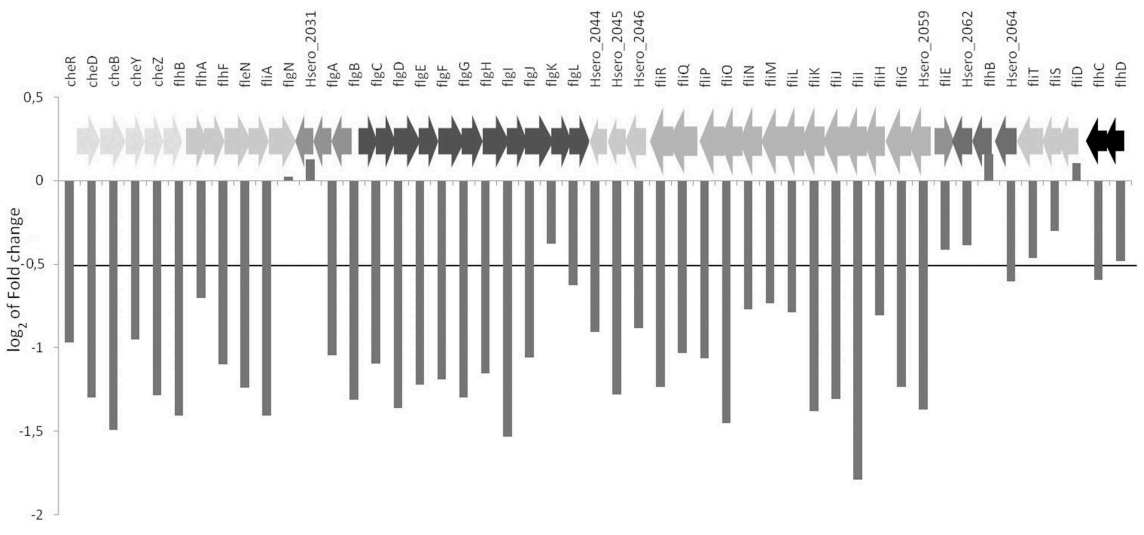

FIGURE 4 | Differential expression of flagellar genes in the presence of naringenin. The value represents the $\log_2$ of fold change of genes. Genes of the same color are in the same operons.

on the stimulus (Ferrandez et al., 2002; Guvener et al., 2006).

In bacteria, flagella genes are regulated in response to environmental changes. These genes are found in operons that are divided in three temporally regulated transcriptional classes: early (class 1), middle (class 2), and late (class 3) (Komeda, 1986; Kutsukake et al., 1994). *H. seropedicae* has at least 46 genes involved in flagella biosynthesis, assembly and structure. *H. seropedicae* early genes homologous to the class 1 *flhC* and *flhD*, to middle genes class 2 *flgA*, *flgBCDEFGHI*, *flhB*, *fliA*, *fliD*, *fliFGHIJK*, *fliOPQR*, and late genes of class 3 *tsr*, *cheA*, *cheRBYZ* are all repressed in the presence of naringenin (**Figure 4**, Figure S1B). The FlhCD proteins are sigma 70 dependent transcriptional activators of class 2 promoters (Kutsukake et al., 1994; Liu and Matsumura, 1994) and FliA protein is a flagella alternative sigma factor – σ^{28} (Ohnishi et al., 1990). FliA has been shown to be involved in transcription of flagella, chemotaxis, and motility genes and the decrease in the expression of this protein could be responsible for the decrease in expression of middle and late flagella genes and chemotaxis genes (Iriarte et al., 1995).

Naringenin regulates flagellar genes expression in other bacteria. The transcriptome profile of *Salmonella typhimurium* LT2 revealed that 24 genes of pathogenicity island 1 and 17 genes involved in flagellar and motility were repressed in the presence of naringenin (Vikram et al., 2011). Flagellar genes were also downregulated in *A. caulinodans* by naringenin (Tsukada et al., 2009) and *Pseudomonas syringae* pv. tomato DC3000 by phloretin (Vargas et al., 2013). In *Bacillus subtilis* OKB105 chemotaxis and motility genes were downregulated in response to rice seedlings (Xie et al., 2015), suggesting that decrease of motility in the presence of root exudate maybe be involved in the establishment of interaction with the plant. Signal molecules released by plants direct the bacteria toward the root in a process dependent on chemotaxis and cell motility. At this initial stage the concentration of signal compounds are low and the bacteria follow a concentration gradient and bacteria motility depends on flagella-driven motility. Upon reaching root surface the bacteria would attach and reduce flagella gene expression and motility may depend on other means more appropriate for this new environment, such as type IV *pilli*-dependent swarming. Alternatively flavonoids such as naringenin acting as an anti-microbial agent targets the flagella, as suggested for *P. syringae* (Vargas et al., 2013).

Downregulation of flagella and chemotaxis genes indicated that naringenin might reduce *H. seropedicae* motility. This hypothesis was tested by measuring the motility of *H. seropedicae* in the presence of naringenin. The results demonstrated that naringenin impairs *H. seropedicae* motility

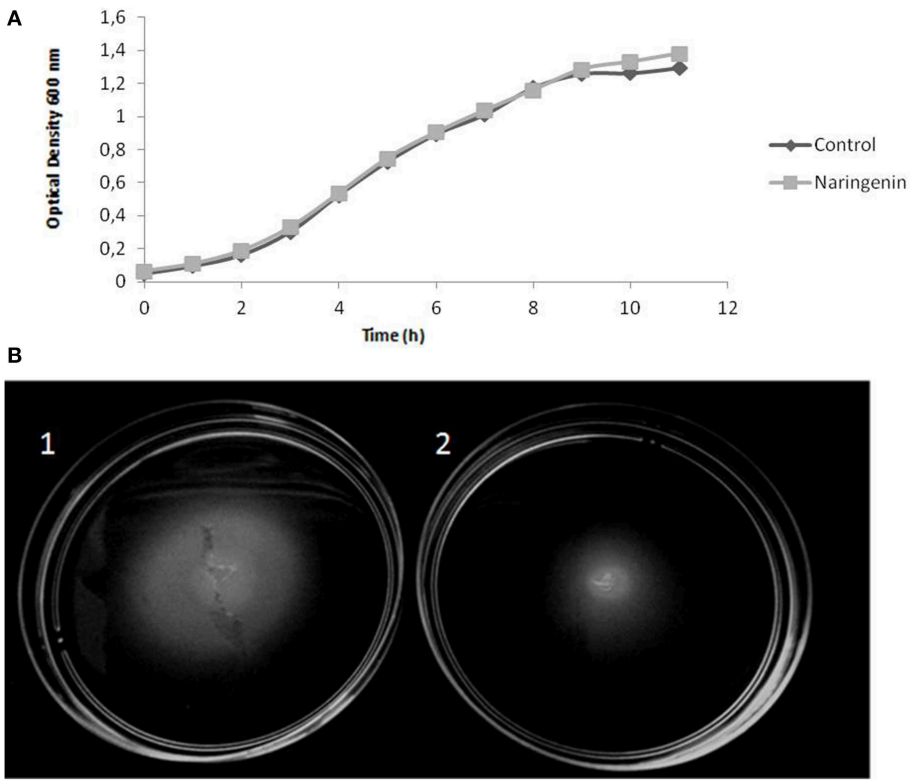

FIGURE 5 | Motility of *H. seropedicae* SmR1 is reduced by the presence of naringenin. (A) Growth curve of *H. seropedicae* SmR1 in liquid NFbHPN-malate. **(B)** Motility of *H. seropedicae* SmR1 in semi-solid NFbHPN-malate in the absence (1) or presence (2) of 100 μM naringenin. Growth halos in semi-solid medium of ten replicates were analyzed by ImageJ software. Control = 1.00 ± 0.15; with naringenin = 0.70 ± 0.14, the values are arbitrary units in relation to the mean of the control condition.

(**Figure 5B**) without affecting the growth in liquid medium (**Figure 5A**).

Aromatic Compounds Metabolism Is Induced by Naringenin

H. seropedicae genome sequence analysis showed the existence of genes involved in aromatic compounds metabolism such as catechol (*cat*), benzoate (*ben*), 4-hydroxybenzoate (*pob*), phenylacetate (*paa*), and protocatechuate (*pca*) metabolism (Pedrosa et al., 2011). These compounds can be metabolized to tricarboxylic acid intermediates.

In *H. seropedicae* the expression of *pcaJIF* and *catCD* genes increased by 3 -7 fold in the presence of naringenin, these genes are involved in the conversion of muconolactone to 3-oxoadipyl-Coa a pathway of the catechol metabolism. The expression of *paaBC* and *Hsero_4130* also increased in the presence of naringenin. These three genes are probably organized in an operon with other *paa* genes. The *paa*, *pca*, and *cat* genes may be involved in naringenin intermediates degradation.

Another important system influenced by naringenin treatment was the multidrug efflux. *H. seropedicae* genome has five regions containing genes *acrAB;* these regions were named Cluster I, II, III, IV, and V. In this study, *acrA* and *acrB* of the cluster II were induced 7.5 and 3.2-fold, respectively. In *S. typhimurium* LT2 the genes *acrAB* were also induced 3-fold in the presence of naringenin (Vikram et al., 2010). Other genes involved in multidrug transport efflux were also induced by naringenin such as *ompC* (2.4-fold) and *Hsero_1358* (3.15-fold). Multidrug transporter efflux pump provides low level of resistance to alkaline dyes, detergents and antibiotics. Induction of this efflux pump by naringenin suggests activation of the drug resistance system.

We found 35 ABC-transporter gene clusters differentially expressed in the presence of naringenin, being 29 downregulated and 6 upregulated (Table S1). The main group downregulated are amino acid and sugar transporter with a putative aromatic amino acid transporter system (∼7-fold down-regulated) and a sugar transporter repressed 4-fold. Among the upregulated ABC transporter we found mainly anion transporters such as sulfate, phosphate and alkanesulfanates. A proteomics approach revealed that *Bradyrhizobium japonicum* strains differentially expressed three periplasmic amino acid binding proteins of ABC-transporter systems in the presence of genistein (Batista and Hungria, 2012). The reason for this effect is not known.

In this study we provided a comprehensive view of a *H. seropedicae* transcriptome in the presence of naringenin. We have defined in detail the RNA populations found in *H. seropedicae* in the presence and absence of the flavonoid. The data obtained from this study enabled us to infer some aspects of the metabolism of the bacteria in the presence of naringenin. Expression of genes related to bacterial flagella biosynthesis, flagella motor activity, and chemotaxis were repressed by naringenin, and this repression is predicted to have negative effects on flagella synthesis and bacterial motility. Biosynthesis of peptidoglycan is also inhibited by narigenin, whereas expression of a multidrug transport efflux pump is activated. The data suggest that in the presence of naringenin *H. seropedicae* triggers a concerted change in gene expression probably related to defense mechanisms.

Acknowledgments

This work was supported by the Brazilian Program of National Institutes of Science and Technology-INCT/Brazilian Research Council-CNPq/MCT, Fundação Araucaìria and CAPES. We would like to thank Dr. Marshall Geoffrey Yates for reading the manuscript. We are also thankful to Roseli A. Prado, Julieta Pie and Marilza D. Lamour for technical assistance.

Supplementary Material

The Supplementary Material for this article can be found online at: http://journal.frontiersin.org/article/10.3389/fmicb.2015.00491/abstract

References

Anders, S., and Huber, W. (2010). Differential expression analysis for sequence count data. *Genome Biol.* 11:R106. doi: 10.1186/gb-2010-11-10-r106

Ardissone, S., Kobayashi, H., Kambara, K., Rummel, C., Noel, K. D., Walker, G. C., et al. (2011). Role of BacA in lipopolysaccharide synthesis, peptide transport and nodulation by *Rhizobium* sp. NGR234. *J. Bacteriol.* 193, 2218–2228. doi: 10.1128/JB.01260-10

Baggerly, K., Deng, L., Morris, J., and Aldaz, C. (2003). Differential expression in SAGE: accounting for normal between-library variation. *Bioinformatics* 19, 1477–1483. doi: 10.1093/bioinformatics/btg173

Baldani, V. L. D., Baldani, J. I., and Dobereiner, J. (2000). Inoculation of rice plants with the endophytic diazotrophs *Herbaspirillum seropedicae* and *Burkholderia* spp. *Biol. Fertil. Soils* 30, 485–491. doi: 10.1007/s003740050027

Balsanelli, E., Tuleski, T. R., Baura, V. A., Yates, M. G., Chubatsu, L. S., Pedrosa, F. O., et al. (2013). Maize root lectins mediate the interaction with *Herbaspirillum seropedicae* via N-acetyl glucosamine residues of lipopolysaccharides. *PLoS ONE* 8:e77001. doi: 10.1371/journal.pone.0077001

Bastián, F., Cohen, A., Piccoli, P., Luna, V., Baraldi, R., and Bottini, R. (1998). Production of indole-3-acetic acid and gibberellins A1 and A3 by *Acetobacter diazotrophicus* and *Herbaspirillum seropedicae* in chemically-defined culture media. *Plant Growth Reg.* 24, 7–11.

Batista, J. S. S., and Hungria, M. (2012). Proteomics reveals differential expression of proteins related to a variety of metabolic pathways by genistein-induced *Bradyrhizobium japonicum* strains. *J. Proteomics* 75, 1211–1219. doi: 10.1016/j.jprot.2011.10.032

Boneca, I. G., Dussurget, O., Cabanes, D., Nahori, M. A., Sousa, S., Lecuit, M., et al. (2007). A critical role for peptidoglycan *N*-deacetylation in *Listeria* evasion from the host innate immune system. *Proc. Natl. Acad. Sci. U.S.A.* 104, 997–1002. doi: 10.1073/pnas.0609672104

Broughton, W. J., Jabbouri, S., and Perret, X. (2000). Keys to symbiotic 279 harmony. *J. Bacteriol.* 182, 5641–5652. doi: 10.1128/JB.182.20.5641-5652.2000

Cesco, S., Neumann, G., Tomasi, N., Pinton, R., and Weisskopf, L. (2010). Release of plant-borne flavonoids into the rhizosphere andtheir role in plant nutrition. *Plant Soil* 329, 1–25. doi: 10.1007/s11104-009-0266-9

Cordeiro, F. A., Tadra-Sfeir, M. Z., Huergo, L. F., Pedrosa, F. O., Monteiro, R. A., and Souza, E. M. (2013). Proteomic analysis of *Herbaspirillum seropedicae* cultivated in the presence of sugar cane extract. *J. Proteome Res.* 12, 1142–1150. doi: 10.1021/pr300746j

Erbs, G., and Newman, M. A. (2012). The role of lipopolysaccharide and peptidoglycan, two glycosylated bacterial microbe-associated molecular patterns (MAMPs), in plant innate immunity. *Mol. Plant Pathol.* 13, 95–104. doi: 10.1111/j.1364-3703.2011.00730.x

Erbs, G., Silipo, A., Aslam, S., De Castro, C., Liparoti, V., and Flagiello, A. (2008). Peptidoglycan and muropeptides from pathogens *Agrobacterium* and *Xanthomonas* elicit plant innate immunity: structure and activity. *Chem. Biol.* 15, 438–448. doi: 10.1016/j.chembiol.2008.03.017

Ferrandez, A., Hawkins, A. C., Summerfield, D. T., and Harwood, C. S. (2002). Cluster II *che* genes from *Pseudomonas aeruginosa* are required for an optimal chemotactic response. *J. Bacteriol.* 184, 4374–4383. doi: 10.1128/JB.184.16.4374-4383.2002

Gough, C., Galera, C., Vasse, J., Webster, G., Cocking, E. C., and Dénarié, J. (1997). Specific flavonoids promote intercellular root colonization of *Arabidopsis thaliana* by *Azorhizobium caulinodans* ORS571. *Mol. Plant. Microbe Interact.* 10, 560–570. doi: 10.1094/MPMI.1997.10.5.560

Guvener, Z. T., Tifrea, D. F., and Harwood, C. S. (2006). Two different *Pseudomonas aeruginosa* chemosensory signal transduction complexes localize to cell poles and form and remould in stationary phase. *Mol. Microbiol.* 61, 106–118. doi: 10.1111/j.1365-2958.2006.05218.x

Gyaneshwar, P., James, E. K., Reddy, P. M., and Ladha, J. K. (2002). *Herbaspirillum* colonization increases growth and nitrogen accumulation in aluminium-tolerant rice varieties. *New Phytol.* 154, 131–145. doi: 10.1046/j.1469-8137.2002.00371.x

Iriarte, M., Stainier, I., Mikulskis, A. V., and Cornelis, G. R. (1995). The *fliA* gene encoding sigma 28 in *Yersinia enterocolitica*. *J. Bacteriol.* 177, 2299–2304.

Jofré, E., Fischer, S., Príncipe, A., Castro, M., Ferrari, W., Lagares, A., et al. (2009). Mutation in a D-alanine D-alanine ligase of *Azospirillum brasilense* Cd results in an overproduction of exopolysaccharides and a decreased tolerance to saline stress. *FEMS Microbiol. Lett.* 290, 236–246. doi: 10.1111/j.1574-6968.2008.01421.x

Klassen, G., Pedrosa, F. O., Souza, E. M., Funayama, S., and Rigo, L. U. (1997). Effect of nitrogen compounds on nitrogenase activity in *Herbaspirillum seropedicae* strain SMR1. *Can. J. Microbiol.* 43, 887–891. doi: 10.1139/m97-129

Komeda, Y. (1986). Transcriptional control of flagellar genes in *Escherichia coli* K-12. *J. Bacteriol.* 168, 1315–1318.

Kutsukake, K., Minamino, T., and Yokoseki, T. (1994). Negative regulation by *fliD*, *fliS*, and *fliT* of the export of the flagellum-specific anti-sigma factor, FlgM, in *Salmonella typhimurium*. *J. Bacteriol.* 176, 7625–7629.

Liu, X., and Matsumura, P. (1994). The FlhD/FlhC complex, a transcriptional activator of the *Escherichia coli* flagellar class II operons. *J. Bacteriol.* 176, 7345–7351.

Livak, K. J., and Schmittgen, T. D. (2008). Analyzing real-time PCR data by the comparative C(T) method. *Nat. Protoc.* 3, 1101–1108. doi: 10.1038/nprot.2008.73

Mortazavi, A., Williams, B. A., McCue, K., Schaeffer, L., and Wold, B. (2008). Mapping and quantifying mammalian transcriptomes by RNA-Seq. *Nat. Methods* 5, 621–628. doi: 10.1038/nmeth.1226

Muchova, K., Wilkinson, A. J., and Barak, I. (2011). Changes of lipid domains in *Bacillus subtilis* cells with disrupted cell wall peptidoglycan. *FEMS Microbiol. Lett.* 325, 92–98. doi: 10.1111/j.1574-6968.2011.02417.x

Ohnishi, K., Kutsukake, K., Suzuki, H., and Iino, T. (1990). Gene *fliA* encodes an alternative sigma factor specific for flagellar operons in *Salmonella typhimurium*. *Mol. Gen. Genet.* 221, 139–147. doi: 10.1007/BF00261713

Patin, D., Boniface, A., Kovac, A., Herve, M., and Dementin, S. (2010). Purification and biochemical characterization of Mur ligases from *Staphylococcus aureus*. *Biochimie* 92, 1793–1800. doi: 10.1016/j.biochi.2010.07.009

Pedrosa, F. O., Monteiro, R. A., Wassem, R., Cruz, L. M., Ayub, R. A., and Colauto, N. B. (2011). Genome of *Herbaspirillum seropedicae* strain SmR1, a specialized diazotrophic endophyte of tropical grasses. *PLoS Genet.* 7:e1002064. doi: 10.1371/journal.pgen.1002064

Pereira, M., Parente, J. A., Bataus, L. A., Cardos, D. D., Soares, R. B., and Soares, C. M. (2004). Chemotaxis and flagellar genes of *Chromobacterium violaceum*. *Genet. Mol. Res.* 3, 92–101.

Ramos, H. C., Rumbo, M., and Sirard, J. C. (2004). Bacterial flagellins: mediators of pathogenicity and host immune responses in mucosa. *Trends Microbiol.* 12, 509–517. doi: 10.1016/j.tim.2004.09.002

Rasband, W. S. (1997). *ImageJ*. Bethesda, MD: U. S. National Institutes of Health. Available online at: http://imagej.nih.gov/ij/

Tadra-Sfeir, M. Z., Souza, E. M., Faoro, H., Müller-Santos, M., Baura, V. A., Tuleski, T. R., et al. (2011). Naringenin regulates expression of genes involved in cell wall synthesis in *Herbaspirillum seropedicae*. *Appl. Environ. Microbiol.* 77, 2180–2183. doi: 10.1128/AEM.02071-10

Tatusov, R. L., Koonin, E. V., and Lipman, D. J. (1997). A genomic perspective on protein families. *Science* 278, 631–637. doi: 10.1126/science.278.5338.631

Tsukada, S., Aono, T., Akiba, N., Lee, K. B., Liu, C. T., Toyazaki, H., et al. (2009). Comparative genome-wide transcriptional profiling of *Azorhizobium caulinodans* ORS571 grown under free-living and symbiotic conditions. *Appl. Environ. Microbiol.* 75, 5037–5046. doi: 10.1128/AEM.00398-09

Vargas, P., Farias, G. A., Nogales, J., Prada, H., Carvajal, V., Baron, M., et al. (2013). Plant flavonoids target *Pseudomonas syringae* pv. tomato DC3000 flagella and type III secretion system. *Environ. Microbiol. Rep.* 5, 841–850. doi: 10.1111/1758-2229.12086

Vikram, A., Jayaprakasha, G. K., Jesudhasan, P. R., Pillai, S. D., and Patil, B. S. (2010). Suppression of bacterial cell-cell signaling, biofilm formation and type III secretion system by citrus flavonoids. *J. Appl. Microbiol.* 109, 515–527. doi: 10.1111/j.1365-2672.2010.04677.x

Vikram, A., Jesudhasan, P. R., Jayaprakasha, G. K., Pillai, S. D., Jayaraman, A., and Patil, B. S. (2011). Citrus flavonoid represses Salmonella pathogenicity island 1 and motility in *S. Typhimurium* LT2. *Int. J. Food Microbiol.* 145, 28–36. doi: 10.1016/j.ijfoodmicro.2010.11.013

Webster, G., Jain, V., Davey, M. R., Gough, C., Vasse, J., Dénarié, J., et al. (1998). The flavonoid naringenin stimulates the intercellular colonization of wheat roots by *Azorhizobium caulinodans*. *Plant Cell Environ.* 21, 373–383. doi: 10.1046/j.1365-3040.1998.00278.x

Xie, S., Wu, H., Chen, L., Zang, H., Xie, Y., and Gao, X. (2015). Transcriptome profiling of *Bacillus subtilis* OKB105 in response to rice seedlings. *BMC Microbiol.* 15:21. doi: 10.1186/s12866-015-0353-4

Conflict of Interest Statement: The authors declare that the research was conducted in the absence of any commercial or financial relationships that could be construed as a potential conflict of interest.

frontiers in
MICROBIOLOGY

HYPOTHESIS AND THEORY ARTICLE
published: 12 January 2015
doi: 10.3389/fmicb.2014.00776

Mutualism–parasitism paradigm synthesized from results of root-endophyte models

Keerthi G. Mandyam[1] and Ari Jumpponen[2]*

[1] *Department of Agriculture, Alcorn State University, Lorman, MS, USA*
[2] *Division of Biology, Ecological Genomics Institute, Kansas State University, Manhattan, KS, USA*

Edited by:
Mysore V. Tejesvi, University of Oulu, Finland

Reviewed by:
Laila Pamela Partida-Martinez, Centro de Investigación y de Estudios Avanzados del Instituto Politécnico Nacional, Mexico
Erik Limpens, Wageningen University, Netherlands

***Correspondence:**
Ari Jumpponen, Division of Biology, Ecological Genomics Institute, Kansas State University, Manhattan, KS 66506, USA
e-mail: ari@ksu.edu

Plant tissues host a variety of fungi. One important group is the dark septate endophytes (DSEs) that colonize plant roots and form characteristic intracellular structures – melanized hyphae and microsclerotia. The DSE associations are common and frequently observed in various biomes and plant taxa. Reviews suggest that the proportion of plant species colonized by DSE equal that colonized by AM and microscopic studies show that the proportion of the root system colonized by fungi DSE can equal, or even exceed, the colonization by AM fungi. Despite the high frequency and suspected ecological importance, the effects of DSE colonization on plant growth and performance have remained unclear. Here, we draw from over a decade of experimentation with the obscure DSE symbiosis and synthesize across large bodies of published and unpublished data from *Arabidopsis thaliana* and *Allium porrum* model systems as well as from experiments that use native plants to better resolve the host responses to DSE colonization. The data indicate similar distribution of host responses in model and native plant studies, validating the use of model plants for tractable dissection of DSE symbioses. The available data also permit empirical testing of the environmental modulation of host responses to DSE colonization and refining the "*mutualism-parasitism-continuum*" paradigm for DSE symbioses. These data highlight the context dependency of the DSE symbioses: not only plant species but also ecotypes vary in their responses to populations of conspecific DSE fungi – environmental conditions further shift the host responses similar to those predicted based on the *mutualism-parasitism-continuum* paradigm. The model systems provide several established avenues of inquiry that permit more detailed molecular and functional dissection of fungal endophyte symbioses, identifying thus likely mechanisms that may underlie the observed host responses to endophyte colonization.

Keywords: *Arabidopsis thaliana*, dark septate endophyte, mutualism, parasitism, population inference, symbiosis

INTRODUCTION

Dark septate endophyte (DSE) fungi colonize plant roots and form characteristic structures – melanized hyphae and microsclerotia – and often have variable effects on plant growth. This inter- and intraspecific variability in host responses has been hypothesized to be central to plant community structuring by mycorrhizal fungi (Wilson and Hartnett, 1998; Hartnett and Wilson, 1999; van der Heijden, 2002). Similarly, the variability in host responses to DSE fungi may promote selection mosaics proposed for ectomycorrhizal symbioses (Piculell et al., 2008).

An issue that has remained under continuous debate is whether the DSE symbiosis should be considered beneficial to the host plant or rather as a weak parasitism (Jumpponen, 2001; Addy et al., 2005; Mandyam and Jumpponen, 2005; Alberton et al., 2010; Newsham, 2011; Mayerhofer et al., 2013). The general host responses to DSE fungi have remained difficult to discern, partly because of their wide variability, partly because of independent small studies that draw conclusions based on a limited number of fungal individuals. Here we aim to synthesize various bodies of data to better resolve the host responses to the colonization by these abundant fungi as well as to discern some abiotic controls that may lead to shifts in these observed host responses. Results from studies that use model and native plant systems provide unique empirical insights into the variability in host responses to DSE fungi drawn from populations of conspecific fungi. We argue that these data permit empirical evaluation of the "*mutualism-parasitism-continuum*" paradigm (Johnson et al., 1997; Saikkonen et al., 1998). We conclude by describing a general neutral null-hypothesis of host responses to fungal symbionts applicable beyond the DSE symbiosis. The mutualism–parasitism paradigm has been used as a general framework to understand the mycorrhizal symbioses that have – similarly to DSE symbioses – been considered variable when observed in different hosts or compared under different abiotic conditions.

DARK SEPTATE ENDOPHYTES – WHAT ARE THEY?

Research on DSE fungal has a long history. Melin (1922) described a melanized sterile fungus – *Mycelium radicis-atrovirens* – that he isolated from ectomycorrhizal roots of conifers. These isolates colonized roots intracellularly, suggesting an association distinct from

ectomycorrhizae. To emphasize the distinction from mycorrhizas, Melin called this association a "*pseudomycorrhiza*." More recently, similar melanized root-associations have been reported from a vast variety of host plants (>600 plant species representing >100 families), biomes, and ecosystems (Jumpponen and Trappe, 1998b; Mandyam and Jumpponen, 2005; Kageyama et al., 2008). The lists of plants with such root-colonization have been expanded with each study that records the presence of indicative structures within host roots (e.g., Kovacs and Szigetvari, 2002).

Dark septate endophytes are a miscellaneous group of mainly ascomyceteous root-colonizing fungi characterized by melanized cell walls and intracellular colonization of healthy plants (Jumpponen and Trappe, 1998b). Early stages of intracellular colonization often include non-pigmented hyphae into which the melanins are deposited later. These difficult to visualize hyphae (see Barrow and Aaltonen, 2001; Barrow, 2003) may also indicate different consortia of root-inhabiting fungi altogether (Porras-Alfaro et al., 2008; Khidir et al., 2010). In addition to potentially biome specific fungal guilds and inconsistent semantics, the research on root-associated endophytes is further burdened by lack of taxonomic cohesion, polyphyletic evolutionary origins of the DSE fungi, and their variable ecological or physiological functions (Caldwell et al., 2000; Addy et al., 2005; Grünig et al., 2008). However, the DSE fungi form melanized inter- and intracellular hyphae and melanized microsclerotia that are indicative and characteristic morphological structures in the host roots (Jumpponen and Trappe, 1998b; Rodriguez et al., 2009; Mandyam et al., 2010).

ABUNDANCE OF DSE FUNGI

Compared to better known mycorrhizal symbioses or the vertically transmitted systemic foliar endophytes, the root-associated fungal endophytes have received very little attention (Rodriguez et al., 2009). This is a serious gap in our understanding of the fungal associations, because the DSE fungi are common in many ecosystems including those in the Antarctic, Arctic, boreal, subtropical, and temperate regions (Mandyam and Jumpponen, 2005; Kageyama et al., 2008). The research gap is further highlighted by studies that compare host colonization by the root endophytes and mycorrhizal fungi in various habitats. The rare studies that estimate the root colonization by both mycorrhizal and endophytic fungi indicate that the DSE fungi are possibly as abundant as mycorrhizas (Mandyam and Jumpponen, 2008; Dolinar and Gaberscik, 2010; Zhang et al., 2010), if not more so (Mandyam and Jumpponen, 2008). Despite their apparent great abundance, functions of the DSE fungi, particularly their general effects on the colonized hosts, have not been resolved.

MUTUALISM-PARASITISM-CONTINUUM PARADIGM

The mechanisms and their magnitudes that alter interspecific interactions are central in ecology (Thompson et al., 2001). Research on mycorrhizal fungi has been pivotal in developing an understanding of the variability in presumed mutualisms (Sapp, 2004). The "*mutualism-parasitism-continuum*" is a paradigm established as a framework to explain why symbiotic associations may deviate from mutualisms to parasitisms (Francis and Read, 1995; Saikkonen et al., 1998; Jones and Smith, 2004). According to this paradigm, compatible host-fungus associations produce host responses that are flanked at one end by obligate mutualisms in which hosts fail to survive in absence of their fungal partners and at another end by parasitisms that lead to the death of a host plant. While the position of each compatible host-fungus association along this continuum is interesting and perhaps context-dependent (Karst et al., 2009), it is imperative that we understand the underlying controls of the variability in these symbioses. These controls include, but are not limited to, biotic variability of the component fungi (Munkvold et al., 2004; Grünig et al., 2008; Mandyam et al., 2012, 2013) or host plants (Jones et al., 1990; Thomson et al., 1994; Karst et al., 2009; Hoeksema et al., 2010) as well as abiotic variability in the availability of light or nutrients or in the stress under which the host-fungus symbiosis is evaluated (Johnson et al., 1997; Redman et al., 2001; Rodriguez et al., 2008; Johnson, 2010).

We describe, reanalyze, and synthesize studies conducted utilizing model plant systems and then use those data to infer general host responses to DSE fungi. We further evaluate the applicability of these model plant systems via comparisons with native plants. Our data clearly indicate that while the host species identities are important, so are the host and fungal genotypes and broad functional groupings (e.g., forb vs. grass; Mandyam et al., 2012). Additional experiments indicate – consistently with predictions of the mutualism-parasitism-continuum framework – that host responses in these associations can be modulated by abiotic conditions.

HOST RESPONSES TO DSE

The DSE fungi may either inhibit or enhance host plant growth (Jumpponen, 2001; Mandyam and Jumpponen, 2005; Grünig et al., 2008; Alberton et al., 2010; Newsham, 2011; Mandyam et al., 2012, 2013; Mayerhofer et al., 2013). The mechanisms that lead to the variable host responses are uncertain but often speculated in conjunction with inoculation experiments. Similarly to both arbuscular mycorrhizal and ectomycorrhizal symbioses where host responses have been considered context-dependent (Karst et al., 2008; Hoeksema et al., 2010), host responses to DSE fungi vary between host species and between coarse functional groupings (Mandyam et al., 2012). In contrast to interspecific variability, intraspecific variability is often discussed but rarely addressed (Piculell et al., 2008; Karst et al., 2009; Mandyam et al., 2013). Empirical evaluation of host responses within and among species to populations of conspecific fungi allow for assessment of intraspecific components of both hosts and fungi in DSE symbiosis (Mandyam et al., 2013).

In addition to the inter- and intraspecific variability among the plants (Piculell et al., 2008; Karst et al., 2009) and fungal symbionts (Munkvold et al., 2004; Mandyam et al., 2012), the potential drivers of the variable host responses – whether negative or positive – include competition with more serious root parasites and pathogens, facilitation of host nutrient uptake, or modulation by environmental stressors such as shade, drought, salinity, and nutrient depletion (Johnson et al., 1997; Kageyama et al., 2008; Rodriguez et al., 2008; Hoeksema et al.,

2010). Endophyte competition with antagonistic fungi is evidenced by the upregulation of plant defense pathways as a result of endophyte colonization (Mandyam and Jumpponen, 2014) and may lead to growth promotion if the cost of combined colonization is lesser than the cost of antagonist colonization alone (Mandyam and Jumpponen, 2005). Like in mycorrhizal symbioses (Hoeksema et al., 2010), facilitation of nutrient uptake is supported by increases in N or P contents and concentrations in the tissues of inoculated hosts (Jumpponen et al., 1998; Newsham, 2011). While this function is attractive mechanism for the growth stimulation in DSE symbiosis (see Newsham, 2011), it suffers from lack of evidence for any perifungal interface through which the nutrient exchange between the host and fungus would take place (Yu et al., 2001). Finally, analogously to the symbiosis between *Curvularia* and *Dichanthelium* (Redman et al., 1999), other endophytes – including DSE – may lead to modulation of plant environmental tolerances (Mandyam and Jumpponen, 2005) that may improve survival and performance during periods of stress.

Generalizations about the functional attributes of DSE fungi are complicated by their taxonomic diversity and the limited overlap in the communities across biomes (Addy et al., 2005; Kageyama et al., 2008; Herrera et al., 2010a). Recent meta-analyses of a limited number of available studies (Alberton et al., 2010; Mayerhofer et al., 2013) suggested that while host growth responses to colonization by DSE fungi were variable, they tended to be negative. In contrast to those meta-analyses, Newsham (2011) concluded that the outcomes of the DSE inoculation depended on the form of nitrogen supplied during the experiment (organic vs. inorganic) highlighting again the environmental context dependency of the symbiosis. Similarly to these conclusions, Mayerhofer et al. (2013) underline the impact of experimental designs or conditions that may confound the observed variability in plant responses. Overall, the three meta-analyses on the functional attributes of the DSE fungi indicate the difficulty of providing strong and meaningful conclusions on the DSE symbiosis highlighting the importance of ambitious empirical studies that evaluate broader selections of hosts and fungi under consistent experimental conditions. The difficulty of arriving at meaningful conclusions is further exaggerated by the diversity of distinct unrelated fungi involved in these associations. Furthermore, predictions on the relative importance of different environmental parameters that may modulate the host responses stem from isolated studies that use small subsets of plants and often only one or two strains of fungi. We urge the use of large numbers of conspecific fungal strains in more ambitious tractable empirical studies that use model plants followed by confirmatory experiments that utilize native plants.

DEBATE ON HOST RESPONSES TO DSE COLONIZATION

Because of the contrasting results from experiments in which host plants are inoculated with the DSE fungi, their effect on the host performance has remained open to debate. Jumpponen (2001) proposed that because these associations lead to host responses ranging from inhibition of growth and performance to occasionally substantial increases in growth, the DSE symbiosis should be considered similarly to mycorrhizal associations. This argument relies on the "*mutualism-parasitism-continuum*" paradigm. Addy et al. (2005) reviewed the fungal associations best exemplifying the DSE symbioses and concluded that – in contrast to Jumpponen (2001) – the DSE fungi are more appropriately characterized as weak parasites than as mutualists within the *mutualism-parasitism-continuum*. The absence of host-derived perifungal membrane and its interfacial matrix structurally support this argument. While meta-analyses (Alberton et al., 2010; Mayerhofer et al., 2013) that summarized results from inoculation experiments concluded that on average the DSE tended to reduce host growth, others (Newsham, 2011) have provided contrasting conclusions. Perhaps the underlying reasons for these contrasts lies indeed in the variability in the experimentation (Mayerhofer et al., 2013).

Here, we contribute to this debate by drawing from more than a decade of continuous research effort and synthesize large bodies of accumulated published and unpublished data. We include a number of concerted, uniform experiments utilizing *Allium* and *Arabidopsis* models; complementary experiments with native hosts; and, experiments that evaluate the environmental modulation of the symbiosis. While this synthesis focuses explicitly on the DSE symbiosis, the neutral null hypotheses, the population-centered approaches, and the environmental modulation of the symbioses are broadly applicable to other symbiotic systems.

MODEL PLANT RESPONSES TO INOCULATION WITH DSE FUNGI

We define the DSE symbiosis narrowly and consider only those species or fungal strains that form the characteristic DSE structures (i.e., intracellular microsclerotia). This approach omits many hyaline root-associated fungi (RAF) that have been frequently observed, particularly in (semi-)arid ecosystems (e.g., Herrera et al., 2010b). As a result, we primarily focus on *Periconia macrospinosa* and its close relatives from the prairie ecosystems (Mandyam et al., 2010) and acknowledge that our experiments do not include other common DSE fungi such as *Phialocephala fortinii* or *Cadophora finlandica* (formerly *Phialophora finlandica*) that tend to be common in boreal/temperate forest ecosystems (Jumpponen and Trappe, 1998b; Jumpponen, 2001; Grünig et al., 2008).

All fungi isolated from host roots neither produce DSE structures nor stimulate host growth (Jumpponen, 2001; Kageyama et al., 2008; Mandyam et al., 2010; Knapp et al., 2012). While some of the fungi isolated from roots behave like pathogens (Kageyama et al., 2008; Mandyam et al., 2010; Tellenbach et al., 2011), the commonly isolated DSE species tend to lead to host responses that range from growth inhibition to growth stimulation as one would predict based on the *mutualism-parasitism-continuum* paradigm. It is the heterogeneity of the fungi that can be isolated from the roots or detected in them molecularly that presents a challenge in the endophyte research. Isolation of fungal strains and fulfilling the Koch's postulates are mandatory steps to convincingly confirm that acquired isolates are indeed responsible for producing the indicative DSE structures in the roots (Mandyam et al., 2010; Jumpponen et al., 2011a; Knapp et al., 2012). Molecular studies of the root-associated fungal communities particularly

suffer from the inability to unequivocally detect endophytes (Jumpponen et al., 2011a,b), despite their occasionally high occurrence in many plant species (Mandyam and Jumpponen, 2008; Mandyam et al., 2012).

A typical experiment in which hosts have been inoculated with DSE fungi includes only very few fungal strains (e.g., Jumpponen and Trappe, 1998a; Jumpponen et al., 1998; Newsham, 1999; Vohnik et al., 2005; Usuki and Narisawa, 2007; Hou and Guo, 2009; Yuan et al., 2010) and only recently have more ambitious studies that include multiple hosts and/or fungal strains emerged (see Mandyam et al., 2012, 2013; Tellenbach and Sieber, 2013). Comparisons of conspecific individuals within common DSE species (*Periconia*) from tallgrass prairie clearly indicate that inoculation with different fungal individuals leads to different host responses in model (Mandyam et al., 2013) and non-model systems (Mandyam et al., 2012). Similarly, host responses to Helotialean DSE fungi also differ supporting the notion that there are differences among the DSE species (Jumpponen and Trappe, 1998a; Jumpponen, 2001; Tellenbach et al., 2011). While inoculation experiments may suffer from limited inferential capacity and extrapolation to natural conditions, these controlled experiments are mandatory to better understand host responses in absence of complex biotic and abiotic interactions.

The model plant *Arabidopsis thaliana* is subject to colonization by a variety of bacterial (Bulgarelli et al., 2012) and fungal endophytes (Garcia et al., 2013), including fungi that occupy root and rhizosphere (Mandyam et al., 2013; Mandyam and Jumpponen, 2014). As such, *A. thaliana* and its endophytes may provide a model for exploring endophyte associations in a well-defined system (Garcia et al., 2013). Mandyam et al. (2013) utilized a closed petri plate system that permitted 6–8 weeks incubation of *A. thaliana* with a minimal contamination risk. These experiments standardly used pairs of experimental treatments that were either mock-inoculated with a disk from fungal medium (fungus-free control) or inoculated with *P. macrospinosa*. While such experiments are tedious to set up and demand substantial growth room capacity, they benefit greatly from simple statistical inference on the host responses to the presence of the endophyte fungus. Furthermore, these experiments easily lend themselves for advanced classroom settings. We were fortunate to conduct a total of 157 such experiments (a total of 3,140 experimental units) with the assistance of more than thirty senior undergraduate students at Kansas State University. These experiments lend further support to conclusions in Mandyam et al. (2013): while the model plant responses to a population of endophytes may be variable and include several examples of symbioses that enhance host growth, on average the host responses are negative and the host growth is inhibited relative to the fungus-free controls (**Figure 1**).

While the variability in host responses to different DSE species is expected, the intraspecific variability in host responses to inoculation has received far less attention. Published data indicate that host responses are variable, often ranging from reduction in host growth to significant increases in the host biomass (Fernando and Currah, 1996; Mandyam et al., 2010, 2012). We have explored this topic extensively using two model systems (*Allium porrum* and *A. thaliana*; Kageyama et al., 2008; Mandyam et al., 2010, 2013): data show substantial intraspecific variability, even when the host genetic background is controlled (Mandyam et al., 2013). Taken together, these data lay a unique empirical foundation that clearly shows the dangers of making conclusions about a diverse guild of fungi without including a broad enough sampling of individuals drawn from a given population.

HOST CONTROL OF RESPONSES TO DSE INOCULATION

The principles that govern the assembly of host-specific endophyte communities from the general and more diverse soil communities remain poorly understood. Yet, co-occurring, adjacent hosts select root-associated community constituents from bulk soil so that the endophyte communities are distinct from bulk soil, lower

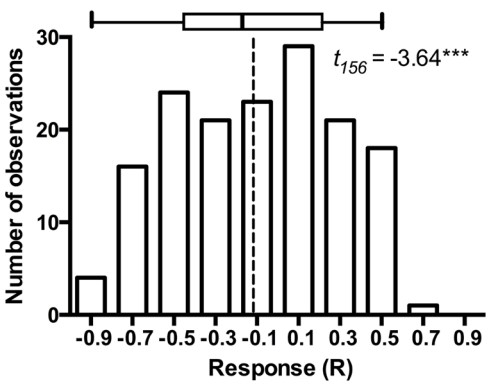

FIGURE 1 | Frequency distribution of *Arabidopsis* responses to inoculation in 157 experiments that paired *Arabidopsis thaliana* either inoculated with *Periconia macrospinosa* or with sterile fungal medium (mock-control). The experimental procedures are described in full detail in Mandyam et al. (2013). Response (R) to inoculation indicates the difference between the control and inoculated plants relative to control (inoculated < control) or inoculated plants (control < inoculated; Klironomos, 2003). *t*-test on the mean of 157 experiments indicates that average response to inoculation is negative ($P < 0.0001$) suggesting thus an overall parasitic association. The box identifies median, quartiles and 95% confidence intervals. Dashed line identifies the mean response across all 157 experiments.

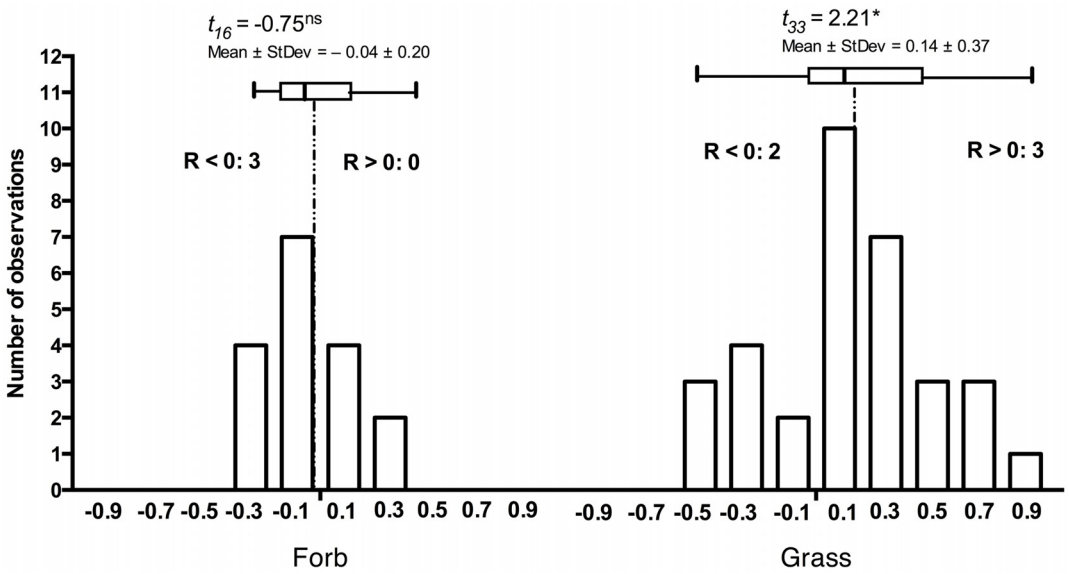

FIGURE 2 | Frequency distribution of responses in 17 forb and 33 grass *Periconia macrospinosa* inoculation experiments. Each experiment paired experimental units inoculated either with *Periconia macrospinosa* or with sterile fungal medium (mock-control). The data were extracted from Mandyam et al. (2010, 2012) and analyses follow those described in Mandyam et al. (2013). Response (R) to inoculation indicates the difference between the control and inoculated plants relative to control (inoculated < control) or inoculated plants (control < inoculated; Klironomos, 2003). The grasses tended to respond positively (*t*-test, $P < 0.05$), whereas the forb response did not differ from zero. Inserts indicate the number of experiments where significant (ANOVA, $P < 0.05$) positive (R > 0) or negative (R < 0) responses were observed.

in diversity (Lundberg et al., 2012; Bodenhausen et al., 2013), and may differ in composition among hosts. Naturally, host species differ in their susceptibility and responses to DSE (Mandyam et al., 2012). Although responses to root-associated endophytes often appear context-dependent, grass hosts are more extensively colonized in the laboratory and in the field when compared to dicotyledonous hosts (Mandyam et al., 2012). Similarly, the grass hosts tend to respond more positively to inoculation than forbs (**Figure 2**) suggesting that host responses may correlate with host evolutionary history or perhaps even suggest co-evolution of grasses and the abundant DSE fungi in grassland ecosystems.

Experiments with model plants indicate that not only do the host species differ in their responses, but also that *Arabidopsis* ecotypes that have very limited genotypic variability differ in their responses to DSE fungi (**Figure 3**). More importantly, it is rare that one fungal strain leads to similar host responses across different *Arabidopsis* accessions. Taken together, these findings suggest that host responses to DSE fungi vary among fungal strains and perhaps also among host genetic backgrounds. These findings clearly demonstrate that growth promoting fungal strains are present in environmental samples (Gentili and Jumpponen, 2006), but that the host responses may depend on the host genotype and are therefore often unpredictable.

VALIDATION OF THE MODEL SYSTEM RESULTS WITH NATIVE PLANTS

It is arguable whether the results from model plant systems apply to native hosts (Mandyam and Jumpponen, 2014). In addition to the experiments exploiting model plants (Mandyam et al., 2010, 2013; Mandyam and Jumpponen, 2014), we have conducted more limited experiments with eighteen native plant species common in the tallgrass prairie ecosystem where the fungal strains originate (Mandyam et al., 2010, 2012). While none of these datasets is quite as large as those accumulated with the *Allium* or *Arabidopsis* models, they nonetheless allow mapping of the native host responses into the *mutualism-parasitism-continuum* that serves as a central framework for this synthesis. These analyses demonstrate that the native plants span a range of responses similar to the model species (**Figure 2**), thus validating the predictions derived from the model systems. One of the native plants (the dominant native tallgrass prairie grass, *Andropogon gerardi*) allows analyses focusing on the responses to different conspecific strains of *P. macrospinosa* (**Figure 4**). These results indicate that – within a population of native conspecific host plants, host responses to DSE inoculation are as variable as they are in the model systems and span a full range from parasitism to mutualism. However, it is important to bear in mind that, across broader plant functional groupings, results indicate that none of the dicotyledonous hosts responded positively to inoculation with DSE fungi and three responded negatively (**Figure 2**). In contrast, three of the eight grass species responded positively, whereas two responded negatively (**Figure 2**). Taken together, our observations support the notion that grasses are more readily colonized by DSE fungi and that they tend to derive a greater benefit from the DSE symbioses than the forbs do.

ENVIRONMENTAL MODULATION OF THE DSE SYMBIOSIS

In mycorrhizal symbioses, the host plant tends to gain less from trading the carbon for the mycorrhiza-derived nutrients if the soil nutrients are in high supply (Koide, 1991; Schwartz and

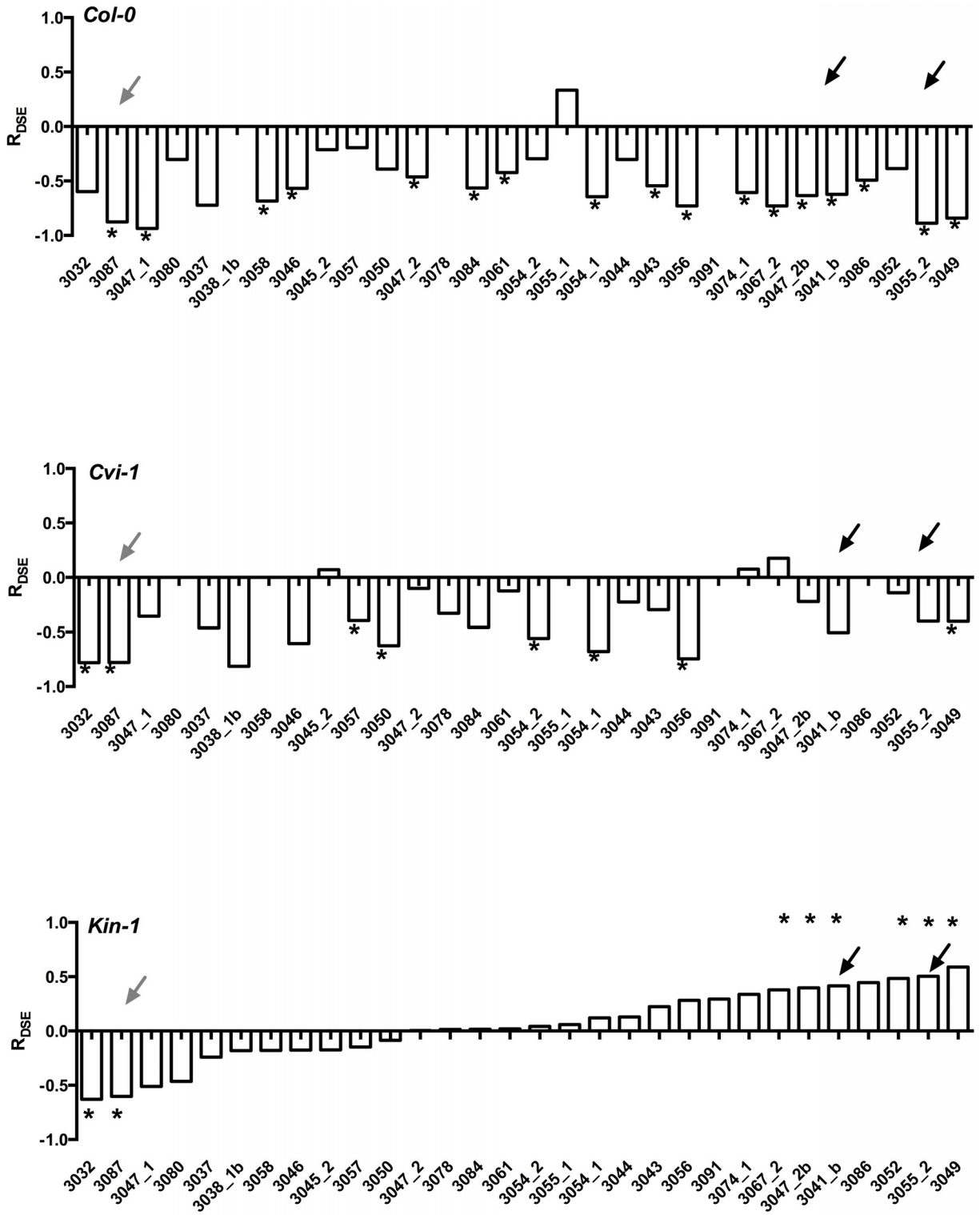

FIGURE 3 | Responses of three *Arabidopsis thaliana* accessions (*Col-0, Cvi-1, Kin-1*) to inoculation with 25 strains of *Periconia macrospinosa*. The analyses follow those described in Mandyam et al. (2013). Response (R) to inoculation indicates the difference between the control and inoculated plants relative to control (inoculated < control) or inoculated plants (control < inoculated; Klironomos, 2003). Values above x-axis indicate a positive response, values below negative. Gray arrows indicate responses consistent across the three accessions, black arrows responses that range from negative to positive depending on the host accession. Asterisks indicate significant difference between the control and inoculated plants (ANOVA, $P < 0.05$). Figure is redrawn from Figure 2 in Mandyam et al. (2013).

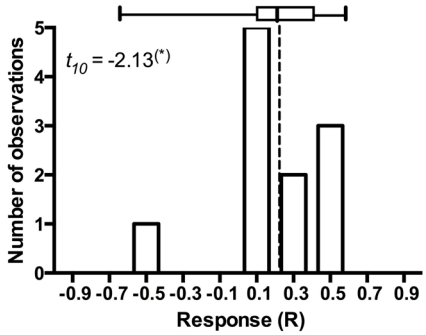

FIGURE 4 | Frequency distribution of *Andropogon gerardi* responses in eleven *Periconia macrospinosa* inoculation experiments. The data were extracted from Mandyam et al. (2010, 2012). Response (R) to inoculation indicates the difference between the control and inoculated plants relative to control (inoculated < control) or inoculated plants (control < inoculated; Klironomos, 2003). Host response is marginally significantly (*t*-test, $P < 0.10$) positive and includes one potential outlier that deviates from the majority of experiments.

Hoeksema, 1998; Jones and Smith, 2004; Hoeksema et al., 2010). We conducted a series of experiments, again with a large numbers of senior undergraduate students, in which model plant *A. thaliana* responses to DSE inoculation were evaluated under different environmental conditions. These studies indicate that the host responses to inoculation are insensitive to the nutrient availability (50% greater addition of Murashige and Skoog basal salt mixture) or elevated temperatures (∼5°C increase using a horticultural heating mat) as inferred from the non-significant interactions between the inoculation and environmental variable (data not shown). In contrast – and as predicted by the *mutualism-parasitism-continuum* paradigm – experiments in which energy flow (light) into the system was controlled by shading (half of the experimental units were individually covered with a horticultural shade cloth) indicate that the relative cost of symbiosis increases when availability of light and resultant energy is reduced (**Figure 5**). These experiments utilized a petri plate design identical to those in Mandyam et al. (2013) and illustrate the ease of conducting model plant experiments that permit testing hypotheses on environmental modulation of host responses expediently under tightly controlled experimental conditions.

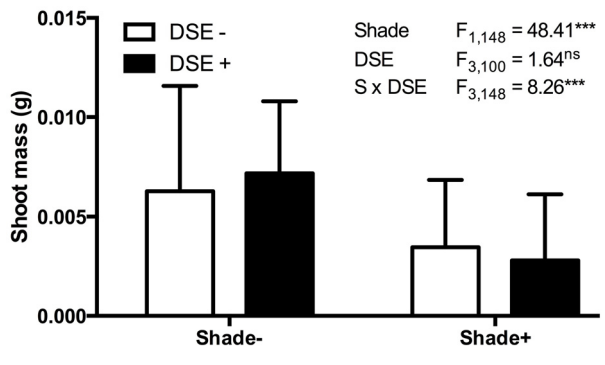

FIGURE 5 | *Arabidopsis* biomass response to inoculation with *Periconia macrospinosa* and shading. A total of 160 plants were included in paired experiments ($n = 20$ for each experiment), in which half were inoculated with living fungal culture, half with fungus free medium (see Mandyam et al., 2013 for details). Half of each inoculation treatment was covered with commercial shade cloth and half were left uncovered. Shoot biomass values were $\log_{10}$ transformed and analyzed for main effects (shade, inoculation) and their interaction in a mixed model ANOVA, where each paired experiment was assigned as a random effect. Significant shade and interaction terms (ANOVA, $P < 0.0001$) indicate lesser biomass accumulation in shade and suggest a greater relative cost of inoculation under low light levels.

THE MODEL

We propose a model that provides insight into how the host response to DSE fungi depends on the host species or ecotype and how these relationships respond to environmental variability. This model can be generally utilized for evaluation of the *mutualism-parasitism-continuum* paradigm. The proposed model rests on an assumption that – overall – the host responses to conspecific individuals drawn at random from a population of endophytic fungi are approximately normally distributed (**Figure 6**). It is of note that the larger model plant data sets generally support this assumption (**Figure 1**). This model also allows for an explicit articulation of the null-hypothesis of no response to inoculation and subsequent evaluation of this null-hypothesis. While it is not possible to predict host's response to any one fungal strain/individual, the responses may range from strong inhibition or promotion of host performance and an average response for the population can be estimated (see **Figure 1**). Analyses of the model and native plant data strongly indicate that both positive and negative responses occur. Further, the overall, average response to a population of fungi or across host

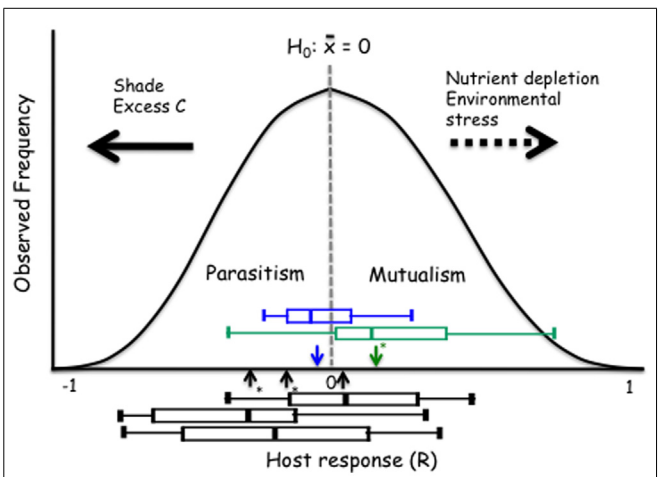

FIGURE 6 | Proposed model with the null hypothesis (H_0) of no response to inoculation. The black boxes show the range of responses of the three *Arabidopsis* accessions **(Figure 3)**. The green and blue boxes identify grass and forb responses, respectively. Horizontal arrows show predicted (dashed) or observed and supported (solid) responses to environmental controls. The boxes identify median, quartiles and 95% confidence intervals for three *Arabidopsis* accessions (Cvi-1, Col-0, and Kin-1 from left to right), grass (green) and forb (blue) experiments. Arrows indicate the mean response for the *Arabidopsis*, grass and forb experiments; asterisks indicate when the mean is different from zero (*t*-test; $P < 0.05$).

ecotypes can be evaluated by testing the general null-hypothesis that the mean host response equals zero. Average host responses that exceed zero can be considered mutualisms, whereas a negative mean response suggests a parasitic, non-beneficial association (**Figure 6**).

Our model also allows evaluation and visualization of hypotheses on environmental modulation of these symbioses. The empirical data presented above show that – consistently with the mutualism–parasitism paradigm – reduction in the light levels shift the outcome of the symbiosis toward parasitism. While there is no empirical data to support shifts toward mutualism, increasing nutrient depletion (e.g., P for AM symbiosis) or environmental stress (temperature in *Dichanthelium–Curvularia* symbiosis; Redman et al., 1999) can be predicted to lead to a greater benefit derived from symbiosis (**Figure 6**).

The empirical data and the model that we present here focus on root-associated DSE fungi. However, the model and its predictions are applicable more broadly to other host-fungus associations. The general model proposed here serves as a general tool to visualize and evaluate outcomes of symbioses when adequate numbers of conspecifics can be drawn from a population. We envision the use of this model and the predictions on the shifts as a result of environmental modulation to be particularly valuable when the outcomes of symbioses are evaluated under shifting environmental conditions. The proposed model thus allows for visualization of the variable host responses to a population of fungi and the modulation of these responses when the environmental conditions change.

DISSECTING THE DSE SYMBIOSIS USING GENOMIC TOOLS

While the host growth responses to fungal inoculations have dominated research in the past, the next-generation chip and sequencing tools have revolutionized the depth at which the symbioses can be queried. Transcriptome analyses of various plant-microbe symbioses including many mutualisms [arbuscular mycorrhiza (AM), ectomycorrhiza (ECM), plant growth promoting bacteria (PGPR), nitrogen fixing bacteria] have been dissected by the use of microarrays available for model plants (e.g., *Arabidopsis*, tomato, maize, wheat, *Medicago*, soybean). Examples of such studies include AM-tomato (Fiorilli et al., 2009; Salvioli et al., 2012); AM-*Medicago* (Hohnjec et al., 2005; Küster et al., 2007); legume root nodulation – soybean-*Bradyrhizobium japonicum* (Brechenmacher et al., 2008) or *Medicago* nodulation (El Yahyaoui et al., 2004; Küster et al., 2004); ECM symbiosis (Johansson et al., 2004; Le Quéré et al., 2005); *Frankia–Alnus* symbiosis (Alloisio et al., 2010); *Arabidopsis–Trichoderma sp.* (Mathys et al., 2012; Morán-Diez et al., 2012; Brotman et al., 2013); *Arabidopsis*-PGPR (Wang et al., 2005; Lakshmanan et al., 2013; Spaepen et al., 2014); fungal or viral pathogens of *Arabidopsis* (Postnikova and Nemchinov, 2012; Pierce and Rey, 2013; Schuller et al., 2014); and, wheat-powdery mildew (Xin et al., 2012) or wheat-*Fusarium* head blight (Golkari et al., 2007).

Despite the availability of innumerable molecular tools for *Arabidopsis*, its use to query root-associated, mycorrhizal symbioses is difficult because *Arabidopsis* is inherently non-mycorrhizal. However, the recent discovery of non-mycorrhizal Sebacinalean fungal symbiosis in *Arabidopsis* (Weiss et al., 2011), the *Arabidopsis* mutualism with *Piriformospora indica* (Peskan-Berghöfer et al., 2004), and the susceptibility of *Arabidopsis* to colonization of variety of endophytes (Garcia et al., 2013; Mandyam et al., 2013) have facilitated the use of the *Arabidopsis* model for studying such fungal symbioses. It must be kept in mind that host colonization occurs despite a sophisticated plant immune system, likely suggesting a defined discrimination against potential pathogens and simultaneous facilitation mutualist and commensal colonization (Lundberg et al., 2012).

The *Arabidopsis–Piriformospora* model has permitted the characterization of unique biphasic colonization mechanism of *Piriformospora* hitherto unknown in other symbioses, extensive role of plant hormones in defense signaling, induced systemic resistance, mechanisms of growth promotion, and differential gene expression during colonization (see review in Mandyam and Jumpponen, 2014). This model has provided vital insights into mechanisms that maintain this mutualism: *P. indica* colonization (i) induces production of indole-3-acetaldoxime (IAOx)-derived compounds in the early stages of colonization (Nongbri et al., 2012) and elevates cellular Ca^{2+} for production of IAOx-derived metabolites (Vadassery et al., 2009a); (ii) suppresses defenses involved in oxidative burst by invoking the 'PLD-PDK1-OXI1' (phospholipase D, 3-phosphoinosilide-dependent kinase, oxidative signal inducible 1) cascade by triggering phosphatidic acid synthesis and upregulating OXI1 and PDK genes (Camehl et al., 2011); (iii) upregulates genes MDAR2 (monodehydroascorbate reductase) and DHAR5 (dehydroascorbate reductase) of the ascorbate–glutathione cycle offering protection from oxidative burst and suppressing defense gene expression that can shift the interaction from mutualism to parasitism (Vadassery et al., 2009b); and, (iv) controls ethylene signaling (Camehl et al., 2010; Khatabi et al., 2012).

Host metabolism and nutrition can also control the fungal interaction with the host. The control on fungal lifestyle and colonization strategies is exemplified by the generalist *P. indica*'s symbiosis with *Arabidopsis* and *Hordeum vulgare* (barley; Lahrmann et al., 2013). Although the symbiosis is generally beneficial, *P. indica* maintains a predominantly biotrophic lifestyle in *Arabidopsis*. Contrastingly, in *Hordeum*, *P. indica* switches from biotrophy during early colonization phase (3 days post-inoculation – dpi) to saprotrophy during late colonization phase (14 dpi). The host-dependent fungal lifestyles or colonization strategies adopted by *P. indica* in respective hosts are accompanied by (i) cytological distinctions including the formation of secondary thin hyphae (SH), host cell wall appositions (papillae) and host cell death and autofluorescence in *Hordeum* – whereas in *Arabidopsis*, SH, papillae and host cell death are absent; (ii) transcriptional changes in *P. indica* with (a) larger number of fungal genes differentially regulated during early colonization in *Arabidopsis* than in *Hordeum* and vice-versa during late colonization; (b) induction of larger number of fungal effectors such as small secreted proteins (SSPs that control colonization by targeting host defense signal transduction and metabolism) in *Hordeum* than in *Arabidopsis*, most of which encoded for hydrolytic enzymes in *Hordeum* especially during late colonization phase; (c) lesser expression of fungal genes involved in host cell wall and lipid degradation in *Arabidopsis* than in *Hordeum*; (d) induction of

fungal amino acid biosynthesis genes in *Arabidopsis* and cell wall polysaccharide metabolic genes in *Hordeum*, coinciding with late colonization phase; and, (iii) distinctly different fungal nitrogen metabolism in *Hordeum* and *Arabidopsis* during late colonization phase exemplified by (a) differences in fungal PiAMT1 (a high-affinity ammonium transporter and downstream signaling under N starvation) expression and (b) free amino acid levels in the host: in *Arabidopsis*, low fungal PiAMT1 expression and high free host amino acid concentrations suggest *Arabidopsis* supply of nitrogen – especially asparagine and glutamine – to the fungus, whereas in *Hordeum*, high PiAMT1 expression and low free host amino acid concentrations – especially asparagine and glutamine – indicated onset of N starvation to the fungus and coincided with the switch to saprotrophic lifestyle. RNAi silencing studies further support the conclusions of host metabolism control on fungal lifestyles during the intracellular colonization. Inhibition of fungal PiAMT1 expression by RNAi did not alter the biotrophic fungal colonization in *Arabidopsis* symbiosis implying host nitrogen supply to fungal symbiont. In contrast, RNAi suppressed-PiAMT1 *P. indica* symbiosis with *Hordeum* during the late colonization was accompanied by increased fungal colonization and increased free host amino acids resulting in a prolonged the fungal biotrophic phase. Overall, studies by Lahrmann et al. (2013) show that fungal nitrogen sensor (PiAMT1 specifically) is not required for biotrophic growth but mandatory for the switch from biotrophy to saprotrophy. These results imply that fungal recognition of host metabolic cues to modulate lifestyle strategies in a dynamic environment. As summarized in Mandyam and Jumpponen (2014), the detailed molecular dissection of *P. indica* mutualism was largely attributable to the simplicity of growing the hosts and availability of a variety of molecular tools, mutants, and databases for *Arabidopsis*.

The DSE symbiosis and its range within the *mutualism-parasitism-continuum* remain unresolved; the *Arabidopsis* model likely serves among the optimal candidates to shed further light toward better resolving this symbiosis. *Arabidopsis* hosts a large number of bacteria and fungi (Lundberg et al., 2012; Bodenhausen et al., 2013; Mandyam and Jumpponen, 2014) and forms DSE symbiosis in the laboratory, greenhouse, and field (Mandyam et al., 2013). Preliminary analyses of the differential gene regulation of the *Arabidopsis*-DSE symbiosis using Affymetrix ATH1 microarrays suggested that this interaction is perhaps most similar to *Trichoderma* symbiosis and/or root endophytes including rhizobacteria and mycorrhizae (Mandyam and Jumpponen, 2014). These symbioses appear to share considerable similarities in the types of upregulated genes and include many involved in metabolism, hormonal control, stress, and defenses. However, further in-depth studies similar to those conducted with *P. indica* are required to further dissect the DSE symbiosis. The studies conducted with *Piriformospora* and model plants are likely applicable and serve as a model to design informative new experiments to address specific aspects of other endophyte symbioses. For example, the colonization mechanism and biotrophic lifestyle of a rice DSE fungus *Harpophora oryzae* was concluded to be similar to that of *P. indica* (Lahrmann et al., 2013; Su et al., 2013; Xu et al., 2014).

The introduction of next generation sequencing (NGS) technologies has opened a great potential to expediently and cost-effectively explore genomics and transcriptomics of non-model plants and/or fungi. To exemplify, Sebastiana et al. (2014) used 454-pyrosequencing to analyze the transcriptome of cork oak, *Quercus suber*, in symbiosis with the ectomycorrhizal fungus *Pisolithus tinctorius*. They observed more than 2,000 genes that were differentially regulated in mycorrhizal roots compared to non-mycorrhizal controls. The fungal colonization altered root cell wall biosynthesis (short root formation and lateral root hair decay), altered flavonoid biosynthesis, and activated secretory pathways. Importantly, the expression of many genes with putative roles in nutrient transfer were altered (upregulation of genes involved in hexose transport and delivery to apoplast plus genes involved in starch biosynthesis and metabolism; activation of genes involved in nitrogen assimilation; upregulation of sugar transporters; downregulation of ammonium, most amino acid transporters, and inorganic phosphate transporters; and, upregulation of a polyamine transporter). Additionally, several plant defense genes were differentially regulated and represented categories similar to those in other symbioses such as AM and nitrogen fixing root nodules. Recently, additional studies utilizing NGS technologies have revealed the likely evolution of mutualistic DSE fungus (*H. oryzae*) from a pathogenic ancestor: Xu et al. (2014) found (i) genome of *H. oryzae*, a mutualistic DSE of rice (Yuan et al., 2010; Su et al., 2013), to be 8% larger than closely related plant pathogens (*Magnaporthe oryzae*, *Magnaporthe poae*, and *Gaeumannomyces graminis*); (ii) high degree of macrosynteny between *H. oryzae* and *M. poae* or *G. graminis* with ancestral state reconstruction analyses suggesting that divergence of hosts resulted in differentiation among the pathogens (*M. oryzae*, *M. poae*, *G. graminis*) and the endophyte (*H. oryzae*); (iii) high number of transposable elements in *H. oryzae* likely driving *H. oryzae* genome evolution; (iv) loss of 73% of genes in 'lipid transport and metabolism' cluster likely required for appressorium-mediated colonization of leaves in the endophyte *H. oryzae* compared to the pathogen *M. oryzae*; (v) differences in the number of G-protein-coupled receptors suggesting differing responses of *H. oryzae* and *M. oryzae* to host extracellular signals; (vi) differences in nutritional preferences of *H. oryzae* and *M. oryzae* with opposite expression patterns of cell wall-degrading enzymes; (vii) differential expression of defense related-genes in *H. oryzae* and *M. oryzae* with suppression of virulence-related genes in *H. oryzae*; and, (viii) the ability of *H. oryzae* to trigger plant hormone production and the resultant growth promotion. Studies such as these demonstrate the great promise that the rapidly evolving genome and transcriptome analysis tools bear for detailed dissection of the endophyte symbioses.

The efforts that combine model plants and genomic tools are likely to further our understanding of DSE symbiosis and clarify the DSE interaction with host plants with regard to the *mutualism-parasitism-continuum*. Unlike AM, DSE fungi are not phylogenetically cohesive. Thus, genomic studies with only a handful of taxa can obfuscate their lifestyle designation. It is important to bear in mind the diversity and complexity of the associations included into the DSE symbioses. For example, *P. fortinii* s.l-*Acephala applanata* complex (PAC) is the dominant

group of DSE fungi in conifers of Northern Hemisphere (Stoyke et al., 1992; Addy et al., 2000). In contrast, *P. macrospinosa* and its close relatives are likely the most common DSE fungi in North American and European grasslands (Mandyam et al., 2010; Knapp et al., 2012). Including a variety of taxa and individuals from target ecosystems is the key to drawing meaningful inferences on a broad and likely diverse guild of fungi. Collections of large numbers of conspecific DSE fungi from an ecosystem are valuable in clarifying these obscure endophyte symbioses. For example, transcriptome characterization and comparisons of conspecific DSE fungi eliciting distinct growth responses on *Arabidopsis* ecotypes (Mandyam et al., 2013) can provide molecular clues about the relative importance of the host and fungal genotype controls over the outcome of symbiosis. Genomic and molecular data highlight the host-dependent nitrogen metabolism in the control of fungal lifestyle (Lahrmann et al., 2013). Meta-analyses have suggested that nitrogen supply likely impacts the outcome of DSE symbiosis (Newsham, 2011) and observational studies suggest that nitrogen fertilization can affect DSE colonization in the field (Mandyam and Jumpponen, 2008). These studies suggest complex and perhaps non-additive controls of DSE symbiosis: the outcomes are likely controlled in part by host genotype, in part by fungal genotype (Mandyam et al., 2013), and in part by environmental modulators. Yet, these complex systems suggest that the combined genotypic controls may prove valuable in dissecting the genomic factors involved in DSE nitrogen metabolism. Finally, the wealth of naturally occurring pairings of DSE fungi and host plants can provide insightful and beneficial experimental tools to ground-truth the conclusions from model systems. The exponential advances in NGS technologies permit the expedient and cost-effective genomic interrogations of the DSE symbiosis in model and non-model plants alike.

CONCLUSION

Here we present arguments based on host growth responses and the potential for molecular dissection of an obscure endophyte symbiosis to better elucidate the ecological and molecular drivers underlying host responses to poorly known fungal symbionts. Our extensive experiments with model and non-model plants indicate a distribution of host responses to colonization and led to a proposal of a null model that permits testing hypotheses on host responses to a population of endophytic fungi as well as generating easily testable hypotheses on the shifts in these responses under altered environmental conditions. We further highlight examples of recent studies that have identified molecular cues and mechanisms underlying the host responses to fungal symbionts and vice-versa. It is the combination of the power of simple model systems and the ground-truthing those conclusions in relevant native plant systems that are likely to best elucidate the drivers and mechanisms of obscure and poorly understood symbioses. The findings of these studies can be coupled with deep interrogations of host and fungal transcriptomes to elucidate the mechanisms that underlay the observed host growth responses.

ACKNOWLEDGMENTS

Studies on which this contribution is based were supported by the National Science Foundation Grants No. 0344838 and 0221489 (to Ari Jumpponen). We were fortunate to have a large number of Kansas State University students and co-workers assist us in experimentation and data acquisition. We wish to acknowledge Bethany Beckman, Joseph Bloomfield, Chad Fox, Jacob Elder, Jennifer Engel, Joseph Foster, Amanda Ernlund, John Girvin, Jacob Hadle, Becki Hastings, Sally Hermann, Stacey Kageyama, Steve Keim, William Klobasa, Jason Knudson, Erich Langenstroer, Tyler Lanning, Andrew Mandracchia, Patrick McClung, Jordan Metcalf, Chris Miller, Stephanie Mitchell, Melanie Moore, Lindsey Onley, Jesse Ostrander, Paul Ragusa, Amanda Riffel, Kaitlyn Schaller, Zach Starr, Brad Sullivan, Justin Trowbridge, Keith Unruh-Carey, Justin Walters, Casey Weber, Casey Wolosyn, Matthew Wymore, Stacey Yadon, and Ziyi Wang for their contributions. Publication of this article was funded in part by the Kansas State University Open Access Publishing Fund. This is Kansas Agricultural Experimental Station publication #15-233-J.

REFERENCES

Addy, H. D., Hambleton, S., and Currah, R. S. (2000). Distribution and molecular characterization of the root endophyte *Phialocephala fortinii* along an environmental gradient in the boreal forest of Alberta. *Mycol. Res.* 104, 1213–1221. doi: 10.1017/S0953756200002896

Addy, H. D., Piercey, M. M., and Currah, R. S. (2005). Microfungal endophytes in roots. *Can. J. Bot.* 83, 1–13. doi: 10.1139/b04-171

Alberton, O., Kuyper, T. W., and Summerbell, R. C. (2010). Dark septate root endophytic fungi increase growth of Scots pine seedlings under elevated CO_2 through enhanced nitrogen use efficiency. *Plant Soil* 328, 459–470. doi: 10.1007/s11104-009-0125-8

Alloisio, N., Queiroux, C., Fournier, P., Pujic, P., Normand, P., Vallenet, D., et al. (2010). The *Frankia alni* symbiotic transcriptome. *Mol. Plant Microbe Interact.* 23, 593–607. doi: 10.1094/MPMI-23-5-0593

Barrow, J. R. (2003). Atypical morphology of dark septate fungal root endophytes of *Bouteloua* in arid southwestern U.S.A. rangelands. *Mycorrhiza* 13, 239–247. doi: 10.1007/s00572-003-0222-0

Barrow, J. R., and Aaltonen, R. E. (2001). Evaluation of the internal colonization of *Atriplex canescens* (Pursh) Nutt. roots by dark septate fungi and the influence of host physiological activity. *Mycorrhiza* 11, 199–205. doi: 10.1007/s005720100111

Bodenhausen, N., Horton, M. W., and Bergelson, J. (2013). Bacterial communities associated with the leaves and the roots of *Arabidopsis thaliana*. *PLoS ONE* 8:e56329. doi: 10.1371/journal.pone.0056329

Brechenmacher, L., Kim, M. Y., Benitez, M., Li, M., Joshi, T., Calla, B., et al. (2008). Transcription profiling of soybean nodulation by *Bradyrhizobium japonicum*. *Mol. Plant Microbe Interact.* 21, 631–645. doi: 10.1094/MPMI-21-5-0631

Brotman, Y., Landau, U., Cuadros-Inostroza, Á., Tohge, T., Fernie, A. R., Chet, I., et al. (2013). *Trichoderma*-plant root colonization: escaping early plant defense responses and activation of the antioxidant machinery for saline stress tolerance. *PLoS Pathog.* 9:e1003221. doi: 10.1371/journal.ppat.1003221

Bulgarelli, D., Rott, M., Schleappi, K., ver Loren van Themaat, E., Ahmadinejad, N., Assenza, F., et al. (2012). Revealing structure and assembly cues for *Arabidopsis* root-inhabiting bacterial microbiota. *Nature* 487, 91–95. doi: 10.1038/nature11336

Caldwell, B. A., Jumpponen, A., and Trappe, J. M. (2000). Utilization of major detrital substrates by dark-septate, root endophytes. *Mycologia* 92, 230–232. doi: 10.2307/3761555

Camehl, I., Drzewiecki, C., Vadassery, J., Shahollari, B., Sherameti, I., Forzani, C., et al. (2011). The OXI1 kinase pathway mediates *Piriformospora indica*-induced growth promotion in *Arabidopsis*. *PLoS Pathog.* 7:e1002051. doi: 10.1371/journal.ppat.1002051

Camehl, I., Sherameti, I., Venus, Y., Bethke, A., Varma, A., Lee, J., et al. (2010). Ethylene signaling and ethylene- targeted transcription factors are required to balance beneficial and nonbeneficial traits in the symbiosis between the endophytic fungus *Piriformospora indica* and *Arabidopsis thaliana*. *New Phytol.* 185, 1062–1073. doi: 10.1111/j.1469-8137.2009.03149.x

Dolinar, N., and Gaberscik, A. (2010). Mycorrhizal colonization and growth of *Phragmites australis* in an intermittent wetland. *Aquat. Bot.* 93, 93–98. doi: 10.1016/j.aquabot.2010.03.012

El Yahyaoui, F., Küster, H., Ben Amor, B., Hohnjec, N., Pühler, A., Becker, A., et al. (2004). Expression profiling in *Medicago truncatula* identifies more than 750 genes differentially expressed during nodulation, including many potential regulators of the symbiotic program. *Plant Physiol.* 136, 3159–3176. doi: 10.1104/pp.104.043612

Fernando, A. A., and Currah, R. S. (1996). A comparative study of the effects of the root endophytes Leptodontidium orchidicola and *Phialocephala fortinii* (Fungi Imperfecti) on the growth of some subalpine plants in culture. *Can. J. Bot.* 74, 1071–1078. doi: 10.1139/b96-131

Fiorilli, V., Catoni, M., Miozzi, L., Novero, M., Accotto, G. P., and Lanfranco, L. (2009). Global and cell-type gene expression profiles in tomato plants colonized by an arbuscular mycorrhizal fungus. *New Phytol.* 184, 975–987. doi: 10.1111/j.1469-8137.2009.03031.x

Francis, R., and Read, D. J. (1995). Mutualism and antagonism in the mycorrhizal symbiosis, with special reference to impacts on plant community structure. *Can. J. Bot.* 73, S1301–S1309. doi: 10.1139/b95-391

Garcia, E., Alonso, A., Platas, G., and Sacristan, S. (2013). The endophytic mycobiota of *Arabidopsis thaliana*. *Fungal Divers.* 60, 71–89. doi: 10.1007/s13225-012-0219-0

Gentili, F., and Jumpponen, A. (2006). "Potential and possible uses of bacterial and fungal biofertilizers," in *Handbook of Microbial Biofertilizers*, eds M. K. Rai and A. Basra (New York: Haworth), 1–28.

Golkari, S., Gilbert, J., Prashar, S., and Procunier, J. D. (2007). Microarray analysis of *Fusarium graminearum*-induced wheat genes: identification of organ-specific and differentially expressed genes. *Plant Biotechnol. J.* 5, 38–49. doi: 10.1111/j.1467-7652.2006.00213.x

Grünig, C. R., Queloz, V., Sieber, T. N., and Holdenrieder, O. (2008). Dark septate endophytes (DSE) of the *Phiolocephala fortinii* s.l. – *Acephala applanata* species complex in tree roots: classification, population biology, and ecology. *Botany* 86, 1355–1369. doi: 10.1139/B08-108

Hartnett, D. C., and Wilson, G. W. T. (1999). Mycorrhizae influence plant community structure and diversity in tallgrass prairie. *Ecology* 80, 1187–1195. doi: 10.1890/0012-9658(1999)080[1187:MIPCSA]2.0.CO;2

Herrera, J., Khidir, H. H., Eudy, D. M., Porras-Alfaro, A., Natvig, D. O., and Sinsabaugh, R. L. (2010a). Shifting fungal endophyte communities colonize *Bouteloua gracilis*: effect of host tissue and geographical distribution. *Mycologia* 102, 1012–1026. doi: 10.3852/09-264

Herrera, J., Poudel, R., Nebel, K. A., and Collins, S. (2010b). Precipitation increases the abundance of some groups of root-associated fungal endophytes in a semiarid grassland. *Ecosphere* 2:50.

Hoeksema, J. D., Chaudhary, V. B., Gehring, C. A., Johnson, N. C., Karst, J., Koide, R. T., et al. (2010). A meta-analysis of context-dependency in plant response to inoculation with mycorrhizal fungi. *Ecol. Lett.* 13, 394–407. doi: 10.1111/j.1461-0248.2009.01430.x

Hohnjec, N., Vieweg, M. F., Pühler, A., Becker, A., and Küster, H. (2005). Overlaps in the transcriptional profiles of *Medicago truncatula* roots inoculated with two different *Glomus* fungi provide insights into the genetic program activated during arbuscular mycorrhiza. *Plant Physiol.* 137, 1283–1301. doi: 10.1104/pp.104.056572

Hou, X., and Guo, S. (2009). Interaction between a dark septate endophytic isolate from *Dendrobium* sp. and roots of *D. nobile* seedlings. *J. Integr. Plant Biol.* 51, 374–381. doi: 10.1111/j.1744-7909.2008.00777.x

Johansson, T., Le Quéré, A., Ahren, D., Söderström, B., Erlandsson, R., Lundeberg, J., et al. (2004). Transcriptional responses of *Paxillus involutus* and *Betula pendula* during formation of ectomycorrhizal root tissue. *Mol. Plant Microbe Interact.* 17, 202–215. doi: 10.1094/MPMI.2004.17.2.202

Johnson, N. C. (2010). Resource stoichiometry elucidates the structure and function of arbuscular mycorrhizas across scales. *New Phytol.* 185, 631–647. doi: 10.1111/j.1469-8137.2009.03110.x

Johnson, N. C., Graham, J. H., and Smith, F. A. (1997). Functioning of mycorrhizal associations along the mutualism-parasitism continuum. *New Phytol.* 135, 575–586. doi: 10.1046/j.1469-8137.1997.00729.x

Jones, M. D., Durall, D. M., and Tinker, P. B. (1990). Phosphorus relationships and production of extramatrical hyphae by 2 types of willow ectomycorrhizas at different soil phosphorus levels. *New Phytol.* 115, 259–267. doi: 10.1111/j.1469-8137.1990.tb00451.x

Jones, M. D., and Smith, S. E. (2004). Exploring functional definitions of mycorrhizas: are mycorrhizas always mutualisms? *Can. J. Bot.* 82, 1089–1109. doi: 10.1139/b04-110

Jumpponen, A. (2001). Dark septate endophytes – are they mycorrhizal? *Mycorrhiza* 11, 207–211. doi: 10.1007/s005720100112

Jumpponen, A., Kageyama, S. A., and Mandyam, K. G. (2011a). "Isolation of fungal root endophytes, molecular screening, and testing of Koch's Postulates," in *Prospects and Applications for Plant-Associated Microbes. A Laboratory Manual, Part B: Fungi*, eds A. M. Pirttilä and S. Sorvari (Piikkiö: BioBien Innovations (BBi)), 28–33.

Jumpponen, A., Kageyama, S. A., and Mandyam, K. G. (2011b). "Identification of root-associated fungal endophytes," in *Prospects and Applications for Plant-Associated Microbes. A Laboratory Manual, Part B: Fungi*, eds A. M. Pirttilä and S. Sorvari (Piikkiö: BioBien Innovations (BBi)), 173–176.

Jumpponen, A., and Trappe, J. M. (1998a). Performance of *Pinus contorta* inoculated with two strains of root endophytic fungus *Phialocephala fortinii*: effects of resynthesis system and glucose concentration. *Can. J. Bot.* 76, 1205–1213. doi: 10.1139/b98-098

Jumpponen, A., and Trappe, J. M. (1998b). Dark-septate root endophytes: a review with special reference to facultative biotrophic symbiosis. *New Phytol.* 140, 295–310. doi: 10.1046/j.1469-8137.1998.00265.x

Jumpponen, A., Trappe, J. M., Mattson, K. G., and Trappe, J. M. (1998). Mycorrhizal functioning of *Phialocephala fortinii*: interactions with soil nitrogen and organic matter. *Mycorrhiza* 7, 261–265. doi: 10.1007/s005720050190

Kageyama, S. A., Mandyam, K. G., and Jumpponen, A. (2008). "Diversity, function and potential applications of the root-associated endophytes," in *Mycorrhiza – State of the Art, Genetics and Molecular Biology, Eco-Function, Biotechnology, Ecophysiology, Structure and Systemetics*, ed. A. Varma (Berlin: Springer-Verlag), 29–59.

Karst, J., Jones, M. D., and Turkington, R. (2009). Ectomycorrhizal colonization and intraspecific variation in growth responses of lodgepole pine. *Plant Ecol.* 200, 161–165. doi: 10.1007/s11258-008-9443-9

Karst, J., Marczak, L., Jones, M. D., and Turkington, R. (2008). The mutualism-parasitism continuum in ectomycorrhizas: a quantitative assessment using meta-analysis. *Ecology* 89, 1032–1042. doi: 10.1890/07-0823.1

Khatabi, B., Molitor, A., Lindermayr, C., Pfiffi, S., Durner, J., von Wettstein, D., et al. (2012). Ethylene supports colonization of plant roots by the mutualistic fungus *Piriformospora indica*. *PLoS ONE* 7:e35502. doi: 10.1371/journal.pone.0035502

Khidir, H. H., Eudy, D. M., Porras-Alfaro, A., Herrera, J., Natvig, D. O., and Sinsabaugh, R. L. (2010). A general suite of fungal endophytes dominate the roots of two dominant grasses in a semiarid grassland. *J. Arid. Environ.* 74, 35–42. doi: 10.1016/j.jaridenv.2009.07.014

Klironomos, J. N. (2003). Variation in plant response to native and exotic arbuscular mycorrhizal fungi. *Ecology* 84, 2292–2301. doi: 10.1890/02-0413

Knapp, D. G., Pintye, A., and Kovacs, G. M. (2012). The dark side is not fastidious – dark septate endophytic fungi of native and invasive plants of semiarid sandy areas. *PLoS ONE* 7:e32570. doi: 10.1371/journal.pone.0032570

Koide, R. T. (1991). Nutrient supply, nutrient demand and plant-response to mycorrhizal infection. *New Phytol.* 117, 365–386. doi: 10.1111/j.1469-8137.1991.tb00001.x

Kovacs, G. M., and Szigetvari, C. (2002). Mycorrhizae and other root-associated fungal structures of the plants of a sandy grassland on the Great Hungarian Plain. *Phyton* 42, 211–223.

Küster, H., Hohnjec, N., Krajinski, F., El, Y. F., Manthey, K., Gouzy, J., et al. (2004). Construction and validation of cDNA-based Mt6k-RIT macro- and microarrays to explore root endosymbioses in the model legume *Medicago truncatula*. *J. Biotechnol.* 108, 95–113. doi: 10.1016/j.jbiotec.2003.11.011

Küster, H., Vieweg, M. F., Manthey, K., Baier, M. C., Hohnjec, N., and Perlick, A. M. (2007). Identification and expression regulation of symbiotically activated legume genes. *Phytochemistry* 68, 8–18. doi: 10.1016/j.phytochem.2006.09.029

Lahrmann, U., Ding, Y., Banhara, A., Rath, M., Hajirezaei, M. R., Döhlemann, S., et al. (2013). Host-related metabolic cues affect colonization strategies of a root endophyte. *Proc. Natl. Acad. Sci. U.S.A.* 110, 13965–13970. doi: 10.1073/pnas.1301653110

Lakshmanan, V., Castaneda, R., Rudrappa, T., and Bais, H. P. (2013). Root transcriptome analysis of *Arabidopsis thaliana* exposed to beneficial *Bacillus subtilis* FB17

rhizobacteria revealed genes for bacterial recruitment and plant defense independent of malate efflux. *Planta* 238, 657–668. doi: 10.1007/s00425-013-1920-2

Le Quéré, A., Wright, D. P., Söderström, B., Tunlid, A., and Johansson, T. (2005). Global patterns of gene regulation associated with the development of ectomycorrhiza between birch (*Betula* Roth.) and *Paxillus involutus* (Batsch) Fr. *Mol. Plant Microbe Interact.* 18, 659–673. doi: 10.1094/MPMI-18-0659

Lundberg, D. S., Lebeis, S. L., Paredes, S. H., Yourstone, S., Gehring, J., Malfatti, S., et al. (2012). Defining the core *Arabidopsis thaliana* root microbiome. *Nature* 487, 86–90. doi: 10.1038/nature11237

Mandyam, K., and Jumpponen, A. (2005). Seeking the elusive function of the root-colonising dark septate endophytic fungi. *Stud. Mycol.* 53, 173–189. doi: 10.3114/sim.53.1.173

Mandyam, K., and Jumpponen, A. (2008). Seasonal and temporal dynamics of arbuscular mycorrhizal and dark septate endophytic fungi in a tallgrass prairie ecosystem are minimally affected by nitrogen enrichment. *Mycorrhiza* 18, 145–155. doi: 10.1007/s00572-008-0165-6

Mandyam, K., and Jumpponen, A. (2014). "Unraveling the dark septate endophyte functions: insights from the *Arabidopsis* model," in *Advances in Endophytic Research*, eds V. C. Verma and A. C. Gange (Berlin: Springer-Verlag), 115–141.

Mandyam, K., Fox, C., and Jumpponen, A. (2012). Septate endophyte colonization and host responses of grasses and forbs native to a tallgrass prairie. *Mycorrhiza* 22, 109–119. doi: 10.1007/s00572-011-0386-y

Mandyam, K., Loughin, T., and Jumpponen, A. (2010). Isolation and morphological and metabolic characterization of common endophytes in annually burned tallgrass prairie. *Mycologia* 102, 813–821. doi: 10.3852/09-212

Mandyam, K., Roe, J., and Jumpponen, A. (2013). *Arabidopsis thaliana* model system reveals a continuum of responses to root endophyte colonization. *Fungal Biol.* 117, 250–260. doi: 10.1016/j.funbio.2013.02.001

Mathys, J., De Cremer, K., Timmermans, P., van Kerckhove, S., Lievens, B., Vanhaecke, M., et al. (2012). Genome-wide characterization of ISR induced in *Arabidopsis thaliana* by *Trichoderma hamatum* T382 against *Botrytis cinerea* infection. *Front. Plant Sci.* 3:108. doi: 10.3389/fpls.2012.00108

Mayerhofer, M. S., Kernaghan, G., and Harper, K. A. (2013). The effects of fungal root endophytes on plant growth: a meta-analysis. *Mycorrhiza* 23, 119–128. doi: 10.1007/s00572-012-0456-9

Melin, E. (1922). On the mycorrhizas of *Pinus sylvestris* L. and *Picea abies* Karst.: a preliminary note. *J. Ecol.* 9, 254–257. doi: 10.2307/2255406

Morán-Diez, E., Rubio, B., Domínguez, S., Hermosa, R., Montea, E., and Nicolás, C. (2012). Transcriptomic response of *Arabidopsis thaliana* after 24 h incubation with the biocontrol fungus *Trichoderma harzianum*. *J. Plant Phys.* 169, 614–620. doi: 10.1016/j.jplph.2011.12.016

Munkvold, L., Kjoller, R., Vestberg, M., Rosendahl, S., and Jakobsen, I. (2004). High functional diversity within species of arbuscular mycorrhizal fungi. *New Phytol.* 164, 357–364. doi: 10.1111/j.1469-8137.2004.01169.x

Newsham, K. K. (1999). *Phialophora graminicola*, a dark septate fungus, is a beneficial associate of the grass *Vulpia ciliata* ssp *ambigua*. *New Phytol.* 144, 517–524. doi: 10.1046/j.1469-8137.1999.00537.x

Newsham, K. K. (2011). A meta-analysis of plant responses to dark septate root endophytes. *New Phytol.* 190, 783–793. doi: 10.1111/j.1469-8137.2010.03611.x

Nongbri, P., Johnson, J. M., Sherameti, I., Glawischnig, E., Halkier, B. A., and Oelmüller, R. (2012). Indole-3-acetaldoxime-derived compounds restrict root colonization in the beneficial interaction between *Arabidopsis* roots and the endophyte *Piriformospora indica*. *Mol. Plant Microbe Interact.* 25, 1186–1197. doi: 10.1094/MPMI-03-12-0071-R

Peskan-Berghöfer, T., Shahollari, B., Giong, P. H., Hehl, S., Markert, C., Blanke, V., et al. (2004). Association of *Piriformospora indica* with *Arabidopsis thaliana* roots represents a novel system to study beneficial plant-microbe interactions and involves early plant protein modifications in the endoplasmic reticulum and at the plasma membrane. *Physiol. Plant.* 122, 465–477. doi: 10.1111/j.1399-3054.2004.00424.x

Piculell, B. J., Hoeksema, J. D., and Thompson, J. N. (2008). Interactions of biotic and abiotic environmental factors in an ectomycorrhizal symbiosis, and the potential for selection mosaics. *BMC Biol.* 6:23. doi: 10.1186/1741-7007-6-23

Pierce, E. J., and Rey, M. E. C. (2013). Assessing global transcriptome changes in response to South African cassava mosaic virus [ZA-99] infection in susceptible *Arabidopsis thaliana*. *PLoS ONE* 8:e67534. doi: 10.1371/journal.pone.0067534

Porras-Alfaro, A., Herrera, J., Sinsabaugh, R. L., Odenbach, K. J., Lowrey, T., and Natvig, D. O. (2008). Novel root fungal consortium associated with a dominant desert grass. *Appl. Environ. Microbiol.* 74, 2805–2813. doi: 10.1128/AEM.02769-07

Postnikova, O. A., and Nemchinov, L. G. (2012). Comparative analysis of microarray data in *Arabidopsis* transcriptome during compatible interactions with plant viruses. *Virol. J.* 9:101. doi: 10.1186/1743-422X-9-101

Redman, R. S., Dunigan, D. D., and Rodriguez, R. J. (2001). Fungal symbiosis from mutualism to parasitism: who controls the outcome, host or invader? *New Phytol.* 151, 705–716. doi: 10.1046/j.0028-646x.2001.00210.x

Redman, R. S., Litvintseva, A., Sheehan, K. B., Henson, J. M., and Rodriguez, R. J. (1999). Fungi from geothermal soils in Yellowstone National Park. *Appl. Environ. Microbiol.* 65, 5193–5197.

Rodriguez, R. J., Henson, J., van Volkenburgh, E., Hoy, M., Wright, L., Beckwith, F., et al. (2008). Stress tolerance in plants via habitat-adapted symbiosis. *ISME J.* 2, 404–416. doi: 10.1038/ismej.2007.106

Rodriguez, R. J., White, J. F. Jr., Arnold, A. E., and Redman, R. S. (2009). Fungal endophytes: diversity and functional roles. *New Phytol.* 182, 314–330. doi: 10.1111/j.1469-8137.2009.02773.x

Saikkonen, K., Faeth, S., Helander, M., and Sullivan, T. (1998). Fungal endophytes: a continuum of interactions with host plants. *Ann. Rev. Ecol. Syst.* 29, 319–343. doi: 10.1146/annurev.ecolsys.29.1.319

Salvioli, A., Zouari, I., Chalot, M., and Bonfante, P. (2012). The arbuscular mycorrhizal status has an impact on the transcriptome profile and amino acid composition of tomato fruit. *BMC Plant Biol.* 12:44. doi: 10.1186/1471-2229-12-44

Sapp, J. (2004). The dynamics of symbiosis: an historical overview. *Can. J. Bot.* 82, 1046–1056. doi: 10.1139/b04-055

Schuller, A., Kehr, J., and Ludwig-Müller, J. (2014). Laser microdissection coupled to transcriptional profiling of *Arabidopsis* roots inoculated by *Plasmodiophora brassicae* indicates a role for brassinosteroids in clubroot formation. *Plant Cell Physiol.* 55, 392–411. doi: 10.1093/pcp/pct174

Schwartz, M. W., and Hoeksema, J. D. (1998). Specialization and resource trade: biological markets as a model of mutualisms. *Ecology* 79, 1029–1038. doi: 10.1890/0012-9658(1998)079[1029:SARTBM]2.0.CO;2

Sebastiana, M., Vieira, B., Lino-Neto, T., Monteiro, F., Figueiredo, A., Sousa, L., et al. (2014). Oak root response to ectomycorrhizal symbiosis establishment: RNA-Seq derived transcript identification and expression profiling. *PLoS ONE* 9:e98376. doi: 10.1371/journal.pone.0098376

Spaepen, S., Bossuyt, S., Engelen, K., Marchal, K., and Vanderleyden, J. (2014). Phenotypical and molecular responses of *Arabidopsis thaliana* roots as a result of inoculation with the auxin-producing bacterium *Azospirillum brasilense*. *New Phytol.* 201, 850–861. doi: 10.1111/nph.12590

Stoyke, G., Egger, K. N., and Currah, R. S. (1992). Characterization of sterile endophytic fungi from the mycorrhizae of sub-alpine plants. *Can. J. Bot.* 70, 2009–2016. doi: 10.1139/b92-250

Su, Z.-Z., Mao, L.-J., Li, N., Feng, X.-X., Yuan, Z.-L., Wang, L.-W., et al. (2013). Evidence for biotrophic lifestyle and biocontrol potential of dark septate endophyte *Harpophora oryzae* to rice blast disease. *PLoS ONE* 8:e61332. doi: 10.1371/journal.pone.0061332

Tellenbach, C., Grünig, C., and Sieber, T. N. (2011). Negative effects on survival and performance of Norway spruce seedlings colonized by dark septate root endophytes are primarily isolate dependent. *Environ. Microbiol.* 13, 2508–2517. doi: 10.1111/j.1462-2920.2011.02523.x

Tellenbach, C., and Sieber, T. N. (2013). Do colonization by dark septate endophytes and elevated temperature affect pathogenicity of oomycetes? *FEMS Microbiol. Ecol.* 82, 157–168. doi: 10.1111/j.1574-6941.2012.01415.x

Thompson, J. N., Reichman, O. J., Morin, P. J., Polis, G. A., Power, M. E., Sterner, R. W., et al. (2001). Frontiers of ecology. *Bioscience* 51, 15–24. doi: 10.1641/0006-3568(2001)051[0015:FOE]2.0.CO;2

Thomson, B. D., Grove, T. S., Malajczuk, N., and Hardy, G. E. S. J. (1994). The effectiveness of ectomycorrhizal fungi in increasing the growth of *Eucalyptus globulus* Labill in relation to root colonization and hyphal development in soil. *New Phytol.* 126, 517–524. doi: 10.1111/j.1469-8137.1994.tb04250.x

Usuki, F., and Narisawa, H. (2007). A mutualistic symbiosis between a dark septate endophytic fungus, Heteroconium chaetospira, and a nonmycorrhizal plant, Chinese cabbage. *Mycologia* 99, 175–184. doi: 10.3852/mycologia.99.2.175

Vadassery, J., Ranf, S., Drzewiecki, C., Mithöfer, A., Mazarsa, C., Scheel, D., et al. (2009a). A cell wall extract from the endophytic fungus *Piriformospora indica* promotes growth of *Arabidopsis* seedlings and induces intracellular calcium elevation in roots. *Plant J.* 59, 193–206. doi: 10.1111/j.1365-313X.2009.03867.x

Vadassery, J., Tripathi, S., Prasad, R., Varma, A., and Oelmüller, R. (2009b). Monodehydroascorbate reductase 2 and dehydroascorbate reductase 5 are crucial for a mutualistic interaction between *Piriformospora indica* and *Arabidopsis*. *J. Plant Physiol.* 166, 1263–1274. doi: 10.1016/j.jplph.2008.12.016

van der Heijden, M. G. A. (2002). "Arbuscular mycorrhizal fungi as a determinant of plant diversity: in search for underlying mechanisms and general principles," in *Mycorrhizal Ecology*, eds M. G. A. van der Heijden and I. R. Sanders (Berlin: Springer-Verlag), 243–266.

Vohnik, M., Albrechtova, J., and Vosatka, M. (2005). The inoculation with *Oidiodendron maius* and *Phialocephala fortinii* alters phosphorus and nitrogen uptake, foliar C:N ratio and root biomass distribution in *Rhododendron* cv. Azurro. *Symbiosis* 40, 87–96.

Wang, Y., Ohara, Y., Nakayashiki, H., Tosa, Y., and Mayama, S. (2005). Microarray analysis of the gene expression profile induced by the endophytic plant growth-promoting rhizobacteria, *Pseudomonas fluorescens* FPT9601-T5 in *Arabidopsis*. *Mol. Plant Microbe Interact.* 18, 385–396. doi: 10.1094/MPMI-18-0385

Weiss, M., Sykorova, Z., Garnica, S., Riess, K., Martos, F., Krause, C., et al. (2011). Sebacinales everywhere: previously overlooked ubiquitous fungal endophytes. *PLoS ONE* 6:e16793. doi: 10.1371/journal.pone.0016793

Wilson, G. W. T., and Hartnett, D. C. (1998). Interspecific variation in plant responses to mycorrhizal colonization in tallgrass prairie. *Am. J. Bot.* 85, 1732–1738. doi: 10.2307/2446507

Xin, M., Wang, X., Peng, H., Yao, Y., Xie, C., Han, Y., et al. (2012). Transcriptome comparison of susceptible and resistant wheat in response to powdery mildew infection. *Genomics Proteomics Bioinformatics* 10, 94–106. doi: 10.1016/j.gpb.2012.05.002

Xu, X.-H., Su, Z.-Z., Wang, C., Kubicek, C. P., Feng, X.-X., Mao, L.-J., et al. (2014). The rice endophyte *Harpophora oryzae* genome reveals evolution from a pathogen to a mutualistic endophyte. *Sci. Rep.* 4:a5783. doi: 10.1038/srep05783

Yu, T., Nassuth, A., and Peterson, R. L. (2001). Characterization of the interaction between the dark septate fungus *Phialocephala fortinii* and *Asparagus officinalis* roots. *Can. J. Microbiol.* 47, 741–753. doi: 10.1139/cjm-47-8-741

Yuan, Z., Lin, F., Zhang, C., and Kubicek, C. P. (2010). A new species of *Harpophora* (Magnaporthaceae) recovered from healthy wild rice (*Oryza granulata*) roots, representing a novel member of a beneficial dark septate endophyte. *FEMS Microbiol. Lett.* 307, 94–101. doi: 10.1111/j.1574-6968.2010.01963.x

Zhang, H., Tang, M., Chen, H., Wang, Y., and Ban, Y. (2010). Arbuscular mycorrhizas and dark septate endophytes colonization status in medicinal plant *Lycium barbarum* L. in arid Northwestern China. *African J. Microbiol. Res.* 4, 1914–1920.

Conflict of Interest Statement: The authors declare that the research was conducted in the absence of any commercial or financial relationships that could be construed as a potential conflict of interest.

Received: 20 October 2014; accepted: 17 December 2014; published online: 12 January 2015.

Citation: Mandyam KG and Jumpponen A (2015) Mutualism–parasitism paradigm synthesized from results of root-endophyte models. Front. Microbiol. ***5****:776. doi: 10.3389/fmicb.2014.00776*

This article was submitted to Plant-Microbe Interaction, a section of the journal Frontiers in Microbiology.

frontiers in Microbiology

METHODS
published: 28 September 2015
doi: 10.3389/fmicb.2015.01033

Phenotype MicroArrays as a complementary tool to next generation sequencing for characterization of tree endophytes

*Kathrin Blumenstein[1†], David Macaya-Sanz[2†], Juan A. Martín[2], Benedicte R. Albrectsen[3,4] and Johanna Witzell[1,5]**

[1] Southern Swedish Forest Research Centre, Swedish University of Agricultural Sciences, Alnarp, Sweden, [2] Department of Natural Systems and Resources, School of Forest Engineers, Technical University of Madrid, Madrid, Spain, [3] Department of Plant Physiology, Umeå Plant Science Centre, Umeå University, Umeå, Sweden, [4] Department of Plant and Environmental Sciences, University of Copenhagen, Copenhagen, Denmark, [5] School of Forest Sciences, Faculty of Science and Forestry, University of Eastern Finland, Joensuu, Finland

OPEN ACCESS

Edited by:
Mysore V. Tejesvi, University of Oulu, Finland

Reviewed by:
Vijai Kumar Gupta, NUI Galway, Ireland
Liliana Maria Cano, North Carolina State University, USA

***Correspondence:**
Johanna Witzell, Southern Swedish Forest Research Centre, Swedish University of Agricultural Sciences, Box 49, 23053 Alnarp, Sweden
johanna.witzell@slu.se

[†]*These authors are joint first authors.*

Specialty section:
This article was submitted to Plant Biotic Interactions, a section of the journal Frontiers in Microbiology

Received: *17 May 2015*
Accepted: *11 September 2015*
Published: *28 September 2015*

Citation:
Blumenstein K, Macaya-Sanz D, Martín JA, Albrectsen BR and Witzell J (2015) Phenotype MicroArrays as a complementary tool to next generation sequencing for characterization of tree endophytes. Front. Microbiol. 6:1033. doi: 10.3389/fmicb.2015.01033

There is an increasing need to calibrate microbial community profiles obtained through next generation sequencing (NGS) with relevant taxonomic identities of the microbes, and to further associate these identities with phenotypic attributes. Phenotype MicroArray (PM) techniques provide a semi-high throughput assay for characterization and monitoring the microbial cellular phenotypes. Here, we present detailed descriptions of two different PM protocols used in our recent studies on fungal endophytes of forest trees, and highlight the benefits and limitations of this technique. We found that the PM approach enables effective screening of substrate utilization by endophytes. However, the technical limitations are multifaceted and the interpretation of the PM data challenging. For the best result, we recommend that the growth conditions for the fungi are carefully standardized. In addition, rigorous replication and control strategies should be employed whether using pre-configured, commercial microwell-plates or in-house designed PM plates for targeted substrate analyses. With these precautions, the PM technique is a valuable tool to characterize the metabolic capabilities of individual endophyte isolates, or successional endophyte communities identified by NGS, allowing a functional interpretation of the taxonomic data. Thus, PM approaches can provide valuable complementary information for NGS studies of fungal endophytes in forest trees.

Keywords: fungal phenotype, nutrient utilization, fungus–fungus interactions, phenolic compounds, Biolog PM

Introduction

The increasing interest in endophyte communities of plants, including those of forest trees, is fueled by the apparent potential of the endophytes to shape and modulate the stress tolerance in host plants, directly by priming or elevating defence responses in the plant (Rodriguez and Redman, 2008; Eyles et al., 2010; Albrectsen and Witzell, 2012; Witzell et al., 2014) or indirectly through competition for substrates (Blumenstein et al., 2015). Moreover, endophytes are explored as a potent source of new solutions, based on metabolites and enzymes, for industrial, pharmaceutical,

or agricultural purposes (Rodrigues et al., 2000; Schulz et al., 2002; Rančić et al., 2006; Gaur et al., 2010). Investigations of endophytes have traditionally been constrained by the difficulty of deciphering the global endophyte communities that are hidden inside the plants and capturing the target species to cultures for functional studies at organismal level. Recent methodological advances may solve some of these problems. For instance, improvements in standard isolation and culturing processes are feasible (Kaewkla and Franco, 2013), and the accumulating information from next generation sequencing (NGS) studies is likely to support discovery of new endophytic species (Toju et al., 2013), and provide information about their characters (Lim et al., 2010). However, while the genomic NGS analyses now provide powerful tools for global high throughput analyses of endophyte communities (Unterseher et al., 2012), they are still limited by the need of conducting a destructive extraction procedure that creates a snapshot of the point-in-time status in the samples (Greetham, 2014). There is also an increasing need to calibrate the NGS-community profiles with relevant taxonomic identities of the microbes, and to further associate these identities with the corresponding functional traits.

The functional traits of organisms are expressed as phenotypic attributes, jointly defined by the genome and the environment (cf. Houle et al., 2010). In fact, it is the phenotypic characters that make up the desired outcome of any selection process and also the key to understanding the biological complexity (Houle et al., 2010; Cabrera-Bosquet et al., 2012). Adequate and reliable phenotyping is thus a crucial task, if we want to utilize the functional traits of endophytes for practical applications. In general, modern strategies for high throughput phenotyping of organisms (phenomics) include application of computer vision, imaging of cell traits using visible light, NIR and fluorescent imaging technology and reporter gene expression (Houle et al., 2010), but effective application of these methods in studies of the functional traits of endophytes is not uncomplicated. The taxonomic and morphological diversity and the physiological versatility of fungal endophytes further complicate the acquirement of biologically relevant information about their phenotypes. For instance, a major challenge in studies of fungal phenotypes is the indeterminate growth of the fungi, with mycelium that forms colonies and is composed of hyphae as the basic units (Davidson, 1998; Falconer et al., 2005). Moreover, the analysis is complicated by the fact that the fungal hyphae may behave collectively rather than as isolated modules, reacting to the conditions across the whole colony (Falconer et al., 2005). In the case of endophytic fungi, these challenges are magnified further, because the endophytes thrive inside the tissues and are often reluctant to be cultured on artificial media. Consequently, any phenotyping of fungal isolates is usually done using low throughput morphological or physiological measurements that despite their great value are often cumbersome.

An emerging method that seems to have a realistic potential to provide at high throughput information about the phenotypes of microbial isolates is the Phenotype MicroArray (PM) technique. This technique relies on microtiter-plate-based substrate utilization assays (Bochner and Savageau, 1977; Bochner, 1989; Bochner et al., 2001). PM technique provides (semi-)high throughput assays for characterization and monitoring the cellular phenotypes of pure cultures or communities in an environmental sample (Borglin et al., 2012). The cellular responses, i.e., respiration or growth, can be monitored over a period of time, which makes it possible to capture some of the metabolic dynamics of the target cells (Bochner et al., 2001). The method thus allows construction of specific metabolic fingerprints that can be used for identification of microbes with desired traits, e.g., for industrial applications (Greetham, 2014). So far, however, the method has mainly been used in studies of bacteria. For example, Dong et al. (2010) applied PM for identification of bacterial strains with capacity for converting a novel precursor into an anti-cholesterol drug. Recently, however, the method has gained popularity also in studies of fungi, including endophytes (Atanasova and Druzhinina, 2010; Blumenstein et al., 2015). For example, PM technology has been used to optimize growth media for production of secondary metabolites by filamentous fungi (Singh, 2009).

The aim of this method paper is to illustrate how PM methods can be applied in studies on the ecology and utilization potential of forest tree endophytes, and validate the performance and reliability of these methods. In particular, we report experiences from two procedures, one where we used pre-configured, commercially available PM arrays to evaluate nutritional niches of endophytes and pathogens sharing the same host plant (Procedure I; part of the results modified from Blumenstein et al., 2015), and another where we used an in-house configured PM array to test the sensitivity of endophytes to a set of carbon sources and inhibitory substrates (phenolic compounds), which were interesting for our research questions but not available among the preconfigured, commercially available arrays (Procedure II). Finally, we discuss the benefits and limitations of the PM approach in studies on the ecological role of tree endophytes and their utilization in practical applications.

Materials and Methods

Procedure I: Utilization of Pre-configured Biolog PM Plates for Comparison of Nutritional Niches of Endophytes and Pathogens

Selection of the Fungi for the Studies

We employed PM technique in studies where the aim was to experimentally explore the competitive interactions between pathogens and endophytes that co-exist in time and space in trees. For this purpose, the carbon and nitrogen substrate utilization patterns of two pathogens (causal agents of Dutch elm disease, *Ophiostoma novo-ulmi* and *O. ulmi*) and four endophyte species (see below) were studied. Three isolates per each of the *Ophiostoma*-species were purchased from CBS-KNAW Fungal Biodiversity Center, Netherlands, or originated from the mycology library of Spanish elm breeding program (Solla et al., 2008). Three of the studied endophytic fungi were isolated earlier from elm trees (*Ulmus* sp.) (Martín et al., 2013). Two of them, *Monographella nivalis* var. *neglecta* (three

isolates) and *Pyrenochaeta cava* (two isolates) have earlier shown chemical antagonism against the pathogenic *O. novo-ulmi*. They both inhabit elm bark and xylem where interspecific competition for the niche might occur (Martín et al., 2015). The third fungus, *Aureobasidium pullulans* (three isolates), was included in the tests as an example of a ubiquitous, "generalist" fungus, with potentially broad nutritional niche. In nitrogen utilization tests, also a common biocontrol fungus, *Trichoderma harzianum* (MB#340299, purchased from CBS - KNAW Fungal Biodiversity Center, Netherlands) was included for comparison. All fungi were cultivated on malt extract agar (MEA) and 26°C following the recommended protocol (Biolog Inc.). Occasional light exposure was not excluded during the experiment period.

Preparation of Inoculum

For preparation of homogenous inoculum, we developed the following protocol that is carried out under sterile conditions. In order to obtain pure fungal mass and to avoid any contamination of agar in the inoculation fluid (IF), fungi were cultivated on semi-permeable cellophane membrane on MEA. After incubation at 26°C (10–15 days depending on species' individual growth rate), the fungal mass was lifted from the cellophane membrane with a cotton swab. Material from 2 to 5 agar plates per isolate was found to contain sufficient fungal material for the tests. The material was transferred into 2 mL Eppendorf vials and manually homogenized with a pestle together with 500 μL of Biolog FF-IF. When a thick suspension was obtained, it was poured over cotton wool on a metal sieve placed over a beaker. By adding 1–3 mL FF-IF, the material was flushed through the cotton. The longer fungal hyphae and bigger cell aggregates were collected into the cotton wool, and a dense, homogenous solution containing fungal spores and small aggregates of mycelial cells was collected underneath the sieve. The viability of the cells in the suspension immediately after the collection procedure was tested by spreading 200 μL aliquots of the cell stock suspension on MEA plates. The viability of the cells in the suspension immediately after the cell collection procedure was tested by spreading 200 μL aliquots of the suspension on MEA plates. After 3–4 days incubation, outgrowing mycelium was visually checked for development and purity.

Using a turbidimeter, the optical density of the inoculum was adjusted to 62% by adding small amounts from the cell suspension. Depending on the species, 400 μL^{-1} mL of cell stock suspension per 17 mL FF-IF was used. Then, following the protocol from the manufacturer, solutions of glucose, sodium sulfate, and potassium phosphate were added. The final inoculum was transferred into a sterile reservoir for multichannel pipettes, and 100 μL of suspension was pipetted into each PM array well. The suspension was added to plates on the same day than it was prepared.

In order to count the colony forming units (CFU) of the inoculum, an aliquot of 100 μL was pipetted into Petri dishes containing MEA, gently tilting the dish with sterile glass beads to evenly distribute the fluid on the agar surface. After 3–4 days incubation, the CFU was determined.

Pre-configured Biolog Phenotype MicroArrays

The commercially available, pre-configured Biolog Phenotype MicroArrays (Biolog Inc., Harvard, CA, USA) are composed of microtiter plates with one negative control well and 95 wells pre-filled with a nutrient source (e.g., C,N,P,S, amino acids) or substrates leading to inhibitory conditions (pH, NaCl, antibiotics) in a dried state. The substrate rehydrates after the target cell suspension, mixed with an IF at a standardized cell density, is inserted in each well. The IF provided by Biolog contains nutrients or chemicals (e.g., C, N, P, S, K, Na, Mg, Ca, Fe, amino acids, purines, pyrimidines, and vitamins) at sufficient levels to maintain cell viability. Through this combination (a nutrient source or an inhibitory compound and IF), unique culture conditions are created for the inoculated cells (Bochner, 2009).

The phenotypic response, i.e., how the cells respond to the conditions, is monitored by the change of color or turbidity in each well. The IF contains a tetrazolium salt, which is reduced by the action of dehydrogenases and reductases of the prokaryote and yeast cells, yielding a purple formazan dye. This color reaction is irreversible, and thus the more intensive the stronger the organism is able to catabolize the provided substrate in the well. In other words, a color reaction indicates that the inoculated cells are actively metabolizing a substrate in the well, while the lack of color change implies that the cells are not able to utilize the substrate. The rate and extent of color formation in each well can be monitored at 490 nm and recorded by the OMNILOG instrument (Bochner, 2003), a specialized instrumentation provided by Biolog. Kinetic response curves can be generated for each well and used for cellular phenotype comparisons. Alternatively, color change can be recorded spectrophotometrically (Atanasova and Druzhinina, 2010), or by visual observations (Bochner et al., 2001). While the color reaction is most convenient for bacteria, the growth response of filamentous fungi can be recorded as change in the optical density at 750 nm (OD750) (Tanzer et al., 2003; Druzhinina et al., 2006; Seidl et al., 2006). Measurements of growth can also be conducted at 590 nm (Blumenstein et al., 2015), which yield results that are comparable to 750 nm.

In our Procedure I, we examined the nutritional niche of endophytes and pathogens with the Biolog plates: PM1 and 2A, that represent 190 carbon sources (95 on each plate) (Blumenstein et al., 2015) and PM3B with 95 nitrogen sources. Three (carbon-source studies, Blumenstein et al., 2015) or two (nitrogen-source studies) replicate plates were used.

Measurements and Data-Analysis

Data for fungal activity was obtained through measurements of OD at 590 nm (PM1 and PM 2A, Blumenstein et al., 2015) or 750 nm (PM3B) using a spectrophotometer with microplate format compatibility (SPECTROstar Nano BMG Labtech) every 24 h for 10 days. The first reading (T = 0) was done at approximately 30 min after the plates were inoculated with the fungal IF. In the PM3A (nitrogen test), the content of six randomly chosen wells of all 30 plates was placed on MEA plates after 360 h when the final reading was done in order to control possible contaminations and vitality of cells. The purity of the

developing mycelium was observed during the seven following days.

Differences in OD for specific substrates were tested using standard ANOVA analyses. Global differences in substrate use were compared by implementing multivariate statistics or by calculation of a niche overlap index (NOI) which compares the number of substrates used and the intensity by which they are used between two strains of fungi (Blumenstein et al., 2015). The competitiveness of the focal fungus against another fungus, or the effectiveness of a potential biocide chemical, may thus be evaluated (Blumenstein et al., 2015).

Examples of the Application Potential of Pre-configured PMs: Nutritional Niche Studies with Elm (Ulmus sp.) Endophytes and Pathogens

Pre-configured PM plates were used to examine whether the carbon-substrate utilization profiles of elm endophytes differ from those of the Dutch elm disease pathogen (Blumenstein et al., 2015). The basic hypothesis to be tested was that endophytes with good potential as biocontrol agents should be able to effectively compete with the pathogen for carbon, but that a successful pathogen might also be superior competitor for nutrients against endophytes. Here, we discuss part of the results from the earlier study by Blumenstein et al. (2015). In ongoing studies, we are applying preconfigures PMs to study the same aspects in competition for nitrogen substances and present here some of the findings from these studies.

Procedure II: In-house Configured PM Array to Test the Sensitivity of Endophytes to a Set of Inhibitory Substrates

Experimental Aim and Selection of the Fungi for the Studies

In order to explore the role of fungal endophytes in the early stages of wood degradation, we employed a combination of NGS and PM approaches. Endophytic fungi were isolated from the wood (including phloem and xylem, but excluding external bark) of *Eucalyptus globulus* and *E. camadulensis* twigs, 1–2 cm in diameter, collected in 2012 and 2013 from different provinces across Spain (five sites in five provinces, three trees per site). The collection was done in spring and the twigs were transported to the laboratory and stored at 4°C. On the same day or the day after, the twigs were surface sterilized with subsequent immersions (30 s in 70% ethanol, 5 min in 4% bleach and 15 s in 70% ethanol), followed by 15 min drying at room temperature. Then, the twigs were peeled with a sterilized scalpel to remove the external bark and 1–2 mm thick slices were excised and placed on 90 mm Petri dishes (four explants per dish). We used five different culture media: MEA, potato dextrose agar, yeast extract agar, rose Bengal chloramphenicol agar, and eucalypt sapwood agar (10% w/v eucalypt sapwood, and 3% w/v agar). During the following two weeks, emerging colonies were transferred into new MEA dishes for preparation of inoculum (see below). By DNA sequencing of the ITS region and searching for matches in the GenBank database (NCBI, Bethesda MD, USA) through BLAST algorithm (Martín et al., 2015) we identified the most probable family of each strain. Fifteen eucalypt endophyte isolates were used for test this procedure, belonging fourteen to the phylum Ascomycota and the remaining one to the phylum Basidiomycota. The ascomycetes were two sordariomycetes (orders Hypocreales and Microascales), one incertae sedis and the rest dothideomycetes. These last belonged to the families Dothioraceae (four strains), Pleosporaceae (three strains), Phaeosphaeriaceae (order Pleosporales), Lophiostomataceae, Botryosphaeriaceae, and Davidiellacea. Additionally, we included in our study *Trichoderma* sp., *Pycnoporus sanguineus* and *Trametes* sp. isolates, commonly used as model fungi, from our mycology library. The species *P. sanguineus* and *Trametes* sp. are basidiomycetes of the order Polyporales.

Preparation of Inoculum

The selected isolates were cultured in Petri dishes on an autoclaved cellophane sheet over MEA medium (darkness, 25°C). After a week, the fungal biomass was harvested by rubbing with a sterilized scalpel and transferring the fungal tissue into a sterile centrifuge tube (15 mL) with a known volume of sterile distilled water. Centrifuge tubes were weighed before and after introduction of the tissue to calculate the weight of the added biomass. Then, the content of the centrifuge tube was homogenized using a sterilized tissue grinder, first with a large clearance pestle and then with a small clearance one (∼20 strokes with each). The homogenate was inserted back into the centrifuge tube and stored at 4°C until use. The concentration of fungal tissue in the suspension was calculated and the suspension was diluted to 1 g/L before pipetting into the PM plates.

In-house Configured PMs

Optical 96-well, round-bottom, sterile polystyrene plates (Deltalab, Barcelona, Spain) were used in the modified PM tests. Each well was first filled with 60 μL of liquid basal culture media (35 μL for inhibition tests; see below), composed by autoclaved Murashige and Skoog (MS) salts (1x; ref. n. 0926230; MP Biochemicals; Santa Ana, CA, USA), Biolog Redox Dye E (2x; ref. n. 74225; Biolog Inc., Hayward, CA, USA), and filtered 1-metoxy-5-methylphenazine methosulfate (1.5 mg/l; ref n. A3799; Applichem, Darmstadt, Germany). We prepared the plates by pouring into each well 50 μL of MS salt solution (2x; i.e., two times as concentrated as the standard recipe; 25 μL of MS salt solution (4x) and glucose 1 M of C atoms for inhibition tests; see below), 10 μL of dye mix, which contained Biolog Redox Dye E (20x; provided by the manufacturer at 100x; this reagent's final concentration was 2x) and of 1-metoxy-5-methylphenazine methosulfate (15 mg/L). MS salts are normally used to plant tissue *in vitro* culture, thus we expected they would also be appropriated for endophyte fungi. Biolog Redox Dye E is recommended by the manufacturer for assays with fungi. It changes its color from transparent to violet when reduced, in a similar way than the classical tetrazolium dye. The mediator 1-methoxy-5-methylphenazine methosulfate enhances the change of color.

After adding these components, each well was supplemented with selected substances (see the details below). Combinations of two groups of substances were tested: carbon sources and inhibitors (phenolic compounds). For testing the effect of seven

different carbon sources (cellobiose, galactose, glucose, sucrose, xylose, pectin, and starch) on the growth of the fungi, we supplemented the media with 20 μL of carbon source solution, to reach a final concentration 0.25 M of C atoms in each well. For testing the possible inhibitory effect on the fungi by 10 phenolic compounds that have been associated to tree resistance as metabolites or external treatments (Witzell and Martín, 2008; Martín et al., 2010): chlorogenic, tannic, and gallic acids; the simple phenolics o-cresol, carvacrol, thymol, and phenyl alcohol, and the flavonoids catechins, myricetin, and quercetin). We supplemented the media with 50 μL of inhibitor solutions (2x). Water-insoluble compounds could dissolved in 10% ethanol (v/v; for stock solution: 2x), 25% methanol (v/v; for the stock solution: 5x), or an alkaline solution (0.01 M NaOH for the stock solution: 5x). To neutralize the alkalinity of the latter media, 10 μL of 0.02 M HCl was added into the wells before inoculation. To test how these solvents affect fungal metabolism, solutions of glucose and sucrose with all these three solvents were prepared to control their possible effect (see Effect of additive solvents).

After addition of the test substances, water was added to fill the volume in each cell to 90 μL. Finally, from a suspension of 1 g/L of homogenized fungal biomass (see above), 10 μL was added into each well, making up a final concentration of 0.1 mg of fungal biomass per mL.

The thermotolerant solutions (carbon sources, tannic, salicylic, and gallic acids) were sterilized by autoclaving and the thermolabile or volatile substances and the substances dissolved in alcoholic solution (chlorogenic acid, flavonoids, and simple phenols) were filtered through disposable, sterile cellulose acetate syringe filters of 0.2 μm pore size. Water was always deionized and autoclaved prior to use. All the operations were done under axenic conditions in a laminar flow chamber.

The PM plates (a total of 30) were composed following four general principles. First, each combination of carbon source or secondary metabolite with a fungal strain was replicated in three separate wells. Second, with few justified exceptions (see Unintentional Chemical Interactions), all wells of a single plate had the same concentration of inhibitory substances, ethanol, or methanol, whenever present. Third, all the treatments included one negative control with the relevant conditions, but fungal inoculum substituted by water, and another one containing inoculum, but the carbon source/secondary metabolite substituted by water. The first was used to calculate the net absorbance (see below), while the second was used as a reference to compare between different endophytic strains. Fourth, all plates were cultivated in the dark at 25°C.

Measurements and Data-analysis

The following aspects that have relevance for the applicability of PMs in our studies on tree endophytes were evaluated from the in-house configurated PMs.

Stability/repeatability

To evaluate the stability and repeatability of the designed configuration, we repeated assays with carbon sources (cellobiose, galactose, glucose, sucrose, xylose, pectin, and starch) with a six months interval, using the freshly prepared inocula of five eucalypt endophyte strains and a model fungus (*Trichoderma sp.*).

Unintentional chemical interactions on PM plates – volatility and unexpected color changes in the medium

Our preliminary tests indicated that certain volatile metabolites might affect cells in neighboring wells in a plate where no such substance had been added. This unwanted effect was evaluated in a plate as described above, where the first three columns were supplemented with 1 g/L (final concentration) of the simple phenol *o*-cresol, while the rest of columns were not. All wells possessed glucose 0.25 M of carbon atoms. In each row one different fungal strain was inoculated, except the last one that was a negative control.

Preliminary tests also indicated that in some inhibitory compound tests the culture media unexpectedly changed color to orange (note that dye should change to violet) when in contact with certain inhibitory substances and certain strains. To explore this phenomenon, we performed a test to infer if this change of color could be because the strains used certain phenolic chemicals as carbon sources. We tested thirteen endophyte strains (selected from the Spanish tree endophyte collection) and the two Polyporales model fungi in media with chlorogenic acid, gallic acid, and tannic acid (1 g/L final concentration, solved in water), salicylic acid (0.02 g/L, in water) and catechins (1 g/L final concentration, solved in ethanol) with glucose. Absorbance was later measured at $\lambda = 405$ nm and $\lambda = 630$ nm.

Effect of additive solvents

Because some of the phenolic compounds had to be dissolved in solvents (see above), we wanted to test if these affected fungal activity. Thus, we tested the same set of strains as in the preceding assay, in four solvents (ethanol, methanol, NaOH+HCl as described above, and water) with added sugar in the form of either glucose or sucrose (0.25 M of carbon atoms). To the basal culture media (MS salts+dye mix) we supplemented with glucose and 5% ethanol or water or with sucrose (0.25 M of carbon atoms) and methanol 5%, NaOH+HCl 0.002 M (i.e., saline solution) or water. Growth in the media with ethanol, methanol, and saline solution were compared to the growth in water.

Data analysis

We defined and calculated the following parameters from the absorbance reads: (i) gross absorbance (A_λ): the mean of the three technical replicates (same conditions in three different wells) for each substance tested, measured at a given λ; (ii) net absorbance ($A'_\lambda = A_\lambda - A_{\lambda\,neg}$): the difference between the gross absorbance and its negative control (water instead of fungal inoculum, $A_{\lambda\,neg}$); (iii) cumulated growth ($A^d{}_\lambda = A'_\lambda{}^d - A'_\lambda{}^0$): net absorbance at day d ($A'_\lambda{}^d$) minus net absorbance at day 0 ($A'_\lambda{}^0$); and (iv) relative growth (ρ_λ): the ratio between the cumulated growth in two different substances ($A^d{}_{\lambda\ subst1} : A^d{}_{\lambda\ subst2}$), usually one of them taken as reference (glucose or sucrose). Comparisons between different strains were done in terms of their relative growth, and therefore the negative control was not considered in comparisons. Standard analyses of Pearson correlation, one-factor ANOVA and Principal Component

Analysis were carried out in STATISTICA V8.0 (StatSoft Inc., Tulsa, OK, USA).

Examples of the Application Potential of In-house Configured PMs: Chemical Sensitivity of Eucalypt (*Eucalyptus* sp.) Endophytes

Phenolic compounds have been identified as potential plant internal defenses and as external inducers of plant defenses (Witzell and Martín, 2008; Martín et al., 2010). However, little is still known about the possible responses of endophytes to these chemicals. Thus, the in-house configuration of PMs with phenolic compounds was designed to evaluate the role of these compounds for individual endophyte species, with the underlying hypothesis the compounds would show inhibitory effects on fungi, but that the effect would show strain- and compound-specificity. Specifically, we performed an inhibition test of four phenolic compounds (phenol, *o*-cresol, thymol, and carvacrol) and two flavonoids (quercetin and myricetin) on the same 15 strains tested above plus a negative control without inoculum. Final concentrations were 0.1 g/L for the phenols and 0.01 g/L for the flavonoids. Flavonoids and carvacrol were dissolved in ethanol, whereas the other phenolics were dissolved in water. We incorporated the results on this assay to the ones on the test we did to research on undesired changes of color (inhibitory substances: chlorogenic, salicylic, gallic and tannic acids, and catechins). We only took into account measures at $\lambda = 630$ nm to minimize interferences of undesired color changes.

Optical densities were measured in a microplate absorbance reader ELx808 (BIOTEK, Winooski, VT, USA). We measured at $\lambda = 405$, 490, and 630 nm, and at 0, 1, 2, 3, 4, 5, 7, 9, and 11 days after inoculation (dai). Wavelengths were selected in order to detect if the absorbance shifts were due to an increase in the turbidity, a change of color due to Biolog Redox Dye, or a change of color by other causes. Single measurement was considered sufficient, because variation between repeated, consecutive measurements were found to be negligible in preliminary tests (Macaya-Sanz, personal observation) Absorbance measurements were stored using the software KCjunior provided by the plate reader's manufacturer. The plates were also photodocumented at 0, 5, and 11 dai.

The absorbance values at all the wavelengths, but especially at shorter ones, were due to increase of turbidity of the medium and the cumulative quantity of redox reactions (reflected in the change of color of the Redox Dye), i.e., two interrelated processes, and were thus considered a proxy of the catabolic activity and the vegetative growth of the fungi.

Results

Standardization of Inoculum (Procedure I and II)

Adequate quality inoculum for PM tests was achieved from the studied endophytes through both procedures. In Procedure I, the inoculum concentration was determined by transmittance, whereas in Procedure II, the inoculum was standardized by biomass. Standard culture conditions were used for studied fungi in both Procedures (I and II), resulting in adequate amount of viable fungal biomass.

In Procedure II studies, we found that fungal inocula lost vitality after a month storage at 4°C, showing clearly reduced growth rate (Macaya-Sanz, personal observation). All the inocula were, however, alive after the storage period.

In Procedure I, the test for the CFU in the inoculum gave varying results for the different species. For instance, CFU for *A. pullulans* was about 400 CFU per 100 μL (**Figure 1A**), whereas for *O. ulmi* the number of growing colonies was too dense to be counted (**Figure 1B**). Bacterial or fungal contaminations were not detected among the growth recovered from the randomly chosen wells.

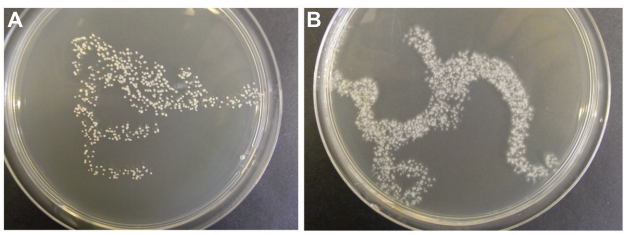

FIGURE 1 | Examples of fungal inoculum (100 μL, i.e., the volume injected into one well) applied to an agar plate for testing the development of CFU. *Aureobasidium pullulans* **(A)** and *Ophiostoma ulmi* **(B)**.

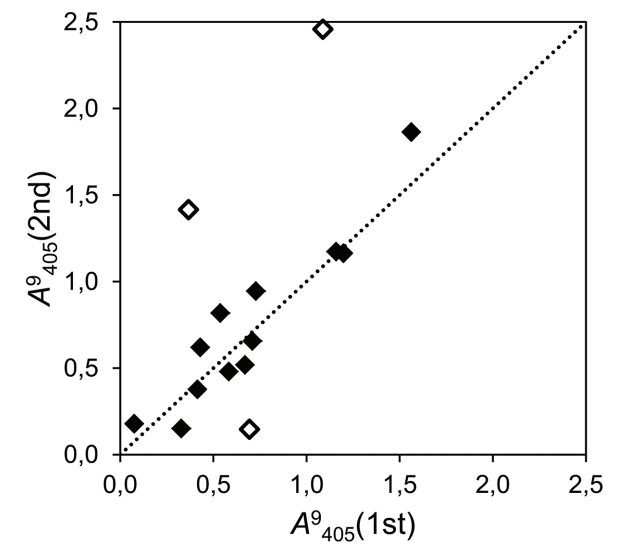

FIGURE 2 | Correlation plot of two independent assays of cumulative growth with glucose as the only carbon source (time point 9 days after inoculation (dai), $\lambda = 405$ nm) with 15 fungal strains, of which 13 were isolated as endophytes ($r^2 = 0.485$; $P = 0.004$). The dotted line represents the bisector of slope $b = 1$. Dots close to this line produced even results in both assays (filled dots). Empty dots indicate deviating strains.

Technical Challenges with In-house Configurated PMs (Procedure II)

The repeated assays showed that the precision of the in-house configurated PMs was moderate. In the experiment which tested 15 strains in glucose (**Figure 2**), the correlation was moderate ($r^2 = 0.485$) but significant ($P = 0.004$), and the slope of the regression line was close to the unity ($b = 1.17$). Nevertheless, ignoring the results of three strongly deviating strains (marked with blank dots in **Figure 2**), the correlation grew to $r^2 = 0.889$ and the regression slope shifted slightly toward one ($b = 1.10$).

The repeated assays where six strains were tested on seven carbohydrates, the precision (measured as correlation of cumulated growth) was extremely high ($r^2 > 0.9$) in some of them, whereas almost negligible in others. Intriguingly, carbon sources where the standard deviation of the absorbance was low (i.e., the different response to the carbon source of the tested strains), displayed a reduced correlation. The carbon sources with high correlation also presented high standard deviation and values of linear regression slope close to the unity (**Table 1**). However, a couple of carbon sources did not follow this pattern (especially, xylose).

Our tests with *o*-cresol indicate that there is a risk that the volatile compounds cause unintentional effects in the neighboring wells: we found that the fungal growth was severely reduced in the adjacent wells and visibly limited in the next columns (**Figure 3**).

Our tests confirmed that unexpected color change (to orange) occurred only in certain combinations of strain and inhibitory substances. The combination of certain strains with the four tested secondary metabolites (salicylic acid, tannic acid, chlorogenic acid, gallic acid, and catechins) resulted in change of color to yellow–orange in last three of them. Occasional change of color was also found in tannic acid assays. This change of color was measurable as a shift in the ratio between absorbance at wavelength $\lambda = 405$ nm and at $\lambda = 630$ nm. In the cases were a change of color occurred, the absorbance at $\lambda = 405$ nm increased abnormally, and the ratio $\lambda = 405$ to $\lambda = 630$ was not conserved (**Figure 4**). Such color change did not occur when other strains were combined with these metabolites or when the strains were growing without these substrates.

Tests with different solvents showed that some of them have a strong effect on the activity of the strains. Alkaline solution, which was neutralized with an acid, did not affect the activity of the strains (**Figure 5A**), while 5% methanol in water (v/v) induced a general decrease in the growth of all the endophytic strains (**Figure 5B**). Ethanol (5% in water, v/v) had an inconsistent effect on strains, decreasing the growth in some of them, but promoting it in others (**Figure 5C**).

TABLE 1 | Correlations between the growth of six fungal strains on seven different carbon sources at 9 days after inoculation (dai; λ = 405 nm) in two independent assays with identical conditions.

Carbon source	$A^9_{405}(1)$	$A^9_{405}(2)$	σ	r^2	*P*	*b*
Cellobiose	1,258	0,830	0.433	0.179	0.403	0.5555
Galactose	0,747	0,849	0.165	0.002	0.940	–0.0361
Glucose	0,916	0,859	0.275	0.039	0.708	0.1372
Sucrose	0,646	0,658	0.381	0.986	0.0001	1.1845
Xylose	1,073	0,723	0.385	0.009	0.857	0.0681
Pectin	0,219	0,474	0.359	0.910	0.012	1.0413
Starch	0,860	0,341	0.441	0.977	0.001	0.6013

The second and third columns display the mean of the cumulated growth of the six strains for the first and second assays, respectively. The fourth column shows the standard deviation (σ) of the pooled measurements from both assays. The fifth and sixth columns display the determination coefficient between two assays (r^2) and its level of significance (P). The last column presents the slope of the regression line (b). Note that carbon sources with lower standard deviation have low correlations between assays. However, not all the carbon sources with higher standard deviation present high correlations.

Application of PM to Forest Tree Endophyte Studies

Procedure I – Comparison of Nutrient Utilization Patterns

With the goal of studying the potential of endophytes in biocontrol, we used PM data to compare the nutritional preferences of a pathogen and endophytes that co-colonize the same host (**Figure 6**, data modified from Blumenstein et al., 2015). The comparison showed that all tested fungi were able to use all of the four tri-and tetrasaccharides tested (**Figure 6**). On the other hand, the endophyte *M. nivalis* was able to use a broader array of available amino acids (96%) and other acids (69%) as compared to the pathogen (56 and 49%, correspondingly) and *A. pullulans* had generally low preference for acids, utilizing 15% of the available amino acids and less than 1% of the other acids (**Figure 6**). Moreover, the endophytes were able to use all available phenolics (5 out of 5) while the pathogen could only use 60% of them (3 out of 5).

Phenotype MicroArray technique also allowed us to observe the effect of substrates on the morphology of the tested fungi. In particular, nitrogen sources seemed to induce varying morphological responses. For instance, only little fungal mass was produced when *T. harzianum* grew on cytidine or cytosine (**Figure 7**). Tyramine and formamide triggered production of in green fungal mass, whereas acetamide resulted in yellow, and adenosine yellow–green, fungal mass. Guanine induced formation of dense, dark green fungal mass in *T. harzianum*.

Procedure II – Targeted Test of Chemical Sensitivity

The measurements of the inhibitory effects of eleven substances on fifteen fungal strains (13 of them endophytes) were analyzed by means of Principal component analysis. The two main principal components collated the fungi following its phylogenetic relations (**Figure 8**).

Discussion

Benefits of PM Approach in Endophyte Studies

Our studies demonstrate that the PM approach is a useful tool to investigate the cellular phenotypes of forest tree endophytes at semi-high throughput rate and in a standardized manner, and to functionally interpret the taxonomic data generated by NGS. For instance, in a recent study exploring the role of endophytes in the

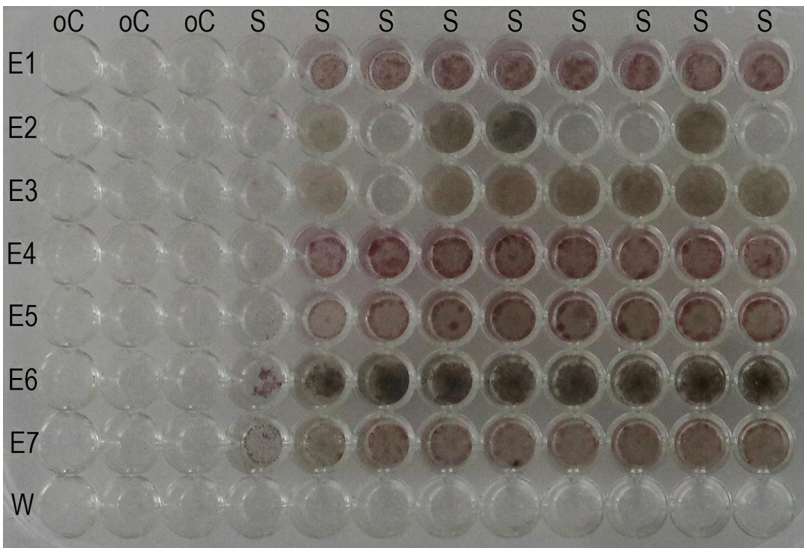

FIGURE 3 | Effect of volatile inhibitory substances on adjacent cells. All the wells of the plate were supplemented with the standard basal medium. In each row, cell suspension of one endophyte strain was added, excluding the last row one where water was added. In the first three columns, the phenolic compound *o*-cresol was incorporated to a final concentration of 1 g/L. Note that the fungi in the fourth and fifth columns were partially inhibited in their growth. E = endophyte; W = water; S = standard basal medium; oC = standard basal medium supplemented with *o*-cresol.

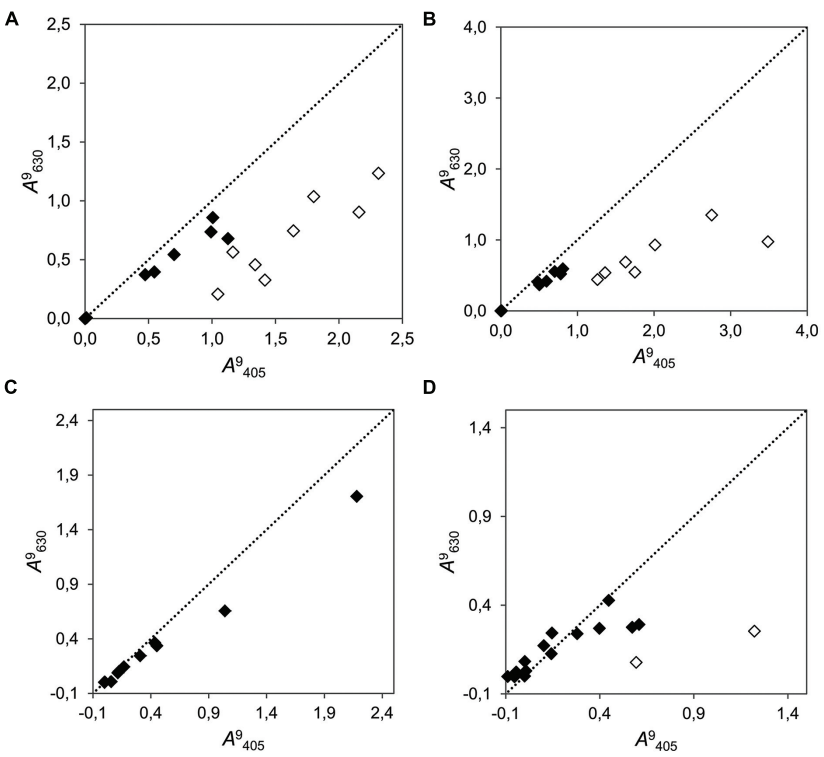

FIGURE 4 | Correlation plots of the cumulative growth (measured at λ = 405 nm vs. λ = 630 nm at time point 9 dai) of 15 fungi in media supplemented with four different phenolic compounds. (A) Chlorogenic acid ($r^2 = 0.683$; $b = 0.430$); **(B)** Gallic acid ($r^2 = 0.788$; $b = 0.321$); **(C)** Salicylic acid ($r^2 = 0.992$; $b = 0.460$); and **(D)** (+)-catechin ($r^2 = 0.407$; $b = 0.240$). The dotted line represents the bisector of slope $b = 1$. Dots close to this line produced even results when measured with both wavelengths (filled dots). Empty dots indicate strains in which an unexpected change of color to yellow–orange was visually evident. Note that it is not expected that points aggregate to the bisector, because the measurements at different wavelengths need not to be alike, regardless of the undesired color change.

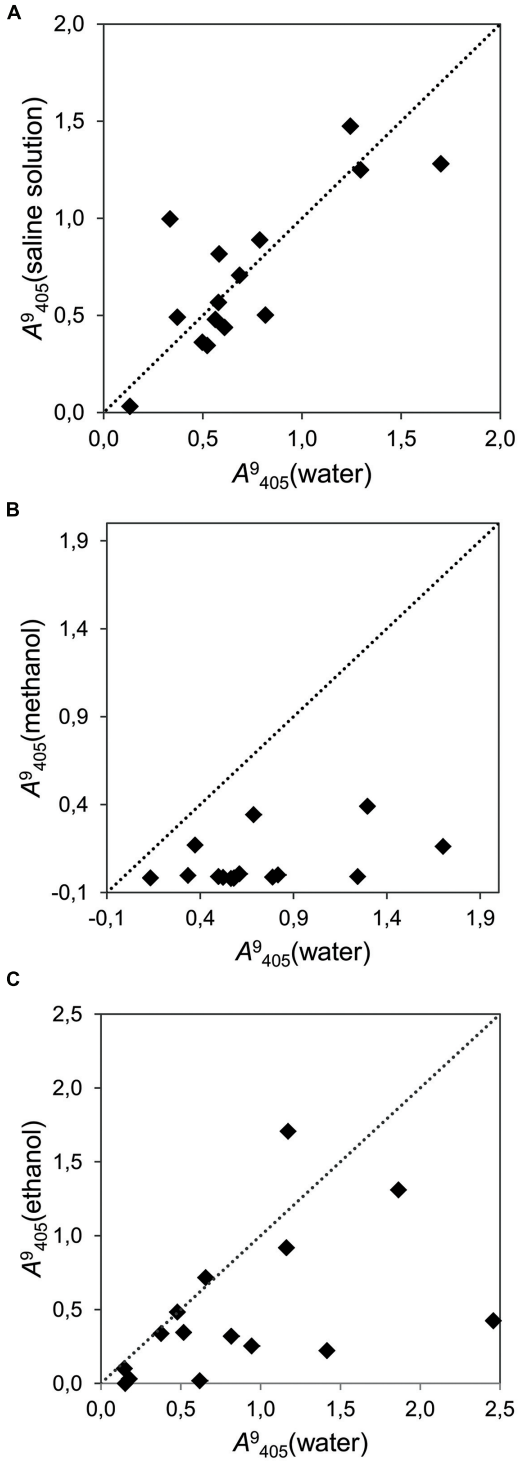

FIGURE 5 | Correlation plot reflecting the effects of different solvents on the cumulative fungal growth (time point 9 dai, λ = 405 nm) of 15 fungal strains. Each dot represents one strain. The dotted line represents the bisector of slope $b = 1$. Placement of dots under this line indicates inhibition by the tested solvent. **(A)** Growth in a saline solvent (NaOH+HCl) versus water with sucrose as carbon source ($r^2 = 0.634$); **(B)** Growth in methanol versus water with sucrose as carbon source ($r^2 = 0.178$); **(C)** Growth in ethanol or water with glucose as carbon source ($r^2 = 0.230$).

Dutch elm disease complex, we were able to identify nutritional niche overlap as a potential mechanism of interaction between the pathogen and potential antagonist endophytes (Blumenstein et al., 2015). This information will assist selection of candidate endophytes for biocontrol purposes. Moreover, we successfully applied PM to characterize the degradation capabilities of the main fungal taxa operating during the first stages of eucalypt wood decay (Macaya-Sanz et al., 2014). In that work, a succession of the most abundant endophyte fungi present during the first 70 days of wood degradation was monitored through pyrosequencing fungal ITS1 region. The resulting operational taxonomic units (OTUs) frequencies varied in time, and certain endophyte OTUs orders were abundant at the beginning of the degradation. Furthermore, the PM analysis showed that these orders are able to effectively degrade lignin-like substances, while other OTUs prevailed at the end and were favored by presence of lignin degradation by-products. This information may be valuable for wood processing industries, but it can also add to the current scientific discourse about the role of microbes as regulators of carbon balance in forest ecosystems (Hiscox et al., 2015) and support the decision making regarding conservation of biodiversity in our forests. Thus, PM techniques are useful tools for both basic and applied research, and can be successfully applied in highly different research fields, such as plant protection, wood material research, and conservation ecology.

Based on our experiences, we conclude that the general benefits of PM approach include its great versatility that allows various research questions to be addressed in a same experiment (e.g., testing of competitive relationships between fungal strains along with gaining information about their sensitivity to individual chemical compounds), testing of a broad array of different compounds and concentrations, and a higher throughput of samples, as compared with earlier methods that have been used in studies of fungal phenotypes (Yourman et al., 2001; Atallah et al., 2011). A great advantage was also that the phenotypic responses are recorded quantitatively and stored electronically (Bochner, 2003; Bochner et al., 2010). If the technical challenges and limitations are properly acknowledged (see below), PM approach opens new experimental possibilities for tree-endophyte research.

Technical Challenges with PM Method

One of the fundamental challenges when working with fungi in the PM procedure is to prepare a representative, homogenous and viable inoculum. Part of this challenge is because the external growth conditions can strongly modulate the quality and quantity of inoculum. Fungi are known to show great phenotypic plasticity in their responses to their immediate growth environment (see, e.g., Rohlfs, 2015, and references therein). In accordance with this expectation, also our results from the nitrogen tests (Procedure I, **Figure 7**) witness how strongly the substrate can affect fungal morphology, which in turn is a product of the fungal metabolism. Moreover, we found a marked loss of vitality during long term storage, possibly because the month of storage promoted the strains to enter latent stages, from which the fungi could not completely recover on the MS medium. Thus, the conditions

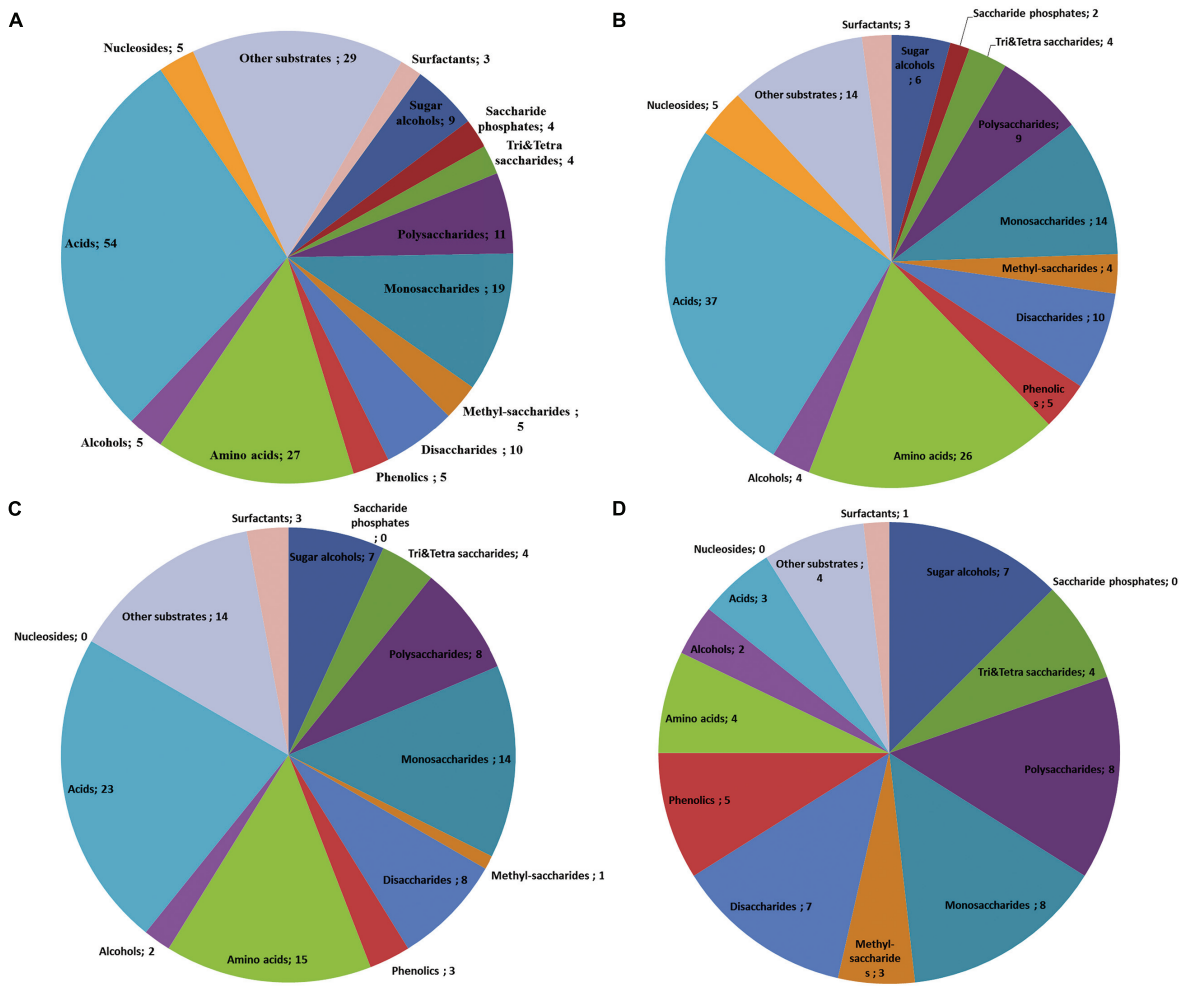

FIGURE 6 | Venn-diagrams show the utilization patterns of carbon sources (divided in chemical groups) of three fungi as indicated by the color development data on BIOLOG plates Phenotype MicroArray (PM) 1 and 2A. All available substrates divided in chemical groups (number of individual compounds after the semicolon; **A**). Substrate utilization pattern by the endophyte *Monographella nivalis* var *neglecta* – a strong *in vitro* competitor of the pathogen, occupying the same niches in the tree and utilizing carbon sources more efficient than the pathogen **(B)**, the pathogen causing Dutch elm disease, *O. novo-ulmi* **(C)** and *Aureobasidium pullulans* **(D)**, a ubiquitous fungus with no detected competitive relation to the pathogen *in vitro* (Data modified from Blumenstein et al., 2015).

before preparation of inoculum may influence the responses of fungal cells on PM plates through metabolic carry-over effects. As a first step when using PM approach, whether it is in-house or pre-configured PM plates, we thus recommend careful standardization and documentation of the pre-inoculum growth conditions for the fungi, to ensure the repeatability of analyses.

Standardization of growth conditions may, however, also add bias to the analysis, given the strain-specific preferences for optimal growth. Indeed, in both procedures (I and II), we found evidence for strain-specificity in fungal responses. For instance, the above mentioned conditioning effects of pre-inoculum preparation growth environment could be highly genotype-specific because the nutritional niches of the strains differ (Blumenstein et al., 2015). Therefore, the possible carry-over effect of culturing conditions may be a factor that needs to be taken into consideration in particular when comparing interspecific differences. In our studies, we pre-cultured all fungi on MEA and at 26°C even though their individual growth preferences may differ. Ideally, the species-specific nutrient utilization patterns detected through PM analysis should be validated using inoculum collected from colonies of the same isolates that have been cultured under a well-defined set of pre-conditions that cover the realistic regimes in physicochemical environment (light, temperature, pH, etc.). Standardization of the pre-inoculum preparation conditions could also be done on strain-specific basis, ensuring the strain-specific maximum growth rate. An interesting possibility with PM could also be to study the possible carryover effects with the goal of gaining a better understanding of how we could better gear the fungal phenotypes for different industrial or pharmaceutical purposes.

Intriguingly, we also observed (Procedure II) how complex strain-specific interactions with the chemical environment were

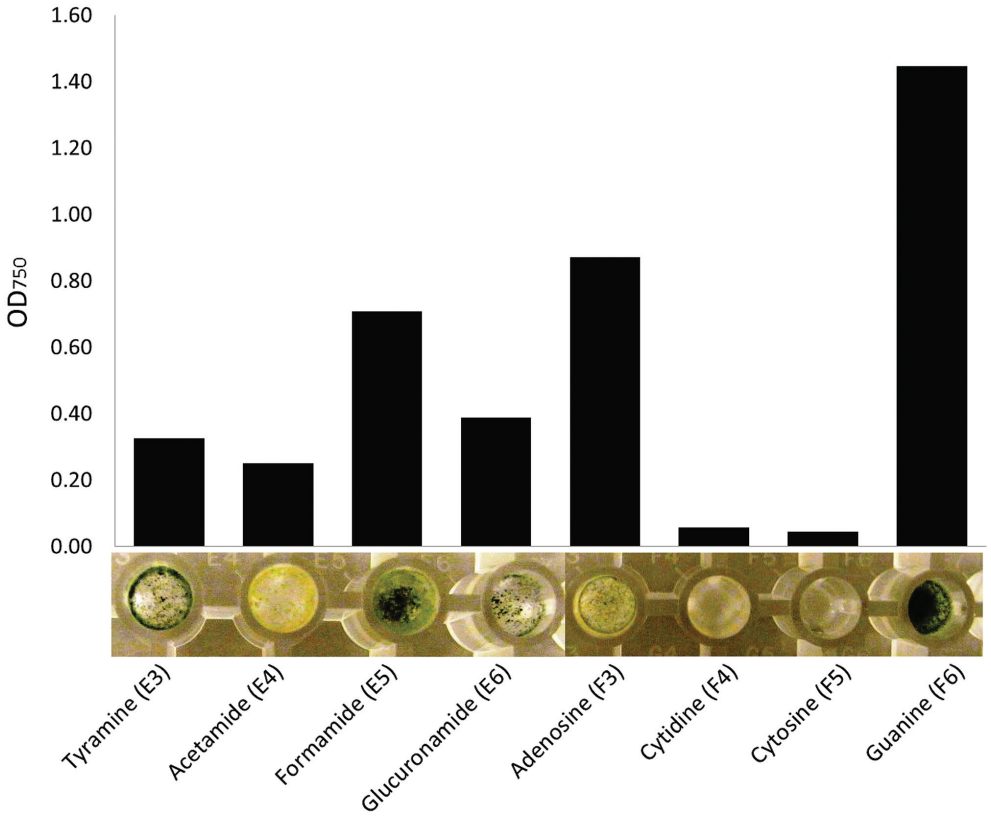

FIGURE 7 | An assortment of nitrogen sources leading to clearly visible differences in optical density (750 nm) and morphology of the fungal mass of *Trichoderma harzianum*. Measurement at 144 h after inoculation to the plates (bars represent the mean of readings from two plates).

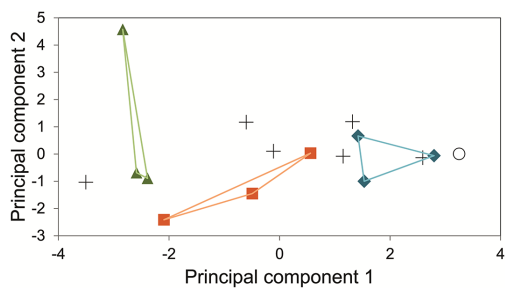

FIGURE 8 | Principal Component analysis of the cumulative growth (time point 9 dai, λ = 630 nm) of 15 fungal strains in an array of in-house PM supplemented with 11 inhibitory substances and glucose. Green triangles indicate three strains of the family Dothioraceae. Orange squares represent members of the order Pleosporales (families Pleosporaceae and Phaeosphaeriaceae). Blue diamonds for the basidiomycetes assayed. Crosses represent a variety of ascomycetous endophytic fungi (Davidiellaceae, Lophiostomataceae, Botryosphaeriaceae, two sordariomycetes, and one *incertae sedis*). Empty circle represents the negative control without inoculum. Principal component 1 explains 42.76% and principal component 2 does 21.50%.

expressed as unexpected color changes in the wells (**Figure 4**). The orange color is characteristic for oxidation of phenols (Holderbaum et al., 2010) and could thus be indication of fungal, extracellular phenolase activity. Another possibility is that the chemical environment induced the fungi to produce colored substances (Velmurugan et al., 2010). Thus, in order to avoid confounding effects of such within-well processes, it is necessary to carefully plan the positive and negative controls in each in-house array. Moreover, new research is needed to better understand the metabolic processes in fungal cells as they grow in the wells.

The second essential step in use of PM approach is to establish an inoculum preparation routine that ensures good viability and accurate and repeatable quantification of inoculum. Our method for preparing a homogenous inoculum (Procedure I) resulted in dense emergence of hyphae on the Petri dishes within 2–4 days, indicating that the process did not negatively affect the viability of the cells. According to the manufacturer's protocol, the density of the IF should be set to 62% transmittance, conveniently measured from inoculum fluid tubes with the original Biolog turbidimeter. Bochner (2009) states that technically one cell per well would be adequate, but recommends 100 cells per 100 μL for the inoculum. For bacterial cells, a concentration of approximately 10^6 cells/mL is a common standard (e.g., Bourne et al., 2012). For fungi, Atanasova and Druzhinina (2010) recommend an adjusted cell density ranging from 1.25×10^5 to 5×10^5 spores/mL, depending on the tested fungus to guarantee repeatable OD measurements.

Insam et al. (1996), however, suggest that instead of total counts, viable counts for microorganisms should be used, or the biomass should be standardized. In our Procedure II, we used biomass standardization. This method is practical in particular for those endophytes that do not readily sporulate in cultures. However, the proportion of metabolically non-active biomass (e.g., non-active hyphal segments) should ideally be controlled as a part of the protocol, by microscopic examination or by determining the CFU of the inoculum. For adequate repeatability of the results, efforts should be made to guarantee that the inoculum prepared from different isolates of a same species contain a comparable CFU/mL and that each well contains at least 100 cells per well (Bochner, 2009).

The third crucial step in PM analyses, in particular when working without the OMNILOG instrumentation and software, is to decide the time points of interest for data collection. There is a temporal dynamic in the substrate use by the cells, which is a fundamental to the evaluation of cell phenotypes. The reaction in the wells is often characterized by a lag-period that can last up to 2–4 days. After that the reaction develops and finally tends to saturate. In the case of the fungi that we have studied the saturation often started after 96 h from the start of the inoculation period. Hierarchical cluster analysis proved to be a useful tool for determination of the appropriate time for downstream analyses of the substrate use by the fungi (Blumenstein et al., 2015). In cases where such clear cluster separation of the replicate measurements does not exist, the readings that represent the highest degree of strain separation could be chosen for further analyses. In our Procedure I studies, we found that the readings for the studied fungi (a pathogen and three fungal endophytes) were most reliable between 168 and 240 h after incubation. We also found that viable cells could be recovered from the wells even after 360 h on the plates. An intriguing option to further utilize PM technique would be to extract the fungal biomass in the wells in the end of an incubation period and study, e.g., using chromatography and molecular approaches, how growth on a single substrate might affect the capacity of fungal cells to accumulate specific chemicals, or express certain genes.

For the in-house configured PMs, we also identify a fourth crucial step: Our Procedure II studies demonstrated that the repeatability and reliability of the in-house arrays can only be ensured through a careful design that acknowledges the specific characters of the studied chemicals. For instance, the volatility of a compound dispensed in a certain well could affect fungal growth in surrounding wells (e.g., observed in adjacent wells to inhibitory, volatile *o*-cresol; **Figure 3**). Thus, when analyzing the chemical sensitivity of volatile substances, a preferable approach seems to be dispensing the same concentration of the volatile substance in question in all the wells of the microplate in order to avoid unintentional cross-well effects.

Challenges in Interpretation of the Biolog Data

The PM technique is a powerful tool to estimate the relative speed of substrate use for particular fungi. However, the interpretation of the between-species difference in the speed of substrate use is not straightforward. A change is absorbance values can be interpreted as a proxy of metabolic activity, but it is risky to propose narrower views. The change of color could be produced by a shift in the tetrazolium dye due to respiration, by an increase of turbidity through fungal body proliferation or even by change of the medium color after production of metabolites by the fungi. Such mélange of processes makes it challenging to contrast different organisms in a fine scale. The inconsistency of results in the repeated assays where six strains were tested on seven carbohydrates (**Table 1**) may reflect such blended processes that interplayed with the inherent variations in the enzymatic activities of the fungi (e.g., van den Brink and de Vries, 2011). Thus, until refinement, the procedure is best suited for studies on general metabolic trends.

Despite the uncertainty, the proxy of metabolic activity can be valuable additional information, e.g., in studies addressing the potential endophyte-based applications (see Benefits of PM Approach in Endophyte Studies). In our recent study (Protocol I; Blumenstein et al., 2015), we used pre-configured PMs to deepen our understanding of the mechanisms of antagonism by potential biocontrol endophytes, identified on basis of field correlations and laboratory tests. In this case, the PM data allowed us to nuance the emerging picture of the potential of endophytes in biocontrol: we could conclude that the antagonistic effect of an endophyte against a pathogen may be due to several, simultaneous or parallel mechanisms (chemical antagonism and competition for nutrients). PM analysis also provided information about the possible ecological strategies of the fungi. In particular, we found that the ubiquitous *A. pullulans* is a slow substrate user with a relatively high tolerance to potentially antifungal compounds such as phenolics (**Figure 6**), whereas the biologically more specialized species *M. nivalis* var. *neglecta* and *P. cava*, were capable of faster catabolism of certain substrates, e.g., monosaccharides, polysaccharides and acids, but were less tolerant to phenolics as compared to *A. pullulans*. These results indicate that while *M. nivalis* var. *neglecta* and *P. cava* may be superior competitors in sugar- and acid-rich environments, *A. pullulans* may have an ecological strategy that permits it to remain active even on nutritionally more reluctant substrates that might cause other fungi to starve or become intoxicated. Given that *M. nivalis* var. *neglecta* and *P. cava* have been identified as potent inhibitors of a vascular pathogen of the host species, elms (Blumenstein et al., 2015), this information might help to set chemical quality targets for the elm trees that are most receptive for biocontrol through these endophytes. Similarly, the protocol II study showed that the phylogeny could be considered as a proxy of the fungal response to plant secondary metabolite. This kind of results, in combination with NGS analyses, can provide novel information about the mechanisms behind the structure and functions of endophyte communities in trees.

The obviously artificial growth environment in PM plate wells, and the distant resemblance of preconfigured plates with the substrate availability under natural conditions, may obviously obscure the interpretations. We only see the response to one isolated substrate in each well on a PM plate. In nature, however, fungal cells inside the plant tissues will exist in a chemical environment that is likely to constantly and gradually change.

This dynamicity will be caused both by the metabolism of the plant and by the endophytic inhabitants, and the composition of the substrate, as well as the fungal community, will continuously be altered. Similar successions have been studied for macro-organisms including fungi and insects in decaying leaf litter (Hättenschwiler et al., 2005) or the succession of saprotrophic organisms in dead woods of forests (Bader et al., 1995, Similä et al., 2003). As one of the functions of endophytic fungi is likely that of a decomposer (Schulz and Boyle, 2005), the conversion from one substrate to another by the help of a fungi will likely determine the succession of endophyte function in a plant both during its life as well as during its after life.

In natural conditions, variations in species-specific infection mode and presence of specific endophytes are also determining the use of substrates by a fungus, which, in turn, will affect the succession of endophytes (Heilmann-Clausen and Boddy, 2005). Thus, the order in which endophytic fungi enter the host plant may also determine the activity and importance of subsequent endophytes in that plant. It further suggests that there is plasticity in how the fungi may make use of the plant, in the sense that some individual species may play different roles depending on when they enter the scene. A certain fungal endophyte may therefore be plastic in the ecological role they play, which may further complicate the interpretations of the biological significance of the phenotypic responses detected in PM plates.

Conclusion

The technical challenges of the PM method are multifaceted and the interpretation of PM data is not straightforward. Thus, ideally, extensive validation through carefully standardized pre-conditions for the fungal growth and careful replication and control well strategies are needed for successful PM analyses, whether the studies use preconfigured or in-house designed PM plates. However, it is evident that the PM technique may significantly help to bridge the genotype–phenotype gaps for the culturable fraction of endophytic fungi. Despite the above-mentioned challenges, PM analyses can provide unique knowledge about functional properties of individual strains and species, and thereby contribute to the knowledge pool that is needed for a more comprehensive understanding of the associations between the NGS-profiles and functional fungal biodiversity.

Acknowledgments

This work was supported by the research project CTQ2011-28503-C02-02 (Ministerio de Economía y Competitividad, Spain) to DM-S and JM, Erasmus Mundus Joint Doctoral Programme FONASO fellowship to KB, and VINNMER Marie Curie International Qualification grant (2011-01350) to JW.

References

Albrectsen, B. R., and Witzell, J. (2012). "Disentangling functions of fungal endophytes in forest trees," in *Fungi: Types, Environmental Impact and Role in Disease*, eds A. Paz Silva and M. Sol (Huntington, NY: Nova Science Publishers), 235–246.

Atallah, Z. K., Maruthachalam, K., Vallad, G. E., Davis, R. M., Klosterman, S. J., and Subbarao, K. V. (2011). Analysis of *Verticillium dahliae* suggests a lack of correlation between genotypic diversity and virulence phenotypes. *Plant Dis.* 95, 1224–1232. doi: 10.1094/PDIS-02-11-0110

Atanasova, L., and Druzhinina, I. S. (2010). Global nutrient profiling by Phenotype MicroArrays: a tool complementing genomic and proteomic studies in conidial fungi. *J. Zhejiang Univ. Sci. B* 11, 151–168. doi: 10.1631/jzus.B1000007

Bader, P., Jansson, S., and Jonsson, B. G. (1995). Wood-inhabiting fungi and substratum decline in selectively logged boreal spruce forests. *Biol. Conserv.* 72, 355–362. doi: 10.1016/0006-3207(94)00029-P

Blumenstein, K., Albrectsen, B., Martin, J., Hultberg, M., Sieber, T., Helander, M., et al. (2015). Nutritional niche overlap potentiates the use of endophytes in biocontrol of a tree disease. *BioControl* 60, 655–667. doi: 10.1007/s10526-015-9668-1

Bochner, B. R. (1989). Sleuthing out bacterial identities. *Nature* 339, 157–158. doi: 10.1038/339157a0

Bochner, B. R. (2003). New technologies to assess genotype-phenotype relationships. *Nat. Rev. Genet.* 4, 309–314. doi: 10.1038/nrg1046

Bochner, B. R. (2009). Global phenotypic characterization of bacteria. *FEMS Microbiol. Rev.* 33, 191–205. doi: 10.1111/j.1574-6976.2008.00149.x

Bochner, B. R., Gadzinski, P., and Panomitros, E. (2001). Phenotype microarrays for high-throughput phenotypic testing and assay of gene function. *Genome Res.* 11, 1246–1255. doi: 10.1101/gr.186501

Bochner, B., Gomez, V., Ziman, M., Yang, S., and Brown, S. D. (2010). Phenotype MicroArray profiling of *Zymomonas mobilis* ZM4. *Appl. Biochem. Biotechnol.* 161, 116–123. doi: 10.1007/s12010-009-8842-2

Bochner, B. R., and Savageau, M. A. (1977). Generalized indicator plate for genetic. Metabolic, and taxonomic studies with microorganisms. *Appl. Environ. Microbiol.* 33, 434–444.

Borglin, S., Joyner, D., Deangelis, K. M., and Et, A. (2012). Application of phenotypic microarrays to environmental microbiology. *Curr. Opin. Biotechnol.* 23, 41–48. doi: 10.1016/j.copbio.2011.12.006

Bourne, C. R., Wakeham, N., Bunce, R. A., Berlin, K. D., and Barrow, W. W. (2012). Classifying compound mechanism of action for linking whole cell phenotypes to molecular targets. *J. Mol. Recognit.* 25, 216–223. doi: 10.1002/jmr.2174

Cabrera-Bosquet, L., Crossa, J., von Zitzewitz, J., Serret, M. D., and Luis Araus, J. (2012). High-throughput phenotyping and genomic Selection: the frontiers of crop breeding converge. *J. Integr. Plant Biol.* 54, 312–320. doi: 10.1111/j.1744-7909.2012.01116.x

Davidson, F. A. (1998). Modelling the qualitative response of fungal mycelia to heterogeneous environments. *J. Theor. Biol.* 195, 281–292. doi: 10.1006/jtbi.1998.0739

Dong, H. P., Liu, Z. Q., Zheng, Y. G., and Shen, Y. C. (2010). Novel biosynthesis of (R)-ethyl-3-hydroxyglutarate with (R)-enantioselective hydrolysis of racemic ethyl 4-cyano-3-hydroxybutyate by *Rhodococcus erythropolis*. *Appl. Microbiol. Biotechnol.* 87, 1335–1345. doi: 10.1007/s00253-010-2584-5

Druzhinina, I. S., Schmoll, M., Seiboth, B., and Kubicek, C. P. (2006). Global carbon utilization profiles of wild-type, mutant, and transformant strains of *Hypocrea jecorina*. *Appl. Environ. Microbiol.* 72, 2126–2133. doi: 10.1128/AEM.72.3.2126-2133.2006

Eyles, A., Bonello, P., Ganley, R., and Mohammed, C. (2010). Induced resistance to pests and pathogens in trees. *New Phytol.* 185, 893–908. doi: 10.1111/j.1469-8137.2009.03127.x

Falconer, R. E., Bown, J. L., White, N. A., and Crawford, J. W. (2005). Biomass recycling and the origin of phenotype in fungal mycelia. *Proc. Biol. Sci.* 272, 1727–1734. doi: 10.1098/rspb.2005.3150

Gaur, R., Singh, R., Gupta, M., and Gaur, M. K. (2010). *Aureobasidium pullulans*, an economically important polymorphic yeast with special reference to pullulan. *Afr. J. Biotechnol.* 9, 7989–7997.

Greetham, D. (2014). Phenotype microarray technology and its application in industrial biotechnology. *Biotechn. Lett.* 36, 1153–1160. doi: 10.1007/s10529-014-1481-x

Hättenschwiler, S., Tiunov, A. V., and Scheu, S. (2005). Biodiversity and litter decomposition interrestrial ecosystems. *Annu. Rev. Ecol. Evol. Syst.* 36, 191–218. doi: 10.1146/annurev.ecolsys.36.112904.151932

Heilmann-Clausen, J., and Boddy, L. (2005). Inhibition and stimulation effects in communities of wood decay fungi: exudates from colonized wood influence growth by other species. *Microbial. Ecol.* 49, 399–406. doi: 10.1007/s00248-004-0240-2

Hiscox, J., Savoury, M., Vaughan, I. P., Müller, C. T., and Boddy, L. (2015). Antagonistic fungal interactions influence carbon dioxide evolution from decomposing wood. *Fungal Ecol.* 14, 24–32. doi: 10.1016/j.funeco.2014.11.001

Holderbaum, D. F., Kon, T., Kudo, T., and Guerra, M. P. (2010). Enzymatic browning, polyphenol oxidase activity, and polyphenols in four apple cultivars: dynamics during fruit development. *HortScience* 45, 1150–1154.

Houle, D., Govindaraju, D. R., and Omholt, S. (2010). Phenomics - the next challenge. *Nat. Rev. Genet.* 11, 855–866. doi: 10.1038/nrg2897

Insam, H., Amor, K., Renner, M., and Crepaz, C. (1996). Changes in functional abilities of the microbial community during composting of manure. *Microbial. Ecol.* 31, 77–87. doi: 10.1007/BF00175077

Kaewkla, O., and Franco, C. M. M. (2013). Rational approaches to improving the isolation of endophytic Actinobacteria from Australian native trees. *Microbial. Ecol.* 65, 384–393. doi: 10.1007/s00248-012-0113-z

Lim, Y., Kim, B., Kim, C., Jung, H., Kim, B.-S., Lee, J.-H., et al. (2010). Assessment of soil fungal communities using pyrosequencing. *J. Microbiol.* 48, 284–289. doi: 10.1007/s12275-010-9369-5

Macaya-Sanz, D., del-Barrio-Duque, A., and Martín, J. A. (2014). Fungal endophyte dynamics and functions in the early steps of degradation of eucalypt twigs. *Presentation at XVI International Congress on Molecular Plant-Microbe Interactions. 6-10 July,* Rhodes. 501.

Martín, J. A., Macaya-Sanz, D., Witzell, J., Blumenstein, K., and Gil, L. (2015). Strong in vitro antagonism by elm xylem endophytes is not accompanied by temporally stable in planta protection against a vascular pathogen under field conditions. *Eur. J. Plant Pathol.* 142, 185–196. doi: 10.1007/s10658-015-0602-2

Martín, J. A., Solla, A., Witzell, J., Gil, L., and Concepcion Garcia-Vallejo, M. (2010). Antifungal effect and induction of elm resistance towards Dutch elm disease fungi by salicylic acid and carvacrol. *Eur. J. Phytopathol.* 127, 21–32.

Martín, J. A., Witzell, J., Blumenstein, K., Rozpedowska, E., Helander, M., Sieber, T. N., et al. (2013). Resistance to Dutch elm disease reduces presence of xylem endophytic fungi in elms (*Ulmus* spp.). *PLoS ONE* 8:e56987. doi: 10.1371/journal.pone.0056987

Rančić, A., Soković, M., Karioti, A., Vukojević, J., and Skaltsa, H. (2006). Isolation and structural elucidation of two secondary metabolites from the filamentous fungus *Penicillium ochrochloron* with antimicrobial activity. *Environ. Toxicol. Pharmacol.* 22, 80–84. doi: 10.1016/j.etap.2005.12.003

Rodrigues, K. F., Hesse, M., and Werner, C. (2000). Antimicrobial activities of secondary metabolites produced by endophytic fungi from *Spondias mombin*. *J. Basic Microbiol.* 40, 261–267. doi: 10.1002/1521-4028(200008)40:4<261::AID-JOBM261>3.3.CO;2-4

Rodriguez, R., and Redman, R. (2008). More than 400 million years of evolution and some plants still can't make it on their own: plant stress tolerance via fungal symbiosis. *J. Exp. Bot.* 59, 1109–1114. doi: 10.1093/jxb/erm342

Rohlfs, M. (2015). Fungal secondary metabolite dynamics in fungus–grazer interactions: novel insights and unanswered questions. *Front. Microbiol.* 5:788. doi: 10.3389/fmicb.2014.00788

Schulz, B., and Boyle, C. (2005). The endophytic continuum. *Mycol. Res.* 109, 661–686. doi: 10.1017/S095375620500273X

Schulz, B., Boyle, C., Draeger, S., Rommert, A. K., and Krohn, K. (2002). Endophytic fungi: a source of novel biologically active secondary metabolites. *Mycol. Res.* 106, 996–1004. doi: 10.1017/S0953756202006342

Seidl, V., Druzhinina, I. S., and Kubicek, C. P. (2006). A screening system for carbon sources enhancing β-N-acetylglucosaminidase formation in *Hypocrea atroviridis* (*Trichoderma atroviride*). *Microbiology* 152, 2003–2012. doi: 10.1099/mic.0.28897-0

Similä, M., Kouki, J., and Martikainen, P. (2003). Saproxylic beetles in managed and seminatural Scots pine forests: quality of dead wood matters. *For. Ecol. Manage.* 174, 365–381. doi: 10.1016/S0378-1127(02)00061-0

Singh, M. P. (2009). Application of Biolog FF MicroPlate for substrate utilization and metabolite profiling of closely related fungi. *J. Microbiol. Methods* 77, 102–108. doi: 10.1016/j.mimet.2009.01.014

Solla, A., Dacasa, M. C., Nasmith, C., Hubbes, M., and Gil, L. (2008). Analysis of Spanish populations of *Ophiostoma ulmi* and *O. novo-ulmi* using phenotypic characteristics and RAPD markers. *Plant Pathol.* 57, 33–44. doi: 10.1111/j.1365-3059.2007.01692.x

Tanzer, M. M., Arst, H. N., Skalchunes, A. R., Coffin, M., Darveaux, B. A., Heiniger, R. W., et al. (2003). Global nutritional profiling for mutant and chemical mode-of-action analysis in filamentous fungi. *Funct. Integr. Gen.* 3, 160–170. doi: 10.1007/s10142-003-0089-3

Toju, H., Yamamoto, S., Sato, H., Tanabe, A. S., Gilbert, G. S., and Kadowaki, K. (2013). Community composition of root-associated fungi in a Quercus-dominated temperate forest: "codominance" of mycorrhizal and root-endophytic fungi. *Ecol. Evol.* 3, 1281–1293. doi: 10.1002/ece3.546

Unterseher, M., Petzold, A., and Schnittler, M. (2012). Xerotolerant foliar endophytic fungi of *Populus euphratica* from the Tarim River basin. Central China are conspecific to endophytic ITS phylotypes of *Populus tremula* from temperate Europe. *Fungal Divers.* 54, 133–142.

van den Brink, J., and de Vries, R. P. (2011). Fungal enzyme sets for plant polysaccharide degradation. *Appl. Microbiol. Biotechnol.* 91, 1477–1492. doi: 10.1007/s00253-011-3473-2

Velmurugan, P., Lee, Y. H., Venil, C. K., Lakshmanaperumalsamy, P., Chae, J.-C., and Oh, B.-T. (2010). Effect of light on growth, intracellular and extracellular pigment production by five pigment-producing filamentous fungi in synthetic medium. *J. Biosci. Bioengin.* 109, 346–350. doi: 10.1016/j.jbiosc.2009.10.003

Witzell, J., and Martín, J. A. (2008). Phenolic metabolites in the resistance of northern forest trees to pathogens – past experiences and future prospects. *Can. J. For. Res.* 38, 2711–2727. doi: 10.1139/X08-112

Witzell, J., Martín, J. A., and Blumenstein, K. (2014). "Ecological aspects of endophyte-based biocontrol of forest diseases," in *Advances in Endophytic Research*, eds V. C. Verma and A. C. Gange (Berlin: Springer), 321–333.

Yourman, L. F., Jeffers, S. N., and Dean, R. A. (2001). Phenotype instability in *Botrytis cinerea* in the absence of benzimidazole and dicarboximide fungicides. *Phytopathology* 91, 307–315. doi: 10.1094/Phyto.2001.91.3.307

Conflict of Interest Statement: The authors declare that the research was conducted in the absence of any commercial or financial relationships that could be construed as a potential conflict of interest.

frontiers in
MICROBIOLOGY

ORIGINAL RESEARCH ARTICLE
published: 03 March 2015
doi: 10.3389/fmicb.2015.00138

Plant genotype-specific archaeal and bacterial endophytes but similar *Bacillus* antagonists colonize Mediterranean olive trees

***Henry Müller*[1]*, *Christian Berg*[2], *Blanca B. Landa*[3], *Anna Auerbach*[4], *Christine Moissl-Eichinger*[4,5,6] and *Gabriele Berg*[1]**

[1] *Institute of Environmental Biotechnology, Graz University of Technology, Graz, Austria*
[2] *Botanical Garden, Institute of Plant Sciences, University of Graz, Graz, Austria*
[3] *Institute for Sustainable Agriculture, Spanish National Research Council, Córdoba, Spain*
[4] *Department for Microbiology and Archaea Center, University of Regensburg, Regensburg, Germany*
[5] *Department of Internal Medicine, Medical University of Graz, Graz, Austria*
[6] *BioTechMed, Graz, Austria*

Edited by:
Mysore V. Tejesvi, University of Oulu, Finland

Reviewed by:
David John Studholme, University of Exeter, UK
Johann Weber, University of Lausanne, Switzerland

****Correspondence:***
Henry Müller, Graz University of Technology, Institute of Environmental Biotechnology, Petersgasse 12/I, 8010 Graz, Austria
e-mail: henry.mueller@tugraz.at

Endophytes have an intimate and often symbiotic interaction with their hosts. Less is known about the composition and function of endophytes in trees. In order to evaluate our hypothesis that plant genotype and origin have a strong impact on both, endophytes of leaves from 10 *Olea europaea* L. cultivars from the Mediterranean basin growing at a single agricultural site in Spain and from nine wild olive trees located in natural habitats in Greece, Cyprus, and on Madeira Island were studied. The composition of the bacterial endophytic communities as revealed by 16S rRNA gene amplicon sequencing and the subsequent PCoA analysis showed a strong correlation to the plant genotypes. The bacterial distribution patterns were congruent with the plant origins in "Eastern" and "Western" areas of the Mediterranean basin. Subsequently, the endophytic microbiome of wild olives was shown to be closely related to those of cultivated olives of the corresponding geographic origins. The olive leaf endosphere harbored mostly *Proteobacteria*, followed by *Firmicutes, Actinobacteria,* and *Bacteroidetes*. The detection of a high portion of archaeal taxa belonging to the phyla *Thaumarchaeota, Crenarchaeota,* and *Euryarchaeota* in the amplicon libraries was an unexpected discovery, which was confirmed by quantitative real-time PCR revealing an archaeal portion of up to 35.8%. Although the function of these Archaea for their host plant remains speculative, this finding suggests a significant relevance of archaeal endophytes for plant–microbe interactions. In addition, the antagonistic potential of culturable endophytes was determined; all isolates with antagonistic activity against the olive-pathogenic fungus *Verticillium dahliae* Kleb. belong to *Bacillus amyloliquefaciens*. In contrast to the specific global structural diversity, BOX-fingerprints of the antagonistic *Bacillus* isolates were highly similar and independent of the olive genotype from which they were isolated.

Keywords: endophytes, *Olea europaea,* Archaea, antagonistic bacteria, *Verticillium dahliae*

INTRODUCTION

Olive trees (*Olea europaea* L.) represent one of the most ancient domestic plants, which have characterized the Mediterranean landscape since ancient times (Zohary and Spiegel-Roy, 1975). Olives originated from Asia and spread from Iran, Syria, and Palestine to the rest of the Mediterranean basin 6,000 years ago (Breton et al., 2008, 2009). The species *O. europaea* L. is classified as wild, referred to as oleaster (subsp. *europaea* var. *sylvestris*), and as cultivated (subsp. *europaea* var. *europaea*) types (Green, 2002). The domestication and breeding history of olive trees has not been fully described to date. Ancestral wild gene pools from three long-term refugia (the Near East, the Aegean area, and the Strait of Gibraltar) have provided the essential foundations for cultivated olive breeding (Besnard et al., 2013). At present, a long list of genotypes cultivated in the Mediterranean basin exists (Lumaret and Quazzani, 2001; Díaz et al., 2006; Díez et al., 2011). According to their gene pools olive cultivars can be divided into three main groups related to the region of origin "Eastern," "Central," and "Western" (Haouane et al., 2011). Today, olive trees represent one of the most important oil crops world-wide, delivering monounsaturated fatty acid and antioxidant-containing olive oil, which serves as the major fatty component of the Mediterranean diet. In 2013, on an area of 10.2 Mio ha 20.3 Mio t of olives was harvested world-wide and showed in the last few years a strong upward trend (FAOSTAT, 2014). However, olive production in the Mediterranean region is affected by several diseases. *Verticillium* wilt, caused by *Verticillium dahliae* Kleb., is currently the most devastating disease correlated with low yield and high rates of tree loss (López-Escudero and Mercado-Blanco, 2011). Since no resistant varieties and effective

fungicides exist, biological control using the naturally occurring antagonistic potential against pathogens is a potentially viable and environmentally friendly alternative (Jiménez-Díaz et al., 2011). Although several successful example studies were published for the pathosystem olive-*Verticillium* (Prieto and Mercado-Blanco, 2008; Maldonado-González et al., 2013, 2015), inconsistent effects in the field are one hurdle along the path towards commercialization. Microbiome-based biocontrol strategies can solve these problems (Berg et al., 2013; Berg, 2014) but have not yet been established.

Endophytes that live inside plants do not cause harm to the plants and are characterized by an intimate interaction with their hosts (Hallmann et al., 1997; Hardoim et al., 2008; Reinhold-Hurek and Hurek, 2011). Endophytes with antagonistic activity against pathogens are promising candidates for biocontrol strategies against *Verticillium* because they colonize the same niche and can compete directly with the pathogen. The endophytic microbiome shows great diversity, which is influenced by the site and growth stage of the host plants as well as fulfilling important functions for its host including the promotion of plant growth, protection against biotic, and abiotic stress as well as the production of essential secondary metabolites (Ryan et al., 2008; Berg, 2009; Alavi et al., 2013). Although a large diversity of microorganisms can live endophytically, mainly bacteria, in particular *Alphaproteobacteria,* were identified as plant inhabitants (Bulgarelli et al., 2013). In contrast, much less is known about endophytic Archaea. Archaea represent the so-called third domain of life, and have only recently been described as important component of the moderate environment and the human microbiome (Probst et al., 2013). A few very recent publications have mentioned internal plant tissue colonization by members of the Archaea (Ma et al., 2013; Oliveira et al., 2013), but their distribution, significance, function, and activity remains unclear. In addition, the endophytic microbiota of trees has undergone less investigation and nothing is known about the associated microorganisms within olive trees. Our hypothesis has been that a positive identification of olive-associated endophytic communities depends on whether their patterns are found to correspond with their geographical origin. Because of the longevity and the high genetic variability of oleasters and cultivars, olives might have a specific but stable community of microbes over periods and ranges and should contain a high diversity of microbes, especially with antagonistic potential against *V. dahliae* (Aranda et al., 2011).

The objective of this study was to determine and compare the structure of endophytic microbiota of 10 *O. europaea* L. cultivars from the Mediterranean basin at one agricultural site in Spain and from nine wild olive trees located in natural habitats in Greece, Cyprus, and on Madeira Island by a set of molecular and isolation-dependent methods. Moreover, the study addressed the question what factors shape the endophytic microbiome and, in particular, whether the bacterial and archaeal communities reflects the different geographic origins of the investigated olive genotypes. The results will be used to reveal influences on the tree microbiome but also to develop successful biocontrol strategies against *Verticillium* wilt in olives.

MATERIALS AND METHODS

SAMPLING STRATEGY

Cultivated and wild olive trees from different regions were sampled. The samples of the cultivated olives were taken at a single experimental orchard at the 'Venta del Llano' Research Station (IFAPA, Andalusia Regional Government) in Mengibar (Jaén province, southern Spain). The field was established 22 years ago using olive planting stocks of the same age of different cultivars of various Mediterranean origins (Palomares-Rius et al., 2012). From four trees of selected cultivars, vegetative branches and adherent leaves were sampled in May 2009 (**Table 1**). Always the terminal ends (10 cm) from four of the youngest branches around an individual tree were taken and pooled. For the sampling surface-disinfected gloves and scissors as well as sterile bags were used. Leaves and boughs of wild olives were collected from Cyprus (February, 2009), Greece (May, 2009), and Madeira (August, 2009). Samples from olive cultivars in Mengibar were chilled and processed within one day, whereas the material from wild olives were stored and transported under cooled condition until processing within at least four days.

DNA EXTRACTION

For the isolation of microorganisms, 10 g of leaves and boughs from each composite sample of individual trees were surface-sterilized for 5 min using sodium hypochlorite (3% active chlorine) and washed three times with autoclaved water. After the

Table 1 | Sample designation, cultivar, and geographical origin used in this study.

Sample designation	Cultivar	Origin	Coordinates
SP3	Arbequino	Spain	37°56′26.62″ N, 03°47′06.78″ W
SP5	Ocal	Spain	37°56′26.62″ N, 03°47′06.78″ W
I2	Leccino	Italy	37°56′26.62″ N, 03°47′06.78″ W
GR1	Koroneiki	Greece	37°56′26.62″ N, 03°47′06.78″ W
GR2	Kalamata	Greece	37°56′26.62″ N, 03°47′06.78″ W
TUN1	Chétoni	Tunisia	37°56′26.62″ N, 03°47′06.78″ W
SI1	Trylia	Syria	37°56′26.62″ N, 03°47′06.78″ W
MO1	Picholine Marrocaine	Morocco	37°56′26.62″ N, 03°47′06.78″ W
PO1	Galega	Portugal	37°56′26.62″ N, 03°47′06.78″ W
FR1	Aglandau	France	37°56′26.62″ N, 03°47′06.78″ W
CY1	Wild	Cyprus	35°04′09.64″ N, 32°18′00.28″ E
CY2	Wild	Cyprus	35°05′01.13″ N, 32°18′00.10″ E
CY3	Wild	Cyprus	34°46′06.99″ N, 32°54′08.96″ E
CY4	Wild	Cyprus	34°46′41.94″ N, 32° 54′53.76″ E
GR(w)1	Wild	Greece	38°12′04.84″ N, 22°06′05.22″ E
GR(w)2	Wild	Greece	38°12′06.01″ N, 22°06′01.38″ E
GR(w)3	Wild	Greece	38°10′00.54″ N, 22°06′05.88″ E
GR(w)4	Wild	Greece	38°10′04.68″ N, 22°06′36.42″ E
M1	Wild	Madeira	32°44′13.37″ N, 17°12′34.77″ W

addition of 5 mL of sterile water the samples were pestled and 2 mL of the suspension was transferred in a 2 mL tube, and centrifuged at 16.500 × *g* for 15 min at 4°C. The supernatant was discarded and the pellet was stored at −21°C. Total DNA of bacterial and fungal consortia was extracted using the FastDNA® Spin Kit for Soil (MP Biomedicals, Santa Ana, CA, USA) according to the manufacturer's protocol.

STRUCTURE OF ENDOPHYTIC BACTERIAL COMMUNITIES REVEALED BY ILLUMINA MiSeq AMPLICON SEQUENCING

To analyze the taxonomic composition of the endophytic bacterial communities an amplicon sequencing approach using Illumina's MiSeq platform was applied for three biological replicates per studied cultivar or oleaster. The hypervariable V4 region of the 16S rRNA gene was amplified according to the protocol described by Caporaso et al. (2012) using the region specific primer pair 515f and 806r that included Illumina cell flow adaptors and sample-specific barcodes. The PCR reaction mixture (30 µl) contained 1x Taq&Go (MP Biomedicals, Illkirch, France), 0.25 mM of each primer and 1 µl of template DNA (94°C for 3 min, 32 cycles of 94°C for 45 s, 60°C for 1 min, 72°C for 18 s, and final elongation at 72°C for 10 min). Products from three independent PCR runs for each sample were pooled in equal volumes and purified by employing the Wizard SV Gel and PCR Clean-Up System (Promega, Madison, WI, USA). After spectrophotometrical measurement of DNA concentrations (Nanodrop 2000, Thermo Scientific, Wilmington, DE, USA) equimolar aliquots of all samples were combined for amplicon sequencing using Illumina MiSeq v2 (250 bp paired end) conducted by (LGC Genomics, Berlin, Germany). Raw sequencing data preparation included demultiplexing (CASAVA data analysis software, Illumina), clipping of sequencing adapters (TruSeq, Illumina), joining read pairs (FLASH 1.2.4, Magoc and Salzberg, 2011) with a minimum overlap of 10 bases and maximum mismatch density of 0.25, and sorting according to sample-specific barcodes. Prior to the next step, reads from biological replicates from each cultivar/oleaster were joined (Supplementary Table S1). Resulting reads were quality (Phred score ≥ 20) and length filtered (290–300 bp) using scripts provided by the open source software package QIIME 1.8.0 (http://qiime.sourceforge.net). Chimeric sequences were discarded after *de novo* detection based on USEARCH 6.1 (Edgar et al., 2011). UCLUST algorithm using default parameters was applied to cluster remaining reads to operational taxonomic units (OTUs) at 97% similarity (Edgar, 2010) followed by taxonomic assignment of representative sequences by RDP naïve Bayesian rRNA classifier (Wang et al., 2007) based on the reference database Greengenes release gg_13_8_99 (DeSantis et al., 2006). Archaeal reads were additionally classified using Silva's SINA aligner (Pruesse et al., 2012). Prior to further analysis all reads assigned to plant plastids (chloroplasts and mitochondria) were discarded from datasets. The number of sequences of each sample was normalized to the lowest number of read counts by randomly selecting subsets of sequences by a custom Perl script (10-times random sampling followed by subset formation). Principal Coordinate Analysis (PCoA) was performed to assess the beta diversity based on the calculation of the weighted normalized UniFrac distance matrix (Lozupone and Knight, 2005). The study is registered as NCBI BioProject PRJNA272855, the metadata for each sample are available at NCBI in the BioSample database (accession numbers SAMN03287521 – 33), and the sequence data are deposited in NCBI's Short Read Archive (SRA) under accession numbers SRR1781607, SRR1781712, SRR1781720, SRR1781736, SRR1781767, SRR1781768, SRR1781984, SRR1781986, SRR1781987, SRR1781988, SRR1781989, SRR1781990, and SRR1782571.

QUANTIFICATION OF ARCHAEA POPULATION BY QUANTITATIVE REAL-TIME PCR (qPCR)

Bacteria- and archaea-directed quantitative real-time PCR (qPCR) was performed as described earlier, with primer pairs 338 bf/517 ur and 344 af/517 ur, respectively, (final primer concentration: 300 nM; Probst et al., 2013). The primer sequences are as follows: Primer 338 bf (5′→ 3′): ACTCCTACGGGAGGCAGCAG (El Fantroussi et al., 1999), primer 517 ur (5′→ 3′): GWATTACCGCGGCKGCTG (Amann et al., 1995), primer 344 af (5′→ 3′): ACGGGGYGCAGCAGGCGCGA (Raskin et al., 1994). For each of the four biological replicates per olive sample, three technical qPCR replicates were carried out, using 1 µl of template DNA. Standard curves were developed from PCR products of the 16S rRNA gene of *Staphylococcus warneri* and *Nitrosopumilus maritimus*. The mean of the triplicates was calculated. The archaeal portion was calculated as part of the total 16S rRNA gene signatures retrieved (archaeal plus bacterial signals).

ISOLATION OF ENDOPHYTES FROM OLIVES AND SCREENING FOR ANTAGONISTIC ACTIVITY TOWARDS *V. dahliae*

Bacterial isolates were obtained by plating aliquots of suspensions from plant materials on R2A (Difco, Detroit, MI, USA) and Kings B (containing 20 g proteose pepton, 15 ml glycerin, 1.5 g K_2HPO_4, 1.5 g $MgSO_4 \times 7\ H_2O$, 20 g agar per liter). The antagonistic activity of randomly selected isolates displaying morphologically distinct colonies (five to seven isolates each olive cultivar) towards the soilborne pathogen *V. dahliae* V25 was assessed by dual culture *in vitro* assay (Berg et al., 2005). Representative antagonistic isolates were characterized by BOX fingerprinting and partial 16S rRNA sequencing as described by Berg et al. (2005).

RESULTS

COMPOSITION OF ENDOPHYTIC MICROBIAL COMMUNITIES IN OLIVE TREES

The number of reads obtained by amplicon sequencing ranged from 210 to 1583 per olive cultivar (Supplementary Table S1). Based on the taxonomic classification of representative sequences from all OTUs, the composition of bacterial communities was revealed at phylum and class level (**Figures 1A,B**). Although PCR primers targeting eubacterial 16S rRNA genes were applied, a notable number of reads was assigned to the archaeal domain. Among all analyzed olive genotypes, the bacterial phylum *Proteobacteria* (21.3–69.6%) and the archaeal phyla *Thaumarchaeota* (0.6–51.7%) and *Crenarchaeota* (1.9–28.6%) predominated. Less abundant taxa that were detected in all samples belonged to *Firmicutes* (2.5–11.0%), *Euryarchaeota* (1.0–13.7%), and *Bacteroidetes* (0.4–13.4%). At class level all microbiomes contained representatives of *Alpha-*, *Beta-* ,and *Gammaproteobacteria* (4.9–17.9%,

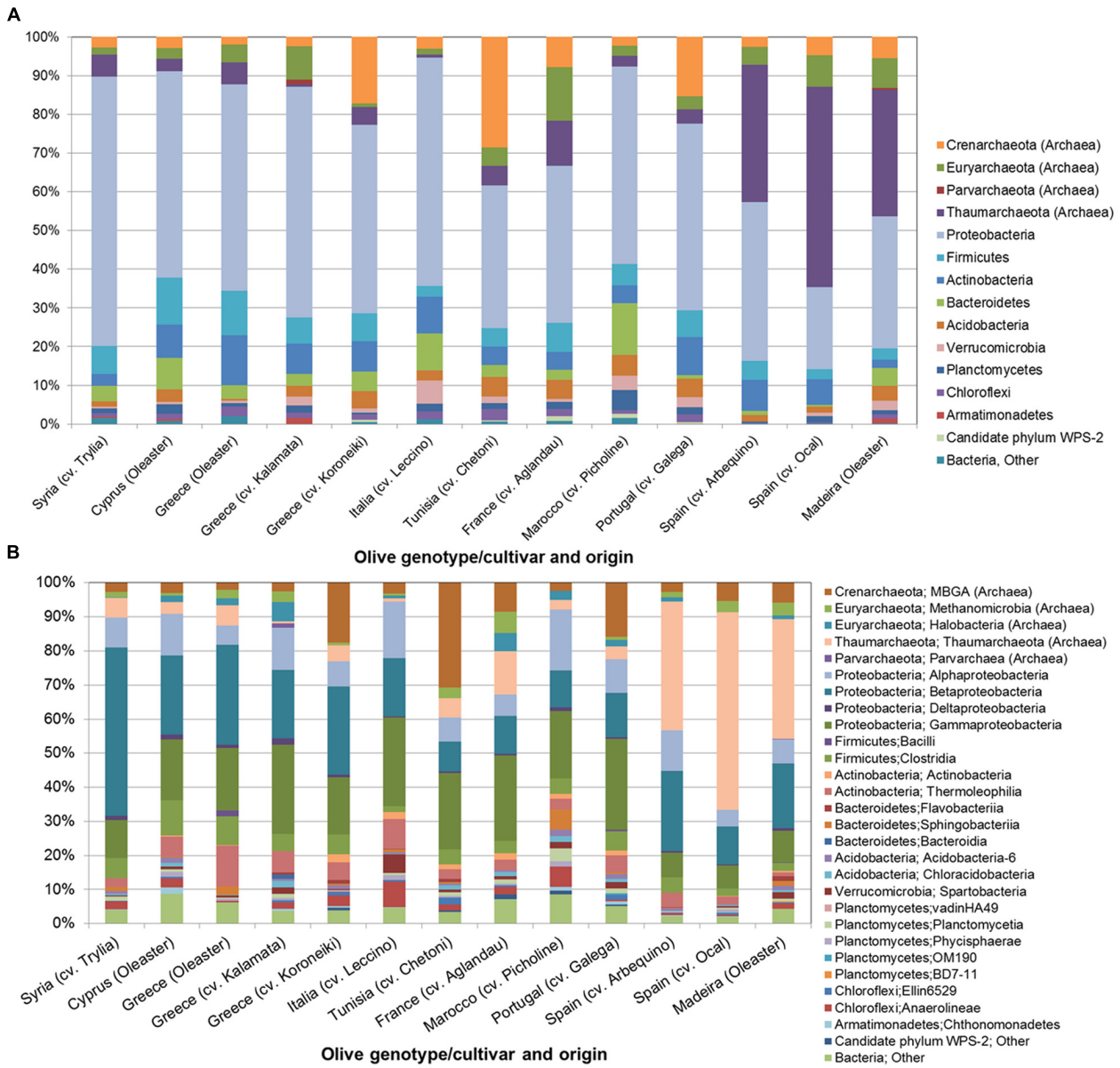

FIGURE 1 | Structure of the microbial communities in the endosphere of different olive cultivars revealed by Illumina MiSeq 16S rRNA gene amplicon sequencing at phylum (A) and class level (B).

8.8–49.4% and 6.7–26.6%), the archaeal classes *Thaumarchaeota* (0.6–58.1%) and MBG group A (2.0–30.7%), and *Bacilli* (1.8–10.3%). Out of 1,595 detected OTUs five OTUs were shared by all olive cultivars representing 9.8 to 61.0% of respective read counts (**Figure 2**). The putative core microbiome consisted of the betaproteobacterial *Pelomonas* sp. (10.7%) and *Ralstonia* sp. (2.2%), the thaumarchaeal candidate genus *Nitrososphaera* (8.6%), and the gammaproteobacterial *Pseudomonas* sp. (2.6%) and *Actinobacter* sp. (2.6%).

Apart from commonalities, the analysis of the microbial endophytic communities indicated a high degree of cultivar and regional specificity. PCoA plot deduced from the distance matrix calculated by the weighted normalized UniFrac algorithm using phylogenetic information demonstrates a general clustering according to the geographic or cultural origin (**Figure 3**). Whereas the Western and Eastern olives are clearly distinguishable, the samples from the central Mediterranean basin (Tunisia, Italy, and France) were more similar to western (in case of Tunisia and France) or to eastern (Italy) olive cultivars. The exception could be explained by ancestors from a different region. The communities of wild olives sampled in Cyprus and Greece grouped closely within the cultivars originated from the same region. The microbiome of the oleaster from Madeira shares the most similarity to the olives from Spain, suggesting a cultural relationship. Analysis

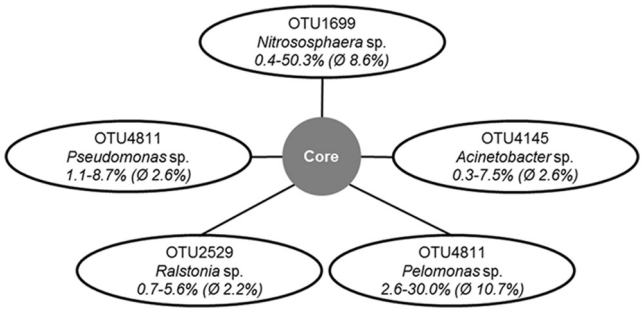

FIGURE 2 | Operational taxonomic units (OTUs) and their taxonomic affiliations representing the putative core microbiome in the endospheres of all studied olive samples. The numbers indicate the maximum, minimum and average of relative abundances of the respective OTU throughout the read libraries.

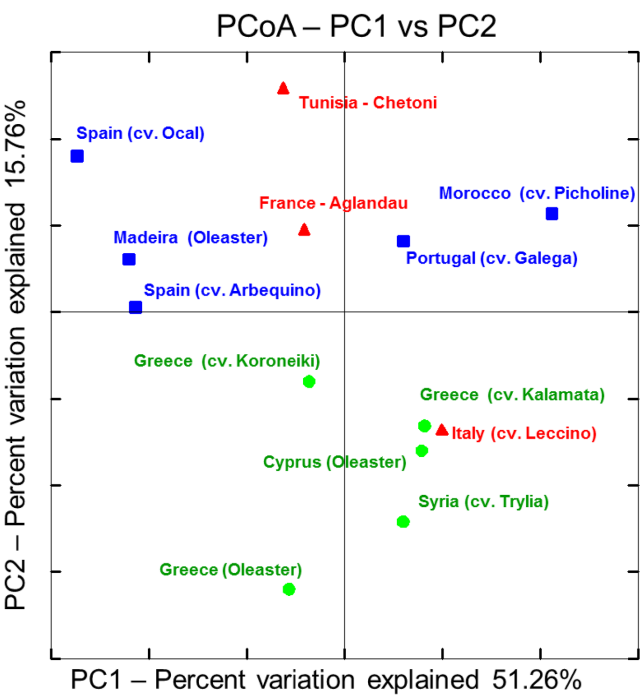

FIGURE 3 | Principal Coordinate Analysis (PCoA) plot deduced from weighted normalized UniFrac distance matrix calculated from OTU distribution obtained from 16S amplicon sequencing using Illumina's MiSeq platform: Olive cultivar accessions were classified into three main geographical regions. ■ – Western Mediterranean. ▲ – Central Mediterranean. ● – Eastern Mediterranean.

of the community composition measured by the UniFrac distances between the three regional groups showed that microbiomes from Western Mediterranean olives differed significantly from those of eastern cultivars and oleasters ($P = 0.03$), whereas there was no statistically significant differences between observed UniFrac distances from central and eastern olive groups or between central and western olive clusters.

The divergence of the microbial communities of olives from certain regions may be explained by variable abundances as well as by the presence and absence of particular taxonomic groups. **Figure 4** illustrates bacterial and archaeal orders identified in eastern and western olive trees with different relative abundances at a ratio higher than two. The bacterial orders *Chthonomonadales*, *Chloroflexi,* the candidate order CFB-26 and *Elusimicrobiales* were found exclusively in olive cultivars or oleasters originating in eastern Mediterranean regions. Among the most abundant eastern olive orders, *Burkholderiales* (2.0x), *Lactobacillales* (2.1x), *Actinomycetales* (2.4x) and *Enterobacteriales* (2.7x) were observed to be in increased numbers. In contrast, mainly archaeal orders were found in western olives. Here, *Crenarchaeales* were found exclusively, and the orders *Nitrososphaerales* (7.0x) and *Crenarchaeota* candidate order NRP-J (2.7x) were more dominant.

ARCHAEAL POPULATION DENSITY AND COMMUNITY STRUCTURE

The structure and abundances of cultivars were analyzed in more detail because they appeared to be particularly well colonized by Archaea. The population density was quantified by qPCR (**Figure 5**), reaching up to 4×10^4 copies per ng template DNA. 35.8% of all microbial 16S rRNA gene copies detected in the Spanish cultivar Ocal where found to be archaeal. It should be noted that because the eubacterial primers used also target plastid DNA, the relative abundances are likely to be higher than indicated by these measurements. The analysis of the amplicon library revealed a high proportion of endophytic Archaea in olive leaf tissues which account for 5.3 to 67.3% of total reads. The majority of archaeal reads were assigned to the phylum *Euryarchaeota* represented by the orders *Halobacteriales* and *Methanomicrobiales*, the phylum *Thaumarchaeota* with representatives in *Nitrososphaerales* and soil group I.1.b (*Nitrososphaera*) and I.1.c, and the *Crenarchaeota* candidate order NRP-J (**Figure 6**).

ANTAGONISTIC ACTIVITY OF ENDOPHYTIC BACTERIAL STRAINS FROM OLIVE TREES

To assess the antagonistic potential of endophytes against *V. dahliae,* bacteria were isolated and tested on their *in vitro* antagonistic activity. The culturable bacterial population was 1.9×10^5 colony forming units (CFU) g^{-1} fw^{-1} on average without any statistically significant differences between wild and cultivated olives (data not shown). Altogether, 80 randomly isolated strains were investigated regarding their antagonistic activity against the pathogen, from which 11.3% showed high antagonistic potential. Although bacteria were isolated from olive trees from different regions, those with high antagonistic activity showed highly similar fingerprints (analyzed by BOX patterns) suggesting that they belong to a similar genotype. The 16S rRNA gene of one representative strain from nine positively tested strains and was therefore sequenced and assigned to *Bacillus amyloliquefaciens* by blastn analysis (closest match: NR_116022.1, 99% identity).

DISCUSSION

The structure of the endophytic microbiome of the 10 different olive cultivars correlated with their (breeding) geographical origin and was confirmed by the similarity of their microbiome structures shown by the nine wild oleasters from each region. In contrast, the function – we analyzed the antagonistic activity of endophytic

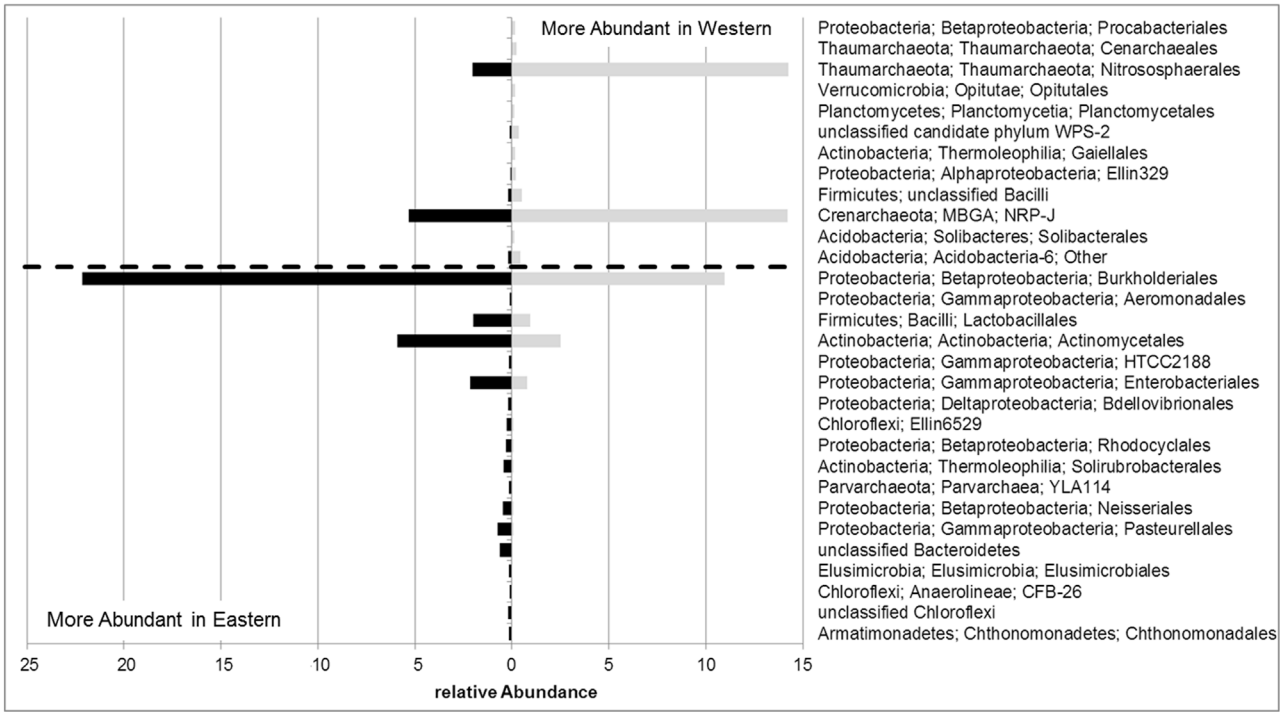

FIGURE 4 | Relative abundances of bacterial and archaeal orders with at least twofold differences in the endosphere of olive trees from eastern or western Mediterranean regions.

isolates against the pathogenic fungus *V. dahliae* – was derived from the same bacterial genus *Bacillus*. Here, no impact of the region or breeding history was found. Moreover, *B. amyloliquefaciens* strains isolated from different cultivars and regions showed similar molecular fingerprints which suggested a close functional relationship.

We confirmed our hypothesis that olive trees and their endophytic microbiome can be divided at least into the major regions "Eastern" and "Western," whereas the microbial populations of the three "Central" cultivars resemble those of one the other two zones. The microbial communities of the wild olives and of the cultivars from the corresponding regions were closely related. A high level of similarity between the microbial composition of wild trees from Cyprus and Greece and the cultivars with western origins were found. Additionally, the wild trees from Madeira possessed endophytes that were similar to the cultivars Arbequino and Ocal (Spain). These results show that compared to the influence of the olive genotype the prevailing soil and climate conditions at the sampling sites and the geographical distances of 1000s of kilometers have a negligible effect on the endophytic communities in leaves. Redford et al. (2010) found similar results by studying the phyllosphere of the *ponderosa* pine; however, several studies described the influence of environmental conditions on endophytic communities (Rosenblueth and Martínez-Romero, 2006). The abundance of the bacterial community depends on the age of the leaves and the endophytic diversity and was related to leaf traits of the tropical plant species *Coccoloba cereifera* (Sanchez-Azofeifa et al., 2012). Because the olive belongs to the evergreen tree species, the endophytic microbial diversity may be stable over longer periods of time.

Endophytes can promote the growth of plants and/or suppress phytopathogens (Backman and Sikora, 2008; Hardoim et al., 2008); however, the antagonistic part of the microbiome in this study was highly similar for all investigated genotypes. Only members of the *Firmicutes* group were found which are well-known as potent antagonists and biocontrol agents (Emmert and Handelsman, 1999). Molecular fingerprints and amplicon libraries confirmed the highly similar structure for all *Firmicutes* (data not shown). In amplicon libraries they present a proportion of less than 5%. The low proportion of potential antagonists within the culturable bacterial endophytes may be one reason for the high susceptibility of olive trees to *V. dahliae*. *B. amyloliquefaciens* has been identified as the most important antagonistic species within the genus *Bacillus* which is well-known as a biological control agent (Marten et al., 2000; Kloepper et al., 2004) and a good colonizer of the olive rizosphere and rhizoplane (Aranda et al., 2011). To date, biological control approaches against *V. dahliae* in olive have targeted Gram-negative antagonists such as *Pseudomonas* and *Serratia* (Mercado-Blanco et al., 2004; Prieto and Mercado-Blanco, 2008; Prieto et al., 2009). Our results suggest that Gram-positive bacteria such as *Bacillus* from oleasters may also be an interesting option for biocontrol (Aranda et al., 2011).

The high proportion of archaeal 16S rRNA genes found in the endosphere of olive trees was the most interesting finding from our study. In a recent study (Cáliz et al., under revision) showed that rhizosphere of olive cultivars in southern Spain

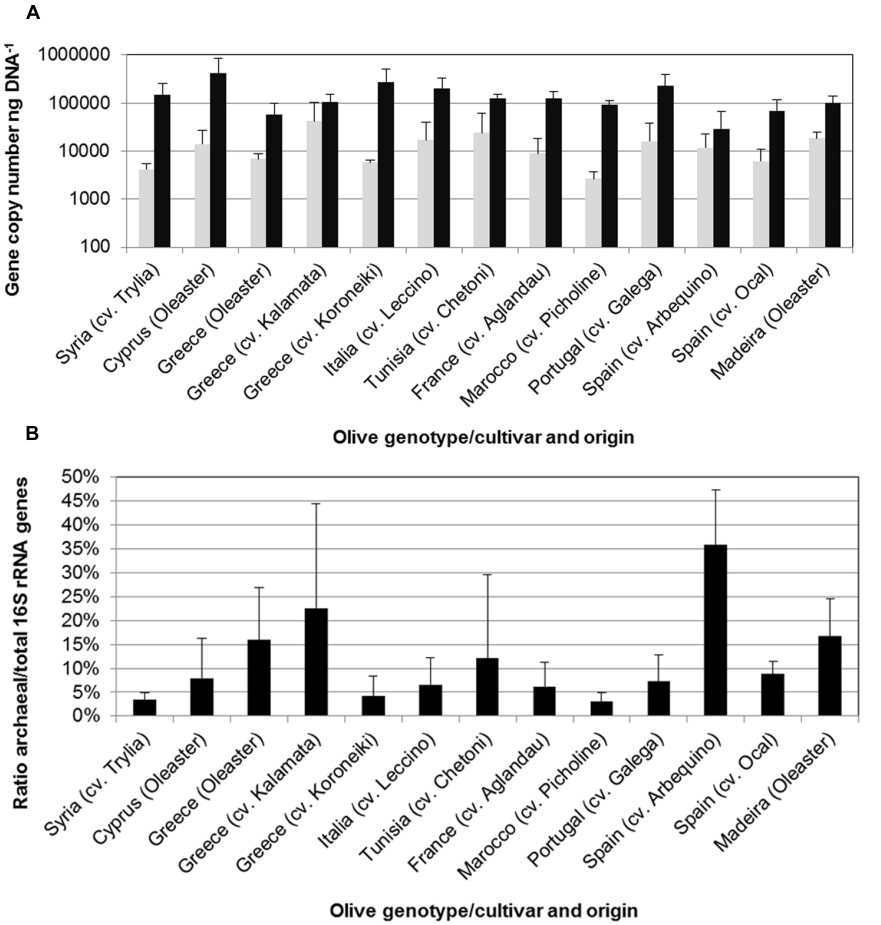

FIGURE 5 | Number of archaeal (gray bars) and total prokaryotic (black bars) 16S rRNA copies per ng template DNA (A) and proportion of archaeal 16S rRNA of total prokaryotic 16S rRNA gene copies (B) determined by quantitative real-time PCR (qPCR). Error bars indicate confidence intervals at $P = 0.05$.

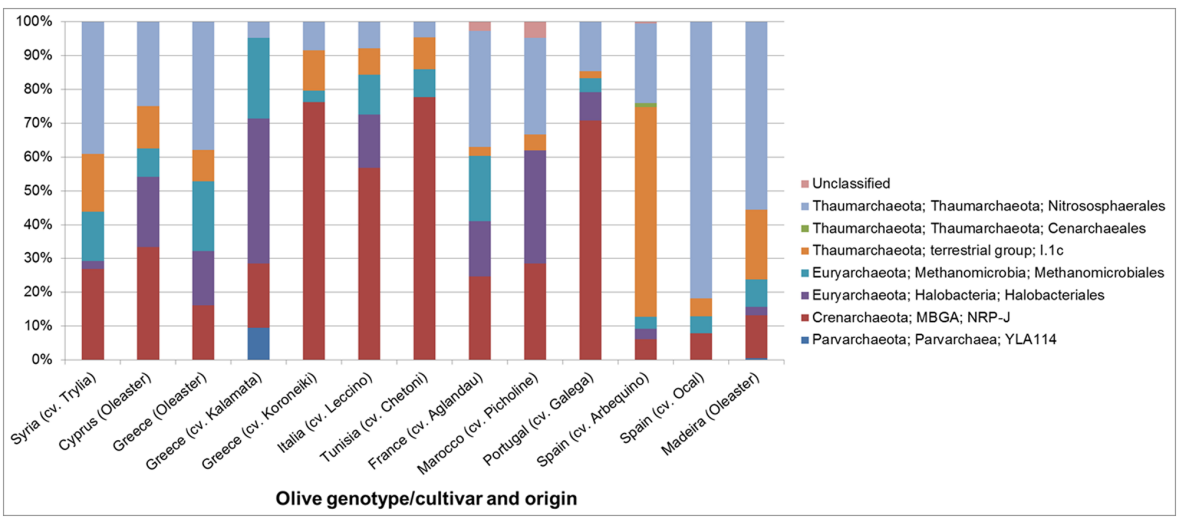

FIGURE 6 | Structure of the archaeal communities in the endosphere of different olive cultivars at order level revealed by Illumina MiSeq 16S rRNA gene amplicon sequencing.

is mainly colonized by members of archaea belonging to 1.1b *Thaumarchaeota* (soil crenarchaeota group) closely related to the genus *Nitrososphaera*, with much less numbers of *Euryarchaeota* of the groups *Halobacteria, Methanomicrobia*, and *Thermoplasmata* indicating that olive select specific groups of Archaea as endophytes or that only specific groups of Archaea are adapted to live within olive tissues. Earlier studies on other plants indicate internal tissue colonization by members of Archaea, e.g., in *Phragmites australis* and *Coffea arabica* (Ma et al., 2013; Oliveira et al., 2013), and give comparably low numbers for their abundance (Redford et al., 2010; Finkel et al., 2011; Knief et al., 2012). In this study, we proof the presence of archaeal signatures in endophytic microbial communities from olive leafs, and propose a larger role of these microbes therein. *Thaumarchaeota* have been described as significant component in soil microbial community and even in the human skin microbiome (Probst et al., 2013). Due to their ammonia-oxidizing capability, they influence the local ammonia-availability and pH, which could help to defend pathogenic microorganisms and to maintain the healthy (endophytic) microbiome. Although the function of these Archaea remains speculative, this finding suggests the existence of an undiscovered action/mechanism that is essential to a more in-depth understanding of plant-archaea and human-archaea interactions.

ACKNOWLEDGMENTS

We would like to thank Katja A. Maurer (Graz), who contributed to the sampling, DNA extraction and isolation of the antagonistic strains during her master thesis at TU Graz. Furthermore, we would like to thank Timothy Mark (Graz) for English revision. This study was partly funded by the binational exchange program between Austria and Spain "Wissenschaftlich-Technische Zusammenarbeit" (WTZ) and 'Acciones Integradas.'

SUPPLEMENTARY MATERIAL

The Supplementary Material for this article can be found online at: http://www.frontiersin.org/journal/10.3389/fmicb.2015.00138/abstract

REFERENCES

Alavi, P., Starcher, M. R., Zachow, C., Müller, H., and Berg, G. (2013). Root-microbe systems: the effect and mode of interaction of stress protecting agent (SPA) *Stenotrophomonas rhizophila* DSM14405T. *Front. Plant Sci.* 4:141. doi: 10.3389/fpls.2013.00141

Amann, R. I., Ludwig, W., and Schleifer, K. H. (1995). Phylogenetic identification and in situ detection of individual microbial cells without cultivation. *Microbiol. Rev.* 59, 143–169.

Aranda, S., Montes-Borrego, M., Jiménez-Díaz, R. M., and Landa, B. B. (2011). Microbial communities associated with the root system of wild olives (*Olea europaea* L. subsp. *europaea* var. *sylvestris*) are good reservoirs of bacteria with antagonistic potential against *Verticillium dahliae*. *Plant Soil* 343, 329–345. doi: 10.1007/s11104-011-0721-2

Backman, P. A., and Sikora, R. A. (2008). Endophytes: an emerging tool for biological control. *Biol. Control* 46, 1–3. doi: 10.1016/j.biocontrol.2008.03.009

Berg, G. (2009). Plant–microbe interactions promoting plant growth and health: perspectives for controlled use of microorganisms in agriculture. *Appl. Microbiol. Biotechnol.* 84, 11–18. doi: 10.1007/s00253-009-2092-7

Berg, G. (2014). Beyond borders: investigating microbiome interactivity and diversity for advanced biocontrol technologies. *Microb. Biotechnol.* doi: 10.1111/1751-7915.12235 [Epub ahead of print].

Berg, G., Krechel, A., Ditz, M., Sikora, R. A., Ulrich, A., and Hallmann, J. (2005). Endophytic and ectophytic potato-associated bacterial communities differ in structure and antagonistic function against plant pathogenic fungi. *FEMS Microbiol. Ecol.* 51, 215–229. doi: 10.1016/j.femsec.2004.08.006

Berg, G., Zachow, C., Müller, H., Phillips, J., and Tilcher, R. (2013). Next-generation bio-products sowing the seeds of success for sustainable agriculture. *Agronomy* 3, 648–656. doi: 10.3390/agronomy3040648

Besnard, G., Khadari, B., Navascués, M., Fernández-Mazuecos, M., El Bakkali, A., Arrigo, N., et al. (2013). The complex history of the olive tree: from late quaternary diversification of Mediterranean lineages to primary domestication in the northern Levant. *Proc. R. Soc. B Biol. Sci.* 280, 1471–2954. doi: 10.1098/rspb.2012.2833

Breton, C., Pinatel, C., Médail, F., Bonhomme, F., and Bervillé, A. (2008). Comparison between classical and Bayesian methods to investigate the history of olive cultivars using SSR-polymorphisms. *Plant Sci.* 175, 524–532. doi: 10.1016/j.plantsci.2008.05.025

Breton, C., Terral, J. F., Pinatel, C., Médail, F., Bonhomme, F., and Bervillé, A. (2009). The origins of the domestication of the olive tree. *C. R. Biol.* 332, 1059–1064. doi: 10.1016/j.crvi.2009.08.001

Bulgarelli, D., Schlaeppi, K., Spaepen, S., van Themaat, E. V. L., and Schulze-Lefert, P. (2013). Structure and functions of the bacterial microbiota of plants. *Annu. Rev. Plant Biol.* 64, 807–838. doi: 10.1146/annurev-arplant-050312-120106

Caporaso, J. G., Lauber, C. L., Walters, W. A., Berg-Lyons, D., Huntley, J., Fierer, N., et al. (2012). Ultra-high-throughput microbial community analysis on the Illumina HiSeq and MiSeq platforms. *ISME J.* 6, 1621–1624. doi: 10.1038/ismej.2012.8

DeSantis, T. Z., Hugenholtz, P., Larsen, N., Rojas, M., Brodie, E. L., Keller, K., et al. (2006). Greengenes, a chimera checked 16S rRNA gene database and workbench compatible with ARB. *Appl. Environ. Microbiol.* 72, 5069–5072. doi: 10.1128/AEM.03006-05

Díaz, A., Rosa, R., Martín, A., and Rallo, P. (2006). Development, characterization and inheritance of new microsatellites in olive (*Olea europaea* L.) and evaluation of their usefulness in cultivar identification and genetic relationship studies. *Tree Genet. Genomes* 2, 165–175. doi: 10.1007/s11295-006-0041-5

Díez, C. M., Trujillo, I., Barrio, E., Belaj, A., Barranco, D., and Rallo, L. (2011). Centennial olive trees as a reservoir of genetic diversity. *Ann. Bot.* 108, 797–807. doi: 10.1093/aob/mcr194

Edgar, R. C. (2010). Search and clustering orders of magnitude faster than BLAST. *Bioinformatics* 26, 2460–2461. doi: 10.1093/bioinformatics/btq461

Edgar, R. C., Haas, B. J., Clemente, J. C., Quince, C., and Knight, R. (2011). UCHIME improves sensitivity and speed of chimera detection. *Bioinformatics* 27, 2194–2200. doi: 10.1093/bioinformatics/btr381

El Fantroussi, S., Verschuere, L., Verstraete, W., and Top, E. M. (1999). Effect of phenylurea herbicides on soil microbial communities estimated by analysis of 16S rRNA gene fingerprints and community level physiological profiles. *Appl. Environ. Microbiol.* 65, 982–988.

Emmert, E. A., and Handelsman, J. (1999). Biocontrol of plant disease: a (gram-) positive perspective. *FEMS Microbiol. Lett.* 171, 1–9. doi: 10.1111/j.1574-6968.1999.tb13405.x

Finkel, O. M., Burch, A. Y., Lindow, S. E., Post, A. F., and Belkin, S. (2011). Geographical location determines the population structure in phyllosphere microbial communities of a salt-excreting desert tree. *Appl. Environ. Microbiol.* 77, 7647–7655. doi: 10.1128/AEM.05565-11

FAOSTAT. (2014). *Agricultural Production Database*. Available at: http://faostat3.fao.org (accessed October 23, 2014).

Green, P. S. (2002). A revision of *Olea* L. (Oleaceae). *Kew Bull.* 57, 91–140. doi: 10.2307/4110824

Hallmann, J., Quadt-Hallmann, A., Mahaffee, W., and Kloepper, J. (1997). Bacterial endophytes in agricultural crops. *Can. J. Microbiol.* 43, 895–914. doi: 10.1139/m97-131

Haouane, H., El Bakkali, A., Moukhli, A., Tollon, C., Santoni, S., Oukabli, A., et al. (2011). Genetic structure and core collection of the World Olive Germplasm Bank of Marrakech: towards the optimized management and use of Mediterranean olive genetic resources. *Genetica* 139, 1083–1094. doi: 10.1007/s10709-011-9608-7

Hardoim, P. R., van Overbeek, L. S., and van Elsas, J. D. (2008). Properties of bacterial endophytes and their proposed role in plant growth. *Trends Microbiol.* 16, 463–471. doi: 10.1016/j.tim.2008.07.008

Jiménez-Díaz, R. M., Olivares-García, C., Landa, B. B., del Mar Jiménez-Gasco, M., and Navas-Cortés, J. (2011). Region-wide analysis of genetic diversity in *Verticillium dahliae* populations infecting olive in southern Spain and agricultural factors influencing the distribution and prevalence of vegetative compatibility groups and pathotypes. *Phytopathology* 101, 304–315. doi: 10.1094/PHYTO-07-10-0176

Kloepper, J. W., Ryu, C.-M., and Zhang, S. (2004). Induced systemic resistance and promotion of plant growth by *Bacillus* spp. *Phytopathology* 94, 1259–1266. doi: 10.1094/PHYTO.2004.94.11.1259

Knief, C., Delmotte, N., Chaffron, S., Stark, M., Innerebner, G., Wassmann, R., et al. (2012). Metaproteogenomic analysis of microbial communities in the phyllosphere and rhizosphere of rice. *ISME J.* 6, 1378–1390. doi: 10.1038/ismej.2011.192

López-Escudero, F. J., and Mercado-Blanco, J. (2011). *Verticillium* wilt of olive: a case study to implement an integrated strategy to control a soil-borne pathogen. *Plant Soil* 344, 1–50. doi: 10.1007/s11104-010-0629-2

Lozupone, C., and Knight, R. (2005). UniFrac: a new phylogenetic method for comparing microbial communities. *Appl. Environ. Microbiol.* 71, 8228–8235. doi: 10.1128/AEM.71.12.8228-8235.2005

Lumaret, R., and Quazzani, N. (2001). Ancient wild olives in Mediterranean forests. *Nature* 413, 700. doi: 10.1038/35099680

Ma, B., Lv, X., Warren, A., and Gong, J. (2013). Shifts in diversity and community structure of endophytic bacteria and archaea across root, stem and leaf tissues in the common reed, *Phragmites australis*, along a salinity gradient in a marine tidal wetland of northern China. *Antonie Van Leeuwenhoek* 104, 759–768. doi: 10.1007/s10482-013-9984-3

Magoc, T., and Salzberg, S. (2011). FLASH: fast length adjustment of short reads to improve genome assemblies. *Bioinformatics* 27, 2957–2963. doi: 10.1093/bioinformatics/btr507

Maldonado-González, M. M., Prieto, P., Ramos, C., and Mercado-Blanco, J. (2013). From the root to the stem: interaction between the biocontrol root endophyte *Pseudomonas fluorescens* PICF7 and the pathogen *Pseudomonas savastanoi* NCPPB 3335 in olive knots. *Microb. Biotechnol.* 6, 275–287. doi: 10.1111/1751-7915.12036

Maldonado-González, M. M., Schilirò, E., Prieto, P., and Mercado-Blanco, J. (2015). Endophytic colonization and biocontrol performance of *Pseudomonas fluorescens* PICF7 in olive (*Olea europaea* L.) are determined neither by pyoverdine production nor swimming motility. *Environ. Microbiol.* doi: 10.1111/1462-2920.12725 [Epub ahead of print].

Marten, P., Smalla, K., and Berg, G. (2000). Genotypic and phenotypic differentiation of an antifungal biocontrol strain belonging to *Bacillus subtilis*. *J. Appl. Microbiol.* 89, 463–471. doi: 10.1046/j.1365-2672.2000.01136.x

Mercado-Blanco, J., Rodríguez-Jurado, D., Hervás, A., and Jiménez-Díaz, R. M. (2004). Suppression of *Verticillium* wilt in olive planting stocks by root-associated fluorescent *Pseudomonas* spp. *Biol. Control* 30, 474–486. doi: 10.1016/j.biocontrol.2004.02.002

Oliveira, M. N., Santos, T. M., Vale, H. M., Delvaux, J. C., Cordero, A. P., Ferreira, A. B., et al. (2013). Endophytic microbial diversity in coffee cherries of *Coffea arabica* from southeastern Brazil. *Can. J. Microbiol.* 59, 221–230. doi: 10.1139/cjm-2012-0674

Palomares-Rius, J. E., Castillo, P., Montes-Borrego, M., Müller, H., and Landa, B. B. (2012). Nematode community populations in the rhizosphere of cultivated olive differs according to the plant genotype. *Soil Biol. Biochem.* 45, 168–171. doi: 10.1016/j.soilbio.2011.11.009

Prieto, P., and Mercado-Blanco, J. (2008). Endophytic colonization of olive roots by the biocontrol strain *Pseudomonas fluorescens* PICF7. *FEMS Microbiol. Ecol.* 64, 297–306. doi: 10.1111/j.1574-6941.2008.00450.x

Prieto, P., Navarro-Raya, C., Valverde-Corredor, A., Amyotte, S. G., Dobinson, K. F., and Mercado-Blanco, J. (2009). Colonization process of olive tissues by *Verticillium dahliae* and its in planta interaction with the biocontrol root endophyte *Pseudomonas fluorescens* PICF7. *Microb. Biotechnol.* 2, 499–511. doi: 10.1111/j.1751-7915.2009.00105.x

Probst, A. J., Auerbach, A. K., and Moissl-Eichinger, C. (2013). Archaea on human skin. *PLoS ONE* 8:e65388. doi: 10.1371/journal.pone.0065388

Pruesse, E., Peplies, J., and Glöckner, F. O. (2012). SINA: accurate high-throughput multiple sequence alignment of ribosomal RNA genes. *Bioinformatics* 28, 1823–1829. doi: 10.1093/bioinformatics/bts252

Raskin, L., Stromley, J. M., Rittmann, B. E., and Stahl, D. A. (1994). Group-specific 16S rRNA hybridization probes to describe natural communities of methanogens. *Appl. Environ. Microbiol.* 60, 1232–1240.

Redford, A. J., Bowers, R. M., Knight, R., Linhart, Y., and Fierer, N. (2010). The ecology of the phyllosphere: geographic and phylogenetic variability in the distribution of bacteria on tree leaves. *Environ. Microbiol.* 12, 2885–2893. doi: 10.1111/j.1462-2920.2010.02258.x

Reinhold-Hurek, B., and Hurek, T. (2011). Living inside plants: bacterial endophytes. *Curr. Opin. Plant Biol.* 14, 435–443. doi: 10.1016/j.pbi.2011.04.004

Rosenblueth, M., and Martínez-Romero, E. (2006). Bacterial endophytes and their interactions with hosts. *Mol. Plant Microbe Interact.* 19, 827–837. doi: 10.1094/MPMI-19-0827

Ryan, R. P., Germaine, K., Franks, A., Ryan, D. J., and Dowling, D. N. (2008). Bacterial endophytes: recent developments and applications. *FEMS Microbiol. Lett.* 278, 1–9. doi: 10.1111/j.1574-6968.2007.00918.x

Sanchez-Azofeifa, A., Oki, Y., Fernandes, G., Ball, R. A., and Gamon, J. (2012). Relationships between endophyte diversity and leaf optical properties. *Trees* 26, 291–299. doi: 10.1007/s00468-011-0591-5

Wang, Q., Garrity, G. M., Tiedje, J. M., and Cole, J. R. (2007). Naïve Bayesian classifier for rapid assignment of rRNA sequences into the new bacterial taxonomy. *Appl. Environ. Microbiol.* 73, 5261–5267. doi: 10.1128/AEM.00062-07

Zohary, D., and Spiegel-Roy, P. (1975). Beginnings of fruit growing in the old world. *Science* 31, 319–327. doi: 10.1126/science.187.4174.319

Conflict of Interest Statement: The authors declare that the research was conducted in the absence of any commercial or financial relationships that could be construed as a potential conflict of interest.

Received: 17 November 2014; accepted: 05 February 2015; published online: 03 March 2015.

Citation: Müller H, Berg C, Landa BB, Auerbach A, Moissl-Eichinger C and Berg G (2015) Plant genotype-specific archaeal and bacterial endophytes but similar Bacillus antagonists colonize Mediterranean olive trees. Front. Microbiol. ***6****:138. doi: 10.3389/fmicb.2015.00138*

This article was submitted to Plant-Microbe Interaction, a section of the journal Frontiers in Microbiology.

frontiers in Microbiology

ORIGINAL RESEARCH
published: 19 May 2015
doi: 10.3389/fmicb.2015.00427

Seasonal variation of bacterial endophytes in urban trees

Shu Yi Shen and Roberta Fulthorpe *

Department of Physical and Environmental Sciences, University of Toronto Scarborough, Toronto, ON, Canada

Bacterial endophytes, non-pathogenic bacteria residing within plants, contribute to the growth and development of plants and their ability to adapt to adverse conditions. In order to fully exploit the capabilities of these bacteria, it is necessary to understand the extent to which endophytic communities vary between species and over time. The endophytes of *Acer negundo*, *Ulmus pumila,* and *Ulmus parvifolia* were sampled over three seasons and analyzed using culture dependent and independent methods (culture on two media, terminal restriction fragment length polymorphism, and tagged pyrosequencing of 16S ribosomal amplicons). The majority of culturable endophytes isolated were Actinobacteria, and all the samples harbored *Bacillus*, *Curtobacterium, Frigoribacterium, Methylobacterium, Paenibacilllus,* and *Sphingomonas* species. Regardless of culture medium used, only the culturable communities obtained in the winter for *A. negundo* could be distinguished from those of *Ulmus* spp. In contrast, the nonculturable communities were dominated by Proteobacteria and Actinobacteria, particularly *Erwinia, Ralstonia,* and *Sanguibacter* spp. The presence and abundance of various bacterial classes and phyla changed with the changing seasons. Multivariate analysis on the culture independent data revealed significant community differences between the endophytic communities of *A. negundo* and *Ulmus* spp., but overall season was the main determinant of endophytic community structure. This study suggests studies on endophytic populations of urban trees should expect to find significant seasonal and species-specific community differences and sampling should proceed accordingly.

Keywords: bacterial endophytes, endophytes, seasonal variation, species variation, trees

OPEN ACCESS

Edited by:
Mysore V. Tejesvi, University of Oulu, Finland

Reviewed by:
Scott Clingenpeel, Department of Energy Joint Genome Institute, USA
Andrea Campisano, Fondazione Edmund Mach, Italy
Carolin Frank, University of California, Merced, USA

***Correspondence:**
Roberta Fulthorpe, Fulthorpe Laboratory, Department of Physical and Environmental Sciences, University of Toronto Scarborough, 1265 Military Trail, Toronto, ON M1C 1A4, Canada
fulthorpe@utsc.utoronto.ca

Specialty section:
This article was submitted to Plant-Microbe Interaction, a section of the journal Frontiers in Microbiology

Received: *17 November 2014*
Accepted: *22 April 2015*
Published: *19 May 2015*

Citation:
Shen SY and Fulthorpe R (2015) Seasonal variation of bacterial endophytes in urban trees. Front. Microbiol. 6:427. doi: 10.3389/fmicb.2015.00427

Introduction

Bacterial endophytes are bacteria extracted from healthy looking, surface-sterilized plants (Hallmann et al., 1997). These bacteria can offer advantages to their hosts such as increasing nutrient acquisition including non-nodular nitrogen fixation, growth and development promotion through mechanisms such as production of growth factors, stress tolerance, pathogen and disease resistance, and contaminant degradation (Cook et al., 1995; Adhikari et al., 2001; Strobel et al., 2004; Moore et al., 2006; Ryan et al., 2008; Doty et al., 2009). The early literature on bacterial endophytes was dominated by studies on plants of agricultural importance such as rice (Sun et al., 2008), wheat (Conn and Franco, 2004), soybeans (Okubo et al., 2009), corn (Figueiredo et al., 2009), and potatoes (Garbeva et al., 2001). While agricultural species are still the main focus, a great deal of work on the endophytes of trees has been carried out, primarily because of the importance of trees for the production of biomass for biofuels and to phytoremediation efforts.

Because of their importance to both enterprises, *Populus* species have been heavily researched at the "microbiome" level (Hacquard and Schadt, 2015). Draft genomes have been prepared for several *P. deltoides* endophytes (Brown et al., 2012). In this group genetic markers indicative of plant senstive quorum sensing have been found (Schaefer et al., 2013). Taghavi et al. (2009) isolated 78 strains from poplar and willow trees, and sequenced four for genome characterization and gfp labeling—finding an *Enterobacter* sp st 638 that enhanced the growth of hybrid poplar cuttings. The fixation of nitrogen appears to be a common trait in endophytes. Doty et al. (2009) found numerous diazotrophic endophytes in *Populus trichocarpa* and *Salix sitchensis*. A diazotrophic and IAA producing *Burkholderia vietnamiensis* strain was isolated in *P. trichocarpa* (cottonwood), and its inoculation into Kentucky Bluegrass enhanced the grasses' nitrogen content and growth (Xin et al., 2009). More recently inocula derived from nutrient stressed poplar were shown to promote growth through N fixation (Knoth et al., 2014). Lodgepole pine seedlings (*Pinus contortia*) led to the isolation of *Paenibacillus polymyxa P32b-2R* that can fix nitrogen in pine and also western red cedar (Anand and Chanway, 2013; Anand et al., 2013). Other plant growth enhancing traits have been documented in poplar and other trees. Endophyte community structure seems to affect the ease of cultivation of *Prunus avium* (sweet cherry) cultivars (Quambusch et al., 2014). Mediterranean pines were found to harbor obligatory *Enterobacter cloacae*- some strains of which could produce indole-3-acetic acid (IAA) in lab culture (Madmony et al., 2005). Large portions of representative strains isolated from *P. euphratica* could enhance wheat germination under salt stress (Ju et al., 2014).

Endophytes that can assist plant growth on contaminated sites and that can contribute to the degradation of specific pollutants have been isolated from trees. The endosphere of *Acer pseudoplatanus* growing at a TNT contaminated site has yielded a consortium of strains (*Pseudomonas*, *Stenotrophomonas chelatiphaga,* and *Variovorax ginsengisol*a) that can detoxify TNT and promote growth of bent grass (*Agrostis capillaris*) (Thijs et al., 2014). *Enterobacter* sp st. PDN3 was isolated from hybrid poplar and shown to reduce TCE in the lab without any inducing substrate (Kang et al., 2012). van Aken et al. (2004) found a methane degrading methylobacterium (*Methylobacterum populi* sp. Strain BJ00) in hybrid poplar. Studies have shown that trees can act as hosts of degradative endophytes and/or degradative genetic material derived from elsewhere. The endophyte *Pseudomonas* sp. strain PD1 reduces phenanthrene toxicity via its degradation when inoculated into willows and grasses (Khan et al., 2014). Inoculation of poplar with *B. fungorum* DBT1 enhanced tolerance of the trees to PAH's (Andreolli et al., 2013). TCE remediation was enhanced in poplar by inoculation with *P. putida* W619-TCE, carrying a transferable plasmid that could move TCE metabolic activity to the endogenous endophytic population (Weyens et al., 2009). Taghavi et al. (2005) described the horizontal gene transfer of an introduced toluene degradation plasmid (pTOM-Bu61) amongst endophytic bacteria in a poplar strain, in both the presence and absence of toluene.

We were interested in looking for endophytic contributions to hydrocarbon degradation at a contaminated site in Toronto. Early reconnaissance of the site revealed the presence of numerous tree species and so we were first faced with practical questions such as how many tree species to investigate, how many individuals, and with what level of replication, and how often? But knowledge gaps exist in our understanding of the degree of host specificity found in endophytes—do plant species harbor specific endophytes, or can they act as hosts to any endophytic bacteria? How much do endophytic communities change over time? Studies on the determinants of endophyte community structure have focused typically on non-woody, agricultural plants and most of these involved the use of culture dependent methods (Adams and Kloepper, 2002; Kuklinsky-Sobral et al., 2004). Significant differences have been found in the endophytic community of different crop cultivars (van Overbeek and van Elsas, 2008; Manter et al., 2010). The diversity of bacteria in the grape endosphere has been shown to be highly dependent on season (Baldan et al., 2014; Bulgari et al., 2014), as have those of elm (Mocali et al., 2003). Contradicting results have been found by different authors, but these results were dependent on the methods used to analyze the communities. Izumi et al. (2008) found no difference in the endophytic communities of pine, birch and rowan trees in a European forest, although DGGE analysis was used that may have included organelle contamination (Izumi et al., 2008). By contrast, Ulrich et al. (2008) detected differences between the endophytic communities of poplar clones. Carrell and Frank (2014) found that pine and spruce species in the same nutrient limited environment had species specific endophytes communities, but nonetheless shared a dominant diazotrophic *Gluconacetobacter* species.

We undertook a characterization of the sources of variation in the endophytic communities of three tree species (*Acer negundo*, *Ulmus parvifolia,* and *Ulmus pumila*) growing at a hydrocarbon contaminated site. We do not report on the degradative or other functional traits of the endophytes here, but rather indicate the relative importance of species and season to endophyte community structure. This knowledge is key to (1) the design of good sampling strategies, (2) the prediction of the fate of introduced endophytes to different species, and (3) assess the fate of genetic material that may be expected to transfer into a dynamic community structure. To this end we used both culture dependent and independent methods.

Materials and Methods

Sample Collection and Surface Sterilization

Three branches from three individuals of each tree species—*A. negundo* (Manitoba Maple), *U. parvifolia* (Chinese Elm), and *U. pumila* (Siberian Elm) were collected in three seasons from an abandoned hydrocarbon contaminated site in Toronto, Ontario, Canada (43° 22′ 38″ N, 79° 18′ 34″ N). Samples were collected in February, July and October 2012, representing the seasons Winter, Summer and Fall, respectively. At the time of sampling, the outside temperature was as follows: Winter: −2°C, Summer: 22°C, and Fall: 11°C. Branches of roughly 1.5–2.0 cm in diameter were collected and the leaves and smaller branches were removed.

The branches were subjected to a detergent wash, rinsed in tap and distilled water before being cut into sections ~ 9 cm in length. They were surface sterilized through successive washes in 70% ethanol, 0.1% Tween 20, and 1.5% bleach solutions. The sections were rinsed three times with sterile distilled water to remove any residual bleach. The effectiveness of the surface sterilization was assessed by spread plating the final water wash and imprinting the washed samples onto agar plates.

Culturable Endophyte Extraction, Isolation, and Identification

Isolation of Endophytes

The periderm of the sterilized branches was removed before the tissue was preweighed in a sterile tube, then homogenized in a sterilized Waring Blender jar at 20,000 rpm with 60 mL of 50 mM Tris-HCl solution for 1 min. The homogenized plant tissue was filtered through 8 layers of sterile cheesecloth and the liquid macerate was collected. The macerate was centrifuged at 600 g for 5 min to pellet plant tissue and the supernatant was centrifuged at 10,000 g for 10 mins to pellet the bacterial cells. The bacterial cells were resuspended in 1 mL of 50 mM Tris-HCl solution, and 100 μL was spread plated onto replicate Reasoner's 2A (R2A, Sigma-Aldrich Canada Co.) and Tryptic Soy Agar (TSA) media plates. The remainder of the macerate, including plant tissue, was used for DNA extraction. The media plates were incubated at 28°C for a period of 7 days to 1 month. For each branch processed, colony types were categorized by color/colony morphologies—each type was counted and a representative was taken for purification and identification.

Identification of Isolates

Lysates were created from colonies of isolates by boiling. Approximately 2 uL of fresh (1–2 day old) colony material was added to 100 μL of sterile distilled water and boiled for 5 min. For each isolate, one microliter of the boiled lysate was used as a template for amplification of ribosomal 16S gene fragments (16S rRNA) using primers 27F (5′- AGAGTTTGA TYMTGGCTCAG -3′) and 1492R (5′-TACCTTGTTACGACT T-3′). The PCR amplifications were carried out in a PTC-200 thermal cycler (MJ Research Inc.) with the following conditions: initial denaturation at 95°C for 5 min followed by 35 cycles of: denaturation at 95°C for 1 min, annealing at 56°C for 1 min and extension at 72°C for 1 min; final extension at 72°C for 10 mins. The amplicons were PCR purified using the GenElute PCR cleanup kit (Sigma-Aldrich Canada Co.) and sent to The Centre for Applied Genomics (TCAG,Toronto, Canada) for Sanger sequencing. The obtained sequences were submitted to the RDP database and BLAST (NCBI) in order to determine the potential identity of the bacteria based on minimum 99% similarity to database 16S rRNA sequences.

Culture Independent Endophyte Community Extraction and Analysis

DNA Extraction of Endophytic Community

Plant macerates were used to extract total tissue DNA using the FastDNA SPIN Kit (MP Biomedicals) following manufacturer's instructions with a couple of modifications. The modifications included the addition of 100 μL of protein precipitation solution (PPS) solution into the lysing tube and 2 additional SEW-SM washes.

Enzymatic Digestion, DGGE, PCR Amplification, and T-RFLP Analysis

Direct amplification of plant DNA tissue using universal bacteria primers produced amplicons dominated by plant organelle sequences (plastids and mitochondria). The primers 799F (5′-AACMGGATTAGATACCCKG-3′: Chelius and Triplett, 2001) and 783R (Sakai et al., 2004–an equimolar mixture of 783R-a (5′-CTACCAGGGTATCTAATCCTG-3′), 783R-b 5′-CTACCG GGGTATCTAATCCCG-3′), and 783R-c (5′-CTACCCGGGTAT CTAATCCGG-3′), have been offered as a means of excluding plastids and mitochondria. Through preliminary testing we have found the effectiveness of 799F primer is dependent on the genotype of the plant and resulted in very minimal amplification of the bacterial sequences in our plant samples. This is similar to what has been previously found by Rasche et al. (2006) in their study of sweet pepper shoots. For this reason, an enzymatic digestion protocol was developed to try to bypass the problem of plastid contamination. Based on the fact that chloroplast 16S rRNA sequences have a *Pvu*II restriction site downstream of the binding site of 27F primer and a *Msc*I restriction site upstream of the binding site of 1492R primer, predigesting genomic DNA with those restriction enzymes should inhibit the amplification of plastid products from 27F to 1492R, allowing only the amplification of bacterial 16S rRNA and its subsequent analysis by molecular methods.

This method was initially tested on a couple of samples using DGGE as a preliminary visualization tool to determine how effective the method was. Using the previously extracted DNA from *A. negundo*, *U. parvifolia,* and *U. pumila* from Summer 2012, DNA from each sample was digested with the *Pvu*II and *Msc*I (NEB Canada). The samples were digested for 3 h at 37°C, followed by incubation at 80°C for 20 min to inactivate the enzymes. One microliter of the digested products was used as template for PCR reactions using primers 27F and 1492R following the previously mentioned conditions. The PCR products were visualized in 1.5% agarose gels and bands of 1500 bp in size were excised and gel purified with QIAEX II Gel Extraction Kits (Qiagen, Canada).

The gel-purified products were used as templates for the following PCR reaction using primers341F-GC (5′- CGCCCGC CGCGCGCGGCGGGCGGGGCGGGGGCACGGGGGGCCTA CGGGAGGCAGCAG-3′) and MOD783R (equimolar concentrations of primer 783RA and primer 783RC- a modification of primers by Sakai et al., 2004). For the amplification, 20 μL PCR reactions were carried out in a PTC-200 thermal cycler (MJ Research Inc.) with the following conditions: initial denaturing at 95°C for 5 min followed by 35 cycles of: denaturing at 95°C for 1 min, annealing at 56°C for 1 min and extension at 72°C for 1 min; final extension at 72°C for 10 mins. The PCR products were checked on 1% agarose gels before the remainder of the PCR products was run in a DGGE gel. The DGGE ge lwas gel was a 6% polyacrylamide gel consisting of a 40–70% denaturing solution gradient and it

was run in a DGGE-2001 Tank (C.B.S. Scientific Co, Del Mar, California) with 0.5 X Tris-acetate-EDTA buffer, for 20 h at 70V and 58°C. The gel was stained in ethidium bromide for 30 min before it was visualized under UV light.

Once the enzymatic predigestion was tested, subsequently for each sample, up to 1 μg genomic DNA was digested using 1U each of restriction enzymes *Pvu*II and *Msc*I for 16 h at 37°C. The digested genomic DNA was used as template for the 16S rRNA PCR reaction using a forward primer labeled with 5′-fluorescein amidite dye (27F-FAM from LifeTechnologies, Canada) and a reverse primer labeled with 5′–hexachlorofluorescein dye (1492R-Hex from LifeTechnologies, Canada). The PCR reactions were carried out in 20 μL reaction volumes following the previously mentioned PCR conditions. For T-RFLP (terminal restriction fragment length polymorphism) analysis the amplicons were digested with 1 U *Msp*I restriction enzyme (Thermo Scientific) for 3 h at 37°C followed by inactivation through incubation at 80°C for 20 min. The digested PCR amplicons were sent to the Agriculture and Food Laboratory (AFL) at the University of Guelph for analysis. Only fragments between 60–1200 bp with fluorescence signals greater than 100 units were included in the output from AFL. The Microsoft Excel macro Treeflap (Rees et al., 2004) from http://urbanstreams.net/index.php/the-treeflap-macro/, was used to round the fragment sizes to the nearest base pair and align the fragments of the same size from different samples, generating a cohesive table of the different fragments sizes and their relative heights in each sample. Fragments in the dataset in the range of 335–338 and 400–403 bp were assumed to represent potential mitochondrial fragments and plastid fragments and omitted from the data. Fragments sizes that had less than 1% abundance or that appeared in less than three samples were removed to account for any background noise generated during the PCR reaction, sequencing artifacts or rare members of the communities.

Pyrosequencing and Analysis

For the pyrosequencing analysis of the culture independent community, equimolar subsets of the digested genomic DNA from the same plants and seasons were pooled together to create 9 plant/season samples. These 9 pools were submitted for 454 pyrosequencing using a Roche 454 FLX titanium instrument at MR DNA (Molecular Research LP) using barcoded facility primers 27Fmod (5′- AGRGTTTGATCMTGGCTCAG-3′) and 530R (5′- CCGCNGCNGCTGGCAC-3′). The data were analyzed using programs in the QIIME pipeline (Caporaso et al., 2010). Sequences with high error content were removed with Denoiser (Reeder and Knight, 2010), placed into OTU's of 97% similarity using UCLUST (Edgar, 2010) while omitting any reads belonging to mitochondria and chloroplast from the analysis. Sequences were rarified to 2000 per sample and the taxonomy was assigned through the use of the Greengenes Database (DeSantis et al., 2006) files from May 2013. The analysis of this data revealed that although this method allowed for the detection of bacterial species found in the samples, plastid 16S rRNA fragments were still amplified in the sample. We decided to try the plastid and mitochondrial oligonucleotide blockers designed by Lundberg et al. to inhibit the amplification of these organelle sequences in the sample (Lundberg et al., 2013). The blockers were used following their specifications. In brief, the oligonucleotide blockers were added to the PCR reaction at a final concentration of 0.5 μM, with primers 27F and 1492R. The PCR was carried out with the previously mentioned conditions with the addition step of 78°C for 30 s prior to the primer annealing step and the reaction was carried out for 25 cycles. The PCR amplicons were gel size selected (for ∼1500 bp) and purified with QIAEX II Gel Extraction Kits (Qiagen, Canada). The amplicons from the same plants and seasons were pooled together and submitted for 454 pyrosequencing using the same machine and primers previously mentioned. This data was analyzed using the same method previously mentioned with the sequences rarified to 10,000.

Community and Statistical Analysis

All of the community and statistical analyses were performed using packages in R 2.15.2 (R Core Team, 2012). The culturable community consisted of the bacteria isolated from the plant macerate and their respective abundances relative to the total amount of bacteria isolated from the same sample. Two communities were generated for each sample as the plant macerate was cultured on R2A and TSA media. The nonculturable community assessed through the use of T-RFLP, relied on the phylotypes in the form of different terminal fragment (T-RFs) detected by the autosequencer and their respective abundance in the sample. The species richness and the species diversity, based on the Shannon index, were determined for each sample. The homoscedascity and the normality of each variable was checked through the use of Levene's test and Shapiro's test (lawstat package, Noguchi et al., 2009). If the data were determined to be homogeneous and normally distributed, ANOVA (analysis of variation) tests were conducted. In the cases where the data were not homogeneous and/or normally distributed after transformation, Kruskal-Wallis tests were conducted. The culturable and nonculturable endophytic community compositions were compared between the different tree species and seasons by using Bray-Curtis dissimilarity matrices, non-metric multidimensional scaling (NMDS, ecodist package, Goslee and Urban, 2007) analysis and permutation multivariate analysis of variance (ADONIS) using functions found in the vegan package (Oksanen et al., 2012). ADONIS analyses were run with 1000 permutations.

Results

Culturable Isolates and Community Analysis

We used two different media to represent both low nutrient (R2A) and rich media (TSA) to allow for the detection of a wide variety of bacteria. Through the culturing of the plant macerates on the two media, the total amount of culturable bacteria obtained from each plant sample per season ranged from 10^3 to 10^7 colony-forming units (cfu) per gram of fresh tissue. There were significantly higher total counts in all species in the Fall compared to the other seasons ($p < 0.05$). However, neither total bacterial counts, species richness, nor species

diversities (Shannon Index) were different between media types (**Supplementary Figure 1**).

A total of 31 different bacterial genera were cultured using the two media from all plant samples combined as shown in **Table 1**. *Variovorax* spp. and *Amnibacterium* spp. could only be isolated from *A. negundo* while *Rhizobium* spp. and *Rathayibacter* spp. were only isolated from *U. parvifolia*. Some bacterial genera were isolated from all the plant species, throughout all 3 seasons: *Bacillus* spp., *Curtobacterium* spp., *Frigoribacterium* spp. *Methylobacterium* spp., *Paenibacillus* spp., and *Sphingomonas* species. All of the genera identified belonged to one of the following phyla: Actinobacteria, Firmicutes, Bacteroidetes, Deinococcus-Thermus, and Proteobacteria. A breakdown of the relative abundances of the culturable endophytic isolates based on class per plant and season is shown in **Figure 1**. The majority of the isolates were from the phylum Actinobacteria, making up 62% and 63% of total bacterial isolated in R2A media and TSA media, respectively. Under the phylum Proteobacteria, bacteria specifically belonging to the class of Alphaproteobacteria, Betaproteobacteria and Gammaproteobacteria were found. Differences in the media used resulted in a higher percentage of Alphaproteobacteria isolated on R2A whereas a higher percentage of Gammaproteobacteria were isolated on TSA. It also made a difference in the actual isolates obtained as *Amnibacterium* spp., *Pseudoclavibacter* spp., and *Rhizobium* spp. were only cultured on TSA whereas *Deinococcus* spp., *Mesorhizobium* sp., and *Variovorax* spp. were only cultured on R2A. There were other noticeable changes in the cultured endophytes such as fewer Firmicutes and Gammaproteobacteria in the Summer and Fall relative to Winter samples, and an increase of Bacteroidetes bacteria cultured in the Fall. 16S sequence data for these isolates can be found in GenBank accessions KP889009-KP889059.

In addition to the bacteria that could be isolated and identified, there were a variety of bacteria that initially grew on the spread plates of the plant macerates but would not subsequently grow on subculture. These unidentified bacteria accounted for 6% and 13% of the total bacterial count isolated from R2A and TSA, respectively.

For both media, NMDS analysis resulted in visible clustering of *A. negundo* samples away from *U. parvifolia* and *U. pumila* samples in all seasons (**Supplementary Figure 2**). However ADONIS testing showed that only the Winter samples exhibited significant differences in the culturable community of *A. negundo* from *Ulmus* spp. (**Table 2**). The *U. parvifolia* community isolated in R2A media in each season was statistically different from the other seasons, whereas in TSA only the community in the Winter was statistically different from the other seasons. For *U. pumila* and *A. negundo* the Fall samples were found to be distinguishable from the other seasons.

TABLE 1 | Cumulative list of identified bacterial endophytes and their corresponding bacterial class, isolated from *A. negundo, U. parvifolia,* and *U. pumila* branches from Winter, Summer, and Fall.

Bacterial Class	Bacterial Genera	
Actinobacteria	*Agrococcus* sp. *Amnibacterium* sp.***T, A*** *Arthrobacter* sp. *Brevibacterium* sp. *Curtobacterium* sp. *Friedmanniella* spp. *Frigoribacterium* spp. *Geodermatophilus* sp. *Kineococcus* sp.	*Kocuria* sp. *Microbacterium* spp. *Nocardioides* sp. *Patulibacter* sp.* *Plantibacter* sp. *Pseudoclavibacter* spp.***T*** *Rathayibacter* sp.***B*** *Sanguibacter* spp.
Bacilli	*Bacillus* spp. *Paenibacillus* spp. *Staphylococcus* spp.	
Flavobacteriia	*Chryseobacterium* sp.	
Deinococci	*Deinococcus* sp.***R***	
Alphaproteobacteria	*Mesorhizobium* sp.***R*** *Methylobacterium* spp. *Paracoccus* sp. *Rhizobium* sp.***T, B*** *Sphingomonas* spp.	
Betaproteobacteria	*Variovorax* sp.***R, A***	
Gammaproteobacteria	*Pseudomonas* spp. *Stenotrophomonas* sp. *Xanthomonas* spp.	

Not previously mentioned in literature as endophyte.* ***T**, Isolated only from TSA media;* ***R****, Isolated only from R2A media;* ***A****, Isolated only from Acer negundo;* ***B****, Isolated only from Ulmus parvifolia.*

Culture-Independent Community Analysis

Use of Predigested DNA Samples for T-RFLP Community Analysis

Initial testing of the enzymatic predigestion of total DNA was originally conducted on extracted DNA from the three plant

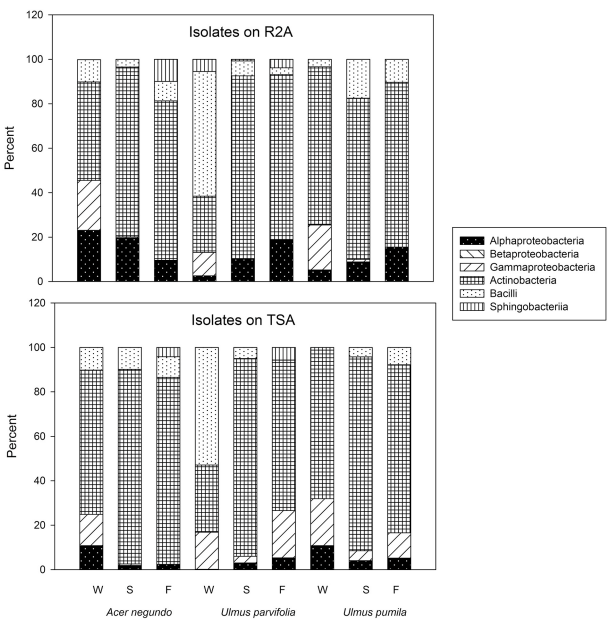

FIGURE 1 | Percent abundance of cultural bacteria in phyla/classes. W, Winter; S, Summer; F, Fall.

TABLE 2 | Results of ADONIS test run on endophytic communities obtained from culture based methods (R2A and TSA) and culture independent method (T-RFLP).

	Category	Subsequent testing	*p*-value	Distinguishable component
R2A	Season	*A. negundo*	0.001*	Fall
		U. parvifolia	0.001*	Winter, Summer Fall
		U. pumila	0.034*	Fall
	Plant	Winter	0.014*	*A. negundo*
		Summer	0.47	
		Fall	0.16	
TSA	Season	*A. negundo*	0.31	
		U. parvifolia	0.002*	Winter
		U. pumila	0.10	
	Plant	Winter	0.013*	*A. negundo*
		Summer	0.60	
		Fall	0.13	
TRFLP	Season	*A. negundo*	0.001*	Summer
		U. parvifolia	0.004*	Fall
		U. pumila	0.013*	Summer
	Plant	Winter	0.001*	*A. negundo*
		Summer	0.042*	*A. negundo*
		Fall	0.025*	*A. negundo*

*Testing of significant difference determined through the use of pairwise comparisons and bonferroni correction. * Significant p-values.*

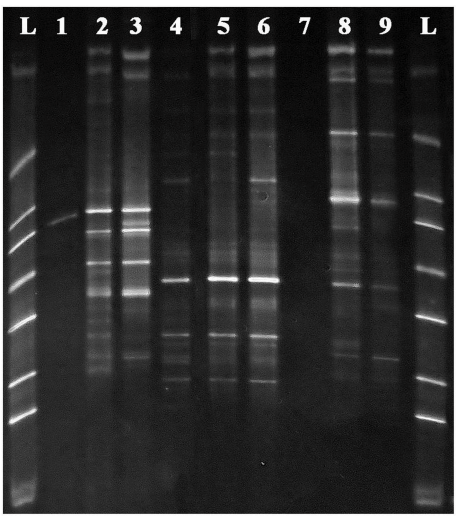

FIGURE 2 | DGGE gel of 341GC-MOD783R PCR amplifications on DNA samples from (1) original *Acer negundo* DNA, (2) *Msc*I digested *Acer negundo* DNA, (3) *Pvu*II digested *Acer negundo* DNA, (4) original *Ulmus parvifolia* DNA, (5) *Msc*I digested *Ulmus parvifolia* DNA, (6) *Pvu*II digested *Ulmus parvifolia* DNA, (7) original *Ulmus pumila* DNA, (8) *Msc*I digested *Ulmus pumila* DNA, (9) *Pvu*II digested *Ulmus pumila* genomic DNA and L–DGGE ladder. Note products are all bacterial due to use of 783 primer, but are not well amplified from undigested targets.

species examined in this study. The results of this testing are shown in **Figure 2**, which shows a DGGE analysis of the amplicons obtained from undigested original samples and those digested by either *Pvu*II or *Msc*I using the primers 341GC-MOD783R that do not target organelles. The figure demonstrates that bacterial fragment amplifications were poor prior to pre-digestion of the template, presumably because of organelle DNA dominance in the samples. The number of bacterial bands detected was either the same as the original undigested samples or in cases where there was minimal to no amplification, it improved the amplification of bacterial sequences present in the sample.

T-RFLP Community Analysis

The examination of the T-RFLP communities resulted in the detection of mean of 27 (+/- standard deviation of 14) phylotypes per sample. These phylotype numbers should be assumed to be underestimates or minimums, as the removal of small fragments and fragments with small peak heights might have deleted data on more than just artifacts. Data on phylotype richness and diversities are shown in **Supplementary Figure 3**. There were 5 phylotypes found to be common to all branches sampled. The sizes of the phylotypes were as follows: 61 bp, 119 bp, 128 bp, 488 bp, and 612 bp.

A. negundo samples had higher phytotype richness than *Ulmus* samples ($p < 0.05$). NMDS and ADONIS analysis of T-RFLP based community compositions showed that regardless of the season the samples were from, *A. negundo* samples were always statistically distinct from those of *U. parvifolia* and *U. pumila* (**Table 2**, **Figure 3**). However no significant differences were found between the communities of *U. parvifolia* and *U. pumila* samples in any season.

When grouped according to their plant species, the NMDS analyses showed that Summer samples typically clustered apart from those from Winter and Fall (**Supplementary Figure 4**). The ADONIS test showed that there was a significant difference between the community profiles of the samples collected in the Summer compared to those collected in Winter and Fall for the *A. negundo* and the *U. pumila* samples ($p < 0.05$). For *U. parvifolia*, it was found that the community profiles of the samples collected in the Fall were significantly different from those collected in Winter and Summer.

Pyrosequencing Data

The amount of reads that were obtained from the pyrosequencing of pooled samples varied between samples, as did the amount of reads that came from plant organelles. The latter averaged 41% when using predigested template DNA and 46% when using the blocker oligonucleotide method (**Table 3**). We attribute some sample to sample differences in the release of plastids from plant cells to seasonal differences in plant cell wall resistances in the extraction method. When sequences were grouped by phyla (class in case of proteobacteria), some differences between the two organelle avoiding techniques are seen (See **Figure 4**). Phylum/Proteobacterial Class assignments are highly correlated between the methods in seven of the 9 pooled samples analyzed,

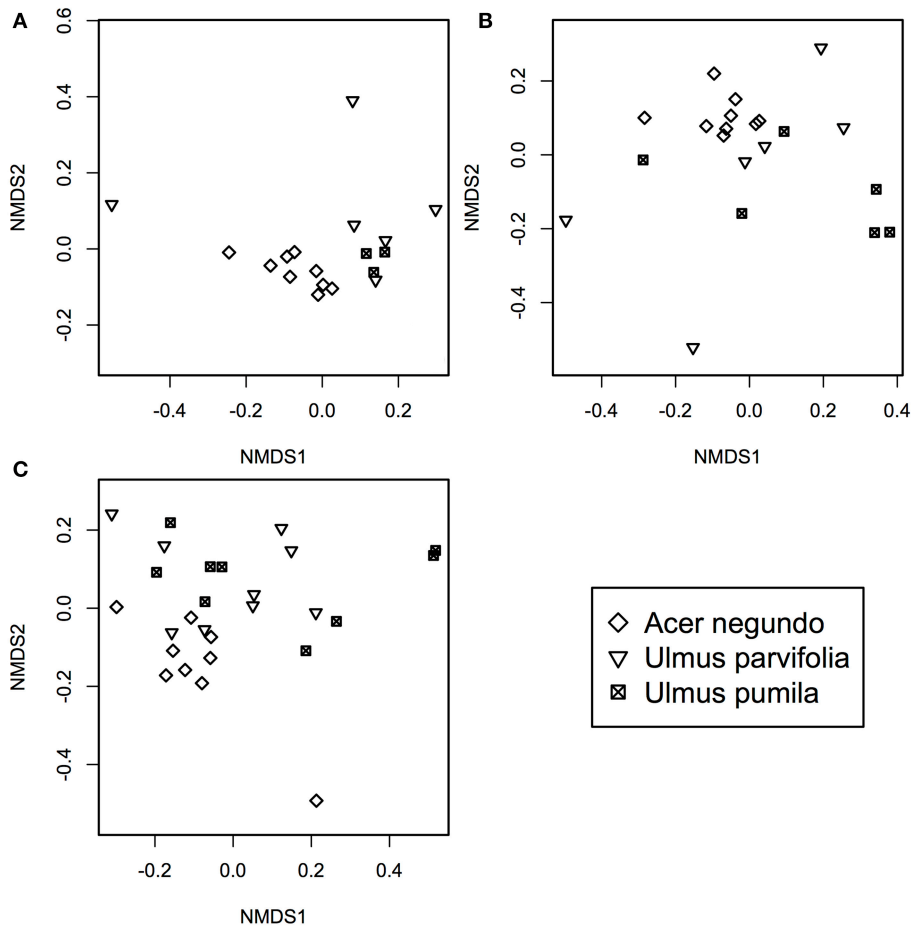

FIGURE 3 | NMDS plots of bacterial community profile of *A. negundo*, *U. parvifolia*, and *U. pumila* generated using T-RFLP community data converted to a Bray-Curtis dissimilarities matrices for (A) Winter 2012 (stress value = 0.05), (B) Summer 2012 (stress value = 0.04), and (C) Fall 2012 (stress value = 0.10).

but there is poor correlation in two of the pools. We did not obtain enough reads from the Fall *U. parvifolia* digested template to perform analyses (**Table 3**). Where the correlations were poor, it was largely due to differing relative abundances of the proteobacterial classes. Both methods clearly show however that the Summer samples see high levels of Actinobacteria, while the Fall and Winter samples are dominated by Proteobacteria. Data have been deposited in Genbank under SRA Study number SRP055785.

The dominant OTUs found for each plant species in each season are shown in **Figure 5**, along with their relative abundances. In this figure OTU's are named at the highest level of classification obtainable, at the genus level where possible, but at family or order where not. Of particular interest is the dominance of *Sanguibacter sp.* in all three species during the summer. When an *in silico* digest to mimic T-RFLP was carried out using a python script on the OTUs obtained from the pyrosequencing, there were some OTUs that matched the dominant T-RFLP phylotype fragments. These included OTUs that corresponded to bacteria from the order Rhizobiales (T-RFLP fragment 128 bp), and *Ralstonia* spp. (T-RFLP fragment 488 bp).

Discussion

It is clear from this work that the main determinant of the endophyte community structures in these tree species is the season. Our work involved the study of both culture dependent and independent methods and shows the latter to be more sensitive to seasonal differences (**Table 2**). Studies on the leaf phyllosphere of *Asclepias viridis* (Ding et al., 2013), the endophytes of maple tree sap (Filteau et al., 2010) and the buds of Scots pine trees (Pirttilä et al., 2005) have also noted a strong seasonal effect. The diversity of bacteria in the grape endosphere has been shown to be highly dependent on season (Baldan et al., 2014; Bulgari et al., 2014). In these studies, the research has involved the use of a variety of methods including T-RFLP for the study of the endophytes in leaves, PCR fingerprinting for the study of maple tree sap and 16S rRNA specific probes for the study of the buds of Scots. There is another study that has looked at variation of root and stems of 2 elm species (*U. japonica* and hybrid "Lobel",) which corroborates with our research (Mocali et al., 2003) even though it was entirely based on culturable endophytes.

TABLE 3 | Comparison of the 454 tagged pyrosequencing of the pooled samples from the same species and the same season, generated through either pre-digestion of the DNA using restriction enzymes (*Pvu*II and *Msc*I) or oligonucleotide blockers designed to inhibit the amplification of plastid and mitochondrial 16S rRNA.

Species	Season	Digest	Digest	Blocker	Blocker	Phyla
		Reads	%Org	Reads	%Org	Correlation
Acer negundo	W	32260	86.75	24090	67.25	0.99
	S	20959	2.05	19744	2.3	1.00
	F	11789	82.35	16821	68.3	0.95
Ulmus parvifolia	W	4520	17.9	14121	13.35	0.97
	S	4752	22.05	12535	22.15	0.44
	F	11	–	21735	79.25	NA
Ulmus pumila	W	4520	32.7	19486	64.4	0.07
	S	3987	36.35	14330	14.8	0.96
	F	2299	49.45	22677	83.65	0.88

The OTUs from both sample sets were rarified to 2000 when estimating organelle read content.

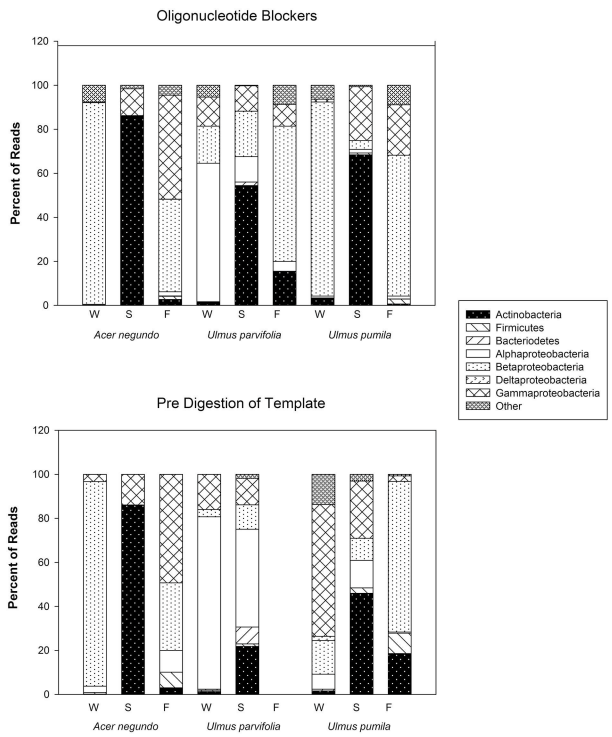

FIGURE 4 | Bacterial phyla, and class for Proteobacteria, and their relative abundances found in the amplicon sequences generated from pre-digested templates and from reactions involving the use of blocker oligonucleotides (see text).

Seasonal community changes could be due to temperature optima of the bacteria or the changing physiology of these temperate deciduous trees which reflects their respective growth phases and external temperatures (Jansson and Douglas, 2007). Changes in the concentrations of soluble sugars, proteins, amino acids, organic acids, and other nutrients in the plant will affect the community (Cox and Stushnoff, 2001; Li et al., 2004; Renaut et al., 2005). Similarly, the carbon source in different plant species varies in the form of different nonreducing sugars, oligosaccharides, sugar alcohols, starch, and other polysaccharides that are present (Bloom et al., 1985). This would explain why after season, the tree genus impacts strongest on the endophytic community. It has also been suggested that the plant host plays an active role in the colonization of the endophytes by attracting specific bacteria, through the release of certain compounds via their roots (de Weert et al., 2002; Compant et al., 2005), or by enhancing or diminishing their colonization in the plant, through plant defense response and generation of phytohormones (Miché et al., 2006; Shah, 2009).

The effect of the tree genus on the endophytic community was clearly seen in the T-RFLP analysis of the endophytic community, but not in the culture collection. This reflects the drawbacks of the culture dependent method where bacteria do not all necessarily grow in the same type of media and a wide variety of them cannot be further isolated and purified. This might be why Izumi et al. (2008) did not see any differences between endophytic communities of three quite different tree species, as their methods relied on incubating plant material in TSB before plating on TSA. However, using four different media, Moore et al. (2006) were able to detect differences in the endophytes of hybrid Poplar cultivars growing intermingled on the same site. They also noted that no genotype (as determined by BOX fingerprints) existed in more than one tree zone (i.e., roots, rhizosphere, stems, and leaves) suggesting strong niche specialization in these bacteria. This supports previous studies that involved studying agricultural plant endophytes using culturable methods, where the plant genotype and cultivar affected the colonization of endophytes, such as in cotton plants (Adams and Kloepper, 2002), soybean (Okubo et al., 2009), and peas (Elvira-Recuenco and van Vuurde, 2000).

Even though different communities were detected through the use of molecular methods, further analysis of the T-RFLP profiles of the endophytes communities revealed the presence of 5 phylotypes common to all branches sampled regardless of season and plant species. These T-RFs could potentially represent a core group of bacteria phylotypes at this site. Mengoni et al. (2009) noted a very small group of T-RFLP fragments were found common amongst highly variable leaf-associated communities within one species. Carrell and Frank (2014) found that pine and spruce species in the same nutrient limited environment had species specific endophytes communities, but nonetheless shared a dominant diazotrophic *Gluconacetobacter* species. This does support the notion of both specific endophyte-plant relationships coexisting with more generalist endophytes that might confer special adaptive traits to their plant hosts.

The shared phylotypes seen in our study were detected as terminal restriction fragments generated based on polymorphisms specific only to *Msp*I cut sites in bacterial 16S rRNA. As one fragment (phylotype) in a T-RFLP analysis can result from more than one bacterial species or genera, we

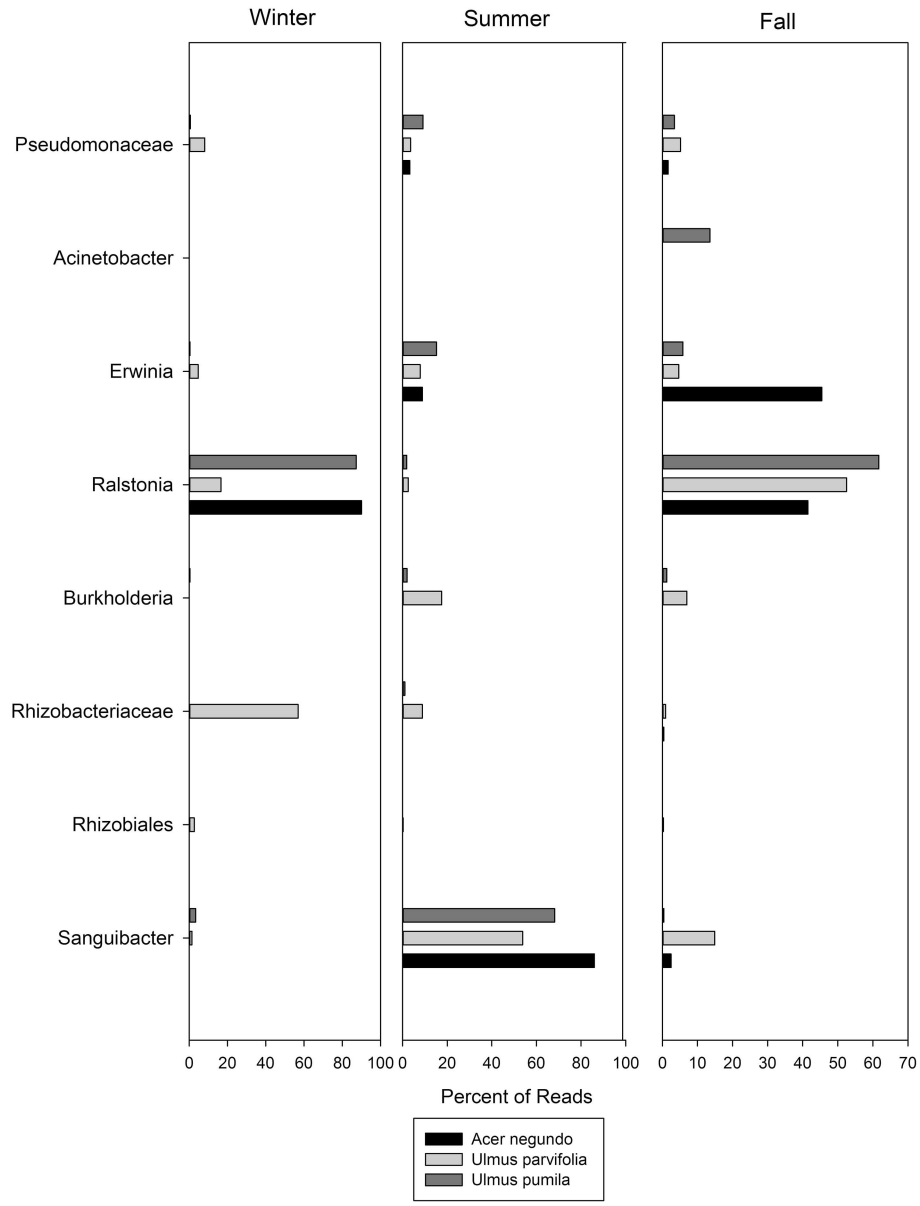

FIGURE 5 | The most abundant OTUs found in the pyrosequencing data along with their relative abundances through the seasons. Names are given for the closest level of classification available in database.

are likely underestimating diversity and also the number of possible shared bacterial genera (Abdo et al., 2006; Schütte et al., 2008). Based on the pyrosequencing data, these core bacterial phylotypes may correspond to *Pseudomonas* spp (although rare in the pyrosequence data), *Ralstonia* spp. and bacteria from the order Rhizobiales.

Culturing the endophytes on R2A and TSA resulted in the isolation of bacterial genera that have been previously been found in the internal tissues or phyllosphere of other crops and trees. In all the samples analyzed, the common presence of bacterial species from *Bacillus* spp., *Curtobacterium* spp., and *Sphingomonas* spp. was similar to for two elm species by Mocali et al. (2003). The majority of the identified cultured bacteria endophytes were classified under the phylum Actinobacteria, making up 62% and 63% of total bacterial isolated in R2A media and TSA media, respectively. The dominance of Actinobacteria has been previously seen in the study of endophytic communities including those of poplar trees (Ulrich et al., 2008), corn (Chelius and Triplett, 2001), wheat (Coombs and Franco, 2003), and *Arabidopsis thaliana* (Bulgarelli et al., 2012). Studies on Actinobacteria endophytes noted their roles as biological control agents (Coombs et al., 2004) and producers of novel natural products (Qin et al., 2012). In addition to these species we also isolated *Patulibacter* sp. which has been previously only been isolated from soil samples (Takahashi et al., 2006).

We were successful in revealing the dominant bacteria from these tree tissues by modifying our amplification procedures prior to pyrosequencing. Both the use of the predigested templates and organelle sequence blocking oligonucleotides were effective in yielding large numbers of bacterial reads. Pyrosequencing of amplicons from plant tissues without such template or primer modifications typically yields more than 90% organelle reads (Gottel et al., 2011; Lucero et al., 2011). However organelle reads were not eliminated by either method. For our predigestion method we speculate this was due to incomplete digestion caused by template abundance or methylation or perhaps to the amplification of organelle chimeras. In the case of the oligonucleotide blockers, their concentration might need optimization in the face of large amounts plant DNA. It is useful to note that the proportion of organelle sequences obtained by the two methods were significantly correlated ($r = 0.76$, $p < 0.05$), suggestive of a template effect (i.e., abundance of organelle targets). Nevertheless our work revealed the importance of some key genera to these trees.

The genus *Sanguibacter* was abundant in all three plant species in the Summer season. *Sanguibacter* is an Actinobacteria as were many of our isolates, but it did not appear in culture. Only two previous studies report *Sanguibacter* as an endophyte–Ulrich et al. (2008) cultured members of this genus from poplar trees and Mastretta et al. (2009) isolated some from seeds of *Nicotiana tabacum* growing at an industrial sewage sludge site. The *Sanguibacter* strain isolated from *N. tabacum* was found to be cadmium tolerant and when used to inoculate other *N. tabacum* plants exposed to different cadmium levels, it was found to increase the development of shoots and roots. Other than this, all *Sanguibacter* isolates have been reported from soils, sands, sediments or even blood and milk.

The pyrosequencing reads also revealed an abundance of Betaproteobacteria in the Winter and Fall samples with the majority of these OTUs corresponding to the genus *Ralstonia*. The *Ralstonia* genus is best known for including the wilt pathogen *R. solanacearum*, but our sequence data do not indicate that particular species was present. *Ralstonia* endophytes have been reported in grapevines (Campisano et al., 2014), in lettuce (Jackson et al., 2013) and in cowpea nodules (Sarr et al., 2010). The presence of the Gammaproteobacteria detected in the Summer and Fall corresponded to OTUs belonging to the genera *Erwinia* and unknown members of *Pseudomonaceae*. *Pseudomonas* spp. have been found to be make up the majority of genera analyzed in the maple sap microbiota (Mengoni et al., 2009) and also in the analysis of the poplar tree endophytes isolates (Moore et al., 2006). Some *Pseudomonas* are plant growth promoting strains (Kuklinsky-Sobral et al., 2004). However the role that each of these genera may play in the biology of these trees requires further research as ribosomal sequences can not reveal much about function, particularly where mobile elements might be involved.

Understanding the variation in the endophytic community allows for optimal sampling for the survey of endophytes and their capabilities in any vegetative community. The original choice of these trees for study was based on their location; they occupy an urban site contaminated by both petroleum and chlorinated solvents. However before investigating the potential role of these tree endophytes in any degradation of these organic contaminants, we needed to know how representative any isolated species might be. Now we know that the dominant strains can differ substantially over the seasons, and less so between species, we can better contextualize any beneficial functions these species might have. This study reveals that a better understanding of the potential role of *Sanguibacter* is warranted if we are to have insights into summer processes. Therefore it is necessary to study the endophytic communities of different types of plants through different seasons to fully appreciate the range of possible plant-endophyte interactions.

Acknowledgments

We are grateful for NSERC Discovery Grant support to RF.

Supplementary Material

The Supplementary Material for this article can be found online at: http://journal.frontiersin.org/article/10.3389/fmicb.2015.00427/abstract

Supplementary Figure 1 | Richness (number of species) and Shannon Diversity of culturable isolates obtained.

Supplementary Figure 2 | Visual analysis of the culturable bacterial community profiles collected from R2A and TSA media. Top plots: NMDS plot of the data obtained on R2A media, stress value = 0.343. Bottom plots: NMDS plot of data obtained on TSA media, stress = 0.350. Tree species symbols: ○– *Acer negundo*, Δ– *Ulmus parvifolia* and + – *Ulmus pumila*. Season symbols: square – Winter, inverted triangle Summer and cross in box Fall.

Supplementary Figure 3 | Average number of phylotypes detected and calculated Shannon phylotypes diversity indices according to terminal restriction fragments obtained with forward labeled fragments and reverse labeled fragments, for each tree species and season.

Supplementary Figure 4 | NMDS analysis of bacterial community profiles from the entire forward T-RFs dataset (stress value = 0.322); and from the entire reverse T-RFs data profiles (stress value = 0.346). Tree species symbols: Δ– *Acer negundo*, ○– *Ulmus parvifolia* and + – *Ulmus* pumila. Season symbols: square – Winter, inverted triangle Summer and cross in box Fall.

References

Abdo, Z., Schüette, U. M. E., Bent, S. J., Williams, C. J., Forney, L. J., and Joyce, P. (2006). Statistical methods for characterizing diversity of microbial communities by analysis of terminal restriction fragment length polymorphisms of 16S rRNA genes. *Environ. Microbiol.* 8, 929–938. doi: 10.1111/j.1462-2920.2005.00959.x

Adams, P., and Kloepper, J. (2002). Effect of host genotype on indigenous bacterial endophytes of cotton (*Gossypium hirsutum* L.). *Plant Soil* 240, 181–189. doi: 10.1023/A:1015840224564

Adhikari, T. B., Joseph, C. M., Yang, G., Phillips, D. A., and Nelson, L. M. (2001). Evaluation of bacteria isolated from rice for plant growth promotion and biological control of seedling disease of rice. *Can. J. Microbiol.* 47, 916–924. doi: 10.1139/w01-097

Anand, R., and Chanway, C. (2013). N-2-fixation and growth promotion in cedar colonized by an endophytic strain of *Paenibacillus polymyxa*. *Biol. Fert. Soil.* 49, 235–239. doi: 10.1007/s00374-012-0735-9

Anand, R., Grayston, S., and Chanway, C. (2013). N-2-Fixation and seedling growth promotion of Lodgepole Pine by endophytic *Paenibacillus polymyx. Microbiol. Ecol.* 66, 369–374. doi: 10.1007/s00248-013-0196-1

Andreolli, M., Lampis, S., Poli, M., Gullner, G., Biro, B., and Vallini, G. (2013). Endophytic Burkholderia fungorum DBT1 can improve phytoremediation efficiency of polycyclic aromatic hydrocarbons. *Chemosphere* 92, 688–694. doi: 10.1016/j.chemosphere.2013.04.033

Baldan, E., Nigris, S., Populin, F., Zottini, M., Squartini, A., and Baldan, B. (2014). Identification of culturable bacterial endophyte community isolated from tissues of *Vitisvinifera "Glera"*. *Plant Biosyst.* 148, 508–516. doi: 10.1080/11263504.2014.916364

Bloom, A., Chapin, F. III, and Mooney, H. (1985). Resource limitation in plants - an economic analogy. *Annu. Rev. Ecol. Syst.* 16, 363–392. doi: 10.1146/annurev.ecolsys.16.1.363

Brown, S. D., Sagar, M. U., Klingeman, D. M., Johnson, C. M., Martin, S. L., Land, M. L., et al. (2012). Twenty-one genome sequences from Pseudomonas species and 19 genome sequences from diverse bacteria isolated from the rhizosphere and endosphere of Populus deltoides. *J. Bacteriol.* 194, 5991–5993. doi: 10.1128/JB.01243-12

Bulgarelli, D., Rott, M., Schlaeppi, K., Ver Loren van Themaat, E., Ahmadinejad, N., Assenza, F., et al. (2012). Revealing structure and assembly cues for Arabidopsis root-inhabiting bacterial microbiota. *Nature* 488, 91–95. doi: 10.1038/nature11336

Bulgari, D., Casati, P., Quaglino, F., and Bianco, P. A. (2014). Endophytic bacterial community of grapevine leaves influenced by sampling date and phytoplasma infection process. *BMC Microbiol.* 14:198. doi: 10.1186/1471-2180-14-198

Campisano, A., Antonielli, L., Pancher, M., Yousaf, S., Pindo, M., and Pertot, I. (2014). Bacterial Endophytic Communities in the Grapevine Depend on Pest Management. *PloS ONE* 9:e112763. doi: 10.1371/journal.pone.0112763

Caporaso, J., Kuczynski, J., and Stombaugh, J. (2010). QIIME allows analysis of high- throughput community sequencing data. *Nat. Methods* 7, 335–336. doi: 10.1038/nmeth.f.303

Carrell, A. A., and Frank, A. C. (2014). Pinus flexilis and Piceae engelmannii share a simple and consistent needle endophyte microbiota with a potential role in nitrogen fixation. *Front. Microbiol.* 5:333. doi: 10.3389/fmicb.2014.00333

Chelius, M. K., and Triplett, E. W. (2001). The Diversity of Archaea and Bacteria in Association with the Roots of *Zea mays* L. *Microb. Ecol.* 41, 252–263. doi: 10.1007/s002480000087

Compant, S., Duffy, B., Nowak, J., Clement, C., and Barka, E. A. (2005). Use of Plant Growth-promoting bacteria for biocontrol of plant diseases: principles, mechanisms of action, and future prospects. *Appl. Environ. Microbiol.* 71, 4951–4959. doi: 10.1128/AEM.71.9.4951-4959.2005

Conn, V., and Franco, C. (2004). Analysis of the endophytic actinobacterial population in the roots of wheat (*Triticum aestivum* L.) by terminal restriction fragment length polymorphism and sequencing of 16S rRNA clones analysis of the endophytic actinobacterial population in the roots. *Appl. Environ. Microbiol.* 70, 1787–1794. doi: 10.1128/AEM.70.3.1787-1794.2004

Cook, R. J., Thomashow, L. S., Weller, D. M., Fujimoto, D., Mazzola, M., Bangera, G., et al. (1995). Molecular mechanisms of defense root disease by rhizobacteria against. *Proc. Natl. Acad. Sci. U.S.A.* 92, 4197–4201. doi: 10.1073/pnas.92.10.4197

Coombs, J. T., and Franco, C. M. M. (2003). Isolation and identification of actinobacteria from surface-sterilized wheat roots isolation and identification of actinobacteria from surface-sterilized wheat roots. *Appl. Environ. Microbiol.* 69, 5603–5608. doi: 10.1128/AEM.69.9.5603-5608.2003

Coombs, J. T., Michelsen, P. P., and Franco, C. M. M. (2004). Evaluation of endophytic actinobacteria as antagonists of Gaeumannomyces graminis var. *tritici* in wheat. *Biol. Control* 29, 359–366. doi: 10.1016/j.biocontrol.2003.08.001

Cox, S. E., and Stushnoff, C. (2001). Temperature-related shifts in soluble carbohydrate content during dormancy and cold acclimation in *Populus tremuloides*. *Can. J. For. Res.* 31, 730–737. doi: 10.1139/x00-206

de Weert, S., Vermeiren, H., Mulders, I. H. M., Kuiper, I., Hendrickx, N., Bloemberg, G. V., et al. (2002). Flagella-driven chemotaxis towards exudate components is an important trait for tomato root colonization by Pseudomonas fluorescens. *Mol. Plant. Microbe. Interact.* 15, 1173–80. doi: 10.1094/MPMI.2002.15.11.1173

DeSantis, T. Z., Hugenholtz, P., Larsen, N., Rojas, M., Brodie, E. L., Keller, K., et al. (2006). Greengenes, a chimera-checked 16S rRNA gene database and workbench compatible with ARB. *Appl. Environ. Microbiol.* 72, 5069–5072. doi: 10.1128/AEM.03006-05

Ding, T., Palmer, M. W., and Melcher, U. (2013). Community terminal restriction fragment length polymorphisms reveal insights into the diversity and dynamics of leaf endophytic bacteria. *BMC Microbiol.* 13:1. doi: 10.1186/1471-2180-13-1

Doty, S. L., Oakley, B., Xin, G., Kang, J. W., Singleton, G., Khan, Z., et al. (2009). Diazotrophic endophytes of native black cottonwood and willow. *Curr. Microbiol.* 47, 23–33. doi: 10.1007/BF03179967

Edgar, R. C. (2010). Search and clustering orders of magnitude faster than BLAST. *Bioinformatics* 26, 2460–2461. doi: 10.1093/bioinformatics/btq461

Elvira-Recuenco, M., and van Vuurde, J. W. (2000). Natural incidence of endophytic bacteria in pea cultivars under field conditions. *Can. J. Microbiol.* 46, 1036–1041. doi: 10.1139/w00-098

Figueiredo, J., Gomes, E., Guimaraes, C. T., Lana, U. G. P., Teixeira, M. A., Bressan, W., et al. (2009). Molecular analysis of endophytic bacteria from the genus Bacillus isolated from tropical maize (*Zea mays* L.). *Brazilian J. Microbiol.* 40, 522–534. doi: 10.1590/S1517-83822009000300014

Filteau, M., Lagacé, L., LaPointe, G., and Roy, D. (2010). Seasonal and regional diversity of maple sap microbiota revealed using community PCR fingerprinting and 16S rRNA gene clone libraries. *Syst. Appl. Microbiol.* 33, 165–173. doi: 10.1016/j.syapm.2010.02.003

Garbeva, P., Overbeek, L. S., Vuurde, J. W. L., and Elsas, J. D. (2001). Analysis of endophytic bacterial communities of potato by plating and Denaturing Gradient Gel Electrophoresis (DGGE) of 16S rDNA Based PCR Fragments. *Microb. Ecol.* 41, 369–383. doi: 10.1007/s002480000096

Goslee, S. C., and Urban, D. L. (2007). The ecodist package for dissimilarity-based analysis of ecological data. *J. Stat. Softw.* 22. Available online at: http://www.jstatsoft.org/v22/i07

Gottel, N. R., Castro, H. F., Kerley, M., Yang, Z., Pelletier, D. A., Podar, M.,et al. (2011). Distinct microbial communities within the endophere and rhizosphere of *Populus deltoides* roots across contrasting soil types. *Appl. Environ. Microbiol.* 77, 5934–5944. doi: 10.1128/AEM.05255-11

Hacquard, S., and Schadt, C. W. (2015). Towards a holistic understanding of the beneficial interactions across the Populus microbiome. *New Phytol.* 205, 1424–1430 doi: 10.1111/nph.13133

Hallmann, J., Quadt-Hallmann, A., Mahaffee, W. F., and Kloepper, J. W. (1997). Bacterial endophytes in agricultural crops. *Can. J. Microbiol.* 43, 895–914. doi: 10.1139/m97-131

Izumi, H., Anderson, I., Killham, K., and Moore, E. (2008). Diversity of predominant endophytic bacteria in European deciduous and coniferous trees. *Can. J. Microbiol.* 54, 173–179. doi: 10.1139/W07-134

Jackson, C. R., Randolph, K. C., Osborn, S. L., and Tyler, H. L. (2013). Culture dependent and independent analysis of bacterial communities associated with commercial salad leaf vegetables. *BMC Microbiology* 13:274. doi: 10.1186/1471-2180-13-274

Jansson, S., and Douglas, C. J. (2007). Populus: a model system for plant biology. *Annu. Rev. Plant Biol.* 58, 435–458. doi: 10.1146/annurev.arplant.58.032806.103956

Ju, Z., Ouyang, L., and Zhang, L. (2014). Endophytes Community of *Populus euphratica* Oliv and the strains improving the salt tolerance of plants. *J. Pure Appl. Microbiol.* 8, 43–52.

Kang, J. W., Khan, Z., and Doty, S. L. (2012). Biodegradation of trichloroethylene by an endophyte of hybrid Poplar. *Appl. Environ. Microbiol.* 78, 3504–3507. doi: 10.1128/AEM.06852-11

Khan, Z., Roman, D., Kintz, T., Alas, M. D., Yap, R., and Doty, S. (2014).Degradation, phytoprotection and phytoremediation of phenanthrene by endophyte *Pseudomonas putida*, PD1. *Environ. Sci. Tech.* 48, 12221–12228. doi: 10.1021/es503880t

Knoth, J. L., Kim, S.-H., Ettl, G. J., and Doty, S. L. (2014). Biological nitrogen fixation and biomass accumulation within poplar clones as a result of inoculations with diazotrophic endophyte consortia. *New. Phytol.* 201, 599–609. doi: 10.1111/nph.12536

Kuklinsky-Sobral, J., Araújo, W. L., Mendes, R., Geraldi, I. O., Pizzirani-Kleiner, A. A., and Azevedo, J. L. (2004). Isolation and characterization of soybean-associated bacteria and their potential for plant growth promotion. *Environ. Microbiol.* 6, 1244–1251. doi: 10.1111/j.1462-2920.2004.00658.x

Li, C., Junttila, O., and Palva, E. (2004). Environmental regulation and physiological basis of freezing tolerance in woody plants. *Acta Physiol. Plant* 26, 213–222. doi: 10.1007/s11738-004-0010-2

Lucero, M. E., A., Unc, P., cooke, S., and Dowd, S., Sun (2011). Endophyte microbiome diversity in micropropagated *Atriplex canescens* and *Atriplex torreyi* var *griffithsii*. *PLoS ONE* 6:e17693. doi: 10.1371/journal.pone.0017693

Lundberg, D. S., Yourstone, S., Mieczkowski, P., Jones, C. D., and Dangl, J. L. (2013). Practical innovations for high-throughput amplicon sequencing. *Nat. Methods* 10, 999–1002. doi: 10.1038/nmeth.2634

Madmony, A., Chernin, L., Pleban, S., Peleg, E., and Riov, J. (2005). Enterobacter cloacae, an obligatory endophyte of pollen grains of mediterranean pines. *Folia. Microbiol.* 50, 209–216. doi: 10.1007/BF02931568

Manter, D. K., Delgado, J. A., Holm, D. G., and Stong, R. A. (2010). Pyrosequencing reveals a highly diverse and cultivar-specific bacterial endophyte community in potato roots. *Microb. Ecol.* 60, 157–66. doi: 10.1007/s00248-010-9658-x

Mastretta, C., Taghavi, S., van der Lelie, D., Mengoni, A., Galardi, F., Gonnelli, C., et al. (2009). Endophytic bacteria from seeds of nicotiana tabacum can reduce cadmium phytotoxicity. *Int. J. Phytoremediation* 11, 251–267. doi: 10.1080/15226510802432678

Mengoni, A., Pini, F., Huang, L.-N., Shu, W.-S., and Bazzicalupo, M. (2009). Plant-by-plant variations of bacterial communities associated with leaves of the nickel hyperaccumulator *Alyssum bertolonii Desv*. *Microb. Ecol.* 58, 660–667. doi: 10.1007/s00248-009-9537-5

Miché, L., Battistoni, F., Gemmer, S., Belghazi, M., and Reinhold-Hurek, B. (2006). Upregulation of jasmonate-inducible defense proteins and differential colonization of roots of Oryza sativa cultivars with the endophyte Azoarcus sp. *Mol. Plant Microbe. Interact.* 19, 502–11. doi: 10.1094/MPMI-19-0502

Mocali, S., Bertelli, E., Di Cello, F., Mengoni, A., Sfalanga, A., Viliani, F., et al. (2003). Fluctuation of bacteria isolated from elm tissues during different seasons and from different plant organs. *Res. Microbiol.* 154, 105–114. doi: 10.1016/S0923-2508(03)00031-7

Moore, F. P., Barac, T., Borremans, B., Oeyen, L., Vangronsveld, J., van der Lelie, D., et al. (2006). Endophytic bacterial diversity in poplar trees growing on a BTEX-contaminated site: the characterisation of isolates with potential to enhance phytoremediation. *Syst. Appl. Microbiol.* 29, 539–556. doi: 10.1016/j.syapm.2005.11.012

Noguchi, K., Hui, W. L. W., Gel, Y. R., Gastwirth, J. L., and Miao, W. (2009). *lawstat: An R Package for Biostatistics, Public Policy, and Law*. Available online at: http://cran.r-project.org/package=lawstat

Oksanen, J., Blanchet, F. G., Kindt, R., Legendre, P., Minchin, P. R., O'Hara, R. B., et al. (2012). *vegan: Community Ecology Package*. Available online at: http://cran.r-project.org/package=vegan

Okubo, T., Ikeda, S., Kaneko, T., Eda, S., Mitsui, H., Sato, S., et al. (2009). Nodulation-dependent communities of culturable bacterial endophytes from stems of field-grown Soybeans. *Microbes Environ.* 24, 253–258. doi: 10.1264/jsme2.ME09125

Pirttilä, A. M., Pospiech, H., Laukkanen, H., Myllylä, R., and Hohtola, A. (2005). Seasonal variations in location and population structure of endophytes in buds of Scots pine. *Tree Physiol.* 25, 289–297. doi: 10.1093/treephys/25.3.289

Qin, S., Chen, H.-H., Zhao, G.-Z., Li, J., Zhu, W.-Y., Xu, L.-H., et al. (2012). Abundant and diverse endophytic actinobacteria associated with medicinal plant Maytenus austroyunnanensis in Xishuangbanna tropical rainforest revealed by culture-dependent and culture-independent methods. *Environ. Microbiol. Rep.* 4, 522–531. doi: 10.1111/j.1758-2229.2012.00357.x

Quambusch, M., Pirttila, A. M., Tejesvi, M. V., Winkelmann, T., and Bartsch, M. (2014). Endophytic bacteria in plant tissue culture: differences between easy- and difficult-to-propagate *Prunus avium* genotypes. *Tree Physiol.* 34, 524–535. doi: 10.1093/treephys/tpu,027

R Core Team (2012). *R: A Language and Environment for Statistical Computing. R Foundation for Statistical Computing*. Vienna: Austria. Available online at: http://www.r-project.org/

Rasche, F., Trondl, R., Naglreiter, C., Reichenauer, T. G., and Sessitsch, A. (2006). Chilling and cultivar type affect the diversity of bacterial endophytes colonizing sweet pepper (*Capsicum anuum* L.). *Can. J. Microbiol.* 1045, 1036–1045. doi: 10.1139/w06-059

Reeder, J., and Knight, R. (2010). Rapidly denoising pyrosequencing amplicon reads by exploiting rank-abundance distributions. *Nat. Methods* 7, 668–669. doi: 10.1038/nmeth0910-668b

Rees, G. N., Baldwin, D. S., Watson, G. O., Perryman, S., and Nielsen, D. L. (2004). Ordination and significance testing of microbial community composition derived from terminal restriction fragment length polymorphisms: application of multivariate statistics. *Antonie Van Leeuwenhoek* 86, 339–347. doi: 10.1007/s10482-004-0498-x

Renaut, J., Hoffmann, L., and Hausman, J.-F. (2005). Biochemical and physiological mechanisms related to cold acclimation and enhanced freezing tolerance in poplar plantlets. *Physiol. Plant.* 125, 82–94. doi: 10.1111/j.1399-3054.2005.00554.x

Ryan, R. P., Germaine, K., Franks, A., Ryan, D. J., and Dowling, D. N. (2008). Bacterial endophytes: recent developments and applications. *FEMS Microbiol. Lett.* 278, 1–9. doi: 10.1111/j.1574-6968.2007.00918.x

Sakai, M., Matsuka, A., Komura, T., and Kanazawa, S. (2004). Application of a new PCR primer for terminal restriction fragment length polymorphism analysis of the bacterial communities in plant roots. *J. Microbiol. Methods* 59, 81–89. doi: 10.1016/j.mimet.2004.06.005

Sarr, P. S., Yamakawa, T., Asatsuma, S., Fujimoto, S., and Sakai, M. (2010). Investigation of endophytic and symbiotic features of Ralstonia sp. TSC1 isolated from cowpea nodules. *Afr. J. Microbiol. Res.* 4, 1959–1963.

Schaefer, A. L., Lappala, C. R., Morlen, R. P., Pelletier, D. A., Lu, T.-Y., Lankford, P. K., et al. (2013). LuxR- and LuxI-type quorum-Sensing circuits are prevalent in members of the Populus deltoides microbiome. *Appl. Environ. Microbiol.* 79, 5745–5752. doi: 10.1128/AEM.01417-13

Schütte, U. M. E., Abdo, Z., Bent, S. J., Shyu, C., Williams, C. J., Pierson, J. D., et al. (2008). Advances in the use of terminal restriction fragment length polymorphism (T-RFLP) analysis of 16S rRNA genes to characterize microbial communities. *Appl. Microbiol. Biotechnol.* 80, 365–380. doi: 10.1007/s00253-008-1565-4

Shah, J. (2009). Plants under attack: systemic signals in defence. *Curr. Opin. Plant Biol.* 12, 459–64. doi: 10.1016/j.pbi.2009.05.011

Strobel, G., Daisy, B., Castillo, U., and Harper, J. (2004). Natural products from endophytic microorganisms. *J. Nat. Prod.* 67, 257–268. doi: 10.1021/np030397v

Sun, L., Qiu, F., Zhang, X., Dai, X., Dong, X., and Song, W. (2008). Endophytic bacterial diversity in rice (*Oryza sativa* L.) roots estimated by 16S rDNA sequence analysis. *Microb. Ecol.* 55, 415–424. doi: 10.1007/s00248-007-9287-1

Taghavi, S., Barac, T., Greenberg, B., Borremans, B., Vangronsveld, J., and van der Lelie, D. (2005). Horizontal gene transfer to endogenous endophytic bacteria from poplar improves phytoremediation of toluene. *Appl. Environ. Microbiol.* 71, 8500–8505. doi: 10.1128/AEM.71.12.8500-8505.2005

Taghavi, S., Garafolal, C., Monchyl, S., Newman, L., Hoffman, A., Weyens, H., et al. (2009). Genome survey and characterization of endophytic bacteria exhibiting a beneficial effect on growth and development of Poplar trees. *Appl. Environ. Microbiol.* 75, 748–757 doi: 10.1128/AEM.02239-08

Takahashi, Y., Matsumoto, A., Morisaki, K., and Omura, S. (2006). Patulibacter minatonensis gen. nov., sp. nov., a novel actinobacterium isolated using an agar medium supplemented with superoxide dismutase, and proposal of Patulibacteraceae fam. nov. *Int. J. Syst. Evol. Microbiol.* 56, 401–406. doi: 10.1099/ijs.0.63796-0

Thijs, S., Van Dillewijn, P., Sillen, W., Truyens, S., Holtappels,M., D'Haen, J., et al. (2014). Exploring the rhizospheric and endophytic bacterial communities of *Acer pseudoplatanus* growing on a TNT-contaminated soil: towards the development of a rhizocompetent TNT-detoxifying plant growth promoting consortium. *Plant Soil* 385, 15–36. doi: 10.1007/s11104-014-2260-0

Ulrich, K., Ulrich, A., and Ewald, D. (2008). Diversity of endophytic bacterial communities in poplar grown under field conditions. *FEMS Microbiol. Ecol.* 63, 169–180. doi: 10.1111/j.1574-6941.2007.00419.x

van Aken, B., Peres, C. M., Doty, S. L., Yoon, J. M., and Schnoor, J. L. (2004). *Methylobacterium populi* sp nov., a novel aerobic, pink-pigmented, facultatively methylotrophic, methane-utilizing bacterium isolated from poplar trees (*Populus deltoides x nigra* DN340). *Int. J. Syst. Evol. Micriobol.* 54, 1191–1196. doi: 10.1099/ijs.0.02796-0

van Overbeek, L., and van Elsas, J. D. (2008). Effects of plant genotype and growth stage on the structure of bacterial communities associated with potato (*Solanum tuberosum* L.). *FEMS Microbiol. Ecol.* 64, 283–96. doi: 10.1111/j.1574-6941.2008.00469.x

Weyens, N., Taghavi, S., Barac, T., van der Lelie, D., Boulet, J., Artois, T., et al. (2009). Bacteria associated with oak and ash on a TCE-contaminated site: characterization of isolates with potential to avoid evapotranspiration of TCE. *Environ. Sci. Pollut. Res. Int.* 16, 830–843. doi: 10.1007/s11356-009-0154-0

Xin, G., Zhang, G., Kang, J. W., Staley, J. T., and Doty, S. L. (2009). A diazotrophic, indole-3-acetic acid-producing endophyte from wild cottonwood. *Biol. Fert. Soils* 45, 669–674. doi: 10.1007/s00374-009-0377-8

Conflict of Interest Statement: The authors declare that the research was conducted in the absence of any commercial or financial relationships that could be construed as a potential conflict of interest.

frontiers in
MICROBIOLOGY

ORIGINAL RESEARCH ARTICLE
published: 05 September 2014
doi: 10.3389/fmicb.2014.00427

The biocontrol endophytic bacterium *Pseudomonas fluorescens* PICF7 induces systemic defense responses in aerial tissues upon colonization of olive roots

Carmen Gómez-Lama Cabanás, Elisabetta Schilirò, Antonio Valverde-Corredor and Jesús Mercado-Blanco*

Lab Plant-Microbe Interactions, Department of Crop Protection, Institute for Sustainable Agriculture, Agencia Estatal Consejo Superior de Investigaciones Científicas (CSIC), Córdoba, Spain

Edited by:
Anna Maria Pirttilä, University of Oulu, Finland

Reviewed by:
Dale Ronald Walters, Scottish Agricultural College, Scotland
Nai-Chun Lin, National Taiwan University, Taiwan

***Correspondence:**
Jesús Mercado-Blanco, Lab Plant-Microbe Interactions, Department of Crop Protection, Institute for Sustainable Agriculture, Agencia Estatal Consejo Superior de Investigaciones Científicas (CSIC), Avda. Menéndez Pidal, Campus 'Alameda del Obispo' s/n, Apartado 4084, 14080 Córdoba, Spain
e-mail: jesus.mercado@ias.csic.es

Pseudomonas fluorescens PICF7, a native olive root endophyte and effective biocontrol agent (BCA) against Verticillium wilt of olive, is able to trigger a broad range of defense responses in root tissues of this woody plant. In order to elucidate whether strain PICF7 also induces systemic defense responses in above-ground organs, aerial tissues of olive plants grown under non-gnotobiotic conditions were collected at different time points after root bacterization with this endophytic BCA. A suppression subtractive hybridization (SSH) cDNA library, enriched in up-regulated genes, was generated. This strategy enabled the identification of 376 ESTs (99 contigs and 277 singlets), many of them related to response to different stresses. Five ESTs, involved in defense responses, were selected to carry out time-course quantitative real-time PCR (qRT-PCR) experiments aiming to: (1) validate the induction of these genes, and (2) shed light on their expression pattern along time (from 1 to 15 days). Induction of olive genes potentially coding for lipoxygenase 2, catalase, 1-aminocyclopropane-1-carboxylate oxidase, and phenylananine ammonia-lyase was thus confirmed at some time points. Computational analysis also revealed that different transcription factors were up-regulated in olive aerial tissues (i.e., JERF, bHLH, WRKY), as previously reported for roots. Results confirmed that root colonization by this endophytic bacterium does not only trigger defense responses in this organ but also mounts a wide array of systemic defense responses in distant tissues (stems, leaves). This sheds light on how olive plants respond to the "non-hostile" colonization by a bacterial endophyte and how induced defense response can contribute to the biocontrol activity of strain PICF7.

Keywords: *Olea europea*, biological control, endophyte, *Pseudomonas fluorescens*, systemic defense response, qRT-PCR, Verticillium wilt

INTRODUCTION

Olive (*Olea europaea* L.) is an emblematic woody plant in the Mediterranean Basin. Its cultivation for millennia has shaped a characteristic agro-ecosystem in the region, representing a traditional agricultural activity with indisputable social, economical, and historical relevance (Caballero and del Río, 2008). From the original domestication and cultivation area, olive cropping is expanding to other climatically-favorable geographical areas around the globe (Barranco et al., 2008). Moreover, consumption of olive oil, the major product extracted from olive drupe, is gaining interest because of the increasing body of knowledge showing its beneficial effects for human health compared to other fat diet (Pauwels, 2011). The traditional landscape of olive orchards found throughout the Mediterranean Basin is progressively changing toward more productive cropping systems with high tree densities (up to 2000 trees/ha) (Navarro and Parra, 2008; Rallo et al., 2012; Connor et al., 2014). These changes lead to an increasing demand for nursery-produced planting material that must be pathogen-free certified and/or protected against pathogen attacks (Tjamos, 1993; López-Escudero and Mercado-Blanco, 2011).

Among the biotic constraints affecting olive cultivation, the soil-borne fungus *Verticillium dahliae* Kleb., causal agent of Verticillium wilt of olive (VWO), is considered the most threatening disease in many areas where this tree is cultivated. During the last two decades, the incidence of VWO has increased considerably. This could be due to factors such as (i) the use of pathogen-infested soil or infected propagation material, (ii) the pathogen's dispersal efficacy, (iii) the abuse on fertilization and irrigation, (iv) variable edaphic and climatic factors, (v) the high genetic/pathogenic diversity found within pathogen populations (i.e., defoliating [D] and non-defoliating [ND] pathotypes), or (vi) the changes in cultivation systems (López-Escudero and Mercado-Blanco, 2011). These factors, among others, makes VWO very difficult to control. Thus, the current spread of the disease and the severity of its attacks can only be effectively

confronted by implementing an integrated disease management strategy (López-Escudero and Mercado-Blanco, 2011). A promising control tool within this strategy is the use of microbial antagonists effective against *V. dahliae*, particularly at the nursery stage (Mercado-Blanco et al., 2004).

Some plant growth promoting rhizobacteria (PGPR) are able to protect their hosts against phytopathogens displaying biocontrol activity (Van Loon, 2007; Beneduzi et al., 2012). This positive effect can be exerted through different mechanisms such as root architecture modification (Vacheron et al., 2013), production of antibiotics (Beneduzi et al., 2012), and/or triggering a specific defense signaling pathway known as induced systemic resistance (ISR) (Bakker et al., 2007). The possibility to exploit ISR within integrated control strategies has been proposed elsewhere (Ramamoorthy et al., 2001; Zehnder et al., 2001). ISR is phenotypically similar to systemic acquired resistance (SAR), a response activated, for instance, after a first infection by an incompatible necrotizing pathogen (Durrant and Dong, 2004). Nevertheless, the signal transduction pathway and the molecular basis underlying both responses are different. In SAR, defense reactions such as hypersensitive response (HR), salicylic acid (SA) biosynthesis or induction of pathogenesis-related (PR) proteins are characteristic (Andreu et al., 2006). In contrast, ISR depends on pathways regulated by the plant hormones ethylene (ET) and jasmonic acid (JA), and include the induction of enzymatic activities related to phenylalanine ammonia-lyase (PAL) synthesis, among others (Sena et al., 2013). Both pathogenic and beneficial bacteria can cause responses such as plant cell wall reinforcement and production of phytoalexins and PR proteins, consistent with the fact that SAR and ISR represent an enhanced basal plant resistance, and that plant hormone(s)-mediated cross talk is taking place between both mechanisms (Pieterse et al., 2009, 2012).

One of the most promising biocontrol agents (BCA) so far studied for the biocontrol of VWO is *Pseudomonas fluorescens* PICF7. Strain PICF7 is a indigenous colonizer of olive roots, an *in vitro* antagonist of *V. dahliae*, and an effective BCA against VWO caused by the D pathotype in young, nursery-produced olive plants (Mercado-Blanco et al., 2004; Prieto et al., 2009). Our previous works have also demonstrated that PICF7 is able to endophytically colonize olive root tissues under different experimental conditions (Prieto and Mercado-Blanco, 2008; Prieto et al., 2009, 2011). Bacterial endophytes, likely present in all plant species (Rosenblueth and Martínez-Romero, 2006; Hardoim et al., 2008; Reinhold-Hurek and Hurek, 2011), offer an interesting potential to be used in agricultural biotechnology. They can exert plant growth promotion and biocontrol activity and, in addition, are adapted to the ecological niche (plant tissues) where their beneficial effects can be deployed (Mercado-Blanco and Lugtenberg, 2014). Living inside the plant means that endophytes must be able to counteract defense responses deployed by the host against their colonization. This scenario likely implies an as yet poorly-understood modulation of the plant immune response enabling endophytes to be recognized and tolerated by the host plant as "friendly" invasors (Reinhold-Hurek and Hurek, 2011; Zamioudis and Pieterse, 2012; Mercado-Blanco and Lugtenberg, 2014).

Our knowledge on the genetic basis underlying the interaction between endophytes and their hosts is still very limited (Bordiec et al., 2010; Reinhold-Hurek and Hurek, 2011). Nevertheless, some studies have shown that inner colonization of plant tissues by bacterial endophytes triggers, among other changes, a wide range of defense responses (Wang et al., 2005; Conn et al., 2008). Our previous works have demonstrated that colonization by *P. fluorescens* PICF7 induced a broad set of defense responses in olive root tissues, including genes related to ISR and SAR (Schilirò et al., 2012). Indeed, root colonization of "Arbequina" plants by this BCA produced the differential expression of genes involved in processes such as plant hormones and phenylpropanoids biosynthesis and PR proteins, as well as the up regulation of several transcription factors implicated in systemic defensive responses (WRKY5, bHLH, ARF2, GRAS1) (Schilirò et al., 2012).

In this study, we aimed to elucidate whether systemic defense responses are also triggered in aerial olive tissues upon root inoculation with strain PICF7. We also aimed to figure out whether these responses are similar to the transcriptional changes observed in roots during the interaction with this endophyte. Whereas, our main objective was to unravel the broad genetic changes taking place in above-ground tissues, we also focused on the time-course expression of specific defense genes. Thus, expression of genes potentially coding for olive lipoxygenase (*LOX-2*), phenylalanine ammonia lyase (*PAL*), acetone cyanohydrin lyase (*ACL*), all of them previously reported to be induced in olive roots upon PICF7 inoculation, as well as a catalase (*CAT*), and 1-aminocyclopropane-1-carboxylate oxidase (*ACO*), was studied. Results showed that strain PICF7 was able to trigger a wide array of systemic defense responses in aerial olive tissues, some of them being previously reported to be induced in roots. This points out to the ability of PICF7 to elicit broad transcriptional changes, mostly of defensive nature, at distant parts of the plant. Remarkably, the genetic changes here reported have been unraveled in a plant-microbe interaction poorly investigated so far; that is, between a woody plant of commercial interest (olive) and an effective biocontrol endophytic bacterium. Furthermore, we have implemented a non-gnotobiotic experimental set-up, a more natural scenario not frequently used in this type of studies.

MATERIALS AND METHODS

PLANT MATERIAL, *PSEUDOMONAS FLUORESCENS* PICF7 ROOT TREATMENT, AND mRNA PURIFICATION

Aerial olive tissues used in this study originated from plants used in an experimental set-up described by Schilirò et al. (2012). Olive plants (cv. Arbequina, 3-month-old) were propagated in a commercial nursery located in Córdoba province (Southern Spain). Prior to bacterial treatment, plants were acclimated for three weeks in a growth chamber under conditions described below. Inoculum of strain PICF7 (Mercado-Blanco et al., 2004) was prepared as described by Prieto and Mercado-Blanco (2008). "Arbequina" plants were manipulated and their root systems bacterized in a suspension of PICF7 cells (15 min, $1{\cdot}10^8$ cells ml^{-1}) as previously described (Schilirò et al., 2012). Roots of control plants (non-bacterized) were dipped in 10 mM $MgSO_4{\cdot}7\ H_2O$. Then, plants were individually transplanted into

polypropylene pots containing an autoclaved sandy substrate (Prieto and Mercado-Blanco, 2008). Plants were maintained at controlled conditions (23 ± 1°C, 60–90% relative humidity, 14-h photoperiod of fluorescent light at 360 μE m^{-2}) during 21 days (Schilirò et al., 2012). In order to alleviate stress of plants after manipulation, inoculation, and transplanting, the above-mentioned photoperiod was enlarged progressively until reaching 14-h daylight.

To obtain a broad range of differentially-expressed (induced) genes, the whole aerial part (stems plus leaves) of each olive plant was sampled at different times after treatments. Therefore, aerial tissues were collected at 0 h, 5 h, 10 h, 24 h and 2, 3, 4, 7, 10, 12, 15, 18, and 21 days (two plants/time point) for both inoculated (bacterized) and non-inoculated (control) plants. Aerial tissues of 52 plants (26 bacterized and 26 control) were sampled, rapidly frozen using liquid nitrogen, and stored at −80°C until used. Total RNA of each sample was extracted according to Asif et al. (2000). The removal of contaminating genomic DNA was carried out by DNaseI treatment (Roche Applied Science, Mannheim, Germany) according to the manufacturer's instructions. All RNA samples corresponding to each treatment (bacterized and non-bacterized plants) were pooled separately to obtain two independent RNA pools prior to mRNA purification. Poly A+ mRNA was purified from approximately 400 μg of total RNA of each pool using the Dynabeads® mRNA Purification Kit (Dynal Biotech, Oslo, Norway) according to the manufacturer's indications. Purity and quality of mRNA samples were verified by both agarose gel electrophoresis and spectrophotometry using a ND-1000 Spectrophotometer (NanoDrop Technologies, Wilmington, DE).

GENERATION OF A "SUPPRESSION SUBSTRACTIVE HYBRIDIZATION" cDNA LIBRARY ENRICHED IN INDUCED GENES OF OLIVE AERIAL TISSUES, CLONING AND SEQUENCING

A cDNA library was constructed by using the "Suppression Subtractive Hybridization" (SSH) technology (Diatchenko et al., 1996) in order to clone and identify genes up-regulated in aerial tissues during the interaction of *P. fluorescens* PICF7 with olive roots. SSH allows enrichment and cloning of less abundant transcripts through amplification and normalization of subtracted cDNAs. The cDNA library was generated using the PCR-Select™ cDNA Subtraction Kit (BD Biosciences, Palo Alto, CA) according to the manufacturer's instructions and as previously described by Schilirò et al. (2012). Briefly, cDNAs were separately synthesized from 2 μg of mRNA of each PICF7-inoculated (tester) and control (driver) plant, digested with *RsaI* and ligated to adaptors 1 and 2R. To enrich differentially-expressed sequences, two rounds of hybridization and PCR amplification were carried out. Advantage® 2 PCR Kit (BD Biosciences) was used for PCR amplifications in total volume of 50 μL. The amplification program was: denaturation for 5 min at 94°C, followed by 33 cycles of 30 s at 94°C, 45 s at 55°C and 1 min at 72°C and a final extension step of 10 min at 72°C. To check the efficiency of subtraction a 308-bp fragment was amplified using the primer pair Act1-fw: 5′-GCTTGCTTATGTTGCTCTCGAC-3′/Act1-rv: 5′-TGATTTCCTTGCTCATACGGTC-3′) belonging to the constitutively expressed (housekeeping) β-actin gene from olive (Acc. No. AF545569) (**Table 1**), whose expression was checked not to be influenced by strain PICF7 inoculation (Schilirò et al., 2012).

Products resulting from SSH (cDNAs) were ligated in the pGEM-T Easy Vector (Promega, Madison, WI) and cloned into *Escherichia coli* CH3-Blue competent cells (Bioline, London, UK) according to manufacturer's specifications. Positive colonies based on white/blue color selection were grown in 96-well microtiter plates contained LB medium with 100 mg L^{-1} and were incubated at 37°C for 22 h. Lastly, forward T7 universal primer was employed to isolate and sequence 1344 bacterial clones from the SSH library. Sequencing of DNAs was performed at a commercial service (Sistemas Genómicos S.L., Valencia, Spain).

BIOINFORMATICS ANALYSIS OF EXPRESSED SEQUENCE TAGS

Contaminating vector and adaptors sequences were identified and eliminated from each Expressed Sequence Tags (ESTs) by mass alignment using the "CLC Main Workbench 6.8.1" (CLC bio, Aarhus, Denmark) software. Sequences showing low quality or length (<100 bp) were excluded from the analysis ("sequence trimming" step). The "CLC Main Workbench 6.8.1" software was used to assemble the EST data set, aiming to find contiguous sequences and redundancy. Computational annotation of ESTs obtained during olive-PICF7 interaction was carried out by using the open software "Blast2GO version 2.7.0" (Conesa et al., 2005) available at http://www.blast2go.com/b2ghome. Homologies were checked in the non-redundant (nr) GenBank protein database by running the Blastx algorithm (Altschul et al., 1990) with the *E*-value set to 1.0E-3 and the High-scoring Segment Pairs (HSP) length cutoff fixed to 33 (as previously implemented by Schilirò et al., 2012).

The "Blast2GO software v.2.7.0" was used to perform Gene Ontology (GO) analysis from retrieved database matches. Functional annotation of all sequences was carried out using default parameters. InterPro Scan (Zdobnov and Apweiler, 2001) was used to associate functional information and GO terms to the protein of interest by using the specific tool implemented in the Blast2GO software with the default parameters. Finally, the "Augment Annotation by ANNEX" function was used to improve the annotation profiles information. The GOslim "goslim_plant.obo" was run to achieve specific plant GO terms by means of a plant-specific reduced version of the GO (available at http://www.arabidopsis.org/). Enzyme mapping of annotated sequences was retrieved by direct GO to Enzyme annotation and used to query the Kyoto Encyclopedia of Genes and Genomes (KEGG—http://www.genome.jp/kegg/) to define the main metabolic pathways involved. The distribution of hits obtained against entries for other plants within the NCBI database was used to get a descriptive view of the newly generated dataset.

DATA VALIDATION AND TIME-COURSE GENE EXPRESSION PROFILE

A selection of up-regulated ESTs identified by the Blast2GO tool was used for validation by quantitative real-time PCR (qRT-PCR) experiments. Five transcripts from the whole dataset of nr sequences found to be up-regulated and belonging to key biosynthetic and metabolic pathways were chosen (*LOX-2*, *PAL*,

Table 1 | List of selected transcripts induced in olive aerial tissues upon *P. fluorescens* PICF7 colonization used in qRT-PCR experiments.

Clone ID	Putative gene	Process	Primer pair	Amplicon length (bp)	Linear equation (1)	R^2(1)	PCR efficiency(1)
AU12-D10T7	1-Aminocyclopropane-1-carboxylate oxidase	Ethylene biosynthesis	Fw: CTCAAGTTGATCCCCAAT Rv: GCATTCCATGGCTCTAAA	231	$Y = -3.430 + 29.271$	0.994	95.7
AU03-E02T7	Phenylananine ammonia-lyase	Phenylpropanoids biosynthesis	Fw: ACATAGGAGGACCAAACAA Rv: GTAGGATAAAGGGACAAGAT	280	$Y = -3.394 + 29.944$	0.991	97.1
AU06-H07T7	Catalase	Oxidation-reduction	Fw: CCCAGGATCTCTACGATT Rv: TCTGGAGCATCTTGTCAT	273	$Y = -3.371 + 22.018$	0.993	98.0
AU13-A07T7	Lipoxygenase 2	Linolenic acid metabolism	Fw: GAGACATCACCAATCCAT Rv: CCAGCACCACATCTATTT	141	$Y = -3.413 + 29.253$	0.989	96.3
AU04-G10T7	Acetone cyanohydrin lyase	Salicylic acid-binding protein 2	Fw: GAAAGAGATGGAGACGGAA Rv: ACACAGGGAAATGCATCAAA	246	$Y = -3.141 + 32.360$	0.994	108.2
AF545569 (2)	*Olea europea* beta-actin (act1)	Cytoskeletal integrity	Fw: GCTTGCTTATGTTGCTCTCGAC Rv: TGATTTCCTTGCTCATACGGTC	308	$Y = -3.341 + 28.428$	0.990	99.2

*For all transcripts, relative expression (RE) analysis was repeated at least two times in independent qRT-PCR experiments (see text and **Figure 4**). Clone ID, gene name, biological process, primers sequences, amplicon length, linear equations, correlation coefficients (R^2), and PCR efficiencies are indicated (Fw: Forward; Rv: Reverse). AU, Arbequina aerial tissues induced gene; (1) Linear equation R^2 coefficient and PCR efficiency correspond to a representative qRT-PCR assay performed (2): olive act-1 gene used as reference to normalize relative expression (Gene Bank Accession Number). doi: 10.1371/journal.pone.0048646.t003.*

ACL, *CAT*, and *ACO*). Moreover, these ESTs fulfilled the criteria of >100-bp long and *E*-value ≤ 1.0E-3 Selected genes were tested by qRT-PCR at four different times to assess their expression patterns in above-ground organs at different time points after inoculation of roots with strain PICF7. Specific primer pairs for these five sequences (**Table 1**) were designed using the "CLC Main Workbench 6.8.1" (CLC bio) software and tested for their specificity in a temperature range (53 to 63°C) by conventional PCR. To find the appropriate range of concentrations at which target cDNA, specific qRT-PCR assays were conducted using cDNAs synthesized from 10-fold serially diluted (1 μg, 100 ng, 10 ng, 1 ng, 100 pg) RNA samples. Standard curves were generated for each selected transcript using reverse transcribed cDNA from serial dilutions (300 ng, 30 ng, 3 ng, 0.3 ng) of remnant samples of total RNA not used for SSH and that were properly stored at −20°C. Gene expression of selected genes was measured at four different times: 1, 3, 7, and 15 days after inoculation (DAI) with PICF7. Ct values and the logarithm of cDNA concentrations were linearly correlated for each of the examined genes and PCR efficiencies were calculated by iQ5 optical system software v.2.1 (BioRad, Hercules, CA). Synthesis of cDNA was performed using the "iScript cDNA Synthesis Kit" (BioRad) from 100 ng of total RNA in each of four different times assayed, and following the manufacturer's procedure. qRT-PCR experiments and analyses were done in a thermal cycler iQ5 Real-Time PCR System (BioRad) provided with a 96-well sample block. For each selected gene, expression was quantified at least two times in independent qRT-PCR experiments, and three replicas per point studied and per plate were routinely included.

All qRT-PCR reactions were performed containing 2 μL of cDNA, 0.5 μM of each primer, 10 μL of 2 × iQ™ SYBRH Green Supermix (BioRad) and H_2O up to a total volume of 20 μL. The following parameters were used in all reactions: 94°C for 5 min, 50 cycles of 94°C for 30 s, 55°C for 30 s, and 72°C for 40 s. Linear equations, correlation coefficients (R^2) and reaction efficiencies were estimated for each transcript. Melting curves of qRT-PCR products were assessed from 55 to 95°C to confirm the amplification of single PCR bands. For all samples reaction protocol was as follows: 5 min at 95°C for initial denaturation, cooling to 55°C and melting from 55 to 95°C with a 0.5°C transition rate every 10 s.

The *O. europaea* β-actin gene was used as housekeeping gene to normalize data obtained from qRT-PCR assay and was amplified in the same conditions above described. Relative expression (RE) levels at different times were calculated according to Livak and Schmittgen (2001). The average of each expression gene fold change was categorized as follows: "low" ≥−1.0 to ≤1.0; "medium" ≥−2.0 to <−1.0 or >1.0 to ≤2.0; "high," <−2.0 or >2.0 (Kim et al., 2008). All relative expression data in four different times for each gene were represented in a graphic as means ± STD of at least two separate experiments, each performed with triplicate samples. A paired sample *T*-test was performed to determine whether there was significant difference between the average values of each relative gene expression independent experiment (between plates). For all genes tested there was no significant difference between experiments ($P > 0.05$). *T*-test analysis was performed using the Statistix software (Version 9.0 for Windows).

ACCESSION NUMBERS

ESTs reported in this study have been deposited in the dbESTs database of the National Center for Biotechnology Information (NCBI) under GenBank accession numbers JZ534362 (dbEST_Id 78897695)—JZ534925 (dbEST_Id 78898258).

RESULTS

CONSTRUCTION AND CHARACTERIZATION OF A cDNA LIBRARY OF OLIVE GENES INDUCED IN AERIAL TISSUES UPON COLONIZATION OF ROOTS BY *P. FLUORESCENS* PICF7

A cDNA library enriched in olive transcripts up-regulated in aerial tissues after root inoculation with the biocontrol endophytic strain PICF7 was generated. A total number of 1344 ESTs were sequenced. Eventually, ESTs in the cDNA library were assembled into 99 distinct contigs (average length of 443 bp) and 277 singlets (average length of 338 bp) to provide a set of 376 unigenes differentially expressed (induced) in above-ground organs during PICF7-olive roots interaction. Despite the fact that the number of ESTs sequenced in this study was higher than that from root tissues (904 ESTs, Schilirò et al., 2012), the number of up-regulated unigenes found in aerial tissues was lower than in roots (445 ESTs, Schilirò et al., 2012).

Querying (Blastx) the nr NCBI database allowed the attribution of homologous hits for 71.8% of the ESTs. Hits distribution of the complete EST set against sequences from different plant species are shown in **Figure 1**. In particular, 130 ESTs (34.6% of the whole ESTs set) correspond to coding sequences previously identified in genomes of woody plants such as grape vine (*Vitis vinifera* L., 69 hits), western balsam poplar (*Populus trichocarpa* Torr. and A.Gray, 29 hits), castor bean (*Ricinus communis* L., 16 hits), and olive (16 hits) (**Figure 1** and **Table 2**). *E*-values for this homology analysis ranged from 5.02E-3 to 1.06E-139. Only 4.3% of the 376 unigenes showed significant homology with olive genes in the databases [NCBI dbEST (http://www.ncbi.nlm.nih.gov/dbEST/)] (**Table 2**), indicating an as yet important lack of genetic/genomic information for this relevant woody crop (last search perfomed on May 2014). Finally, a total of 106 unigenes (28.2% of induced transcripts found in this work) were of unknown function.

Analysis of the 376 olive ESTs showed that many of the ESTs identified as induced in aerial olive tissues during the interaction of PICF7 in roots were related with plant responses to different stimuli and stresses (biotic, abiotic, endogenous, extracellular, or/and external). For instance, genes potentially coding for a 14-3-3-protein [EST sequence name AU11-F06] (response to stress), CAT [AU03-B01] (response to stress and abiotic, extracellular and endogenous stimuli), ACO [AU12-D10], phosphatase 2c [AU02-A06], and glycine rich RNA binding [AU01-H12] (response to stress, abiotic, biotic, and endogenous stimuli), PAL [AU03-E02] and ACL [AU04-G10] (response to pathogens), LOXs [AU13-A01; AU13-A07] (response to stress, biotic, and abiotic stimuli), were found to be up-regulated. Some of the ESTs were different kind of calcium (Ca^{2+})-binding proteins that could be related with plant defense reaction, e.g., Ca^{2+}-binding protein cm127 [AU-C172], calreticulin [AU02-C02], calreticulin-3 parcial [AU07-B01], calmodulin (CaM) [AU-C96], and ef hand family protein [AU01-G11]. A complete list of ESTs identified as induced in above-ground organs after inoculation of olive roots with *P. fluorescens* PICF7 is shown in Table S1 as supplementary information for the reader. In addition, Table S2 displays contigs identified with their corresponding contiguous/overlapping ESTs. ESTs with unknown functions were not included in these tables. Results revealed that only a small percentage of induced unigenes (26 out of 376, representing 7.18% of all transcripts) were found in both the cDNA libray of aerial tissues (this study) and that one previously reported for root tissues (Schilirò et al., 2012) (**Table 3**). In particular, 4 out of the 26 putative proteins shared the same accession number when a blastx analysis was performed: serine protease (CAA07250), CAT (CAB56850), cyclophilin (ABS30424), and ef hand family protein (XP_002319225). Three of these proteins seem to be related to defensive response in plants. Thus, CAT and ef hand family protein take part in Ca^{2+} metabolism, biotic and abiotic stress (Day et al., 2002; Yang and Poovaiah, 2002). On the other hand, cyclophilin belongs to a family of immunosuppressant receptors called immunophilins that is expressed during pathogenic infection and abiotic stress condition (Romano et al., 2004).

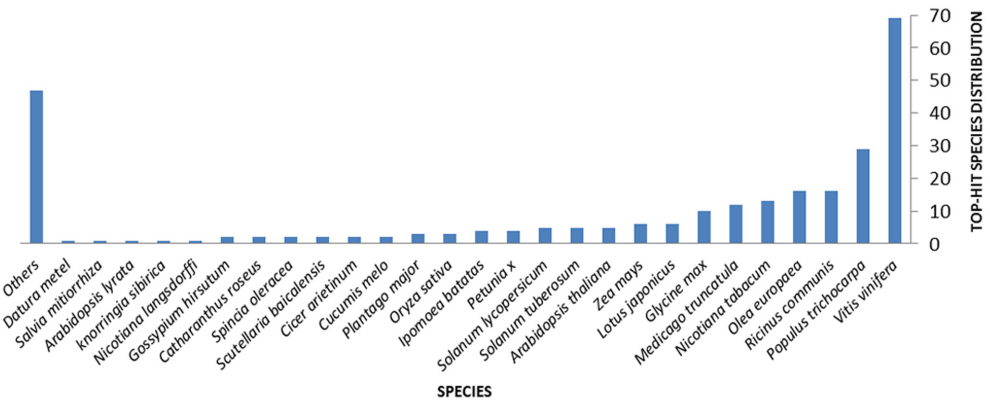

FIGURE 1 | Distribution of hits of the complete assembly obtained against sequences available in Uniprot for different plant species.

Table 2 | List of induced EST sequences identified after Blastx analysis as homologous to olive (*Olea europaea* L.) genes previously indexed in databases.

EST sequence name	Putative protein function	Accession number	*E*-Value
AU01-B01T7	protein	AF28695	2,6E-47
AU01-D04T7	beta-glucosidase g1	AAL93619	2,70E-61
AU02-A03T7	low-temperatura inducible	ABS72020	1,93E-60
AU02-A05T7	beta-glucosidase d4	ACD43481	6,73E-55
AU02-C12T7	ribulose bisphosphate carboxylase oxygenase activase chloroplastic-like	ABS72022	5,37E-23
AU02-E06T7	chloroplast ribulose- -bisphosphate carboxylase oxygenase small subunit	ABS71998	1,93E-12
AU03-F12T7	psa1 protein	ABU39903	4,26E-48
AU04-G06T7	thaumatin-like protein	ACZ57583	5,98E-26
AU05-F08T7	1-deoxy-d-xylulose 5-phosphate reductoisomerase	AFS28671	3,75E-59
AU08-E04T7	cytochrome p450	AFS28690	8,09E-63
AU11-A01T7	auxin-induced protein pcnt115	ABS72001	2,29E-15
AU13-A01T7	loxc homolog	ADC43485	1,02E-61
AU13-A07T7	lipoxygenase	ADC43484	8,73E-25
AU13-E01T7	serine hydroxymethyltransferase	ABS72016	1,60E-86
AU-C1	bark storage protein a-like	AFP49328	1,95E-120
AU-C172	calcium-binding protein cml27	Q9M7R0	4,58E-61

IDENTIFICATION OF DEFENSE RESPONSES INDUCED IN AERIAL TISSUES DURING OLIVE ROOT-PICF7 INTERACTION.

Analysis of the EST set by the Blast2GO software enabled annotation of expressed sequences according to the terms of the three main GO vocabularies, i.e., "biological process" (BP), "molecular function" (MF), and "cellular component" (CC). GO annotation was only feasible for 67.8% of the sequences, i.e., 121 ESTs (106 assigned to "unknown" category and 15 assigned to "predicted" category) were automatically excluded from this functional classification by the program. Since a number of transcripts were identified by different GO terms, the mapped ESTs distribution for BP, MF and CC main categories shown in **Figure 2** resulted in more than 376 sequences. The distribution of assignments into the GO categories "level 3" was 208 (BP), 192 (MF), and 150 (CC). Regarding to BP main GO vocabulary, transcripts representing GO terms categories non-related to plant defense processes (e.g., macromolecule metabolic process, developmental maturation, pigment accumulation, chromosome segregation and microtubule-based process), were grouped as "other" (**Figure 2**, BP).

Concerning to plant defense-related categories, ESTs found to be induced in above-ground organs upon *P. fluorescens* PICF7 olive root colonization, were assigned to processes such as "response to stress" (81 unigenes), "response to chemical stimulus" (79 unigenes), "response to abiotic stimulus" (63 unigenes), "oxidation-reduction process" (51 unigenes), "response to biotic stimulus" (33 unigenes), or "response to other organism" (32 unigenes). GO terms included CATs [AU03-B01], proteins involved in the phenylpropanoid pathway (PAL [AU03-E02], reductase [AU01-H12], lactoperoxidase [AU02-F09; AU-C159], dehydrogenase [AU08-A06]) (**Figure 3**), ET biosynthesis (ACO [AU12-D10]) or terpenoids biosynthesis (reductoisomerase [AU-C168]), ACL (AU04-G10), linolenic acid metabolism (monoxygenase [AU05-F07], and LOXs [AU13-A01; AU13-A07]). In addition, we identified transcripts belonging to different classes of PR proteins such as thaumatin-like protein (PR-5) (AU04-G06) or PR protein STH2 (PR-10) (AU05-F04).

For the main GO vocabulary term MF 33 different categories could be identified for "level 3." The four main categories were "hydrolase activity" (58 unigenes, i.e., epoxide hydrolase 2-like [AU02-A10], raffinose synthase [AU03-E11]), tubby-like f-box protein 8-like [AU09-B03] or alpha beta hydrolase domain [AU-C51]) "ion binding" and "small molecule binding" (with 57 unigenes, i.e., LOXs [AU13-A01; AU13-A07], ACO [AU12-D10], nucleoside diphosphate kinase [AU12-B11] or serine hydroxymethyltransferase [AU13-E01]) and 54 unigenes, i.e., cysperoxiredoxin [AU02-F09], serine hydroxymethyltransferase [AU13-E01], or nucleoside diphosphate kinase [AU12-B11]) and "oxidoreductase activity" (37 unigenes, i.e., phosphoglycerate mutase [AU05-D07], ACO [AU12-D10], histidinol dehydrogenase [AU01-F08] or cytochrome p450 [AU08-E04]) (**Figure 2**, MF).

Finally, most of the unigenes identified for the main GO term vocabulary CC were assigned to: "cell part" (185 unigenes, i.e., protein ET insensitive [AU08-H12], phosphoribulokinase precursor [AU07-H02], CAT [AU03-B01], thiredoxin-like protein [AU02-C01], ribosomal protein s1 [AU04-C09]), "membrane-bounded organelle" (155 unigenes, i.e., loxc homolog [AU13-A01], cytochrome b6 [AU-C41], photosystem i reaction center subunit n [AU14-C11], nucleoporin autopeptidase [AU12-C08]), and "organelle part" (103 unigenes, i.e., auxin response factor 9 [AU01-H05], transcription factor bHLH 110-like [AU02-B01]) (**Figure 2**, CC).

TIME-COURSE OF EXPRESSION AND VALIDATION ANALYSIS OF SELECTED DEFENSE RESPONSE OLIVE GENES INDUCED BY STRAIN PICF7

A qRT-PCR time-course study was carried out to validate gene expression of five selected genes identified as induced in olive aerial tissues and present in the generated EST library: *ACO*

Table 3 | Putative protein functions identified in *Pseudomonas fluorescens* PICF7-induced EST sequences in both roots and aerial tissues of olive (*Olea europaea* L.).

Putative protein function	EST name sequence (root)	Accession number (root)	EST name sequence (aerial tissues)	Accesion number (aerial tissues)
blight-associated protein p12	ARBRI-4_T7_B03	EAZ09461	AU02-F12T7	ADG29118
phenylalanine ammonia-lyase	ARBRI-C73	BAA95629	AU02-E02T7	ABS58596
Catalase	ARBRI-C50, ARBRI-2_T7_C02, ARBRI-2_T7_C12, ARBRI-10_T7_B01	AAC19397, ABM47415, NP_001048861, CAB56850*	AU03-B01T7, AU06-H07T7	CBA13361, CAB56850*
glutamate decarboxylase	ARBRI-6_T7_E02	XP_002528515	AU04-A03T7	XP_003538378
thaumatin-like protein	ARBRI-C25	AAK59275	AU04-G06T7	ACZ57583
acetone cyanohydrin lyase	ARBRI-C140	AAR87711	AU04-G10T7	Q6RYA0
cytochrome p450	ARBRI-C12, ARBRI-C53, ARBRI-C103, ARBRI-6_T7_B02	P93531, ABC68413, CBI30225, CBI19610	AU09-G05T7, AU08-E04T7, AU02-H09T7	XP_003610581, AFS28690, AAZ07706
zinc finger	ARBRI-5_T7_A10, ARBRI-7_T7_H04	AAD02556, ABN08073	AU09-E09T7, AU08-B12T7	XP_002265999, XP_002336150
serine protease	ARBRI-C113	CAA07250*	AU11_H05T7	CAA07250*
beta-galactosidase	ARBRI-C68, ARBRI-4_T7_B06	ADV41669, ABN08770	AU12_A03T7	BAH03319
ubiquitin-like protein	ARBRI-4_T7_G02	XP_002866079	AU12_C05T7	AAZ82816
lipoxygenase	ARBRI-2_T7_F05	ACG56281	AU13_A07T7	ACD43484
nac domain ipr003441	ARBRI-1_T7_D12	XP_002512632	AU13_D11T7, AU04-B01T7	XP_002284654, AAM34770
serine hydroxymethyltransferase	ARBRI-C184	CBI17302	AU13_E01T7	ABS72016
glutamine synthetase	ARBRI-C29	AAK08103	AU14_E11T7	BAD94507
60s acidic ribosomal protein p0	ARBRI-C109	XP_002268645	AU-C208	ABB29933
superoxide dismutase	ARBRI-C52, ARBRI-7_T7_A02	ADX36104, CAE54085	AU-C109	AAO16563
cyclophilin	ARBRI-C70	ABS30424*	AU04-A01T7	ABS30424*
ring finger and chy zinc finger domain-containing protein	ARBRI-C157	AAD02556	AU01-B06T7	XP_002268193
f-box family protein	ARBRI-2_T7_H04	XP_002307387	AU01-G09T7	AAZ81591
glutathione s-transferase	ARBRI-3_T7_D07, ARBRI-6_T7_B12	XP_002328824, ADB85090	AU02-E11T7	P46423
cysteine proteinase precursor	ARBRI-C1	BAF46302	AU01-C03T7	ABK93575
phospholipase d	ARBRI-3_T7_E12	ACG63795	AU07-D08T7	AFK36876
ef hand family protein	ARBRI-8_T7_D07	XP_002319225*	AU01-G11T7	XP_002319225*
calmodulin	ARBRI-C191	NP_001131288	AU-C96	AAD10247
14-3-3 protein	ARBRI-1_T7_H06	AAY67798	AU11-F06T7	ADK93080

*Sequence names, putative protein functions and accession numbers are indicated. *ESTs identified with the same accession number in two different libraries (from roots and aerial tissues).*

[AU12-D10], *PAL* [AU03-E02], *CAT* [AU03-B01], *LOX-2* [AU13-A07], and *ACL* [AU04-G10]. Moreover, we aimed to analyze the gene expression pattern along time: i.e., at 1, 3, 7, and 15 DAI of strain PICF7 in olive roots.

qRT-PCR experiments validated the results from the generated SSH cDNA library for four (*ACO*, *PAL*, *CAT*, and *LOX-2*) of the five selected genes, although gene expression patterns varied along time (**Figure 4**). Linear equations, correlation coefficients (R^2) and PCR efficiencies for each case are shown in **Table 3**. The relative fold changes were assigned to three categories of up-regulation: high ($>+2$), medium ($>+1.0$ to $\leq+2.0$) and low (≥-1.0 to $\leq+1.0$), according to Kim et al. (2008).

Overall, results showed a decrease in the transcription level of the analyzed genes 3 days after PICF7 inoculation, and an increase 7 days after introducing the BCA in the olive root system (**Figure 4**). In three out of the five studied genes we observed up-regulation with maximal expression at 7 DAI, two of them (*PAL* and *CAT*) up-regulated at a high-level and one (*ACO*) at a medium-level (estimated fold change of PAL [+2.62], ACO [+1.93], and *CAT* [+2.57] log units compared with the control, non-bacterized samples) (**Figure 4**). The increase of *LOX-2* gene expression level was confirmed at 7 and 15 DAI ([+0.66] and [+1.84], respectively; **Figure 4**). Finally, up-regulation of the putative *ACL* gene could not be corroborated by qRT-PCR

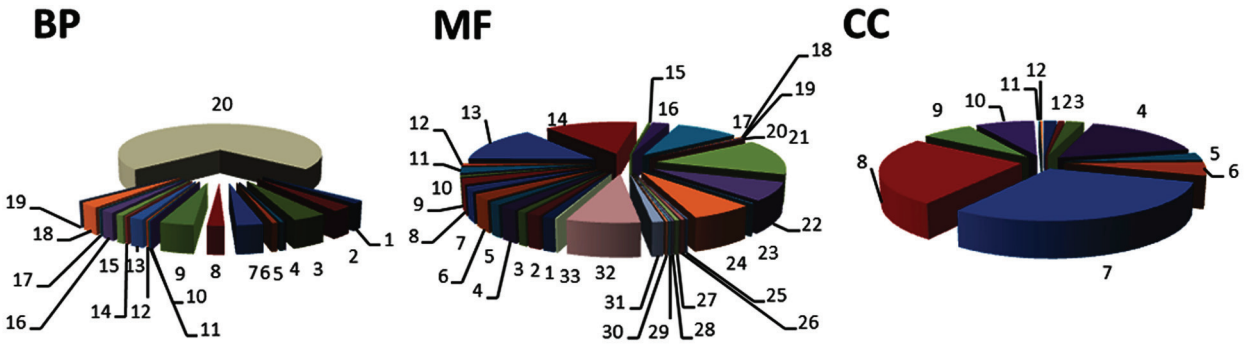

	Go Term BP	No. Unigenes
1	Response to endogenous stimulus	29
2	Cellular response to stimulus	53
3	Response to stress	81
4	Interspecies interaction	2
5	Cell death	10
6	Response to external stimulus	14
7	Response to abiotic stimulus	63
8	Cell communication	40
9	Response to chemical stimulus	79
10	Tropism	3
11	Immune effector process	3
12	Detection of stimulus	4
13	Response to biotic stimulus	33
14	Methylation	5
15	Immune response	19
16	Response to other organism	32
17	Hormone metabolic process	2
18	Oxidation-reduction process	51
19	Cell-cell signaling	2
20	Other	1310

	Go Term MF	No. Unigenes
1	Sequence DNA binding transcription factor activity	5
2	Signal transducer activity	6
3	Peroxidase activity	4
4	Isomerase activity	8
5	Ligase activity	6
6	Transmembrane transporter activity	11
7	Structural constituent of ribosome	9
8	Cofactor binding	10
9	Lipid binding	3
10	Enzyme inhibitor activity	1
11	Substrate-specific transporter activity	10
12	Carbohydrate binding	4
13	Ion binding	57
14	Small molecule binding	54
15	Electron transporter (cytochrome b6/f complex)	1
16	Tetrapyrrole binding	10
17	Oxidoreductase activity	37
18	Electron transporter (noncyclic electron transport)	1
19	Enzyme activator activity	1
20	Xenobiotic transporter activity	1
21	Hydrolase activity	58
22	Protein binding	30
23	Selenium binding	1
24	Nucleic acid binding	27
25	Chromatin binding	1
26	Superoxide dismutase activity	2
27	Metal cluster binding	2
28	Oxygen binding	1
29	Electron transporter (cyclic electron transport)	1
30	Pattern binding	1
31	Lyase activity	5
32	Transferase activity	31
33	Carboxylic acid binding	1

	Go Term CC	No. Unigenes
1	Cell-cell junction	11
2	Outer membrane	5
3	Apoplast	15
4	Organelle part	103
5	Vesicle	18
6	Non-membrane-bounded organelle	32
7	Cell part	185
8	Membrane-bounded organelle	155
9	Membrane part	43
10	Protein complex	49
11	Protein-DNA complex	1
12	Coated membrane	2

FIGURE 2 | "Level 3" Gene Ontology (GO) terms distribution of 376 unigenes induced in olive (*Olea europaea* L.) aerial tissues colonized by *Pseudomonas fluorescens* PICF7. Expressed Sequences Tags (ESTs) were categorized using the "Blast2GO" software according to the terms of the three main GO vocabularies: (BP) "biological processes," (MF) "molecular functions," and (CC) "cellular components." The category "Other" in the main GO vocabulary term "biological processes" clusters 1310 of the transcripts analyzed.

analysis, since this transcript showed a down regulation in all measured times (−0.14, −3.02, −1.24, and −2.80) (**Figure 4**).

DISCUSSION

Plants can deploy a range of chemical and physical defense barriers to minimize or overcome damages produced at the primary site where any given biotic and/or abiotic stress is acting. Because defense is metabolically costly, plants have evolved inducible defensive mechanisms that can be activated or amplified in response to stress (Walters and Heil, 2007). Specific signals can "prime" plant tissues, preparing them for an augmented response to confront future damage without direct activation of costly

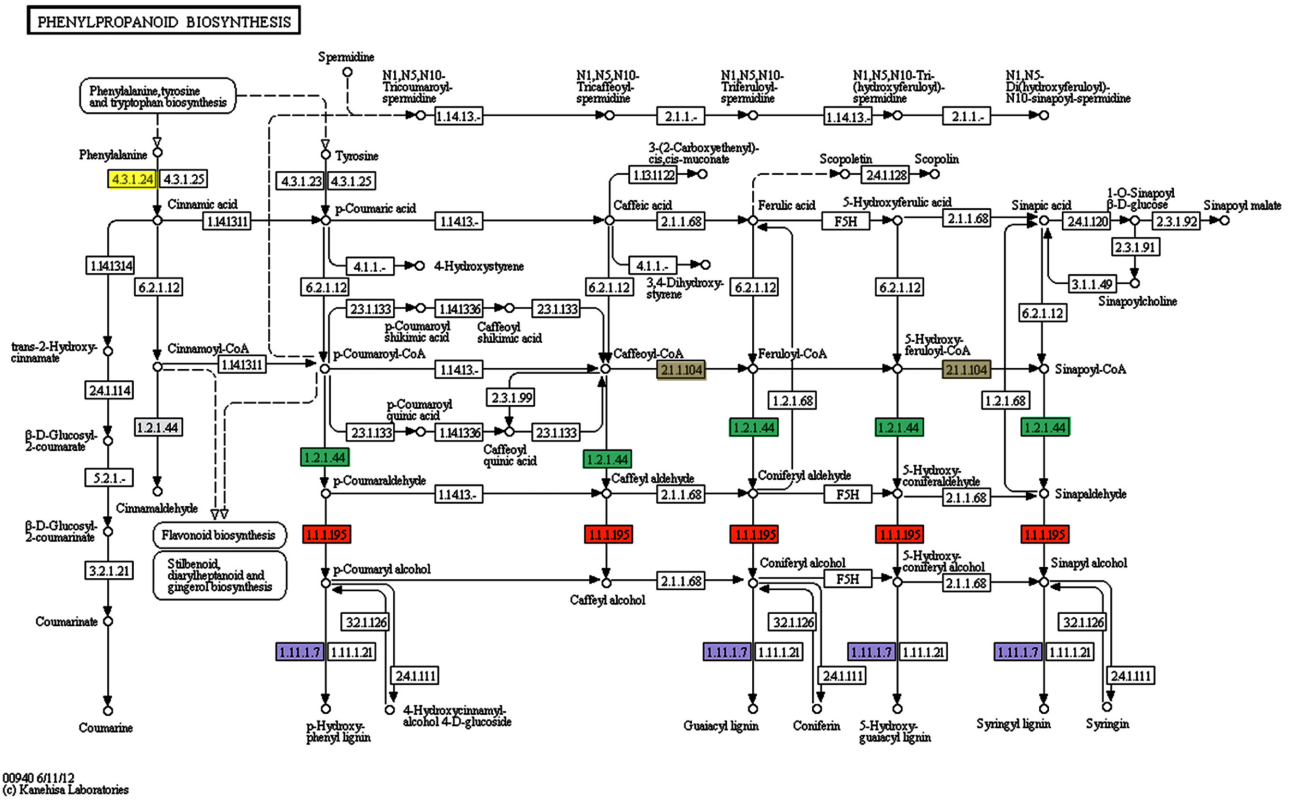

FIGURE 3 | Patway map from KEGG for the phenylpropanoid biosynthesis pathway. Several genes involved in this pathway have been found to be induced in olive roots (Schilirò et al., 2012) and/or aerial tissues (this study) upon *Pseudomonas fluorescens* PICF7 root inoculation. The enzymes reductase (1.2.1.44) (green rectangles) induced in aerial tissues, the cinnamyl-alcohol deydrogenase (1.1.1.95) (orange rectangles), the lactoperoxidase (1.11.1.7) (violet rectangles), the phenylalanine ammonia-lyase (4.3.1.5)* induced in roots and aerial tissues, and the caffeoyl-CoA Omethyltransferase (2.1.1.104) (gray rectangles) induced in roots, are mapped. *Phenylalanine ammonia-lyase (EC4.3.1.5) is now divided into three different enzymes: EC4.3.1.23 (tyrosine ammonia-lyase), EC4.3.1.24 (phenylalanine ammonia-lyase), and EC4.3.1.25 (phenylalanine/tyrosine ammonia-lyase) according to IUBMB Enzyme Nomenclature (http://www.chem.qmul.ac.uk/iubmb/enzyme/EC4/3/1/5.html). Yellow rectangle is phenylalanine ammonia-lyase.

defense mechanisms (Conrath, 2009; Jung et al., 2009). In addition, plants have developed countermeasures aimed to halt the dispersal of deleterious (micro)organisms therefore preventing further damage at distant parts (Gaupels and Vlot, 2012). On the other hand, beneficial soil-borne microorganisms, such as mycorrhizal fungi and PGPR, can induce systemic plant immunity (Van Loon et al., 1998; Pozo and Azcon-Aguilar, 2007; Zamioudis and Pieterse, 2012). Plants thus must deal with a broad range of microorganisms (deleterious and beneficial) that interact with them at any time thereby influencing their defense response (Van der Putten et al., 2001; Stout et al., 2006; Poelman et al., 2008). Hence, plants need efficient regulatory mechanisms to effectively adapt to different trophic interactions. In this scenario, crosstalk among hormone-signaling pathways provides plants a powerful regulatory potential to defend themselves against a range of invaders (Reymond and Farmer, 1998; Kunkel and Brooks, 2002; Bostock, 2005; Pieterse and Dicke, 2007; Pieterse et al., 2009).

A functional genomics study was conducted to shed light on potential systemic genetic responses taking place in aerial tissues during the interaction between the biocontrol endophyte *P. fluorescens* PICF7 and olive root tissues. Computational analysis revealed that 376 transcripts were induced upon PICF7 treatment, and that many of them were potentially involved in plant defense and response to different kind of stresses. This demonstrates that PICF7 is able to mount systemic defense responses at distant tissues from its natural colonization niche (roots). Strain PICF7 was previously shown to effectively colonized inner root tissues with no evidence of translocation to above-ground organs (Prieto and Mercado-Blanco, 2008; Prieto et al., 2009, 2011; Maldonado-González et al., 2013). Therefore, the effective biocontrol displayed by PICF7 against VWO (Mercado-Blanco et al., 2004; Prieto et al., 2009), which can be explained by the induction of defense response at the root level (Schilirò et al., 2012), seems also to operate systemically. Furthermore, some of the genes involved in defense response here reported were also up-regulated in root tissues (Schilirò et al., 2012). This suggests that strain PICF7 could potentially be an effective BCA against olive pathogens other that *V. dahliae* through an ISR mechanism. However, root inoculation of *in vitro*-propagated olive plants with PICF7 did not hinder olive knot (caused by *Pseudomonas savastanoi* pv. savastanoi) development in stems (Maldonado-González et al., 2013). Thus, while PICF7 is able to trigger a range

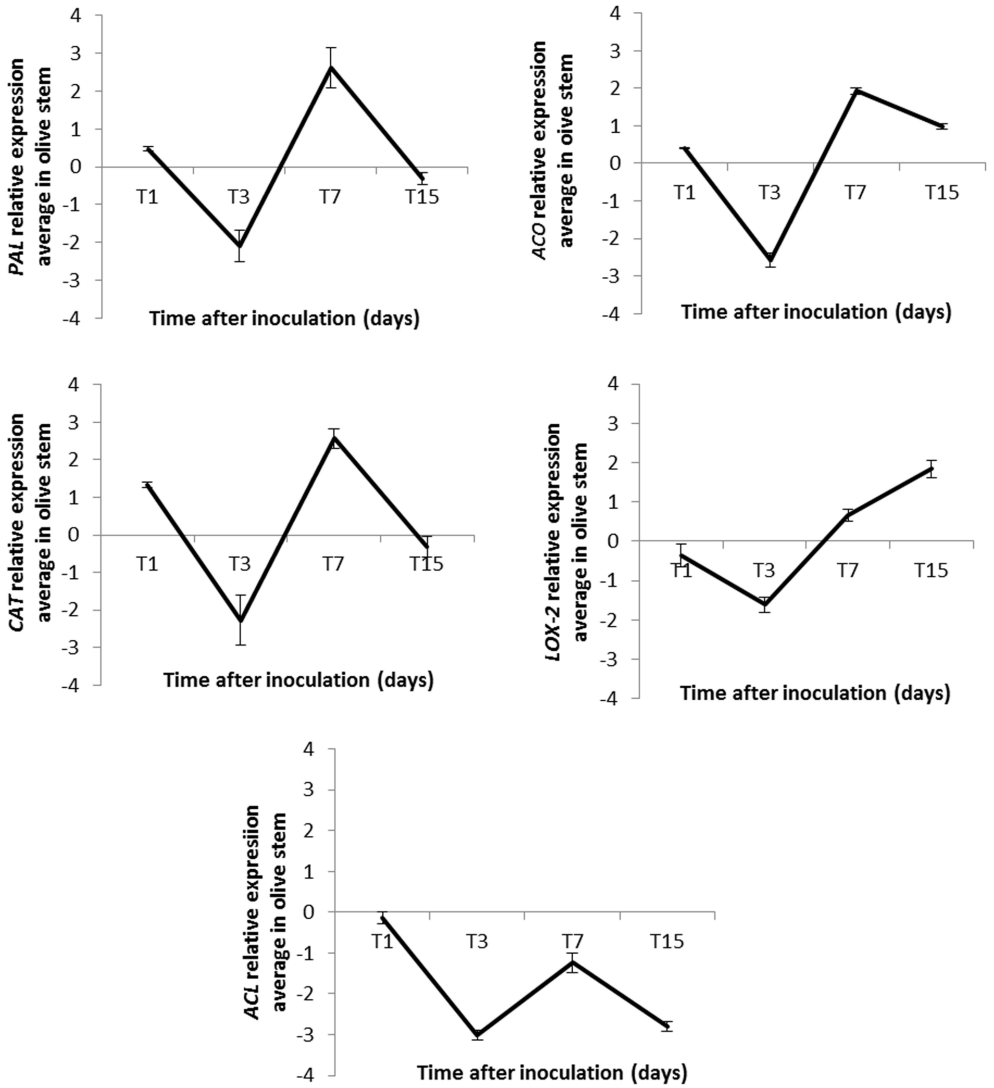

FIGURE 4 | Relative expression (RE) average of five genes identified as up-regulated in stems of inoculated "Arbequina" olive plants at different time points after *Pseudomonas fluorescens* PICF7 inoculation in roots. *PAL*, phenylananine ammonia-lyase; *ACO*, 1-aminocyclopropane-1-carboxylate oxidase; *CAT*, catalase; *LOX-2*, lipoxygenase 2; *ACL*, acetone cyanohydrin lyase. Error bars represent the STD from at least two independent experiments. RE values ($\log_2$ fold-change values) were calculated according to the $2^{-\Delta\Delta Ct}$ method (Livak and Schmittgen, 2001).

of systemic defense responses, they seem to be ineffective at least against this phytopathogenic bacterium.

Our results indicated that, among others, genes involved in plant hormones and phenylpropanoids biosynthesis (i.e., *PAL*, *ACL*, *LOX-2*, etc.), oxidative stress (*CAT*), and Ca^{2+} metabolism (CaM, glutamate descarboxylase, or an ef hand family protein) implicated in systemic defensive responses are induced in aerial olive tissues during the interaction of PICF7 with olive roots. Besides, several transcription factors related to plant defense were found as up-regulated, i.e., JERF [implicated in regulation of plant stress and response to fungal disease attack (Zhang et al., 2004)], WRKY [global regulators of host responses following challenge by phytopathogenic organisms (Pandey and Somssich, 2009)], and bHLH [involved in response to pathogen (Van Verk et al., 2009)]. Among the ample set of transcripts found to be up-regulated in the generated SSH library, we selected for validation purpose and to assess expression pattern along time five genes related with plant defense responses. ACC oxidase (ACO) catalyzes the final step in the biosynthesis of ET, known as the "stress hormone" which is regulated by diverse environmental factors, including (a)biotic stresses (Wang et al., 2002). For instance, *ACO* mRNA levels, as well as ACO activity, can be elevated under phytopathogen attacks (Díaz et al., 2002; Iwai et al., 2006). Moreover, it has been proved that *ACO* gene silencing can affect the susceptible host response to pathogen (Shan and Goodwin, 2006). Our results indicate that a putative olive *ACO* [AU12-D10] was moderately up-regulated in aerial tissues upon root colonization by PICF7, suggesting an ET-mediated systemic defense response

triggered when a beneficial bacterial endophyte is introduced in the root system.

CATs are involved in decomposition of H_2O_2 into H_2O and O_2. A close interaction has been reported between intracellular H_2O_2 and cytosolic Ca^{2+} concentration in response to both biotic and abiotic stresses (Rudd and Franklin-Tong, 2001; Yang and Poovaiah, 2002; White and Broadley, 2003). These studies indicate that an increase in cytosolic Ca^{2+} boosts the generation of H_2O_2. The Ca^{2+}-binding protein CaM activates some plant CATs in the presence of Ca^{2+}. Yang and Poovaiah (2002) proposed that increased cytosolic Ca^{2+} has a dual role. For positive regulation, extracellular signals trigger an influx of Ca^{2+} which increases H_2O_2 levels; for negative regulation, Ca^{2+} binds to CaM, and this complex stimulates CAT activity leading to the rapid degradation of H_2O_2. The increase in H_2O_2 can enhance the Ca^{2+} influx by activating the Ca^{2+} channel (Pei et al., 2000). Our results showed that a putative olive *CAT* [AU03-B01] was highly induced (+2.57) at 7 DAI. Besides, a *CAT* gene (same accession number) was also up-regulated in olive roots (Schilirò et al., 2012). Interestingly, CaM and other Ca^{2+}-related proteins have been found to be induced in olive aerial tissues as well (i.e., CaM [AU-C96], ef hand family protein [AU01-G11] and calreticulin [AU02-C02]). This suggests that the complex Ca^{2+}/CaM can decrease H_2O_2 levels in plants by stimulating CATs activities and hence their possible role in plant defense responses (Yang and Poovaiah, 2002). It might well be that olive plants first react (even systemically) to the invasion of PICF7 by the induction of *CAT*. However, this response seems to be attenuated at later times (15 DAI). It is tempting to speculate that the decrease in *CAT* expression (also observed for other validated genes) could be due to the fact that this endophytic bacterium is eventually recognized by the host plant as a non-hostile microorganism, enabling its endurance inside the plant. Alternatively, strain PICF7 might counteract this defense response by deploying an as yet unidentified mechanism(s).

The activation of systemic resistance by non-pathogenic rhizobacteria has been also associated with the induction of LOX activity in plants such as bean (*Phaseolus vulgaris* L.) and tomato (*Solanum lycopersicum* Mill) (Blée, 2002; Silva et al., 2004; Ongena et al., 2007). Plant LOX catalyzes incorporation of O_2 in polyunsaturated fatty acids to yield the corresponding fatty acid hydroperoxides. These are related to substrates for other enzymes leading to the production of JAs involved in signaling events and regulation of plant defense gene expression (Feussner and Wasternack, 2002; Shah, 2005). A putative olive *LOX-2* [AU13-A07], involved in linolenic acid metabolism (Siedow, 1991), was found to be up-regulated at latter times after bacterization (15 DAI, +1.84). Another *LOX*, implicated in JA biosynthesis, was found to be up-regulated in olive roots (Schilirò et al., 2012). This fact further supports the possible role of PICF7 in triggering olive defense response not only in roots but also in above-ground tissues.

A putative olive *ACL* [AU04-G10] was found to be induced in aerial tissues by the SSH approach implemented in this study. Up regulation of *ACL* was previously reported in root tissues upon strain PICF7 colonization (Schilirò et al., 2012). Therefore, ACL activity seems to be induced at both local and systemic levels in olive plants when interacting with PICF7. This enzyme is involved in the catabolism of cyanogenic glycosides (Trummler and Wajant, 1997) which play pivotal roles in the organization of chemical defense systems in plants against pathogens and herbivores and in plant-insect interactions (Ganjewala et al., 2010). However, induction of *ACL* [AU04-G10] was not validated at the time points checked by qRT-PCR experiments. A possible explanation for this outcome is that *ACL* is induced in a very transient way and/or at very specific time points other than those assessed in this study.

The expression pattern of a gene coding for a putative olive *PAL* [AU03-E02] was also evaluated. *PAL* genes can be induced by wounding, low temperature, pathogen attack, and other stress conditions (Collinge and Slusarenko, 1987; Wu and Lin, 2002), and activation of the phenylpropanoids pathway in plants is linked to diverse stress situations (Gómez-Vásquez et al., 2004). The induction of the *PAL* gene [both in roots (Schilirò et al., 2012) and aerial tissues(this study)] in olive upon PICF7 treatment suggests that this defense response pathway, as others analyzed in this study, is a consequence of PICF7 colonization being recognized as a stressful situation by the host plant, at least transiently (maximum relative expression at 7 DAI, +2.62). On the other hand, PAL activation can play a role in biocontrol activity displayed by strain PICF7, as reported for other plant-endophyte interactions (Benhamou et al., 1996a,b; Ramamoorthy et al., 2002).

Our previous results have shown that root colonization by PICF7 induced a broad range of defense response genes in root tissues (Schilirò et al., 2012). This present study demonstrates that many of these responses are also systemically up-regulated in aerial tissues: genes involved in plant hormones and phenylpropanoids biosynthesis, PR proteins, and several transcription factors involved in systemic defensive responses. In fact, 26 up-regulated transcripts detected in aerial tissues were annotated with the same putative function than that of genes induced in olive roots upon PICF7 colonization (i.e., PAL, ACL, CAT, LOX, 14-3-3 protein, CaM, thaumatin-like protein, etc.) (**Table 3**). Our study therefore provides a database of differentially-expressed transcripts deserving future research. It constitutes an excellent starting point for in-depth genetic analysis to further characterize the interaction between plants and beneficial bacterial endophytes. Some genes could possibly constitute specific markers distinguishing this type of plant-microbe interaction from other trophic scenarios such as plant-pathogen and/or plant-symbiont interactions. Alternatively, commonalities among these interactions could also be uncovered. For instance, a putative gene coding for a 14-3-3 protein was found to be up regulated in both roots (Schilirò et al., 2012) and aerial tissues (this study) upon PICF7 root colonization (**Table 3**). Manosalva et al. (2011) have reported that a rice 14-3-3 protein (GF14e) negatively affected the induction of plant defense response genes, cell death and disease resistance in this host. It would be interesting to investigate whether the induction of this gene in olive might contribute to facilitate endophytic colonization by PICF7 because of defense responses mediated by SA or reactive oxygen species (as cell death or SAR) are being attenuated by this protein.

Interestingly enough, all transcripts evaluated by qRT-PCR showed a decrease in their relative expression at 3 DAI and an increase at 7 DAI. We do not have a clear answer for this fluctuation. Without ruling out other explanations, a possible reason could be that plants were not exposed to a complete day-light period along the first 5 days of the bioassay. Indeed, in order to protect plants from excessive light stress after uprooting, cleaning and inoculation procedures, the day–night cycle was progressively applied until reaching the complete 14-h photoperiod (see Materials and Methods). Little is known about how external abiotic factors, for instance light exposure and intensity, can influence the ability of plants to defend from biotic stresses. A few reports point to a light dependency of distinct defense responses in different systems (Graham and Graham, 1996; Asai et al., 2000; Brodersen et al., 2002). Zeier et al. (2004) reported that whereas *PAL* transcripts accumulated in Arabidopsis leaves 2–6 h post infection with *P. syringae* pv. maculicola (avrRpm1) under medium or high light conditions, they failed to do so at dark. Therefore, light (duration and intensity) could play an important regulatory role influencing disease resistance responses. On the other hand, the observed overall increase in transcripts level at 7 DAI could be related to the moment in which plant defense responses here analyzed reached their maximum expression level in aerial tissues in response to root bacterial colonization. The subsequent decrease observed at 15 DAI could indicate that the presence of this endophytic bacterium in roots is somehow recognized as "non-hostile." Therefore, initially-induced defense responses are eventually modulated/attenuated allowing the establishment of this beneficial association, as reported elsewhere (Plucani do Amaral et al., 2014).

In summary, we have demonstrated that PICF7 is able to activate an array of defense pathways not only in olive root tissues (Schilirò et al., 2012) but also at distant parts of the plant. This is one of the first studies demonstrating that root colonization by a beneficial endophyte triggers systemic responses. Moreover, this has been accomplished in a woody plant such as olive and using non-gnotobiotic conditions. On the one hand, our functional genomics approach can shed light on how the plant broadly and systemically respond to a specific interaction (i.e., colonization by a beneficial endophytic bacterium), a trophic scenario poorly investigated within plant-microbe interactions studies. Olive plants seem to react to a "non-hostile" colonization by deploying several defense responses that eventually must be modulated or attenuated to ensure penetration, colonization, and survival of PICF7 cells inside root tissues. Alternatively, PICF7 can also be able to counteract these responses by specific, unidentified traits enabling this bacterium to be recognized as a harmless invader. On the other hand, the genetic responses triggered by PICF7, even at distant tissues, may explain its biocontrol activity. How effective and durable are these responses and what are the bacterial traits involved in the endophytic lifestyle of PICF7 are matters of ongoing studies.

ACKNOWLEDGMENTS

Research supported by grants P07-CVI-02624 and P12-AGR-667 from Junta de Andalucía (Spain) and AGL2009-07275 from Spanish MICINN/MINECO, both co-financed by The European Regional Development Fund of the European Union.

SUPPLEMENTARY MATERIAL

The Supplementary Material for this article can be found online at: http://www.frontiersin.org/journal/10.3389/fmicb.2014.00427/abstract

REFERENCES

Altschul, S. F., Gish, W., Miller, W., Myers, E. W., and Lipman, D. J. (1990). Basic local alignment search tool. *J. Mol. Biol.* 215, 403–410. doi: 10.1016/S0022-2836(05)80360-2

Andreu, A., Guevara, M., Wolski, E., Daleol, G., and Caldiz, D. (2006). Enhancement of natural disease resistance in potatoes by chemicals. *Pest Manag. Sci.* 62, 162–170. doi: 10.1002/ps.1142

Asai, T., Stone, J. M., Heard, J. E., Kovtun, Y., Yorgey, P., Sheen, J., et al. (2000). Fumonisin B1-induced cell death in Arabidopsis protoplasts requires jasmonate-, ethylene-, and salicylate-dependent signaling pathways. *Plant Cell* 12, 1823–1836. doi: 10.1105/tpc.12.10.1823

Asif, M. H., Dhawan, P., and Nath, P. (2000). A simple procedure for the isolation of high quality RNA from ripening banana fruit. *Plant Mol. Biol. Rep.* 18, 109–115. doi: 10.1007/BF02824018

Bakker, P. A. H. M., Pieterse, C. M. J., and Van Loon, L. C. (2007). Induced systemic resistance by fluorescent *Pseudomonas* spp. *Phytopathology* 97, 239–243. doi: 10.1094/PHYTO-97-2-0239

Barranco, D., Fernández-Escobar, R., and Rallo, L. (2008). *El Cultivo del Olivo*. Madrid: Ediciones Mundi-Prensa y Junta de Andalucía.

Beneduzi, A., Ambrosini, A., and Passaglia, L. M. P. (2012). Plant growth-promoting rhizobacteria (PGPR): their potential as antagonists and biocontrol agents. *Genet. Mol. Biol.* 35, 1044–1051. doi: 10.1590/S1415-47572012000600020

Benhamou, N., Bélanger, R. R., and Paulitz, T. C. (1996b). Induction of differential host responses by *Pseudomonas fluorescens* in Ri T-DNA-transformed pea roots after challenge with *Fusarium oxysporum* f. sp. pisi and Pythium ultimum. *Phytopathology* 86, 1174–1185. doi: 10.1094/Phyto-86-1174

Benhamou, N., Kloepper, J. W., Quadt-Hallmann, A., and Tuzun, S. (1996a). Induction of defense-related ultrastructural modification in pea root tissues inoculated with endophytic bacteria. *Plant Physiol.* 112, 919–929.

Blée, E. (2002). Impact of phyto-oxylipins in plant defense. *Trends Plant Sci.* 7, 315–322. doi: 10.1016/S1360-1385(02)02290-2

Bordiec, S., Paquis, S., Lacroix, H., Dhondt, S., Ait Barka, E., Kauffmann, S., et al. (2010). Comparative analysis of defence responses induced by the endophytic plant growth-promoting rhizobacterium *Burkholderia phytofirmans* strain PsJN and the non-host bacterium *Pseudomonas syringae* pv. pisi in grapevine cell suspensions. *J. Exp. Bot.* 62, 595–603. doi: 10.1093/jxb/erq291

Bostock, R. M. (2005). Signal crosstalk and induced resistance: straddling the line between cost and benefit. *Annu. Rev. Phytopathol.* 43, 545–580. doi: 10.1146/annurev.phyto.41.052002.095505

Brodersen, P., Petersen, M., Pike, H. N., Olszak, B., Skov-Petersen, S., Oedum, N., et al. (2002). Knockout of Arabidopsis Accelerated-cell-death11 encoding a sphingosine transfer protein causes activation of programmed cell death and defense. *Genes Dev.* 16, 490–502. doi: 10.1101/gad.218202

Caballero, J. M., and del Río, C. (2008). "Métodos de multiplicación," in *El Cultivo del Olivo*, *6th Edn.*, eds D. Barranco, R. Fernández-Escobar, and L. Rallo (Madrid: Junta de Andalucía and Ediciones Mundi-Prensa), 93–125.

Collinge, D. B., and Slusarenko, A. J. (1987). Plant gene expression in response to pathogens. *Plant Mol. Biol.* 9, 389–410. doi: 10.1007/BF00014913

Conesa, A., Götz, S., Garcia-Gomez, J. M., Terol, J., Talon, M., and Robles, M. (2005). Blast2GO: a universal tool for annotation, visualization and analysis in functional genomics research. *Bioinformatics* 21, 3674–3676. doi: 10.1093/bioinformatics/bti610

Conn, V. M., Walker, A. R., and Franco, C. M. M. (2008). Endophytic actinobacteria induce defense pathways in *Arabidopsis thaliana*. *Mol. Plant Microb. Interact.* 21, 208–218. doi: 10.1094/MPMI-21-2-0208

Connor, D. J., Gómez-del-Campo, M., Rousseaux, M. C., and Searles, P. S. (2014). Structure, management and productivity of hedgerow olive orchards. A review. *Sci. Hortic.* 169, 71–93. doi: 10.1016/j.scienta.2014.02.010

Conrath, U. (2009). "Priming of induced plant defence responses," in *Advances in Botanical Research*, ed L. C. Van Loon (Oxford: Elsevier), 361–395.

Day, I. S., Reddy, V. S., Ali, G. S., and Reddy, A. S. (2002). Analysis of EFhand-containing proteins in Arabidopsis. *Genome Biol.* 3:RESEARCH0056. doi: 10.1186/gb-2002-3-10-research0056

Diatchenko, L., Lau, Y. F., Campbell, A. P., Chenchik, A., Moqadam, F., Huang, B., et al. (1996). Suppression subtractive hybridization: a method for generating differentially regulated or tissue-specific cDNA probes and libraries. *Proc. Natl. Acad. Sci. U.S.A.* 9, 6025–6030. doi: 10.1073/pnas.93.12.6025

Díaz, J., ten Have, A., and van Kan, J. A. L. (2002). The role of ethylene and wound signaling in resistance of tomato to *Botrytis cinerea*. *Plant Physiol.* 129, 1341–1351. doi: 10.1104/pp.001453

Durrant, W. E., and Dong, X. (2004). Systemic acquired resistance. *Annu. Rev. Phytopathol.* 42, 185–209. doi: 10.1146/annurev.phyto.42.040803.140421

Feussner, I., and Wasternack, C. (2002). The lipoxygenase pathway. *Annu. Rev. Plant Biol.* 53, 275–297. doi: 10.1146/annurev.arplant.53.100301.135248

Ganjewala, D., Kumar, S., Devi, S. A., and Ambika, K. (2010). Advances in cyanogenic glycosides biosynthesis and analyses in plants: a review. *Acta Biol. Szeged.* 54, 1–14.

Gaupels, F., and Vlot, A. C. (2012). "Plant defense and long-distance signaling in the phloem," in *Phloem: Molecular Cell Biology, Systemic Communication, Biotic Interactions*, eds G. A. Thompson and A. J. E. Van Bel (Hoboken, NJ: Wiley-Blackwell), 227–247. doi: 10.1002/9781118382806.ch11

Gómez-Vásquez, R., Day, R., Bushmann, H., Randles, S., Beeching, J. R., and Cooper, R. M. (2004). Phenylpropanoids, phenylalanine ammonia lyase and peroxidases in elicitor-challenged cassava (*Manihot esculenta*) suspension cells and leaves. *Ann. Bot.* 94, 87–97. doi: 10.1093/aob/mch107

Graham, T. L., and Graham, M. Y. (1996). Signaling in soybean phenylpropanoid responses (dissection of primary, secondary, and conditioning effects of light, wounding, and elicitor treatments). *Plant Physiol.* 110, 1123–1133.

Hardoim, P. R., van Overbeek, L. S., and van Elsas, J. D. (2008). Properties of bacterial endophytes and their proposed role in plant growth. *Trends Microbiol.* 16, 463–471. doi: 10.1016/j.tim.2008.07.008

Iwai, T., Miyasaka, A., Seo, S., and Ohashi, Y. (2006). Contribution of ethylene biosynthesis for resistance to blast fungus infection in young rice plants. *Plant Physiol.* 142, 1202–1215. doi: 10.1104/pp.106.085258

Jung, H. W., Tschaplinski, T. J., Wang, L., Glazebrook, J., and Greenberg, J. T. (2009). Priming in systemic plant immunity. *Science* 324, 89–91. doi: 10.1126/science.1170025

Kim, J. H., Yu, J., Mahoney, N., Chan, K. L., Molyneux, R. J., Varga, J., et al. (2008). Elucidation of the functional genomics of antioxidant-based inhibition of aflatoxin biosynthesis. *Int. J. Food Microbiol.* 122, 49–60. doi: 10.1016/j.ijfoodmicro.2007.11.058

Kunkel, B. N., and Brooks, D. M. (2002). Cross talk between signaling pathways in pathogen defense. *Curr. Opin. Plant Biol.* 5, 325–331. doi: 10.1016/S1369-5266(02)00275-3

Livak, K. J., and Schmittgen, T. D. (2001). Analysis of relative gene expression data using real-time quantitative PCR and the $2^{-\Delta\Delta Ct}$. *Methods* 25, 402–408. doi: 10.1006/meth.2001.1262

López-Escudero, F. J., and Mercado-Blanco, J. (2011). Verticillium wilt of olive: a case study to implement an integrated strategy to control a soil-borne pathogen. *Plant Soil* 344, 1–50. doi: 10.1007/s11104-010-0629-2

Maldonado-González, M. M., Prieto, P., Ramos, C., and Mercado-Blanco, J. (2013). From the root to the stem, interaction between the biocontrol root endophyte *Pseudomonas fluorescens* PICF7 and the pathogen *Pseudomonas savastanoi* NCPPB 3335 in olive knots. *Microb. Biotechnol.* 6, 275–287. doi: 10.1111/1751-7915.12036

Manosalva, P. M., Bruce, M., and Leach, J. E. (2011). Rice 14-3-3 protein (GF14e) negatively affects cell death and disease resistance. *Plant J.* 68, 777–787. doi: 10.1111/j.1365-313X.2011.04728.x

Mercado-Blanco, J., and Lugtenberg, B. J. J. (2014). Biotechnological applications of bacterial endophytes. *Curr. Biotechnol.* 3, 60–75. doi: 10.2174/2211550113026660038

Mercado-Blanco, J., Rodríguez-Jurado, D., Hervás, A., and Jiménez-Díaz, R. M. (2004). Suppression of Verticillium wilt in olive planting stocks by root-associated fluorescent *Pseudomonas* spp. *Biol. Control.* 30, 474–486. doi: 10.1016/j.biocontrol.2004.02.002

Navarro, C., and Parra, M. A. (2008). "Plantación," in *El cultivo del olivo*, eds D. Barranco, R. Fernández-Escobar, and L. Rallo (Madrid: Ediciones Mundi-Prensa y Junta de Andalucía), 189–238.

Ongena, M., Jourdan, E., Adam, A., Paquot, M., Brans, A., Joris, B., et al. (2007). Surfactin and fengycin lipopeptides of *Bacillus subtilis* as elicitors of induced systemic resistance in plants. *Environ. Microbiol.* 9, 1084–1090. doi: 10.1111/j.1462-2920.2006.01202.x

Pandey, S. P., and Somssich, I. E. (2009). The role of WRKY transcription factors in plant immunity. *Plant Physiol.* 150, 1648–1655. doi: 10.1104/pp.109.138990

Pauwels, E. K. J. (2011). The protective effect of the Mediterranean diet: focus on cancer and cardiovascular risk. *Med. Princ. Pract.* 20, 103–111. doi: 10.1159/000321197

Pei, Z. M., Murata, Y., Benning, G., Thomine, S., Klusener, B., Allen, G. J., et al. (2000). Calcium channel activated by hydrogen peroxide mediated abscisic acid signalling in guard cells. *Nature* 406, 731–734. doi: 10.1038/35021067

Pieterse, C. M. J., and Dicke, M. (2007). Plant interactions with microbes and insects: from molecular mechanisms to ecology. *Trends Plant Sci.* 12, 564–569. doi: 10.1016/j.tplants.2007.09.004

Pieterse, C. M. J., Leon-Reyes, A., Van der Ent, S., and Van Wees, S. C. M. (2009). Networking by small-molecule hormones in plant immunity. *Nat. Chem. Biol.* 5, 308–316. doi: 10.1038/nchembio.164

Pieterse, C. M. J., van der Does, D., Zamioudis, C., Leon-Reyes, A., and van Wees, S. C. M. (2012). Hormonal modulation of plant immunity. *Annu. Rev. Cell Dev. Biol.* 28, 489–521. doi: 10.1146/annurev-cellbio-092910-154055

Plucani do Amaral, F., Cavalheiro, J., Slahl, V., and Maisonnave, A. C., (2014). Gene expression analysis of maize seedlings (DKB240 variety) inoculated with plant growth promoting bacterium *Herbaspirillum seropedicae*. *Symbiosis* 62, 41–50. doi: 10.1007/s13199-014-0270-6

Poelman, E. H., Van Loon, J. J. A., and Dicke, M. (2008). Consequences of variation in plant defense for biodiversity at higher trophic levels. *Trends Plant Sci.* 13, 534–541. doi: 10.1016/j.tplants.2008.08.003

Pozo, M. J., and Azcon-Aguilar, C. (2007). Unraveling mycorrhiza-induced resistance. *Curr. Opin. Plant Biol.* 10, 393–398. doi: 10.1016/j.pbi.2007.05.004

Prieto, P., and Mercado-Blanco, J. (2008). Endophytic colonization of olive roots by the biocontrol strain *Pseudomonas fluorescens* PICF7. *FEMS Microb. Ecol.* 64, 297–306. doi: 10.1111/j.1574-6941.2008.00450.x

Prieto, P., Navarro-Raya, C., Valverde-Corredor, A., Amyotte, S. G., Dobinson, K. F., and Mercado-Blanco, J. (2009). Colonization process of olive tissues by Verticillium dahliae and its in planta interaction with the biocontrol root endophyte *Pseudomonas fluorescens* PICF7. *Microb. Biotechnol.* 2, 499–511. doi: 10.1111/j.1751-7915.2009.00105.x

Prieto, P., Schilirò, E., Maldonado-González, M. M., Valderrama, R., Barroso-Albarracín, J. B., and Mercado-Blanco, J. (2011). Root hairs play a key role in the endophytic colonization of olive roots by *Pseudomonas* spp. with biocontrol activity. *Microb. Ecol.* 62, 435–445. doi: 10.1007/s00248-011-9827-6

Rallo, G., Agnese, C., Minacapilli, M., and Provenzano, G. (2012). Comparison of SWAP and FAO agro-hydrological models to schedule irrigation of wine grapes. *J. Irrig. Drain. Eng.* 138, 581–591. doi: 10.1061/(ASCE)IR.1943-4774.0000435

Ramamoorthy, V., Raguchander, T., and Samiyappan, R. (2002). Induction of defense related proteins in tomato roots treated with *Pseudomonas fluorescens* Pf1 and *Fusarium oxysporum* f. sp. *lycopersici*. *Plant Soil* 239, 55–68. doi: 10.1023/A:1014904815352

Ramamoorthy, V., Viswanathan, R., Raguchander, T., Prakasam, V., and Samiyappan, R. (2001). Induction of systemic resistance by plant growth promoting rhizobacteria in crop plants against pests and diseases. *Crop Prot.* 20, 1–11. doi: 10.1016/S0261-2194(00)00056-9

Reinhold-Hurek, B., and Hurek, T. (2011). Living inside plants: bacterial endophytes. *Curr. Opin. Plant Biol.* 14, 1–9. doi: 10.1016/j.pbi.2011.04.004

Reymond, P., and Farmer, E. E. (1998). Jasmonate and salicylate as global signals for defense gene expression. *Curr. Opin. Plant Biol.* 1, 404–411. doi: 10.1016/S1369-5266(98)80264-1

Romano, P. G. N., Horton, P., and Gray, J. E. (2004). The Arabidopsis cyclophilin gene family. *Plant Physiol.* 134, 1268–1282. doi: 10.1104/pp.103.022160

Rosenblueth, M., and Martínez-Romero, E. (2006). Bacterial endophytes and their interactions with hosts. *Mol. Plant-Microbe Interact.* 19, 827–837. doi: 10.1094/MPMI-19-0827

Rudd, J. J., and Franklin-Tong, V. E. (2001). Unravelling response-specificity in Ca^{2+}signalling pathways in plant cells. *New Phytol.* 151, 7–33. doi: 10.1046/j.1469-8137.2001.00173.x

Schilirò, E., Ferrara, M., Nigro, F., and Mercado-Blanco, J. (2012). Genetic responses induced in olive roots upon colonization by the biocontrol endophytic bacterium *Pseudomonas fluorescens* PICF7. *PLoS ONE* 7:e48646. doi: 10.1371/journal.pone.0048646

Sena, A. P. A., Chaibub, A. A., Côrtes, M. V. C. B., Silva, G. B., Silva-Lobo, V. L., Prabhu, A. S., et al. (2013). Increased enzymatic activity in rice leaf blast suppression by crude extract of *Epicoccum* sp. *Trop. Plant Pathol*. 38, 387–397. doi: 10.1590/S1982-56762013005000028

Shah, J. (2005). Lipids, lipases, and lipid-modifying enzymes in plant disease resistance. *Annu. Rev. Phytopathol*. 43, 229–260. doi: 10.1146/annurev.phyto.43.040204.135951

Shan, X. C., and Goodwin, P. H. (2006). Silencing an ACC oxidase gene affects the susceptible host response of *Nicotiana benthamiana* to infection by *Colletotrichum orbiculare. Plant Cell Rep*. 25, 241–247. doi: 10.1007/s00299-005-0063-8

Siedow, J. N. (1991). Plant lipoxygenase: structure and function. *Annu. Rev. Plant Physiol. Plant Mol. Biol.* 42, 145–188. doi: 10.1146/annurev.pp.42.060191.001045

Silva, H. S. A., Romeiro, R. D. S., Macagnan, D., Halfeld-Vieira, B. D. A., Pereira, M. C. B., and Mounteer, A. (2004). Rhizobacterial induction of systemic resistance in tomato plants: non-specific protection and increase in enzyme activities. *Biol. Control*. 29, 288–295. doi: 10.1016/S1049-9644(03)00163-4

Stout, M. J., Thaler, J. S., and Thomma, B. P. H. J. (2006). Plant-mediated interactions between pathogenic microorganisms and herbivorous arthropods. *Annu. Rev. Entomol.* 51, 663–689. doi: 10.1146/annurev.ento.51.110104.151117

Tjamos, E. C. (1993). Prospects and strategies in controlling Verticillium wilt of olive. *Bull. OEPP/EPPO Bull.* 23, 505–512. doi: 10.1111/j.1365-2338.1993.tb01361.x

Trummler, K., and Wajant, H. (1997). Molecular cloning of acetone cyanohydrin lyase from flax (*Linum usitatissimum*). Definition of a novel class of hydroxynitrile lyases. *J. Biol. Chem.* 272, 4770–4774. doi: 10.1074/jbc.272.8.4770

Vacheron, J., Desbrosses, G., Bouffaud, M. L., Touraine, B., Moënne-Loccoz, Y., Muller, D., et al. (2013). Plant growth-promoting rhizobacteria and root system functioning. *Front. Plant Sci.* 4:356. doi: 10.3389/fpls.2013.00356

Van der Putten, W. H., Vet, L. E. M., Harvey, J. A., and Wäckers, F. L. (2001). Linking above- and belowground multitrophic interactions of plants, herbivores, pathogens, and their antagonists. *Trends Ecol. Evol.* 16, 547–554. doi: 10.1016/S0169-5347(01)02265-0

Van Loon, L. C. (2007). Plant response to plant-growth-promoting rhizobacteria. *Eur. J. Plant Pathol*. 119, 243–254. doi: 10.1007/s10658-007-9165-1

Van Loon, L. C., Bakker, P. A. H. M., and Pieterse, C. M. J. (1998). Systemic resistance induced by rhizosphere bacteria. *Ann. Rev. Phytopathol.* 36, 453–483. doi: 10.1146/annurev.phyto.36.1.453

Van Verk, M. C., Gatz, C., and Linthorst, H. J. M. (2009). "Transcriptional regulation of plant defense responses," in *Advances in Botanical Research*, ed L. C. Van Loon (Oxford: Academic Press), 397–438.

Walters, D., and Heil, M. (2007). Costs and trade-offs associated with induced resistance. *Physiol. Mol. Plant Pathol*. 71, 3–17. doi: 10.1016/j.pmpp.2007.09.008

Wang, K. L., Li, H., and Ecker, J. R. (2002). Ethylene biosynthesis and signaling networks. *Plant Cell*. 14, S131–S151. doi: 10.1105/tpc.001768

Wang, Y. Q., Ohara, Y., Nakayashiki, H., Tosa, Y., and Mayama, S. (2005). Microarray analysis of the gene expression profile induced by the endophytic plant growth-promoting rhizobacteria, *Pseudomonas fluorescens* FPT9601-T5 in Arabidopsis. *Mol. Plant-Microbe Interact.* 18, 385–396. doi: 10.1094/MPMI-18-0385

White, P. J., and Broadley, M. R. (2003). Calcium in plants. *Ann. Bot.* 92, 487–511. doi: 10.1093/aob/mcg164

Wu, J. Y., and Lin, L. D. (2002). Ultrasound-induced stress responses of Panax ginseng cells: enzymatic browning and phenolics production. *Biotechnol. Progr.* 18, 862–866. doi: 10.1021/bp0255210

Yang, T., and Poovaiah, B. W. (2002). Hydrogen peroxide homeostasis: activation of plant catalase by calcium/calmodulin. *Proc. Natl. Acad. Sci. U.S.A*. 99, 4097–4102. doi: 10.1073/pnas.052564899

Zamioudis, C., and Pieterse, C. M. J. (2012). Modulation of host immunity by beneficial microbes. *Mol. Plant-Microbe Interact*. 25, 139–150. doi: 10.1094/MPMI-06-11-0179

Zdobnov, E. M., and Apweiler, R. (2001). InterProScan - an integration platform for the signature-recognition methods in InterPro. *Bioinformatics* 17, 847–848. doi: 10.1093/bioinformatics/17.9.847

Zehnder, G. W., Murphy, J. F., Sikora, E. J., and Kloepper, J. W. (2001). Application of rhizobacteria for induced resistance. *Eur. J. Plant Pathol*. 107, 39–50. doi: 10.1023/A:1008732400383

Zeier, J., Pink, B., Mueller, M. J., and Berger, S. (2004). Light conditions influence specific defense responses in incompatible plantpathogen interactions: uncoupling systemic resistance from salicylic acid and PR-1 accumulation. *Planta* 219, 673–683. doi: 10.1007/s00425-004-1272-z

Zhang, H., Huang, Z., Xie, B., Chen, Q., Tian, X., Zhang, X., et al. (2004). The ethylene-, jasmonate-, abscisic acid- and NaCl-responsive tomato transcription factor JERF1 modulates expression of GCC box-containing genes and salt tolerance in tobacco. *Planta* 220, 262–270. doi: 10.1007/s00425-004-1347-x

Conflict of Interest Statement: The authors declare that the research was conducted in the absence of any commercial or financial relationships that could be construed as a potential conflict of interest.

Received: 09 June 2014; accepted: 29 July 2014; published online: 05 September 2014.
*Citation: Gómez-Lama Cabanás C, Schilirò E, Valverde-Corredor A and Mercado-Blanco J (2014) The biocontrol endophytic bacterium Pseudomonas fluorescens PICF7 induces systemic defense responses in aerial tissues upon colonization of olive roots. Front. Microbiol. **5**:427. doi: 10.3389/fmicb.2014.00427*
This article was submitted to Plant-Microbe Interaction, a section of the journal Frontiers in Microbiology.

frontiers in Microbiology

ORIGINAL RESEARCH
published: 12 May 2015
doi: 10.3389/fmicb.2015.00440

The genomes of closely related *Pantoea ananatis* maize seed endophytes having different effects on the host plant differ in secretion system genes and mobile genetic elements

Raheleh Sheibani-Tezerji[1,2], *Muhammad Naveed*[1†], *Marc-André Jehl*[2], *Angela Sessitsch*[1], *Thomas Rattei*[2*] and *Birgit Mitter*[1*]

[1] Bioresources Unit, Health and Environment Department, AIT Austrian Institute of Technology GmbH, Tulln, Austria, [2] Division of Computational System Biology, Department of Microbiology and Ecosystem Science, University of Vienna, Vienna, Austria

The seed as a habitat for microorganisms is as yet under-explored and has quite distinct characteristics as compared to other vegetative plant tissues. In this study, we investigated three closely related *P. ananatis* strains (named S6, S7, and S8), which were isolated from maize seeds of healthy plants. Plant inoculation experiments revealed that each of these strains exhibited a different phenotype ranging from weak pathogenic (S7), commensal (S8), to a beneficial, growth-promoting effect (S6) in maize. We performed a comparative genomics analysis in order to find genetic determinants responsible for the differences observed. Recent studies provided exciting insight into the genetic drivers of niche adaption and functional diversification of the genus *Pantoea*. However, we report here for the first time on the analysis of *P. ananatis* strains colonizing the same ecological niche but showing distinct interaction strategies with the host plant. Our comparative analysis revealed that genomes of these three strains are highly similar. However, genomic differences in genes encoding protein secretion systems and putative effectors, and transposase/integrases/phage related genes could be observed.

Keywords: seed endophyte, *Pantoea ananatis*, comparative genomics, plant growth promotion

OPEN ACCESS

Edited by:
Anna Maria Pirttilä, University of Oulu, Finland

Reviewed by:
Laila Pamela Partida-Martinez, Centro de Investigaciones Avanzadas del Instituto Politecnico Nacional, Mexico
David John Studholme, University of Exeter, UK

***Correspondence:**
Thomas Rattei, Division of Computational Systems Biology, Department of Microbiology and Ecosystem Science, University of Vienna, Althanstrasse 14, 1090 Vienna, Austria
thomas.rattei@univie.ac.at;
Birgit Mitter, Unit of Bioresources, Health and Environment Department, AIT Austrian Institute of Technology GmbH, Konrad Lorenz Strasse 24, 3430 Tulln, Austria
birgit.mitter@ait.ac.at

†Present Address:
Muhammad Naveed, Institute of Soil and Environmental Sciences, University of Agriculture Faisalabad, Faisalabad, Pakistan

Specialty section:
This article was submitted to Plant-Microbe Interaction, a section of the journal Frontiers in Microbiology

Received: *30 January 2015*
Accepted: *23 April 2015*
Published: *12 May 2015*

Citation:
Sheibani-Tezerji R, Naveed M, Jehl M-A, Sessitsch A, Rattei T and Mitter B (2015) The genomes of closely related Pantoea ananatis maize seed endophytes having different effects on the host plant differ in secretion system genes and mobile genetic elements. Front. Microbiol. 6:440. doi: 10.3389/fmicb.2015.00440

Introduction

Bacterial endophytes have been defined as "bacteria, which for all or part of their life cycle invade the tissues of living plants and cause unapparent and asymptomatic infections entirely within plant tissues, but cause no symptoms of disease" (Wilson, 1995). Based on this definition, endophytes are clearly distinct from plant pathogens. However, bacteria can exist in plants in quiescence but proliferate and become detrimental to the host under certain conditions such as plant growth perturbations (Kloepper et al., 2013). Moreover, plant-pathogen interactions are often plant species specific and bacteria that are pathogenic to one plant species can exhibit an endophytic lifestyle in other plants (Bashan et al., 1982). On the other hand, it has been shown that plants respond differently to endophytes and plant pathogens (Bordiec et al., 2011). A promising approach in

revealing differences in the host interaction strategies of pathogens and plant beneficial bacteria might be the comparison of functionalities and gene content of closely related bacterial strains that show different modes of interaction with host plants. Genome sequencing provides detailed information on the genes present in bacteria and offers a basis for comparative genomics that aids in revealing differences in the host interaction strategies of pathogens and plant growth promoting bacteria.

The seed as a habitat for microorganisms is under-explored, although the first report of bacteria colonizing seeds dates back to the 1970s (Mundt and Hinkle, 1976). Only few studies have been performed on seed endophytes (Compant et al., 2011; Johnston-Monje and Raizada, 2011; Hardoim et al., 2012) and the origin of endophytes is under debate. A few studies suggest that at least some bacterial endophytes are vertically transmitted (Johnston-Monje and Raizada, 2011). The seed has quite distinct characteristics as compared to other vegetative plant tissues and one would expect that it also harbors distinct microbial communities. Based on cultivation-based analysis it has been reported that Gammaproteobacteria represent the most abundant class of maize seed endophytes, comprising mostly *Pantoea* and *Enterobacter* (Johnston-Monje and Raizada, 2011). Similarly, Rijavec et al. (2007) identified *Pantoea* as a major genus among endophytes isolated from maize seeds.

Pantoea ananatis is a bacterial species that was originally discovered in pineapple in the Philippines, in 1928 (Serrano, 1928). Members of this species have been shown to infect many mono- and dicotyledonous plant species, such as onion, rice, melon, sudan grass, tomato, and sorghum (Stall et al., 1969; Wells et al., 1987; Gitaitis and Gay, 1997; Azad et al., 2000; Cother et al., 2004; Cota et al., 2010). In maize *P. ananatis* is the causing agent of the foliar disease termed maize white spot disease (Paccola-Meirelles et al., 2001). *P. ananatis* strains display a wide range of ecological versatility, as they are commonly recovered from water, soil, insects, and plants (De Maayer et al., 2014). Depending on their host and ecological niches, *P. ananatis* strains can show different life styles such as mutualistic, saprophytic and pathogenic life styles (Coutinho and Venter, 2009). De Maayer et al. (2012a) showed that the Large Pantoea Plasmid (LLP-1) plays a crucial role in niche adaption and functional diversification of the genus *Pantoea*. By analyzing the pan-genome of eight sequenced *P. ananatis* strains De Maayer et al. (2014) identified a large number of proteins in this species with orthologs restricted to bacteria associated either with plants, animals or insects. The mechanisms of the diverse interactions between *P. ananatis* and the host are still poorly understood and only little is known on the genetic traits underlying plant pathogenic or beneficial activity. Shyntum et al. (2014) showed that type IV section system could play a role in pathogenicity and niche adaptation. Genome analysis of the plant growth promoting strain *P. ananatis* B1-9 that has been isolated from the rhizosphere of green onions in Korea indicates that the strain lacks traits related to pathogenicity. Furthermore, it harbors genes that are putatively involved in plant growth stimulation and yield improvement (Kim et al., 2012).

In this work, we studied three endophytic *P. ananatis* strains (S6, S7, S8) isolated from maize seeds. Although they were isolated from seeds of healthy plants, they showed distinct characteristics in regard to plant growth and health. Strain S6 exhibited clear beneficial effects on maize growth, whereas S8 had hardly any effect and is considered as neutral and S7 caused disease symptoms known from *P. ananatis* infections. Therefore, this closely related group of strains represents a promising model to unravel genetic determinants in *P. ananatis* responsible for beneficial and pathogenic effects. Consequently, we functionally characterized the strains by testing for various known plant growth-promoting characteristics as well as for their effect on plant growth, and performed a comparative genome analysis to elucidate genetic features determining the type of plant-microbe interaction.

Materials and Methods

Maize Varieties and Seed Surface Sterilization

Seeds of the maize cultivars (Helmi, Morignon, Pelicon, and Peso) were obtained from local farmers in Seibersdorf, Austria. Maize seeds with no cracks or other visible deformations were surface-sterilized with 70% ethanol for 3 min and 5% sodium hypochlorite for 5 min, and followed by repeated washing with sterile distilled water (3 times for 1 min). The efficacy of surface sterilization was checked by plating 3–5 seeds and aliquots of the final rinse onto 10% tryptic soy agar plates, and incubated for 3 days at $28 \pm 1^{\circ}$C. The medium was checked daily for bacterial or fungal growth.

Isolation of Endophytic Bacteria from Maize Seeds

Seed-borne bacteria were isolated following the procedure described by Rijavec et al. (2007) with some modifications. For isolation, 50 surface-sterilized seeds of each cultivar were crushed and blended aseptically in 90 mL of half strength nutrient broth (Difco, Detroit, Michigan) for 5 min. The blend was then incubated at room temperature for 4 h on a rotary shaker (VWR International GmbH, Austria) at 100 r min^{-1}. Half strength nutrient broth containing 200 mg/L cycloheximide was inoculated with a series of the incubation mixture (10:1 mL ratio) and further incubated for 4 days on a rotary shaker at room temperature. Aliquots were taken from Erlenmeyer flasks with observed microbial growth and plated onto R2A (Difco, Detroit, Michigan). Plates were incubated at 28°C for 24–48 h. One hundred colonies were picked, and pure cultures were obtained by further streaking on agar plates. Single colonies were picked, inoculated in LB broth and incubated with shaking at 28°C for 24–48 h. Bacterial strains were preserved at −80°C as saturated cultures containing 20% (w/v) glycerol.

Partial 16S rRNA Gene Sequencing

For phylogenetic identification of maize seed endophytes we performed partial 16S rDNA (V1 to V3) PCR and sequencing as described by Reiter and Sessitsch (2006). Sequencing was performed by LGC Genomics (Berlin, Germany).

Preparation of Inoculum

Inoculum of the selected strains (S6, S7, S8) were prepared in 100 mL 10% tryptic soy broth in 250 mL Erlenmeyer flasks

and incubated at 28 ± 2°C for 48 h in an orbital shaking incubator (VWR International, GmbH) at 180 r min^{-1}. The optical density of the broth was adjusted to 0.5 measured at λ 600 nm using spectrophotometer (Gene Quant Pro, Gemini BV, The Netherlands) to obtain an uniform population of bacteria [10^8–10^9 colony-forming units (CFU) mL^{-1}] in the broth at the time of inoculation.

Testing the Effect of Endophytic Strains on Maize Under Axenic Conditions

Seeds were surface-sterilized by dipping them in 70% ethanol for 3 min and then in a 5% sodium hypochlorite solution for 5 min and subsequently thoroughly washing with sterilized distilled water. The efficacy of surface sterilization was checked by plating seeds, and aliquots of the final rinse onto 10% tryptic soy agar. Samples were considered to be successfully sterilized when no colonies were observed on the tryptic soy agar plates after inoculation for 3 days at 28°C. Surface-disinfected seeds of three maize cultivars (DaSilvie, Kaleo, and Mazurka) were immersed in the bacterial suspensions for 1 h. For the uninoculated control, sterilized tryptic soy broth was used for the seed treatment. Fifteen seeds per treatment were planted in plastic trays with sterilized compost (Blumenerde, COMPO SANA®) and trays were arranged using a randomized design with 3 replications resulting in total number of 45 seeds per treatment. The experiment was conducted for 24 days and data of shoot and root length as well as biomass were recorded.

Functional Characterization of Seed Endophytic Bacteria

Phenotypic, Physiological, and Biochemical Characterization

Color and shape of bacterial colonies, growth behavior in different pHs, salt concentrations and C sources as well as aggregate and biofilm formation and motility were tested following the procedures described by Naveed et al. (2014). Biochemical testing of oxidase, catalase, gelatin hydrolysis, and casein hydrolysis activity of the selected strains was performed according to Naveed et al. (2014).

Plant Growth Promoting Activities

Strains were tested for activities known to be involved in plant growth regulation and/or rhizosphere competence such as ACC-deaminase activity, auxin production, phosphate solubilization (organic/inorganic P) and siderophore production as well as ammonia, hydrogen cyanide and PHB production as described by Naveed et al. (2014).

Cell Wall-degrading Activities

Bacterial cell wall hydrolyzing activities such as amylase, cellulase, chitinase, lipase, pectinase, phosphatase, protease, and xylanase were screened on diagnostic plates as described by Naveed et al. (2014).

Antibiotic Resistance of the Isolates

Antibiotic resistance was tested individually on tryptic soy agar plates containing the antibiotics ampicillin, cycloheximide, gentamycin, kanamycin, chloramphenicol, rifampicin, spectinomycin, streptomycin or tetracycline respectively at the following concentrations: 25, 50, 75, 100 μg ml^{-1}. The plates were incubated at 28 ± 2°C for 5 days and resistance was observed in terms of bacterial growth.

Antagonistic Activities Against Plant Pathogens

The antagonistic activities of bacterial isolates were screened against plant pathogenic fungi (Fusarium caulimons, Fusarium graminarium, Fusarium oxysporum, Fusarium solani, Rhizoctonia solani, Thielaviopsis basicola) and oomycetes Phytophthora infestans, Phytophthora citricola, Phytophthora cominarum). Antagonistic activity of the bacterial isolates against fungi and oomycetes was tested by the dual culture technique on potato dextrose agar (PDA) and yeast malt agar (YMA) media as described by Naveed et al. (2014).

Statistical Analyses

The data of plant growth parameters and colonization were subjected to analyses of variance (ANOVA). The means were compared with Least Significant Difference (LSD) testing ($p < 0.05$) to detect statistical significance among treatments (Steel et al., 1997). Statistical analyses were conducted using SPSS software version 19 (IBM SPSS Statistics 19, USA).

Genomic DNA Isolation for Sequencing

For DNA isolation, the bacterial strains were grown by loop-inoculating one single colony in 5 mL LB broth. The bacterial cultures were incubated at 28 ± 2°C overnight at 180 rpm in a shaking incubator. The overnight cultures were used to inoculate 50 mL fresh LB broth and again incubated at 28 ± 2°C overnight at 180 rpm in a shaking incubator. Bacterial cells were harvested by centrifugation at 4700 rpm for 10 min at 4°C. DNA was extracted from bacterial cell pellets according to the following protocol: The cell pellet was washed with 5 mL lysis buffer (0.1 M NaCl; 0.05 M EDTA, pH 8.0), resuspended in 4 mL lysis buffer containing lysozyme (20 mg mL-1; Roche Diagnostics, Mannheim, Germany) and incubated at 37°C for 20 min. Then 300 μl of 10% sarkosyl was added and placed on ice for 5 min. DNA was extracted with phenol-chloroform-isoamylalcohol (25:24:1, Fluka, Sigma-Aldrich Co.) and re-extracted with chloroform (1:1, Merck, Darmstadt, Germany) followed by precipitation with 0.1 volume of 3 M sodium acetate (pH 5.2) and 2.5 volume of ice-cold absolute ethanol (Merck, Darmstadt, Germany) at −20°C overnight. DNA pellets were washed with 1 ml of 70% ethanol and dissolved in 100 μL TE buffer (10 mM Tris-HCl, pH 7.5; 1 mM EDTA, pH 8·0). DNA was treated with RNase A (final concentration 0.2 gl −1; Invitrogen, Carlsbad, CA) for 90 min at 37°C. DNA quality was analyzed by electrophoresis (80 V) on 0.8% (w/v) agarose gels stained with ethidium bromide. DNA concentration was measured using a NanoDrop 1000 spectrophotometer (Thermo Scientific, Wilmington, DE, USA).

Genome Sequencing, Assembly and Genome Alignment of *P. ananatis* S6, S7, and S8 Strains

Genome sequencing of the three strains of *P. ananatis* (S6, S7, and S8) was done by GATC Biotech AG (Konstanz, Germany) using

a Roche/454 GS-FLX system. After sequencing, pairwise analysis of average nucleotide identity (ANI) was performed between the *P. ananatis* strains with closed genome sequences and the strains S6, S7, and S8 draft genomes individually as described previously (Goris et al., 2007).

The raw reads from sequencing projects have been deposited at the European Nucleotide Archive (ENA, http://www.ebi.ac.uk/ena/data/view/) under the following project accession numbers: *P. ananatis* S6, PRJEB7511; *P. ananatis* S7, PRJEB7512, and *P. ananatis* S8, PRJEB7513. Genome assemblies are available in ENA under accession numbers CVNF01000001 to CVNF01000077 for *P. ananatis* S6, CVNG01000001 to CVNG01000071 for *P. ananatis* S7 and CVNH01000001 to CVNH01000061 for *P. ananatis* S8. The contigs were assembled using AMOScmp comparative assembler (Pop et al., 2004) and the Roche GS de novo assembler package (Newbler v2.6) in the 454 GS-FLXTM system (http://www.454.com/), indipendently. For AMOScmp assembly, four complete genomes of *P. ananatis* strains (*P. ananatis* AJ13355, *P. ananatis* LMG20103, *P. ananatis* LMG5342 and *P. ananatis* PA13) were used as potential reference genomes. As the assemblies based on *P. ananatis* AJ13355 resulted into highest coverage and mapping quality, this genome was used as reference genome for AMOScmp. The result of quality and coverage control of the assembly of each *P. ananatis* genome sequence was calculated using Qualimap v.1.0 (Garcia-Alcalde et al., 2012). In repetitive regions, such as rRNA operons, the assembly was further evaluated based on the read coverage distribution. Whole genome comparisons between *P. ananatis* S6, S7, and S8 strains were performed using Mauve v.2.3.1 (Darling et al., 2004). In Mauve, the Progressive Mauve algorithm was used to order the contigs against *P. ananatis* AJ13355 as reference genome. Genome assemblies are accessible via http://fileshare.csb.univie.ac.at/pantoea/.

Overview of *P. ananatis* Genomes Used in the Current Study

Five complete genomes of *P. ananatis* strains with different life styles and environmental origin were used in the comparative genomics and phylogenetic analysis. *P. ananatis* PA13 (accession numbers CP003085 and CP003086) is known as a pathogen of rice causing grain and sheath rot (Choi et al., 2012). *P. ananatis* AJ13355 (accession numbers AP012032 and AP012033) shows saprophytic life style and was isolated from soil (Hara et al., 2012). *P. ananatis* LMG20103 (accession number CP001875) is a pathogenic strain causing the severe blight and dieback of *Eucalyptus* (De Maayer et al., 2010). *P. ananatis* LMG5342 (accession numbers HE617160 and HE617161) is an opportunistic human pathogen reported from clinical isolations (De Maayer et al., 2012b). *P. vagans* C9-1 (accession numbers CP002206, CP001893, CP001894, and CP001895) is known as a common plant epiphyte (Smits et al., 2010).

Phylogenetic Analysis

We constructed a phylogenetic tree for *P. ananatis* S6, S7, S8 and the *Pantoea* genomes mentioned above. *P. vagans* C9-1 was included as outgroup. Mauve v2.3.1 (Darling et al., 2004) was used to identify specific and shared SNPs between all compared genomes. The alignments of the genomes were checked manually to eliminate possible false positive SNPs in less conserved regions, particularly if they occur in direct neighborhood of insertions and deletions. The obtained SNPs were filtered based on the position of phylogenetic markers of *P. ananatis* AJ13355 as reference [identified by AMPHORA2; Wu and Scott (2012)] to get the core SNPs of the genome sequences of *P. ananatis* strains. Afterwards, the phylogenetic tree was computed with Geneious 8.0 (Kearse et al., 2012) using 1000 runs for bootstrapping.

Genome Annotation

Gene prediction and annotation were obtained from the in-house ConsPred workflow. ConsPred consists of two phases: *ab initio* as well as homology-based predictions. *Ab initio* predictions are followed by Genemark.hmm (Lukashin and Borodovsky, 1998), Glimmer (Delcher et al., 2007), Prodigal (Hyatt et al., 2010), Critica (Badger and Olsen, 1999) and additional homology based information derived from a BLAST search against the NCBI non-redundant sequence database (NR) (Sayers et al., 2012). Protein domains were predicted by InterProScan (Zdobnov and Apweiler, 2001). For protein sequences without significant hits in NR, functional annotation of protein-coding genes was obtained by a similarity search against the UniProt/SwissProt database (Uniprot consortium, 2009). Non protein-coding elements such as tRNA and rRNA were predicted using tRNAScan and RNAmmer tools, respectively (Lowe and Eddy, 1997; Lagesen et al., 2007). Non-coding RNA genes (ncRNAs) were identified and annotated by a search against RFAM database (Griffiths-Jones et al., 2005).

To check for the completeness of housekeeping genes in the genomes of strains S6, S7, and S8 we used AMPHORA2 (Wu and Scott, 2012) with 31 bacterial phylogenetic marker genes for inferring phylogenetic information.

Plasmid Sequence Alignment Analysis

To identify the plasmid sequences within the assembled contigs we compared the plasmid sequence of the closest reference genome (*P. ananatis* AJ13355) to the assembly of *P. ananatis* S6, S7 and S8 strains using Mauve v2.3.1 (Darling et al., 2004).

To visualize the coverage of the plasmids in the draft genome sequences, the plasmid sequence of *P. ananatis* AJ13355 were used as reference for comparative circular alignments of the three *P. ananatis* S6, S7, and S8 strains using the BLAST Ring Image Generator (Stothard and Wishart, 2005; Alikhan et al., 2011).

Comparative Genome Analyses

Identification of Orthologous Groups

Paralogous and orthologous clusters were identified using OrthoMCL (Li et al., 2003) using the predicted proteomes of seven *P. ananatis* strains (*P. ananatis* AJ13355, *P. ananatis* LMG20103, *P. ananatis* LMG5342, *P. ananatis* PA13 and *P. ananatis* S6, S7, and S8 strains) which initially required an all-vs.-all blastp (E-value cut-off of 1×10^{-5}). Then the mcl clustering algorithm was used to deduce the relationship between genes.

Identification of Eukaryotic-like Protein Domains

To identify eukaryotic-like protein domains (ELDs) in protein sequences in the genomes of strains S6, S7, and S8, those genomes were included in the individual ELD calculation procedure of the Effective web-portal (Jehl et al., 2011). The approach detects protein domains that are present in eukaryotic organisms and significantly enriched in pathogenic and symbiotic compared to non-pathogenic, non-host-associated bacteria. Using default settings, all eukaryotic-like protein domains with an enrichment score greater or equal to 4 were considered for comparison regarding functional differences in *P. ananatis* strains of diverse phenotype.

Results

Selection of Strains and Effects of Maize Seed Endophytes on Maize Seedling Growth

In a previous study, we isolated 90 bacterial strains from seeds of healthy maize plants grown at organic farming fields in Austria. Thirty-seven of these strains shared highest 16S rDNA sequence homology with *P. ananatis* strains (data not shown). Ten strains were randomly selected and tested for effects on seedling growth of maize grown in sterile hydroponic cultures (for a description see Naveed et al., 2014). Along with strains that did not influence maize seedling growth we found one strain with clear detrimental effect and other strains that promoted maize seedling growth (data not shown). One representative of each group was selected and further tested on maize grown in compost. Strain S6 significantly increased seedling growth in all three maize cultivars tested compared to the control (Figure S1; **Table 1**). Depending on the plant variety root- and shoot-dry biomass was increased up to 47 and 41%, respectively. Root and shoot length was increased up to 57 and 41%, respectively. Strain S8 showed positive effects on plant growth in cultivar DaSilvie only but did not significantly affect growth of the cultivars Kolea and Mazurka (**Table 1**). In contrast, strain S7 had a negative effect on seedling growth in all the maize cultivars with the effect being significant in DaSilvie and Kolea and less pronounced in Mazurka (**Table 1**; Figure S1). Apart from reduced biomass S7 treated plants showed white streaks on leaves (Figure S2).

Functional Characterization of Maize Seed Isolates Based on *in vitro* Assays

A range of activities known to contribute to plant growth promotion, stress tolerance or biocontrol was tested. The results of functional characterization are summarized in **Table 2**. All strains exhibited ACC-deaminase activity and showed auxin, NH_3 and siderophore production (qualitative). All three strains showed P-solubilization and were able to produce AHL and PHB. S6, S7, and S8 behaved similar in tests for motility and chemotaxis as well as the biochemical characters mentioned in **Table 2**. No strain produced EPS in our assays. Lipase, pectinase, phosphatase and xylanase activity was detected in all strains, whereas none of the strains showed amylase, cellulose, chitinase or protease activity. Strain S6 showed *in vitro* antagonistic activity against all bacterial pathogens tested but *F. solani*. Strain S7 inhibited growth of *F. oxysporum*, *T. basicola,* and *P. citricola* in our assays, whereas strain S8 negatively affected growth of *F. graminarium*, *F. oxysporum*, *R. solani,* and *P. citricola.*

Genome Sequences of *P. ananatis* Strains S6, S7, and S8

Genomic DNA of strains S6, S7, and S8 was sequenced and the generated raw reads represented 230, 76, and 79 million bases respectively (**Table 3**). The number of sequenced reads varied from 570,490 in strain S6 with an average length of 406 bp to 174,500 and 179,051 in S7 and S8 respectively, with an average length of 441 bp in both strains.

The pairwise comparision of average nucleotide identity (ANI) of the draft genomes of strains S6, S7, and S8 with the *P. ananatis* AJ13355 genome showed that the similarity of the analyzed strains and strain AJ13355 exceeds 99% (Supplementary Table 1).

Comparative sequence assembly was performed by AMOScmp program (Pop et al., 2004) as a conservative method that uses the most similar available complete genome

TABLE 1 | Effect of inoculation with seed-associated endophytic bacteria on root/shoot length and biomass of maize seedlings.

Strains	DaSilvie	Kaleo	Mazurka	DaSilvie	Kaleo	Mazurka
	Root length (cm)			Shoot length (cm)		
Control	16.67 fgh[a]	15.67 gh	19.00 ef	27.67 bcd	24.67 ef	25.33 def
P. ananatis S6	25.67 ab	24.50 bc	27.33 a	34.66 a	34.97 a	34.83 a
P. ananatis S7	16.33 fgh	15.00 h	17.67 fgh	26.67 cde	26.33 cde	23.33 f
P. ananatis S8	20.67 de	18.00 fg	21.38 de	30.00 b	28.33 bc	27.00 bcd
	Root dry biomass (mg)			Shoot dry biomass (mg)		
Control	20.98 cde	20.49 de	22.78 bcd	229.31 e	224.38 e	248.75 bcd
P. ananatis S6	29.57 a	30.09 a	30.51 a	323.11 a	324.00 a	330.42 a
P. ananatis S7	18.78 ef	17.23 f	21.24 cde	199.29 f	191.18 f	232.45 de
P. ananatis S8	24.02 b	22.03 bcd	23.39 bc	256.45 bc	241.25 cde	262.89 b

[a] *Means sharing same letter(s) do not differ significantly at P = 0.05.*

TABLE 2 | Physico-chemical and growth-promoting characteristics of maize seed-borne endophytic bacteria.

Characteristics	*P. ananatis* S6	*P. ananatis* S7	*P. anantis* S8
PHENOTYPIC CHARACTERIZATION			
Colony color	Yellow	Yellow	Yellow
Colony morphology	Round	Round	Round
BACTERIAL GROWTH CONDITIONS			
Temperature			
4°C	+	+	+
42°C	–	–	–
NaCl			
2%	+	+	+
6%	+	+	+
pH:			
5	+	+	+
12	+	+	+
MOTILITY/CHEMOTAXIS[a]			
Swimming	+	+	+
Swarming	++	+	+
Twitching	+	+	+
Biofilm formation			
OD (600 nm)	0.95 ± 0.08	0.89 ± 0.07	0.92 ± 0.06
Biofilm (595 nm)	0.08 ± 0.01	0.07 ± 0.01	0.06 ± 0.01
Aggregate stability (%)	32.61 ± 2.13	28.61 ± 1.93	30.61 ± 2.01
BIOCHEMICAL CHARACTERIZATION[b]			
Catalase	+	+	+
Oxidase	–	–	–
Casein	–	–	–
Gelatin	3.5 ± 0.15	2.9 ± 0.10	3.2 ± 0.12
Methanol	–	–	–
Ethanol	–	–	–
GROWTH PROMOTING CHARACTERIZATION[a]			
ACC-deaminase activity	+	+	+
Auxin production (IAA equivalent μg mL^{-1})			
Without L-TRP	0.87 ± 0.55	0.68 ± 0.52	0.78 ± 0.54
With L-TRP	32.67 ± 3.17	27.45 ± 2.89	30.89 ± 3.17
P-solubilization (Inorganic/organic P)			
$Ca_3(PO_4)_2$	1.6 ± 0.10	1.2 ± 0.14	1.4 ± 0.14
$CaHPO_4$	1.5 ± 0.08	1.0 ± 0.06	1.2 ± 0.08
Ca-Phytate	2.5 ± 0.11	2.0 ± 0.10	2.3 ± 0.11
Na-Phytate	1.4 ± 0.06	0.9 ± 0.02	1.0 ± 0.06
Exopolysaccharide	–	–	–
HCN production	–	–	–
NH_3 production	+	+	+
Siderophore	–	–	–
AHL	+	+	+
PHB	+	+	+
ENZYME HYDROLYZING ACTIVITY[a] **(COLON DIAMETER CM)**			
Amylase	–	–	–
Cellulase	–	–	–
Chitinase	–	–	–
Lipase	2.2 ± 0.09	1.8 ± 0.08	2.0 ± 0.09
Pectinase	1.5 ± 0.11	1.2 ± 0.04	1.0 ± 0.05
Phosphatase	1.6 ± 0.08	1.3 ± 0.07	1.0 ± 0.08
Protease	–	–	–
Xylanase	1.3 ± 0.09	0.8 ± 0.02	1.0 ± 0.06
ANTIBIOTIC RESISTANCE (μg mL^{-1})			
Ampicillin	–	–	–
Gentamycin	–	–	–
Kanamycin	–	–	–
Chloramphenicol	–	–	–
Rifampicin	–	–	–
Spectinomycin	–	–	–
Streptomycin	–	–	–
Tetracycline	–	–	–
ANTI-FUNGAL ACTIVITY (COLON DIAMETER cm)			
F. caulimons	2.0 ± 0.05	–	–
F. graminarium	1.2 ± 0.04	–	1.0 ± 0.04
F. oxysporum	1.0 ± 0.03	1.0 ± 0.03	1.0 ± 0.03
F. solani	–	–	–
R. solani	1.8 ± 0.07	–	1.5 ± 0.06
T. basicola	1.2 ± 0.05	1.2 ± 0.05	–
ANTI-OOMYCETE ACTIVITY			
P. infestans	3.4 ± 0.11	–	–
P. citricola	3.5 ± 0.09	3.0 ± 0.09	3.0 ± 0.12
P. cominarum	2.8 ± 0.08	–	–

[a] *Results in characterization table are of 4–6 replicates.*
[b] *–, absent; +, present.*

sequence as a reference to assemble the 454 reads (**Table 3**). The *P. ananatis* S6, S7, and S8 draft genomes consist of 93, 92, and 63 contigs, respectively, and range from 4.3 to 4.6 Mb in length.

De novo assembly resulted in almost the same coverage assembly but less assembly score and N50 value in comparison to AMOScmp assembler.

The comparison of draft genome assembly for *P. ananatis* S6, S7, and S8 against *P. ananatis* AJ13355 as reference genome are shown in **Figure 1**, illustrating a higher degree of genome conservation among the strains S6, S7, S8, as compared to *P. ananatis* AJ13355 (**Figure 1**). Phylogenetic analysis revealed a close relationship between strains S6, S7, S8, and the other four genomes of *P. ananatis* in comparison to *P. vagans* (**Figure 2**).

Genome Annotation of *P. ananatis* S6, S7, and S8 Strains

The genome annotation of *P. annanatis* S6, S7, and S8 resulted in different numbers of protein-coding genes. The genome of strain S6 consists of 4.375 predicted coding sequences (CDSs), while S7 and S8 contain 4.516 and 4.528 predicted CDSs, respectively (**Table 4**). Seven 16S rRNA, seven 23S rRNA and eight 5S rRNA genes are encoded in each of the *P. annanatis* strains. In total all tRNA genes for 33 different anticodons were found in all *P. annanatis* strains. The results of annotation analysis of three *P. ananatis* S6, S7, and S8 strains and reannotation of *P. ananais*

TABLE 3 | Genome characteristics of sequencing and assembly of three strains of *P. ananatis* S6, S7, and S8.

Species	Strain	Total nucleotides (bp)	Total reads	Average length
SEQUENCING STATISTICS				
P. ananatis	S6	231,806,398	570,490	406
P. ananatis	S7	76,917,000	174,500	441
P. ananatis	S8	79,039,900	179,051	441

Species	Strain	# Contigs	N50	Total size	Assembly Score	Average Coverage
COMPARATIVE ASSEMBLY STATISTICS (AMOScmp)						
P. ananatis	S6	93	127341	4361793	5972420241	43.08
P. ananatis	S7	92	134747	4553649	6669462411	13.62
P. ananatis	S8	63	178470	4618012	13082168280	14.38

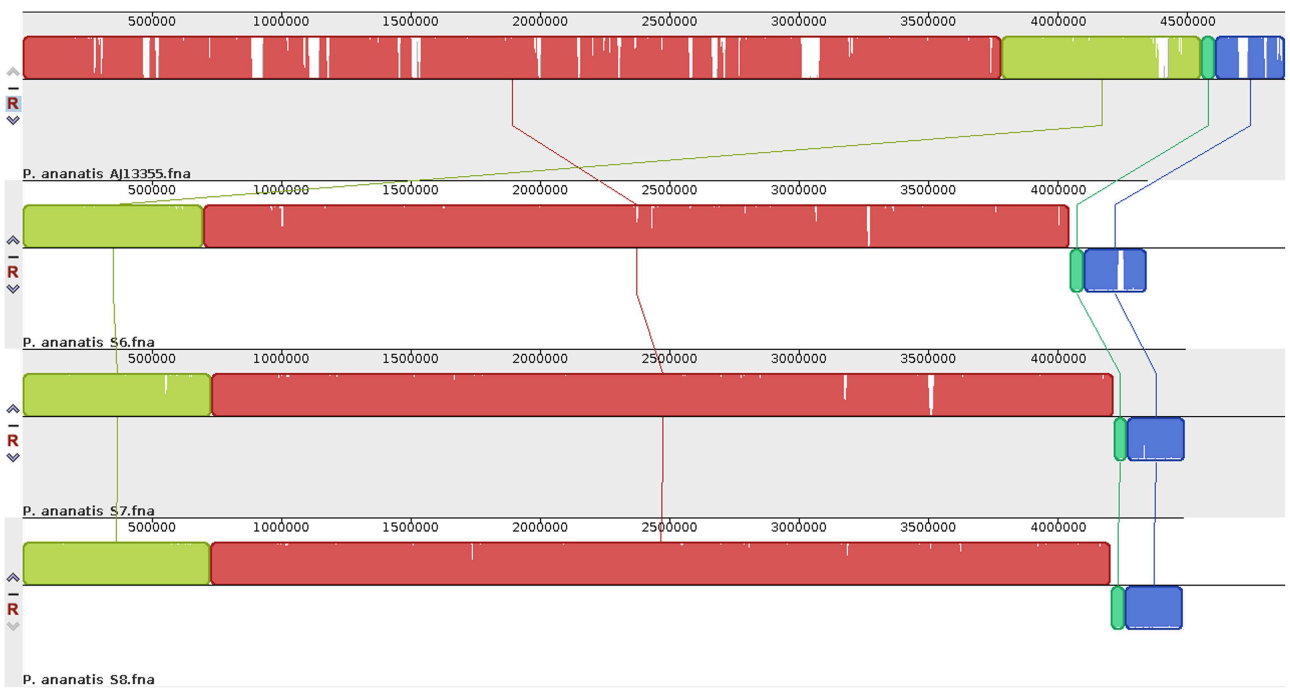

FIGURE 1 | Genome-scale comparison for draft genome sequences of the three *P. ananatis* strains (S6, S7, and S8) and complete genome sequence of *P. ananatis* AJ13355. Homologous DNA regions among the strains are marked by the same colored blocks, while gaps correspond to non-homologous regions. The figure was generated using nucleotide sequences of the genomes using Mauve v2.3.1.

strains (*P. ananatis* AJ13355, *P. ananatis* LMG20103, *P. ananatis* LMG5342, and *P. ananatis* PA13) are summarized in **Table 4**.

The fact that tRNA genes for all essential amino acids, the 16S rRNA gene and 31 housekeeping genes were found in the draft genomes of strains S6, S7, and S8 indicates that the genomes are close to complete. Moreover, the overall pattern of distribution of housekeeping genes and the gene copy number are identical to other members of the *Enterobacteriaceae* family.

To verify the sequence quality generated by 454 sequencing technology we identified putative pseudogenes represented by frameshifts in the draft genomes of *P. ananatis*. The low number of pseudogenes in the genomes of strains S6, S7, and S8 (11, 13, and 11 respectively) indicated that the genome draft has sufficient quality for further comparative genomics analysis (**Table 4**).

Plasmid Sequence Alignment Analysis

Five, six, and seven contigs in *P. ananatis* S6, S7, and S8 genome sequences, respectively, were homologous with the plasmid sequence of *P. ananatis* AJ13355 (Supplementary Table 2). In total, 287, 271, and 276 genes were identified in the plasmid contigs of strains S6, S7, and S8. The core factors identified on the large universal *Pantoea* plasmid LPP-1 (De Maayer et al., 2012a) such as genes coding for thiamine biosynthesis proteins (*thiOSF*), pigment biosynthetic protiens (*crtEXYIBZ*), arbutin/cellobiose/salicin transport and catabolism

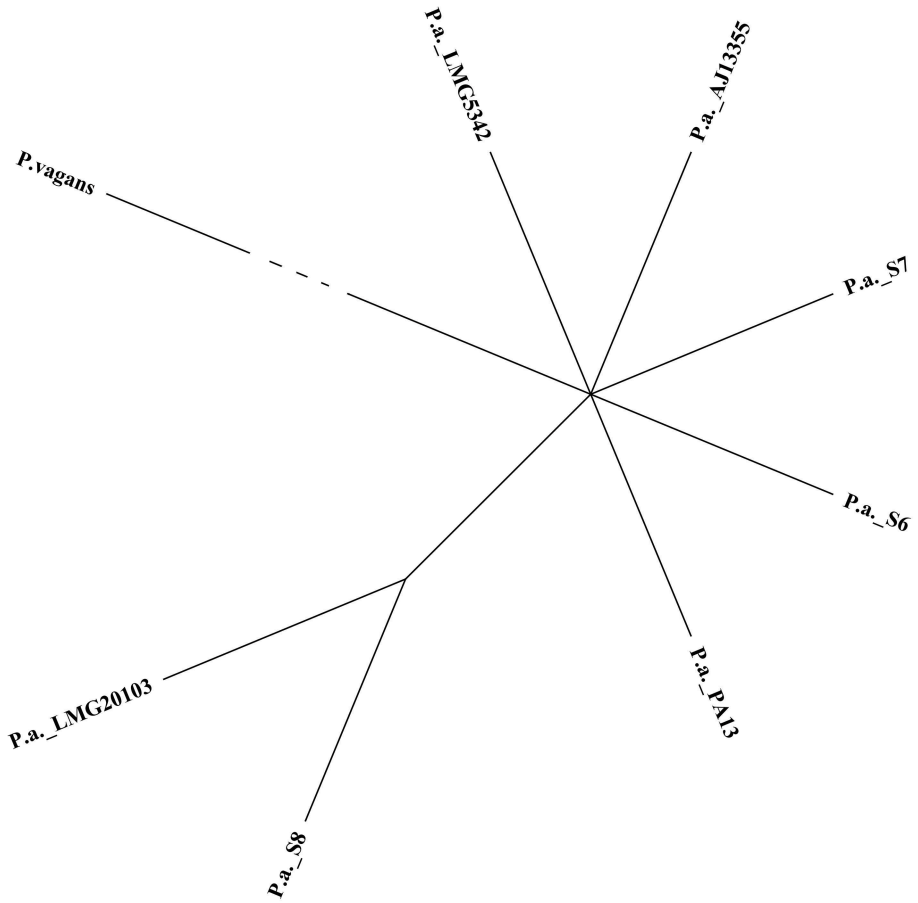

FIGURE 2 | Phylogenetic trees of three strains of *P. ananatis* S6, S7 and S8 with four closed genomes from *Pantoea* genus. *Pantoea vagans* was included as an out group (edge has been shortened).

TABLE 4 | Comparison of (A) draft genome annotation of three *P. ananatis* S6, S7, and S8 strains and (B) re-annotation of four complete genome of *P. ananatis* strains.

	Species	Strain	GC content (%)	#CDS	tRNA	rRNA			ncRNA	Pseudogenes
						5S	16S	23S		
(A)	*P. ananatis*	S6	54	4375	69	8	7	7	144	11
	P. ananatis	S7	54	4516	68	8	7	7	143	13
	P. ananatis	S8	54	4528	68	8	7	7	142	11
(B)	*P. ananatis*	AJ13355	54	4977	78	8	7	7	167	21
	P. ananatis	LMG5342	53	5010	77	8	7	7	154	12
	P. ananatis	LMG20103	54	4715	70	8	7	7	154	24
	P. ananatis	PA13	54	5038	83	8	7	7	167	13

components (*ascBFG*), malate:quinone oxidoreductase (*mqo*), 1,3-diaminopropane production (dat, ddc) and branched-chain amino acid transport protein (*azlDC*) are present on the plasmid sequences of *P. ananatis* S6, S7, and S8 (Supplementary Table 1).

Comparative circular blast alignments of the plasmid sequences in **Figure 3** shows high homology between plasmid sequences of *P. ananatis* S6, S7, and S8 as compared to the *P. ananatis* AJ13355 plasmid sequence (Stothard and Wishart, 2005; Alikhan et al., 2011) (**Figure 3**).

Comparative Genomics Analysis

To identify the core *P. ananatis* genome, we clustered orthologous groups from genes predicted in the seven *P. ananatis* genomes of this study (*P. ananatis* AJ13355, *P. ananatis*

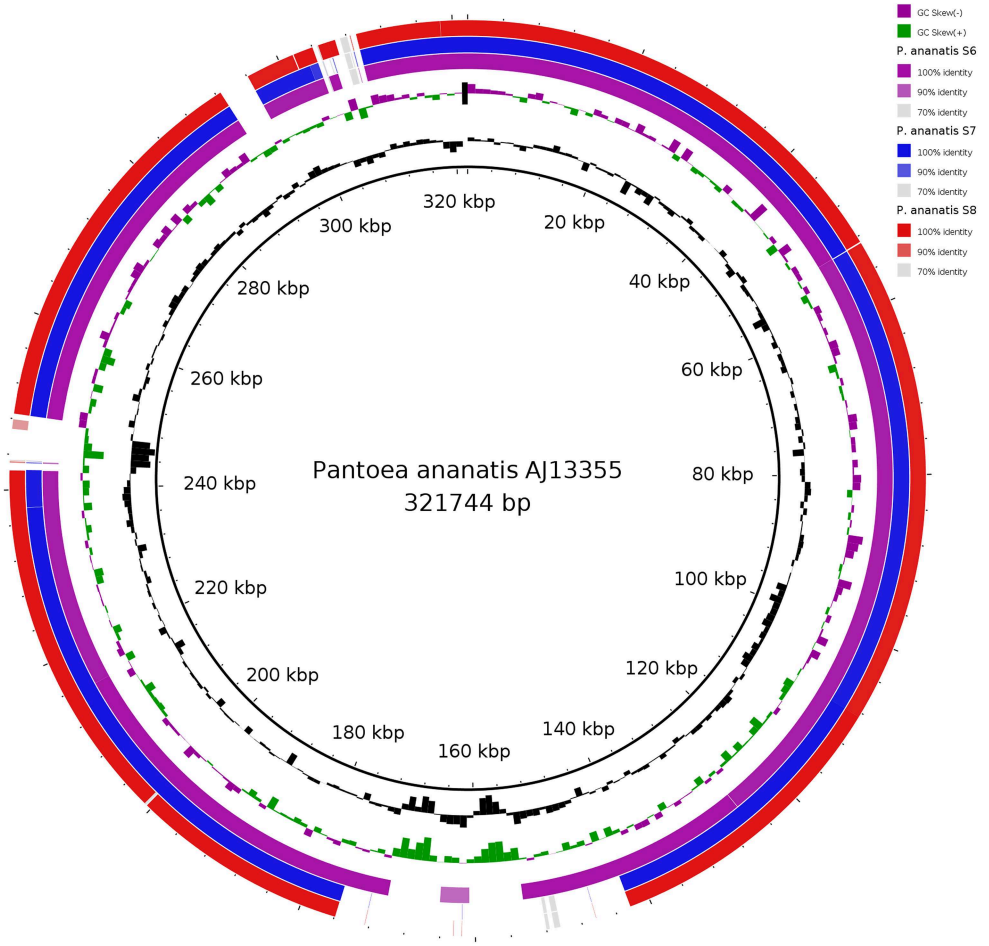

FIGURE 3 | Comparison of the circular genome map of plasmid sequences of three *P. ananatis* S6, S7, and S8 genome structures with the known *P. ananatis* AJ13355 plasmid sequence as reference genome using blast ring image generator (BRIG). The inner circle shows the scale (bp). The first and the second rings show the GC content (black) and GC skew (purple/green), respectively, with respect to the reference genome. The 3rd, 4th, and 5th rings show BLAST comparisons of *P. ananatis* strains S6, S7, and S8 plasmid sequences, respectively.

LMG20103, *P. ananatis* LMG5342, *P. ananatis* PA13 and strains S6, S7, S8) using OrthoMCL (Li et al., 2003). Of the total 33,159 protein-coding genes in all *P. ananatis* strains, 31,987 genes clustered into 4959 gene families. Out of these, 27,578 genes representing 3785 gene families, were common to all *P. ananatis* strains, hereafter referred to as the core *P. ananatis* proteome (**Figure 4**). Fifty-three clusters were shared between *P. ananatis* S6 and S7. *P. ananatis* S7 and S8 have 207 clusters in common while *P. ananatis* S6 and S8 shared 79 clusters (**Figure 5**).

Gene Functional Classification of *P. ananatis* Strains

To understand the functions of shared and specific genes between the *P. ananatis* strains, we analyzed the functional categories of the respective *P. ananatis* gene clusters based on the NOG annotations (Jensen et al., 2008).

As expected, the core *P. ananatis* genes were categorized in functions involved in metabolism, cellular processes and signaling activity, information storage and processing (Supplementary Tables 3, 5). The beneficial *P. ananatis* S6 specific genes encode proteins with putative functions in metabolism, signal transduction and information storage and processing. Whereas, pathogenic *P. ananatis* S7 specific genes were specifically involved in cell cycle control, cell division, chromosome partitioning and amino acid transport. The commensal *P. ananatis* S8 specific genes were responsible for transcription and amino acid transport (Supplementary Tables 4, 6).

Functional Annotation of *P. ananatis* Strains

Functional annotations of orthologous groups on the predicted proteomes of S6, S7, and S8 and the published *P. ananatis* genomes revealed functions that were common within all the

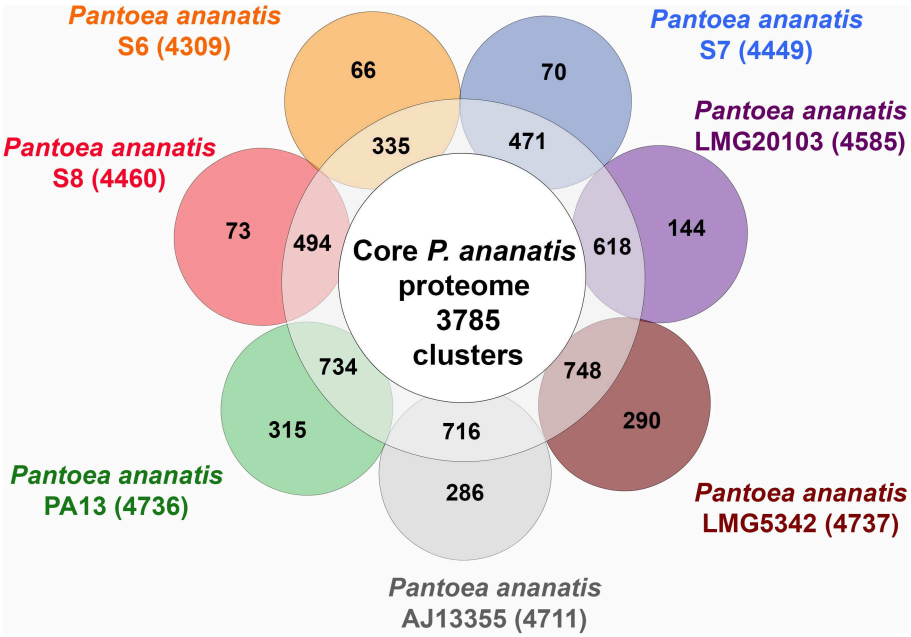

FIGURE 4 | Clusters of orthologous gene families in seven *P. ananatis* strains identified by OrthoMCL. The inner circle shows the core proteome shared between all strains. The numbers of gene clusters shared between specific strains are shown in the ring. The specific proteins for each strain are indicated in each of the outer circles. The numbers outside the Venn diagram show the total number of genes (in parentheses) for each strain.

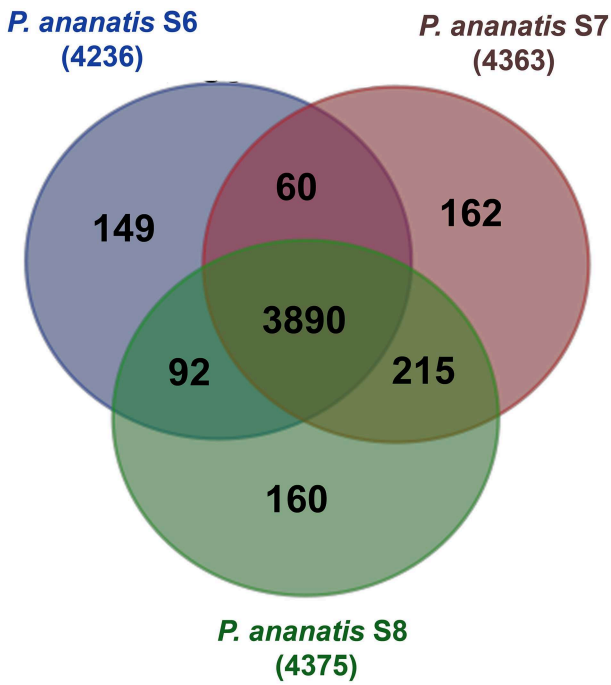

FIGURE 5 | Venn diagram of OrthoMCL cluster distribution across three *P. ananatis* S6, S7, and S8 strains identified by OrthoMCL. The number of core proteome clusters, gene families shared between the species and the specific proteins for each strain is indicated in each of the components. The numbers outside the Venn diagram show the total number of genes (in parentheses) for each strain.

genomes. This analysis also indicated gene families that cause differences among the strains on the functional level. The distribution of genes in COG functional categories is shown in **Figure 6**.

Type IV pilus biogenesis proteins such as *PilNQCWTZ*, type IV pilus secretin *PilQ*, pili assembly chaperone and prepilin type IV endopeptidase were found in the core proteome of *P. ananatis* strains (Supplementary Table 5). Interestingly, two genes related to pili assembly chaperon and fimbrial-type adhesion (the uncharacterized fimbrial chaperone *YhcA* and *F17a-A* fimbrial protein) were found in all *P. ananatis* strains but missing from beneficial *P. ananatis* S6 and two other genes related to the pili (fimbrial chaperone *YfcS* and chaperone protein *PapD*) were absent in pathogenic *P. ananatis* S7 but found in all other *P. ananatis* strains (Supplementary Table 7; **Figure 6B**).

Transposases related proteins such as tyrosine recombinase *XerD*, tyrosine recombinase *XerC* and site-specific recombinase *XerD* were identified in the core proteome of all *P. ananatis* strains. The only difference seen was the*YhgA*-like transposase that was found only in the commensal *P. ananatis* S8 (Supplementary Tables 5, 6; **Figures 6A,C**).

Virulence associated genes on mobile genetic elements showed that phage/bacteriophage related proteins such as bacteriophage P2 (*GpU*), bacteriophage tail protein *Gp41* and phage tail tape measure protein are present in *P. ananatis* S7 and S8 and all other *P. ananatis* strains but do not have orthologs in the beneficial *P. ananatis* strain S6. The bacteriophage T7, Gp4, DNA primase/helicase is presented only in commensal *P. ananatis* S8 strain. Orthologous for integrases were not found in

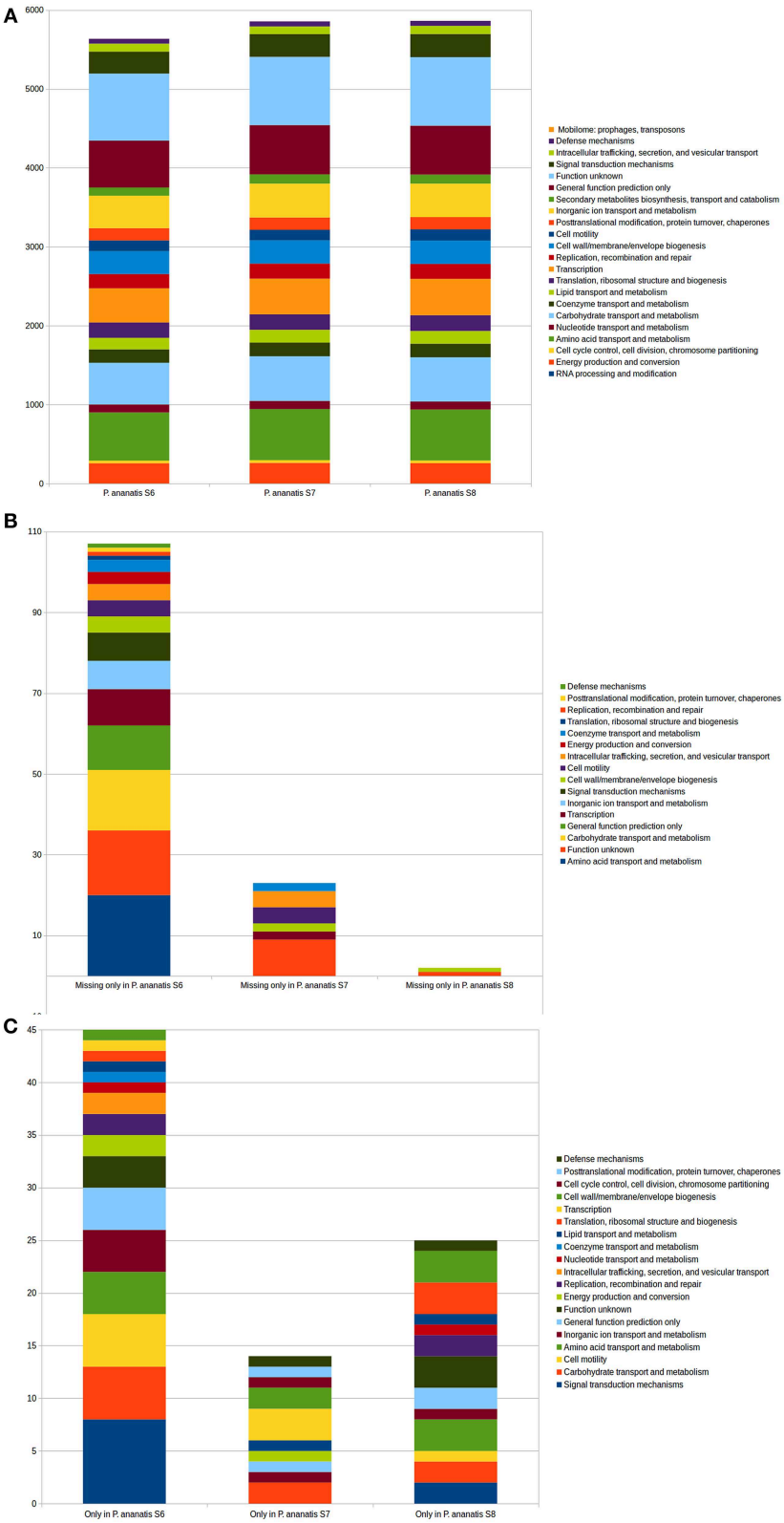

FIGURE 6 | Functional COG categories in the genomes of the three *P. ananatis* strains S6, S7, and S8. (A) Comparison of the COG categories in the genomes of the three *P. ananatis* strains S6, S7, and S8. **(B)** The COG categories that present in two of the *P. ananatis* strains but are absent in the third strain (S6, S7, or S8). **(C)** The COG categories existing in only one of the *P. ananatis* strains (S6, S7, or S8).

the beneficial strain S6 but were presented in the other strains (Supplementary Tables 6, 7; **Figures 6B,C**).

The chemotaxis related proteins such as chemotaxis methyl-accepting receptor (*CheR*) and chemotaxis proteins (*CheVWY*) were identified in the core proteome of the *P. ananatis* strains. The methyl-accepting chemotaxis signaling proteinI *TSR* is missing in the beneficial *P. ananatis* S6 strain but this strain contains the methyl-accepting chemotaxis signaling protein (*MCP*) which has the same activity in transducing the signal to downstream signaling proteins in the cytoplasm (Supplementary Tables 5, 6; **Figures 6A,C**).

The orthologous groups that are related to flagellar structures in the core *P. ananatis* proteome consists of flagella basal body P-ring formation proteins FlgAC; flagellar assembly proteins *FliH*; flagellar basal body rod protein components *FlaE, FlgJ*; flagellar hook-basal body complex proteins *FliELK*, *FlgCK* and flagellar biosynthesis proteins *FlhAQRO*. Other main flagellar related proteins are *FliJ*, *FlhE* flagellar motor protein MotA/MotB and *FliNGMSTZ* identified in the core proteome of *P. ananatis* strains (Supplementary Table 5; **Figure 6A**).

Gene families for T6SS loci were found on the core proteome of all seven *P. ananatis* strains investigated in this study. These common genes encoding *DotU* (COG2885), ATPase *ClpV1* (COG0542), FHA domain-containing protein (COG3456), *IcmF* (COG3523), lipoprotein *SciN* (COG3521), lysozyme-related protein (*impF*) (COG3518), OmpA/MotB domain (COG3455), T6SS RhsGE-associated *Vgr* family subset (COG3501), T6SS-associated *BMAA0400* (COG3913), T6SS -associated *ImpA* (COG3515) and *Hcp1* (COG3157) (Supplementary Table 5; **Figure 6A**). Our analysis showed also that the outer component of the T6SS, which consist of two proteins, *VgrG* (COG3501) and *Hcp* (COG3157) have also been identified as secreted effectors of the T6SS in some of the *P. ananatis* strains (Supplementary Table 7; **Figure 6B**). The effector protein genes *hcp*1, *hcp*1_2, and *hcp*1_3 loci are presented in six *P. ananatis* strains but absent in the pathogenic strain *P. ananatis* S7 (**Table 5**). The *HcpC* as major exported protein is missing in commensal *P. ananatis* S8 and pathogenic strains *P. ananatis* S7 and LMG5342, however it was present in the beneficial S6 strains, *P. ananatis* AJ13355 and pathogenic strains of *P. ananatis* PA13 and *P. ananatis* LMG20103 (Supplementary Table 7; **Figure 6B**).

Eukaryotic-like Protein Domains in *P. ananatis* Strains

We identified eukaryotic-like protein domains (ELDs) in strains S6, S7, and S8 by applying the prediction framework of the Effective web-portal (Jehl et al., 2011). The prediction assigns a eukaryotic-like domain enrichment score (ELD score) to each protein domain, reflecting the maximal enrichment of that domain in any pathogen or symbiont compared to the background frequency of the protein domain in non-pathogenic, non-host-associated bacteria. A high ELD score equals strong enrichment of the protein domain in pathogenic/symbiotic bacteria and suggests an important functional role of the secreted protein in the interaction with the host cell. All ELDs with a significant ELD score greater or equal to 4 were considered to investigate the genomic variance of *P. ananatis* strains S6, S7, and S8 that cause different phenotypes in the host plant.

In summary, 29 different ELDs were predicted (**Table 6**). The majority, i.e., 26 ELDs are shared between all three genomes, supporting the assumption of a high average functional similarity of effector proteins. One eukaryotic-like protein domain, the tRNA delta-isopentenylpyrophosphate (IPP) transferase domain (PF01715) was exclusively found in the genome of the beneficial maize seed strain *P. ananatis* S6. IPP transferases are involved in the modification of tRNAs and convert A(37) to isopentenyl A(37). Another one was unique in the pathogenic strain S7 and contains the C terminal part of a GMP synthase (PF00958). This enzyme belongs to the family of ligases and is involved the biosynthesis of the nucleic acid guanine. A eukaryotic-like domain containing the signature of the collagen-binding domain of bacterial collagenases (PF12904) was found in S7, S8 and all other *P. ananatis* genomes but was absent in S6.

Discussion

The genus *Pantoea* comprises bacteria that are frequently associated with eukaryotic hosts such as plants but strains, even those belonging to the same species (such as *P. ananatis*), have different type of interactions with their host ranging from pathogenicity to mutualism (De Maayer et al., 2014). In our study

TABLE 5 | Hemolysin co-regulated effector proteins (Hcp) presented in the Type VI secretion system identified in orthologous clusters of *P. ananatis* strains.

P. *ananatis* Strains	T6SS hemolysin co-regulated effector proteins (Hcp)			
	Hcp1 (PAGR_1583)*	**Hcp1_2 (PAGR_1584)***	**Hcp1_3 (IPR008514)**	**HcpC (PAGR_3636)***
S6	BN1182_BN_00010	BN1182_BN_00910	BN1182_BN_00920	BN1182_CY_00040
S7	–	–	–	–
S8	BN1184_BC_00200	BN1184_BC_01090	BN1184_BC_01100	–
AJ13355	PantAJ13_A_20550	PantAJ13_A_21490	PantAJ13_A_21500	PantAJ13_B_01630
PA13	PantPA13_B_18870	PantPA13_B_18000	PantPA13_B_17990	PantPA13_B_41060
LMG20103	PantLMG20_A_26140	PantLMG20_A_27020	PantLMG20_A_27030	PantLMG20_A_46190
LMG5342	PantLMG53_A_18720	PantLMG53_A_17820	PantLMG53_A_17810	–

**Hcp locus tag PAGR-* are reported in Shyntum et al. (2014).*

TABLE 6 | Differences of eukaryotic-like protein domain (ELD) enrichment in *P. ananatis* strains of diverse phenotype.

	Pfam ID	Domain description	ELD Score*
Only in pathogenic *P. ananatis* S7	PF00958	GMP synthase C terminal domain	7
Only in beneficial *P. ananatis* S6	PF01715	IPP transferase	5
missing only in beneficial *P. ananatis* S6	PF12904	Putative collagen-binding domain of a collagenase	6
Shared in all *P. ananatis* S6, S7, and S8 strains	PF14328	Domain of unknown function (DUF4385)	–
	PF14145	YrhK-like protein	–
	PF13718	GNAT acetyltransferase 2	–
	PF13347	MFS/sugar transport protein	–
	PF10685	Stress-induced bacterial acidophilic repeat motif	–
	PF09825	Biotin-protein ligase N terminal	–
	PF09330	D-lactate dehydrogenase membrane binding	–
	PF08351	Domain of unknown function (DUF1726)	–
	PF08125	Mannitol dehydrogenase C-terminal domain	–
	PF07798	Protein of unknown function (DUF1640)	–
	PF07350	Protein of unknown function (DUF1479)	–
	PF06500	Alpha/beta hydrolase-unknown function- DUF1100	–
	PF05870	Phenolic acid decarboxylase (PAD)	–
	PF05704	Capsular polysaccharide synthesis protein	–
	PF05433	Glycine zipper 2TM domain	–
	PF05127	Helicase	–
	PF03825	Nucleoside H+ symporter	–
	PF02551	Acyl-CoA thioesterase	–
	PF01306	LacY proton/sugar symporter	–
	PF01232	Mannitol dehydrogenase Rossmann domain	–
	PF01204	Trehalase	–
	PF01116	Fructose-bisphosphate aldolase class-II	–
	PF00625	Guanylate kinase	–
	PF00328	Histidine phosphatase superfamily (branch 2)	–
	PF00294	pfkB family carbohydrate kinase	–
	PF00070	Pyridine nucleotide-disulphide oxidoreductase	–

**The domains without score have different scores for each P. ananatis strains.*

we showed that genetically closely related *P. ananatis* strains with different effects on plant growth colonize maize seeds.

In our study, the maize seed endophyte *P. ananatis* S6 showed clear beneficial effects on maize growth, while strain S7 induced weak pathogenicity symptoms. *P. ananatis* S8 had hardly any effect and can be considered as commensal. The pan genome of eight *P. ananatis* genomes indicated as open pan genome that they can colonize and exploit several different environmental niches by De Maayer et al. (2014). As three *P. ananatis* strains (S6, S7, and S8) are also capable to colonize inside maize seeds and interact with their host, we can expect that the pan genome of these strains can be defined as open pan genome.

Our comparative analysis showed that an average of 85–87% of CDSs predicted for each individual strain of *P. ananatis* S6, S7, and S8 have orthologs encoded by the genomes of the other strains (*P. ananatis* AJ13355, *P. ananatis* LMG20103, *P. ananatis* LMG5342 and *P. ananatis* PA13). These results suggest that the core genomes of strains S6, S7, and S8 strains are highly conserved (**Figure 1**). Despite the overall high degree of similarity between the core genomes of the three maize seed endophytes, we found differences in transposase/integrases/phage related genes, type VI secretion system, and eukaryotic-like protein domains. Similarly, the analysis of the open pan-genome of eight sequenced genomes of *P. ananatis* indicated that between 89.3 and 95.7% of the proteins are common between all strains and they are important for metabolism and cellular processes (De Maayer et al., 2014).

Genes of the accessory genome of selected *P. ananatis* strains analyzed by De Maayer et al. (2014) encoded mainly poorly characterized proteins including transposases, integrases, and mobile genetic elements. The role of horizontal gene transfer in the diversification of *P. ananatis* strains was suggested (De Maayer et al., 2014). Similarly, phage related genes were reported to have a significant role in transferring pathogenicity factors to their bacterial host and thereby to affect bacterial evolution (Lima-Mendez et al., 2008). Due to the differences found in regard mobile genetic elements such as integrase genes, transposase genes and phage related genes, our study confirms a potential role of these elements in the diversification of related strains colonizing the same

ecological niche. An over-representation of transposase genes and mobile elements also indicates the genomes' potential for acquisition of novel functions. The reduced number of mobile elements in *P. ananatis* S6 on the other hand could indicate high stability of its genome, implying good adaption to the habitat.

De Maayer et al. (2012a) proposed the Large Pantoea Plasmid (LLP-1) as genetic determinant of niche adaption and functional diversification of the genus *Pantoea*. All three maize seed endophytes S6, S7, and S8 contain a LLP-1 plasmid and no differences in LPP-1 related genes were found between the genomes of these strains and the core genome of *P. ananatis*. Our analysis revealed further that genes encoding the pigment biosyntetic (*CrtEXYIBZ*) and thiamine biosynthesis (*ThiOSGF*) proteins are present on the plasmid of *P. ananatis* S6, S7, and S8 (Supplementary Table 1). These genes are among those genes identified by De Maayer et al. (2014) to be specific for plant-associated bacteria (PAB) among *P. ananatis*. In addition, the core proteome of the maize seed *P. ananatis* strains contains PAB-specific CDs with prediction functions in metabolism and transport of carbohydrates, iron uptake and metabolism, and carbon, nitrogen and energy sources (De Maayer et al., 2014). In conclusion, our findings support the concept of functional diversification of the species *P. ananatis* proposed by De Maayer et al. (2014).

The T6SS is one of the most studied secretion system in *P. ananatis* (Coutinho and Venter, 2009; De Maayer et al., 2011; Shyntum et al., 2014). Three T6SS loci (T6SS-1, -2, and –3) have been described in *P. ananatis* strains, translocating effectors into the host plant (De Maayer et al., 2011; Shyntum et al., 2014). The T6SS-1 locus is found on the genomes of all *P. ananatis* strains, while T6SS-2 is restricted to pathogenic strains of *P. ananatis*. The presence of T6SS-1 and T6SS-2 in both pathogenic and non-pathogenic *P. ananatis* strains support the idea that the T6SS itself is not necessarily a determinant of pathogenicity and could play a role in competition against other microorganisms, fitness or niche adaptation (Weber et al., 2009; English et al., 2012; Shyntum et al., 2014). T6SS-3 was found to be mainly restricted to *P. ananatis* AJ13355, *P. ananatis* LMG 20103, and *P. ananatis* PA4 (De Maayer et al., 2014).

Beside the T6SS loci related genes VgrG and Hcp genes are present in the maize seed *P. ananatis* strains. The VgrG genes were found in S6, S7, and S8, whereas differences were seen in the presence of hemolysin co-regulated effector proteins (Hcp) between these three strains. A recent study showed that three *hcp* genes exist in *P. ananatis* strains comprising *hcp*-1, *hcp*-2 (having homologs in all sequenced strains of *P. ananatis*) and *hcp*-3 genes (found in *P. ananatis* PA13) (Shyntum et al., 2014). The *hcp*-3 gene is highly divergent from *hcp*-1, *hcp*-2, and the T6SS associated *hcp* genes (Shyntum et al., 2014). The plant-beneficial strain S6 has orthologs with all *hcp* genes identified in the orthologous gene families, while plant-pathogenic strain S7 has no orthologs for *hcp* genes. HcpC is presented in all *P. ananatis* strains but it is missing from S7 and S8 strains. This Hcp protein is located on the plasmid sequence of this strain. Paralogs of *hcp* influence bacterial motility, protease production and biofilm formation (Sha et al., 2013). A potential role of *Hcp* and V*gr*G proteins in host interaction is not described. As all *hcp* genes are present in other *P. ananatis* strains (ranging from pathogenic to saprophytic life style), the *hcp* genes in in the beneficial *P. ananatis* strain S6 might not be responsible for the differences in the phenotype of plant-microbe interaction of the three maize seed strains S6, S7, and S8.

The analysis of effector candidates containing eukaryotic-like protein domains (ELDs) revealed varying molecular repertoire in the genomes of the three maize seed *P. ananatis* strains. The plant-beneficial strain S6 carries a gene for a tRNA delta-isopentenylpyrophosphate (IPP) transferase domain which is not present in the strains S7 and S8. In *E. coli* this enzyme is involved in increasing spontaneous mutation frequency when cells need to adapt to environmental stress (Connolly and Winkler, 1989). Moreover, tRNA modifications mediated by tRNA delta-isopentenylpyrophosphate (IPP) transferase are required for virulence in *Shigella flexneri* by regulating posttranscriptional expression of the regulatory gene *virF* (Durand et al., 1997). The collagen-binding domain of bacterial collagenases is missing in the beneficial *P. ananatis* S6, although present in S7 and S8. This domain is a major component of the extracellular matrix (ECM) and plays a role in cell attachment, haemostasis, differentiation and bacterial adhesion in human and plant pathogens (Foster and Hook, 1998). Interestingly, in *Yersinia enterocolitica* it is a part of the pathogenic bacterial strategy for avoiding host response (Nummelin et al., 2004). The GMP synthase domain exclusively found in the pathogenic *P. ananatis* strain S7 is known to play an important role in cell-to-cell signaling in regulation of virulence in the plant pathogen *Xanthomonas campestris* (Ryan et al., 2006a). This domain is also involved in aggregative behavior, adhesion, biofilm formation, and the virulence of animal and plant pathogens (Ryan et al., 2006b). The role of these EDLs in the interaction of the three maize seed strains *P. ananatis* S7, S8, and S9 with maize plants remains unclear and merits further investigation.

Overall, our study showed that groups of bacterial endophytes with highly related genotypes but different phenotypes in terms of effects on host plants may exist in the same ecological niche. It can be expected that seed endophytes colonize, at least to a certain extent, plants derived from these seeds. Consequently, both, potential plant pathogens and mutualistic endophytes, may be together transmitted to the developing plant.

To predict the phenotype of plant-microbe interactions from traits manifested on the genome of bacteria is an attractive idea and would very much facilitate efforts in selecting microbial inoculants for improved plant production in sustainable agriculture. However, given the high genomic similarity between strains showing distinct phenotypes in regard to their interaction with plants, we conclude that plant pathogenicity and mutualism in *P. ananatis* may be based on rather subtle differences, e.g., on the expression of genes leading to plant defense reactions. Plant-bacteria interactions, irrespectively of whether pathogenic or beneficial must be considered as a multi-dimensional system and the expression of pathogenic or beneficial effects might depend on a multitude of parameters such as the

plant/bacterial physiology, environmental conditions and/or a very fine-tuned interaction between bacterial elicitors and plant response.

Acknowledgments

This work was supported by grants provided by the FWF (National Science Foundation, grant no. P22867-B16 and P26203-B22). The maize seeds of cultivars Kaleo and Mazurka used in this experiment were kindly provided by DOW AgroSciences, Neusiedl am See, Austria and cultivar DaSilvie was kindly provided by Saatbau Linz, Austria.

Supplementary Material

The Supplementary Material for this article can be found online at: http://journal.frontiersin.org/article/10.3389/fmicb.2015.00440/abstract

References

Alikhan, N.-F., Petty, N., Ben Zakour, N., and Beatson, S. (2011). BLAST Ring Image Generator (BRIG): simple prokaryote genome comparisons. *BMC Genomics* 12:402. doi: 10.1186/1471-2164-12-402

Azad, H., Holmes, G., and Cooksey, D. (2000). A new leaf blotch disease of sudangrass caused by Pantoea ananas and Pantoea stewartii. *Plant Dis.* 84, 973–979. doi: 10.1094/PDIS.2000.84.9.973

Badger, J. H., and Olsen, G. J. (1999). CRITICA: coding region identification tool invoking comparative analysis. *Mol. Biol. Evol.* 16, 512–524. doi: 10.1093/oxfordjournals.molbev.a026133

Bashan, Y., Diab, S., and Okon, Y. (1982). Survival ofXanthomonas campestris pv.vesictoria in pepper seeds and roots in symptomless and dry leaves in non-host plants and in the soil. *Plant Soil* 68, 161–170. doi: 10.1007/BF02373702

Bordiec, S., Paquis, S., Lacroix, H., Dhondt, S., Ait Barka, E., Kauffmann, S., et al. (2011). Comparative analysis of defence responses induced by the endophytic plant growth-promoting rhizobacterium Burkholderia phytofirmans strain PsJN and the non-host bacterium Pseudomonas syringae pv. pisi in grapevine cell suspensions. *J. Exp. Bot.* 62, 595–603. doi: 10.1093/jxb/erq291

Choi, O., Lim, J. Y., Seo, Y. S., Hwang, I., and Kim, J. (2012). Complete genome sequence of the rice pathogen *Pantoea ananatis* strain PA13. *J. Bacteriol.* 194, 531. doi: 10.1128/JB.06450-11

Compant, S., Mitter, B., Colli-Mull, J. G., Gangl, H., and Sessitsch, A. (2011). Endophytes of grapevine flowers, berries, and seeds: identification of cultivable bacteria, comparison with other plant parts, and visualization of niches of colonization. *Microb. Ecol.* 62, 188–197. doi: 10.1007/s00248-011-9883-y

Connolly, D. M., and Winkler, M. E. (1989). Genetic and physiological relationships among the miaA gene, 2-methylthio-N6-(delta 2-isopentenyl)-adenosine tRNA modification, and spontaneous mutagenesis in Escherichia coli K-12. *J. Bacteriol.* 171, 3233–3246.

Cota, L., Costa, R., Silva, D., Parreira, D., Lana, U., and Casela, C. (2010). First report of pathogenicity of *Pantoea ananatis* in sorghum (Sorghum bicolor) in Brazil. *Australas. Plant Dis. Notes* 5, 120–122. doi: 10.1071/DN10044

Cother, E., Reinke, R., Mckenzie, C., Lanoiselet, V., and Noble, D. (2004). An unusual stem necrosis of rice caused by Pantoea ananas and the first record of this pathogen on rice in Australia. *Australas. Plant Pathol.* 33, 495–503. doi: 10.1071/AP04053

Coutinho, T. A., and Venter, S. N. (2009). *Pantoea ananatis*: an unconventional plant pathogen. *Mol. Plant Pathol.* 10, 325–335. doi: 10.1111/j.1364-3703.2009.00542.x

Darling, A., Mau, B., Blattner, F., and Perna, N. (2004). Mauve: multiple alignment of conserved genomic sequences with rearrangements. *Genome Res.* 14, 1394–1403. doi: 10.1101/gr.2289704

Delcher, A. L., Bratke, K. A., Powers, E. C., and Salzberg, S. L. (2007). Identifying bacterial genes and endosymbiont DNA with Glimmer. *Bioinformatics* 23, 673–679. doi: 10.1093/bioinformatics/btm009

De Maayer, P., Chan, W., Blom, J., Venter, S., Duffy, B., Smith, T., et al. (2012a). The large universal Pantoea plasmid LPP-1 plays a major role in biological and ecological diversification. *BMC Genomics* 13:625. doi: 10.1186/1471-2164-13-625

De Maayer, P., Chan, W., Rezzonico, F., Buhlmann, A., Venter, S., Blom, J., et al. (2012b). Complete genome sequence of clinical isolate *Pantoea ananatis* LMG5342. *J. Bacteriol.* 194, 1615–1616. doi: 10.1128/JB.06715-11

De Maayer, P., Chan, W., Venter, S., Toth, I., Birch, P., Joubert, F., et al. (2010). Genome sequence of *Pantoea ananatis* LMG20103, the causative agent of Eucalyptus blight and dieback. *J. Bacteriol.* 192, 2936–2937. doi: 10.1128/JB.00060-10

De Maayer, P., Chan, W. Y., Rubagotti, E., Venter, S. N., Toth, I. K., Birch, P. R., et al. (2014). Analysis of the *Pantoea ananatis* pan-genome reveals factors underlying its ability to colonize and interact with plant, insect and vertebrate hosts. *BMC Genomics* 15:404. doi: 10.1186/1471-2164-15-404

De Maayer, P., Venter, S., Kamber, T., Duffy, B., Coutinho, T., and Smits, T. (2011). Comparative genomics of the type VI secretion systems of Pantoea and Erwinia species reveals the presence of putative effector islands that may be translocated by the VgrG and Hcp proteins. *BMC Genomics* 12:e576. doi: 10.1186/1471-2164-12-576

Durand, J. M., Bjork, G. R., Kuwae, A., Yoshikawa, M., and Sasakawa, C. (1997). The modified nucleoside 2-methylthio-N6-isopentenyladenosine in tRNA of Shigella flexneri is required for expression of virulence genes. *J. Bacteriol.* 179, 5777–5782.

English, G., Trunk, K., Rao, V., Srikannathasan, V., Hunter, W., and Coulthurst, S. (2012). New secreted toxin and immunity proteins encoded within the Type VI secretion system gene cluster of Serratia marcescens. *Mol. Microbiol.* 86, 921–936. doi: 10.1111/mmi.12028

Foster, T. J., and Hook, M. (1998). Surface protein adhesins of Staphylococcus aureus. *Trends Microbiol.* 6, 484–488. doi: 10.1016/S0966-842X(98)01400-0

Garcia-Alcalde, F., Okonechnikov, K., Carbonell, J., Cruz, L. M., Gotz, S., Tarazona, S., et al. (2012). Qualimap: evaluating next-generation sequencing alignment data. *Bioinformatics* 28, 2678–2679. doi: 10.1093/bioinformatics/bts503

Gitaitis, R. D., and Gay, J. D. (1997). First report of a leaf blight, seed stalk rot, and bulb decay of onion by pantoea ananas in Georgia. *Plant Dis.* 81, 1096–1096. doi: 10.1094/PDIS.1997.81.9.1096C

Goris, J., Konstantinidis, K. T., Klappenbach, J. A., Coenye, T., Vandamme, P., and Tiedje, J. M. (2007). DNA-DNA hybridization values and their relationship to whole-genome sequence similarities. *Int. J. Syst. Evol. Microbiol.* 57, 81–91. doi: 10.1099/ijs.0.64483-0

Griffiths-Jones, S., Moxon, S., Marshall, M., Khanna, A., Eddy, S. R., and Bateman, A. (2005). Rfam: annotating non-coding RNAs in complete genomes. *Nucleic Acids Res.* 33, D121–D124. doi: 10.1093/nar/gki081

Hara, Y., Kadotani, N., Izui, H., Katashkina, J., Kuvaeva, T., Andreeva, I., et al. (2012). The complete genome sequence of *Pantoea ananatis* AJ13355, an organism with great biotechnological potential. *Appl. Microbiol. Biotechnol.* 93, 331–341. doi: 10.1007/s00253-011-3713-5

Hardoim, P. R., Hardoim, C. C., Van Overbeek, L. S., and Van Elsas, J. D. (2012). Dynamics of seed-borne rice endophytes on early plant growth stages. *PLoS ONE* 7:e30438. doi: 10.1371/journal.pone.0030438

Hyatt, D., Chen, G. L., Locascio, P. F., Land, M. L., Larimer, F. W., and Hauser, L. J. (2010). Prodigal: prokaryotic gene recognition and translation initiation site identification. *BMC Bioinformatics* 11:119. doi: 10.1186/1471-2105-11-119

Jehl, M. A., Arnold, R., and Rattei, T. (2011). Effective–a database of predicted secreted bacterial proteins. *Nucleic Acids Res.* 39, D591–D595. doi: 10.1093/nar/gkq1154

Jensen, L. J., Julien, P., Kuhn, M., Von Mering, C., Muller, J., Doerks, T., et al. (2008). eggNOG: automated construction and annotation of orthologous groups of genes. *Nucleic Acids Res.* 36, D250–D254. doi: 10.1093/nar/gkm796

Johnston-Monje, D., and Raizada, M. N. (2011). Conservation and diversity of seed associated endophytes in Zea across boundaries of evolution,

ethnography and ecology. *PLoS ONE* 6:e20396. doi: 10.1371/journal.pone.0020396

Kearse, M., Moir, R., Wilson, A., Stones-Havas, S., Cheung, M., Sturrock, S., et al. (2012). Geneious basic: an integrated and extendable desktop software platform for the organization and analysis of sequence data. *Bioinformatics* 28, 1647–1649. doi: 10.1093/bioinformatics/bts199

Kim, H. J., Lee, J. H., Kang, B. R., Rong, X., Mcspadden Gardener, B. B., Ji, H. J., et al. (2012). Draft genome sequence of *Pantoea ananatis* B1-9, a nonpathogenic plant growth-promoting bacterium. *J. Bacteriol.* 194, 729. doi: 10.1128/JB.06484-11

Kloepper, J. W., Mcinroy, J. A., Liu, K., and Hu, C.-H. (2013). Symptoms of fern distortion syndrome resulting from inoculation with opportunistic endophytic fluorescent *Pseudomonas* spp. *PLoS ONE* 8:e58531. doi: 10.1371/journal.pone.0058531

Lagesen, K., Hallin, P., Rodland, E. A., Staerfeldt, H. H., Rognes, T., and Ussery, D. W. (2007). RNAmmer: consistent and rapid annotation of ribosomal RNA genes. *Nucleic Acids Res.* 35, 3100–3108. doi: 10.1093/nar/gkm160

Li, L., Stoeckert, C. J. Jr., and Roos, D. S. (2003). OrthoMCL: identification of ortholog groups for eukaryotic genomes. *Genome Res.* 13, 2178–2189. doi: 10.1101/gr.1224503

Lima-Mendez, G., Van Helden, J., Toussaint, A., and Leplae, R. (2008). Prophinder: a computational tool for prophage prediction in prokaryotic genomes. *Bioinformatics* 24, 863–865. doi: 10.1093/bioinformatics/btn043

Lowe, T. M., and Eddy, S. R. (1997). tRNAscan-SE: a program for improved detection of transfer RNA genes in genomic sequence. *Nucleic Acids Res.* 25, 0955–0964. doi: 10.1093/nar/25.5.0955

Lukashin, A., and Borodovsky, M. (1998). GeneMark.hmm: new solutions for gene finding. *Nucleic Acids Res.* 26, 1107–1115. doi: 10.1093/nar/26.4.1107

Mundt, J. O., and Hinkle, N. F. (1976). Bacteria within ovules and seeds. *Appl. Environ. Microbiol.* 32, 694–698.

Naveed, M., Mitter, B., Yousaf, S., Pastar, M., Afzal, M., and Sessitsch, A. (2014). The endophyte *Enterobacter* sp. FD17: a maize growth enhancer selected based on rigorous testing of plant beneficial traits and colonization characteristics. *Biol. Fertil. Soils* 50, 249–262. doi: 10.1007/s00374-013-0854-y

Nummelin, H., Merckel, M. C., Leo, J. C., Lankinen, H., Skurnik, M., and Goldman, A. (2004). The Yersinia adhesin YadA collagen-binding domain structure is a novel left-handed parallel β-roll. *EMBO J.* 23, 701–711. doi: 10.1038/sj.emboj.7600100

Paccola-Meirelles, L. D., Ferreira, A. S., Meirelles, W. F., Marriel, I. E., and Casela, C. R. (2001). Detection of a bacterium associated with a leaf spot disease of maize in Brazil. *J. Phytopathol.* 149, 275–279. doi: 10.1046/j.1439-0434.2001.00614.x

Pop, M., Phillippy, A., Delcher, A. L., and Salzberg, S. L. (2004). Comparative genome assembly. *Brief. Bioinform.* 5, 237–248. doi: 10.1093/bib/5.3.237

Reiter, B., and Sessitsch, A. (2006). Bacterial endophytes of the wildflower Crocus albiflorus analyzed by characterization of isolates and by a cultivation-independent approach. *Can. J. Microbiol.* 52, 140–149. doi: 10.1139/w05-109

Rijavec, T., Lapanje, A., Dermastia, M., and Rupnik, M. (2007). Isolation of bacterial endophytes from germinated maize kernels. *Can. J. Microbiol.* 53, 802–808. doi: 10.1139/W07-048

Ryan, R. P., Fouhy, Y., Lucey, J. F., Crossman, L. C., Spiro, S., He, Y.-W., et al. (2006a). Cell–cell signaling in Xanthomonas campestris involves an HD-GYP domain protein that functions in cyclic di-GMP turnover. *Proc. Natl. Acad. Sci. U.S.A.* 103, 6712–6717. doi: 10.1073/pnas.0600345103

Ryan, R. P., Fouhy, Y., Lucey, J. F., and Dow, J. M. (2006b). Cyclic Di-GMP signaling in bacteria: recent advances and new puzzles. *J. Bacteriol.* 188, 8327–8334. doi: 10.1128/JB.01079-06

Sayers, E. W., Barrett, T., Benson, D. A., Bolton, E., Bryant, S. H., Canese, K., et al. (2012). Database resources of the National Center for Biotechnology Information. *Nucleic Acids Res.* 40, D13–D25. doi: 10.1093/nar/gkr1184

Serrano, F. (1928). Bacterial fruitlet brown-rot of pineapple in the Philippines. *Phil. J. Sci.* 36, 271–305.

Sha, J., Rosenzweig, J., Kozlova, E., Wang, S., Erova, T., Kirtley, M., et al. (2013). Evaluation of the roles played by Hcp and VgrG type 6 secretion system effectors in Aeromonas hydrophila SSU pathogenesis. *Microbiology* 159, 1120–1135. doi: 10.1099/mic.0.063495-0

Shyntum, D., Venter, S., Moleleki, L., Toth, I., and Coutinho, T. (2014). Comparative genomics of type VI secretion systems in strains of *Pantoea ananatis* from different environments. *BMC Genomics* 15:163. doi: 10.1186/1471-2164-15-163

Smits, T., Rezzonico, F., Kamber, T., Goesmann, A., Ishimaru, C., Stockwell, V., et al. (2010). Genome sequence of the biocontrol agent Pantoea vagans C9-1. *J. Bacteriol.* 192, 6486–6487. doi: 10.1128/JB.01122-10

Stall, R. E., Alexander, L. J., and Hall, C. B. (1969). Effect of tobacco mosaic virus and bacterial infections on occurrence of graywall of tomato (Erwinia ananas). *Fla State Hort. Soc. Proc* 81, 157–161.

Steel, R. G. D., Torrie, J. H., and Dicky, D. A. (1997). *Principles and Procedures of Statistics: a Biometrical Approach, 3rd Edn.* Singapore: McGraw Hill Book Int. Co.

Stothard, P., and Wishart, D. S. (2005). Circular genome visualization and exploration using CGView. *Bioinformatics* 21, 537–539. doi: 10.1093/bioinformatics/bti054

Uniprot consortium. (2009). The universal protein resource (UniProt) *Nucleic Acids Res.* 37, D169–D174. doi: 10.1093/nar/gkn664

Weber, B., Hasic, M., Chen, C., Wai, S., and Milton, D. (2009). Type VI secretion modulates quorum sensing and stress response in Vibrio anguillarum. *Environ. Microbiol.* 11, 3018–3028. doi: 10.1111/j.1462-2920.2009.02005.x

Wells, J., Sheng, W., Ceponis, M., and Chen, T. (1987). Isolation and characterization of strains of Erwinia ananas from honeydew melons. *Phytopathol* 77, 511–514. doi: 10.1094/Phyto-77-511

Wilson, D. (1995). Endophyte: the evolution of a term, and clarification of its use and definition. *Oikos* 73, 274–276. doi: 10.2307/3545919

Wu, M., and Scott, A. J. (2012). Phylogenomic analysis of bacterial and archaeal sequences with AMPHORA2. *Bioinformatics* 28, 1033–1034. doi: 10.1093/bioinformatics/bts079

Zdobnov, E., and Apweiler, R. (2001). InterProScan - an integration platform for the signature-recognition methods in InterPro. *Bioinformatics* 17, 847–848. doi: 10.1093/bioinformatics/17.9.847

Conflict of Interest Statement: The authors declare that the research was conducted in the absence of any commercial or financial relationships that could be construed as a potential conflict of interest.

frontiers in Microbiology

ORIGINAL RESEARCH
published: 26 May 2015
doi: 10.3389/fmicb.2015.00419

Whole-genome comparative analysis of virulence genes unveils similarities and differences between endophytes and other symbiotic bacteria

*Sebastiàn Lòpez-Fernàndez, Paolo Sonego, Marco Moretto, Michael Pancher, Kristof Engelen, Ilaria Pertot and Andrea Campisano **

Research and Innovation Center, Fondazione Edmund Mach, Trento, Italy

OPEN ACCESS

Edited by:
Mysore V. Tejesvi, University of Oulu, Finland

Reviewed by:
Eric Kemen, Max Planck Institute for Plant Breeding Research, Germany
Dario Cantu, University of California Davis, USA

****Correspondence:***
Andrea Campisano, Department of Sustainable Agroecosystems and Bioresources, Research and Innovation Center, Fondazione Edmund Mach. Via E. Mach 1, San Michele All'adige, Trento 38010 Italy
andrea.campisano@fmach.it

Specialty section:
This article was submitted to Plant-Microbe Interaction, a section of the journal Frontiers in Microbiology

Received: *23 January 2015*
Accepted: *21 April 2015*
Published: *26 May 2015*

Citation:
Lòpez-Fernàndez S, Sonego P, Moretto M, Pancher M, Engelen K, Pertot I and Campisano A (2015) Whole-genome comparative analysis of virulence genes unveils similarities and differences between endophytes and other symbiotic bacteria. Front. Microbiol. 6:419. doi: 10.3389/fmicb.2015.00419

Plant pathogens and endophytes co-exist and often interact with the host plant and within its microbial community. The outcome of these interactions may lead to healthy plants through beneficial interactions, or to disease through the inducible production of molecules known as virulence factors. Unravelling the role of virulence in endophytes may crucially improve our understanding of host-associated microbial communities and their correlation with host health. Virulence is the outcome of a complex network of interactions, and drawing the line between pathogens and endophytes has proven to be conflictive, as strain-level differences in niche overlapping, ecological interactions, state of the host's immune system and environmental factors are seldom taken into account. Defining genomic differences between endophytes and plant pathogens is decisive for understanding the boundaries between these two groups. Here we describe the major differences at the genomic level between seven grapevine endophytic test bacteria, and 12 reference strains. We describe the virulence factors detected in the genomes of the test group, as compared to endophytic and non-endophytic references, to better understand the distribution of these traits in endophytic genomes. To do this, we adopted a comparative whole-genome approach, encompassing BLAST-based searches through the GUI-based tools Mauve and BRIG as well as calculating the core and accessory genomes of three genera of enterobacteria. We outline divergences in metabolic pathways of these endophytes and reference strains, with the aid of the online platform RAST. We present a summary of the major differences that help in the drawing of the boundaries between harmless and harmful bacteria, in the spirit of contributing to a microbiological definition of endophyte.

Keywords: comparative genomics, virulence, core genome, endophyte, synteny, niche occupation

Introduction

After the breakthrough of Koch's molecular postulates (Falkow, 2004), bacteriology has been challenged by a new definition of "pathogen." The fact that horizontal gene acquisition may confer virulence traits to harmless bacteria (Charpentier and Courvalin, 1999; Rosas-Magallanes et al., 2006; Kelly et al., 2009) is changing the dogma on the separation between beneficial or detrimental microorganisms. The interaction in microbial communities can also trigger the disease process

(Shankar et al., 2014) and recently a shift of the paradigm from "pathogens" to "pathobiome" was proposed (Vayssier-Taussat et al., 2014). This is especially true for those microorganisms inhabiting complex communities in the gastrointestinal tract of mammals (Britton and Young, 2012), insect guts (Cariveau et al., 2014), in soils and in the phyllosphere, rhizosphere, and endosphere of plants (Troxler et al., 1997; Christensen et al., 1998). Recent studies have cleared that imbalances in host-associated microbial populations, in signaling within bacterial communities and in the immune state of the host play a crucial role in pathogenicity and in disease development (Monack et al., 2004; Parker and Sperandio, 2009; Cardenas et al., 2012).

Plant-borne bacteria can live on the surface or inside their hosts, establishing bonds at different levels, ranging from a loose, free-living lifestyle in the vicinity of the host, to a tight association inside tissues (Little et al., 2008). In the latter case they can live intercellularly or intracellularly without causing any apparent damage or disruption to the plant's homeostasis. Bacteria with this lifestyle are defined as endophytes (Reinhold-Hurek and Hurek, 2011). An endophytic lifestyle benefits a microorganism by providing shelter, facilitating access to carbon sources and increasing its overall fitness. In turn, endophytes may improve plant health and competitiveness by synthesizing molecules involved in plant protection against pests and pathogens (Clarke et al., 2006), nitrogen fixation (Hurek et al., 2002), and induction or enhancement of plant defense mechanisms (Iniguez et al., 2005; Bordiec et al., 2011).

In spite of the experimental evidence showing that many endophytes are beneficial to plants, so far scientists have not succeeded in singling out specific traits that could help categorize bacteria as endophytic organisms. On the other hand, for plant and animal pathogens, genes, and gene families associated with virulent phenotypes have been identified in the past. Several examples exist, including the locus of enterocyte effacement (LEE) in *E. coli* that produces the enterohemorragic phenotype on the gastrointestinal tract (Elliott et al., 2000), the *cag* pathogenicity island in *Helicobacter pylori* responsible for the initiation of the inflammatory response in bacterially-induced gastric ulcers (Backert et al., 2004), or the *hrp* pathogenicity island in the plant pathogenic *Erwinia amylovora*, that encodes a type III secretion system enabling the bacterium to infect the host, ultimately leading to the blighting of tissues and development of disease (Oh et al., 2005).

While endophytes might possess a genetic weaponry similar to that of virulent microorganisms, its expression and regulatory mechanisms are different (Xu et al., 2014), and the coordination of activities and cell to cell communication in the community greatly explains these differences between mutualistic and pathogenic bacteria. This makes the boundaries between the two lifestyles diffuse (Clay and Schardl, 2002; Schulz and Boyle, 2005; Zuccaro et al., 2011; Dubois et al., 2012). For example, the construction of mutants unable to synthesize type IV pili in *Xyllela fastidiosa*, a well-known plant pathogen, showed the impairment for its basipetal translocation in grapevine and a diminished colonization rate, making it more similar to a symbiont (Meng et al., 2005). The analysis of colonization traits and the evaluation of the production of endoglucanases and endopolygalacturonases also showed that the *Burkholderia phytofirmans* strain PsJN indeed utilizes cell-wall degrading enzymes to colonize grapevine tissues (Compant et al., 2005). This phenotype is widespread among pathogens as a means of colonizing plants, thus showing that the definition of endophytes is still *per se* imprecise.

Genome sequencing has become increasingly accessible and the abundance of genomic data is undoubtedly improving our understanding of the evolution of traits involved in mutualism and parasitism (Parkhill et al., 2003; De Maayer et al., 2010; Kahlke et al., 2012). In addition to this, the annotation of genomes and the discovery of biochemical pathways *in silico* has proven a promising tool for bioprospecting in unexplored habitats (Ahmed, 2009). Comparative genomics analyzes several genomes simultaneously to find similarities and differences between them and to study traits that could be further manipulated in the lab by means of genetic engineering (Suen et al., 2010). Genome alignment, synteny plots and core and accessory genome elucidation are basic tools for the genomic study of microorganisms and have proved to be useful in biotechnology (Bentley and Parkhill, 2004; Binnewies et al., 2006).

The increasing knowledge of the composition and organization of chromosomes of endophytes is ultimately providing a body of data large enough to explain complex traits such as plant growth promotion, biocontrol, and symbiosis-specific attributes in different bacteria-plant symbiosystems (Amadou et al., 2008; Fouts et al., 2008; Yan et al., 2008; Tian et al., 2012). To give an example, the analysis of the genome of *B. phytofirmans* PsJN, a grapevine colonizing Gram negative bacterium, has revealed the mechanisms the endophyte uses to colonize the plants. These include bacterial polymer-degrading enzymes, siderophores, and several protein secretion systems (Mitter et al., 2013). These colonization mechanisms are the same used by pathogens to infect plants.

Most of the comparative genomics analyses carried out on endophytes have focused on showing similarities in beneficial traits (Sugawara et al., 2013). Fewer have addressed the main commonalities between endophytes and pathogens. Virulence traits shared by pathogenic bacteria and endophytes could be a milestone for the understanding of adaptation to different hosts and lead to the inception of new tools for the control of detrimental organisms or for improving the performance of beneficial symbionts.

In this work we sequenced the genomes of seven bacterial endophytes isolated from Italian grapevine, belonging to the genera *Enterobacter*, *Erwinia,* and *Pantoea*. We used the sequenced genomes to make comparisons with twelve available genomes of bacteria belonging to the same taxa, but having different lifestyles (endophytic, epiphytic, pathogenic to humans, or pathogenic to plants). Our aim was to determine whether or not the genomes of these endophytes resembled those of organisms engaged in other lifestyles (especially the genomes of pathogens) and whether we could single out specific characteristics of endophytism.

Materials and Methods

Bacterial Strains Used in this Study

We sequenced the genome of seven bacterial endophytes isolated from Italian *Vitis vinifera* (*Enterobacter ludwigii*. EnVs6, *En. ludwigii*. EnVs2, *En. ludwigii*. LecVs2, *Erwinia* sp. ErVv1, *Pantoea vagans*. PaVv1, *P. vagans*. PaVv7 *P. vagans* PaVv9) belonging to the family Enterobacteriaceae. The strains were previously characterized in terms of plant growth promotion, antibiotic resistance, exoenzyme production, *N*-acyl homoserine lactone production, and biocontrol activity against plant pathogens (Campisano et al., 2015). Of these seven strains (henceforth referred to as "test strains"), three belong to the genus *Entoerobacter,* three to the genus *Pantoea*, and one to the genus *Erwinia* (**Table 1**). Twelve available genome sequences of reference strains (four for each genus mentioned above), including either or both human-, plant-pathogenic, endophytic or epiphytic strains, were selected for genome comparison and served as controls for the purpose of this work (*En. cloacae* subsp. *cloacae* ATCC 13047, *En. asburiae* LF7a, *En. aerogenes* KCTC 2190, *En.* sp. 638, *P. agglomerans* 299R, *P. ananatis* LMG 20103, *P. ananatis* PA13, *P. vagans* C9-1, *Er. billingiae* Eb661, *Er. amylovora* ATCC 49946, *Er. pyrifoliae* Ep1-96, *Er. pyrifoliae* Ejp617). We chose four reference genomes for each genus because their sequences are complete and available online. The ecology and properties of these strains (henceforth referred as "reference strains") have also been studied previously. The identity and genomic characteristics of these strains are summarized in **Table 1** and in Supplementary Table ST1.

DNA Extraction, Genome Sequencing and Assembly

The test strains were grown in nutrient broth (NB; Oxoid, United Kingdom) at 200 r.p.m on a SI600R rotatory incubator (MID SCI, USA) at 30 ± 2°C until an OD_{600} value of 0.8. Bacterial cells were pelleted on an ANNITA PK12 R bench centrifuge (ALC International, Italy) for 5 min at 10,000 r.c.f. The pellet was washed with sterile phosphate buffer saline (PBS) 1× and DNA was extracted using the RBC real genomics DNA extraction kit (RBCBiosciences, China) according to the manufacturer's instructions. DNA concentration was estimated using a Nanodrop 8000 UV-VIS spectrophotometer (Thermo Scientific, Germany). DNA integrity and the absence of RNA contamination were checked by electrophoresis on a 1% agarose gel. Sequencing libraries were constructed using the Nextera DNA Sample Prep Kit (Illumina, Inc., USA) according to the manufacturer's instructions. DNA-seq libraries were pooled at 10-plex level of multiplexing and sequenced paired-end 100 bp on a HiSeq2000 Illumina sequencer at IGA Technology Services (Udine, Italy). Raw images were processed using Illumina Pipeline version 1.8.2.

The assembly of the genomes from test strains was performed as follows. Three of the genomes (EnVs6, ErVv1, and PaVv9) were assembled using the A5 pipeline release 20140401 (Tritt et al., 2012); other four assemblies (PaVv7, EnVs2, LecVs2, and PaVv1) were produced using the SOAPdenovo software, version 2.04 (Luo et al., 2012). The assemblies were done using the two aforementioned pipelines as they provided the optimal number of contigs and N50, after testing different methods. Quality of the sequences was evaluated using the quality assessment tool for genome assemblies (QUAST) to produce metrics of quality using two different assembly pipelines (Alexey et al., 2013).

Annotation and Subsystem Analysis

Genomes were annotated using the Prokaryotic Genome Annotation System (PROKKA) (Seemann, 2014). To eliminate the bias of different annotation systems employed, test and reference genomes were all submitted to the online platform RAST (Rapid Annotation using Subsystem Technology) version 2.0.

We chose six RAST subsystems central to our analysis (cell wall and capsule, iron acquisition and metabolism, chemotaxis, phages and mobilome, regulation and cell signaling, virulence and disease) to build a presence/absence map through a series of Perl® scripts (Wall et al., 2000), which summarize all pairwise comparisons into a unique list, including all genes assigned to the chosen subsystems. A list of genes common to all compared genomes was compiled using a custom script in R version 3.0.2 (R Core Team, 2013).

Phylogeny

We retrieved the sequences of the test strains' 16S rDNA genes from RAST and confirmed that they were identical to those previously deposited in GenBank (Campisano et al., 2015). We then used the 16S rDNA sequences downloaded from RAST to perform a blastn search against the NCBI database (Wheeler et al., 2007), and aligned them with the closest sequences from the database using the clustalW algorithm implemented in the software bioedit version 7.2.5 (Hall, 1999).

We reconstructed the phylogeny using the tree-building algorithm Neighbour-Joining with the Jukes-Cantor distance estimator implemented in MEGA6 version 6.0.6 (Tamura et al., 2013). We assigned the phylogeny, when possible, to the species level.

Whole-genome Comparison

We used several methods for whole-genome comparison to identify similarities and differences between each test strain's genome and reference genome in the same genus. First we retrieved the assembled genomes from RAST and aligned them against one reference genome for each genus using MAUVE version 2.3.1 (Darling et al., 2004). Following this step we performed a multiple whole–genome alignment using the progressive alignment algorithm implemented in MAUVE. We used the output of this alignment to check for rearrangements in each genome.

Syntheny plots were constructed as had been done previously (Husemann and Stoye, 2010) by aligning regions of the test and reference genomes that differed by no more than 8% and shared at least 44 overlapping 11mers no more distant from each other than 64 nucleotides. All regions were aligned and displayed in r2cat (Husemann and Stoye, 2010). We drew several plots to check for syntheny against reference strains with different degrees of relatedness, for each of the three genera under study.

TABLE 1 | Characteristics of the genomes used in this study.

Species	Habitat/host	Lifestyle	Chromosome size (bp)	G + C content (%)	Number of ORF*	References
En. cloacae subsp. *cloacae* ATCC 13047	Human	Pathogenic humans	5,314,588	54.79	5518	Ren et al., 2010
En. asburiae LF7a	Human	Pathogenic humans	5,012,130	53.84	4612	Brenner et al., 1986
En. aerogenes KCTC 2190	Human	Pathogenic humans	5,280,350	54.8	4912	Shin et al., 2012
En. sp. 638	Poplar	Endophytic	4,518,712	52.98	4240	Taghavi et al., 2010
Er. billingiae Eb661	Pear tree	Epiphytic	5,100,168	55.2	4587	Kube et al., 2010
Er. amylovora ATCC 49946	Apple tree	Pathogenic plant	3,805,874	53.5	3483	Sebaihia et al., 2010
Er. pyrifoliae Ep1-96	Pear tree	Pathogenic plant	4,026,322	53.4	3645	Kube et al., 2010
Er. pyrifoliae Ejp617	Pear tree	Pathogenic plant	3,909,168	53.64	3873	Park et al., 2011
P. agglomerans 299R	Pear tree	Endophytic	4,581,483	54.29	4194	Remus-Emsermann et al., 2013
P. ananatis LMG 20103	Eucalyptus tree	Pathogenic plant	4,690,000	53.69	4241	De Maayer et al., 2010
P. ananatis PA13	Rice plants	Pathogenic plant	4,586,378	53.66	4372	Choi et al., 2012
P. vagans C9-1	Apple tree	Epiphytic	4,025,000	55.09	4619	Smits et al., 2010
En. ludwigii. EnVs6	Grapevine plants	Endophytic	5,220,112	54.62	4809	This study
En. ludwigii EnVs2	Grapevine plants	Endophytic	5,067,900	53.98	4649	This study
En. ludwigii LecVs2	Grapevine plants	Endophytic	5,285,925	54.59	4886	This study
Er. sp. ErVv1	Grapevine plants	Endophytic	4,719,019	54.6	4207	This study
P. vagans PaVv1	Grapevine plants	Endophytic	4,850,774	55.14	4453	This study
P. vagans PaVv7	Grapevine plants	Endophytic	4,879,255	55.22	4470	This study
P. vagans PaVv9	Grapevine plants	Endophytic	9,754,510	54.65	9466	This study

**ORF stands for open reading frames.*

We constructed a circular genomic map for each genome using the BLAST Ring Image Generator (BRIG, version 0.95; Alikhan et al., 2011). Each circular genomic map was drawn using the genome of one reference strain (henceforth referred to as "alignment reference genome") on a local BLAST + basis, with standard parameters (50% lower – 70% upper cut-off for identity and *E*-value of 10). For the genus *Enterobacter* we used the fully sequenced genome of the poplar endophyte *Enterobacter* sp. 638 as a reference to align all genomes under this genus. For the genus *Erwinia* we used the sequenced genome of *Er. amylovora* ATCC 49946. For *Pantoea* we used the genome sequence of the biocontrol agent *P. vagans* C9-1. The ring color gradients correspond to varying degrees of identity of BLAST matches. Circular genomic maps also include information on GC skew and GC content.

Clustering of Orthologous Families

In order to depict the core and accessory genome in each genus, we performed a reciprocal best hit search using the OrthoMCL software release five (Li et al., 2003). For this we downloaded the predicted coding sequences (CDS) of the reference and the test strains and performed a blastp search against each other with an *E*-value cut-off of 10^{-5} and a sequence coverage higher than 50%, as reported previously (Li et al., 2013). We used a series of built-in scripts to (i) parse, (ii) upload to the MySQL relational database, (iii) perform a reciprocal best hit analysis to form pairs of sequences, and to (iv) normalize the *E*-values for all the pairs formed. Normalization of *E*-values was done by by averaginf all recent orthologs (in paralogs) and dividing each pair of orthologs by the average Finally, using the Markov Cluster Algorithm (MCA) program, the sequences were distributed in orthologous families using 1.5 as the inflation value. We calculated the pangenome size as the sum of the CDS in all the genomes and the accessory genome size (within each genus and for each species) as the difference between the pangenome and the core genome. We assigned functions to all orthologous families and filtered virulence functions using a set of Perl® scripts. We also used a list of keywords to query for virulence functions in the orthologous families and to calculate the number of matches of those functions, using custom bash commands.

Secretion System Analysis

The Lawrence Livermore national laboratory virulence database (MvirDB; Zhou et al., 2007) and the virulence factors of pathogenic bacteria database (VFDB; Chen et al., 2012) contain hundreds of gene annotations related to virulence determinants of bacteria and have been curated since 2007. We used these resources to download datasets of virulence genes (either validated or predicted). We chose a set of bacterial secretion systems (ranging from type I to type VII) to locate secretion system genes in the genomes of the test strains. The matching results were drawn in a presence/absence map.

CRISPRs and Phage Presence

To evaluate the presence of CRISPRs (Clustered Regularly Interspaced Short Palindromic Repeats) we analyzed the assembled genomes of the seven test strains using the CRISPR Recognition Tool CRT (Bland et al., 2007). Also we search for putative phage sequences in the test strains in the online tool PHAST (Zhou et al., 2011).

Results

Sequencing and Assembly of Endophytic Genomes

The characteristics of the genomes sequenced in this study, including length, GC content and amount of transfer, and ribosomal RNA genes are summarized in **Table 1** and in Supplementary Table ST1. The sequencing of the 16S rDNA revealed that the test strains under the genus *Enterobacter* are closely related to *En. ludwigii*; strain ErVv1 under the genus *Erwinia* is related to *Er. amylovora* and *Er. tasmaniensis,* while the *Pantoea* test strains are closely related to *P. vagans* (Supplementary Figure SF1). The sequencing data is deposited in the EMBL-EBI repository (https://www.ebi.ac.uk/ena) with accession numbers PRJEB8251 (EnVs6); PRJEB8253 (EnVs2); PRJEB8254 (LecVs2); PRJEB8255 (PaVv1); PRJEB8258 (PaVv7); PRJEB8259 (PaVv9); and PRJEB8284 (ErVv1).

To optimize the assembly procedure, we compared the performance of two different pipelines (A5 and SOAPdenovo) through the online tool QUAST (Supplementary Table ST2). The realignments of the reads showed consistently good results with high realignment percentages and the distribution of the insert sizes within the limits of the suggested values from the sequencing provider (∼600/800 bp). The Log Aaverage Probability (LAP) scores (Ghodsi et al., 2013) from the different assemblies for the same organism were also very close, showing that both pipelines produced comparable results. We used this scores and the N50 values to choose which assembly pipeline to use. For strain LecVs2, pipeline A5 did not produce any results. Thus, we used the Velvet pipeline (Zerbino and Birney, 2008) to assemble the genome and compared it with the SOAPdenovo assember. Quality analysis showed that differences between the two pipelines were minimal as presented in Supplementary Table ST2. Scripts to build up the assemblies are deposited and publicly available at the github online public repository (at the address https://github.com/pochotustra/genomics_endophytes.git as Supplementary Material SM1-4

Comparison of Genome Structure between Endophytic and Non-Endophytic Genomes

A visual inspection of the circular alignment of genomes under the genus *Enterobacter* (**Figures 1A, B**) highlights that two of the test genomes (EnVs2 and LecVs2) are similar to the alignment reference genome of endophytic strain 638, while the test strain EnVs6 is similar to the reference genomes of human pathogens (ATCC 13047, LF7a, and KCTC 2190). The region between 1–800 kbp is well conserved in all three test isolates (EnVs6, EnVs2, and LecVs2). The rest of the chromosome is more variable, with regions where the identity between EnVs2 and LecVs2 reaches up to a 70% while the test strain EnVs6 aligns better with the genomes of pathogens (ATCC 13047, LF7a, and KCTC 2190). A positive to negative GC skew at position 1 corresponds to the origin of replication and the switch at 2200 kbp may account for the replication terminus. Regions at 2800–2880 and 3120–3200 kbp have higher content of GC. Several regions in the genome of test strains (EnVs2 and LecVs2) are syntenic with the genome of the alignment reference genome of endophytic strain 638. For strain EnVs6 however this synteny is less conspicuous as it is made evident in the alignment plot (Supplementary Figures SF2A–C). Regions between 240–280 kbp and between 4040–4080 kbp in the test strains (EnVs2, EnVs6, and LecVs2) show an identity higher than 70% to the alignment reference genome of strain 638. In these regions we located genes related to the thiamin biosynthesis (the thiamin phosphate pyrophosporilase and the thiamin biosynthesis gene *thiC*) and several genes of the *yjb* operon that regulate the synthesis of a stress-induced exopolysaccharide in *E. coli* (Ionescu et al., 2008). We also found that more than 10 regions in the genome of strain 638 and of the test strains (EnVs2 and LecVs2) are absent in the pathogenic reference strains and in one test strain (ATCC 13047, LF7a, KCTC 2190, and EnVs6). These missing regions contain several enzymes involved in nitrogen assimilation including genes coding for a 2,3,4,5-tetrahydropyridine-2,6-dicarboxylate *N*-succinyltransferase, a uridylyltransferase and several enzymes for the synthesis of the core carbohydrate 3-deoxy-D-manno-octulosonic acid (KDO).

In the genus *Erwinia* a positive to negative GC skew at position 1 in **Figure 1C** corresponds to the origin of replication and a positive to negative GC switch at approximately 1920 kbp corresponds to the replication terminus in all the genomes compared. We found seven positions with higher GC contents in regions 440–480, 600–960, 1280–1320, 1640–1720, 2200–2640, 2880–2920, and 3340–3400 kbp. These regions contain several virulence factors including *vgrG, virB* and several *imp* all genes related to the type VI secretion system (Filloux et al., 2008). Also, several genes of the biotin biosynthesis pathway and a few DNA repair genes like the methylated DNA protein cysteine methyltransferase are found in these regions, according to the location on the genome of the alignment reference genome ATCC 49946.

A qualitative interpretation of the plots suggests that the genome of strain ErVv1 is similar to that of the alignment reference genome ATCC 49946 and they share several regions that are not present in the other genomes compared. Conversely, the reference strains Ep1-96, Eb661, and Ejp617 are more similar to each other. The more evident gaps highlighting the missing regions are visible at positions 40–60, 440–530, 2400–2440, 2920–2960, 3120–3160, 3220–3240, and 3360–3400 kbp (**Figure 1C**). Synteny plots constructed for the test strain genomes under taxa *Erwinia* show a high degree of homology with the alignment reference genome. The number of insertions or deletions is low, which is confirmed by the continuity in the plots. For strain ErVv1 the number of discontinuities is higher (6 regions of the genome being separated by indels; Supplementary Figure SF2D**).**

In **Figure 1D** we compare test and reference strains of the *Pantoea* group. The test strains PaVv1 and PaVv9 are similar to the C9-1 strain used as alignment reference genome, while the test strain PaVv7 is very similar to the genomes of pathogens PA13 and LMG20103. We found regions with higher GC content at positions 960–1120, 1800–2200, 2560–2600, and 2840–2920 kbp. The GC switches at 1440 kbp (positive to negative) and at 3480 kbp (negative to positive) may represent

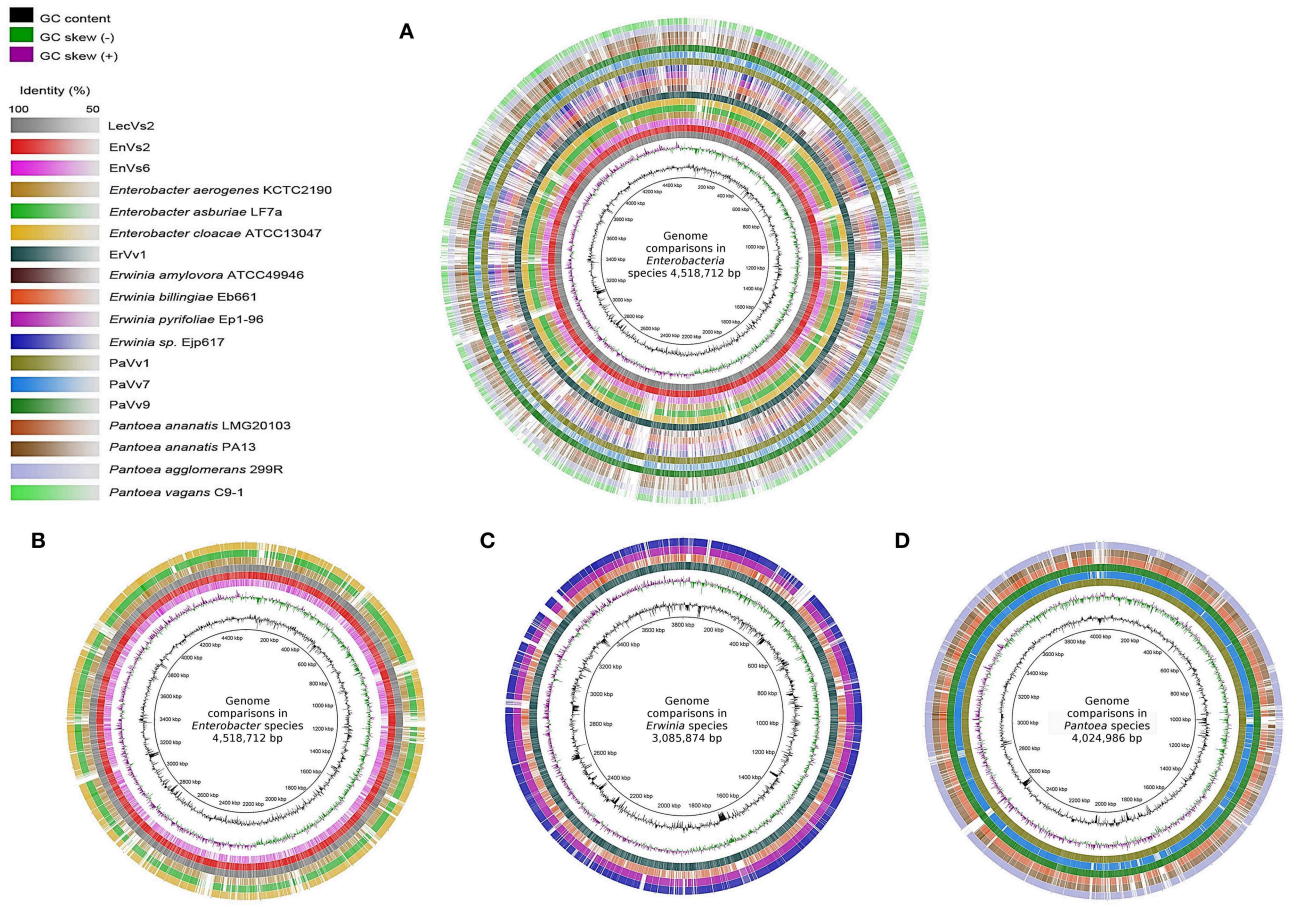

FIGURE 1 | Whole-genome comparisons in three genera of Enteobacteria. The color intensity in each ring represents the BLAST match identity. **(A)** whole-genome comparison of all the strains considered in this work. **(B)** Whole-genome comparisons in *Enterobacter*, from outer to inner ring: *En. cloacae* subsp. *cloacae* ATCC 13047, *En. asburiae* LF7a, *En. aerogenes* KCTC 2190, *En. ludwigii* LecVs2, *En. ludwigii* EnVs2, *En. ludwigii* EnVs6; reference genome: *Enterobacter* sp. 638. **(C)** Whole-genome comparisons in Erwinia, from outer to inner ring: *Er.* ErVv1, *Er. pyrifoliae* Ejp617, *Er. pyrifoliae* Ep1-96, *Er. billingiae* Eb661; reference genome: *Er. amylovora* ATCC 49946. **(D)** whole-genome comparisons in *Pantoea*, from outer to inner ring: *P. agglomerans* 299R, *P. ananatis* PA13, *P. ananatis* LMG 20103, *P. vagans* PaVv9, *P. vagans* PaVv7, *P. vagans* PaVv1; reference genome: *P vagans* C9-1.

the origin of replication and replication terminus, respectively (**Figure 1D**). The sequence identity between the test strains (PaVv1, PaVv7, and PaVv9) and the alignment reference genome C9-1 is high throughout the alignment and can reach peaks of up to 100%. This is more evident in the regions between 200–1700 and 2400–4000 kbp. Several regions shared between the alignment reference genome and the test strains are instead absent in the genomes of pathogens PA13 and LMG20103. The genes differentially present in these regions are involved in cysteine metabolism, isoprenoid biosynthesis and in the transport and metabolism of D-glucarate (ascorbic acid biosynthesis).

Synteny plots made for *Pantoea* show homology of test strains to the alignment reference genome C9-1. We located two exceptional re-arrangements (indels) in strains PaVv9 and PaVv1 that are not present in strain PaVv7 (Supplementary Figures SF2E–G).

Commonalities and Differences in the Core and Accessory Genome of Enterobacterial Strains

Genus Enterobacter

Our analysis shows that the core genome in this taxon comprises 2468 orthologous genes that correspond to 53% of the pangenome (**Figure 2A** and Supplementary Figure SF3). Venn diagrams show genes exclusively shared between test strains and either of the reference genomes. In strains EnVs6, EnVs2, and LecVs2, the number of genes shared exclusively with the endophytic reference strain 638 was 149, 127, and 150, respectively. The number of genes shared exclusively with the pathogenic reference strain (ATCC 13047) was 254, 257, and 256, respectively (**Figure 3A**).

In the genus *Enterobacter*, the abundance of genes in each category (see Supplementary Table ST3 for a list of categories used) was similar in all genomes (**Figure 4**). The cell signaling and two-component system genes are present in all of the strains

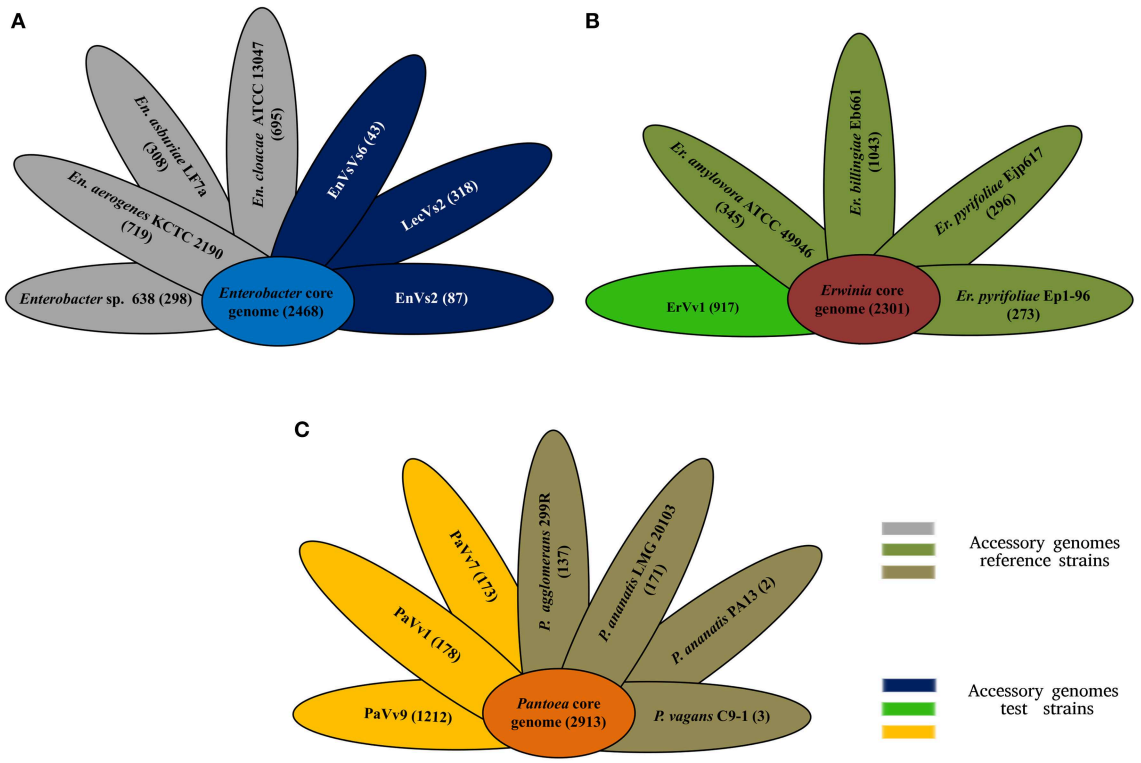

FIGURE 2 | Core and accessory genome size. (A) Core (sky blue) and accessory genome size of reference (gray petals) and test (deep blue) strains of the genus *Enterobacter*. **(B)** Core (terracotta) and accessory genomes of reference (olive petals) and test (bright green petals) strains of the genus *Erwinia*. **(C)** Core (orange) and accessory genomes of reference (brown petals) and test (yellow petals) strains of the genus *Pantoea*. Numbers indicate genes counts.

analyzed. In these systems, transcriptional regulators belonging to the LysR and GntR families (Fujita and Fujita, 1987; Maddocks and Oyston, 2008) are the most important. We found a conserved set of about 40 genes devoted to the synthesis of cell wall and capsule that are shared among all *Enterobacter* genomes under analysis. Among these, we highlight the presence of *rlpB*, *rcsF*, *lptA*, *lptC* and the organic solvent tolerance protein *lptD*a set of genes involed in LSP biosynthesis (McCandlish and Silhavy, 2007) and the oxidoreductases *mviM* and *mviN*, necessary for murein synthesis (Inoue et al., 2008). We found an average of 51.8 flagellar genes across the *Enterobacter* genomes with a maximum in the reference pathogenic strain ATCC 13047. A set of genes that belong to the *che* operon for chemotaxis signaling and to the twitching motility apparatus are also present in the core genome. The number of genes related to pathogenicity mechanisms was slightly higher in the genomes of the test strains LecVs2 and EnVs6 and in the genome of the reference genome ATCC 13047. Among these genes we emphasize the presence of a virulence sensor related to the *bvgS* sensor kinase and of *arnC* belonging to the polymixin resistance group. We report the presence of a type 1 secretion system agglutinin of the RTX family (Linhartová et al., 2010) and members of a tripartite multidrug resistance system. Some of the genes in this category are also related to the type II secretion systems and genes for the biogenesis of type IV pilus. The categories with the lowest number of genes were phages and *quorum sensing* in which the highest number of genes among the test strains was in the genome of EnVs6 (**Figure 4**) Several protein coding sequences for phage capsid and phage associated enzymes (terminases and integrases) are shared among all strains. In the *quorum sensing* category we detected the presence of the *sdiA* gene of the orphan *quorum sensing* communication circuit from *E. coli* (Kanamaru et al., 2000). We also located the a *N*-acyl homoserine lactone synthase in all genomes. No AI-2 dependent *quorum sensing* systems were detected in the test strains. We found no variation in the content of siderophore related genes (average 52,14 genes). However, the test strains (EnVs6, EnVs2, and LecVs2) contain a higher number of genes for this category as compared to all the reference strains (**Figure 4**) We found the genes for enterobactin synthesis and some of the genes for hemin metabolism. Also, exo- and endoenzymes are present in the core genome of the *Enterobacter* including the phospholipase A and two hemolysins.

Genus Erwinia

In the genus *Erwinia*, the core genome is constituted by 2301 gene clusters that correspond to the 60% of the pangenome (**Figure 2B** and Supplementary Figure SF3). Venn diagrams in **Figure 3B** show genes exclusively shared between test strains either the endophytic reference genomes or the pathogenic reference genomes. We found that strain ErVv1 shares 133 genes

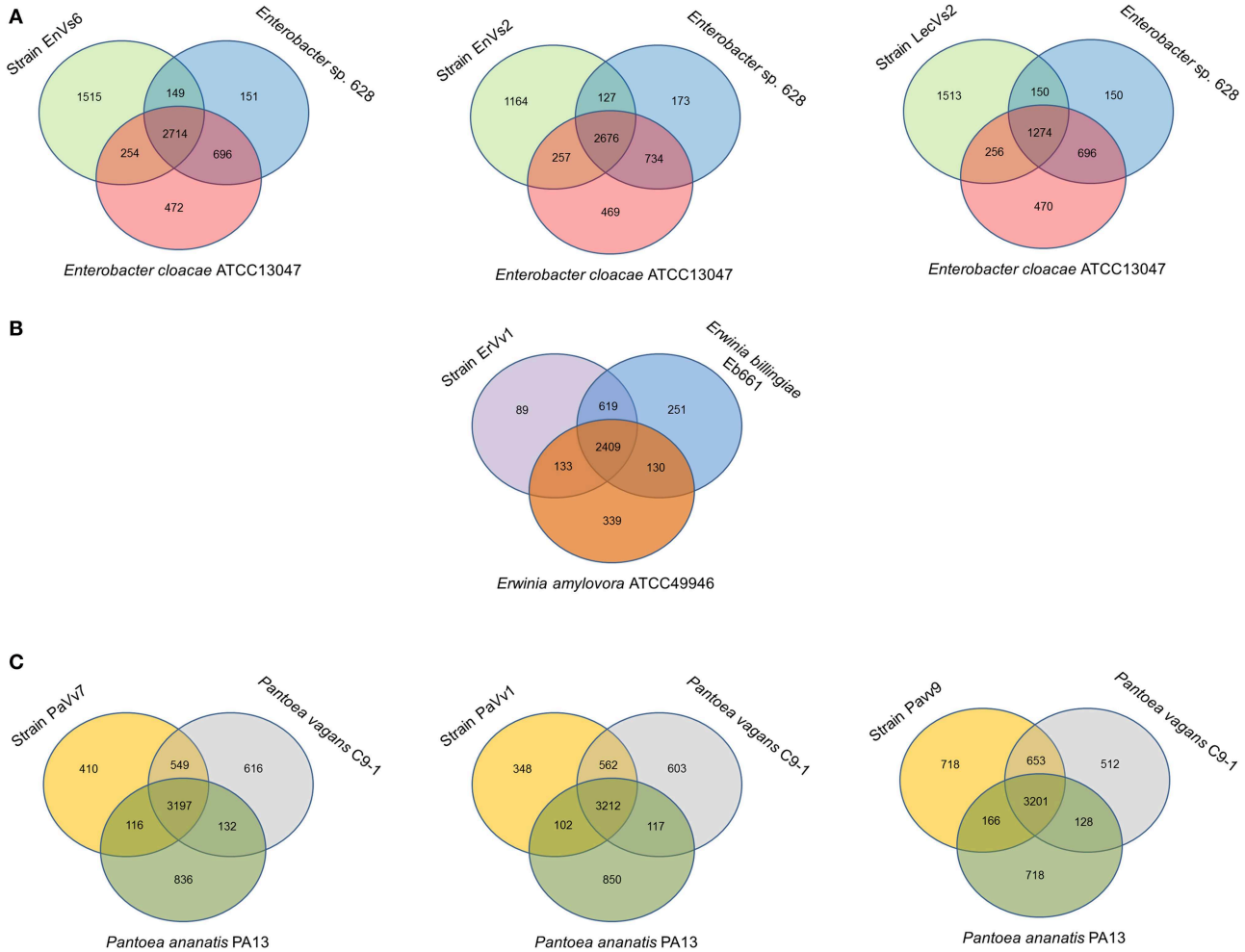

FIGURE 3 | Venn diagrams showing shared and unique genes in *Enterobacteriaceae*. All comparisons are made between the test strains (left circle) with an epiphyte or endophyte (right circle) and a pathogen (lower circle). **(A)** Comparison of strains EnVs6, EnVs2, and LecVs2 with the endophyte *Enterobacter.* sp. 638 and the human pathogen *En. cloacae* ATCC 13047**; (B)** comparison of strain ErVv1 with the epiphyte *Er. billingiae* strain Eb661 and the plant pathogen *Er. amylovora* ATCC 49946; **(C)** comparison of strains PaVv7, PaVv1, and PaVv9 with the epiphyte *P. vagans* C9-1 and the plant pathogen *P. ananatis* PA13. Numbers inside the circles, indicate the genes shared among genomes.

exclusively with the apple tree pathogen ATCC 49946 and shares 619 genes exclusively with the epiphyte Eb661.

The core genome of the genus *Erwinia* defined in this study is populated with cell signaling functions including two component systems sensitive to nitrates, copper and osmolarity (**Figure 4**). We located also two transcriptional factors belonging to the Rrf2 family involved in the metabolism of cysteine (Shepard et al., 2011) and a cyclic AMP regulator of the *crp/fnr* family (Shimada et al., 2011). Among the most important gene functions for cell wall is the regulator in colanic acid synthesis that confers a mucoid phenotype in other taxa. The flagellar machinery is present in all the strains analyzed. As pathogenicity mechanisms we detected multidrug efflux transporters as well as heavy metal detoxification genes including the *arcB* gene (Iuchi et al., 1990) and the cation efflux pump *fieF* (Munkelt et al., 2004); it also bears well-known antibiotic inactivating proteins, including the *ampG* beta lactam activation protein (Lindquist et al., 1993) and both *mdtK* and the multidrug resistance protein D *emrD* (Lomovskaya and Lewis, 1992). Several phage elements and the *sdiA* gene from the *quorum sensing* circuit along with a *N*-acyl homoserine lactone synthase and a homoserine lactone transporter are conserved in all species analyzed. The core genome contains also general mechanisms for iron acquisition that comprise 36 different functions. In the exoenzyme category we found two cellulose synthesis genes, one phospholipase A and a cryptic hemolysin regulator.

Genus Pantoea

In the genus *Pantoea* we found 2913 orthologous families. The core genome corresponds to 60% of the pangenome (**Figure 2C** and Supplementary Figure SF3). Venn diagrams show that strain PaVv7 shares 549 genes exclusively with the symbiont C9-1 while test strains PaVv1 and PaVv9 share 562 and 653, respectively. One-hundred and sixteen genes are shared exclusively between

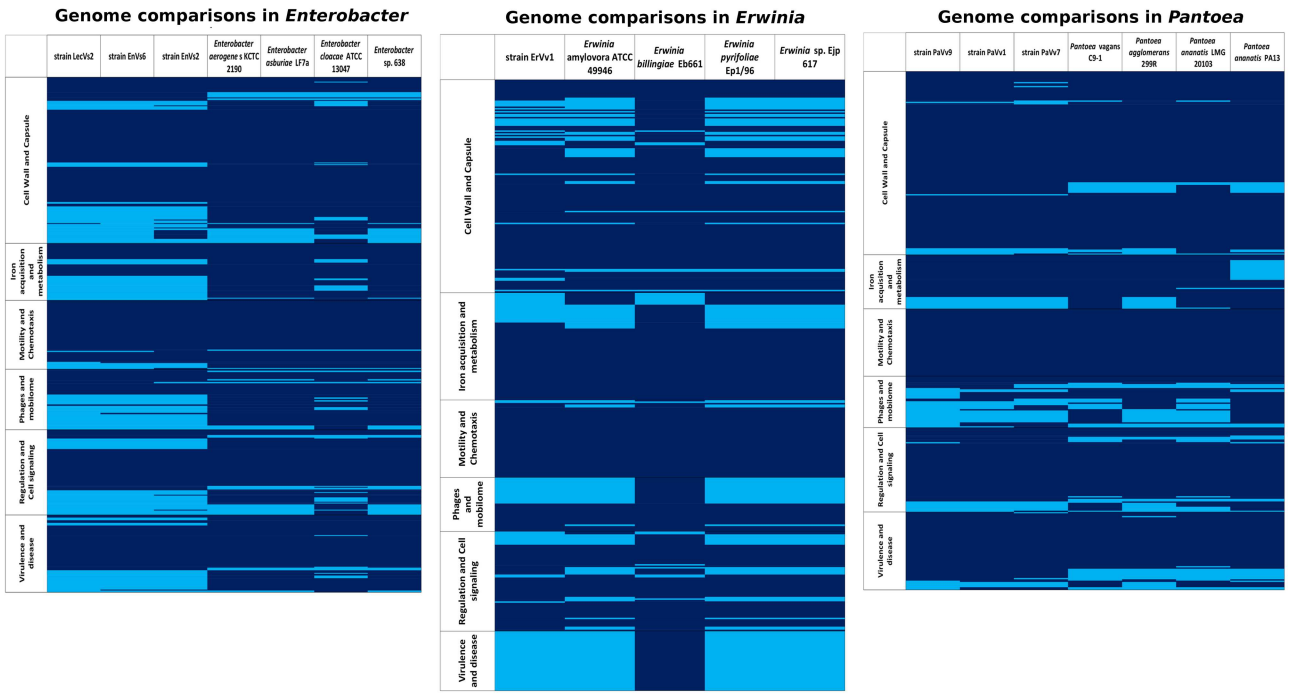

FIGURE 4 | Presence/absence map based on six functional gene categories (from RAST). Rows: within categories, each line represents a gene; deep blue, gene presence; sky blue, gene absence. Columns: each column represents an analyzed genome in the genus *Enterobacter*, *Erwinia,* or *Pantoea*.

the rice pathogen PA13 and the test strain PaVv7 while test strains PaVv1 and PaVv9 share 102 and 166 genes, respectively (**Figure 3C**).

The cell signaling mechanisms in the core genome of *Pantoea* include the diguanylate cyclase mediator of biofilm formation, along with other biofilm-related genes like *rcsB* (Shiba et al., 2006), and one ribose metabolizing gene *rpiR* (Sorensen and Hove-Jensen, 1996). In this category two distinct groups*: one* made of 299R, LMG 20103, PaVv1, and PaVv7 and a second group made of PaVv9, C9-1, and PA13 are well defined (**Figure 4**) The cell wall and capsule functions form the same two groups, in which the second group has a greater number of genes in the core genome (**Figure 4**). The functions for these genes are linked to the synthesis of the exopolysaccharide substance amylovoran and of lipopolysaccharide modifications. The presence of a putative cellulose synthesis gene is consistent in all the species. Among the flagellar genes we were able to recognize three different groups: 299R and LMG20103; PaVv1 and PaVv7; PaVv9, C9-1, and PA13. As for pathogenicity mechanisms, we found that the number of genes in strain PaVv9 is the highest among the test strains (282 genes) and similar to the number found in the reference plant pathogen PA13 (290 genes). Also a high number of genes for flagellum assembly (139 genes), exo- and endo-enzymes (117 genes), capsule (141 genes), and phages (37 genes) is present in this test strain PaVv9 as compared to the other test strains and to some of the reference genomes (**Figure 4**). Inside the core genome, we located the *shlA* gene and several other putative adhesines. We also found the *pilN* gene of pilus biogenesis (Sakai and Komano, 2000) along with the two partner secretion system *tpsA/B* that correspond to a conserved virulence factor for host adhesion and toxicity in bacterial cells (Ur Rahman and Van Ulsen, 2013). Finally, we provide evidence for the presence of the phenazine synthesis gene *phzF* (Parsons et al., 2004). Some of the virulence-related gene products are transmembrane transporters including members of the major facilitator superfamily (MFS) and members of the Tol-Pal system involved in membrane integrity and phage acquisition. The core genome of the *Pantoea* is poor in genes related to iron acquisition although it contains important elements belonging to the ABC transporters and to the TonB-dependent pathway. Also in the core genome of the *Pantoea* species analyzed in our study, several exo- and endo-enzymes were detected. Particularly, we were able to track the *bcs* genes involved in cellulose metabolism. Several regulatory proteases make part of the core genome of the genus. We found *hsl*, *clp*, *lon,* and *fts* present in all the genomes analyzed. We also detected a lipase gene LIP-1 and the collagenase *yhbU* that has been implicated in virulence of several animal pathogens. We report also the finding of a LuxI-type coding gene, similar to the *pagI* synthase and a transcriptional activator belonging to the LuxR family that's related to the *N*-3-oxohexanoyl-L-homoserine lactone quorum-sensing transcriptional activator of *P. agglomerans* (**Figure 4**).

Unique Gene Functions in the Different Lifestyles

Presence/absence maps based on six RAST categories from annotated genomes of test and reference strains were obtained (**Figure 4**). In each genus, a list of shared and unique features of virulence-related genes was drawn (Supplementary Table ST4).

The genomes of both reference and test strains in all genomes contain most of the main functions for cell wall synthesis and flagellum synthesis which are basic for the niche occupation. They are characterized however, by minor differences in which some genes are unique for test strains or for reference strains, respectively.

In the genus *Enterobacter* some genes involved in the modification of lipopolysaccharide as well as genes related to the glicocalix synthesis and modification are lacking in the test strains (Supplementary Table ST5). Genes related to the use of sialic acid are present only in the test and absent in the reference genomes. We also found that genes involved in the metabolism hemin and synthesis of aerobactin are absent in the test and present in the reference genomes. We detected variable content of flagellar genes since test strains possess one component of the flagellum apparatus uniquely present and lack one gene of the *che* group.

In the genus *Erwinia* we highlight four genes that are absent in the genomes of the reference strains with unrelated functions: antibiotic resistance, detoxification of xenobiotics and stress response (Supplementary Table ST6).

In the genus *Pantoea* we stress the presence of genes that are unique only in the test strains. These genes are necessary for plasmid stability and for recognition and resistance to exogenous substances. On the other hand, the test strains lack genes for modification of the KDO in the LPS an one sequence coding for structural components of a phage, that are only present in the reference strains (Supplementary Table ST7).

Other Virulence Determinants: Screening for CRISPRs, Phages, and Secretion Systems

CRISPRs

We identified only two CRISPR systems, located in the genome of strain EnVs6 (**Table 2**). The systems consist of two sets of repeats of approximately 20 nt each. The first set consisting of only three spacers and four repeats and the second system with seven repeats and six spacers. No CRISPRs were identified in the genomes of strains LecVs2, EnVs2, ErVv1, PaVv1, PaVv7, or PaVv9.

Phages

With RAST we observed the presence of several phage-related proteins including the tail and sheath proteins as well as DNA modifying proteins of phage origin (Supplementary Tables ST5–7), We used PHAST to confirm the presence of phages that we were able to identify with RAST. With PHAST we were able to identify 12 intact phages in the genomes of the test strains EnVs6, LecVs2, EnVs2, PaVv9, PaVv1, PaVv7 (Supplementary Table ST8). The phage sequences belong to different types of phages, and are identical to those present in *Enterobacter* genomes deposited in NCBI. The phages do not seem related to one another.

Secretion Systems

We detected some of the components for major secretion system in all test strains (Supplementary Table ST9). In all the test strains we detected some of the flagellar components plus the protein *clpV*. In *Enterobacter*, all test strains contain the hemaglutinin/adhesin gene *shlA* (Poole and Braun, 1988). In *Erwinia* we did not find any common secretion system gene among the test and reference strains and in *Pantoea* test strains we found the protein Sfa3 of the type VI secretion system apparatus in *Pseudomonas aeruginosa* (Sana et al., 2013).

Discussion

In this work we compared the genomes of seven bacterial grapevine endophytes, belonging to three genera of the family Enterobacteriacea using several methods including whole-genome alignments and synteny plots. We selected this taxon because it contains some of the most important human and plant pathogens (*Escherichia coli*, *Salmonella typhimurium*, *Shigella flexneri, Pantoea ananatis,* and *Erwinia amylovora* among several others) but also includes beneficial species. We also calculated the core and accessory genomes and showed that the core genome of three genera of enterobacteria are populated with virulence factors. Further, we provide evidence for ecological genus-level trends in endophytic organisms, reflected in their genomes' organization. We also highlighted a set of genes that are uniquely present in some isolates, that may possibly account for specificity in niche occupation. Finally, using a subsystem categorization of the main virulence traits in annotated genomes, we revealed that endophytes bear a very similar set of virulence traits within their genomes and that the patterns of gene distribution can be comprable to that of pathogens, fulfilling one of the conditions of the pathobiome hypothesis.

Our study clearly shows how, endophytic test genomes are not only similar to reference endophytes but also share several characteristics with pathogenic reference genomes (**Figure 1** and Supplementary Figure SF2). At the structural level, We have demonstrated a high degree of synteny between endophytic test and reference strains (Supplementary Figure SF2) but also a high identity percentage at the genome level between endophytes and symbionts with other lifestyles (**Figure 1**). We hypothesize that these traits reflect the potential of bacterial endophytes to express virulence when associated with their hosts and therefore the similarity of pathogens and endophytes at the genomic level. In *Pantoea* for example, the similarities at the structural level between endophytes and plant pathogens are linked to the absence of regions that contain key enzymes for aminoacid biosynthesis and vitamin production. In *Enterobacter* it is the absence of genes for central metabolism and of some, but not all, genes for exopolysaccharide modification (that are otherwise present in the endophytic reference strain 638) and in *Erwinia* the similarities between test and pathogenic reference genomes are based on the synteny between the genomes of the test strain ErVv1 and the reference strain ATCC 49946 (Supplementary Figure SF2G) and on the presence of virulence genes from pathogenicity islands (a trademark genome arrangement of virulent phenotypes (**Figure 4** and Supplementary Table ST9). These genomic structures might be a sign of lifestyle switching (from endophytes to pathogens and viceversa) when conditions are optimal for such phenomenon. For example, strains that have no enzymes for ascorbic acid production might be prone to take it from the environment, thus scavenging the substrates from the

TABLE 2 | CRISPRs found in the genome of strain EnVs6.

Range	Position	Repeat	Spacer
CRISPR 1 Range: 556393–556547	556393	CGCCATTCATGGCGACCTT	ATTAATGGCCGCACCCTGCCCCG
	556435	CGCCATTCATGGCGACCTT	CTTCTTACACGCACCCAACNTAATCCGTAGGGT
	556487	CGCCATTCATGGCGACCTT	ATTAATGGCCGCACCCTGCCCCG
	556529	CGCCATTCATGGCGACCTT	
CRISPR 2 Range: 2949702–2949985	2949702	ATGTTCACTGTAATCAGTAAA	ACTTGATGACTTTTCTTTCTCAACGCCTA
	2949752	ACATTCACTGTAATCAGTGAA	AACCTTGTGCTCATCATAGACAA
	2949796	AGATTCACTGTAGTCAGTAGA	TGGTTATCGCGCTTCGATTTA
	2949838	ACGTTCACTGTAATCAGTAAG	TCAAATCTGCAACTTCGACAGA
	2949881	ACATTCACTGTAATCAGTAAA	AGTTATGACCCGGAGAAGA
	2949921	ACGTTCACTGTAATCAGCAAA	GCTTGTTTAGTACTTTGATACGA
	2949965	GCGTTCACTGTAATCAGTAAA	

host's cells (Abu Kwaik and Bumann, 2013). Also, the presence of pathogenicity island components might suggest the use of such modules to achieve colonization using a pathogen-like strategy.

Schulz and colleagues proposed in 2005 that the endophytism might be an outcome of the interactions in what has been termed the "disease triangle" (i.e., the endophyte's innate virulence, the immune responses of the host, and several environmental variables). In their studies, they conclude that adaptation of endophytic fungi to plant's organs (a particular biotope) determines the neutral to beneficial association that endophytes hold with their hosts. In the light of our results, we suggest that this state of "balanced antagonism" is dictated extensively by the genomic determinants that permit such adaptation. In that sense, our results provide further evidence to reinforce this model of interactions between endophytes and plants and pave the road to further research toward the understanding of how the balanced antagonism is kept in particular hosts and how adaptation to plant may be key to the transition between pathogenic to endophytic lifestyles.

Our comparisons also show that, endophytes, epiphytes, and pathogens share a wide number of virulence-related genes. We found that core genomes are densely populated with virulence factors. These genes are present in each of the genomes in this study (**Figures 2**, **4**) and they mark a baseline for the existence of a core virulence genome. Furthermore, the virulence-related genes found in the core genomes are conserved within each genus, regardless of pathogenic or endophytic lifestyles (**Figure 4**). For example, the core genome of the genus *Pantoea* is characterized by the largest number of virulence-related genes (**Figure 4**) as a genus-specific characteristic and genes existing in this taxon are not present in the other groups analyzed (**Figure 4** and Supplementary Table ST7). This supports our hypothesis that differences between endophytes and pathogens do not exist *per se*, and demonstrates that the similarities between these two groups are set above the species level. We believe that the most abundant functions in each of the analyzed core genomes are crucial for understanding the balanced antagonism (Schulz et al., 1999) and that these functions point at the co-evolution of endophytes and pathogens. Among these, we suggest that two-component systems (especially those that regulate responses to heavy metals and those that mediate repression of gene expression), genes involved in modification of exopolysaccharide and lipopolysaccharide, genes for antibiotic resistance, efflux pumps, and cellulose metabolism are functions crucial for the endophyte-pathogenic dycotomy. These specific functions are important since they have an impact on pathogenicity as was shown for example, in genes for cellulose synthesis and catabolism (Rajeshwari et al., 2005). Previous research found that mutations in these genes can attenuate the virulent phenotype of some strains (Matthysse et al., 1995) and it is then conceivable that such mutations or downregulation of gene expression may produce an endophytic phenotype as an attenuated virulence state. We extend this rationale to other genes of the core genomes, like those coding for the phospholipase A, a well-known virulence determinant that in human pathogens is activated upon antagonistic antimicrobial activity (Istivan and Coloe, 2006); the *clpV* gene that has been linked to the proper folding of effector proteins in pathogenic strains (Schlieker et al., 2005; Filloux et al., 2008) and those virulence-related genes that are key in regulatory networks in other taxa, including the orphan *quorum sensing* gene s*diA* (Kanamaru et al., 2000) found in all the strains analyzed. Some of these functions appear more frequently in the genomes of microorganisms adopting a specific lifestyle (pathogenicity, endophytism, and other lifestyles), and their abundance may vary accross these groups with specific functions associating to specific lifestyles (Dr Pablo Hardoim, personal communication). Although our methods for calculating virulence factors may have introduced a bias (indeed this could explain why such associations are not clearly emerging from our data), the genes that we have found in this study reflect existing and previously reported functions. Together with the aformentioned findings, our observations are consistent with the emerging idea of pathobiome and "balanced antagonism," by which host-adapted bacteria can play different roles, depending on their relations with the environment.

Complementary to the core genome, the accessory genome reveals differences in niche specialization. Variation in accessory genome size might be related to the endophytic lifestyle, since genome reduction is reported in symbiotic microorganisms (McCutcheon and Moran, 2012). Strain EnVs6 for example,

displays the smallest accessory genome in the *Enterobacter* set of strains (**Figure 2A**), fitting the concept that endophytes have reduced genomes as compared to pathogens. In contrast, the accessory genome of the test strain ErVv1 is large, paralleling the one of the epiphyte strain Eb661 (**Figure 2B**). Also, genome structure in the test strains resembles that of endophytic reference genomes (**Figure 2**) in the number of genes that compose the accessory genome. For example, in **Figure 2A** the accessory genomes of strain EnVs2 and EnVs6 contain lower gene numbers, similar to what happens in the endophytic reference genomes *Enterobacter* sp. 638. The same happens in strain ErVv1, which contains about the same number of genes as the endophytic *E. billingiae* Eb661 (**Figure 2B**) and in strains PaVv1 and PaVv7 that are similar to the endophytic reference *P. agglomerans* 299R (**Figure 2C**). Niche specialization might be related to the abundance of gene functions like the toxin-antitoxin systems (**Figure 4** and Supplementary Table ST5) that are thought to be more abundant in free living engaging bacteria and fewer in other types of lifestyle (Pandey and Gerdes, 2005) and the ABC-type polar amino acid transport system for opine translocation (Moore et al., 1997) that in other taxa is important for selection of bacterial pathogenic subpopulations.

Although we report several functions that are characteristically shared between endophytic test strains and reference strains with other types of lifestyles (pathogens and epiphytes), we present a set of genes that could be found only in the endophytic genomes, either test or reference strains. We are uncertain of how these genes affect virulence in endophytes. As shown in Supplementary Table ST4 the nature of this genes is quite diverse and span from functions related to the normal modification of the cell surface (in the cell wall and capsule category) to the catabolism of by-products of the S-adenosyl cystein pathway (in the regulation and cell signaling category). However, it is yet to be discovered how such modifications might be involved in the mechanisms of colonization or if they are used for beneficial associations or for pathogenicity.

Reinhold-Hurek and Hurek (2011) have highlighted the main characteristics of bacterial endophytes and the challenges for the study of this lifestyle. The term "disarmed pathogen" has arisen for endophytes that certainly hold a virulent background in their genomes while lacking a set of genes allegedly atributed to virulence. Also, these reserchers have proposed that endophytic colonization might be followed by a very mild immune response in the plant due to the presence (or absence) of microbial associated molecular patterns (MAMPs) and that these response, although related to strategies pathogens of colonization, differs in magnitud and perhaps in mechanisms. Our results agree with these points since we have been able to identify the presence of virulence factors that remind the arsenal of pathogenic bacteria (for example the presence of a collection of genes dedictated to the siderophore enterobactin synthesis in *Enterobacter* test strain, Supplementary Table ST5) but we have also shown that some of the endophytic strains lack genes that have been proven to be key for virulence in pathogenic bacteria (for example, genes involved in flagellum assembly that might be triggers of plant's immune responses, Supplementary Table ST9). We propose that some of these traits provide clues on how bacteria with an endophytic lifestyle maintain a symbiotic relation with its host as they are present sometimes only in endophytes and moreover in grape endophytes (test strains). This is the case of endophytic phage sequences (Supplementary Table ST8) which are not rare in the endophytic genomes (Ozer et al., 2014). We speculate that a link between phage sequences and the attenuation of virulence in endophytes might exist given the widespread appearance of such sequences only in the genomes of test strains. Moreover, a genome analysis of the endophytic test strains revealed that the core endophytic genome (i.e., the collection of orthologous genes present only in the endophytic test strains of our set) contains only 536 gene families (the endophytic core genome of our test strains) and is populated with functions related to vitamin synthesis and to cell signaling as well as virulence(data not shown). This suggestins that endophytic only a limited part of the genome of endophytes is dedicated to sych associations and that virulence is a leading trait in that core genome.

Summing up these observations, we suggest that endophytes conserve properties of different lifestyles, including pathogenic traits. This is reflected in the structural organization of the genomes (**Figure 1**) and in the overlapping functions between the test strains and the genomes of plant or animal pathogens, epiphytes, or endophytes (**Figures 3**, **4**). We propose that endophytic and pathogenic lifestyles are composed of a base core virulence genome that might be used and expressed differentially, as has been shown for other taxa (Meysman et al., 2013). While this background virulence genome exists for all species analyzed (**Figure 4**, and Supplementary Table ST9), regardless of their lifestyle, there are devoted genes that permit niche specialization and occupation either in the core and in the accesory genome (**Figure 2** and **Table 1**). This level of genomic organization makes the genomes of the test strains structurally similar to the genome of a strain that fits into one kind of lifestyle (for example strain ErVv1 being similar to the reference alignment genome strain ATCC 13047 in the genomic map of **Figure 1**) while functionally recalling a different lifestyle (for example genes shared between strain ErVv1 and the epiphyte Eb661 in **Figure 3B**). Our findings might also explain intra-genus specificity as shown for test endophytes under genera *Pantoea* and *Erwinia* that share a larger number of genes with the non-pathogenic references, while those under genus *Enterobacter* share more genes with the pathogenic reference genome (**Figure 3**). Lifestyle in pathogens or endophytes might be the outcome of a complex, multifactorial interaction. Our conclusions are consistent with the hypothesis that relationships between environment, host and microorganism(s) contribute to shape the environmental role of microorganisms in this symbiosis, independent of their phylogenetical relatedness. Our research is to the best of our knowledge a pioneer in two regards. First, we are showing similarities between sequenced genomes of endophytic strains from grapevine while also emphasizing on the differences that our endophytic test strains present when compared with organisms spanning other lifestyles. Secondly, we are using comparative genomics to establish a link between the genome content and genome organization of endophytic (beneficial)

organisms with niche occupation, by highlighting the role of specific characteristics of the genome, that lead to different degrees of specialization.

Acknowledgments

We would like to thank Sergio I. Tusso from Uppsala University for support with Perl and Python scripts, Britt Koskella from University of Exeter for the insightful discussions on phages and Pablo Hardoim from University of Algarve for providing unpublished data. This work was funded by Provincia Autonoma di Trento, progetto PAT - Call 2 Team 2009 - Incoming – Mecagrafic. We thank COST Action FA1103 for providing network activities.

Supplementary Material

The Supplementary Material for this article can be found online at: http://journal.frontiersin.org/article/10.3389/fmicb.2015.00419/abstract

References

Abu Kwaik, Y., and Bumann, D. (2013). Microbial quest for food *in vivo*: "nutritional virulence" as an emerging paradigm. *Cell. Microbiol.* 15, 882–890. doi: 10.1111/cmi.12138

Ahmed, N. (2009). A flood of microbial genomes-do we need more? *PLoS ONE* 4:e5831. doi: 10.1371/journal.pone.0005831

Alexey, G., Vladislav, S., Nikolay, V., and Glenn, T. (2013). QUAST: quality assessment tool for genome assemblies. *Bioinformatics* 29, 1072–1075. doi: 10.1093/bioinformatics/btt086

Alikhan, N. F., Petty, N. K., Ben Zakour, N. L., and Beatson, S. A. (2011). BLAST Ring Image Generator (BRIG): simple prokaryote genome comparisons. *BMC Genomics* 12:402. doi: 10.1186/1471-2164-12-402

Amadou, C., Pascal, G., Mangenot, S., Glew, M., Bontemps, C., Capela, D., et al. (2008). Genome sequence of the beta-rhizobium *Cupriavidus taiwanensis* and comparative genomics of rhizobia. *Genome Res.* 18, 1472–1483. doi: 10.1101/gr.076448.108

Backert, S., Schwarz, T., Miehlke, S., Kirsch, C., Sommer, C., Kwok, T., et al. (2004). Functional analysis of the cag pathogenicity island in *Helicobacter pylori* isolates from patients with gastritis, peptic ulcer, and gastric cancer. *Infect. Immun.* 72, 1043–1056. doi: 10.1128/IAI.72.2.1043-1056.2004

Bentley, S. D., and Parkhill, J. (2004). Comparative genomic structure of prokaryotes. *Annu. Rev. Genet.* 38, 771–792. doi: 10.1146/annurev.genet.38.072902.094318

Binnewies, T. T., Motro, Y., Hallin, P. F., Lund, O., Dunn, D., La, T., et al. (2006). Ten years of bacterial genome sequencing: comparative-genomics-based discoveries. *Funct. Integr. Genomics* 6, 165–185. doi: 10.1007/s10142-006-0027-2

Bland, C., Ramsey, T. L., Sabree, F., Lowe, M., Brown, K., Kyrpides, N. C., et al. (2007). CRISPR recognition tool (CRT): a tool for automatic detection of clustered regularly interspaced palindromic repeats. *BMC Bioinformatics* 8:209. doi: 10.1186/1471-2105-8-209

Bordiec, S., Paquis, S., Lacroix, H., Dhondt, S., Ait Barka, E., Kauffmann, S., et al. (2011). Comparative analysis of defence responses induced by the endophytic plant growth-promoting rhizobacterium *Burkholderia phytofirmans* strain PsJN and the non-host bacterium *Pseudomonas syringae* pv. pisi in grapevine cell suspensions. *J. Exp. Bot.* 62, 595–603. doi: 10.1093/jxb/erq291

Brenner, D. J., Mcwhorter, A. C., Kai, A., Steigerwalt, A. G., and Farmer, J. J. III. (1986). Enterobacter asburiae sp. nov., a new species found in clinical specimens, and reassignment of *Erwinia dissolvens* and *Erwinia nimipressuralis* to the genus *Enterobacter* as *Enterobacter dissolvens* comb. nov. and *Enterobacter nimipressuralis* comb. nov. *J. Clin. Microbiol.* 23, 1114–1120.

Britton, R. A., and Young, V. B. (2012). Interaction between the intestinal microbiota and host in *Clostridium difficile* colonization resistance. *Trends Microbiol.* 20, 313–319. doi: 10.1016/j.tim.2012.04.001

Campisano, A., Pancher, M., Puopolo, G., Puddu, A., Lòpez-Fernàndez, S., Biagini, B., et al. (2015). Diversity in endophytic populations reveals functional and taxonomic diversity between wild and domesticated grapevines. *Am. J. Enol. Vitic.* 66, 12–21. doi: 10.5344/ajev.2014.14046

Cardenas, A., Rodriguez, R. L., Pizarro, V., Cadavid, L. F., and Arevalo-Ferro, C. (2012). Shifts in bacterial communities of two Caribbean reef-building coral species affected by white plague disease. *ISME J.* 6, 502–512. doi: 10.1038/ismej.2011.123

Cariveau, D. P., Elijah Powell, J., Koch, H., Winfree, R., and Moran, N. A. (2014). Variation in gut microbial communities and its association with pathogen infection in wild bumble bees (Bombus). *ISME J.* 8, 2369–2379. doi: 10.1038/ismej.2014.180

Charpentier, E., and Courvalin, P. (1999). Antibiotic Resistance in *Listeria* spp. *Antimicrob. Agents Chemother.* 43, 2103–2108.

Chen, L., Xiong, Z., Sun, L., Yang, J., and Jin, Q. (2012). VFDB 2012 update: toward the genetic diversity and molecular evolution of bacterial virulence factors. *Nucleic Acids Res.* 40, D641–D645. doi: 10.1093/nar/gkr989

Choi, O., Lim, J. Y., Seo, Y.-S., Hwang, I., and Kim, J. (2012). Complete genome sequence of the rice pathogen *Pantoea ananatis* strain PA13. *J. Bacteriol.* 194, 531–531. doi: 10.1128/JB.06450-11

Christensen, B. B., Sternberg, C., Andersen, J. B., Eberl, L., Møller, S., Givskov, M., et al. (1998). Establishment of new genetic traits in a microbial biofilm community. *Appl. Environ. Microbiol.* 64, 2247–2255.

Clarke, B. B., White, J. F., Hurley, R. H., Torres, M. S., Sun, S., and Huff, D. R. (2006). Endophyte-mediated suppression of dollar spot disease in fine fescues. *Plant Dis.* 90, 994–998. doi: 10.1094/PD-90-0994

Clay, K., and Schardl, C. (2002). Evolutionary origins and ecological consequences of endophyte symbiosis with grasses. *Am. Nat.* 160(Suppl. 4), S99–S127. doi: 10.1086/342161

Compant, S., Reiter, B., Sessitsch, A., Nowak, J., Clement, C., and Ait Barka, E. (2005). Endophytic colonization of *Vitis vinifera* L. by plant growth-promoting bacterium Burkholderia sp. strain PsJN. *Appl. Environ. Microbiol.* 71, 1685–1693. doi: 10.1128/AEM.71.4.1685-1693.2005

Darling, A. C., Mau, B., Blattner, F. R., and Perna, N. T. (2004). Mauve: multiple alignment of conserved genomic sequence with rearrangements. *Genome Res.* 14, 1394–1403. doi: 10.1101/gr.2289704

De Maayer, P., Chan, W. Y., Venter, S. N., Toth, I. K., Birch, P. R., Joubert, F., et al. (2010). Genome sequence of *Pantoea ananatis* LMG20103, the causative agent of *Eucalyptus* blight and dieback. *J. Bacteriol.* 192, 2936–2937. doi: 10.1128/JB.00060-10

Dubois, T., Faegri, K., Perchat, S., Lemy, C., Buisson, C., Nielsen-Leroux, C., et al. (2012). Necrotrophism is a quorum-sensing-regulated lifestyle in *Bacillus thuringiensis*. *PLoS Pathog.* 8:e1002629. doi: 10.1371/journal.ppat.1002629

Elliott, S. J., Sperandio, V., Giron, J. A., Shin, S., Mellies, J. L., Wainwright, L., et al. (2000). The locus of enterocyte effacement (LEE)-encoded regulator controls expression of both LEE- and non-LEE-encoded virulence factors in enteropathogenic and enterohemorrhagic *Escherichia coli*. *Infect. Immun.* 68, 6115–6126. doi: 10.1128/IAI.68.11.6115-6126.2000

Falkow, S. (2004). Molecular Koch's postulates applied to bacterial pathogenicity–a personal recollection 15 years later. *Nat. Rev. Micro.* 2, 67–72. doi: 10.1038/nrmicro799

Filloux, A., Hachani, A., and Bleves, S. (2008). The bacterial type VI secretion machine: yet another player for protein transport across membranes. *Microbiology* 154, 1570–1583. doi: 10.1099/mic.0.2008/016840-0

Fouts, D. E., Tyler, H. L., Deboy, R. T., Daugherty, S., Ren, Q., Badger, J. H., et al. (2008). Complete genome sequence of the N2-fixing broad host range endophyte *Klebsiella pneumoniae* 342 and virulence predictions verified in mice. *PLoS Genet.* 4:e1000141. doi: 10.1371/journal.pgen.1000141

Fujita, Y., and Fujita, T. (1987). The gluconate operon *gnt* of *Bacillus subtilis* encodes its own transcriptional negative regulator. *Proc. Natl. Acad. Sci. U.S.A.* 84, 4524–4528. doi: 10.1073/pnas.84.13.4524

Ghodsi, M., Hill, C. M., Astrovskaya, I., Lin, H., Sommer, D. D., Koren, S., et al. (2013). *De novo* likelihood-based measures for comparing genome assemblies. *BMC Res. Notes* 6:334. doi: 10.1186/1756-0500-6-334

Hall, T. A. (1999). BioEdit: a user-friendly biological sequence alignment editor and analysis program for Windows 95/98/NT. *Nucleic Acids Symp. Ser.* 41, 95–98.

Hurek, T., Handley, L. L., Reinhold-Hurek, B., and Piche, Y. (2002). *Azoarcus* grass endophytes contribute fixed nitrogen to the plant in an unculturable state. *Mol. Plant-Microbe Interact.* 15, 233–242. doi: 10.1094/MPMI.2002.15.3.233

Husemann, P., and Stoye, J. (2010). r2cat: synteny plots and comparative assembly. *Bioinformatics* 26, 570–571. doi: 10.1093/bioinformatics/btp690

Iniguez, A. L., Dong, Y., Carter, H. D., Ahmer, B. M., Stone, J. M., and Triplett, E. W. (2005). Regulation of enteric endophytic bacterial colonization by plant defenses. *Mol. Plant Microbe Interact.* 18, 169–178. doi: 10.1094/MPMI-18-0169

Inoue, A., Murata, Y., Takahashi, H., Tsuji, N., Fujisaki, S., and Kato, J.-I. (2008). Involvement of an essential gene, *mviN*, in murein synthesis in *Escherichia coli*. *J. Bacteriol.* 190, 7298–7301. doi: 10.1128/JB.00551-08

Ionescu, M., Franchini, A., Egli, T., and Belkin, S. (2008). Induction of the *yjbEFGH* operon is regulated by growth rate and oxygen concentration. *Arch. Microbiol.* 189, 219–226. doi: 10.1007/s00203-007-0311-0

Istivan, T. S., and Coloe, P. J. (2006). Phospholipase A in Gram-negative bacteria and its role in pathogenesis. *Microbiology* 152, 1263–1274. doi: 10.1099/mic.0.28609-0

Iuchi, S., Matsuda, Z., Fujiwara, T., and Lin, E. C. (1990). The *arcB* gene of *Escherichia coli* encodes a sensor-regulator protein for anaerobic repression of the *arc* modulon. *Mol. Microbiol.* 4, 715–727. doi: 10.1111/j.1365-2958.1990.tb00642.x

Kahlke, T., Goesmann, A., Hjerde, E., Willassen, N. P., and Haugen, P. (2012). Unique core genomes of the bacterial family vibrionaceae: insights into niche adaptation and speciation. *BMC Genomics* 13:179. doi: 10.1186/1471-2164-13-179

Kanamaru, K., Kanamaru, K., Tatsuno, I., Tobe, T., and Sasakawa, C. (2000). SdiA, an *Escherichia coli* homologue of quorum-sensing regulators, controls the expression of virulence factors in enterohaemorrhagic *Escherichia coli* O157:H7. *Mol. Microbiol.* 38, 805–816. doi: 10.1046/j.1365-2958.2000.02171.x

Kelly, B. G., Vespermann, A., and Bolton, D. J. (2009). Horizontal gene transfer of virulence determinants in selected bacterial foodborne pathogens. *Food Chem. Toxicol.* 47, 969–977. doi: 10.1016/j.fct.2008.02.007

Kube, M., Migdoll, A. M., Gehring, I., Heitmann, K., Mayer, Y., Kuhl, H., et al. (2010). Genome comparison of the epiphytic bacteria *Erwinia billingiae* and *E. tasmaniensis* with the pear pathogen *E. pyrifoliae*. *BMC Genomics* 11:393. doi: 10.1186/1471-2164-11-393

Li, L., Stoeckert, C. J. Jr., and Roos, D. S. (2003). OrthoMCL: identification of ortholog groups for eukaryotic genomes. *Genome Res.* 13, 2178–2189. doi: 10.1101/gr.1224503

Li, X., Hu, Y., Gong, J., Zhang, L., and Wang, G. (2013). Comparative genome characterization of *Achromobacter* members reveals potential genetic determinants facilitating the adaptation to a pathogenic lifestyle. *Appl. Microbiol. Biotechnol.* 97, 6413–6425. doi: 10.1007/s00253-013-5018-3

Lindquist, S., Weston-Hafer, K., Schmidt, H., Pul, C., Korfmann, G., Erickson, J., et al. (1993). AmpG, a signal transducer in chromosomal beta-lactamase induction. *Mol. Microbiol.* 9, 703–715. doi: 10.1111/j.1365-2958.1993.tb01731.x

Linhartová, I., Bumba, L., Mašín, J., Basler, M., Osička, R., Kamanová, J., et al. (2010). RTX proteins: a highly diverse family secreted by a common mechanism. *FEMS Microbiol. Rev.* 34, 1076–1112. doi: 10.1111/j.1574-6976.2010.00231.x

Little, A. E., Robinson, C. J., Peterson, S. B., Raffa, K. F., and Handelsman, J. (2008). Rules of engagement: interspecies interactions that regulate microbial communities. *Annu. Rev. Microbiol.* 62, 375–401. doi: 10.1146/annurev.micro.030608.101423

Lomovskaya, O., and Lewis, K. (1992). *emr*, an *Escherichia coli* locus for multidrug resistance. *Proc. Natl. Acad. Sci. U.S.A.* 89, 8938–8942. doi: 10.1073/pnas.89.19.8938

Luo, R., Liu, B., Xie, Y., Li, Z., Huang, W., Yuan, J., et al. (2012). SOAPdenovo2: an empirically improved memory-efficient short-read *de novo* assembler. *Gigascience* 1:18. doi: 10.1186/2047-217X-1-18

Maddocks, S. E., and Oyston, P. C. (2008). Structure and function of the LysR-type transcriptional regulator (LTTR) family proteins. *Microbiology* 154, 3609–3623. doi: 10.1099/mic.0.2008/022772-0

Matthysse, A.G., White, S., and Lightfoot, R. (1995). Genes required for cellulose synthesis in Agrobacterium tumefaciens. *J. Bacteriol.* 177, 1069–1075.

McCandlish, A. C., and Silhavy, T. J. (2007). Sugar-coating bacteria with lipopolysaccharides. *Microbe* 2, 289. doi: 10.1128/microbe.2.289.1

McCutcheon, J. P., and Moran, N. A. (2012). Extreme genome reduction in symbiotic bacteria. *Nat. Rev. Microbiol.* 10, 13–26. doi: 10.1038/nrmicro2670

Meng, Y., Li, Y., Galvani, C. D., Hao, G., Turner, J. N., Burr, T. J., et al. (2005). Upstream migration of *Xylella fastidiosa* via pilus-driven twitching motility. *J. Bacteriol.* 187, 5560–5567. doi: 10.1128/JB.187.16.5560-5567.2005

Meysman, P., Sanchez-Rodriguez, A., Fu, Q., Marchal, K., and Engelen, K. (2013). Expression divergence between *Escherichia coli* and *Salmonella enterica* serovar Typhimurium reflects their lifestyles. *Mol. Biol. Evol.* 30, 1302–1314. doi: 10.1093/molbev/mst029

Mitter, B., Petric, A., Shin, M. W., Chain, P. S. G., Hauberg-Lotte, L., Reinhold-Hurek, B., et al. (2013). Comparative genome analysis of *Burkholderia phytofirmans* PsJN reveals a wide spectrum of endophytic lifestyles based on interaction strategies with host plants. *Front. Plant. Sci.* 4:120. doi: 10.3389/fpls.2013.00120

Monack, D. M., Mueller, A., and Falkow, S. (2004). Persistent bacterial infections: the interface of the pathogen and the host immune system. *Nat. Rev. Microbiol.* 2, 747–765. doi: 10.1038/nrmicro955

Moore, L. W., Chilton, W. S., and Canfield, M. L. (1997). Diversity of opines and opine-catabolizing bacteria isolated from naturally occurring crown gall tumors. *Appl. Environ. Microbiol.* 63, 201–207.

Munkelt, D., Grass, G., and Nies, D. H. (2004). The chromosomally encoded cation diffusion facilitator proteins DmeF and FieF from *Wautersia metallidurans* CH34 are transporters of broad metal specificity. *J. Bacteriol.* 186, 8036–8043. doi: 10.1128/JB.186.23.8036-8043.2004

Oh, C. S., Kim, J. F., and Beer, S. V. (2005). The Hrp pathogenicity island of *Erwinia amylovora* and identification of three novel genes required for systemic infectiondouble dagger. *Mol. Plant. Pathol.* 6, 125–138. doi: 10.1111/j.1364-3703.2005.00269.x

Ozer, E. A., Allen, J. P., and Hauser, A. R. (2014). Characterization of the core and accessory genomes of *Pseudomonas aeruginosa* using bioinformatic tools Spine and AGEnt. *BMC Genomics* 15:737. doi: 10.1186/1471-2164-15-737

Pandey, D. P., and Gerdes, K. (2005). Toxin-antitoxin loci are highly abundant in free-living but lost from host-associated prokaryotes. *Nucleic Acids Res.* 33, 966–976. doi: 10.1093/nar/gki201

Park, D. H., Thapa, S. P., Choi, B. S., Kim, W. S., Hur, J. H., Cho, J. M., et al. (2011). Complete genome sequence of Japanese *Erwinia* strain ejp617, a bacterial shoot blight pathogen of pear. *J. Bacteriol.* 193, 586–587. doi: 10.1128/JB.01246-10

Parker, C. T., and Sperandio, V. (2009). Cell-to-cell signalling during pathogenesis. *Cell. Microbiol.* 11, 363–369. doi: 10.1111/j.1462-5822.2008.01272.x

Parkhill, J., Sebaihia, M., Preston, A., Murphy, L. D., Thomson, N., Harris, D. E., et al. (2003). Comparative analysis of the genome sequences of *Bordetella pertussis*, *Bordetella parapertussis* and *Bordetella bronchiseptica*. *Nat. Genet.* 35, 32–40. doi: 10.1038/ng1227

Parsons, J. F., Song, F., Parsons, L., Calabrese, K., Eisenstein, E., and Ladner, J. E. (2004). Structure and function of the phenazine biosynthesis protein PhzF from *Pseudomonas fluorescens* 2-79. *Biochemistry* 43, 12427–12435. doi: 10.1021/bi049059z

Poole, K., and Braun, V. (1988). Iron regulation of *Serratia marcescens* hemolysin gene expression. *Infect. Immun.* 56, 2967–2971.

Rajeshwari, R., Jha, G., and Sonti, R. V. (2005). Role of an in planta-expressed xylanase of *Xanthomonas oryzae* pv. *oryzae* in promoting virulence on rice. *Mol. Plant-Microbe Interact.* 18, 830–837. doi: 10.1094/MPMI-18-0830

R Core Team. (2013). *R: A Language and Environment for Statistical Computing*. Vienna:R Foundation for Statistical Computing. Available online at: http://www.R-project.org/.

Reinhold-Hurek, B., and Hurek, T. (2011). Living inside plants: bacterial endophytes. *Curr. Opin. Plant. Biol.* 14, 435–443. doi: 10.1016/j.pbi.2011.04.004

Remus-Emsermann, M. N., Kim, E. B., Marco, M. L., Tecon, R., and Leveau, J. H. (2013). Draft genome sequence of the phyllosphere model bacterium *Pantoea agglomerans* 299R. *Genome announc.* 1, e00036–e00013. doi: 10.1128/genomeA.00036-13

Ren, Y., Ren, Y., Zhou, Z., Guo, X., Li, Y., Feng, L., et al. (2010). Complete genome sequence of *Enterobacter cloacae* subsp. *cloacae* type strain ATCC 13047. *J. Bacteriol.* 192, 2463–2464. doi: 10.1128/JB.00067-10

Rosas-Magallanes, V., Deschavanne, P., Quintana-Murci, L., Brosch, R., Gicquel, B., and Neyrolles, O. (2006). Horizontal transfer of a virulence operon to the ancestor of *Mycobacterium tuberculosis*. *Mol. Biol. Evol.* 23, 1129–1135. doi: 10.1093/molbev/msj120

Sakai, D., and Komano, T. (2000). The *pilL* and *pilN* genes of IncI1 plasmids R64 and ColIb-P9 encode outer membrane lipoproteins responsible for thin pilus biogenesis. *Plasmid* 43, 149–152. doi: 10.1006/plas.1999.1434

Sana, T. G., Soscia, C., Tonglet, C. M., Garvis, S., and Bleves, S. (2013). Divergent control of two type VI secretion systems by RpoN in *Pseudomonas aeruginosa*. *PLoS ONE* 8:e76030. doi: 10.1371/journal.pone.0076030

Schlieker, C., Zentgraf, H., Dersch, P., and Mogk, A. (2005). ClpV, a unique Hsp100/Clp member of pathogenic proteobacteria. *Biol. Chem.* 386, 1115–1127. doi: 10.1515/BC.2005.128

Schulz, B., and Boyle, C. (2005). The endophytic continuum. *Mycol. Res.* 109, 661–686. doi: 10.1017/S095375620500273X

Schulz, B., Römmert, A.-K., Dammann, U., Aust, H.-J., and Strack, D. (1999). The endophyte-host interaction: a balanced antagonism? *Mycol. Res.* 103, 1275–1283. doi: 10.1017/S0953756299008540

Sebaihia, M., Bocsanczy, A., Biehl, B., Quail, M., Perna, N., Glasner, J., et al. (2010). Complete genome sequence of the plant pathogen *Erwinia amylovora* strain ATCC 49946. *J. Bacteriol.* 192, 2020–2021. doi: 10.1128/JB.00022-10

Seemann, T. (2014). Prokka: rapid prokaryotic genome annotation. *Bioinformatics* 30, 2068–2069. doi: 10.1093/bioinformatics/btu153

Shankar, V., Hamilton, M. J., Khoruts, A., Kilburn, A., Unno, T., Paliy, O., et al. (2014). Species and genus level resolution analysis of gut microbiota in *Clostridium difficile* patients following fecal microbiota transplantation. *Microbiome* 2:13. doi: 10.1186/2049-2618-2-13

Shepard, W., Soutourina, O., Courtois, E., England, P., Haouz, A., and Martin-Verstraete, I. (2011). Insights into the Rrf2 repressor family–the structure of CymR, the global cysteine regulator of *Bacillus subtilis*. *FEBS J.* 278, 2689–2701. doi: 10.1111/j.1742-4658.2011.08195.x

Shiba, Y., Matsumoto, K., and Hara, H. (2006). DjlA negatively regulates the Rcs signal transduction system in *Escherichia coli*. *Genes Genet. Syst.* 81, 51–56. doi: 10.1266/ggs.81.51

Shimada, T., Fujita, N., Yamamoto, K., and Ishihama, A. (2011). Novel Roles of cAMP Receptor Protein (CRP) in regulation of transport and metabolism of carbon sources. *PLoS ONE* 6:e20081. doi: 10.1371/journal.pone.0020081

Shin, S. H., Kim, S., Kim, J. Y., Lee, S., Um, Y., Oh, M. K., et al. (2012). Complete genome sequence of *Enterobacter aerogenes* KCTC 2190. *J. Bacteriol.* 194, 2373–2374. doi: 10.1128/JB.00028-12

Smits, T. H., Rezzonico, F., Kamber, T., Goesmann, A., Ishimaru, C. A., Stockwell, V. O., et al. (2010). Genome sequence of the biocontrol agent *Pantoea vagans* strain C9-1. *J. Bacteriol.* 192, 6486–6487. doi: 10.1128/JB.01122-10

Sorensen, K. I., and Hove-Jensen, B. (1996). Ribose catabolism of *Escherichia coli*: characterization of the *rpiB* gene encoding ribose phosphate isomerase B and of the *rpiR* gene, which is involved in regulation of *rpiB* expression. *J. Bacteriol.* 178, 1003–1011.

Suen, G., Scott, J. J., Aylward, F. O., Adams, S. M., Tringe, S. G., Pinto-Tomás, A. A., et al. (2010). An insect herbivore microbiome with high plant biomass-degrading capacity. *PLoS Genet.* 6:e1001129. doi: 10.1371/journal.pgen.1001129

Sugawara, M., Epstein, B., Badgley, B. D., Unno, T., Xu, L., Reese, J., et al. (2013). Comparative genomics of the core and accessory genomes of 48 *Sinorhizobium* strains comprising five genospecies. *Genome Biol.* 14:R17. doi: 10.1186/gb-2013-14-2-r17

Taghavi, S., van der Lelie, D., Hoffman, A., Zhang, Y.-B., Walla, M. D., Vangronsveld, J., et al. (2010). Genome sequence of the plant growth promoting endophytic bacterium *Enterobacter* sp. 638. *PLoS Genet.* 6:e1000943. doi: 10.1371/journal.pgen.1000943

Tamura, K., Stecher, G., Peterson, D., Filipski, A., and Kumar, S. (2013). MEGA6: molecular evolutionary genetics analysis version 6.0. *Mol. Biol. Evol.* 30, 2725–2729. doi: 10.1093/molbev/mst197

Tian, C., Zhou, Y., Zhang, Y., Li, Q., Zhang, Y., Li, D., et al. (2012). Comparative genomics of rhizobia nodulating soybean suggests extensive recruitment of lineage-specific genes in adaptations. *Proc. Natl. Acad. Sci. U.S.A.* 109, 8629–8634. doi: 10.1073/pnas.1120436109

Tritt, A., Eisen, J. A., Facciotti, M. T., and Darling, A. E. (2012). An integrated pipeline for *de Novo* assembly of microbial genomes. *PLoS ONE* 7:e42304. doi: 10.1371/journal.pone.0042304

Troxler, J., Azelvandre, P., Zala, M., Defago, G., and Haas, D. (1997). Conjugative transfer of chromosomal genes between fluorescent pseudomonads in the rhizosphere of wheat. *Appl. Environ. Microbiol.* 63, 213–219.

Ur Rahman, S., and Van Ulsen, P. (2013). System specificity of the TpsB transporters of coexpressed two-partner secretion systems of *Neisseria meningitidis*. *J. Bacteriol.* 195, 788–797. doi: 10.1128/JB.01355-12

Vayssier-Taussat, M., Albina, E., Citti, C., Cosson, J. F., Jacques, M.-A., Lebrun, M.-H., et al. (2014). Shifting the paradigm from pathogens to pathobiome: new concepts in the light of meta-omics. *Front. Cell. Infect. Microbiol.* 4:29. doi: 10.3389/fcimb.2014.00029

Wall, L., Christiansen, T., and Orwant, J. (2000). *Programming Perl.* California, CA: O'Reilly and Associates, Inc.

Wheeler, D. L., Barrett, T., Benson, D. A., Bryant, S. H., Canese, K., Chetvernin, V., et al. (2007). Database resources of the national center for biotechnology information. *Nucleic Acids Res.* 35, D5–D12. doi: 10.1093/nar/gkm1000

Xu, X.-H., Su, Z.-Z., Wang, C., Kubicek, C. P., Feng, X.-X., Mao, L.-J., et al. (2014). The rice endophyte *Harpophora oryzae* genome reveals evolution from a pathogen to a mutualistic endophyte. *Sci. Rep.* 4:5783. doi: 10.1038/srep05783

Yan, Y., Yang, J., Dou, Y., Chen, M., Ping, S., Peng, J., et al. (2008). Nitrogen fixation island and rhizosphere competence traits in the genome of root-associated *Pseudomonas stutzeri* A1501. *Proc. Natl. Acad. Sci. U.S.A.* 105:5783 7564–7569. doi: 10.1073/pnas.0801093105

Zerbino, D. R., and Birney, E. (2008). Velvet: algorithms for de novo short read assembly using de Bruijn graphs. *Genome. Res.* 18, 821–829. doi: 10.1101/gr.074492.107

Zhou, C. E., Smith, J., Lam, M., Zemla, A., Dyer, M. D., and Slezak, T. (2007). MvirDB–a microbial database of protein toxins, virulence factors and antibiotic resistance genes for bio-defence applications. *Nucleic Acids Res.* 35, D391–D394. doi: 10.1093/nar/gkl791

Zhou, Y., Liang, Y., Lynch, K. H., Dennis, J. J., and Wishart, D. S. (2011). PHAST: A Fast Phage Search Tool. *Nucleic Acids Res.* 39, W347–W352. doi: 10.1093/nar/gkr485

Zuccaro, A., Lahrmann, U., Güldener, U., Langen, G., Pfiffi, S., Biedenkopf, D., et al. (2011). Endophytic life strategies decoded by genome and transcriptome analyses of the mutualistic root symbiont *Piriformospora indica*. *PLoS Pathog.* 7:e1002290. doi: 10.1371/journal.ppat.1002290

Conflict of Interest Statement: The authors declare that the research was conducted in the absence of any commercial or financial relationships that could be construed as a potential conflict of interest.

Advantages of publishing in Frontiers

OPEN ACCESS
Articles are free to read, for greatest visibility

COLLABORATIVE PEER-REVIEW
Designed to be rigorous – yet also collaborative, fair and constructive

FAST PUBLICATION
Average 85 days from submission to publication (across all journals)

COPYRIGHT TO AUTHORS
No limit to article distribution and re-use

TRANSPARENT
Editors and reviewers acknowledged by name on published articles

SUPPORT
By our Swiss-based editorial team

IMPACT METRICS
Advanced metrics track your article's impact

GLOBAL SPREAD
5'100'000+ monthly article views and downloads

LOOP RESEARCH NETWORK
Our network increases readership for your article

Frontiers
EPFL Innovation Park, Building I • 1015 Lausanne • Switzerland
Tel +41 21 510 17 00 • Fax +41 21 510 17 01 • info@frontiersin.org
www.frontiersin.org

Find us on